University *of Ljubljana*
Faculty *of Pharmacy*

SLOVENSKO FARMACEVTSKO DRUŠTVO
SLOVENIAN PHARMACEUTICAL SOCIETY

EUFEPS
EUROPEAN FEDERATION FOR PHARMACEUTICAL SCIENCES

4th BBBB International Conference on Pharmaceutical Sciences

New Trends in Drug Discovery, Delivery Systems and Laboratory Diagnostics

Proceedings

www.bbbb-eufeps.org

September 29 – October 1, 2011 / Bled – SLOVENIA

doi:10.1016/j.ejps.2011.08.002

The 4th BBBB Conference is subsidized by the Slovenian Research Agency.

Spelling mistakes and other errors are under the responsibility of the authors!

New Trends in Drug Discovery, Delivery Systems and Laboratory Diagnostics

The outstanding scientific programme of the 4th BBBB* International Conference on Pharmaceutical Sciences in Bled covers actual aspects of effective and safe drug design, multifactorial approaches to delivery system development, as well as current diagnostic opportunities in laboratory biomedicine. The aim of the conference is to fulfil the needs of pharmaceutical and biomedical scientists in academia, industry, hospitals and laboratories to work hand in hand towards better understanding of disease etiology, towards the development of new drugs and diagnostic markers, and towards the creation of new therapeutic strategies.

The Proceedings include peer-reviewed contributions submitted for the 4th BBBB International Conference. The research reports focus on important new achievements in laboratory biomedicine, medicinal chemistry and pharmaceutical technology. Plenary lectures will highlight interdisciplinary approaches to unsolved challenges: from diagnosis to drug therapy, from past lessons and future perspectives to safer drugs, and from the formulation of macro- through micro- to nanomedicines. The invited lecturers are pioneers and opinion leaders from academia, clinical laboratories and the pharmaceutical industry. Their contributions provide a good scientific introduction to further readings of other research reports and will be presented at the conference either as oral or poster presentations. Authors from 25 countries will be sharing their views and fascinating strategies, all currently in research or under development, to optimise drug discovery, laboratory diagnostics and therapy.

We extend our thanks to all the colleagues who spent time writing or reviewing the submissions for the 4th BBBB International Conference. We hope that the conference and this Special Issue of the European Journal of Pharmaceutical Sciences will inspire new fruitful ideas for further development of advanced medicines and better health care.

Guest Editors

Prof. Dr. Julijana Kristl
Prof. Dr. Janja Marc
Prof. Dr. Danijel Kikelj

* In 2005, The **BBBB International Conferences** were initiated under the auspices of EUFEPS by the joint proposal of four founder countries' associations, the Estonian and the Finnish (**B**altic), the Hungarian (**B**alaton), the Slovenian (**B**led), and the Turkish Pharmaceutical Association (**B**osphorus), in order to organize conferences biennially to share state-of-the-art level information during its scientific programme covering all important aspects of the pharmaceutical sciences.

Conference Chair:
Julijana Kristl, Ljubljana, Slovenia

Conference co-chairs
Danijel Kikelj, Ljubljana, Slovenia
Janja Marc, Ljubljana, Slovenia

Founders of BBBB Conferences
Dominique Duchene, Paris, France
Istvan Hermecz, Budapest, Hungary
Hincal Atilla, Ankara, Turkey
Hans Linden (EUFEPS)
Aleš Mrhar, Ljubljana, Slovenia
Christian R. Noe, Vienna, Austria
Peep Veski, Tartu, Estonia

Scientific Committee
Karmela Barišić, Zagreb, Croatia
Ruggero Bettini, Parma, Italy
Jörg Breitkreutz, Düsseldorf, Germany
Sema Çalis, Ankara, Turkey
Gerhard Ecker, Vienna, Austria
Stanko Gobec, Ljubljana, Slovenia
Gabor L. Kovacs, Pecs, Hungary
Istvan Hermecz, Budapest, Hungary
Albin Kristl, Ljubljana, Slovenia
Gašper Marc, Ljubljana, Slovenia
Aleš Rotar, Novo mesto, Slovenia
Jürgen Siepmann, Lille, France
Vojmir Urlep, Ljubljana; Slovenia
Arto Urtti, Helsinki, Finland
Clive G. Wilson, Glasgow, United Kingdom
Peep Veski, Tartu, Estonia
Jari Yli-Kauhaluoma, Helsinki, Finland

Organizing Committee
Saša Baumgartner (president)
Lucija Peterlin Mašič (president)
Marko Anderluh
Mateja Cegnar
Bojan Doljak
Mirjana Gašperlin
Iztok Grabnar
Janez Kerč
Nataša Karas Kuželički
Aleš Mlinarič
Irena Mlinarič Raščan
Barbara Možina
Aleš Obreza
Tomaž Vovk
Franc Vrečer
Jernej Zadnik

Scientific Committe of the Satellite Symposium
Franc Vrečer (president)
Saša Baumgartner
Sara Cesar
Jernej Zadnik

Secretary of the Conference
Jelka Dolinar

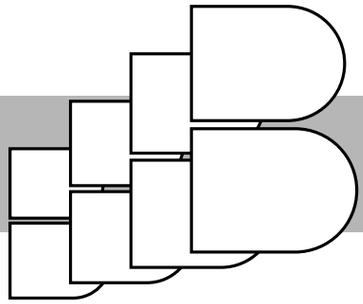

PLENARY LECTURES

OLD AND NEW ALLERGIC DISEASES: FROM DIAGNOSIS TO DRUG THERAPY

Hans-Uwe Simon

Institute of Pharmacology, University of Bern, CH-3010 Bern, Switzerland

Allergic diseases can be considered as hyperresponsiveness of target organs, in which an inflammatory cellular infiltrate is usually present. This hyperresponsiveness may or may not be IgE-mediated. The search of the responsible allergen is important for both diagnosis and therapy. Common allergies are hay fever, bronchial asthma, and atopic dermatitis. Allergen-specific immunotherapy is supposed to induce tolerance in these patients and newly identified molecular and cellular mechanisms (e.g. regulatory T cells) increased our understanding regarding how this treatment works (1). Besides IgE, allergic diseases are often associated with significant eosinophilia. Eosinophils are believed to contribute to organ dysfunction by causing tissue damage. The cationic proteins present within the eosinophil granules are particularly cytotoxic. We have recently observed that eosinophil granule proteins often associate with DNA in the extracellular space (2). These newly identified structures, also called eosinophil extracellular traps, appear to be able to kill pathogens, but may also contribute to tissue pathology (2). Interestingly, we detected eosinophil extracellular traps in biopsies of patients suffering from allergic diseases of the lungs and/or skin (3,4).

Eosinophilic esophagitis represents an emerging new allergic disease. It is a chronic Th2-type inflammatory disease of the esophagus (5,6). The inflammation is driven by both aero- and food allergens. Eosinophilic esophagitis is characterized clinicopathologically by symptoms attributed to esophageal dysfunction in combination with a dense esophageal eosinophilia, both of which are largely refractory to proton pump inhibitors. One serious concern is that unbridled eosinophilic inflammation leads to fibrosis and angiogenesis, with an ensuing mural thickening and loss of elasticity of the esophageal wall. Such a remodeling process has been described in clinical studies as well as in animal models.

There has been recent progress in the treatment of eosinophilic esophagitis. Clinical studies have been performed using both old and new anti-allergic drugs. Topical corticosteroids are highly efficacious in bringing patients in clinical and histological remission (7). They have also been used, although less successfully, as maintenance therapy (8). Corticosteroids were not only useful in reducing symptoms, they also limited tissue damage and esophageal remodeling processes (7,8). Interestingly, specific depleting eosinophils by using anti-IL-5 antibodies as a single treatment was clinically less successful compared with topical corticosteroid therapy, although remodeling was significantly reduced (9). Moreover, neutralization of TNF-alpha, which is highly expressed by epithelial cells of the esophagus (5), by antibody therapy did not seem to be a useful strategy (10).

Taken together, the recent years were witnesses of progress in both understanding and managing of old and new allergic diseases. Future work is required to further reduce the burden of allergic diseases.

REFERENCES

1. T. Bieber, H.-U. Simon: Allergen-specific immunotherapy: current concepts and future directions. Allergy 66 (2011), 709-712.
2. S. Yousefi, J.A. Gold, N. Andina, J.J. Lee, A.M. Kelly, E. Kozlowski, I. Schmid, A. Straumann, J. Reichenbach, G.J. Gleich, H.-U. Simon: Catapult-like release of mitochondrial DNA by eosinophils contributes to antibacterial defense. Nat. Med. 14 (2008), 949-953.
3. D. Simon, S. Hoesli, N. Roth, S. Staedler, S. Yousefi, H.-U. Simon: Eosinophil extracellular DNA traps in skin diseases. J. Allergy Clin. Immunol. 127 (2011), 194-199.
4. R. Dworski, H.-U. Simon, A. Hoskins, S. Yousefi: Eosinophil and neutrophil extracellular DNA traps in human allergic asthmatic airways. J. Allergy Clin. Immunol. 127 (2011), 1260-1266.
5. A. Straumann, M. Bauer, B. Fischer, K. Blaser, H.-U. Simon: Idiopathic eosinophilic oesophagitis is associated with a T-helper 2-type allergic inflammatory response. J. Allergy Clin. Immunol. 108 (2001), 954-961.
6. A. Straumann, H.P. Spichtin, L. Grize, K.A. Bucher, C. Beglinger, H.-U. Simon: Natural history of primary eosinophilic esophagitis: A follow-up of 30 adult patients for up to 11.5 years. Gastroenterology 125 (2003), 1660-1669.
7. A. Straumann, S. Conus, L. Degen, S. Felder, M. Kummer, H. Engel, C. Bussmann, C. Beglinger, A. Schoepfer, H.-U. Simon: Budesonide is effective in adolescent and adult patients with active eosinophilic esophagitis. Gastroenterology 139 (2010), 1526-1537.
8. A. Straumann, S. Conus, L. Degen, C. Frei, C. Bussmann, C. Beglinger, A. Schoepfer, H.-U. Simon: Long-term budesonide maintenance treatment is partially effective for patients with eosinophilic esophagitis. Clin. Gastroenterol. Hepatol. 9 (2011), 400-409.
9. A. Straumann, S. Conus, P. Grzonka, H. Kita, G. Kephart, C. Bussmann, C. Beglinger, D.A. Smith, J. Patel, M. Byrne, H.-U. Simon: Anti-interleukin-5 antibody treatment (mepolizumab) in active eosinophilic oesophagitis: a randomized, placebo-controlled, double-blind trial. Gut 59 (2010), 21-30.
10. A. Straumann, C. Bussmann, S. Conus, C. Beglinger, H.-U. Simon: Anti-TNF-alpha (infliximab) therapy for severe adult eosinophilic esophagitis. J. Allergy Clin. Immunol. 122 (2008), 425-427.

TRANSLATIONAL MEDICINE: HOW TO EXPLAIN VARIABILITY OF *IN VIVO* DRUG EFFECTS BY *IN VITRO* EXPERIMENTS, A RALOXIFENE CASE

A. Mrhar[1*], T. Trdan[1], J. Trontelj[1], B. Stieger[2], J. Marc[3], B. Ostanek[3], A. Zavratnik[4]

[1] University of Ljubljana, Faculty of Pharmacy, Department of Biopharmacy and Pharmacokinetics, Aškerčeva cesta 7, 1000 Ljubljana, Slovenia; [2] University Hospital, Department of Clinical Pharmacology and Toxicology, Raemistrasse 100, 8091 Zurich, Switzerland; [3] University of Ljubljana, Faculty of Pharmacy, Department of Clinical Biochemistry, Ljubljana; [4] University Medical Centre, Department of Endocrinology and Diabetology, Ljubljanska 5, 2000 Maribor, Slovenia.

INTRODUCTION

Raloxifene (Ral) exhibits a large (30-100%) variability in pharmacokinetics (PK) and pharmacodynamics (PD) [1], the source of which is still not known. Absolute oral bioavailability of Ral is very low (2 %) as it is extensively conjugated by the uridine-diphospho-glucuronosyl transferases (UGT) to raloxifene-6-glucuronide (M1), raloxifene-4'-glucuronide (M2) and raloxifene-6,4'-diglucuronide (M3), which undergo an intensive enterohepatic and enteroenteric recirculation [2]. The majority of raloxifene species in the blood represent inactive Ral glucuronides that can be considered a transport form of active Ral. Our main hypothesis was that the large interindividual variability in Ral PK is a consequence of genetic polymorphisms in the genes coding for drug metabolizing enzymes and drug transporters.

MATERIALS AND METHODS

Materials

Human liver microsomes (BD Gentest), raloxifene (Sigma Aldrich), [3H] estrone-3-sulfate (E3S) (PerkinElmer). M1, M2 and M3 were synthesised and characterised in our laboratory.

In vitro study

The models chosen to cover the metabolic conversion and the transport process were:

a) Incubations with human liver microsomes, genotyped for the *UGT1A1*28* polymorphism,
b) Uptake experiments on the CHO cells with hyperexpression of OATP1B1 transporters. The relative inhibition of the uptake of a radioactively labelled model substrate E3S was used as a measure of Ral species – OATP interaction. Indocyanine green (ICG) was used as a positive control for the inhibition of OATP1B1.

In vivo study

The clinical study was performed on 57 postmenopausal osteoporotic women who were started on raloxifene therapy (60mg daily). Before and after 12 months the following measurements were performed: concentration of serum C-terminal telopeptide fragments of type I collagen (CTX), serum bone-specific alkaline phosphatase (BALP), serum osteocalcin (OC), BMD measurement in hip, femoral neck and lumbar spine. Also, blood samples were collected in steady state for the quantification of Ral, M1, M2 and M3

with LC-MS/MS and *UGT1A1* and *SLCO1B1* genotype determination with PCR. The study was approved by the Slovenian National Medical Ethics Committee.

Statistical methods

For determination of genotype influence on PK and PD, ANOVA, t-test and z-test followed by appropriate post-hoc analysis were used. The apparent kinetic parameters K_m, V_{max} and K_{si} were calculated by nonlinear regression using IBM SPSS Statistics 19 (IBM Corporation). Data were fitted to the Michaelis-Menten (for M1) and substrate inhibition equation (for M2) and intrinsic clearance was determined as $Cl_{int}=V_{max}/K_m$.

RESULTS AND DISCUSSION

The main results of our study were two-fold. Firstly, we demonstrated a significant effect of patient's genotype on the activity of UGT1A1 on both the *in vitro* and *in vivo* raloxifene conjugation. Microsomes from *1/*1 homozygotes showed fivefold higher intrinsic clearance than *28/*28 (p=0.003) (Fig. 1). Similarly, patients homozygous for the polymorphic *28 allele showed a doubled raloxifene exposure (558 ± 115 nmol/L compared with 295 ± 43 nmol/L in patients with at least one copy of *1 allele (p=0,012) (Fig. 2A). Likewise, a significant effect of the number of haplotype *1b copies for *SLCO1B1* in the gene coding OATP1B1 on serum concentrations was also observed (Fig. 4A). Higher raloxifene exposure was observed in patients with higher number of *SLCO1B1* *1b copies (Fig. 4A). The *in vivo* effect of *SLCO1B1* polymorphism was explained by the *in vitro* study of OATP1B1-raloxifene species interaction. (Fig. 3).

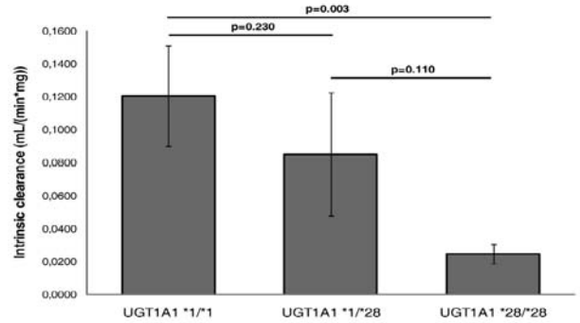

Fig. 1: Raloxifene clearance determined by UGT1A1 genotyped liver microsomes.

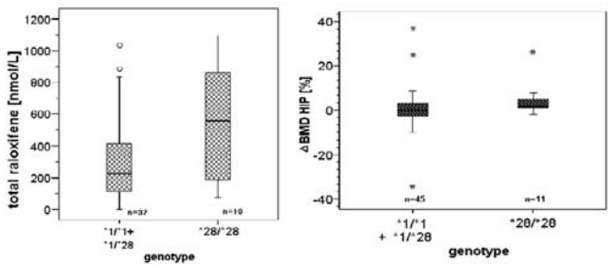

Fig. 2: A: Raloxifene species concentration distribution among the subjects grouped by the presence or absence of the *28 polymorphic allele. B: Distribution of % changes in bone mineral density in HIP after one year of raloxifene therapy in the same two UGT1A1 genotype groups.

Secondly, we have also demonstrated a significant contribution of both the drug metabolizing enzyme and the drug transporter genotype on PD of raloxifene. A significant effect was observed for *UGT1A1**28 polymophism on bone mineral density of hip (Fig. 2B) and for *SLCO1B1* *1b haplotype on CTX (Fig. 4B).

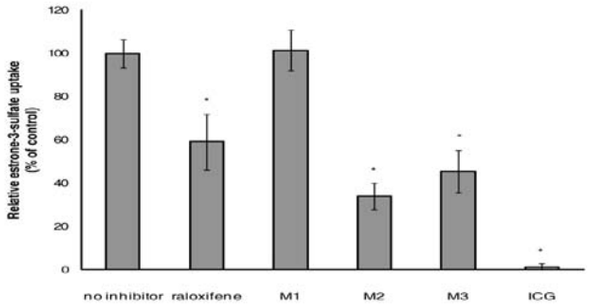

Fig. 3: Inhibitory effects of Ral, M1, M2, M3, ICG on active uptake of E-3-S into CHO cells recombinantly expressing OATP1B1.

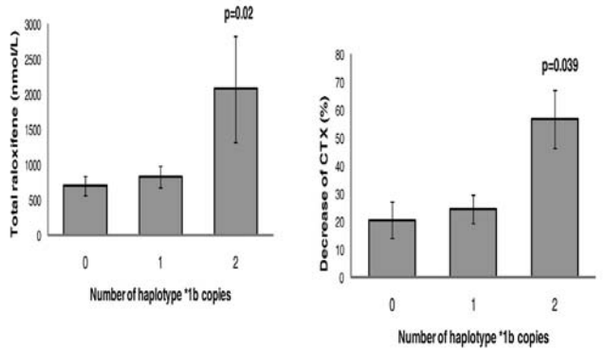

Fig. 4: A: Raloxifene species concentration in serum according to number of SLCO1B1 *1b copies. B: Percentage decrease of CTX after one year of raloxifene according to number of SLCO1B1 *1b copies.

CONCLUSIONS

The synergistic use of *in vitro* models combined with a small-sized *in vivo* study has proven to be highly successful in explaining the observed raloxifene variability. Multidisciplinary approach of translational research yields a greater insight into the complex mechanisms of drug disposition. Finally, the acquired knowledge assures safer, more effective treatment strategies in the clinical setting.

REFERENCES

1. Trontelj J., Marc J., Zavratnik A. et al. Effects of UGT1A1*28 polymorphism on raloxifene pharmacokinetics and pharmacodynamics. Br J. Clin. Pharmacol. 2009;
2. Hochner-Celnikier D. Pharmacokinetics of raloxifene Eur. J. Obstet. Gynecol. Reprod Biol; 1999; 85(1):23-9.

DESIGNING SAFER DRUGS: PAST LESSONS AND FUTURE CHALLENGES

Boyer S.

AstraZeneca R&D, Pepparedsleden 1, 43183 Mölndal, Sweden

Drug discovery should be easy; one only needs to prove that a given medication is effective and that it is safe enough to gain benefits from efficacy without causing excessive harm. This balance of benefit and risk is extremely difficult to establish in most cases. This talk will explore the evaluation of risk/benefit in modern pharmaceutical research in an environment of ever-increasing demands for greater benefit coupled with lower risk.

The factors contributing to these demands include higher hurdles for proof of patient benefit by payers attempting to get the most from their healthcare budgets, but also from regulators, who have assumed a more risk-averse stance in many therapeutic areas. The result is that drugs now take longer to develop and are much more costly to register due to the level of supporting information required. This has resulted in a number of business decisions within the pharmaceutical industry which include abandoning certain therapeutic areas because the burden of proof is prohibitively expensive, closer accounting of return on investment for each project as it progresses from early discovery through to development and finally, assuring the best quality in each project by making strategic investments in quality from the very inception of a new project.

The investment in 'quality' gives a number of advantages. In general there are two primary drivers for investing in better quality material in projects: 1) gaining competitive advantage and 2) lowering the average cost of each project by mitigating the common causes of project failure.

Among the top contributing factors to project 'failure' in the pharmaceutical industry are 1) lack of market potential 2) failure to show adequate beneficial effect and 3) unacceptable safety profile. These three factors, while sometimes contributing to a failure by themselves, most often are linked to each other. Central to these factors is drug safety. Without appropriate safety profiles, projects cannot be developed fully regardless of the anticipated beneficial effects and the potential reimbursement picture.

Assuring that new drug candidates are as safe as possible is a process which requires many different levels of tools and strategies, from the very initiation of the idea of intervening in a biological process to design of the molecule to assessment of toxicity in animals and humans to pharmacovigilance. Each of these aspects of drug safety evaluation demands its own set of questions and its own solutions to information management and analysis to bring as much past information and experience to bear on the project without overwhelming decision-makers with too much information.

Much of the focus of this talk will be on the issue of providing the right information to decision-makers in the area of drug safety. Aspects of drug safety that can directly benefit from better information management range from the choice of therapeutic 'target' to designing the right molecule to better estimation of therapeutic margins to more rigorous analysis of safety data from early clinical trials.

TREATING DEPRESSION: LESSONS FROM HUMAN LYMPHOBLASTOID CELLS

David Gurwitz

Department of Human Molecular Genetics and Biochemistry, Sackler Faculty of Medicine, Tel-Aviv University, Tel-Aviv 69978, Israel

Selective serotonin reuptake inhibitors (SSRIs) are the most commonly used class of antidepressants for treating major depression. However, ~30% of patients do not respond sufficiently to their first-line antidepressant drug treatment and require alternative therapeutics. Genome-wide studies searching for SSRI response DNA biomarkers or studies of candidate serotonin-related genes so far gave inconclusive or contradictory results. As a first step toward studies with patients' lymphocytes, we used the alternative approach of genome-wide transcriptome-based search for SSRI response biomarkers in human lymphoblastoid cell lines (LCLs). We first screened 80 LCLs from healthy adult female individuals for growth inhibition by paroxetine. Fourteen LCLs with extremely high and low sensitivities to paroxetine (7 from each phenotypic group) were chosen for genome-wide expression profiling with Affymetrix microarrays. Genome-wide transcriptomic analysis has identified 158 genes whose levels of expression differed by >1.5-fold and $p<0.005$ between the two paroxetine sensitivity groups, as confirmed by real-time PCR experiments. Among these genes *CHL1* stands is the most promising biomarker, showing 36-fold lower expression in LCLs with high sensitivity to paroxetine. CHL1 codes for a cell adhesion protein implicated in synaptogenesis and maintenance of correct brain circuitry. Its potential as a putative SSRI response biomarker will be explored with clinical samples from major depression patients with known drug response phenotypes. Our method may be applied as a research tool for genome-wide exploration of biomarkers for drugs whose protein targets are expressed by lymphocytes.

NEW GLYCINE TRANSPORTER INHIBITORS: DESIGN, SYNTHESIS AND BIOLOGICAL EVALUATION

P. Matyus[1*], L. G. Jr. Harsing[2], P. Tapolcsanyi[1], A. Kocsis[1], A. Czompa[1], G. Szabo[3], J. Barkoczy[3], K. Nagy[2] and G. Zsilla[2]

[1] Department of Organic Chemistry, Semmelweis University, 1092 Budapest, Hőgyes E. u. 7. Hungary; [2] Department of Pharmacology and Pharmacotherapy, Semmelweis University, 1089 Budapest, Nagyvárad tér 4. Hungary; [3] EGIS Pharmaceuticals Plc. 1106 Budapest, Keresztúri út 30-38. Hungary; [4] Institute of Experimental Medicine, Hungarian Academy of Sciences, 1083 Budapest, Szigony u. 43. Hungary

For the effective treatment of complex symptoms of schizophrenia, there is a great need to develop new types of drugs. The current therapy is mainly based on mixed dopamine D_2 and serotonine 5-HT_{2A} type atypical antipsychotics which, although, such drugs improve positive symptoms of the disease, because of their limited therapeutic scope and unfavorable side effect profile, are far from being optimal. Recently, glycine transporter-1 (GlyT1) inhibition has attracted much attention as a promising new therapeutic strategy for the treatment of schizophrenia, with the expectation of restoring hypofunction of NMDA receptors, thus eliminating negative symptoms of schizophrenia, via increasing levels of NMDA receptor co-agonist glycine within synapses [1]. In fact, sarcosine (*N*-methylglycine), the prototype of GlyT1 inhibitors, proved to be effective in combination with antipsychotics without exerting significant side effects in a six-week double-blind clinical trial [2]. To improve its moderate activity and modest bioavailability, several series of more lipophylic glycine/sarcosine derivatives have been synthesized. In a series of amides of glycine, sarcosine and alanine, there was observed a fairly good inhibition of GlyT1 (Table 1A) [1a]. To obtain more drug-like molecules, some CNS active structural elements were connected to sarcosine. In particular, two new series of compounds were promising, represented by NFPS, N-(3-(4-fluorophenyl)-3-(4-phenyl-phenoxy)-propyl)sarcosine (Allelix) and Org 24461, N-(3-phenyl)-3-(4-trifluoromethyl-phenoxy)propyl)sarcosine (Organon) and their eutomers ALX-5407 and Org-24598, respectively (Figure 1) [1b]. These compounds proved to be even more potent GlyT1 inhibitors, than the previous set of

amides (Table 1B) [1]. Importantly, these compounds also exerted antipsychotic activities and were able to reverse the cognitive deficit induced by phencyclidine in disease-relevant animal models [3,4]. However, their untoward side effects, such as ataxia and especially a decreased respiratory activity, have turned the attention to non-sarcosine-based inhibitors (for some representatives, s. Figure 1) [1b]. This line of research has become undoubtedly more successful so far, since, more recently, a potent, highly selective GlyT1 inhibitor, RG1678 (Figure 1) positively influenced negative symptoms of schizophrenia in a Phase II clinical study, thereby providing a definite proof of concept in human subjects [5]. However, further data are needed to come to a conclusion regarding possible respiratory reduction in a long term application, if it is associated only with the structure of sarcosine or, we think so, it is a mechanism-based side effect, the manifestation of which is dependent on the occupancy of the transporter.

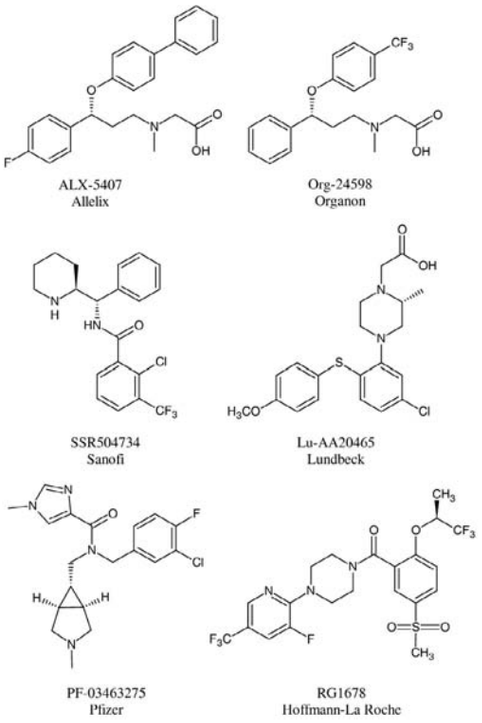

Fig. 1: Some sarcosine and non-sarcosine type GlyT1 inhibitors.

Table 1: Performance of reference compounds in our own assays

A. Aminoacid amides

Compounds	[^{3}H]Gly uptake inhibition (IC_{50} M)
Glycyldodecylamide	3.3×10^{-5}.
D-Alanyldodecylamide	2.3×10^{-5}
Sarcosyldodecylamide	1.6×10^{-5}
Beta-Alanyldodecylamide	2.3×10^{-5}
N-(2-imidazolinyl)-glycyldodecylamide	$>10^{-4}$
[^{3}H]Gly uptake was measured in synaptosomal preparation of rat hippocampus	

B. NFPS and Org24461

Compounds	hGlyT-1b	hGlyT-1a	GlyT-1 synaptosomes
NFPS	4.2×10^{-8}	1.2×10^{-8}	2.4×10^{-8} M
Org24461	10^{-7}	-	1.1×10^{-7} M
hGlyT-1b expressed in CHO cells; hGlyT1a expressed in JAR cells; synaptosomal preparation: rat brain			

A few years ago, we initiated ourselves a research project with the aim to develop novel GlyT1 inhibitors. We focused particularly on structures of NFPS and Organon series of compounds, taking also into consideration that in fluoxetine-based Organon series, GlyT1 inhibitory activity was possible to significantly influence by substituents of the phenoxy group [6]. Utilizing also our previous experiences in the development of CNS-active pyridazines led us to synthesize three new series of compounds, in which we incorporated a pyridazine ring in different ways. In the first series, the sarcosine unit was replaced by a 3(2*H*)-pyridazinone ring through attaching the propyl chain to the amide nitrogen or 5-position of pyridazinone, whereas in the second and third series, the biphenyloxy group was replaced with a 2-aryl-3-oxo-5-pyridazinyloxy or 4-(3-oxopyridazin-5-yloxy)phenoxy substituent, respectively.

In the latter two series, some compounds were found i) to exert strong inhibition of GylT1 (micro/nanomolar IC50 on recombinant hGlyT1 expressed in CHO cells and in rat brain synaptosomal preparations), ii) to enhance extracellular glycine concentrations in conscious rats in striatum, and glycine levels in a microdialysis assay in mice, iii) to reverse phencyclidine-induced hypermotility in mice, an animal model for symptoms of schizophrenia. Moreover, the most active pyridazine derivative did not exhibit i) affinity for a number of receptors and ii) inhibition of GlyT-2 or iii) inhibition of hERG channel in concentrations relevant to the desired pharmacological effect.

REFERENCES

1. For recent reviews, see:
   a. Harsing, L.G., Jr., Juranyi, Z., Gacsalyi, I., Tapolcsanyi, P., Czompa, A., Matyus, P.: Glycine transporter type-1 and its inhibitors. *Curr. Med. Chem*., **2006**, *13*, 1017-1044.
   b. Wolkenberg, S. E., Sur, C. Recent Progress in the Discovery of Non-Sarcosine Based GlyT1 Inhibitors. *Curr. Topics Med. Chem*., **2010**, *10*, 170-186.
2. Tsai, G., Lane, H.Y., Yang, P., Chong, M.Y., Lange N. Glycine transporter I inhibitor, N-methylglycine (sarcosine), added to antipsychotics for the treatment of schizophrenia. *Biol. Psychiatry*, **2004**, *55*, 452–456.
3. Harsing, L.G.,Jr., Gacsalyi,I. Szabo, G., Schmidt, E., Sziray, N., Sebban, C., Tesolin-Decros, B., Matyus, P., Egyed, A., Spedding, M., Levay, G.: The glycine transporter-1 inhibitors NFPS and Org 24461: a pharmacological study. *Pharm. Biochem, Behav*., **2003**, *74*, 811-825.
4. Hashimoto, K., Fujita, Y., Ishima, T., Chaki, S., Iyo, M. Phencyclidine-induced cognitive deficits in mice are improved by subsequent subchronic administration of the glycine transporter1 inhibitor NFPS and D-serine. *Eur. Neuropsychopharmacol*., **2008**, *18*, 414-421.
5. Brown, A., Carlyle, I., Clark, J., Hamilton, W., Gibson, S., Mcgarry, G., McEachen, S., Rae, D., Thorn, S., Walker, G. Discovery and SAR of Org24598 – a selective glycine uptake inhibitor. *Bioorg. Med. Chem. Lett*., **2001**, *11*, 2007-2009.
6. Pinnard, E., Alanine, A., Alberati, D., Bender, M., Borroni, E., Bourdeaux, P., Brom, V., Burner, S., Fischer, H., Hainzl, D., Halm, R., Hauser., N., Jolidon, S., Lengyel, J., Marty, H.P., Meyer, T., Moreau, J.L., Mory, R., Narquizian, R., Nettekoven, M., Norcross, R.D., Puellmann, B., Schmid P., Schmitt, S., Stalder H., Wermouth R., Wettstein, J.G., Zimmerli, D. Selective GlyT1 inhibitors: discovery of [4-(3-(fluoro-5-trifluoromethylpyridin-2-yl)piperazin-1-yl]- [5-methansulfonyl-2-((S)-2,2,2-trifluoro-1-methylethoxy)-phenyl]methanone (RG1678), a promising novel medicine to treat schizophrenia. *J. Med. Chem*., **2010**, *53*, 4603-4614.

FORMULATION OF PROTEIN PHARMACEUTICALS – TRENDS, TRUTHS AND SURPRISES FROM THE LAST 20 YEARS

G. Winter

University of Munich (LMU), Department Pharmacy, Butenandtstr. 5-13, 81377 München, Germany

INTRODUCTION

Recombinant protein pharmaceuticals have matured into a significant part of our drug portfolio today. Their success rate, medically and financially, is incredible and they form with no doubt the fastest growing segment of modern drugs. Along with the research and development on these new biological entities (NBEs) itself, formulations research for biotec drugs has evolved into an exciting new sector of modern pharmaceutics. Since the first recombinant protein product (insulin) was marketed in 1985, protein formulation research took its own interesting path, from rather empiric approaches towards more specific, rational concepts, including also work

on specific dosage forms for targeted and/or sustained delivery. The contribution shall explain some important concepts that have changed over this period of time. Some case studies will highlight novel ideas and either confirm or challenge well known concepts.

RESULTS AND DISCUSSION

The major aim of all formulation work on protein drugs is achieving stability of the drug over an adequate shelf live period. The resulting formulation must of course fulfil all the requirements on safety, handling, costs and, if appropriate, more sophisticated pharmacokinetic/delivery aspects. Already in the 1980ies, basic tasks like minimizing adsorption of low dose proteins on surfaces, stabilization in liquid and freeze dried forms and selecting the right manufacturing were achieved. With that done and more products coming to the market and more sophisticated analytical methods been developed alongside, some unresolved issues remained or "new" challenges arose.

In the following we will concentrate on such topics and explain our experience and actual position. First, one of the most discussed aspects of protein product safety and quality is the issue of unwanted immunogenicity and its correlation to aggregates in the product. For many years, particulate matter in protein solutions has been an issue but only more recently has the public discussion (1,2) moved towards a more critical, complete understanding. The community has learned, that protein aggregates of different size and solubility are hardly detectable and quantifiable with only one method. Therefore we accept today, that "orthogonal" methods have to be used, i.e. methods that complement each other and are using different analytical principles thereby reducing the risk of overlooking certain quality aspects or hunting after artefacts. We have tried to support these efforts by research on flow field flow fractionation, a method that can in the best case fractionate and characterize a wide range of protein aggregates, soluble as well as insoluble matter (3).

Second, one may consider to tough the aggregation aspect already at its roots, namely at the interface of downstream processing of a particular protein and its final formulation. We have worked on that field for about 20 years and are happy to see how close these two steps in the development and production of a modern biopharmaceutical are today. In an ideal case, bulk drug substance solutions are already formulated and stored as such until just filled into vials, leaving practically no gap. Formulations research has even moved into the last steps of downstream processing and we will present some examples how for highly concentrated antibody solutions optimization at that point can improve overall quality (4).

In case of freezes dried products, main concern for decades was and still is the high costs, the long duration of the processes and the inherent technical risk of failure, mostly due to collapse of the cakes. The latter increased over the year due to the fact, that the community has learned after the ground-braking work of Carpenter, Pikal, Franks et al., that glassy sugar matrices are mandatory for the state of the art freeze drying products and such matrices have inherently difficult drying properties. We have done research over significant time on alternative drying technologies, challenging the dogma of elegant, not collapsed cakes and now propose very fast drying cycles with, surprisingly, not compromised but even improved storage stability of the resulting matrices (5).

Another aspect of protein formulation is the use of surfactants. Not only do they minimize adsorption but also significantly reduce aggregation caused by different stress factors, one of them being mechanical stress, e.g. shaking. Much has been published over the years about some drawbacks on the typical surfactant of choice, polysorbate. We now propose to reconsider HP-ß-CD (Hydroxypropyl-ß-cyclodextrin) as a very valid alternative to polysorbates. Interestingly it has a different mechanism of action and exceeds the effect of polysorbate in certain aspects (6).

Finally, a major new trend in modern formulations research for protein drugs is the miniaturising approach. It is always an issue to use as low amounts of drug substance for formulation development as possible, but only recently has the pressure to come to a formulation with minimal amounts increased again. Reason is the insight, that formulation aspects should be included already into the selection process of the drug candidates in cases where several potentially effective drug entities are available but only one should be developed further due to financial restrictions during the costly preclinical, let alone the clinical phase. Two approaches that can also be combined with each other are used today. One is high-throughput formulation studies where as much as possible analytical methods and stress model are applied in well plate format etc. to allow experiments with volumes in the µl range (7). In addition, predictive methods are widely used, where the protein unfolding under stress, e.g. temperature ramping over a few hours is correlated to the long term stability of such a molecule under normal storage conditions (8). Such methods are in part able to save a lot of time and material, especially when they are combined with well plate formats.

Beside these trends on traditional formulations we would like to review a few more recent lipid based depot systems for protein drugs, allowing very long term local and systemic delivery. Some of them have the potential to cure some of the unsuccessful approaches taken over the last 20 years in the design of such depot systems (9,10).

REFERENCES

1. Carpenter et al. J.Pharm.Sci. (2010) 99(5):2200-2208
2. Gabrielson et al. J.Pharm.Sci (2007) 96(2):268-279
3. Fraunhofer et al. EJPB (2004) 58(2):369-383
4. Rosenberg et al. J.Mem.Sci.(2009) 342(1-2):50-59
5. Schersch et al. J.Pharm.Sci. (2010) 99(5):2256-2278
6. Serno et al. J.Pharm.Sci.(2010) 99(3):1193-1206
7. Capelle et al. EJPB (2007) 65(2):131-148
8. Youssef, A. Dissertation, LMU München, 2010
9. Tian et al. JCR (2010) 142(3):319-325
10. Schulze et al. JCR (2009)134(3):177-185

PHTHALEATES AS ENDOCRINE DISRUPTING CHEMICALS AND PHARMACEUTICAL EXCIPIENTS

Filiz Hincal

Hacettepe University, Faculty of Pharmacy, Department of Toxicology, 06100 Ankara, Turkey

Phthalates are synthetic chemicals with a wide spectrum of industrial and commercial appplications. They are the most abundant chemical contaminants in the environment, produced in high volume and used mostly as plasticizers to impart flexibility, transparency and durability to plastics that are widely used in personal care products, food packaging and medical devices, cosmetics, baby feeding tubes, nipples and toys. Phthalates easily released from the plastic matrix into the environment, their metabolites have been detected in virtually all human urine samples tested, indicating widespread exposure (1). Diet is the major route of exposure for phthalates, especially di(2-ethylhexyl)phthalate DEHP (1, 2). But other sources such as fragrance-containing personal care products make a substantial contribution to overall exposure levels (2,3). However, low-molecular-weight phthalates, such as diethyl phthalate (DEP) and dibutyl phthalate (DBP) that are used to make coatings for oral medications, including those designed for timed release or release in the large bowel are considered to be high exposure sources (4).

Phthalates are known as endocrine disrupters and peroxisome proliferators (PP), possess hepatocarcinogenic activity, cause reproductive and developmental toxicity in rodents (5-7). Their inevitable environmental exposures in humans have been suspected to contribute to the increasing incidence of testicular dysgenesis syndrome (TDS) that is a range of reproductive defects including cryptorchidism and hypospadias in

newborn boys, and testicular cancer and reduced sperm quality in adult males. In fact, TDS has been shown to develop in male rats that are exposed to phthalates *in utero* (7,8).

Multiple mechanisms of action were suggested for phthalate effects in the reproductive system, including PP-activated or estrogen receptor-mediated mechanisms, dysregulation of gene-expression pattern, and affecting spermatogenesis by altering the activities of enzymes responsible for the maturation of sperms (9-11). Another ever increasing possibility is the induction of oxidative stress. In fact, free radicals and lipid peroxidation are considered as potentially important mediators in testicular physiology and induce apoptosis in male germ cells; CYP450 enzymes of the steroidogenic pathway are known to produce free radicals under physiological conditions, and testicular oxidative stress has been related to a number of pathological conditions and exposures known to be detrimental to male fertility (12,13). Our recent studies on MA-10 Leydig and LNCaP human prostate cells (14-16) have produced comprehensive data suggesting that at least one of the mechanisms underlying the reproductive toxicity of DEHP is the induction of intracellular ROS and p53, and alterations in intracellular enzymatic and nonenzymatic antioxidants, thus, the production of oxidative stress. Our data have emphasized the importance of the redox status of the testicular cells in which selenium (Se) has a critical role. Accordingly, we have demonstrated that Se supplementation was highly protective against the cytotoxicity and genotoxicity of DEHP in both MA-10 Leydig and LNCaP cells stressing the role of Se as an effective cellular redox regulator. These in vitro findings were also in line with those of our in vivo study (17) that have demonstrated a testosterone lowering effect of DEHP along with other hormonal (LH, and FSH) alterations; disturbed testicular histology with damaged seminiferous tubule epithelium, detachment of spermatogenic cells and disturbed spermato- and spermiogenesis; as well as increased morphologic abnormalities and diminished motility in epididymal sperms. We also showed the influence of Se status on the adverse effects of DEHP in rats, similarly suggesting that DEHP exposure may cause alterations in the cellular redox status in testis and Se provides protection.

Our overall results, along with high plasma levels of DEHP we observed in pubertal gynecomastia patients (18), raise the concern over the potential effects of inevitable phthalate exposures including by their pharmaceutical usage. Such concerns are increasing particularly for the developing reproductive system of male infants and children, and for the pregnant women.

REFERENCES

1. Heudorf et al., Int. J. Hyg. Environ. Health 2007; 210: 623–634.
2. Fromme et al., Env. Int. 2007; 33: 1012-1020.
3. Duty et al., Hum. Reprod. 2005; 20: 604-610.
4. Hernández-Díaz et al., Environ. Health Perspect. 2009; 117: 185–189.
5. Rusyn et al., Crit. Rev. Toxicol. 2006; 36: 459-479.
6. Lyche et al., J. Toxicol. Environ. Health B Crit. Rev. 2009; 12: 225–249.
7. Fisher et al., Hum. Reprod. 2003; 18: 1383–1394.
8. Yiee and Baskin, J. Urol. 2010; 184: 34–41.
9. Gazouli et al., Endocrinology 2002; 143: 2571–2583.
10. Borch et al., Toxicology 2006; 223: 144-155.
11. Barlow et al., Toxicol. Sci. 2003; 7: 431-441.
12. Aitken and Baker, Mol Cell Endocrinol 2006; 250: 66-69.
13. Turner and Lysiak, Androl. 2008; 29: 488-498.
14. Erkekoglu et al., Free Radic. Biol. Med. 2010; 49: 559-566.
15. Erkekoglu et al., Toxicol. Appl. Pharmacol. 2010; 248: 52-62.
16. Erkekoglu et al., Food Chem. Toxicol. 2011; doi: 10.1016/j.fct.2011.04.001.
17. Erkekoglu et al., Drug Chem. Tox. 2011; doi: 10.3109/01480545.2010.547499.
18. Durmaz et al., Pediatrics 2010; 125: 122-129.

THE APPLICATIONS OF NEW IMAGING AND DELIVERY TECHNOLOGIES IN FORMULATION PROTOTYPING

Clive G. Wilson

SIPBS, University of Strathclyde, Glasgow G4 0NR, Scotland, U.K.

INTRODUCTION

Formulations represent the opportunity for a complex interaction in terms of dissolution and deposition. The essence of translational medicine is the feedback between clinical trial and the laboratory bench, utilising the outputs in the pursuit of better *in vitro* or *in silico* correlation. The ability to examine the formulation, particularly with regard to dispersion, or better still targeting, facilitates cycles of optimisation and pharmacometrics. In surgery, clinical diagnosis and bio-chemistry, biological imaging has undergone a revolution in terms of imaging the orientation of molecular motifs, visualising signal pathways and complementing this information with advanced chemical fingerprinting in proteomics and other metabolomics.

Pharmaceutical sciences has utilised tools from these disciplines to understand formulation behaviour and the relationship of physicochemical attributes to the plasma concentration time profile. In the early stages this was confined the identification of 'absorption windows' but more lately endoscopic cameras can been employed to examine precipitation and the behaviour of tablet and capsule coatings in the gut. Quantitative clinical tools such as gamma scintigraphy are the mainstay of measurement by interval or continuous monitoring. These instruments can capture formulation differences occurring in the gastrointestinal tract before the appearance of the active pharmaceutical ingredient in the systemic circulation, especially as blood sampling cannot be continuous (1). Other new tools such as magnetic moment monitoring are widening the possibilities for prototype evaluation and improvement (2). The industry maxim of 'what gets measured, gets fixed" can be applied in pharmaceutical metrics, resulting in faster elimination of poor formulations by understanding *in vivo* performance constraints.

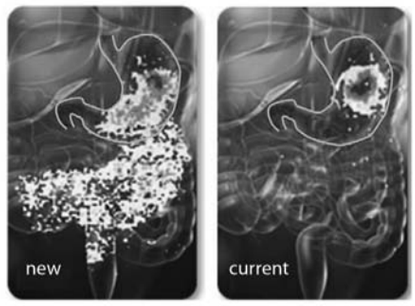

Fig. 1: Dispersion of new and old formulations in the stomach using gamma scintigraphy. Image 5 minutes after swallowing formulations (From Ref 2).

CONCLUSIONS

Adoption of new clinical imaging tools will speed up the process of rational formulation design and allow better discrimination of factors affecting variability in smaller volunteer and patient populations.

REFERENCES

1. Palmer H., Wilson C.G., Clarke C P., Starkey Y L., Clarke G D. (2010). Comparison of a novel fast dissolving acetaminophen tablet formulation (FD-APAP) and standard acetaminophen tablets using gamma scintigraphy and pharmacokinetic studies. Drug Dev. Indust. Pharm. Vol. 37, No. 7 , 747-753.
2. Weitschies W. & Wilson C.G. (2011). In vivo imaging of drug delivery systems in the gastrointestinal tract. Int. J. Pharm. (in press).

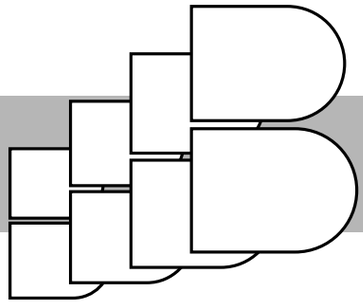

KEYNOTE LECTURES

ADVANCED CELL-BASED THERAPIES

M. Jeras[1, 2, 3*], M. Bergant Marušič[4], M. Gabrijel[2,5], M. Kreft[2,5], R. Zorec[2,5], U. Švajger[1,3]

[1] University of Ljubljana, Faculty of Pharmacy, Aškerčeva cesta 7, 1000 Ljubljana, Slovenia; [2] Celica d.o.o., Tehnološki park 24, 1000 Ljubljana, Slovenia; [3] Blood Transfusion Centre of Slovenia, Šlajmerjeva ulica 6, 1000 Ljubljana, Slovenia; [4] University of Nova Gorica, Faculty of Environmental Sciences, Vipavska 13, Rožna Dolina, 5000 Nova Gorica, Slovenia; [5] Laboratory of Neuroendocrinogy-Molecular Cell Physiology, Institute of Pathophysiology, Medical School, University of Ljubljana, Zaloška cesta 4, 1000 Ljubljana, Slovenia

INTRODUCTION

By definition, advanced therapies are encompassing the emerging gene, somatic cell and tissue-engineered therapeutic products. They are becoming important new alternatives in treatment of various diseases, for example cancer and autoimmune disorders and represent a basis for regenerative medicine. In Europe, this fast evolving field has recently been defined and regulated by the Regulation (EC) No. 1394/2007.

Immunotherapy of cancer is an attractive and perspective part of advanced therapies. A profound knowledge on numerous mechanisms, characteristic of cell biology and physiology, is crucial for successful *ex vivo* preparation and *in vivo* application of selected antigen-specific anti-cancer immune cells, acting as defined therapeutic products. For this purpose technically demanding *in vitro* bioengineering processes, fully considering good manufacturing practice (GMP), have to be in place and applied.

IMMUNOTHERAPY OF CANCER

There is no doubt that cancer is immunogenic. However most of its numerous forms are weak inducers of immune responses and only few, like melanoma and prostate cancer are able to elicit a strong anti-tumor cellular immunity. Beside this drawback there are many additional problems, importantly influencing the success rate of immunotherapy, which should be considered and possibly circumvented, like: quick mutations in genes coding for tumor-associated antigens (TAAs), partial or complete loss of expression of major histocompatibility molecules (MHC) on tumor cells as well as tumor anti-inflammatory microenvironment and presence of various types of tolerogenic and anergic immune cells that are all protecting tumor against the activity of patient's immune system.

Generally two kinds of approaches are used in immunotherapy. The first one is adoptive transfer of *in vitro* pre-expanded effector T lymphocytes that are specifically recognising TAAs, thereby attacking and eliminating cancer cells. Alternatively, *in vitro* prepared dendritic cells (DCs), mostly derived from human monocytes and provided with relevant TAAs, are applied as anti-cancer vaccines, able to reactivate and *de novo* induce anti-tumor immune responses. Both concepts have proven to be safe and sometimes quite successful in numerous clinical studies. As a consequence Provenge®, the first FDA-approved autologous DC-based anti-prostate cancer vaccine has recently been launched in the market (1).

Adoptive transfer of anti-tumor effector T cells

In most cases *in vitro* pre-selected and expanded autologous tumor-infiltrating lymphocytes (TILs) are infused in patients, together with rather high amounts of human recombinant interleukin 2 (IL-2). These cells can be obtained from excised solid tumors, tumor-draining lymph nodes and even from peripheral blood of cancer patients (2, 3). In the latter case their pre-vaccination with TAAs is often required to increase the frequency of circulating anti-tumor T lymphocytes.

For the adoptive transfer of TILs to be successful, first a thorough "cleansing" of patient's immune system has to be carried out by applying a proper non-myeloablative preconditioning regimen. Namely in this way, recipient's tumor-protecting regulatory/suppressor T cells and cytokine sinks, i.e. immune cells that would otherwise compete with the transferred TILs for homeostatic pro-inflammatory cytokines, are greatly reduced (2, 3).

Dendritic cell–based anti-cancer vaccines

DCs are professional antigen presenting cells (APCs) and therefore possess all the necessary machinery for antigen uptake, processing, MHC-restricted presentation, costimulatory signalization and cytokine production. They can be prepared *in vitro* either from bone-marrow-derived $CD34^+$ cells or from easily accessible peripheral blood $CD14^+$ monocytes. The next crucial step needed for providing strong and specific (re)activation of anti-cancer T cells, following their *in vivo* application, is their effective antigen loading. As some TAAs are well defined, synthetic antigenic peptides with high binding affinity to specific MHC class I alleles can be used. More often tumor proteins or whole tumor cell (TC) preparations (apoptotic TCs or TC lysates) are delivered to immature DCs which have a strong capacity to uptake, process and present them as peptide fragments within the context of both, MHC class I and class II molecules. When matured, such TAA-loaded DCs become strong inducers of specific $CD4^+$ and $CD8^+$ T cell immune responses. If sufficient amounts of TCs are available, they can be irradiated and electrofused with DCs to form TC-DC immunohybridomas which combine the whole spectrum of TAAs with strong T-cell stimulatory properties of professional APCs (3, 4). Whenever the amount of tumor tissue is too small for hybridoma preparation, tumor-derived DNA or preferentially RNA can be isolated and transferred into DCs, either in its native or preamplified state (3, 5). In this way specific genetic information for the production of actual TAAs is provided (Fig. 1).

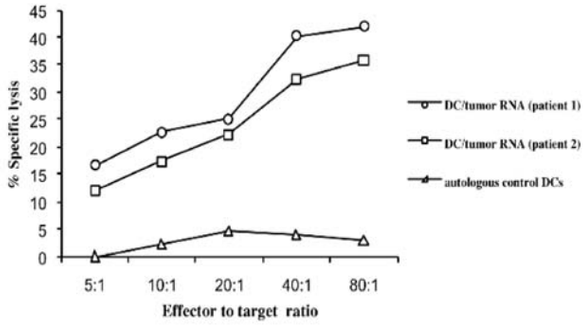

Fig. 1: Specific cytotoxicity of $CD8^+$ T cells induced in vitro by autologous DCs, transfected with patients' tumor RNA.

CONCLUSIONS

Although current results of cancer immunotherapy are promising, there are still many questions to be answered, like for example the use of allogeneic cells.

REFERENCES

1. Kantoff PW, Higano CS, Shore ND, Berger ER, Small EJ, et al. Sipuleucel-T immunotherapy for castration-resistant prostate cancer. N. Engl. J. Med. 2010; 363: 411–422.
2. Rosenberg SA, Dudley ME. Adoptive cell therapy for the treatment of patients with metastatic melanoma. Curr. Opin. Immunol. 2009; 21: 233–240.
3. Jeras M, Bricl I, Zorec R, Švajger U. Induction/engineering, detection, selection, and expansion of clinical-grade human antigen-specific CD8+ cytotoxic T cell clones for adoptive immunotherapy. J. Biomed. Biotechnol. 2010; 2010:705215.
4. Gabrijel M, Bergant M, Kreft M, Jeras M, Zorec R. Fused late endocytic compartments and immunostimulatory capacity of dendritic – tumor cell hybridomas. J. Membrane Biol. 2009; 229: 11-18.
5. Bergant M, Meden L, Repnik U, Sojar V, Stanisavljević D, Jeras M. Preparation of native and amplified tumour RNA for dendritic cell transfection and generation of in vitro anti-tumour CTL responses. Immunobiology 2006; 211: 179-189.

DRUG DELIVERY IN BRAIN AND SPINAL CORD TRAUMA MODEL

H. Eroğlu[1*], E. Nemutlu[2], O. Gürcan[3], O. A. Nacar[4], O. F. Turkoglu[5], E. Bodur[6], M. F. Sargon[7], L. Öner[1]

[1] Department of Pharmaceutical Technology, Faculty of Pharmacy, Hacettepe University, Sıhhiye-Ankara/Turkey; [2] Department of Analytical Chemistry, Faculty of Pharmacy, Hacettepe University, Sıhhiye-Ankara/Turkey; [3] Department of Neurosurgery, Kayseri Research and Education Hospital, Kayseri/Turkey; [5] Department of Neurosurgery, Ankara Numune Research and Education Hospital,Sıhhiye-Ankara/Turkey; [5] Department of Neurosurgery, Atatürk Research and Education Hospital, Sıhhiye-Ankara/Turkey; [6] Department of Biochemistry, Faculty of Medicine, Hacettepe University, Sıhhiye-Ankara/Turkey; [7] Department of Anatomy, Faculty of Medicine, Hacettepe University, Sıhhiye-Ankara/Turkey

Trauma is one of the major problems in surgery that needs special strategies for treatment. In neurosurgery, especially after head and spinal cord injuries, immediate care must be taken into account, since a cascade of events start occur after primary insult. In many trauma incidents, an initial mechanical insult is followed by a sequence of biochemical pathways leading to secondary injury. Free radicals-principally oxygen-react with the membrane phospholipids to cause destruction of both cellular and mitochondrial membranes as well as the blood brain barrier (1-3). In addition, inflammation and edema formation appear to be the fundamental mechanisms of secondary damage. Brain edema, which is an important therapeutic target after traumatic brain injury (TBI) in humans, strongly influences survival and secondary tissue damage during the acute phase after TBI. Traumatic brain injury causes a deficiency of local energy, extracellular glutamate accumulation and excitotoxic lesion, which is reducible by glutamate receptor antagonists. Excitotoxicity on the neuronal cells is partly mediated by the over activation of the N-methly-D-Aspartate type glutamate receptors. This over activation leads to the excessive influx of Ca^{++} through the receptor mediated ion channel and subsequent free radical formation resulting in neuronal cell death in brain and spinal cord tissues named as neurotoxicity (4, 5).

In our research studies, we have investigated the possible neuroprotective efficiencies of some therapeutic agents which are currently used in clinics for other indications. The most significant agent for this purpose was atorvastatin. It is a member of the statin family which has been shown to be neuroprotective after TBI in rats (6, 7). Although the mechanisms that underlie the neuroprotective properties of statins are still not fully elucidated, the most leading mechanism seems to be the pleiotropic effects of statins such as antioxidative and antiinflammatory properties. Therefore, in order to clarify these effects we have investigated the efficiency of atorvastatin administration by the intraperitoneal route on lipid peroxidation and brain edema after traumatic brain injury in rats. The efficiency of atorvastatin was quantified by wet-dry weight method, determination of malondialdehyde amount for lipid peroxidation and ultrastructural evaluation of the recovery after damage by transmission electron microscopy. The results clearly indicated that TBI significantly increased brain edema at 24 hours in rat brain. The ultrastructural findings have also supported the quantitative results. But on the other hand, atorvastatin administered groups showed significantly decreased brain edema and preserved ultrastructural damage This beneficial effect can be mediated not only by lipid peroxidation–altering mechanisms but also may involve other mechanisms such as the inhibition of the inflammatory response, as shown previously (8).

As another part of these multistep study, the efficiency of chitosan microspheres containing cyclosporine-A (Cs-A), which is a cyclic undecapeptide known as a successful immunosuppressant drug used after transplantation, in TBI in rats. Cs-A may be used to inhibit the inflammatory reaction, decrease the free radical formation and lipid peroxidation (9). In many other studies, potential use of immunosuppressant drugs after TBI due to their neuroprotective effects has been investigated (10, 11). The major hypothesis in this part, was the local administration of chitosan microspheres (10 mg/kg Cs-A) with respect to systemic administration (20 mg/kg Cs-A) would be more efficacious, even at the half dose. Chitosan microspheres containing Cs-A were prepared by spray drying method. Microspheres were implanted at the craniectomy area just after trauma formation by modified Feeney method (12). After 24 hours, brain tissues were removed intact. Hemispheres were dissected immediately and kept in liquid nitrogen until analysis. As the results of this part, we have determined that treatment with both systemic (20 mg/kg Cs-A) and encapsulated Cs-A (10 mg/kg) in chitosan microspheres provided a significant reduction in MDA levels ($p<0.05$). In the ultrastuctural evaluation part, mitochondrial damage was evaluated. It was clearly observed that trauma caused significant mitochondrial damage with cloudy swelling and significant cristae appearance. On the other hand, treatment with systemic and encapsulated Cs-A resulted in mitochondria with normal appearance. Although we have implanted microspheres containing Cs-A at the half dose with respect to systemic administration (20 mg/kg), Cs-A microspheres provided comparable results with respect to the systemic administration without any statistical difference ($p>0.05$).

In the third part of this study, we have formulated chitosan microspheres containing atorvastatin calcium and this time neuroprotective efficiency of atorvastatin calcium was investigated by an experimental spinal cord injury (SCI) model. Chitosan microspheres containing atorvastatin calcium microspheres were well characterized and they were implanted at the laminectomy area (1 mg/kg) immediately after trauma. Again 24 hours after injury, motor functions of animals were scored according to modified Tarlov Scale. The spinal cord samples (1cm) were obtained from operated spinal cord area after the animals were sacrificed. In spinal cord tissues tumor necrosis factor (TNF)-α, interleukin (IL)-1β, IL-6 and lipid peroxidation levels were quantified and ultrastructural changes have been investigated. The results of all parameters indicated that microspheres containing atorvastatin calcium were capable of improving functional outcome, attenuating the expression of TNF-α, IL-1β and IL-6; lowering lipid peroxidation levels and maintaining the ultrastructural preservation of the cellular uniformity.

The overall results of the above mentioned experimental studies revealed that Cs-A in TBI and atorvastatin in both TBI and SCI animal models could provide an effective treatment by the inhibition of secondary injury. It was also demonstrated that they preserve cellular uniformity and prevent the damage in mitochondrial structure.

REFERENCES

1. Hall ED, Kupina NC, Althaus JS. Peroxynitrite scavengers for the acute treatment of traumatic brain injury. Ann NY Acad Sci 1999;890:462–8.
2. Lifshitz J, Friberg H, Neumar RW, et al. Structural and functional damage sustained by mitochondria after traumatic brain injury in the rat: evidence for differentially sensitive populations in the cortex and hippocampus. J Cereb Blood Flow Metab 2003;23(2):219–31.
3. Tsubokawa T, Jadhav V, Solaroglu I, et al. Lecithinized superoxide dismutase improves outcomes and attenuates focal cerebral ischemic injury via antiapoptotic mechanisms in rats. Stroke 2007;38(3):1057–62.
4. Lipton SA. Pathologically-activated therapeutics for neuroprotection: mechanism of NMDA receptor block by memantine and S-nitrosylation. Curr Drug Targets 2007;8(5):621-32.
5. Rice AC, Khaldi A, Harvey HB, et al. Proliferation and neuronal differation of mitotically active cells following traumatic brain injury. Exp Neurol 2003;183:406-17.
6. Blanco M, Nombela F, Castellanos M, Rodriguez-Yanez M, et al. Statin treatment withdrawal in ischemic stroke: a controlled randomized study. Neurology 2007;69:904-10.
7. Hong H, Zeng JS, Kreulen DL, et al. Atorvastatin protects against cerebral infarction via inhibition of NADPH oxidase-derived superoxide in ischemic stroke. Am J Physiol Heart Circ Physiol 2006;291:H2210-5.
8. Willerson JT, Ridker PM. Inflammation as a cardiovascular risk factor. Circulation 2004;109:2-10.
9. Diaz-Ruiz A, Rios C, Duarte I, et al. Cyclosporin-A inhibits lipid peroxidation after spinal cord injury in rats. Neurosci Lett 1999;266(1):61–4.
10. Riess P, Bareyre FM, Saatman KE, et al. Effects of chronic, post-injury cyclosporin A administration on motor and sensorimotor function following severe, experimental traumatic brain injury. Restor Neurol Neurosci 2001;18(1):1–8.
11. Sullivan PG, Rabchevsky AG, Hicks RR, et al. Dose–response curve and optimal dosing regimen of cyclosporin A after traumatic brain injury in rats. Neuroscience 2000;101(2): 289–95.
12. Feeney DM, Boyeson MG, Linn RT, Murray HM, Dail WG. Responses to cortical injury: I. Methodology and local effects of contusions in the rat. Brain Res 1981;211(1):67–77.

FROM THE HIGUCHI LAW AND THE LINEAR IVIVC TO FRACTIONAL KINETICS AND THE NONLINEAR IVIVC

Aristides Dokoumetzidis, Panos Macheras*

Faculty of Pharmacy, University of Athens

The pioneering work of T. Higuchi (1) describing the rate of release of a solute from a matrix is considered as the starting point of the rigorous physicochemical and mathematical approaches in oral drug delivery. Since then, both simple and sophisticated models have been developed to predict the release of drug from various dosage forms as a function of time. In parallel, advances in dissolution and oral drug absorption studies have led to the introduction of dissolution tests and the *in vitro in vivo* correlations (IVIVC) in the official compendia. Overall, the understanding of the release mechanism facilitates the design of the pharmaceutical formulation while the development of a validated IVIVC may even lead to a biowaiver status.

The current work focuses on the applications of Monte Carlo simulations for the description of mass transport in drug release as well as the utility of fractal and fractional kinetics for the analysis of biopharmaceutical-pharmacokinetic processes (2-5). All these approaches have been proven suitable for the kinetic study of drug processes under heterogeneous conditions since they capture the anomalous diffusional characteristics of drug both under *in vitro* and *in vivo* conditions (6). A major conclusion from these advances is the validity of the nonlinear character of IVIVC, a special case of which is the routinely used linear IVIVC (7).

REFERENCES

1. Higuchi T., 1961. Rate of release of medicaments from ointment bases containing drugs in suspension. J. Pharm.Sci. 50, 874-875.
2. Kosmidis K. et al, 2003. A re-appraisal of drug release laws using Monte-Carlo simulations: the prevalence of the Weibull function. Pharm. Res. 20, 988-995.
3. Macheras P., Dokoumetzidis A., 2000. On the heterogeneity of drug dissolution and release. Pharm. Res. 17, 108-112.
4. Dokoumetzidis A., Macheras P., 2009. Fractional kinetics in drug absorption and disposition processes. J. Pharmacok. & Pharmacod. 36, 165-178.
5. Dokoumetzidis A., et al, 2010. Fractional Kinetics in Multi-Compartmental Systems. J. Pharmacok. & Pharmacod. 37, 1-18.
6. Dokoumetzidis A., Macheras P., 2011. The changing face of the rate concept in biopharmaceutical sciences: From classical to fractal and finally to fractional. Pharm. Res. 28, 1229-1232.
7. Kytariolos J., et al, 2010. Power law IVIVC: an application of fractional kinetics for drug release and absorption. Europ. J. of Pharm. Sci. 41, 299-304.

NATURAL PRODUCT DRUG DISCOVERY FOR CHLAMYDIA PNEUMONIAE

O. Salin[1], L. Pohjala[1], T. Näreoja[2], P. Vuorela[1*]

[1] Pharmaceutical Sciences, Department of Biosciences, BioCity, Abo Akademi University, Artillerigatan 6 A, FI-20520 Turku, Finland; [2]Laboratory of Biophysics, Cell Biology and Anatomy, Institute of Biomedicine, University of Turku, Artillerigatan 6 A, FI-20520 Turku, Finland.

INTRODUCTION

Chlamydia pneumoniae is a difficult bacterium to treat due to its intracellular habitat and tendency to cause persistent infections refractory to antibiotic treatment at subinhibitory concentrations (1). In addition, it is difficult as a target for drug discovery and development, because it is thus far genetically intractable and highly dependent on the cellular functions of host cells, but does not seem to be dependent on any single function. The bacterium modifies several host cell processes and the persistent infection is firmly linked to development of asthma, atherosclerosis, COPD and Alzheimer's disease, although as acute infection it is recognized as a respiratory pathogen.

The developmental cycle of *C. pneumoniae* has many phases where the organism can be targeted with anti-chlamydial compounds (Fig. 1). However the classical antibiotics target mostly the multiplication phase of the developmental cycle, although they do affect also other phases of the cycle. In the case of *Chlamydia* the multiplication phase is not necessarily the optimal target as the pathogen seems to be accustomed to growth limiting factors and targeting this phase easily causes persistent infection (*e.g.* 2).

Natural phenols have been shown to possess antichlamydial properties *in vitro* (3-5) and *in vivo* (6). *C. pneumoniae* seems to be most vulnerable at the initial contact with host cell and thus natural phenols *e.g.* nutritional polyphenols, may, to some extent, have prophylactic properties being present in tissues already during the initial acute infection (7). In our studies, the natural products have made an excellent source for antichlamydial compounds, as presented here.

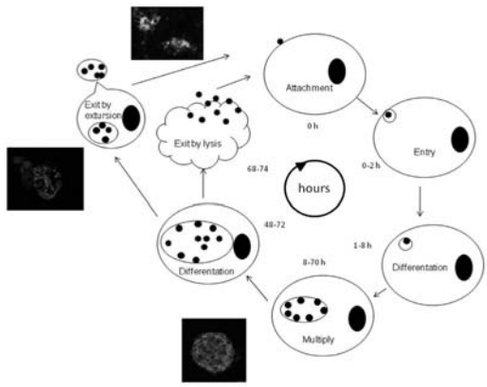

Fig. 1: The normal developmental cycle of *C. pneumoniae* (graphics by Olli Salin and confocal microscopy pictures taken by Tuomas Näreoja).

MATERIALS AND METHODS

The cell-based, 96-wellplate time-resolved fluorometric immunoassay (TR-FIA) according to (8) is usually used as a first screen to give primary information of the antichlamydial effect of the samples. In follow-up studies host cells are infected with *C. pneumoniae* and incubated 72 h, with studied natural products, and the reduction in the number of inclusions is determined from immunofluorescence staining. The details of the method are described in (9). The effect on host cell viability of studied samples is measured with the commercial "CellTiter-Glo® Luminescent Cell Viability Assay" (Promega, Madison, USA).

RESULTS AND DISCUSSION

Several drug discovery and development approaches have been taken to find antichlamydial compounds and to further examine the effects of known inhibitors. We applied rational synthesis, targeted library selection, combination treatment, ethnopharmacological, and epidemiologi-cal approaches to select the material for our antichlamydial studies. We were able to improve the potency of benzimidazole structured antichlamydial compounds by over 10-fold compared to our previous study (10) and identified the structure activity relationship of these compounds (9). We also assayed betulin derivatives against both *C. pneumoniae* and the possible target phospholipase A_2 enzyme (11). Potent inhibitors of *C. pneumoniae* were found, but the inhibition of the bacterium and the target enzyme did not correlate well enough to explain the antichlamydial effect. Our attempt to discover synergetic combinations from doxycycline, calcium modulators, and natural phenols strengthened the assumption that these compounds have dose dependent interactions (unpublished). Most interesting results were gained with *Mentha arvensis* (L.) Lamiaceae extract. The extract was chosen as one of the most potent plant extract against *C.*

pneumoniae assayed in cell culture model (Table 1). The cornmint extract and the compounds within showed remarkable antichlamydial effects in cell cultures, and the extract clearly inhibited the *C. pneumoniae* caused inflammation in mice (unpublished).

CONCLUSIONS

The mechanisms behind the observed antichlamydial properties of the natural products most likely derive from multiple modes of actions as the structural differences of the compounds indicate that they have different targets.

Table 1: Plant extracts causing 100% inhibition of C. pneumoniae growth

Species		Order
Brassica oleracea	wild cabbage	Cruciferae
Citrus sinensis	orange	Rutaceae
Daucus carota	wild carrot	Umbelliferae
Fragaria iinumae	strawberry	Rosaceae
Medicago sativa	alfalfa	Leguminosae
Mentha arvensis	cornmint	Labiateae
Mentha longifolia	home mint	Labiateae
Rosa rugosa	Japanese rose	Rosaceae
Rumex acetocella	Sheeo's sorrel	Polygonaceae
Salvia officinalis	garden salvia	Labiateae
Thymus vulgaris	thyme	Labiateae
Vaccinum myrtillus	blueberry	Ericaceae

REFERENCES

1. Gieffers G, Rupp J, Gebert A, Solbach W, Klinger M, First-choice antibiotics at subinhibitory concentrations induce persistence of *Chlamydia pneumoniae*. Antimicrob. Agents Chemother. 2004; 48: 1402-1405.
2. McCoy A, Maurelli A, Building the invisible wall: updating the chlamydial peptidoglycan anomaly. Trends Microbiol. 2006; 14: 70-77.
3. Alvesalo J, Vuorela H, Tammela P, Leinonen M, Saikku P, Vuorela P, Inhibitory effect of dietary phenolic compounds on *Chlamydia pneumoniae* in cell cultures. Biochem. Pharmacol. 2006; 71: 735-741.
4. Schriever C, Pendland S, Mahady GB. Red wine, resveratrol, *Chlamydia pneumoniae* and the French connection. Atherosclerosis 2003; 171: 379-380.
5. Vuorela H, Vuorela P, Hiltunen R, Leinonen M, Saikku P, Plant-derived and synthetic phenolic compounds and plant extracts, effective in the treatment and prevention of chlamydial infections, WO patent 2002/14464; 2002.
6. Törmäkangas L, Vuorela P, Saario E, Leinonen M, Saikku P, Vuorela H, In vivo treatment of acute *Chlamydia pneumoniae* infection with the flavonoids quercetin and luteolin and an alkyl gallate, octyl gallate, in a mouse model. Biochem. Pharmacol. 2005; 70: 1222-1230.
7. Henning S, Aronson W, Niu Y, Conde F, Lee N, Seeram N, Lee R, Lu J, Harris D, Moro A, Hong J, Pak-Shan L, Barnard J, Ziaee H, Csathy G, Go V, Wang H, Heber D, Tea polyphenols and theaflavins are present in prostate tissue of humans and mice after green and black tea consumption. J. Nutrition 2006; 136: 1839-1843.
8. Tammela P, Alvesalo J, Riihimäki L, Airanne S, Leinonen M, Hurskainen P, Enkvist K, Vuorela P, Development and validation of a time-resolved fluorometric immunoassay for screening of antichlamydial activity using a genus-specific europium-conjugated antibody. Anal. Biochem. 2004; 333: 39-48.
9. Keurulainen L, Salin O, Siiskonen A, Kern JM, Alvesalo J, Kiuru P, Yli-Kauhaluoma, Vuorela P, Design and synthesis of 2-arylbenzimidazoles and evaluation of their inhibitory effect against *Chlamydia pneumoniae*. J. Med. Chem. 2010; 53: 7664-7674.
10. Alvesalo J, Siiskonen A, Vainio M, Tammela P, Vuorela P, Similarity based virtual screening: A tool for targeted library design. J. Med. Chem. 2006; 49: 2353-2356.
11. Salin O, Alakurtti S, Pohjala L, Siiskonen A, Maass V, Maass M, Yli-Kauhaluoma J, Vuorela P, Inhibitory effect of the natural product betulin and its derivatives against the intracellular bacterium *Chlamydia pneumoniae*. Biochem. Pharmacol. 2010; 80: 1141-1151.

DESIGN SRC KINASE INHIBITORS AS A THERAPEUTIC APPROACH FOR CANCER AND METASTASES

Süreyya Ölgen

Ankara University, Faculty of Pharmacy, Department of Pharmaceutical Chemistry, Tandogan-Ankara, 06100, Turkey

Cancer metastasis is a severe problem and therefore discovering key targets as well as developing breakthrough medicines is a big challenge. Src (known as c-Src or Src) is a member of non-receptor tyrosine kinase family that implicates many cellular activities including differentiation, adhesion, migration, cytoskeletal alterations, and proliferation. Another important role of Src is the regulation of vesicle transport and secretion of proteases in osteoclasts. Src plays an important role in genesis and progression of human cancers, including carcinomas of breast, colon, prostate, lung and ovary, and in myeloproliferative disorders. Inhibition of Src kinase has the potential to have a significant impact as a treatment for cancer. According to mechanism of action, Src inhibitors are generally categorized into two major classes: 1) Tyrosine kinase activity inhibitors: ATP binding domain blockers; 2) Protein-protein interaction inhibitors: -SH2, -SH3 or substrate binding domain blocking molecules as protein recognition inhibitors. The most of Src inhibitors are targeted at the ATP-binding site of the catalytic domain of the kinase. These Src inhibitors include heterocyclic ATP analogs, as shown in **Figure 1**: pyrazolo-[2,3-*d*]pyrimidines (PP1 and PP2), pyrrolo-[2,3-*d*]pyrimidines (CGP76030), pyrido-[2,3-*d*]pyrimidines (PD166285), quinoline carbonitriles (SKI606), and olomucines (CGP79883).

Studies of several types of human carcinoma tissue have shown a strong association between Src activity, which modulates the invasiveness and metastasis of carcinoma cells. In an in vitro study, Src inhibition blocked IL-8 induced prostate cancer cell migration and in another mouse models of breast cancer, inhibition of Src tyrosine kinase activity disrupted metastasis. Bone is the primary metastatic site of patients with breast and prostate cancer. A complex interaction between metastatic tumor cells, osteoclasts, and osteoblasts results in the development of bone lesions that cause significant pain and patient morbidity. High levels of Src are found in mature osteoclasts and Src activity is essential for the normal organization of the osteoclast cytoskeleton. Thus, in patient with metastatic bone disease, Src inhibitors could potentially have negative effects not only on osteoclasts, but also on tumour cells and on their interactions with osteoclasts. Because of its role in osteoclast function, Src is a novel target for metastatic cancers. Three agents currently under clinical investigation are dasatinib, saracatinib and bosutinib, which all prevent Src signaling is pivotal to tumor growth, metastasis and bone metabolism for patients with solid tumors, including prostate and breast cancer. Several Src inhibitors have been described to effect anti-invasive, antiproliferative and antimetastatic properties in a number of cancer cell models. Such inhibitors include PP1, PP2, SKI606, PD180970, CGP76030 and AP23464 (**Figure 1**).

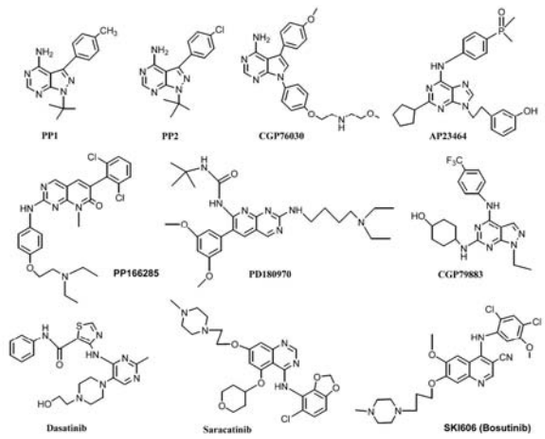

Fig. 1: Chemical structure of small molecule Src inhibitors for cancer and metastasis.

Main topic of this lecture is based on the literature survey and clical studies on Src inhibitors for cancer and metastasis. In addition, design and synthesis of several heterocylic compounds from our laboratory have been described as Src kinase inhibitors.

REFERENCES

1. Sen B, Johnson FM, J. Signal Trans. 2011, doi: 10.1155/2011/865819.
2. Saad F, Lipton A, Cancer Treat. Rev. 2010: 36; 177-184.
3. Rucci N. et al., Anti-Cancer Agents Med. Chem. 2008: 8; 342-349.
4. Sawyer T.K., Expert Opin. Invest. Drugs 2004:13; 1-19.
5. Sakamoto et.al., Jpn. J. Cancer Res.2001: 92, 941-946.

THE MODERN ENDOCRINE LABORATORY: PRINCIPLES AND PITFALLS

Gabor L. Kovacs

Institute of Laboratory Medicine, University of Pecs, Hungary

When the author began his career in 1972 he found a calorimeter in the endocrine lab put out of use just a few years before. The hormone laboratory has changed dramatically since the last 40 years and even more since. Many of the major principles governing clinical endocrinology taken for granted today were established during the last 50 years. In fact, during this period, twelve individuals received individual or shared Nobel Prizes for discoveries directly related to endocrinology and hormone assays. From the tremendous amount of information gathered during half a century, the author has selected a few topics that had a particular impact on the practice of endocrinology and therefore on hormone measurements. These topics include the discovery and identification of brain neuropeptides, the mediation of hormonal action through extra- and intracellular receptors, and the evolution of the concept of free hormones, the role of genetic and epigenetic mechanisms, and the role of post-translational modifications.

We do not have sufficient foresight to extrapolate what endocrinology laboratories will look like in 20 years from now. Part of what we already use, assay formats and automated analyzers, will probably still be around. We may expect improvements in the recipes to eliminate interferences caused by heterophyl antibodies in immunoassays. The problems of cross reactivity for small molecules will eventually be solved by using tandem mass spectrometry technology instead of immunoassays. There is no doubt that the number of definitive methods based on mass spectrometry for biochemical measurements reflects that mass spectrometry is superior to immunoassays for small molecules.

As one of these examples, the pituitary adenylyl cyclase–activating peptide (PACAP) has been involved in a wide variety of physiologic responses and in development, and is therefore believed to act through as many intracellular pathways. PACAP signaling has been described through cAMP, calcium, phospholipase C, and MAPK (and it might also use the NF B signaling pathway), and regulates the expression of many genes. The wide distribution of PACAP and its receptors suggests that the peptide may exert pleiotropic physiological functions. As a matter of fact, PACAP has now been shown to act as a hormone, a neurohormone, a neurotransmitter, and a trophic factor in a number of tissues. Measurement of circulation PACAP levels might be a valuable tool in measuring some adaptive responses of the organism.

Follicular fluid provides an important microenvironment for the proper development of oocytes. It contains a number of biologically active substances including growth factors, cytokines, neutrotransmitters, vasoregulators, enzymes, apoptotic factors and reactive oxygen species. These compounds, acting individually or in concert, constitute a local intra-ovarian regulatory system which has been shown to influence the developmental potential of oocyte/embryo complex. New research horizons appear with the investigation of follicular fluid samples during in vitro fertilization. Besides the neuroendocrine effects of leptin in the control of food intake and energy expenditure, binding of this hormone has been proven in lung, intestine, kidney, liver, skin, stomach, heart, spleen and other organs, suggesting its apheliotropic actions. These include, for example, the role of leptin in the direct regulation of immune cells, pancreatic beta cells, adipocytes, muscle and blood cells and last but not least the oocytes. Thus, leptin and adiponectin appear to act as an endocrine and paracrine factor for the regulation of reproduction.

The discovery of adiponectin occurred at about the same time as the discovery of leptin, but it did not receive major attention in the scientific community for the next few years until its markedly protective role in the pathogenesis of obesity-related disorders was acknowledged. Compared with the aforementioned factors, adiponectin differs in almost all biological properties and effects. Nevertheless, to date, it is the most promising adipocytokine with a sincere potential for developing novel intervention strategies for obesity-related disorders. Recent data suggest that, besides its influence on maternal health, adiponectin can also play a role in maintaining the normal reproductive function, and in the communication between mother and embryo. The influence of adiponectin on ovarian, endometrial and placental functions as well as on early embryo development has been suggested. Like leptin, adiponectin affects oocyte number and functions during in vitro fertilization.

Lab-on-a-chip technologies have a tremendous but unproven potential. Neurons and endocrine cells secrete neurotransmitter and hormones in discrete packets in a process called quantal exocytosis. Electrochemical microelectrodes can detect spikes in current resulting from the oxidation of individual quanta of transmitter only if the electrodes are small and directly adjacent to release sites on the cell. It has been reported the development of a microchip device that uses microfluidic traps to automatically target individual or small groups of cells to small electrochemical electrodes.

Genome-wide mapping of protein–DNA interactions and epigenetic marks are essential for a full understanding of transcriptional regulation. A precise map of binding sites for transcription factors, core transcriptional machinery and other DNA-binding proteins is vital for deciphering the gene regulatory networks that underlie various biological processes. The combination of nucleosome positioning and dynamic modification of DNA and histones has a key role in gene regulation– and guides development and differentiation. Chromatin states can influence transcription directly by altering the packaging of DNA to allow or prevent access to DNA-binding proteins, or they can modify the nucleosome surface to enhance or impede recruitment of effector protein complexes. Recent advances suggest that this interplay between chromatin and transcription is dynamic and more complex than previously appreciated, and there is a growing recognition that systematic profiling of the epigenomes in multiple cell types and stages may be needed for understanding developmental processes and disease states. Taken together, detection of new endocrine biomarkers will be in the focus of research in the next 2-3 decades.

The role of the laboratory specialist in hormone testing has also changed in the last 50 years. For many years, laboratory specialists prepared their own kits. Now, clinical biochemists can make no changes to manufacturers' protocols without risking legal action. Assay development will be concentrated within research and manufacturers' laboratories. Our role will be more devoted to explain the limitations of these assays to clinicians submerged by all kinds of information and – most importantly - to consult with them.

REFERENCES:

1. Yen PM et al. Molecular and Cellular Endocrinology 246 (2006) 121–127.
2. Gu J et al. Clinical Biochemistry 40 (2007) 1386–1391.
3. Diamond EJ et al. Clinical Chemistry 41 (1995) S213-S214.
4. Toldy E et al. Clinica Chimica Acta 352 (2005) 93-104.
5. Pardridge WM, Landaw EM. American Journal of Physiology 258 (1990) 396-397.
6. Ahmed OM et al. International Journal of Developmental Neuroscience 26 (2008) 147–209.
7. Ain KB et al. Journal of Clinical Endocrinology and Metabolism 65 (1987) 689-696.
8. Locsei Z et al. Clinical Biochemistry 42 (2009) 225-228.

DIAGNOSIS OF ATHEROSCLEROTIC CARDIOVASCULAR DISEASE: CAN LABORATORY DO IT BETTER?

D. Černe

University of Ljubljana, Faculty of Pharmacy, Aškerčeva cesta 7, 1000 Ljubljana, Slovenia

Atherosclerotic cardiovascular disease (CVD) is the major cause of premature death in developed countries, important cause of disability and contributes substantially to the escalating costs of health care. The underlying atherosclerosis develops insidiously over many years and is usually advanced by the time that symptoms occur. The mass occurrence of CVD relates strongly to lifestyles and to modifiable physiological and biochemical factors.

Current guidelines on CVD prevention in clinical practice recommend total CVD risk assessment, which means the likelihood of a person developing an acute atherosclerotic event over a defined period of time. This can be easily done by a use of the risk charts (Fig 1), which estimate the 10-year risk of a CVD event (*i.e.* heart attack, stroke). A 10-year risk of CVD death of 5 % or more is arbitrarily considered high risk (1).

Laboratory measurements of serum concentrations of lipids (total, LDL and HDL cholesterol and triglycerides) have important role in CVD risk assessment. Serum total cholesterol concentration is included in all risk charts (beside age, gender, blood pressure and smoking habit) and most recently the novel SCORE risk charts with the use of the ratio total to HDL cholesterol were introduced (1), clearly indicating the importance of decreased serum HDL cholesterol as an independent risk factor for CVD, in addition to increased serum LDL cholesterol concentration. Beside lipids measurements laboratory markers for increased risk of occurrence of diabetes are also recommended, such as serum glucose (1) or HbA1c (2). Diabetes associates with increased risk of CVD death.

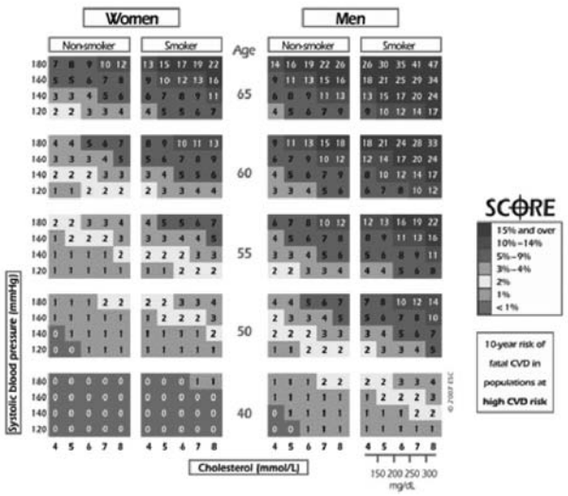

Fig. 1: Risk chart indicating a 10-year risk of CVD death (1).

However, positive predictive value of risk charts currently used in clinical practice is approximately 50 %. That means that in patients assigned to have risk of developing CVD event in the following 10 years roughly half of them will actually develop the event in predetermined period of time. More concerning, sensitivity of these risk charts is considerably below what we expect from a useful screening test and is around 16 % (3). Low sensitivity of the combined score emphasises multifactorial nature of CVD and suggests other factors are involved in the disease which so far have not been measured. This is a reasonable background for intensive search of new risk factors which yielded a long list of so called emerging risk factors for CVD.

As to laboratory CVD risk assessment, several emerging risk factors were proposed, such as serum concentrations of apolipoproteins (*i.e.* apo B and apo A1, as an alternative to measurements of cholesterols and triglycerides), Lp(a) (a distinct lipoprotein resembling LDL with heritability over 90 %), homocystein (an intermediate of methionine metabolism) and various genotype testing. Several studies indicate that these emerging laboratory tests are associated with very small to very significant (magnitude similar to smoking) risk for various CVD. Therefore, they are often recommended to be considered if premature CVD or family history of premature CVD exists (1, 4). However, the latest studies show that these new risk factors add very small incremental risk information or even none in addition to the use of conventional CVD risk charts, or that detailed information on incremental risk prediction beyond traditional risk factors is still lacking. Therefore, it is generally accepted that these new risk factors do not merit consideration for CVD assessment in the asymptomatic adults (2, 5). The only discrepancy in opinion between EU and USA experts is platelet-activating factor acetylhydrolase. While EU guidelines do not pay any attention (1), USA guidelines declare its measurement in plasma as reasonable for CVD assessment in intermediate-risk asymptomatic adults (2).

An alternative could be looking for laboratory tests for early detection of the existing arterial disease rather than looking for laboratory markers for risk that atherosclerosis may develop and progress to the degree of clinical manifestation. Thus, it would be possible to identify those apparently healthy individuals who have asymptomatic arterial disease in order to slow the progression of atherosclerotic disease, to induce regression, and in particular to reduce the risk of clinical manifestations. As an example that this alternative approach may be beneficial is broad application of new imaging techniques in currant guidelines on CVD prevention in asymptomatic adults, such as transthoracic echocardiography to detect left ventricular hypertrophy, carotid artery intima-media thickness, ankle-brachial index, computed tomography for coronary calcium and also myocardial perfusion imaging.

Worryingly, the only sensitive laboratory indicator of the existing atherosclerosis that entered the guidelines on CVD prevention in clinical practice is C-reactive protein (CRP), despite being very unspecific. The latest USA guidelines (2) suggests CRP measurements for CVD prevention in asymptomatic intermediate-risk men (<50 years) and woman (<60 years) and in older subjects with LDL cholesterol <3.5 mmol/L where it can be useful in selecting patients beneficial for statin therapy. Two other non-lipid laboratory indicators of the existing atherosclerosis that entered the current guidelines on CVD prevention are mildly elevated serum creathinine and microalbuminuria (2).

To conclude, future perspective is developing specific laboratory tests for early detection of the existing atherosclerosis. Several biological systems are at considerable scientific interest, *i.e.* laboratory markers for oxidative stress, instability of haemostasis, endothelial damage (VCAM1, ICAM, MCP1), vascular matrix turnover and plaque instability (MMP9).

REFERENCES

1. Graham I, Atar D, Borch-Johnsen K, Boysen G, Burell G *et al.* European guidelines on cardiovascular disease prevention in clinical practice: executive summary. Eur Heart J 2007; 28: 2375–414.
2. Greenland P, Alpert JS, Beller GA, Benjamin EJ, Budoff MJ *et al.* 2010 ACCF/AHA guideline for assessment of cardiovascular risk in asymptomatic adults. J Am Coll Cardiol 2010; 56: e50-103.
3. Cooper JA, Miller GJ, Humphries SE. A comparison of the PROCAM and Framingham point-scoring systems for estimation of individual risk of coronary heart disease in the Second Northwick Park Heart Study. Atherosclerosis 2005; 181: 93-100.
4. Genest JJ Jr, McNamara JR, Upson B, Salem DN, Ordovas JM *et al.* Prevalence of familial hyperhomocyst(e)inemia in men with premature coronary artery disease. Arterioscler Thromb 1991; 11: 1129–36.
5. De Backer G. New European guidelines for cardiovascular disease prevention in clinical practice. Clin Chem Lab Med 2009; 47: 138-42.

SIMULTANEOUS TOPICAL DELIVERY OF VITAMINS C AND E: AN OPPORTUNITY FOR COMBATING PHOTOAGEING?

M. Gašperlin

University of Ljubljana, Faculty of pharmacy, Askerceva 7, 1000 Ljubljana, Slovenia

INTRODUCTION

One of the major contributions to skin (photo)aging, disorders and diseases is oxidative stress caused by UV radiation by inducing reactive oxygen and nitrogen species (1). Free radicals are ubiquitous in our body and are formed under physiological (aerobic metabolism, inflammatory responses) as well as under pathological conditions. Normally their production and elimination are balanced but in the case of excess free radical concentrations (e.g. due to increased production or depletion of antioxidant defence systems) they can cause oxidative damage to DNA, protein and lipids. Therefore successful approach for prevention harmful effects could be to control oxidant/antioxidant balance at the affected site, which can be achieved through external supply of endogenous antioxidants (2).

The aim of this presentation is to show that microemulsions (ME), especially highly viscous ME gels are appropriate carrier systems for simultaneous delivery of two antioxidant vitamins, hydrophilic vitamin C and lipophilic vitamin E into skin to enhance skin antioxidant defence.

MATERIALS AND METHODS

Components of ME

Isopropyl myristate (IPM) was used as lipophilic phase, Tween 40 as surfactant, Imwitor 308 – glyceryl caprylate (Condea, Germany) as cosurfactant and purified water as the hydrophilic phase. α-tocopherol (vitamin E) was incorporated at 1% w/w and ascorbic acid (vitamin C) at 0,4% w/w. All components except Imwitor 308 were from Fluka, Switzerland. The composition of tested ME is given in Table 1.

Table 1: Composition of ME (w/w %).

COMPONENT	w/o ME	o/w ME	gel-like ME
Water	10.0	45.0	60.0
IPM	60.0	25.0	10.0
Tween 40	15.0	15.0	15.0
Imwitor 308	15.0	15.0	15.0

Preparation of ME

The surfactant and cosurfactant were blended in a 1:1 mass ratio to give the surfactant mixture. IPM and water were then added and mixed with a magnetic stirrer for 5 minutes. Vitamin C and E were incorporated by stirring for 30 minutes

Rheological measurements

The absolute dynamic viscosity of ME was determined in a temperature range 20-32°C using a SV-10 Vibro Viscosimeter, A&D Company, Japan

Vitamin C stability

The amount of non-degraded vitamin C at room temperature (22+/-1°C) was determined quantitatively by HPLC immediately after preparation of the sample and subsequently on the 1st, 2nd, 3rd, 7th, 14th and 28th day (3).

Cell toxicity test

The effect of tested formulations on cell viability was evaluated by MTT assay performed according to the method of Mosmann (4). Normal human undifferentiated keratinocytes, NCTC 2544 (Interlab Cell line collection, Genoa, Italy) were used.

The morphology of NCTC 2544 cells was examined by inverted light (Olympus CKX41, Japan) and fluorescence (Olympus IX81, Japan) microscopy.

RESULTS AND DISCUSSION

For successful development of dermal delivery systems it is crucial not only optimizing the formulation to maximize cutaneous drug bioavailability but also to ensure that the formulation is aesthetically acceptable, easy to use and adheres to skin sufficiently. Since ME are by definition low viscous Newtonian fluids, optimizing of rheological behaviour is needed. The most convenient way to increase viscosity is addition of thickeners while an innovative approach could be formation of ME gels which are formed upon the addition of specific amounts of water to liquid o/w ME (5). The viscosity of liquid o/w ME, thickened o/w ME (with 2,5 % of carbomer) and ME gel, shown on Fig.1, is decreasing in the T range 20-32°C. In the case of liquid and thickened o/w ME the decrease is linear, while the viscosity of ME gel decreases drastically with T.

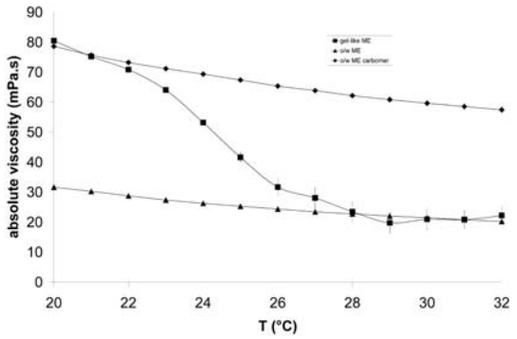

Fig. 1: Temperature dependence of absolute viscosity for ME gel ME, o/w ME and o/w ME carbomer (5)

The incorporation of vitamins E and C into liquid o/w and w/o ME, and into gel-like o/w ME, enhanced their (photo)stability. ME gel was found to be the best protective system for both vitamins. Stability data for vitamin C are presented on Fig 2.

Cell viability after the exposure of tested systems to NCTC 2544 human keratinocytes was higher than 80% and no significant difference was found among tested ME (Fig.3).

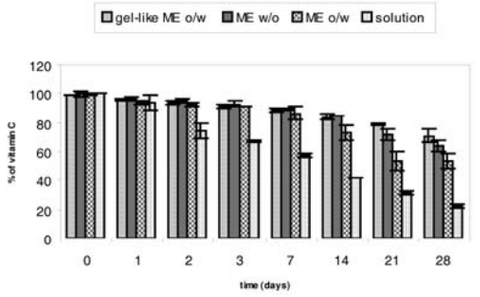

Fig. 2: Fractions of non-degraded vitamin C in tested ME (non-thickened, thickened and gel-like) in comparison with aqueous solution during one-month storage.

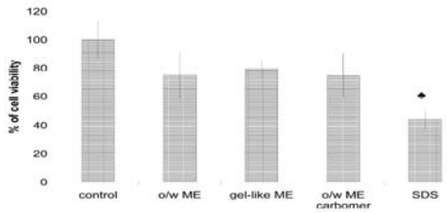

Fig. 3: Cytotoxicity of ME gel, liquid o/w ME and o/w ME thickened with carbomer according to MTT assay. SDS was used as a positive control. ♣ p‹0,05 compared to control

CONCLUSIONS

ME gel with temperature sensitive rheological behaviour has been proved an effective and non-irritant vehicle with functionally suitable consistency for simultaneous topical delivery of a hydrophilic vitamin C and a lipophilic vitamin E.

REFERENCES

1. Callaghan TM, Wilhelm KP. A review of ageing and an examination of clinical methods in the assessment of ageing skin.. Int. J. Cosme.t Sci 2008;30(5):313-22
2. Gasperlin M, Gosenca M. Main approaches for delivering antioxidant vitamins through the skin to prevent skin ageing, Exp. Op. Drug Deliv. 2011. doi: 10.1517/17425247 .2011.581657
3. Rozman B, Gašperlin M. Stability of vitamins E and C in topical microemulsions for combined antioxidant therapy. Drug Del. 2007: 14: 235-245
4. Mosmann, T, Rapid colorimetric assay for cellular growth and survival: Application to proliferation and cytotoxicity assays. J.Immun. Methods. 1983: 65(1-2): 55-63.
5. Rozman B, Zvonar A, Falson F, Gasperlin M. Temperature-sensitive microemulsion gel: an effective topical delivery system for simultaneous delivery of vitamins C and E. AAPS Pharm.Sci.Tech, 2009; 10 (1): 54-61

AMORPHOUS FORMULATION DEVELOPMENT- ADVANTAGES AND DRAWBACKS

K. Kogermann[1], P. Veski[1], J. Rantanen[2], K. Naelapää[1*]

[1] Department of Pharmacy, University of Tartu, Estonia/ Nooruse 1, 50411, Tartu, Estonia; [2] Department of Pharmaceutics and Analytical Chemistry, Faculty of Pharmaceutical Sciences, University of Copenhagen, Denmark/ Universitetsparken 2, Copenhagen, Denmark

INTRODUCTION

Amorphous formulations, especially in case of poorly soluble active pharmaceutical ingredients (APIs), have recently obtained an increased attention. The higher dissolution rate in combination with the enhanced bioavailability is a well recognised benefit of amorphous drug delivery systems (1,2). However, the physical instability because of the high energy state and tendency to recrystallise is the most prevalent issue of concern. Therefore, it must be shown that amorphous component resists the recrystallisation during the shelf-life of the product as well as after administration.

One possible method to improve the stability of amorphous API is to use excipients, e.g. polymers, which increase the glass-transition temperature (T_g) and may chemically interact with the API.

The aim of this study was to investigate the possibilities for stabilisation of an amorphous API by formulating it together with polymers. In addition, stability under different conditions and in simulated gastric fluid was examined.

MATERIALS AND METHODS

Materials

The model API, piroxicam form I (PRXAH), was obtained from Lianyuangang Ruidong International Co.,Ltd (China). Polymers, polyvinylpyrrolidone (PVP) in two different grades 25 (PVP 25) and 90 (PVP 90) (BASF SE, Germany), and methylcellulose (MC) (Shin-Etsu Chemical Co., Ltd) were used as obtained, whereas

Soluplus® (BASF SE, Germany) was pre-milled for one hour in order to decrease the particle size. The simulated gastric fluid used for dissolution and slurry experiments was prepared according to the USP NF 33.

Methods

Preparation of amorphous formulations and their solid state characterisation

Ball-milling (Mixer Mill MM301, Retsch GmbH & Co., Germany) and co-milling at low and room temperature were used for preparation of amorphous formulations. All solid state forms were characterised using XRPD and Raman spectroscopy. Obtained data were analyzed using Simca-P+ software (v.12.0, Umetrics AB, Sweden). Thermal behaviour was investigated by DSC.

Dissolution behaviour of amorphous formulations in gastric fluid

In-line Raman spectroscopy and XRPD equipped with the variable temperature stage were used to monitor the recrystallisation of amorphous piroxicam (PRX) from amorphous PRX-polymer systems as well as from physical mixtures of PRXAH and the respective polymer in slurry with simulated gastric fluid (SGF). Conventional dissolution testing was performed from hard gelatine capsules (USP 33 NF 28, n=3). The relative amount of PRX in each capsule was kept constant (20 mg). Samples were withdrawn every 3 minutes and analyzed using UV-Vis spectrophotometer at 353 nm.

RESULTS AND DISCUSSION

Preparation of amorphous formulations

Amorphous PRX was obtained by ball-milling of PRXAH at low temperature. Due to its instability co-milling approach with polymers was investigated. Several formulations were developed and tested, Tbl. 1.

Table 1: Overview of PRX:polymer ratios used during formulation development. RT: amorphous material was obtained by co-milling at room temperature; LT: amorphous material was obtained by co-milling at low temperature; n/a: given ratio was not tested; not: amorphous material was not obtained during milling.

Polymer/Ratio	1:1	1:2	1:3	1:4
PVP 25	RT	RT	n/a	n/a
PVP 90	RT	RT	n/a	n/a
MC	not	RT	RT	n/a
Soluplus®	not	not	LT	LT

Stability of amorphous formulations during storage

Co-milling enabled to increase the stability of amorphous PRX. Even after six months of storage at room temperature the PRX-PVP formulations in ratios 1:1 and 1:2 were amorphous (Fig. 1). Formulations with MC were stable for three months and with Soluplus® for two months (Fig. 1).

Amorphous formulations in SGF

All amorphous PRX-polymer formulations were tested for stability in SGF. The conversion of amorphous PRX to PRXMH started already after three minutes of testing, Fig. 2a. However, no transformations were detected with physical mixtures of crystalline PRXAH and respective polymer within six hours, Fig. 2b.

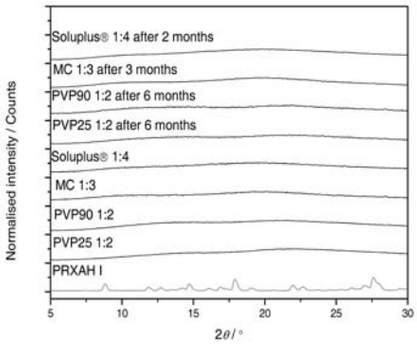

Fig. 1: XRPD patterns of untreated crystalline PRXAH and amorphous co-milled samples, i.e. with PVP 25 1:2; PVP 90 1:2, MC 1:3 and Soluplus® 1:4 on the day of preparation and after storage at room temperature for specified time periods. All patterns are normalised

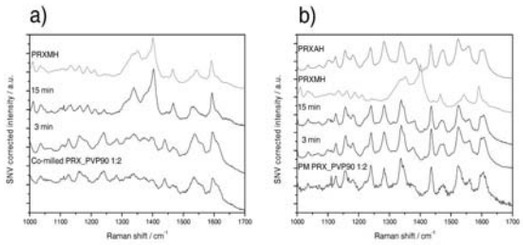

Fig. 2: Recrystallisation behaviour of PRX in SGF from PRX-PVP 90 1:2 co-milled sample and physical mixture (PM), monitored with in-line Raman spectroscopy (n=2), compared to crystalline PRXMH spectrum. All spectra are SNV corrected.

The effect of polymers on the dissolution behaviour of amorphous PRX was not expected. All the polymers tested decreased the dissolution rate of PRX compared to the crystalline PRXAH. Interestingly, the dissolution rate of PRX-Soluplus formulations was the slowest.

CONCLUSIONS

Stable amorphous PRX formulations were obtained by using co-milling approach. The drawback of these drug delivery systems was the fast recrystallisation of amorphous PRX as PRXMH in SGF. Through the formulation screening studies it was possible to identify whether a sophisticated formulation approach is providing the expected solubility and dissolution rate advantages.

ACKNOWLEDGEMENTS

Kristina Predbannikova and Anna Penkina are acknowledged for their work with the formulation development.

REFERENCES

1. Hancock, B.C., Zografi, G. Characteristics and significance of the amorphous state in pharmaceutical systems. J. Pharm. Sci. 1997; 86: 1–12.
2. Serajuddin, A.T.M. Solid dispersion of poorly water-soluble drugs: early promises, subsequent problems, and recent breakthroughs. J. Pharm. Sci., 1999; 88:1058-66.

TOWARD ANTITHROMBOTIC COMPOUNDS WITH DUAL FUNCTION – RECENT DEVELOPMENTS AND FUTURE CHALLENGES

J. Ilaš*, M. Ilič, A. Žula, Ž. Hodnik, D. Kikelj

University of Ljubljana, Faculty of Pharmacy, Aškerčeva cesta 7, 1000 Ljubljana, Slovenia

INTRODUCTION

Cardiovascular diseases with an estimated 17 million deaths yearly or 29% of all deaths are the main cause of death and morbidity globally. There is, therefore, a growing need to discover novel antithrombotic agents as alternatives to existing treatment strategies. Major progress was made in the past decade in developing novel antithrombotic agents, e.g., thrombin inhibitors, inhibitors of factor Xa, tissue factor/factor VIIa inhibitors, and platelet GPIIb/IIIa receptor antagonists. In 2009, two new anticoagulant drugs were introduced to the market, direct thrombin inhibitor *dabigatran* and direct factor Xa inhibitor *rivaroxaban*. However, the disappointing experience with *ximelagatran*, which was withdrawn in 2006 after a short time of use, shows that the search for novel antithrombotic drugs still remains a major challenge to medicinal chemistry.

Efficient combination of anticoagulant and antiplatelet activity in the same molecule would produce a novel type of antithrombotic drug featuring substantial advantages over possible combinations of anticoagulant and antiplatelet agents, including more predictable and less complex pharmacokinetics, lower incidence of side effects, less demanding clinical studies and more straightforward registration procedure, which together could render them the antithrombotic drugs of the future (1).

Our research group has prepared several compounds combining thrombin inhibitory and glycoprotein IIb/IIIa receptor antagonistic activities in the same molecule (2). Generally, compounds possessing thrombin inhibitory and glycoprotein IIb/IIIa receptor antagonistic activities require four moieties; a basic centre which is usually arginine mimetic (in our case benzamidine), a central scaffold (1,4-benzoxazine), an acidic centre (acetate) and an aromatic moiety (benzyl group) (Fig 1) (3).

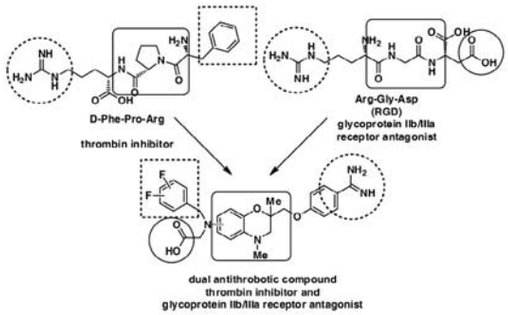

Fig. 1: Design of 1,4-benzoxazine derivatives with thrombin inhibitory and GPIIb/IIIa receptor antagonistic activities.

Main focus was pointed towards optimization of P3 moiety with different combinations of aromatic and carboxyl group moieties. Special focus was put onto various fluorine substituted aromatics (4) with the goal of improving activity, selectivity and pharmacokinetic properties.

On the other hand, we prepared a compound possessing (2-(butyl-sulfonamido)-2-carboxyethyl) moiety, which is found in GPIIb/IIIa antagonist *tirofiban*.

MATERIALS AND METHODS

Chemistry

1,4-Benzoxazine (5) scaffold was prepared from aminonitrophenol. The reduction of ethyl ester and lactam carbonyl groups with borane dimethyl sulfide afforded alcohol which was coupled with 4-cyanophenol under Mitsunobu reaction conditions.

The reduction of nitro group using catalytic hydrogenation, afforded aromatic amines that were *N*-alkylated using various fluorinated benzaldehydes, to afford secondary amines which were alkylated with ethyl bromoacetate or acylated with ethyl oxalyl chloride. Target compounds were prepared from nitriles using the Pinner reaction. Esters were converted to the zwitterionic compounds by alkaline hydrolysis. Compound possessing butyl-sulfonamido moiety was prepared in similar fashion, starting from tyrosine.

Biological Activity

Inhibition of thrombin was used to evaluate anticoagulant activity and inhibition of factor Xa and trypsin was used to assess the selectivity of potential anticoagulants for coagulation enzymes. The enzyme amidolytic method for determining inhibition of thrombin factor Xa and trypsin is based on the spectrophotometric determination (abs. at 405 nm) of the product formed after amide bond cleavage of a chromogenic substrate.

Binding affinities to the integrin GPIIb/IIIa receptor (fibrinogen receptor) involved in platelet aggregation was measured by a solid-phase competitive displacement assay, while inhibition of ADP-induced aggregation of platelets in platelet rich plasma showed antagonistic activity to the integrin GPIIb/IIIa receptor.

RESULTS AND DISCUSSION

We found out that methylenoxy spacer provides optimized flexibility between benzamidine moiety and central 1,4-benzoxazine scaffold to ensure the desired activity on both targets. To improve balanced dual activity on thrombin and platelet GPIIb/IIIa receptor, a compromise concerning flexibility and bulkiness in P3 part containing aromatic and carboxylic acid moieties was sought. Encouraged by promising results of positive effect of introducing fluorine atoms to P3 aromatic ring, we prepared a small series of 1,4-benzoxazine compounds based on our most active compounds. The influence of fluorination on the activity of GPIIb/IIIa receptor antagonist is not described, so we decided to systematically perform full fluorine scan by preparing 3-fluorobenzyl, 4-fluorobenzyl, 3,4-difluorobenzyl, and 3,5-difluorobenzyl substituted compounds. Introduction of fluorine atoms should also have favourable effect on physiochemical properties and improved pharmacokinetic.

CONCLUSIONS

In conclusion, we have described the design, synthesis, and dual activity of several new fluorinated 3,4-dihydro-2*H*-1,4-benzoxazine compounds capable of acting both as thrombin inhibitors and GPIIb/IIIa receptor antagonists and analyzed the structure-activity relationship of combining anticoagulant and antiaggregatory activity into one molecule. We optimized the flexibility between benzamidine moiety and central 1,4-benzoxazine scaffold to ensure the desired activity on both targets. To improve balanced dual activity on thrombin and platelet GPIIb/IIIa receptor, a compromise concerning flexibility and bulkiness in P3 part containing aromatic and carboxylic acid moieties was sought. The introduction of fluorinated benzyl moieties improved the activity on both targets, giving compounds with thrombin K_i inhibitory activity and IC_{50} value for binding affinities to the integrin GPIIb/IIIa receptor in nanomolar range.

REFERENCES

1. P. S. Anderluh, M. Anderluh, J. Ilas, J. Mravljak, M. S. Dolenc, M. Stegnar, D. Kikelj, Journal of Medicinal Chemistry 2005, 48, 3110-3113;
2. J. Ilas, F. Hudecz, H. Suli-Vargha, D. Kikelj, Journal of Peptide Science 2008, 14, 946-953.
3. J. Ilas, Z. Jakopin, T. Borstnar, M. Stegnar, D. Kikelj, Journal of Medicinal Chemistry 2008, 51, 5617-5629;
4. J. A. Olsen, D. W. Banner, P. Seiler, U. Obst Sander, A. D'Arcy, M. Stihle, K. Müller, F. Diederich, Angewandte Chemie 2003, 42, 2507-2511.
5. J. Ilas, P. S. Anderluh, M. S. Dolenc, D. Kikelj, Tetrahedron 2005, 61, 7325-7348.

DEVELOPMENT OF KINASE-SELECTIVE INHIBITORS: CHALLENGES WITH PIM KINASES

P. J. Koskinen[1,2]

[1] Turku Centre for Biotechnology, University of Turku and Åbo Akademi University, Tykistökatu 6B, 20520 Turku, Finland, [2] Department of Biology, 20014 University of Turku, Finland

INTRODUCTION

There has recently been enormous progress in development of small molecule inhibitors against various protein kinases. These include multiple compounds targeting the Pim family of serine/ threonine-specific kinases that have been implicated as therapeutic targets in both hematopoietic malignancies and in solid tumors (1,2). Pim kinases contribute to tumorigenesis e.g. by promoting cell survival and by enhancing resistance of cancer cells against chemotherapy and radiation therapy (3,4,5).

One class of inhibitors against Pim kinases represents ATP-mimetic compounds that form hydrogen bonds with the hinge region of the kinases. Another class of inhibitors consists of ATP-competitive compounds interacting with the ATP-binding pocket. While identification of potent and yet selective inhibitors against any kinase is very challenging, there are several features specific for Pim kinases that may be helpful in development of Pim-specific compounds. First of all, the hinge region of Pim kinases contains a unique sequence with a proline residue that allows formation of only one instead of two hydrogen bonds to ATP or ATP-mimetic compounds. Secondly, due to unusually rigid structures, the active loops of Pim kinases remain constitutively in an open, active confirmation. Thus, whenever Pim kinases are expressed, they are expected to be catalytically active.

In collaboration with several groups of chemists, our group has also been involved in identification and verification of novel Pim-selective small molecule compounds.

MATERIALS AND METHODS

The *in vitro* inhibitory activities of multiple compounds have been pretested against 70 to 90 different kinases in the kinase platform at the Division of Signal Transduction Therapy, University of Dundee, UK. Since some of them have turned out be potent and fairly specific against Pim kinases, we have functionally validated these compounds using both *in vitro* kinase assays and cell-based assays.

For the *in vitro* kinase assays, we have preincubated bacterially produced Pim kinases with either DMSO or inhibitory compounds dissolved in DMSO and have then added radioactive gamma-^{32}P-ATP and bacterially produced Pim substrates. Phosphorylated proteins have been resolved in SDS-PAGE and subjected to autoradiography and quantitation.

For the cell-based assays, we have used a myeloid FDCP1 cell model (3), where the cytokine-independent survival of the cells is dependent on continuous Pim expression and activity. We have grown cells with or without interleukin-3 and various inhibitory compounds and have measured cell viability by the MTT or the Trypan blue exclusion assays, cell migration by wound healing assays and cell invasion by Boyden chamber assays.

RESULTS AND DISCUSSION

Our *in vitro* kinase assays have revealed that some of the tested compounds efficiently block the ability of some or all Pim family kinases to phosphorylate their known substrates such as NFATc1 and Bad (6,7). In cell-based assays, the protective effects of Pim kinases on cytokine-deprived myeloid cells are efficiently abrogated with micromolar concentrations of these compounds, indicating that they can enter the cells and impair the anti-apoptotic effects of Pim kinases. Furthermore, these compounds have helped us to reveal a novel function for Pim kinases in regulation of the metastatic potential of adherent cancer cells. The Pim-inhibitory compounds are able to inhibit migration and invasion of adherent cancer cells, suggesting that they could reduce the ability of these cells to form fatal metastases.

CONCLUSIONS

The novel Pim-selective inhibitors may be used not only as efficient research tools to study Pim functions, but also as promising scaffolds in developing drugs against metastatic tumours overexpressing Pim kinases.

REFERENCES

1. Morwick T. Pim kinase inhibitors: a survey of the patent literature. Expert Opin. Ther. Pat. 2010; 20: 193-212.
2. Brault L, Gasser C, Bracher F, Huber K, Knapp S, Schwaller J. PIM serine/threonine kinases in pathogenesis and therapy of hematological malignancies and solid cancers. Haematologica 2010; 95: 1004–1015.
3. Aho TLT, Sandholm J, Peltola KJ, Mankonen HP, Lilly M, Koskinen PJ. Pim-1 kinase promotes inactivation of the pro-apoptotic Bad protein by phosphorylating it on the Ser112 gatekeeper site. FEBS Lett. 2004; 571: 43–49.
4. Zemskova M, Sahakian E, Bashkirova S, Lilly M. The PIM1 kinase is a critical component of a survival pathway activated by docetaxel and promotes survival of doxotacel-treated prostate cancer cells. J. Biol. Chem. 2008; 283: 20635–20644.
5. Peltola K, Hollmen M, Maula SM, Rainio EM, Ristamäki R, Luukkaa M, Sandholm J, Sundvall M, Elenius K, Koskinen PJ, Grenman R, Jalkanen S. Pim-1 kinase expression predicts radiation response in squamocellular carcinoma of head and neck and is under the control of epidermal growth factor receptor. Neoplasia 2009; 11: 629–636.
6. Santio NM, Vahakoski RL, Rainio EM, Sandholm JA, Virtanen SS, Prudhomme M, Anizon F, Moreau P, Koskinen PJ. Pim-selective inhibitor DHPCC-9 reveals Pim kinases as potent stimulators of cancer cell migration and invasion. Mol. Cancer 2010; 9: 279–291.
7. Vahakoski RL, Kiriazis A, Eerola S, Santio NM, Rainio EM, Aumüller I, Papageorgiou A, Yli-Kauhaluoma J, Koskinen PJ. Manuscript in preparation with a patent pending.

LOW IMMUNOGENICITY OF SALMON FIBRIN GLUE

I. Laidmäe[1,2,*], P. Veski[2], R. Uibo[1]

[1] Immunology Group, IGMP University of Tartu, Ravila Street 19, Tartu 50411, Estonia,
[2] Institute of Pharmacy, University of Tartu, Nooruse Street 1, Tartu 50411, Estonia

INTRODUCTION

Fibrin glue (FG) of thrombin and fibrinogen composition was originally used to minimize blood loss during operations in clinical practice (1). Polymerized fibrin mimics the initial matrix that prevents bleeding and acts as scaffold for cells that initiate tissue repair. There is also a rising interest for using coagulation proteins in haemostatic dressings (2).

Use of FG is accompanied by immunological reactions. A concern, especially with non-autologous proteins, is the potential that antibodies developed in response to the foreign protein may crossreact with endogenous proteins and can lead to coagulation disturbances (3).

Salmon fibrinogen and thrombin are sufficiently similar to human fibrinogen and thrombin to be interchangeable in terms of fibrin polymerization (4).

We evaluate the safety of salmon derived fibrinogen and thrombin as a new source of FG proteins. We evaluate the impact of salmon proteins to host immune system on animal model. Studies regarding host coagulation system parameters, antibody development and possible cross-reaction with host coagulation proteins were done. Also we evaluate the biocompatibility of salmon fibrinogen consisting haemostatic dressing with fibroblasts culture *in vitro*.

MATERIALS AND METHODS

Experimental animals and study design

23 Wistar rats were immunized by intraperitoneal injection of salmon FG (Sea-Run Holdings Inc., ME, USA) on the 2nd and 32nd days. Similar treatment with 0.9% sodium chloride was also done to 23 rats in control group. Plasma from all rats was collected before the immunization and on days 11, 20, 30, 33, 42 and 46.

Coagulation assays

For thrombin time (TT) and prothrombin activity (PT, expressed in international normalized ratio (INR)) evaluations in rats human test kits developed by Diagnostica Stago (Asnieres, France) are readily usable. TT in seconds was measured by the STA-thrombin kit (REF 00611 and REF 00669) and PT and INR by the STA-SPA 50 kit (REF 00105) using the STA Compact apparatus (Diagnostica Stago, Asnieres, France).

Antibody Assays

An ELISA and Western blot analysis for measurement of plasma immunoglobulins (IgG) binding to salmon thrombin (lot#5031, Sea-Run Holdings Inc., ME, USA) and fibrinogen (lot#1289, Sea-Run Holdings Inc., ME, USA) or rat thrombin (T5772, Sigma, USA) and fibrinogen (F6755, Sigma, USA) was used in all experiments. Details of antibody assays are described elsewhere (5).

In vitro cellular biocompatibility

The biocompatibility of the electrospun salmon fibrinogen dressing was evaluated in vitro by measuring fibroblast metabolic activity cultured on the scaffold for 14 days. Human dermal fibroblasts were seeded on the scaffolds placed on the bottom of tissue culture plate wells. On days 2, 4, 8 and 14 two scaffolds were harvested for proliferation measurement. Cellular proliferation was monitored by forming of formazan product (MTS assay, CellTiter 96 Aqueous One Solution Cell Proliferation Assay, Promega Corporation, WI, USA) detected by spectrophotometer.

RESULTS AND DISCUSSION

ELISA tests showed that all rats in the experimental group who were challenged with salmon-derived FG complex preparation developed low antibody (IgG) amounts to the salmon thrombin and fibrinogen after the first intraperitoneal FG application. However, after the second administration of FG, there was a substantial increase in antibody levels (Fig. 1).

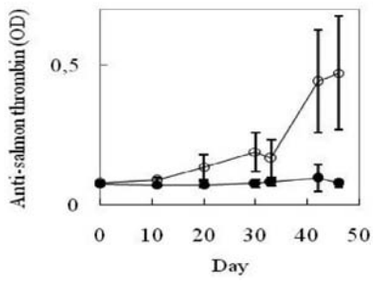

Fig. 1: Antibodies to salmon thrombin in plasma samples taken from 46 rats. Solid symbols are data for samples from control animals and open symbols are from animals treated with salmon fibrin.

Immunoblot studies for anti-rat thrombin or fibrinogen IgG antibodies revealed a very weak reaction with rat thrombin-derived peptides. Reaction to rat thrombin was seen in 4 and a weak reaction against rat fibrinogen

beta chain was seen in 3 out of 23 animals at the 46th day of experiment. In control groups no reactions were seen.

Results from coagulation measurement showed that presence of weakly crossreacting antibodies had no deleterious effects on blood clotting in the experimental rat model. The results of mean TT values are shown in Figure 2. No differences in mean INR values between control group and experimental group rats were seen during the entire course of the experiment. In mean TT values there was slight but statistically significant ($p < 0.001$) drop in experimental group of rats after the second administration of FG, however TT normalized by the end of experiment. No differences in other time points were seen.

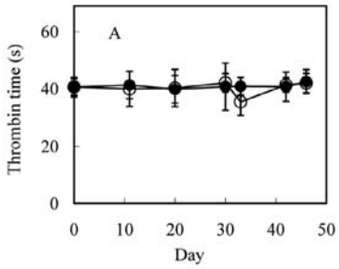

Fig. 2: Thrombin time as measured in plasma samples before and after intra-peritoneal administration of salmon fibrin. Solid symbols are data for control animals and open symbols are mean values from animals treated with salmon fibrin.

Fibroblast proliferation experiment revealed that the nanofibrous salmon fibrinogen dressing supports cell attachment and proliferation during 14 day evaluation, indicating its good biocompatibility.

CONCLUSIONS

Our results show that antibodies of IgG type to salmon fibrinogen and thrombin were detected from experimental animals' plasma after two following administrations of salmon FG. In spite of slight antibody crossreactivity to rat coagulation proteins, these reactions had no inhibitory effect on rats' coagulation profiles. By supporting cellular proliferation salmon fibrin could be utilized as haemostatic dressings.

REFERENCES

1. Dunn CJ, Goa KL. Fibrin sealant: a review of its use in surgery and endoscopy. Drugs. 1999; 58: 863-886.
2. Ahmed TA, Dare E.V, Hincke M. Fibrin: a versatile scaffold for tissue engineering applications. Tissue Eng Part B Rev. 2008; 14: 199-215.
3. Ortel TL, Mercer MC, Thames EH, Moore KD, Lawson JH. Immunologic impact and clinical outcomes after surgical exposure to bovine thrombin. Ann Surg. 2001; 233: 88-96.
4. Wang LZ, Gorlin J, Michaud SE, Janmey PA, Goddeau RP, Kuuse R, Uibo R, Adams D, Sawyer ES. Purification of salmon clotting factors and their use as tissue sealants. Thromb Res. 2000; 100: 537-48.
5. Laidmae I, Salum T, Sawyer ES, Janmey PA, Uibo R. Characterization of the biological effect of fish fibrin glue in experiments on rats: immunological and coagulation studies. J Biomed Mater Res A. 2010; 93: 29-36.

ORAL MODIFIED RELEASE DOSAGE FORMS – QUO VADIS

S. Baumgartner

University of Ljubljana, Faculty of Pharmacy, Aškerčeva 7, 1000 Ljubljana, Slovenia

INTRODUCTION

The development of prolonged release formulations is one of the most important challenges in pharmaceutical research. There are different delivery systems that are under investigation; however, hydrophilic matrices are one of the most widely used for controlling drug release. The mechanisms involved in drug release from these matrix systems are complex and depend on many factors. Therefore, it is essential to have a profound knowledge of these factors to achieve the final goal: to formulate medicines with desired biopharmaceutical and pharmacokinetic parameters.

Further, there is a growing interest in the new concept of chronopharmacology, where pulsatile drug delivery systems that can effectively treat the disease with non-constant dosing therapies, are investigated.

One interesting approach in oral modified release is site specific drug delivery, where definition of the best strategy is difficult due to complexity of the different organs within GI tract. Challenges and opportunities regarding three different approaches will be shortly presented.

Hydrophilic matrix tablets – do we really know them in detail?

Critical factors in drug release from hydrophilic matrices are numerous. Among the most important and well studied are related to polymer properties: polymer molecular weight, its percentage, particle size and similar (1). However, today, there is a growing interest in the research of polymer characteristics on the molecular basis, as for example substituent pattern along the HPMC backbone. Namely, sometimes it is not enough to explain the behaviour of the polymers only by the average degree of polymer substitution. In this way, different batches of HPMC were hydrolyzed by endoglucanase and rather large differences in heterogeneity were found that correlated well to the polymer erosion and drug release. This leads to the conclusion that only by extensive polymer characterization predictable drug release rates from matrix tablets can be obtained (2).

It is known that non-ionic polymers like HPMC are golden standard for formulators of modified release dosage forms. As alternative natural polymers like xanthan or carrageenans are suggested. They are poly-electrolytes that form different complex secondary structures under different environmental conditions, which influences drug release (Fig. 1). For their characterization sophisticated methods like atomic force microscopy (AFM) or nuclear magnetic resonance are necessary (3).

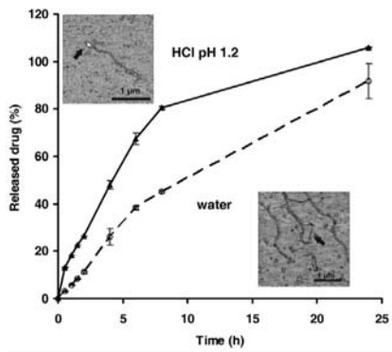

Fig. 1: Drug release from xanthan tablets together with polymer structures imaged by AFM

Pulsatile drug delivery

To design effective pulsatile drug delivery systems, the diseases with established circadian rhythms should be investigated. These include asthma, arthritis, duodenal ulcer, neurological disorder etc. There are various approaches of pulsatile drug delivery systems, which are based on: osmosis; erodible, soluble or rupturable membrane; systems based on capsule. They can be found under different names of chronopharmaceutical technologies (OROS®, CODAS®, etc.). The prime advantage of pulsatile delivery is that drug is released when necessity comes. As a result chance of development of drug resistance or its toxic effects, which are sometimes observed in conventional or prolonged drug release, can be reduced. The

key point of development of these formulations is to find circadian rhythm i.e. suitable indicator which will trigger the release of the drug from device. Besides, there are problems regarding absence of suitable biomaterial that will respond in a proper manner. By selecting optimal time to achieve the desired effect, treatment opportunities may arise and undesired side effects can be minimized (4).

Strategies for site specific drug delivery systems within GIT

The physiology of different organs in GIT and transit patterns of dosage forms are so different that for each organ several strategies to achieve site specific delivery are possible. These are adhesion, chemical modification of drug and/or excipient moieties, technological features of dosage forms, pH variations, etc.

In the mouth fast disintegration of orodispersible delivery systems represents one approach, while on the other hand by adhesion prolonged drug release can be achieved. The adhesive polymers are used for formulation of bioadhesive films, patches, gels or the most popular buccoadhesive tablets, which can be single or multiple layered systems (5).

Stomach is another place, where different strategies were proposed to prolong gastric residence time. On of them is floating ability, which can be effectively achieved by incorporation of gas generating agents. In this way tablets based on HPMC, $NaHCO_3$ and with amoxicyllin were investigated for the treatment of *Helicobacter pylori* infections. Beside good floating properties also proper pH within formed gel layer was established by incorporation of succinic acid or citrate buffer, what enabled longer stability of amoxicillin in acidic environment (Fig 2).

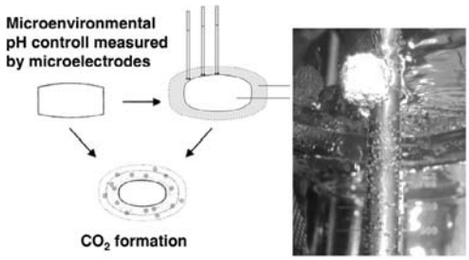

Fig. 2: Floating HPMC tablets with incorporated gas forming agent and pH modifying substances

CONCLUSION

The development of innovative oral modified release dosage forms is still in progress and the most promising approach is under vigorous debate. It should also be emphasized that the more specific is the trigger for drug release, the greater can be inter-subject variability for the successful delivery. Some of the researchers are even prone to develop personalized medicines in oral modified release. However, firstly the paradox between the large benefit to the population versus decreased benefit to the industry should be solved.

REFERENCES

1. Maderuelo C, Zarzuelo A, Lanao JM. Critical factors in the release of drugs from sustained release hydrophilic matrices. J. Control. Release 2011, doi:10.1016/j.jconrel.2011.04.002.
2. Viridén A, Larsson A, Schegerlöf H, Wittgren B. Model drug release from matrix tablets composed of HPMC with different substituent heterogeneity. Int. J. Pharm. 2010; 401: 60-67.
3. Mikac U, Sepe A, Kristl J, Baumgartner S. A new approach combining different MRI methods to provide detailed view on swelling dynamics of xanthan tablets influencing drug release at different pH and ionic strength. J. Control Release 2010; 145: 247-256.
4. Mandal AS, Biswas N, Karim KM, Guha A, Chatterjee S, et al. Drug delivery system based on chronobiology – A review. J. Control Release 2010; 147: 314-325.
5. Pinto JF. Site-specific drug delivery systems within the gastro-intestinal tract: From mouth to the colon. Int. J. Pharm. 2010; 395: 44 – 52.

NATURAL POLYMERS FOR ORAL MODIFIED RELEASE DOSAGE FORMS

M. Pavli

Krka d.d., Novo mesto, Šmarješka cesta 6, 8501 Novo mesto, Slovenia

INTRODUCTION

Natural polymers are widely used in pharmaceutical dosage forms, however their use as modified release agents of active pharmaceutical ingredients still offers a great potential in pharmaceutical development.

Among natural polymers, proteins and polysaccharides are the two groups of the most diverse and complex substances. Both can be obtained from a wide range of natural raw materials including animal connective tissues, microorganisms, land and sea plants (Table 1).

Table 1: Some of the most important natural polymers used for modified drug release according to their origin.

PROTEINS	
Animal	
gelatin	silk
Plant	
zein	
POLYSACCHARIDES	
Animal	
chitosan	
Vegetal	
cellulose	starch
Microbial	
dextran	xanthan
pullulan	gellan
scleroglucan	
Plant/algae	
pectin	inulin
guar gum	karaya gum
locust bean gum	xyloglucan
alginate	carrageenan

These polymers hold advantages over the synthetic polymers, generally because they are nontoxic, less expensive, and freely available. Natural polymers used in the pharmaceutical industry are in majority regarded as GRAS – generally recognized as safe and are thus allowed for human consumption with no special restrictions.

These polymers can also be modified to have tailor-made materials for drug delivery systems and thus can more easily compete with the synthetic excipients available in the market (1).

Very important property of the majority of natural polymers is that they are hydrophilic, water soluble. Thus in contact with water they hydrate and swell, being able to form gel structure under defined conditions. The latter property is often used for modified release of drugs especially in matrix tablets.

Among the variety of oral modified release dosage forms matrix tablets, composed of one or a combination of several biologically acceptable polymers, are to this end the most preferred drug delivery system. Many natural polymers like xanthan, locust bean gum, carrageenans, alginate, guar gum etc. have already proven their potential in the usage in such controlled release dosage forms, where drug release was usually controlled for 6-24 hours. Drug release mechanisms from matrix tablets based on natural polymers are generally the same as from other hydrophilic matrices. The most common controlled release mechanisms are therefore dissolution and diffusion of the drug through the formed gel layer, swelling and erosion of matrix polymers (2). However more complex mechanisms like polymer-drug or polymer-polymer interactions can also take place.

Complex structure that may favor different polymer chain conformations is characteristic for all natural polymers. The type of conformation and, consequently, different interactions between polymer chains significantly affect their properties (3). This can be furthermore exploited in the development of more advanced drug delivery systems. One such system represent matrices based on polyelectrolyte complexes of different natural polymers of opposite charges, like chitosan-carrageenan, chitosan-xanthan (4). In such systems regular characteristics of the matrices are usually completely altered due to interactions between polymers. When needed, such systems can be also used in development of different matrix beads with modified drug release like chitosan-alginate beads.
Some natural polymers, for instance shellac and zein can also provide modified release coatings, others like pectin, chitosan, guar gum, dextran, inulin etc. are capable for colon-specific drug delivery.
Numerous natural polymers have also been investigated for their modified drug release capabilities from nano-, microparticles, microcapsules. Usage of natural polymers as modified release agents, for instance of silk fibroin, has also been increasing in more novel technological procedures like electrospinning.

A major problem concerning modified release dosage forms based on natural polymers is that due to the lack of understanding of their behaviour at the molecular level, it is difficult to predict the properties and susceptibility of these systems to different factors, that may affect the release of active ingredients. In addition, reproducibility of the raw materials properties can be problematic and can significantly contribute to varying biopharmaceutical properties of the final dosage forms.
For the evaluation of these systems conventional analytical methods in pharmaceutical development are often not enough, therefore it is necessary to use the specific analytical methods. Two such methods are texture analyzer (TA) and membrane ion selective electrode (MIE). TA can be used for the evaluation of the gel texture of the matrix tablets, beads, capsules, their mechanical properties, both which can have substantial impact on drug release like in the case of xanthan and locust bean gum matrices (5, 6). MIE on the other hand can be employed for studying interactions between natural polymers like carrageenans and oppositely charged drugs, where drug release is altered due to drug binding to polymers (7). Methods like these therefore allow us to precisely design and achieve desired drug release for the best therapy outcome.

New findings, integration and implementation of scientific knowledge about natural polymers allow us to more successfully develop these complex pharmaceutical delivery systems.
On the other hand genetic engineering could offer us a tremendous opportunity for new functional developments in natural polymers, greater mass production whereas also more standardised products could become available. Standardisation is one of the most important goals to be met in order to achieve higher usage widespread of natural polymers in oral modified release dosage forms.

REFERENCES

1. Bhardwaj TR, Kanwar M, Lal R, et al. Natural gums and modified natural gums as sustained-release carriers. Drug Development and Industrial Pharmacy 2000; 26 (10): 1025-1038.
2. Li X, Jasti RB. Design of controlled release drug delivery systems. New York: McGraw-Hill, 2006: 107-229.
3. Hugerth A, Sundelöf L. The effect of polyelectrolyte counterion specificity, charge density, and conformation on polyelectrolyte-amphiphile interaction: The carrageenan/furcellaran-amitriptyline system. Biopolymers 2001; 58 (2): 186-194.
4. Coviello T, Matricardi P, Marianecci C, Alhaique F. Polysaccharide hydrogels for modified release formulations. Journal of Controlled Release 2007; 119: 5-24.
5. Baumgartner S, Pavli M, Kristl J. Effect of calcium ions on the gelling and drug release characteristics of xanthan matrix tablets. European Journal of Pharmaceutics and Biopharmaceutics 2008; 69 (2): 698-707.
6. Pavli M, Kristl J, Vrečer F, Baumgartner S, et al. The reflection of the texture of swollen polymer matrix on the release of incorporated substance. E-polymers Online ed., http://www.e-polymers.org, 2009, no. 17, 15 p.
7. Pavli M, Vrečer F, Baumgartner S. Matrix tablets based on carrageenans with dual controlled release of doxazosin mesylate. International Journal of Pharmaceutics 2010; 400 (1-2): 15-23.

MODIFICATION OF DRUG RELEASE BY SYNTHETIC OR SEMISYNTHETIC POLYMERS

D. Schmalz

HARKE Pharma GmbH, Xantener Straße 12, 45479 Mülheim a. d. Ruhr, Germany

INTRODUCTION

Cellulosedrivatives, acrylic polymers and polyvinylalkohol are often used in the pharmaceutical industry to modify the solubility, the release and sometimes also the absorbtion of good soluble active pharmaceutical ingredients. Since many years, sustained release formulations, based on diffusion control out of a hydrophilic matrix or diffusion controlling film layers are used to slow down the release of a soluble pharmaceutical ingredient (API).
However, in recent years many new chemical entities (NCE) are poorly soluble. Therefore, the increase of the solubility and the stabilization of a supersaturated solution gain more and more interest.

Sustained release

After a brief introduction into the concept of matrix tablets and the nomenclature, the influence of HPMC content, particle size, viscosity, substitution type, tablet size and compression force on the kinetics of matrix tablets will be discussed.
The concept of PVA based CR-films will be introduced and the role of the layer-thickness will be discussed.
Also acrylic polymers are used to modify the release of API through a film layer. The formulation principles determing the release kinetics will be discussed.

Solubility Enhancement

The concept of solid dispersion (SD) will be discussed using the example of Nifedipin-HPMC-Acetat-Succinat (NF-HPMCAS). Release kinetics of different preparations of SD by solvent evaporation and their stability in supersaturation will be discussed.
Hot Melt Extrusion (HME) offers a new and elegant way to solid dispersion, at least for API with relatively low melting points. Results of HME of the NF-HPMCAS example in a twin screw extruder will be shown and discussed.
HME might release free acids from the applied polymer. Data of such release will be shown and discussed.

SINGLE UNIT VERSUS MULTIPARTICULATE MODIFIED RELEASE DOSAGE FORMS

Klára Pintye-Hódi

Department of Pharmaceutical Technology, University of Szeged, H-6720, Eötvös u. 6., Szeged, Hungary

INTRODUCTION

During the past century, a rapid evolution has been observed in the field of the preparation of solid dosage forms. Besides the conventional preparations, modified release solid dosage forms have been introduced. The advantages of these preparations are as follows:

- less frequent drug intake,
- longer duration of action,
- less side-effects,
- uniform blood concentration,
- better patient compliance.

Modified-release dosage forms may be

- sustained release,
- delayed release, or
- pulsatile release dosage forms.

There are currently many products containing these dosage forms on the market.

Modified release solid dosage forms are available either as a *single-unit* or as a *multiparticulate* form.

SINGLE-UNIT DOSAGE FORMS

The single-unit dosage form is usually a diffusion-controlled system, where the drug is dissolved or dispersed throughout a solid matrix *(monolithic system)*. The release of the drug is controlled either by incorporating a suitable filler within the matrix, or by coating the matrix with a swellable or non-swellable polymer film(s).

This form either passes the gastrointestinal tract as a whole, or gradually becomes smaller due to degradation, or only releases the active ingredient in the intestines.

The drug dissolution is controlled by diffusion or erosion.

In the film-coated dosage form, the drug release is controlled by the properties of polymer films (pH-dependent/independent solubility or ability of diffusion).

In this group, mention must also be made of *oral osmotic systems (OROS),* which may be one-chamber or two-chamber systems. In this case, the drug release is controlled by the force of osmosis, produced in the dosage form on the action of the gastric/intestinal juice in gastrointestinal tract.

A further possibility is the preparation of *bi- or multilayer tablets* through the repeated compression of powders. These tablets allow modulation of the dissolution and release characteristics, and drug combinations with different release profiles.

MULTIPARTICULATE DOSAGE FORMS

The multiparticulate drug delivery systems are divided into numerous functional units, which may be spherical *pellet particles* (in tablet or capsules) or *minitablets* (in capsules).

Pellets are small, free-flowing, spherical particles which can be obtained through the aggregation of fine powders or granulates of active ingredients and excipients by using appropriate technical equipment. They may be matrix pellets or coated pellets. They can be filled into capsules or sachets, or can be pressed into tablets as multiple unit particulate systems *(MUPS).*

Minitablets are small tablets with a diameter of less than 3 mm. They are typically filled into a capsule. It is possible to incorporate many different minitablets with different release properties into a capsule.

In the manufacture of multiparticulate dosage forms there are numerous possibilities through which to influence the kinetics of dissolution and the duration of the effect of drug.

SUMMARY

Finally, it can be concluded that there are a number of possibilities to modify drug release from both single-unit and multiparticulate dosage forms. Choice of the best form depends on the status of the patient and the therapeutic requirements.

EXPERIMENTAL AND THEORETICAL TECHNIQUES FOR CHARACTERIZATION OF ENTERIC AND GIT-INSOLUBLE FILM COATINGS

Z. Abramović*, L. Peternel

Lek Pharmaceuticals d.d., Verovškova 57, 1526 Ljubljana, Slovenia

INTRODUCTION

Polymer blends used for the coatings of solid dosage forms can provide different drug release behavior, e.g. zero-order pulsatile or sigmoidal patterns and are therefore attractive in development of more advanced drug products (1, 2). However the complexity of these systems is higher compared to coatings based on only one polymer (2). Consequently development and optimization of polymer blend coatings is very challenging and too often based on trial-and-error experimentations. Therefore, better understanding of drug release mechanisms through these systems is necessary.

Traditional methodology to investigate characteristics of polymer blends coatings is to formulate dosage form and then investigate dissolution rate using different apparatus and experimental conditions. Drawbacks of this methodology are lack of time and cost effectiveness and on the other hand lack of mechanistically investigation.

Alternative methods for evaluation of polymer blends as potential candidate for desired drug release have to be introduced in drug development process. For better understanding of underlying mechanism of drug release through these films different experimental and theoretical techniques can be used. Particularly high-throughput methods are attractable as they can help us rapidly determine the permeability of drugs through different type of film coatings and recognize potential candidates for further classical testing and optimizations. Some of such potential experimental methods are permeation through thin polymer films using side-by-side diffusion cells, evaluation of weight loss and water uptake of polymer films, studies of mechanical resistance of film coating (1). Theoretical methods such as determination of apparent drug diffusion coefficients within the polymeric systems determined by fitting of Fick's second law of diffusion to experimental results can also help characterize polymer blends coatings.

In this study two possible approaches for determination of fluorescine permeability through polymer mixtures of GIT-insoluble (Eudragit RS) and enteric (Eudragit L) polymers are presented.

MATERIALS AND METHODS

Polymer solutions

Polymer solution were prepared by dissolving Eudragit L 100 (methacrylic acid-ethyl acrylate copolymer 1:1) and Eudragit RS PO (ammonio methacrylate copolymer) in different ratios (100:0, 75:25, 50:50, 40:60, 25:75

and 0:100 w/w) in ethanol/acetone mixture (60:40) in concentration of 7 %. Triethyl citrate was added as plasticizer in concentration of 15 % per dry polymer mass.

Permeability through polymers using Transwell® filter supports
Transwell filter supports made of polycarbonate (pore size = 3 µm, membrane thicknes = 10 µm, Corning) were treated with 20µL of different polymer mixtures. Following addition of polymers, filters were dried and the permeability of fluorescine was investigated. Coated filters were placed in a 24-well microtiterplate in a way to divide each well in a donor and acceptor compartment. A fluorescine in phosphate buffer (pH=7.4) (100 µM) was placed in a donor compartment (1000 µL); in the acceptor compartment phosphate buffer (pH=7.4) was added (250 µL). The microtiterplate was incubated and samples were withdrawn from donor and acceptor compartments. Fluorescine content was determined by UV reader (Safire, Tecan), following permeability coefficient calculation (P_{app}).

Permeability through polymer films using side-by-side diffusion chamber
Polymer films were prepared by applying 0.8 ml of polymer solutions on 2 x 3 cm teflon plate. The films were dried, removed from Teflon and placed in the chamber slide. Fluorescine solution was placed in a donor compartment (2.5 ml); in the acceptor compartment phosphate buffer was added (2.5 mL). Fluorescine flux from donor to acceptor compartment was monitored and samples were withdrawn from both compartments. Fluorescine content was determined and permeability coefficient was calculated.

RESULTS AND DISCUSSION

Permeability through Eudragit RS/L using Transwell® filter supports
Using Transwell filter supports polymers presumably penetrate into filter pores and form thin layer on the top of filter (Fig 1.).
Fluorescine permeated through polymer mixtures where Eudragit L content was greater than 75% (Fig 2). When Eudragit L content in the polymer mixture was less than 50%, fluorescine was not detected in the acceptor chamber. Although significant differences of permeability values were observed between 75:25 and 100:0 treatment groups ($p<0.01$), we were not able to rank order fluorescine permeability through different polymer mixtures due to very small fluorescine flux through mixtures with higher Eudragit RS content. Transwell filter supports in combination with Eudragit RS/L coatings produce just yes/no type of results.

Permeability through Eudragit RS/L using side-by-side diffusion chamber
In contrast to experiment using Transwell filter supports fluorescine permeated in the side-by-side diffusion chambers also through films with Eudragit L content lower than 50% (Fig 2). Unfortunately we could not prepare polymer films with pure Eudragit L or pure Eudragit RS. Film prepared with pure Eudragit RS was too adhered to Teflon plate, on the other hand film prepared with pure Eudragit L was cracked after the placement in the chamber slide. Permeability values differed significantly among all treatment groups ($p<0.01$).

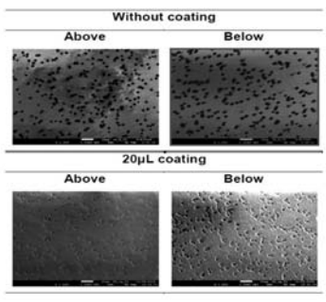

Fig. 1: Images of Transwell polycarbonate filter with and without coating.

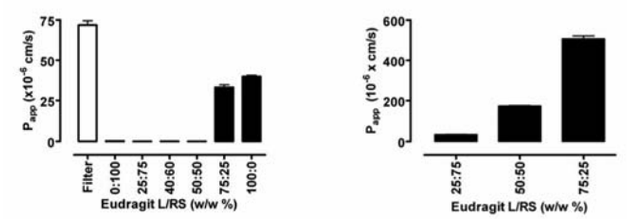

Fig. 2: Permeability (P_{app}) values of fluorescine obtained by Transwell filter supports (left) or side-by-side diffusion chamber (right).

CONCLUSIONS

Described experimental models represent a meaningful way to investigate the behavior of different kind of coatings, what can be usefully applied in the development of controlled release formulations.

REFERENCES

1. Lecomte F, Siepmann J, Walther M et al. Blends of enteric and GIT-insoluble polymers used for film coating: physicochemical characterization and drug release patterns. J. controlled Release. 2003;89:457-471.
2. F. Siepmann, J Siepmann, M Walther et al. Polymer blends for controlled release coating. J. controlled Release. 2008;125:1-15.

BIOPHARMACEUTICAL ASPECTS OF ORAL MODIFIED RELEASE DOSAGE FORMS

M. Bogataj

University of Ljubljana, Faculty of Pharmacy, Aškerčeva cesta 7, 1000 Ljubljana, Slovenia

INTRODUCTION

According to US Pharmacopoeia "a modified-release dosage form is one for which the drug release characteristics of time course and/or location are chosen to accomplish therapeutic or convenience objectives not offered by conventional dosage forms". For this purpose the time to reach therapeutic concentrations and the length of interval during which plasma concentrations are in therapeutic range are controlled. High plasma concentrations, especially in initial phase after administration, which can produce adverse drug effects, can be avoided. Less frequent dosing is also possible what increases patient's compliance. However, one has to be careful when the doses of the drug are larger than those used in immediate release dosage forms. To reach all goals drug has to be released and absorbed in controlled manner over longer period of time.

Biopharmaceutical processes
After oral administration of the dosage form drug is released in gastro intestinal (GI) tract, absorbed and distributed in the blood and tissues, it might be metabolised and in final phase it is eliminated from the body. The processes of distribution, metabolism and elimination depend mostly on the drug itself, while drug release might be controlled by the dosage form and thus might influence also the absorption. The emphasis of this presentation will be on those biopharmaceutical processes where the dosage form plays an important role and on the parameters that influence these processes.

Conditions in GI tract
When talking about the behaviour of the dosage form in GI tract after administration two aspects have to be considered: properties of the dosage

form and the conditions in GI tract. In the present contribution the important conditions in GI tract will be exposed and the behaviour of the dosage form described. Among the most important conditions that influence the behaviour of the dosage form after oral administration is the composition of GI media. Probably the best known are the values of pH but there are less data about buffer capacity, surface tension, ionic strength, exact ionic composition and the presence of other substances. Another important parameter are mechanical influences on the dosage form which are the most intensive during the passage of the dosage form through sphincters; in this regard there might also be difference between tablets and pellets. Transit times through GI tract are also important; tablets which do not disintegrate are transported on all-or-nothing principle, while pellets are frequently transported along the gut in a series of boluses. When the dosage form is taken with food the conditions in GI tract change drastically. The composition of GI media is completely different due to food components and changed secretions. Transit times, the mechanical influences on the dosage form and some other conditions are also changed. And finally, one has to be aware also of great intra and inter-subject variability of all described parameters which may strongly influence the behaviour of the dosage form after administration.

Dissolution / release

All above described parameters might influence strongly the drug dissolution / release and have to be considered when preparing a new formulation. To predict the behaviour of the dosage form after administration well it is necessary to find critical parameters which have the strongest influence and consider them in *in vitro* release evaluation.

Absorption

The described conditions in GI tract are also very important for drug absorption and we have to have in mind that MR dosage forms travel along GI tract and that the drug is intended to be released and absorbed in different parts. However, it is well known that for most drugs their absorption in the stomach is negligible and the most important site for absorption is small intestine, especially the upper part. Some drugs are also efficiently absorbed from colon. However, the fact is that the residence time of the dosage form at the site of absorption frequently determines the absorption time. But many technological approaches have already been developed which can avoid the limitation of GI transit times and enable much longer absorption of the drug.

The components of the dosage form may in some cases also influence the permeability. The most frequent case is when specific substances which can act as absorption enhancers are incorporated in the dosage form; some substances may also influence the processes of active transport. However, the influence of the dosage form on the drug absorption is noticed relatively seldom if compared with its influences on the dissolution.

First pass metabolism

Substances incorporated in the dosage form may sometimes also influence the metabolic processes which take place in intestine. However, like the influence on the permeability also this influence is in most cases connected with incorporation of specific substances and is noticed much rarely than the influences of the dosage form on the drug release.

But even if no components of the MR dosage form influence the first pass metabolism, its extent might be increased and bioavailability decreased in comparison with immediate release dosage form. It might happen when metabolic processes are saturated after immediate release dosage form administration due to high concentrations of the drug. As MR dosage form usually release the drug in lower concentrations for a prolonged period of time the probability to saturate the enzymes becomes lower.

Metabolism, distribution, elimination

The influence of the dosage form and its components on other biopharmaceutical processes i.e. on systemic drug metabolism, distribution and elimination is less probable and it is most frequently expected that these processes do not differ between immediate and modified release dosage forms.

CONCLUSION

The MR dosage forms may assure therapeutic plasma concentrations through prolonged period of time, thus improving therapeutic efficacy and safety of the drug and patient compliance. There are some negative aspects and increased risks connected with MR dosage forms, but by good knowledge of these negative sides and correct and reasonable use of MR dosage forms most of them can be avoided or prevented. It is frequently very difficult to predict the behaviour of MR dosage forms in GI tract as they are exposed to a variety of very variable conditions for a long period of time. However, huge efforts are invested in the development of new technological approaches as well as of new biorelevant testing systems of MR dosage forms. The results can already be seen in increasing number of new efficient MR dosage forms on the market and due to all advantages of MR dosage forms further expansion of their use in already known and in new therapeutic areas can be expected.

REFERENCES

1. Dressman J.B. et al., Pharm Res 1998, 15(1), 11-22.
2. Welling P.G., Pharmacikonetics, ACS, Washington, 1997.
3. Hurst S. et al., Expert Opin Drug Metab Toxicol 2007, 3(4), 469-489.
4. Locatelli I. et al., Expert Opin Drug Deliv 2010, 7(8), 967-976.

STATISTICAL AND MACHINE LEARNING TOOLS IN EVALUATION AND OPTIMIZATION OF MODIFIED RELEASE PRODUCTS

S. Ibrić*, J. Djuriš, J. Parojčić, Z. Djurić

Department of Pharmaceutical Technology, Faculty of Pharmacy, University of Belgrade, Vojvode Stepe 450, 11221 Belgrade, Serbia

DESIGN OF EXPERIMENTS

Development of modified release product, is always a time-consuming and complicated process. In reality, the formulator has to work in a design space that is multi-dimensional and virtually impossible to conceptualize. To date, statistics has been used as one approach to this problem. The recent regulations from the key federal agencies, to apply "Quality by Design (QbD)" paradigm, have pursued researchers in industry to employ experimental designs during drug product development. Experimental design is the strategy for setting up experiments in such a manner that the information is obtained as efficiently and precisely as possible. This method has the advantage of generating clearly expressed models, with associated confidence factors. However, for more than three or four inputs, statistical approaches rapidly become unwieldy, so that the formulator is tempted to oversimplify the problem (for example, restricting a study to three input variables) in order to model it. Statistics also often require the assumption of a functional form (for example, linearity) in order to generate a model and such assumptions can be inappropriate for complex tasks like formulation (1).

ARTIFICIAL NEURAL NETWORKS

An artificial neural network (ANN) is an intelligent non-linear mapping system built to loosely simulate the functions of the human brain. An ANN model consists of many nodes and their connections. Its capacity is

characterized by the structure, transfer function and learning algorithms. Because of their model independence, non-linearity, flexibility, and superior data fitting and prediction ability, ANNs have gained interest in the pharmaceutical field in the past decade. Rigorous regulations in pharmaceutical industry urge for more sophisticated tools that could be used for designing and characterizing dosage forms. It is of great importance to be fully aware of all the factors impacting the process of dosage form manufacturing and, if possible, predict the intensity of these impacts on product characteristics.

Artificial neural networks have been introduced into the field of pharmaceutical technology in 1991 by Hussain and coworkers and gained interest in several pharmaceutical applications. Ever since, they received great attention, especially when it was realized how powerful tools these networks can be. This is especially useful for nonlinear complex problems. It has been shown that many artificial intelligence systems, especially neural networks, can be applied to the fundamental investigations of the effects of formulation and process variables on the delivery system (2).

Design of artificial neural networks has evolved over time making it possible to have networks specialized for solving specific types of problems. A network is fed with data - different inputs and outputs - and let to find some connection between them. Generally, networks can be divided into static and dynamic, but other classifications are also possible. Dynamic neural networks are more advanced than static ones because of the fact that data is stored and elaborated *in time* - the inputs are not independent, moreover they are interacting and influencing each other. Every input is analyzed as a function of the previous one, the network remembers past inputs making the current output integration of past inputs and current response of the system. Past information is therefore used for predicting current and future states of the system. This approach is very useful for analyzing drug release from controlled release pharmaceutical formulations since the amount of drug released is a function where each output depends on the previous input. It is expected that modeling of drug release is more adequate with dynamic than static neural networks (3, 4).

The aim of the presented case study is to expand the utilization of artificial neural networks (ANNs) to prediction of controlled release matrix tablets dissolution profiles on the basis of knowledge of formulation factors (composition), processing parameters and tablets mechanical properties. ANNs of the same topology were developed to model dissolution profiles of different matrix tablets types (hydrophilic/lipid) using formulation composition, compression force used for tableting, tablets porosity and tensile strength as input data. Developed ANN models were used to construct design space in order to elucidate optimal combination of formulation factors and processing parameters to produce desired dissolution profiles. Furthermore, potential application of decision trees in discovering knowledge from experimental data was investigated.

Modeling of drug release for hydrophilic and lipid matrix tablets using dynamic neural networks has been done using Elman's neural network (Fig.1), optimizing the number of neurons in hidden layers, neurons weights and time delay of signals using genetic algorithms.

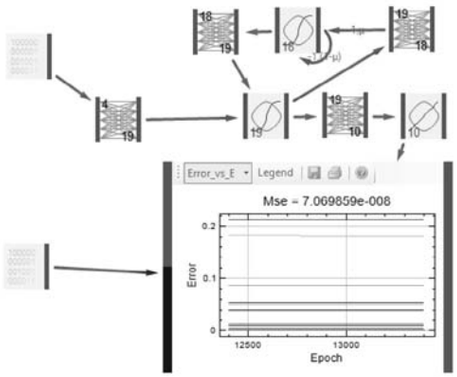

Fig 1: Topology of *Elman's* dynamic network used for modeling of drug release for both hydrophilic and lipid matrix tablets

Obtained results indicate to the possibility of prediction of drug release profiles on the basis of key formulation factors, process parameters and tablet properties. Developed methods allow simple, yet very precise way of drug release predictions for both hydrophilic and lipid matrix tablets having controlled drug release. So far, there have been no methods in the literature that were developed for prediction of drug release regardless the type of matrix system. Therefore, it is to be expected that presented *in silico* tools facilitate implementation of quality by design concept, i.e. description and understanding of design space and quality risk management for formulations and processing parameters being developed.

REFERENCES

1. Lewis G, Mathieu D, Phan-Tan-Luu R, Pharmaceutical Experimental Design, Marcel Dekker, New York, 1999
2. P Barmpalexis, FI Kanaze, K Kachrimanis, E Georgarakis, Artificial neural networks in the optimization of a nimodipine controlled release tablet formulation. Eur. J. Pharm. Biopharm. 2010; 74: 316-323.
3. J Petrović , S Ibrić, G Betz, J Parojčić, Z Djurić, Application of dynamic neural networks in the modeling of drug release from polyethylene oxide matrix tablets. Eur. J. Pharm. Sci., 2009; 38:172-180.
4. Elman JL. Finding structure in time. Cognitive Science,1990; 14(2): 179-211.

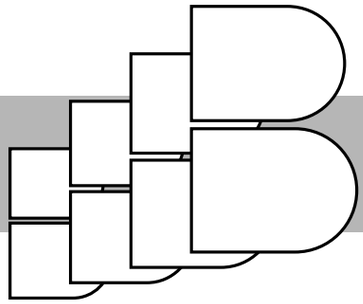

ORAL PRESENTATIONS

THE POTENTIAL OF TANDEM MASS SPECTROMETRY AT THE FIELD OF METABOLIC DISORDERS

S. Murko[1*], B. Repič Lampret[1], T. Battelino[2]

[1]University Children's Hospital, University Medical Centre Ljubljana, Unit for Special Laboratory Diagnostics, Vrazov trg 1, 1000 Ljubljana, Slovenia; [2] University Children's Hospital, University Medical Centre Ljubljana, Department of Endocrinology, Diabetes and Metabolic Diseases, Bohoričeva 20, 1000 Ljubljana, Slovenia

INTRODUCTION

Tandem mass spectrometry (MS/MS) enables the screening of a broad spectrum of metabolic disorders in a single analytical run. These include disorders of amino acids metabolism such as phenylketonuria (PKU) and maple syrup urine disease (MSUD), disorders of fatty acid metabolism (e.g. medium-chain and very-long-chain acylCoA dehydrogenase deficiency; MCAD, VLCAD) as well as organo acidemias such as propionic and methylmalonic acidemia (1, 2). Reliable and simultaneous detection of many target molecules and determination of their concentrations is a great benefit of this technology. MS/MS is the method of choice because of its great sensitivity, selectivity, linearity, robustness and reliability. Because of its high selectivity the application does not require chromatographic separation, enabling very short run times (2 min).

In this report, a method for the determination of 12 amino acids and 25 acylcarnitines in a single run by MS/MS, is presented.

MATERIALS AND METHODS

Materials

MassChrom reagent kit for the LC-MS-MS analysis of Amino Acids and Acylkarnitines from dried blood spot for newborn screening (Chromsystems, 55000/F). Mass spectrometer: 3200 QTRAP LC/MS/MS System (ABSCIEX). HPLC system: Perkin Elmer Series 200

Manual puncher, Thermostable microtiter plates shaker for extraction and derivatisation of the samples: PST-60 HL plus (Biosan).

Sample collection

Whole blood specimens are spotted on filter paper cards (Whatman 903), dried and delivered to the laboratory.

Sample preparation

Extraction: 3 mm dried blood spot disk + 200 µL internal standard → agitation, 600 rpm, 25 min, ambient temperature → centrifugation, 4000 rpm, 2 min → evaporation, 600 rpm, 60 °C to dryness.

Derivatisation to butyric esters : addition of 60 µL derivatisation reagent → incubation, 600 rpm, 20 min, 60 °C → evaporation, 600 rpm, 60 °C to dryness.

Reconstitution: addition of 200 µL reconstitution buffer → agitation, 600 rpm, 1 min.

MS/MS Measuring method

Injection volume: 25 µL

Run time: 1.7 min

Flow rate: isocratic, 100 µL/min

The acycarnitines and amino acids were analysed using a multiple reaction monitoring (MRM) transitions for each parameter. All analytes were quantified using the ratio of the signal intensity of the compound to that of its deuterated internal standard.

RESULTS AND DISCUSSION

In order to confirm the reliability of the proposed method numerous normal and some pathological patient samples were analysed. The out-of-range amino acids or acylcarnitines concentrations were set after determination of our own reference ranges. For this purpose analysis of 130 apparently healthy children were performed. Reference ranges were calculated with the use of statistical programme MedCalc. In Fig.1 and Fig.2 mass spectrum for normal pattern of amino acids and acylcarnitines are given, respectively. All analytes were within reference ranges. In addition, three samples of previously diagnosed patients with phenylketonuria, propionic academia and glutaric academia type I were analysed (Fig.3 to Fig.5). Characteristic markers for acylcarnitine disorder and reference ranges are given in Table 1. Data of Figs.3-5 indicate that specific markers for associate disorder are elevated which confirms the reliability of the method.

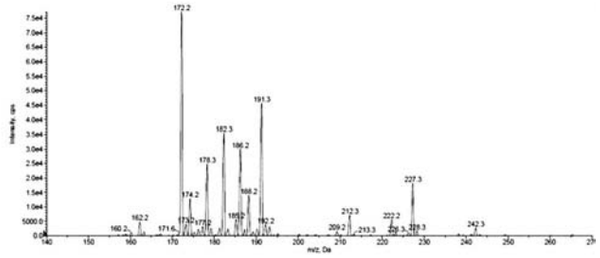

Fig.1: Spectrum of a sample with normal amino acids profile.

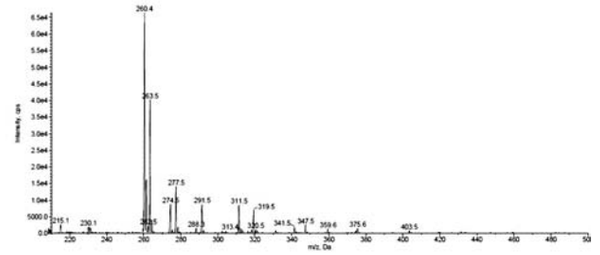

Fig.2: Spectrum of a sample with normal acylcarnitines profile.

Table 1: Acylcarnitine disorder, characteristic marker and reference range.

Marker	Associated disorder	Referenc range
Propionylcarnitine (C3)	Propionic acidemia (PA) Methylmalonic academia (MMA) Multiple carboxylase deficiency (MCD)	0,38-2,02
Glutarylcarnitine (C5DC)	Glutaric acidemia I and II (GA I and II)	0,04-0,11

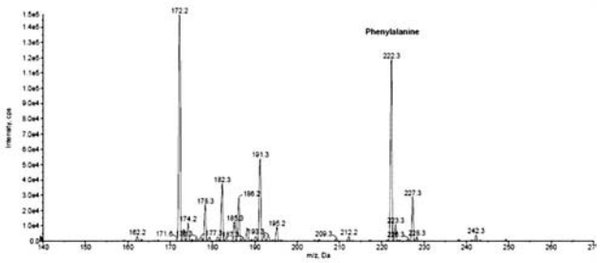

Fig.3: Spectrum of a patient sample with Phenylketonuria (Phenylalanine, m/z=222). Concentration of phenylalanine was 8,0 times above reference range (28-67 µmol/L).

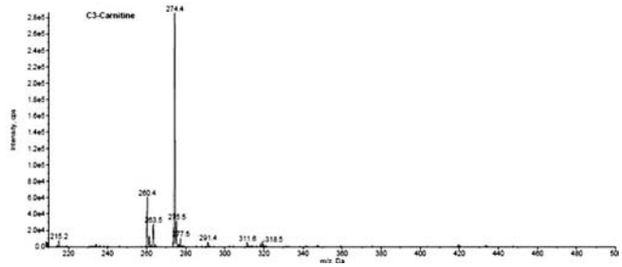

Fig.4: Spectrum of a patient sample with Propionic academia (C3-Carnitine, m/z=274). Concentration of C3-Carnitine was 38,3 times above reference range.

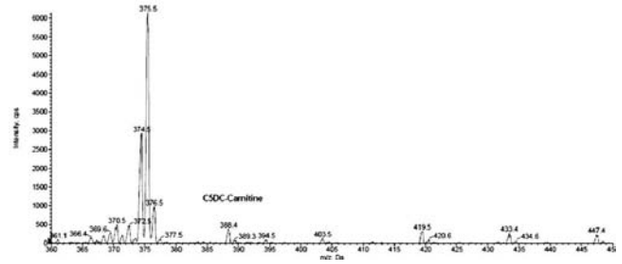

Fig.5: Spectrum of a patient sample with Glutaric academia type (C5DC-Carnitine, m/z=388). Concentration of C5DC-Carnitine was 18,2 times above reference range.

CONCLUSIONS

The proposed MS/MS method enables fast, reliable and accurate determination of the concentrations of amino acids and acylcarnitines from the dried blood spot. This study shows tremendous potential of tandem mass spectrometry in the field of metabolic disorders.

REFERENCES

1. Dietzen DJ et al., National academy of clinical biochemistry laboratory medicine guidelines, Clin.Chem. 2009; 55:9: 1615 – 1626.
2. Instruction manual for LC/MS/MS analysis.

PRO-INFLAMMATORY EFFECTS OF GALECTIN-3 ON MONOCYTIC-MACROPHAGE CELLS

R. Novak, S. Dabelić, J. Dumić*

University of Zagreb, Faculty of Pharmacy and Biochemistry, Department of Biochemistry and Molecular Biology, A. Kovačića 1, 10000 Zagreb, Croatia

INTRODUCTION

Galectin-3 (gal-3), a β-galactoside binding lectin has been recently recognized a potent and very useful diagnostic and prognostic marker for heart failure. In addition, it exerts important roles in many other (patho)physiological processes (adhesion, proliferation, differentiation, apoptosis, inflammation, neoplastic transformation, spreading metastases). Being one of the key lectins of innate and acquired immunity, gal-3 is generally considered a powerful pro-inflammatory signal. However, additional biological characterization of gal-3 is of utmost importance for elucidation of the mechanisms of the processes in which it is involved.
The aim of this study was to ascertain the level of gal-3 expression and explore its role in (patho)physiological processes of monocytic lineage cells.

MATERIALS AND METHODS

We used lipopolysaccharide (LPS) activated and phorbol 12-myristate-13-acetate (PMA) differentiated, THP-1 cells and human monocytes isolated from the buffy coats of healthy volunteers. Flow cytometry and Western blot were used to determine gal-3 expression, while qRT-PCR was used to measure *LGALS3* expression. Dead cells were excluded as 7AAD positive. Using cytokine capture beads and flow cytometry, we studied the effect of recombinant human gal-3 on inflammatory cytokine secretion of classically (M1) or alternatively activated (M2a/M2c) macrophage cells and on the expression of *LGALS3*. PBMC-derived monocytes from healthy volunteers were exposed to macrophage colony-stimulating factor (M-CSF), IFN-γ and LPS to generate M1 cells or granulocyte-macrophage colony-stimulating factor (GM-CSF) and IL-4/IL-10 to generate M2a/M2c cells.

RESULTS AND DISCUSSION

LPS-activated THP-1 cells had markedly up-regulated expression of intracellular gal-3, while the surface level remains largely unchanged. Differentiation of monocytes to macrophages is associated with an increase of surface and total gal-3 expression in respect to the controls. M1 polarization was confirmed by elevated TNF-α, IL-1ß and IL-6 in culture medium and lack of CD206 mannose receptor in respect to M2 macrophages. Our data indicate IL-8 could be considered a novel M1 *vs*. M2 polarization marker. Exogenous gal-3 was shown to effect *LGALS3* expression and to up-regulate IL-6 and IL-8 production in M2a cells and TNF-α, IL-6 and IL-8 production in M2c cells in respect to the control cells, thus skewing M2 cells towards the M1 pro-inflammatory phenotype.
Although further research is needed, collected data provide new insights into gal-3 pro-inflammatory effects and could contribute setting up a platform for development of new anti-inflammatory therapeutic approaches.

SIMULTANEOUS SOLUBILITY DETERMINATIONS OF TWO POORLY SOLUBLE DRUGS FROM THEIR BINARY MIXTURES BY MICRO TENSIOMETRY

L. Peltonen[1*], T. Messiaen, T. Laaksonen, J. Hirvonen

University of Helsinki, Division of Pharmaceutical Technology, P.O. Box 56 (Viikinkaari 5 E), 00014 University of Helsinki, Finland

INTRODUCTION

Solubility of active pharmaceutical ingredients (APIs) is of crucial importance to drug formulations, since low aqueous solubility may limit bioavailability and the possible drug delivery route(s). As the number of poorly water-soluble APIs is growing all the time, better formulations and solubility testing methods are needed. Throughput requirements in solubility testing have also increased, and different miniaturized testing methods on 96-well plate systems have been presented (1,2).
In our earlier studies we have demonstrated the feasibility of micro tensiometric measurements on a 96-well plate as a fast analytical tool for solubility determinations of poorly soluble drug substances (1). The objective of this study was to utilize the surface tension measurements for simultaneous solubility determinations of two individual drug substances from their binary mixtures in aqueous environment.

MATERIALS AND METHODS

Materials

Ibuprofen, rifampicin, spirinolactone (all from Orion Pharma, Espoo, Finland) and indomethacin (Fluka Biochemika, Italy) were used as model drug substances. DMSO (Sigma Aldrich Chemie GmbH, Taufkirchen, Germany) was used as a presolvent. Water used was ultrapure Millipore water (Molsheim, France).

Microtensiometry

Surface tension measurements were performed by Delta-8 multichannel micro tensiometer equipped with wire probes (Kibron Inc., Helsinki, Finland); the technique is related to the Du Noüy ring method. Sample volume was 50 µl. The drugs were first dissolved in a presolvent, and concentration series of drugs in aqueous DMSO were prepared for the analyses.

Equilibration time of 10 minutes before the analysis was allowed in order to let the non-dissolved drug to sediment and the surface to stabilize. The solubility value was achieved from the focal point between the sloping part and the level part of the isotherm (1). After this point, solid and solvated phases are in equilibrium and the amount of free compound(s) constant in the solution. Measurements were performed at room temperature and repeated at least four times.

RESULTS AND DISCUSSION

For testing the feasibility of the micro tensiometry for simultaneous solubility determinations of individual drug materials from binary mixtures, we first analysed different ratios of ibuprofen and indomethacin. Combinations ranging from 1:5 to 5:1 of indomethacin and ibuprofen, respectively, were studied.

From these results, it was clear that two different linear areas on the lowering part of the isotherm can be identified, which were separated by a horizontal section (Fig. 1). The first slope (seen at the lower concentration values) is the result of the presence of indomethacin in the sample.

The solubility value for indomethacin was found to be 0.091 mg/ml (value in a pure indomethacin solution 0.080 mg/ml, respectively). For ibuprofen, the corresponding values were 0.273 mg/ml for a mixture and 0.240 mg/ml for a pure solution. Accordingly, with a single measurement, we were able to determine the solubility values of both the indomethacin and ibuprofen from a mixture.

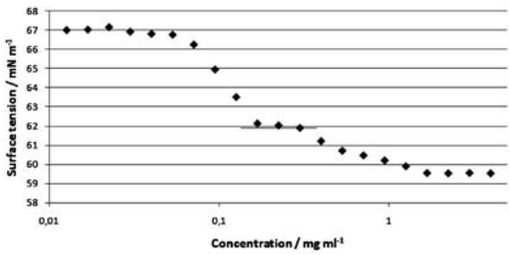

Fig. 1: The surface tension of indomethacin-ibuprofen solution (1:5) as a function of concentration.

Also some other combinations, like rifampicin and spironolactone, were tested and the solubility results from a mixture were in good correlation with pure substances (Fig. 2).

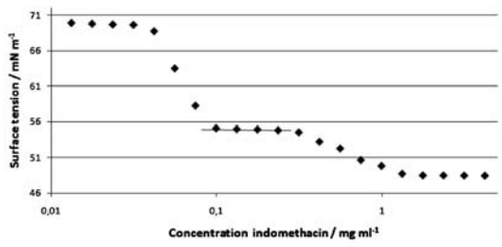

Fig. 2: Surface tension-concentration isotherm for rifampicin-spironolactone mixture.

Adsorption isotherms from binary mixtures with two slopes and a horizontal section between them were obtained, if differences in solubility and drop in surface tension were sufficiently high. When this was the case, it was possible to determine the individual solubility of both the drugs.

CONCLUSIONS

In this study, the feasibility of micro tensiometric measurements for predictive tool in solubility screening tests from binary mixtures was demonstrated. With a single measurement, we were able to determine the solubility values of two different drugs from their binary mixtures.

REFERENCES

1. Heikkilä T, Peltonen L, Taskinen S, Laaksonen T, Hirvonen J. 96-well plate surface tension measurement for fast determination of drug solubility. Letters Drug Des. Discov. 2008; 5: 471-476.
2. Heikkilä T, Karjalainen M, Ojala K, Partola K, Lammert F, Augustijns P, Urtti A, Yliperttula M, Paltonen L, Hirvonen J. Equilibrium drug solubility measurements in 96-well plates reveal similar drug solubilities in phosphate buffer pH 6.8 and human intestinal fluid. Int. J. Pharm. 2011; 405: 132-136.

DESIGN OF A DOSAGE FORM WITH PH-DEPENDENT BIMODAL PULSATILE RELEASE OF CARVEDILOL

B. Kovačič[1,2], O. Planinšek[1*], F. Vrečer[1,2], S. Sotlar[1]

[1] University of Ljubljana, Faculty of pharmacy, Aškerčeva 7, 1000, Slovenia; [2] Krka, d.d., Novo mesto, Šmarješka cesta 6, 8501, Slovenia

INTRODUCTION

Carvedilol is a drug molecule that has a low solubility in gastrointestinal fluids and is extensively metabolized in the liver, which results in absolute bioavailability of less than 30% after oral intake (1). Dosage form which ensures increased dissolution of carvedilol can, as a result, improve its bioavailabilty up to fourfold (2).

Dissolution rate of poorly soluble drug can be improved by various methods; one of them is adsorption and deposition onto high-surface-area carriers (3, 4).

A commercial product (Coreg CR) exhibits a biphasic release of carvedilol. It is available for once-a-day administration as controlled-release oral capsules filled with carvedilol phosphate immediate-release and controlled-release microparticles that are drug-layered and then coated with methacrylic acid copolymers. Slow release and absorption from controlled-release microparticles further increases drug metabolism which results in 15% lower bioavailability when compared to immediate release carvedilol tablets. The aim of this study was to design a once-a-day dosage form which would exhibit bimodal pulsatile release of poorly water soluble drug carvedilol.

MATERIALS AND METHODS

Materials

Carvedilol (CAR) was supplied by Krka, d.d., SI, and used as model drug compound. Neusilin (synthetic amorphous magnesium aluminometasilicate, Fuji Chemical Industry Ltd., JP) was used as a carrier in solid dispersion particles. Tetrahydrofuran (Merck, G) was used as a solvent for preparation of solid dispersion. Eudragit® S 100 (Röhm Gmbh, G) was used as a coating enteric polymer.

Preparation of solid dispersion

0.5 g of CAR was dissolved in 20 ml of tetrahydrofuran and 2.0 g of Neusilin was suspended in solution. Prepared suspension was evaporated by rotary evaporator until dry particles were obtained. Physical mixture was prepared by mixing CAR and Neusilin in a mortar with pestle in same proportion.

Preparation of final dosage form

62.5 mg solid dispersion/physical mixture (corresponding to 12.5 mg CAR), 7.3 mg microcrystalline cellulose and 3.7 mg sodium crosscarmellose were

directly pressed (SP 300, Killian&co., G) into tablets of hardness 50±10 N (VanKel VK200, USA), m=73,5 mg , 2r=6 mm.
Tablets were coated with Eudragit® S 100 dispersion to a target mass gain 30%. Final dosage form consisted of two coated and two uncoated tablets inserted in one hard gelatine capsule size 2 (Capsugel, USA).

SEM imaging
The morphology of CAR, Neusilin, and solid dispersion particles was analyzed using field emission scanning electron microscope (Supra 35 VP, Carl Zeiss, G).

Drug release from solid dispersions and final dosage form
Dissolution studies of solid dispersions were performed in HCl pH 1.2, phosphate buffer pH 4.5 and pH 7.4, with 5% SDS in all media, on a dissolution apparatus, paddle method (Apparatus II, VK7000, USA), 250 ml, 50 rpm, 37°C±0.5. Drug release from final dosage form was evaluated on USP III dissolution apparatus (BioDis, VanKel, USA) in phosphate buffer pH 4.5, pH 5.8, pH 6.8 and pH 7.4, with 5% SDS in all media, 250 ml, 37°C±0.5, 10 dips/min. Samples were UV analyzed at 285 nm (HP DA-UV spectrophotometer, 8453, G).

RESULTS AND DISCUSSION

SEM images of CAR, Neusilin and solid dispersions are shown in Fig. 1. As it can be seen, CAR is in great extent incorporated into porous structure of Neuslin and very few particles of CAR can be seen scattered around or adsorbed on Neusilin surface.

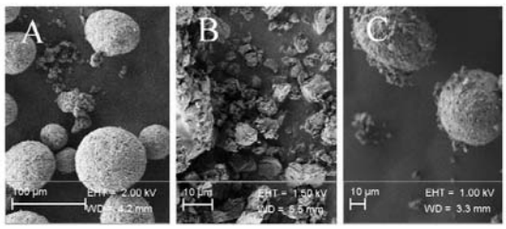

Fig. 1: SEM image of (A) Neusilin, (B) CAR and (C) solid dispersion

Drug release studies reveal that crystalline CAR is poorly soluble, especially in aqueous solution of higher pH. After 120 minutes 77%, 35% and 2% of CAR (25 mg dose) was dissolved in HCl 1.2, phosphate buffer pH 4.5 and pH 7.4, respectively. Preparation of solid dispersion with Neusilin greatly increased CAR dissolution rate; 90-100% of CAR was dissolved in same media (Fig. 2).

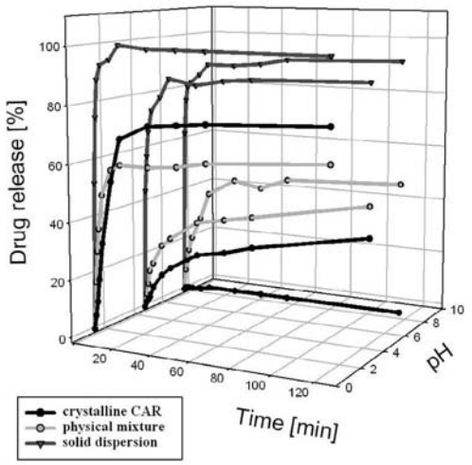

Fig. 2: Comparison of CAR dissolution (crystalline CAR, Physical mixture, solid dispersion) in HCl pH 1.2, phosphate buffer pH 4.5 and pH 6.8, 5% SDS in all media; 25 mg dose.

Drug release from final dosage form was evaluated on apparatus III simulating *in-vivo* fed conditions. Drug release profile at different pH regions is presented in Fig. 3.

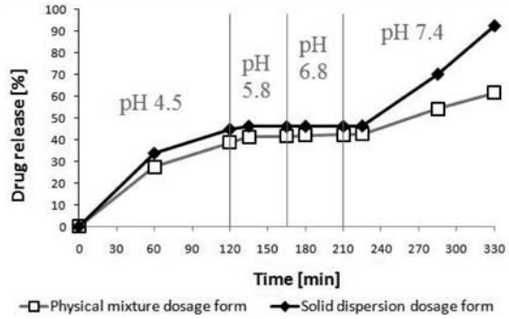

Fig. 3: Dissolution of CAR from final dosage form: pH 4.5 120 min, pH 5.8 45 min, pH 6.8 45 min, pH 7.4 120 min, 5% SDS in all media; 50 mg dose.

CAR in final dosage form exhibits bimodal pulsatile release. First pulse of 25 mg dose from uncoated tablets is released within first 120 minutes at pH 4.5, which is the pH of stomach content after feeding. In fact, the content of stomach becomes more acidic when the food passes through pylorus, but due to enteric polymer coating there is no drug release of remaining 25 mg dose from coated tablets until the pH value rises above 7.0, which happens later on in distant ileum part of intestines. Drug release is faster when solid dispersion is compressed into tablets in comparison to compressed physical mixture, because CAR in solid dispersion is finely dispersed inside porous structure and effectively hydrophilized due to intense interaction with silanol groups (5).

ACKNOWLEDGMENTS

The authors acknowledge to KRKA, d.d., Novo mesto for support in the study. Present work was partly financed by the European Union, European Social Fund.

REFERENCES

1. Morgan T. Clinical pharmacokinetics and pharmacodynamics of carvedilol. Clin Pharmacokinet. 1994; 26: 335-346.
2. Wei L, Sun P, Nie S, Pan W. Preparation and evaluation of SEDDS and SMEDDS containing carvedilol. Drug. Dev. Ind. Pharm. 2005; 31: 785-794.
3. Rupprecht H, Biersack MJ, Kindl G. Freigabe schwer löslicher Substanzen von den Oberflächen partiell belegter Kieselsäuren. Colloid. Polym. Sci. 1974; 252: 415-416
4. Vrečer F. PhD Thesis, University of Ljubljana, 1992,.
5. Kovačič B, Vrečer F, Planinšek O. Solid dispersions of carvedilol with porous silica. Chem. Pharm. Bull. 2011; 9: 427-433.

PLATELET AND SERUM CALCIUM AND MAGNESIUM CONCENTRATION IN SUICIDAL AND NON-SUICIDAL SCHIZOPHRENIC PATIENTS

N. Ruljancic[1*], M. Mihanovic[1], A. Bakliza[1], I. Cepelak[2]

[1] Psychiatric hospital Sveti Ivan, Clinical Laboratory, Jankomir 11, Zagreb, Croatia, [2] Department of Medical Biochemistry and Hematology, Faculty of Pharmacy and Biochemistry, University of Zagreb, A. Kovačića1, Croatia

INTRODUCTION

It is well established that calcium (Ca) plays important role in the regulation of neurotransmitters in the central nervous system (CNS). Main processes modulated by Ca and involved in the aetiology of schizophrenia are alteration in dopamine (DA) and glutamate neurotransmitter system. The DA hypothesis is

hyperactivity of dopaminergic transmission while glutamate postulates hypofunction of glutamate Ca-permeable N-methyl-D-aspartate (NMDA) receptors. Hypotheses of Ca-imbalance are based on examination of platelets in schizophrenic patients and suggested that increased cytosolic Ca may be the primary molecular abnormality (1,2). Intracellular effects of magnesium (Mg) ions are opposite to Ca-ions in competition at K- ion channels, in Na/K-ATP-ase activity, cAMP/cGMP concentration and Ca-ion currents in pre- and postsynaptic membranes.

Antipsychotic drugs with Mg supplement may reverse consequences of abnormalities in Ca-signalling.

SUBJECTS AND METHODS

Subjects

Group of schizophrenic patients was consisted of 23 patients with attempted suicide (S-SCH) and 48 patients without suicidal behaviour (K-SCH) diagnosed according to ICD-10 diagnosis (F20.0) with or without Intentional self-harm (X60-X84). The control group (K) was made of 99 voluntary blood donors. All patients were on psychopharmacological therapy. In Table 1. The features of the study subjects according to psychopharmacological therapy, age and gender have been presented.

Table 1: The features of the study subjects

Group	K	K-SCH	S-SCH
N	99	48	23
Age X±SD	49±11.6	45±12.9	42±15.6
M/F	48/51	28/20	7/16
AA (N)	-	48	23
TA (N)	-	29	6
A (N)	-	32	17

AA - atypical antipsychotic; TA - typical antipsychotic; A- anksiolitics; M/F – male/female; K – control group; K-SCH-non-suicidal patients; S-SCH – suicidal patients.

METHODS

The Mg and Ca concentration in platelets and serum was determined by atomic absorption spectrophotometry on the AAnalyst 200 (Perkin Elmer, USA).

RESULTS

One-way ANOVA test and by manifold application of the SNK post hoc test it has been established higher concentration of platelet Mg (μmol/10^9 platelets) ($p=0.009$, $F=4.89$) and lower concentration of serum Ca concentration (mmol/L) ($p<0.001$, $F=19.18$) in S-SCH group of patients and higher concentration of platelet Ca/Mg ratio in K-SCH group of patients ($p=0.006$, $F=5.37$). The obtained platelet and serum Ca and Mg concentration of the all examines, have been shown in Table 2.

DISCUSSION AND CONCLUSION

The research has shown disbalance of the two electrolytes in platelets of the suicidal and non-suicidal schizophrenic patients. Higher Ca/Mg ratio in platelet of non-suicidal patients confirm indirect higher Ca concentration. Higher Mg concentration in platelet of suicidal patients, considered an Ca antagonist, may represent a compensatory attempt to restrain Ca-activity. The platelet Ca concentration is higher but not statistically significant, while concentration in serum is lower in suicidal patients. DA release is Ca-dependent process triggered by Ca-influx upon activation NMDA receptors or Ca-release from intracellular stores. While inhibition of NMDA receptors reduces Ca-influx through these channels, the overall effect is an increase Ca-level in large neuronal population. This mechanism may facilitate excitotoxic neuronal damage or exaggerated DA release (3,4). From the obtained result we can conclude that Mg supplement with antipsychotics may be beneficial for treatment of schizophrenic patients. Lack of large-scale, double-blinde, placebo controlled clinical trials is the main limited factor in making strong recommendation.

Table 2: Platelet and serum Ca and Mg concentration in all group of examines

Group	K		K-SCH		S-SCH	
Sample	Plt	Ser	Plt	Ser	Plt	Ser
Mg (X±SD)	0,16 0,07	0,95 0,07	0,14 0,07	0,95 0,12	0,23* 0,13	0,92 0,13
Ca (X±SD)	0,35 0,19	2,54 0,14	0,34 0,13	2,40 0,30	0,42 0,17	2,28 • 0,17
Ca/Mg (X ±SD)	2,19 0,54	2,67 0,18	2,61◆ 0,86	2,55 0,24	2,09 0,66	2,52 0,30

K – control group; K-SCH-non-suicidal patients; S-SCH – suicidal patients; *p<0,05 compared to K and K-SCH; •P<0,05 compared to K and K-SCH; ◆p<0,05 compared to K and S-SCH

REFERENCES

1. Ripova D, Strunecka A, Nemcova V, Farska I. Phospholipids and calcium alteration in platelets of schizophrenic patients. Physiol Res 1997;46:59-68.
2. Das I, Khan NS, Puri BK, Soorana SR, deBelleroche J, Hirsch SR. Elevated platelet calcium mobilization and nitric oxide synthase activity may reflect abnormalities in schizophrenic brain. Biochem Biophys Res Commun 1995;212:375-380.
3. Bojarski L, Debowska K, Wojda U. In vitro findings in intracellular calcium homeostasis in schizophrenia. Prog Neuropsychopharmacol Biol Psych 2010;34:1367-1374.
4. Lidow MS. Calcium signalling dysfunction in schizophrenia:a unifying approach. Brain Res Rew 2003;43:70-84.

ANALYSIS OF CARBAMAZEPINE AND ITS ACTIVE METABOLITE IN SALIVA USING HPLC AFTER SOLID-PHASE EXTRACTION

J. Tonic – Ribarska[1*], Z. Sterjev[1], A. Haxhiu[2], Lj. Suturkova[1], S. Trajkovic – Jolevska[1]

[1] Faculty of Pharmacy, University "Ss Cyril and Methodius", Vodnjanska 17, 1000 Skopje, Macedonia, [2] Medical Sciences Faculty, State University of Tetova, Ilinden nn, 1200 Tetovo, Macedonia

INTRODUCTION

Therapeutic drug monitoring (TDM) of antiepileptic drugs (AED) has been used in clinical practice to aid the treatment of patients with epilepsy. Measurements of total drug concentration in blood correlate far better with clinical effect than the drug dose. But, only free drug is pharmacologically active, can interact with a receptor to produce a given pharmacologic and therapeutic effect (1). AED concentrations in saliva were assumed to reflect their free levels in blood and therefore may have greater clinical relevance than total AED concentrations. Furthermore, saliva can be obtained easily with minimal discomfort to the patient. Hence, there has been a great interest in the use of saliva as an alternative matrix for TDM of AEDs (2). Carbamazepine (CBZ) is a first line antiepileptic drug used in the treatment of partial and generalized tonic-clonic seizures. From a clinical standpoint, carbamazepine-10,11-epoxide (CBZ-EP) is the most important metabolite of CBZ, because it is a pharmacologically active compound with anticonvulsant properties, as its parent compound (3).

The purpose of this study was to establish the specific, sensitive, reliable solid-phase extraction followed by RP-HPLC for the simultaneous determination of CBZ and its active metabolite, CBZ-EP, in saliva.

MATERIALS AND METHODS

Chemicals and reagents

BZ, CBZ-EP and nitrazepam (internal standard, IS), were purchased from Sigma-Aldrich, USA. Methanol and acetonitrile, HPLC grade, were obtained from Merck, Germany. For all analysis, HPLC grade water was used. OASIS HLB cartridges (30mg/1mL) used for sample preparation were supplied by Waters, USA.

Saliva samples

Saliva was collected from healthy volunteers and from the epileptic patients under oral chronic CBZ therapy. The saliva samples were frozen at -20ºC until the analysis. The principles embodied in the Helsinki Declaration were adhered to and the Ethics Committee at the Faculty of Pharmacy, Skopje, approved the study.

Preparation of standard solutions

Stock solutions of the analytes (500µg/ml CBZ and 250µg/ml CBZ-EP) and the IS (500µg/ml) were prepared by dissolving each compound in methanol. Working solutions were prepared from stock solutions by dilution with the purified water. Calibration standards were made by spiking the blank saliva aliquots with appropriate volume of working solutions of CBZ and CBZ-EP at 6 different concentrations containing the IS at constant concentration (1µg/ml). The resulting saliva concentration ranges were: 0.1-5µg/ml for CBZ and 0.05-2.5µg/ml for CBZ-EP. Four levels of quality control (QC) samples were prepared at the concentrations of: 0.1, 0.5, 1.0, 2.5 µg/ml for CBZ and 0.05, 0.25, 0.5, 1.25 µg/ml for CBZ-EP, in same way as describe above, and stored at -20ºC until the analysis.

Sample preparation

Preparation of samples was based on the solid-phase extraction (SPE). The collected saliva stored at – 20^{0}C were allowed to thaw at room temperature before centrifuged at 3000 rpm for 15 min. The supernatant from epileptic patient saliva was spiked with 100 µl IS, while the supernatant from blank saliva was previously spiked with analytes. The mixture was vortex-mixed for 30s and loaded into OASIS HLB cartridges previously conditioned with 1ml methanol/water; loading of 1ml saliva sample; washing with 1ml 5% methanol and eluting with methanol.

Chromatographic conditions

The separation was carried out on a Waters HPLC system with reversed-phase column (Zorbax Extend C18, 150 x 4,6 mm, 5µm) using isocratic elution with acetonitrile and water (35:65) as a mobile phase. The temperature was 30°C and UV detection was set at 220 nm. Method validation was developed following the recommendations for validation of bioanalytical methods of EMA guideline (4).

RESULTS AND DISCUSSION

The recovery values of the extraction procedure at four concentration levels were in the range of 98,3%-99,2% for CBZ and 98,1%-99,3% for CBZ-EP.

Under the proposed chromatographic conditions, no interfering peaks were observed in the retention times of analytes.

Calibration curves were set up by plotting the analyte-IS peak area ratios versus the respective analyte concentrations. The correlation coefficient was 0,9991 for CBZ and 0,9987 for CBZ-EP, respectively.

The results for accuracy and precision were within recommended limits.

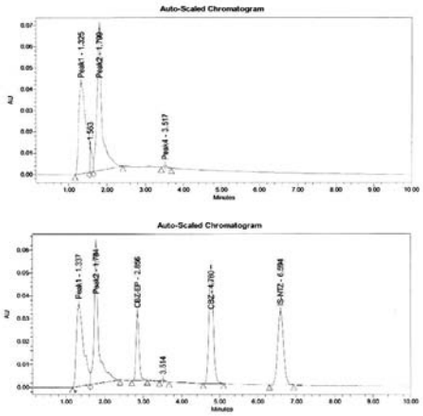

Fig. 1: RP-HPLC chromatograms of: a) blank saliva; b) blank saliva spiked with 2.5µg/ml CBZ, 1.25µg/ml CBZ-EP and 1µg/ml nitrazepam

Table 1: Precision and accuracy of CBZ and CBZ-EP in human saliva

Analyt	Conc µg/ml	Within-run assay (n=5)		Between-run assays (n=15)	
		accuracy (%)	precision (CV%)	accuracy (%)	precision (CV%)
CBZ	2.5	99.1	0.81	98.4	1.02
	1.0	101.2	1.23	98.7	1.16
	0.5	98.9	1.06	97.9	0.92
	0.1	98.3	0.91	102.1	2.11
CBZE	1.25	100.2	2.01	99.0	1.39
	0.5	99.1	1.13	97.5	0.76
	0.25	98.2	0.86	97.8	3.18
	0.05	97.6	2.71	98.8	0.79

Stability studies indicate that stock solutions and saliva samples were stabile under different storage conditions and no stability related problems would be expected during the routine saliva sample analysis.

The proposed method gives satisfactory results when was applied to saliva samples collected from epileptic patients with CBZ therapy.

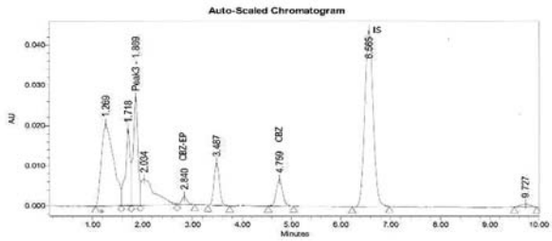

Fig. 2: Representative chromatogram of saliva sample from a patient treated with 600mg/day of CBZ, taken 10h after the last oral administration

CONCLUSIONS

A simple, sensitive, precise and accurate HPLC method has been developed for simultaneous determination of CBZ and CBZ-EP in human saliva after SPE. The proposed method was successfully applied to saliva samples obtained from epileptic patients under CBZ therapy.

REFERENCES

1. Liu H, Delgado M, Therapeutic drug concentration monitoring using saliva samples. Clin. Pharmacokinet. 1999; 36: 453-470
2. Maldonado C, Fagiolino P et al, Therapeutic carbamazepine and valproic acid monitoring in children using saliva as a biologic fluid. J. Epilepsy. Clin. Neurophysiol. 2008;14:55-58
3. Oh E, Ban E et al, Analysis of carbamazepine and its active metabolite, carbamazepine-10,11-epoxide, in human plasma using HPLC. Anal. Bioanal. Chem. 2006; 386; 1931-1936
4. Guideline on validation of bioanalytical methods, European Medicines Agency (EMA), Committee for Medicinal Products for Human Use (CHMP), 2009

PHARMACOGENETICS OF TPMT: SCREENING FOR NEW BIOCHEMICAL FACTORS INFLUENCING TPMT ACTIVITY

A. Šmid[1], M. Milek[1], N. Karas-Kuželički[1], R. Tamm[1], A. Metspalu[1], I. Mlinarič-Raščan[1*]

[1] University of Ljubljana, Faculty of Pharmacy, Aškerčeva cesta 7, 1000 Ljubljana, Slovenia, [2] Estonian Genome Centre and Department of Biotechnology, Institute of Molecular and Cell Biology, University of Tartu, Estonia

INTRODUCTION

The main challenge of chemotherapy is to design individualized dosage regimens to overcome the boundaries of narrow therapeutic index. Both

the efficacy and the toxicity of thiopurine drugs depend largely on the extent of their deactivation by S-methylation. This process is catalyzed by thiopurine S-methyltransferase (TPMT), a genetically polymorphic enzyme. Non-synonymous amino acid substitutions in mutant TPMT allozymes destabilize the protein structure and increase its susceptibility to proteasomal degradation. In homozygous mutants, TPMT activity is low or absent, while heterozygous individuals exhibit intermediate TPMT activity.

In addition to the role played by genotype, TPMT activity is regulated by a complex metabolic network. As an SAM-dependant methyltransferase (MT-ase), TPMT is closely connected to the L-methionine (Met) cycle, the folate pathway, trans-sulfuration and glutathione (GSH) synthesis (Fig. 1).

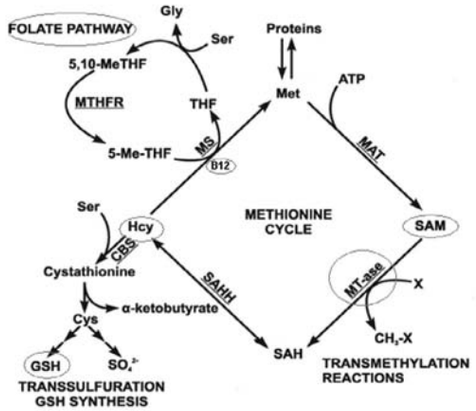

Fig. 1: SAM metabolism, the methionine cycle and related pathways. The analytes under investigation are encircled. 5,10-Me-THF, 5,10-methylenetetrahydrofolate; 5-Me-THF, 5-methyltetrahydrofolate; THF, tetrahydrofolate; MS, methionine synthase; MTHFR, 5,10-methylenetetrahydrofolate reductase; CBS, cystathionine-β-synthase; Cys, cysteine; GSH, glutathione; SAHH, S-adenosylhomocysteine hydrolase; MAT, methionine adenosyltransferase.

Recently, some studies have reported on the post-translational stabilization of TPMT by its co-factor S-adenosylmethionine (SAM) (1) while others demonstrated that mutations in MTHFR, the enzyme involved in SAM biosythesis correlates well with hematotoxic events during ALL treatment, improving the predictive value of TPMT-based genotyping (2, 3).

In this study we investigated the influence of SAM-related metabolites - namely GSH, B12, Hcy and folates- as well as of TPMT genotype and SAM levels, on TPMT activity in healthy individuals.

MATERIALS AND METHODS

Study participants, preparation of hemolysates and genotyping assays.
Blood samples were collected from 154 healthy individuals, donors of the Estonian Gene Bank. Genotyping of TPMT*3 alleles (460G>A – rs1800460, and 719A>G – rs1142345) was carried out by Taqman Genotyping Assays (Applied Biosystems, Foster City, CA) as described previously (2). Hemolysates were prepared in accordance with the previously described procedure (4, 5). An aliquot (0.1 ml) was used for the routine hemoglobin measurement on a Coulter Ac·T Diff analyzer (Beckman Coulter, Brea, CA).

Metabolites and TPMT activity.
TPMT activity and SAM levels in hemolysates were determined using modified versions of the high-performance liquid chromatography (HPLC) methods described previously (1, 5).

GSH levels were determined using the Glutathione Assay Kit from Sigma-Aldrich (St. Louis, Missouri, USA) in accordance with the manufacturer's instructions.

B12, folate and Hcy levels were measured as part of routine blood analysis performed in the United Laboratories of Tartu University Hospital.

Statistical analyses
Correlations were determined by the linear regression model. Statistical analysis was carried out using PASW 18 (SPSS Inc., Chicago, IL, USA).

RESULTS AND DISCUSSION

Biochemical measurements, genotyping and determination of TPMT activity were performed in 154 healthy individuals.

As expected, the results demonstrated significantly higher values of TPMT activity in individuals with wild type TPMT genotype (TPMT*1/1) compared to individuals with heterozygous TPMT genotype (TPMT*3/1) (Fig. 2).

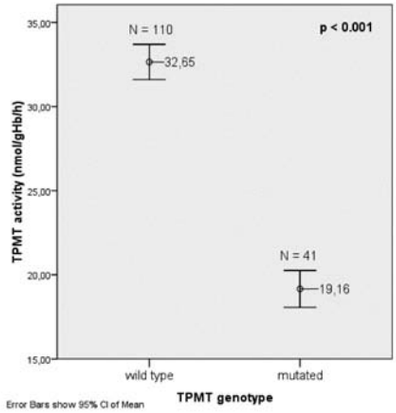

Fig. 2: TPMT activity in individuals with wild type and mutated (heterozygous) TPMT genotype.

Furthermore, the results showed that TPMT activity is influenced not only by TPMT genotype, but also by SAM levels (Fig. 3).

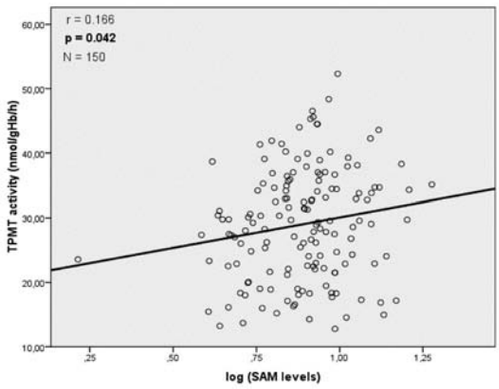

Fig. 3: Correlation between TPMT activity and SAM levels. Hemolysate SAM levels were log-transformed to obtain normal distribution of data. A statistically significant (p=0.042) positive correlation is observed.

In the present set of samples, we could not observe statistically significant correlation between TPMT activity and B12, total folate levels and GSH levels.

CONCLUSIONS

Identifying and understanding the factors influencing TPMT activity are crucial for improving the efficacy and safety of thiopurine therapy. Our study demonstrated that TPMT activity is not influenced by TPMT genotype

alone, but also by SAM levels and therefore indicates SAM as a potential novel biomarker in the individualization of thiopurine therapy.

REFERENCES

1. Milek M, Karas Kuzelicki N, Smid A, et al. S-adenosylmethionine regulates thiopurine methyltransferase activity and decreases 6-mercaptopurine cytotoxicity in MOLT lymphoblasts. Biochem Pharmacol 2009; 77 (12): 1845-53.
2. Karas Kuzelicki N, Milek M, Jazbec J, et al. 5,10-Methylenetetrahydrofolate reductase (MTHFR) low activity genotypes reduce the risk of relapse-related acute lymphoblastic leukemia (ALL). Leuk Res 2009; 33 (10): 1344-8.
3. Karas-Kuzelicki N, Jazbec J, Milek M, et al. Heterozygosity at the TPMT gene locus, augmented by mutated MTHFR gene, predisposes to 6-MP related toxicities in childhood ALL patients. Leukemia 2009; 23 (5): 971-4.
4. Keizer-Garritsen JJ, Brouwer C, Lambooy LH, et al. Measurement of thiopurine S-methyltransferase activity in human blood samples based on high-performance liquid chromatography: reference values in erythrocytes from children. Ann Clin Biochem 2003; 40 (Pt 1): 86-93.
5. Milek M, Murn J, Jaksic Z, et al. Thiopurine S-methyltransferase pharmacogenetics: genotype to phenotype correlation in the Slovenian population. Pharmacology 2006; 77 (3): 105-14.

PENETRATION ENHANCER CONTAINING VESICLES (PEVS) FOR DERMAL DELIVERY OF LIDOCAINE

M. Chessa[1], M. Manconi[1], C. Caddeo[1], C. Celia[2], S. Lampis[3], C. Sinico, A.M. Fadda[1*]

[1] Dept. Farmaco Chimico Tecnologico, University of Cagliari, Via Ospedale 72, 09124 Cagliari, Italy, [2] Dept. Scienze Biofarmacologiche, Faculty of Pharmacy, University "Magna Grecia" Catanzaro, Italy, [3] Dept. Scienze Chimiche, University of Cagliari, ss 554, bivio Sestu, 09042 Monserrato (CA), Italy

INTRODUCTION

The aim of the present study was to develop innovative deformable liposomes for dermal delivery of the local anaesthetic lidocaine (Lid) and to study was the influence of the edge activator structure on the obtained vesicles' properties. Thus, Penetration Enhancer containing Vesicles (PEVs) were prepared by testing five different amphiphilic penetration enhancers as edge activators in the bilayer composition. The penetration enhancers contained the same lipophilic tail (one or more C_8-C_{10} carbon chains), linked to different polar headgroups by an ethereal or estereal linkage.

Lidocaine loading vesicles were prepared by the film hydration method followed by sonication, using a mixture of soy lipids (phosphatidylcholine, phosphatidyl ethanolamine, fatty acids and triglycerides; Phospholipon® 50, P50) as the main bilayer component. Vesicles were thoroughly characterized and tested in *ex vivo* permeation experiments through new born pig skin.

MATERIALS AND METHODS

Materials

Phospholipon®50, mixture of phosphatidyl choline (45%), phosphatidylethanolamine (10-18%), fatty acids and triglycerides, was kindly supplied by Lipoid GmbH (Ludwigshafen, Germany). Oramix CG110 (HLB 16; Or) was from Seppic (Milan, Italy); Labrasol® (HLB 14; Labr), Labrafac™ PG (HLB 2; LabPG), and Labrafac™ CC (HLB 1; LabCC) were a gift from Gattefossè (Saint Priest, France). Lidocaine and all the other products were of analytical grade and were purchased from Sigma-Aldrich (Milan, Italy).

Vesicles preparation and characterization

Multilamellar vesicles (MLVs) were prepared by the thin film method using P50 (60 mg/ml), PE (6mg/ml) and Lid (25 mg/ml). Unilamellar vesicles (UVs) were prepared by sonication of MLVs for 3 minutes using a Soniprep 150 apparatus (MSE, Crowley). Each drug-loaded vesicle suspension was purified from free drug by exhaustive dialysis. Loaded Lid was quantified by HPLC after disruption of vesicles with Triton X-100. Vesicle dispersions were characterized in terms of morphology, size distribution, zeta potential value, and loading capacity by using transmission electron microscopy, dynamic laser light scattering, and HPLC. Vesicle stability was evaluated by a TurbiScan Lab® Expert optical analyzer (Formulaction, France). A detailed investigation of the vesicle structural features, as a function of the components, Lid and PEs, was performed by Small and Wide-Angle X-ray Scattering (SWAXS).

Ex vivo skin permeation studies

Experiments were performed non-occlusively by means of Franz diffusion vertical cells using new-born pig skin. The amount of drug permeated through and deposited into the skin were quantitatively measured. Results are expressed as mean ± standard deviation (6 independent samples).

RESULTS AND DISCUSSION

In previous works, PEVs containing different PEs (transcutol, propylen glycol, Labrasol and Oramix) were prepared and tested as carriers for (trans)dermal delivery of different model drugs (1). PEVs showed to improve dermal delivery of the tested drugs, in comparison with conventional liposomes and commercial formulations. However, PEVs' properties were different and strongly related to the used PE. Therefore, in the present study, Lid loaded vesicles were prepared using different commercially available penetration enhancers with similar chemical structure but different hydrophile/lipophile balance (HLB 1 to 16).

Photon Correlation Spectroscopy results disclosed a small average size (around 150 nm), a narrow size distribution (PI ≈ 0.2), and a negative surface charge ($\zeta \approx$ -50 mV), due to the heterogeneous anionic lipidic fractions in P50 (e.g. fatty acids), which prevented the vesicle aggregation on storage (over a 60-day period at 4 °C) by means of the superficial electrostatic repulsion. The loading capacity (E%) of the vesicles was between 35 and 67%.

The innovative TurbiScan Lab® Expert was used to build up accelerated stability profiles, as it provides early information on destabilization processes occurring in a colloidal suspension (2). Results clearly indicated that no destabilization process occurred, confirming that all the formulations were optimally stable.

The structure and lamellar organization of the vesicle bilayer were investigated by Transmission Electron Microscopy and Small/Wide Angle X-ray Scattering (SWAXS). Whatever the composition of the vesicular dispersion, a diffuse scattering was observed, with low and broad symmetric bump, characteristic for single uncorrelated bilayer of unilamellar vesicles, with the only exception of empty P50 Or-PEVs, whose profile suggested the presence of two populations, uni- and multilamellar vesicles. It is noteworthy that the addition of Lid led to a reduction of lamellarity, suggesting the intercalation of the drug in the phospholipid lamellae.

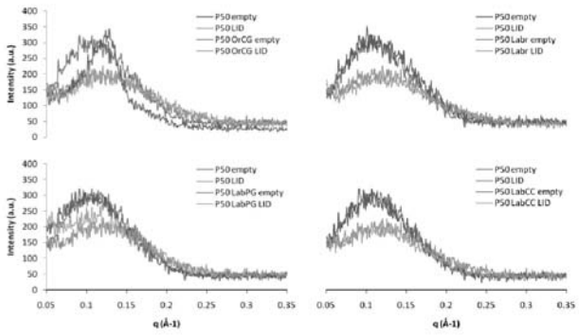

Fig. 1: Small Angle X-ray diffraction (SAXS) patterns of empty or Lid-loaded P50 liposomes and PEVs.

Ex vivo transdermal experiments showed an improved skin deposition of lidocaine when PEVs were used. In particular, PEVs enhanced drug accumulation into stratum corneum and dermis, as compared to

conventional liposomes. Moreover, none of the vesicular preparations were found to determine a systemic drug permeation.

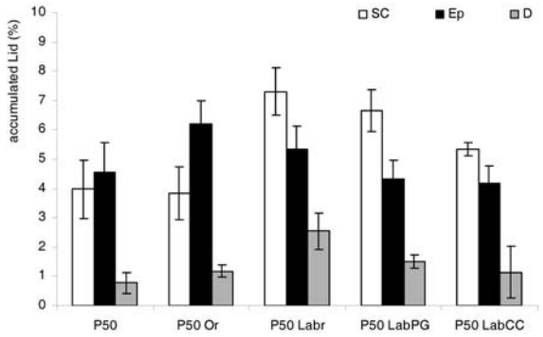

Fig. 2: Lid accumulated into pig skin layers (SC, stratum corneum; Ep, epidermis; D, dermis) after 8-h treatment with P50 vesicles,. Each value is the mean ± S.D. of at least six experimental determinations.

CONCLUSIONS

Results have shown the ability of the tested PEs to give vesicles capable of enhancing Lid dermal delivery. Results have also shown the influence of the used PE on PEVs' properties.

REFERENCES

1. Manconi M, Caddeo C, Sinico C, Valenti D, Mostallino MC, Biggio G, Fadda AM. Eur. J. Pharm. Biopharm. 2011; 78: 27-35.
2. Celia C, Trapasso E, Cosco D, Paolino D, Fresta M. Colloids Surf B Biointerfaces 2009; 72: 155–160.

C16 AND C17-HETEROCYCLE BEARING ANDROSTANES. CYP17 INHIBITION STUDIES AND MULTIPLE EFFECTS ON PROSTATE CANCER CELLS

V. M. Moreira[1,2*], J. A. R. Salvador[2,3], A. Matos Beja[4], J. A. Paixão[4], T. S. Vasaitis[5], V. C. O. Njar[6]

[1] Centro de Química de Coimbra, Faculdade de Ciências e Tecnologia, Universidade de Coimbra, Portugal, [2] Grupo de Química Farmacêutica, Faculdade de Farmácia, Universidade de Coimbra, Portugal, [3] Centro de Neurociências e Biologia Celular, Universidade de Coimbra, Portugal, [4] CEMDRX, Departamento de Física, Faculdade de Ciências e Tecnologia, Universidade de Coimbra, Portugal, [5] Department of Medicine, University of Maryland School of Medicine, Baltimore, MD, USA and Department of Pharmaceutical Sciences, University of Maryland Eastern Shore, Princess Anne, MD, USA, [6] Department of Pharmaceutical Sciences, Jefferson School of Pharmacy, Thomas Jefferson University and Thomas Jefferson University, Kimmel Cancer Center, Philadelphia, USA

INTRODUCTION

Heterocycles are important features of biologically active molecules. Pyrrole, pyrimidine, indole, quinoline and purine are a few classes of heterocycles which have served as platforms for developing pharmaceutical agents for various applications (1). Many important naturally occurring steroids contain one or more heterocyclic ring(s), fused or attached to ring D, formed by modifications of the side chain (2). Moreover, attachment of heterocyclic moieties at diverse positions of the steroid core has provided novel compounds with a diverse range of biological activities including inhibition of cytochrome 17α-hydroxylase-$C_{17,20}$-lyase (CYP17), one of the enzymes involved in androgen biosynthesis in the human body and a valuable target for prostate cancer (PC) treatment (3). Steroidal CYP17 inhibitors bearing *N*-containing heterocyclic moieties linked to the steroid core directly through the nitrogen atom have been shown to have antiandrogenic properties against the androgen-dependent LAPC4 human prostate tumor xenograft, actually being more effective than castration in suppressing its growth (4). We have synthesized and fully characterized C16 and C17 azole-bearing androstanes (5). Some of the C17-substituted compounds were found to inhibit CYP17, bind to the androgen receptor (AR), and block AR-mediated transcription. Moreover, they inhibited the proliferation of LNCaP, PC-3 and LAPC4 cells. The C16-substituted steroids bear privileged heterocyclic moieties attached to C16 via a methine carbon bridge, examples of which, to the best of our knowledge, are non-existent in the literature.

RESULTS AND DISCUSSION

The synthesis of the steroidal C17 2'-methylimidazole derived carbamates **10-18** was based on the reaction of the respective steroidal substrates with 1,1'-carbonylbis(2-methylimidazole) (CBMI), in acetonitrile, at reflux, and was accomplished in high yields (Fig.1).

Compounds **14** and **18** were found to inhibit CYP17 with IC_{50} values of 17.1 and 11.5 mM, respectively. The compounds inhibited mutated-AR mediated transcription at concentrations ranging from 5 to 10 mM.

The Vilsmeier-Hack reaction of the commercially available dehydroepiandrosterone acetate afforded compound **19** which was further reacted with several azoles, in DMF, at reflux, in the presence of K_2CO_3, to afford the 1*H*- and 2*H*-indazoles **21-27** and the *E*/*Z* 16-azolylmethylene-17-oxoandrostanes **28-35** (Fig. 2). The 2*H*-indazole steroids **25-27** inhibited the growth of PC-3 cells in the low micromolar range.

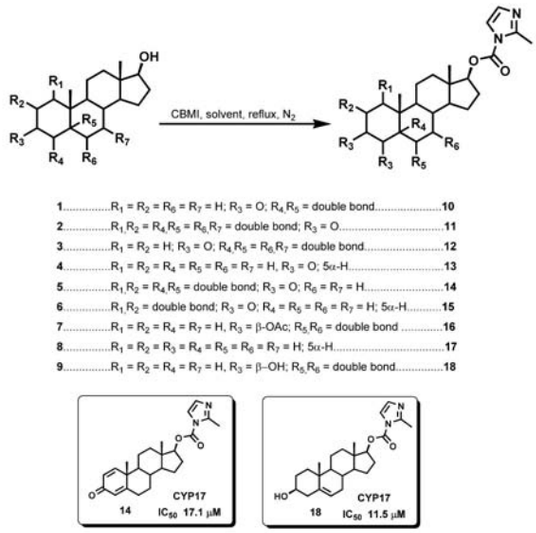

Fig. 1: C17 2'-methylimidazole derived carbamates

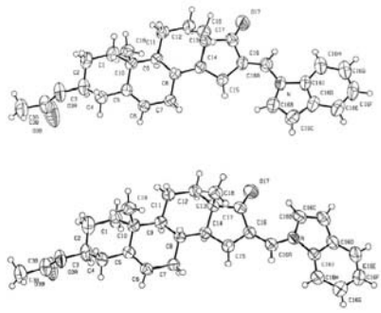

Fig. 2: C16 and C17-azole bearing derivatives

All compounds were fully characterized by 1D and 2D NMR techniques. X-ray diffraction was used to unequivocally assign the *E*/*Z* isomeric pairs (Fig.3).

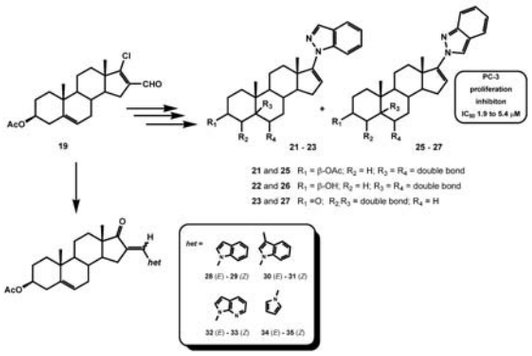

Fig. 3: ORTEP diagram of the E/Z-isomers 28 and 29.

CONCLUSIONS

The synthesis and full structural characterization of C16 and C17-heterocycle bearing androstanes has been accomplished. Some of the compounds inhibited the activity of CYP17, an important target in PC therapy and further demonstrated the ability to block mutated-AR mediated transcription and inhibit the proliferation of PC cell lines. Studies on the biological activities of the novel C16-substituted steroids are ongoing.

ACKNOWLEDGMENTS

Vânia M. Moreira thanks Fundação para a Ciência e a Tecnologia for financial support (SFRH/BD/12508/2003 and SFRH/BPD/45037/2008). Jorge A. R. Salvador thanks Universidade de Coimbra for financial support. Tadas S. Vasaitis was supported in part by US NIH training grant T32 AG000219.

REFERENCES

1. (a) Kidwai M, Venkataramanan R, Mohan R, Sapra P. Cancer chemotherapy and heterocyclic compounds. Curr. Med. Chem. 2002; 9:1209–1228; (b) Preobrazhenskaya M N. Synthesis of heterocyclic medicinal agents at the institute of organic synthesis of the academy of sciences of the Latvian SRR. Chem. Heterocycl. Compd. 1985; 21:13–24.
2. (a) May P M. Comprehensive medicinal chemistry. Oxford: Pergamon Press; 1990. p. 206; (b) Steyn P S, Heerden F R. Bufadienolides of plant and animal origin. Nat. Prod. Rep. 1998; 397–413; (c) Hill R A, Kirk D N, Makin H L J, Murphy G M. Dictionary of steroids. Chapman & Hall; 1991; (d) Takuichi M, Nobuyuki K, Triamcinolone Derivative. JP8073491 (A), 1996.
3. (a) Moreira V M, Salvador J A R, Vasaitis T S, Njar V C. CYP17 inhibitors for prostate cancer treatment – an update. Curr. Med. Chem. 2008; 15:868–99; (b) Vogiatzi P, Claudio PP. Efficacy of abiraterone acetate in post-docetaxel castration-resistant prostate cancer. Expert Rev. Anticancer Ther. 2010; 10:1027–30; (c) Bansal R, Guleria S. Synthesis of 16E-[3-methoxy-4-(2-aminoethoxy)benzylidene]androstene derivatives as potent cytotoxic agents. Steroids 2008; 73:1391–1399.
4. (a) Handratta VD, Vasaitis TS, Njar VC, Gediya LK, Kataria R, Chopra P, et al. Novel C-17-heteroaryl steroidal CYP17 inhibitors/antiandrogens: synthesis, in vitro biological activity, pharmacokinetics, and antitumor activity in the LAPC4 human prostate cancer xenograft model. J. Med. Chem. 2005; 48:2972–2984; (b) Molina A, Belldegrun A. Novel therapeutic strategies for castration resistant prostate cancer. Inhibition of persistent androgen production and androgen receptor mediated signaling. J. Urol. 2011;185:785-794.
5. (a) Moreira VM, Vasaitis TS, Njar VC, Salvador JAR. Synthesis and evaluation of novel 17-indazole androstene derivatives designed as CYP17 inhibitors. Steroids 2007; 72:939–948; (b) ; Moreira VM, Vasaitis TS, Njar VC, Salvador JAR. Synthesis of novel C17 steroidal carbamates. Studies on CYP17 action, androgen receptor binding and function, and prostate cancer cell growth. Steroids 2008; 73:1217-1227; (c) Moreira V M, Salvador J A R, Matos Beja A, Paixão J A. The reaction of azoles with 17-chloro-16-formylandrosta-5,16-dien-3β-yl acetate: Synthesis and structural elucidation of novel 16-azolylmethylene-17-oxoandrostanes. Steroids 2011; 76:582-587.

SYNTHESIS AND ANTIFUNGAL STUDY OF SOME (E) – AND (Z)-4-(ARYLMETHYLENE)-3-ISOCHROMANONES

T. Lóránd[1*], A. Agócs[1], R. Berzaghi[2], J.C. Ribas[2]

[1] Department of Biochemistry and Medicinal Chemistry, University of Pécs, Medical School, Pécs, H-7624 Pécs, Szigeti u. 12, Hungary, [2] Instituto de Biología Funcional y Genómica Edificio Departamental # 222, Campus Miguel de Unamuno, CSIC/Universidad de Salamanca 37007 Salamanca, Spain

INTRODUCTION

Previously we have reported the synthesis of some homoisoflavones as (*E*)-2-(arylmethylene)-1-tetralones, (*E*)-3-(arylmethylene)-4-chromanones and (*E*)-3-(arylmethylene)-1-thiochroman-4-ones. They were screened against human pathogenic yeasts (*Candida spp*.). Some of them showed as high activity as 1.5-6.0 μg/mL (1). An isomeric series, the 4-arylmethylene-3-isochromanones have been prepared by us (2). A second generation of the isochromanones was also synthesized. Our method the solvent free Knoevenagel condensation afforded mostly the *E*- isomer, but the isomeric ratio was highly influenced by the type of aromatic aldehyde. The structure verification was based on ^{1}H NMR, ^{13}C NMR and FT IR methods. With proper choice of the aldehydes we wished to study the structure-activity relationships.

MATERIALS AND METHODS

Materials

The reagents used were purchased from Aldrich Chemical Co. and Fluka and were not further purified. NMR spectra were recorded with ^{UNITY}*INOVA* 400WB (400/100MHz for ^{1}H/^{13}C) spectrometer. Chemical shifts are referenced to Me_4Si (^{1}H) or to the residual solvent signals (^{13}C).
The FT-IR spectra were recorded by an Impact 400 (Nicolet) spectrometer in KBr pellets.

Synthesis - a general procedure for the synthesis of title compounds

A mixture of 3-isochromanone (6.75 mmol), the corresponding aldehyde (6.75 mmol) and five drops of piperidine was stirred at 140 °C under argon for 1 h. The mixture was allowed to cool to room temperature, and the residue was crystallized from ethanol. The products were purified by means of column chromatography.

Antifungal study

The tests have been performed according to literature methods (3-4).

RESULTS AND DISCUSSION

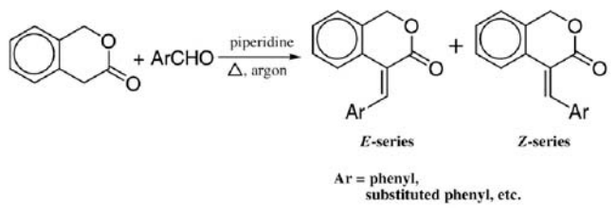

Fig. 1: Synthesis of the title compounds.

The compounds were tested in vivo assays against three fungal species: *S. pombe* (wild type), *S. pombe* (*pbr 1-8*) and *S. pombe* (*pbr 1-6*). The strains that showed sensitivity to some of the compounds were tested for their in vitro GS - β(1-3)glucan synthase - sensitivity.

CONCLUSIONS

The compounds showed only slight antifungal activity, pbr mutants resistant to the known GS antifungals are the sensitive strains to our compounds.

REFERENCES

1. Al-Nakib T M, Lóránd T, Földesi A, Varghese R. The in vitro Antimycotic Activity and Acute Toxicity of Third Generation Benzylidenetetralones and Heteroarylidenetetralones. Med. Print. Pract. 2001; 10: 191-196.
2. Lóránd T, Forgó P, Földesi A, Ősz E, Prókai L. Improved Solvent-free Synthesis and Structure Elucidation of (E)- and (Z)-4-Arylmethylene-3-isochromanones. Eur. J. Org. Chem. 2002; 2996-3003.
3. Perez P, Ribas JC. Cell wall analysis. Methods 2004; 33: 245-251.
4. Martins I, Cortes JCG, Muñoz J, Moreno MB, Ramos M, Clemente-Ramos JA, Duran A, Ribas JC. Differential activities of three families of specific (1,3)glucan synthase inhibitors in wild-type and resistant strains of fission yeast. J. Biol. Chem. 2011; 286: 3484-3496.

DESIGN AND SYNTHESIS OF NEW FLUOROPHORE-NITROXIDE DOUBLE PROBES FOR MEMBRANE SPECTROSCOPY

S. Pajk[1*], M. Garvas[2], J. Štrancar[2] and S. Pečar[1,2]

[1] University of Ljubljana, Faculty of pharmacy, Aškerčeva 7, SI-1000 Ljubljana, [2] Institute Jožef Stefan, Laboratory of biophysics, Jamova cesta 39, SI-1000 Ljubljana

INTRODUCTION

Electron spin resonance (ESR) is commonly employed to study the membrane physical properties that reflect its lateral inhomogeneity (1). A serious drawback of ESR, particularly in its application to cells, is the lack of information on the location of spin probes in the system. Cells comprise many membranes of very different lipid and protein compositions. Because spin probes introduced into the plasma membrane of a cell rapidly undergo spontaneous or catalyzed flip-flop, followed by redistribution to other intracellular membranes, the resulting ESR spectra comprise the superimposition of spectra of several membranes (2).

One possible solution is to couple ESR with fluorescence microscopy, a technique that provides real time visualization together with high sensitivity. In order to realize this approach, a double probe, containing nitroxide and fluorophore moieties in the same molecule, is necessary (Fig. 1).

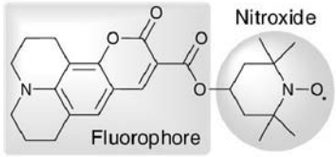

Fig. 1: Example of double nitroxide-fluorophore probe (profluorescent nitroxide).

However, implementation of this idea is hampered by the fact that nitroxides are strong quenchers of fluorescence (3). This phenomenon is exploited by »profluorescent nitroxides«, which are double probes in which the nitroxide serves as a 'molecular switch' that turns on fluorescence intensity by its conversion to a diamagnetic moiety (4).

MATERIALS AND METHODS

Design and synthesis

To overcome the problem of quenching we designed a class of probes in which the fluorophore and nitroxide moieties are as far apart as possible, since contact between the two is a precondition for quenching. Two classes of double probes were made; first based on rhoramine B fluorophore and the second on 7-nitrobenz-2-oxa-1,3-diazol-4-yl (NBD) fluorophore (Fig. 2) (5). Since NBD is more lipophilic than rhodamine B a hydrophilic sugar was inserted between the lipophilic chain bearing the nitroxide and the NBD fluorophore in order to minimize interaction between the two.

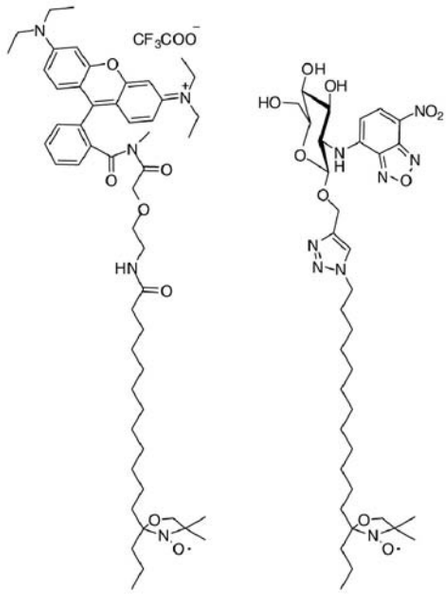

Fig. 2: Examples of double probes based on rhodamine B (left) and NBD (right) fluorophore.

RESULTS AND DISCUSSION

Fluorescence and ESR properties of both classes of probes were studied on liposomes and MCF-7 cells. With both types of probes ESR spectra and corresponding confocal fluorescence images could be obtained in good resolution. However, experiments on MCF-7 cells demonstrated advantageous properties of NBD based double probes over probes based on rhodamine B. Fluorescence microscopy revealed that all NBD based probes we synthesized concentrated specifically in the plasma membrane, with little redistribution to intracellular membranes even after one hour of incubation (Pic. 1.).

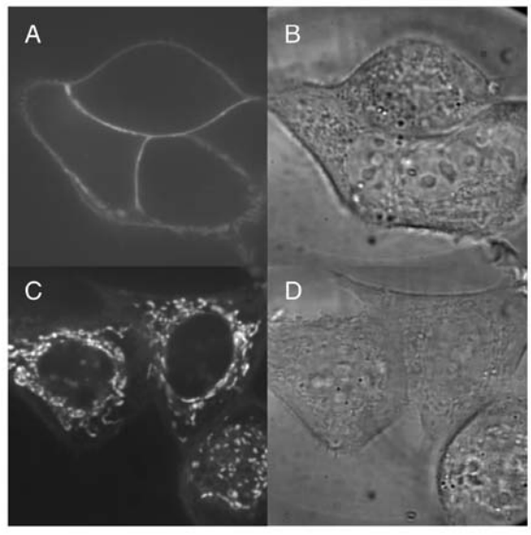

Pic. 1: Confocal fluorescence images (left column) and corresponding bright field images (right column) of MCF-7 cells labelled with NBD based probe (A and B) and rhodamine based probe (C and D).

The preferential localization in plasma membrane should make these probes particularly interesting for research of lipid dynamics and changes that occur during certain cell events e. g. cell signalling.
Because of unique properties of our NBD based probes these were further studied regarding the influence of our design on ESR properties. Tests on liposomes revealed that sugar and NBD moiety have very little influence on the mobility and the ESR signature of probes (Fig. 3.).

Fig. 3: ESR spectra of liposomes labeled with MeFASL(2,11) (a) and NBD based double probe (b).

CONCLUSIONS

We have succeeded in synthesizing new class of double fluorophore-nitroxide probes, based on rhodamine B and NBD fluorophores. Both types of probes and their non-paramagnetic analogues were tested on the MCF-7 cell line by ESR spectroscopy and fluorescence microscopy, providing, for the first time, ESR spectra with corresponding information of the probe's distribution in the cells. Furthermore, early testing on MFC-7 cells showed that our NBD based probes concentrated specifically in plasma membrane with little redistribution to intracellular membranes. Based on these encouraging results, we believe that these double nitroxide-fluorophore probes will open up new possibilities for studying plasma membrane heterogeneity.

REFERENCES

1. Dzikovski B, Freed JH, Begley TP, Membrane Fluidity, John Wiley & Sons, Inc., 2007.
2. Pomorski T, Muller P, Zimmermann B, Burger K, Devaux PF, Herrmann A, Transbilayer movement of fluorescent and spin-labeled phospholipids in the plasma membrane of human fibroblasts: a quantitative approach. J. Cell. Sci. 1996; 109 (Pt 3): 687-698.
3. Likhtenstein GI., Ishii K, Nakatsuji S, Dual chromophore-nitroxides: novel molecular probes, photochemical and magnetic materials. Photochem. Photobiol. 2001; 83(4): 871-881.
4. Likhtenshtein GI, Yamauchi J, Nakatsuji S, Smirnov AI, Tamura R, Nitroxide Spin Probes for Studies of Molecular Dynamics and Microstructure, Wiley-VCH Verlag GmbH & Co. KGaA, 2008.
5. Pajk S, Garvas M, Štrancar J, Pečar S, Nitroxide-fluorophore double probes: a potential tool for studying membrane heterogeneity by ESR and fluorescence. Org. Biomol. Chem. 2011; 9(11): 4150-4159.

ANTIBACTERIAL DRUG THERAPY FOR IMPROVED BURN TREATMENT: LIPOSOMAL HYDROGELS FOR MUPIROCIN

O. Berg[1], J. Hurler[1], N. Škalko-Basnet[*]

Department of Pharmacy, Faculty of Health Sciences, University of Tromsø, Universitetsveinen 57, N-9037 Tromsø, Norway

INTRODUCTION

Trauma to the skin in the form of severe wound, particularly burns, can facilitate colonization of potentially life threatening bacterial infections. To prevent infections of the wounded area, antimicrobial agents are recommended as standard treatment (1). Topical administration of antimicrobial agents, such as mupirocin, can provide local therapy, while avoiding the risks of systemic administration. Mupirocin-in-liposomes-in hydrogels was proposed as advanced delivery system for this purpose. Up to now, no liposomal mupirocin for topical administration has been reported. Hydrogels are one of the most promising wound dressings, and chitosan hydrogels offer additional advantage of chitosan itself having wound healing and antimicrobial properties (2). Mupirocin-containing liposomes incorporated in hydrogels were expected to provide sustained release of incorporated drug, very important feature in improved wound therapy. Moreover, we compared the antimicrobial and drug release characteristics of our newly developed system to marketed product containing mupirocin, namely Bactroban® cream.

MATERIALS AND METHODS

Materials

Mupirocin calcium was kindly provided by GlaxoSmithKline, Zagreb, Croatia and phosphatidylcholine (S-100) was a generous gift from Lipoid, Germany. Chitosan, high molecular weight, was from Sigma-Aldrich Chemistry, St Luis, USA.
Bactroban 2 % (w/w) cream was a product by GlaxoSmithKline, Barnard Castle, UK.
All chemicals used in experiments were of analytical grade. Pig ear skin, was purchased from Nortura, Målselv, Norway.

Methods

Liposomes containing mupirocin were prepared by the modified film method, followed by sonication, and characterized for particle size, polydispersity and encapsulation efficiency (3). Chitosan hydrogels were prepared by the modified method of Cao et al. (4) and liposomes incorporated into hydrogels by hand stirring (5). Liposomal hydrogels were characterized for their textural properties and stability profile on Texture Analyzer TA.XT. (Stable Microsystems, Surrey, UK) as shown in Figure 1.

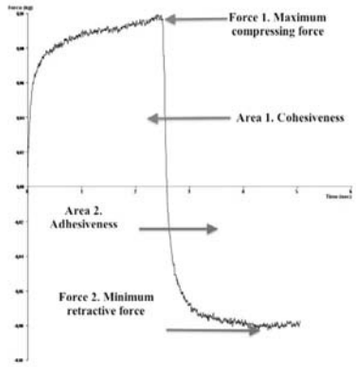

Figure 1: Measured textural properties of hydrogels

All mupirocin formulations were characterized for their antimicrobial properties against *B. subtilis* and *S. aureus* strains.
In vitro and *ex vivo* (pig ear skin) studies were performed on Franz diffusion cells.

RESULTS AND DISCUSSION

MLV liposomes (1 µm) entrapped 74 % of mupirocin, whereas sonicated liposomes (130 nm) contained 49 % of mupirocin, respectively.
Incorporation of liposomes in hydrogels affected original gel cohesiveness and adhesiveness to an acceptable extent. Interestingly, liposomes incorporated in hydrogels were shown to improve the stability of hydrogels, particularly small liposomes.
Microbiological evaluation confirmed antibacterial properties of liposomal hydrogels for mupirocin. The antimicrobial activity was found to correspond to the activity of marketed product.

The drug release profile, in *in vitro* (Table 1) conditions, was found to be depended on the formulation characteristics.

Table 13: Cumulative release profile of mupirocin (n=4)

Type of formulation	Released after 30 min (%)	Released after 7 h (%)	Released after 24 h (%)
gel- N-SL	12.45 ± 2.47	37.65 ± 8.02	43.14 ± 7.41
gel-SL	3.85 ± 0.07	8.89 ± 0.70	9.33 ± 1.23
Bac-cream	5.28 ± 0.89	21.40 ± 3.08	28.62 ± 5.00
d Bac-cream	10.48 ± 1.47	28.94 ± 2.43	42.89 ± 2.66
gel-pg	38.82 ± 1.90	90.46 ± 4.25	90.91 ± 4.57
pg	97.27 ± 1.27	97.33 ± 2.40	100.03 ± 2.34
N-SL	68.79 ± 3.09	103.17 ± 4.11	nd
SL	79.81 ± 5.38	102.09 ± 6.37	nd
gel-N-SL (f+e)	11.04 ± 1.56	32.48 ± 3.00	33.11 ± 2.78

nd= not determined; gels-N-SL= hydrogel with incorporated non-sonicated vesicles; gel-SL= hydrogel with incorporated sonicated vesicles; Bac-cream= Bactroban® cream; d Bac cream= diluted Bactroban cream to the concentration corresponding to liposomal hydrogel concentration of mupirocin; gel-pg= hydrogel containing mupirocin in propylene glycol; pg= mupirocin dissolved in propylene glycol; N-SL= non-sonicated liposomes containing mupirocin; SL= sonicated liposmes containing mupirocin; gel-N-SL (f+e)= hydrogel containing non-sonicated liposomes with unentrapped mupirocin also present in hydrogel.
Mupirocin concentration in all formulations was 505 µg/ml.

Hydrogels clearly prolonged the release of liposomally entrapped mupirocin. The liposomal size was found to affect the release profile of mupirocin (Table 1).
Similar release profiles as observed in the *in vitro* experiments were seen in the experiments on pig ear skin (*ex vivo*).

CONCLUSIONS

We were able to optimize liposomal delivery system for mupirocin destined for wound therapy. By incorporating liposomes-containing mupirocin in chitosan hydrogels, we developed advanced delivery system, with acceptable hydrogel adhesiveness and cohesiveness, and satisfactory stability profile. Microbiological, *in vitro* and *ex vivo* release studies revealed that by manipulating the liposomal characteristics such as vesicle size, it is possible to achieve sustained release of incorporated mupirocin. The comparison with marketed product Bactrocan® cream confirmed the potentials of liposomal hydrogels for mupirocin as promising advanced delivery system in burn therapy.

REFERENCES

1. Frankel, Y.M., Melendez, J.H., Wang, N.Y., Price, L.B., Zenilman, J.M., Lazarus, G.S. Defining wound microbial flora: molecular microbiology opening new horizons. Arch. Dermatol. 2009; 145: 1193-1195.
2. Bhattarai, N., Gunn, J., Zhang M. Chitosan-based hydrogels for controlled, localized drug delivery. Adv. Drug Delivery Rev. 2010; 62: 83-99.
3. di Cagno, M., Styskala J., Hlaváč, J., Brandl, M., Bauer-Brandl, A., Škalko-Basnet, N. Liposomal solubilization of new 3-hydroxy-quinolinone derivatives with promising anticancer activity: a screening method to identify maximum incorporation capacity. J. Liposome Res., 2011, *early online*
4. Cao, Z., Gilbert, R.J., He, W. Simple aragose-chitosan gel composite system for enhanced neuronal growth in three dimensions. Biomacromolecules 2009; 10: 2954-2959.
5. Škalko, N., Čajkovac, M., Jalšenjak, I. Liposomes with metronidazole for topical use: the choice of preparation method and vehicle. J. Liposome Res. 1998; 8: 283-293.

DEVELOPMENT OF "SPONGE-LIKE" DRESSINGS BASED ON CHITOSAN AND HYALURONIC ACID FOR THE DELIVERY OF PLATELET LYSATE TO SKIN WOUNDS

S. Rossi[1], M.C. Bonferoni[1], F. Ferrari[1], G. Sandri[1], C. Del Fante2[1], C. Perotti[2], F. D'Autilia[1], C. Caramella[1*]

[1] Department of Pharmaceutical Sciences, University of Pavia, V.le Taramelli 12, 27100 Pavia, I; [2] Immunohaematology and Transfusion Service and Cell Therapy Unit, Fondazione IRCCS S. Matteo, V.le Golgi, 27100 Pavia, I

INTRODUCTION

Healing of wounds progresses through a series of interdependent and overlapping phases in which cellular and matrix components act together (1). In particular healing is initiated by the secretion in the local environment of a pool of growth factors, cytokines and proteins from the serum and degranulating platelets (2). Platelets constitute a potential source of multiple growth factors and proteins involved in tissue regeneration.
The term platelet lysate (PL) indicates the solution of bioactive molecules obtained by platelet destruction by freeze-thawing usually starting from a platelet rich plasma sample in presence of an anticoagulant agent (3). In the last years chitosan and hyaluronic acid have been demonstrated to improve tissue repairing properties (4, 5). Given these premises, in the present work "sponge-like" dressings based on the combination of PL with chitosan glutamate and hyaluronic acid sodium salt were developed. They were prepared by freeze-drying and characterized for hydration and mechanical properties. Their capability to maintain unaltered PL was assessed by dosing PDGF AB (a representative PL growth factor) by means of ELISA test.

MATERIALS AND METHODS

Materials

Chitosan high MW (MW: 1600 kDA, DD:91% (1568, Giusto Faravelli, Milan, I); Hyaluronic acid sodium salt medium MW (Bioiberica, Barcelona, S); Glutamic acid, Glycine, β-Glycerophosphate (Sigma Chimica, Milan, I). Platelet lysate was prepared from platelet rich plasma obtained from different blood donors.

Dressings without PL (blank samples)

3% (w/w) chitosan glutamate (CSG) and 3% (w/w) sodium hyaluronate (SH) solutions were prepared in distilled water. Glycine (Gly) was added at 2% (w/w) concentration. In the case of CSG solution, pH was adjusted to 6.3 with NaOH 2N. A solution containing CGS 3% (w/w), Gly 2% (w/w) and GP (12% w/w) was also prepared. It was characterized by a pH equal to 6.8. Polymer solutions were diluted 1:1 with saline solution. 4 g of each solution were poured into a plastic cylindrical container (Ø= 40mm), congealed at -40°C overnight and freeze-dried (Heto Dryer, Analitica De Mori, Milan, I) for 24h. "Sponge-like" dressings (40 mm diameter; 5 mm thickness) were hydrated up to 10% water concentration in presence of a saturated NaCl solution.
Hydration properties of dressings were evaluated by means of a modified Enslin apparatus in pH 7.2 phosphate buffer.
Mechanical properties of the dressings were evaluated by means of a tensile apparatus (TAXTplus, ENCO, Spinea, I). In particular, the distance corresponding to the dressing fracture was evaluated.

Dressings loaded with PL

SH /Gly, CGS/Gly, CS /Gly/GP solutions were diluted 1: 1 with PL, congealed and freeze-dried as described in the previous paragraph. Mechanical properties of dressings were evaluated as previously described.
Dressing capability to maintain unaltered PL was assessed by dosing PDGF AB (a representative PL growth factor) by means of ELISA test (6). 300 mg of each polymer solution/PL mixture were freeze-dried and dissolved in 1,9

ml of water and 2 ml of saline solution. The PDGF AB amounts in the dressings were related to the PDGF AB amount in fresh PL. The parameter % PDGF AB was calculated as (PDGF AB amount in the dressings/ PDGF AB amount in fresh PL)*100.

RESULTS AND DISCUSSION

Dressings show different hydration properties: SH/Gly is completely hydrated after 12 min, CSG/Gly maintains its integrity after 6 days and CSG/Gly/GP forms a viscous gel after 24 h (Fig. 1).

For all the dressings the addition of PL produces a decrease in fracture distance, which indicates a decrease in elasticity (Table 1). However, dressings loaded with PL are characterized by distance values higher than 5 mm meaning good elastic properties.

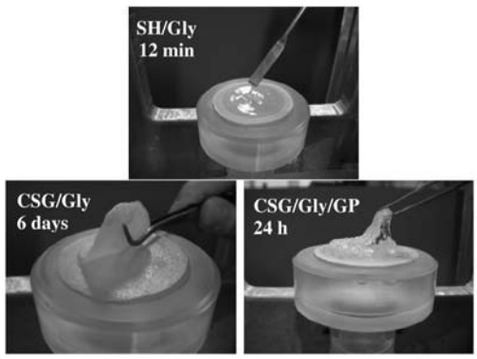

Fig. 1: Pictures of the dressings hydrated with pH 7.2 phosphate buffer.

SH/Gly and CSG/Gly/GP show PDGF AB contents comparable to that of fresh PL (Fig. 2). The lower value observed for CSG/Gly could be due to the low CSG solubility in the saline solution in absence of GP.

Table 1: Fracture distance (mm) observed for the dressings blank and loaded with PL (mean values ± s.e.; n=3)

	SH/Gly	CSG/Gly	CSG/Gly/GP
Blank	16.0 ± 1.0	16.1 ± 0.9	10.5 ± 0.5
Polymer solution/PL 1/1	7.3 ± 0.6	7.6 ± 0.1	5.2 ± 1.2

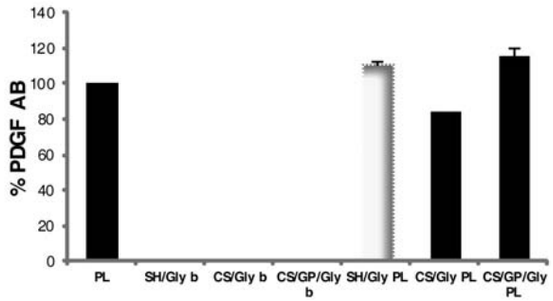

Fig. 2: % PDGF AB obtained for all the dressings (mean values ± s.e.; n=3): b: blank samples; PL: samples loaded with PL.

CONCLUSION

All the dressings show mechanical properties consistent to their application on skin wounds. Depending on their composition, they present different hydration properties that make them suitable for different types of wounds: wet and slight exudative.

Both the polymers employed and the freeze-drying process do not damage the PL growth factors.

REFERENCES

1. Boateng JS, Matthews KH, Stevens HNE, Eccleston GM. Wound healing dressings and drug delivery systems: A review. J. Pharm. Sci. 2008; 97(8): 2892- 2923.
2. Anitua E, Sánchez M, Orive G, Andía I. The potential impact of the preparation rich in growth factors (PRGF) in different medical fields. Biomaterials 2007; 28: 4551-4560.
3. Mazzucco L, Borzini P, Gope R. Platelet-derived factors involved in tissue repair-from signal to function. Transfus Med Rev. 2010; 24: 218-234.
4. Muzzarelli RAA. Chitins and chitosans for the repair of wounded skin, nerve, cartilage and bone. Carbohydrate Polymers 2009; 76: 167-182.
5. Weindl G, Schaller M, Schäfer-Korting M, Korting HC. Hyaluronic acid in the treatment and prevention of skin diseases: molecular biological, pharmaceutical and clinical aspects. Skin Pharmacol Physiol. 2004;17(5): 207-13.
6. Sandri G, Bonferoni MC, Ferrari F, Rossi S, Del Fante C et al. An in situ gelling buccal spray containing platelet lysate for the treatment of oral mucositis. Current Drug Discovery Technology 2011 in press.

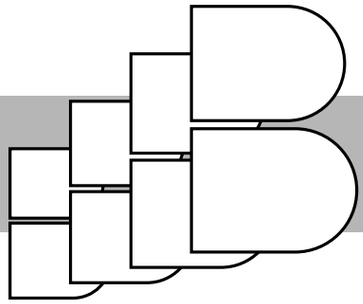

POSTER PRESENTATIONS

DETERMINATION OF URINARY PORPHYRINES IN FAMILIES WITH AUTISTIC MEMBERS

A. France-Štiglic[1*], M. Keržan[2] and J. Osredkar[1]

[1] Clinical Institute of Clinical Chemistry and Biochemistry, University Medical Centre Ljubljana, Njegoševa 4, 1525 Ljubljana, Slovenia; [2] Kobis, d.o.o., Mlakarjeva 26, 1236 Trzin, Slovenia

INTRODUCTION

Autism spectrum disorders (ASD) are pervasive neural developmental disorders with prevalence approximately 9 per 1000 children (1). It is well established that ASD have a strong genetic basis, but there are possible environmental factors that also contribute to ASD such as heavy metals, infections of central neural system, hormones, drugs and other toxins (2).

Emerging evidence support the theory that some ASD cases result from combination of reduced ability to excrete mercury and exposure to mercury at critical developmental periods (3). Mercury in metallic and organic form readily enters all cells, mainly in brain, liver and kidney. In cells it can be easily converted to cationic form and binds to sulfhydryl groups on enzymes and other proteins. In this form it accumulates and remains in the body for a long time. Because of quick mercury shift in cells, its elevated levels in blood and urine remain detectable for only a short period. For this reason some authors propose usage of porphyrin fractions as biological markers to determine toxicological effect of mercury. Porphyrins are derivates of heme synthesis pathway. Blockage of key enzymatic steps, including mercury binding on sulfhydryl groups on these enzymes, results in excess urinary porphyrin excretion and characteristic porphyrin profile with pentacarboxyporphyrin and coproporphyrin elevation (4).

The aim of our study was to investigate concentrations of porphyrin fractions and their profile in spot urine samples of patients with ASD and their first degree relatives. For separation and quantification of urine porphyrin fractions the HPLC technique was used.

MATERIALS AND METHODS

Samples

In our study there were 8 families with at least one autistic member included. Analysis of porphyrins in spot urine samples was performed on 10 ASD family members and on 23 first degree relatives (including parents and siblings). In two of eight families there were two siblings with ASD diagnosis.

Methods

After addition of internal standard to urine samples and centrifugation, separation of porphyrin fractions was performed on a Thermo Scientific Surveyor HPLC (Thermo Fischer Scientific, Waltham, USA) consisted of quaternary low-pressure mixing solvent pump, automatic autosampler, column oven and fluorescence detector with excitation at 394 nm and emission wavelength at 624 nm. Thermostated (30°C) reverse phase column RP 18 (150 x 4,6 mm, 5 µm) and also the Guard column was used.

For separation and porphyrin elution gradient pump was used with two mobile phases. Mobile phase A consisted of methanol (20%) and aqueous buffer (80%), mobile phase B of methanol. For quality control were used ClinChek® Urine controls (Recipe Chemicals + Instruments GmbH, Munich, Germany). Calculation of unknown samples was done by using the external standard method using peak areas.

For normalization of porphyrin fractions urine creatinine values were used. Urine creatinine was measured by a kinetic Jaffé method (Hitachi 917, Hitachi, Tokyo, Japan; reagents from Roche Diagnostics, Mannheim, Germany).

RESULTS AND DISCUSION

After separation there were seen up to six different porphyrin fractions and Internal Standard peak in our chromatogram.

Table 1: Retention times for individual porphyrins

Porphyrin fraction	Retention time (minute)
Uroporphyrin I	5,5
Heptacarboxyporphyrin I	6,7
Hexacarboxyporphyrins	8,1
Internal Standard	9,4
Pentacarboxyporphyrin	10,1
Coproporphyrin I	11,8
Coproporphyrin III	13,0

After separation, concentrations of porphyrin fractions in unknown samples were automatically calculated by calculation unit using the external standard method by comparing peak areas of known samples and according Internal Standard. At the end all porphyrin fraction concentrations were normalized to urine creatinine concentrations.

For evaluation of our results age and gender dependent creatinine adjusted porphyrin values were used as previously published by Woods et al. (5). We found elevated pentacarboxyporphyrin levels in three of eight ASD children (Fig. 1), two of them were siblings and they had also elevated coproporphyrin levels. In a family of third ASD child there was one of six siblings without ASD diagnosis with elevated pentacarboxyporphyrin levels. Other 5 ASD children and 22 first degree relatives had normal pentacarboxyporphyrin values.

Our results are in accordance with a fact that mercury is one of many possible causes that contribute to ASD. In the three cases of ASD with elevated pentacarboxyporphyrin urine levels it is possible that presence of mercury influences the porphyrin pathway to cause characteristically changed urine porphyrin profile. For other ASD cases that have normal pentacarboxyporphyrin levels there are probably different possible environmental factors that contribute to ASD.

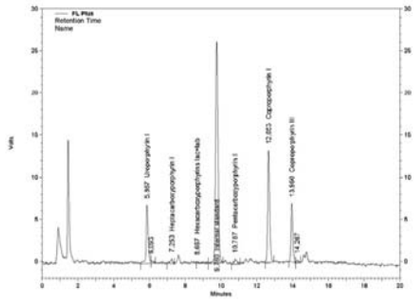

Fig. 1: Urine porphyrin chromatogram of the autistic child where elevated pentacarboxyporphyrin and coproporphyrin levels were found.

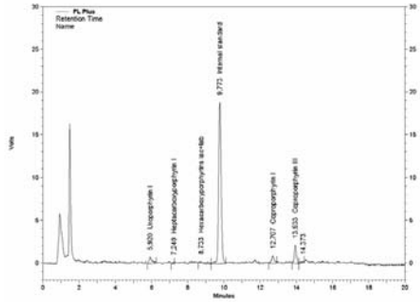

Figure 2: Urine porphyrin chromatogram of the sibling without ASD diagnosis where normal porphyrin levels can be seen.

CONCLUSIONS

Larger study of porphyrins in families with ASD members should be done to confirm our results, possibly with additionally measured mercury and other toxic metals. Other biological markers as urine N-acetyl-β-D-glucosaminidase should also be used.

REFERENCES

1. Centers for Disease Control and Prevention (CDC). Prevalence of autism spectrum disorders - Autism and Developmental Disabilities Monitoring Network, United States, 2006. MMWR Surveill Summ. 2009;58:1-20.
2. Plauche Johnson C, Myers M and the Council on Children With Disabilities. Identification and Evaluation of Children With Autism Spectrum Disorders. Pediatrics. 2007;120:1183-1215.
3. Schultz ST. Does thimerosal or other mercury exposure increase the risk for autism? A review of current literature. Acta Neurobiol Exp (Wars).2010;70:187-95.
4. Geier DA, Geier MR. A prospective assessment of porphyrins in autistic disorders: a potential marker for heavy metal exposure. Neurotox Res. 2006;10:57-64.
5. Woods JS, et al. Urinary porphyrin excretion in normal children and adolescents. Clin Chim Acta. 2009;405:104-9.

SIGNIFICANCE OF S100B PROTEIN DETERMINATION IN DIFFERENTIAL DIAGNOSTICS OF BACTERIAL AND VIRAL MENINGITIS

E. Božnar Alič[1*], A. Jerin[1], M. Jereb[2], J. Osredkar[1]

[1] University Medical Centre Ljubljana, Institute of Clinical Chemistry and Biochemistry, Njegoševa 4, 1525 Ljubljana, Slovenia; [2] University Medical Centre Ljubljana, Department of Infectious Diseases, Japljeva 2, 1000 Ljubljana, Slovenia

INTRODUCTION

S-100 protein is an acid calcium-binding protein synthesized in astroglial cells in all part of the central nervous system (1). In recent years, there have been numerous studies establishing and monitoring the existence of brain damage based on determining the S100B protein biochemical marker in cerebrospinal fluid (CSF) and serum (2, 3, 4,). In the central nervous system the S100B protein is most abundant in astrocytes (5) and after brain damage it is released in CSF and then it passes into systemic circulation in the areas of blood-brain barrier impairment (3, 4). High levels of S100B have been considered as a biomarker that could indicate damage or dysfunction of the central nervous system (5). The purpose of our research was to determine a difference in the S100B protein level in serum and CSF of patients with bacterial and viral meningitis and to establish whether S100B protein concentration is of additional importance for differential diagnosis.

MATERIALS AND METODS

In the prospective study 3 study groups were included: a control group (CG) of patients with no central nervous system infection, a group of patients with tick-borne encephalitis (TBE) confirmed by the demonstration of specific IgM and IgG antibodies in serum samples and a group of patients with bacterial meningitis (BM) confirmed by positive bacterial culture or positive biochemical and cytological criteria (a CSF glucose less than 1.9 mmol/L, a CSF-blood glucose ratio less than 0.23, a CSF protein level greater than 2.2 mmol/L, more than 2000 x 10^6/L CSF
leukocytes, or more than 1180 x 10^6/L polymorphonuclear leukocytes).
The concentration of S-100B protein in CSF and serum were analyzed using a quantitative immunoluminometric assay (Liaison® S100, DiaSorin S.p.A., Saluggia, Italy). The analytical sensitivity of this method was 0,02 µg/L.
Analysis of data was done using SPSS Statistica 17.0 statistical program.

RESULTS AND DISCUSSION

A total of 90 patients were included. 25 patients were diagnosed with bacterial meningitis (median age 55, range 18–85), 35 with tick-borne encephalitis (median age 53, range 15–78) and 30 with no central nervous system infection (median age 51, range 15–77).

Median values of the S100B protein in CSF were 4.21 µg/L (range 1.66–59.00 µg/L) for the bacterial meningitis group, 1.35 µg/L (range 0.67–4.74 µg/L) for tick-borne encephalitis group and 0.85 µg/L (range 0.85–2.21 µg/L) for control group.
All patients with BM had the CSF S100B concentration above cut off value of 1.50 µg/L. 37 % patients with TBE and 10 % patients in the control group had CSF S100B concentration above the cut off value, too. The highest CSF S100B concentration was found in patients with BM and neurological complications and in patients with TBE and meningoencephalitis. With patients having the infection of central nervous system and the S100B protein in cerebrospinal fluid lower than 1.60 µg/L, bacterial infection can be excluded with 100% certainty.
Statistically significant differences in CSF S100B concentration were found between all three groups (TBE/CG $p < 0.001$; BM/CG $p < 0.001$; BM/TBE $p < 0.001$). Concentration of the S100B protein in CSF increased with age in patients with TBE ($p = 0.01$). Increased concentration of S100B protein was in correlation with the increased CSF protein concentration in patients with BM. In the control group increased, CSF S100B concentration was not in correlation with age and routine laboratory parameters.
Median concentration of the S100B protein in the serum of patients with BM was 0.15 µg/L (range 0.04–0.89 µg/L). Patients in the control group had the same median concentration of serum S100B protein than the patients in the TBE group (0.07 µg/L, range 0.03–0.26 for CG and 0.04–0.42 µg/L for TBE group). 48 % patients in the BM group, 20 % patients in the TBE group and 10 % patients in the control group had the serum S100B concentration above the reference value 0.15 µg/L. There were significant differences between the CG and BM group ($p = 0.001$) and TBE and BM group ($p = 0.003$) in serum S100B concentration, but there was no significant difference between the CG and TBE group in S100B concentration in serum ($p = 0.527$). Increased CSF S100B concentration was not in correlation with increased serum S100B concentration in none of our research groups (CG: $p = 0.756$; TBE: $p = 0.309$; BM: $p = 0.309$).

CONCLUSION

The CSF S100B concentration can be used as a biochemical marker to predict more severe form of bacterial and viral meningitis and also as an additional laboratory criterion to distinguish bacterial meningitis from viral meningitis.

REFERENCES

1. Donato R. Functional roles off S100 proteins, calcium-binding proteins of the EF-hand type. Biochemica et Biophysica acta 1999; 1450: 191–231.
2. Gazzolo D, Grutzfeld D, Michetti F, Toesca A, Lituania M, Bruschettini M, Dobrzanska A, Bruschettini P. Increased S100B in Cerebrospinal Fluid of Infants with Bacterial Meningitis: Relationship to Brain Damage and Routine Cerebrospinal Fluid Findings. Clinical Chemistry 2004 50: 941–944.
3. Hamed SA, Hamed AE, Zakary MM. Oxidative Stress and S-100B protein in children with bacterial meningitis. BMC Neurology 2009; 9.
4. Lins H, Wallesch C-W, Wunderlich MT. Sequential analysis of cerebral damage of neurobiochemical markers of cerebral damage in cerebrospinal fluid and serum in CNF infection. Acta Neurol Scand 2005; 112: 303–308.
5. Sindic CJM, Chalon MP, Cambasio CL, Laterre EC, Masson PL. Assessment of damage to the central nervous system by determination of S-100 protein in the cerebrospinal fluid. Journal of Neurology, Neurosurgery, and Psychiatry 1982; 45: 1130–1135.

PPARG PROMOTER POLYMORPHISM IS ASSOCIATED WITH RESPONSIVENESS TO ALENDRONATE TREATMENT IN POSTMENOPAUSAL OSTEOPOROTIC WOMEN

J. Dragojevič[1*], B. Ostanek[1], S. Mencej Bedrač[1], J. Preželj[2], J. Marc[1]

[1] University of Ljubljana, Faculty of Pharmacy, Department of Clinical Biochemistry, Aškerčeva cesta 7, 1000 Ljubljana, Slovenia; [2] University Medical Centre Ljubljana, Department of Endocrinology, Diabetes and Metabolic Diseases, Zaloška cesta 7, 1000 Ljubljana, Slovenia

INTRODUCTION

Osteoporosis is a common skeletal disease characterized by low bone mass and changes of bone micro architecture, caused by the loss of balance between bone resorption by osteoclasts and bone formation by osteoblasts. This results is increased bone fragility and susceptibility to fractures (1). Alendronate is a nitrogen-containing biphosphonate used in osteoporosis treatment and exerts an antiresorptive effect by increasing osteoclast apoptosis. Additionally, an *in vitro* study has shown that alendronate also has an anabolic effect on bone (2). Osteoblasts and adipocytes originate from the common precursor - the mesenchymal stem cell. When human mesenchymal stem cells are treated with alendronate, osteoblastogenesis is induced and adipogenesis is inhibited (2). The main regulator of adipogenesis essential for adipocyte differentiation is the peroxisome-proliferator activated receptor γ (PPARγ). By increasing adipogenesis on account of osteoblastogenesis, PPARγ has been implicated in the pathogenesis of osteoporosis (3). The effect of single nucleotide polymorphisms (SNPs) in the PPARγ coding gene *PPARG* on osteoporosis treatment has not been studied so far. The aim of our preliminary study was to determine whether three SNPs (the promoter rs12497191, Pro12Ala in exon B and His477His in exon 6) influence alendronate treatment in postmenopausal osteoporotic women.

MATERIALS AND METHODS

Patients

Fifty-one postmenopausal women with primary osteoporosis, defined according to WHO criteria (1), were included in the study. None have previously taken any drugs known to influence bone metabolism. All patients received alendronate (10 mg/day), calcium (500 mg/day) and vitamin D (500 IU/day) for one year. The study was approved by the national Medical Ethics Committee of the Republic of Slovenia and written informed consent was obtained.

Bone mineral density (BMD) and biochemical markers of bone turnover

BMD at the lumbar spine (BMD-ls) and total hip (BMD-th) was measured by dual-energy x-ray absorptiometry (QDR-4500, Hologic Inc., Waltham, MA, USA). Biochemical markers of bone turnover plasma osteocalcin, serum bone alkaline phosphatase (BALP) and urine deoxypyridinoline (DPYR) were also measured. All measurements were performed at baseline and after one year of therapy and relative changes were calculated from the data.

Genotyping

DNA was isolated from peripheral blood leukocytes. The rs12497191 SNP was genotyped by high resolution melting analysis with subsequent sequencing of samples representing each of the three possible genotypes. The Pro12Ala and His477His SNPs were genotyped by TaqMan allelic discrimination method.

Statistical analysis

Due to low frequency of mutated homozygotes, subjects were divided into subgroups according to whether they had none or at least one mutated allele. Normality of distribution was checked using Shapiro-Wilk test. Data were analysed using Student's t-test or Mann Whitey test.

RESULTS AND DISCUSSION

Whole study group characteristics are presented in Table 1 and genotype frequencies in Table 2. Genotype subgroups did not differ in age, body mass index (BMI), BMD or biochemical markers of bone turnover at baseline except for His477His CT+TT carriers having lower DPYR than wild-type CC carriers (5.4 vs. 7.6 nmol/mmol creatinine, P=0.014).

Table 1: Whole study group baseline characteristics. Values are means ± SD.

Age (years)	65.4 ± 6.4
BMI (kg/m^2)	26.5 ± 3.7
BMD-th (g/cm^2)	0.738 ± 0.108
BMD-ls (g/cm^2)	0.703 ± 0.074
Osteocalcin (µg/l)	24.2 ± 9.1
BALP (µg/l)	12.5 ± 5.5
DPYR (nmol/mmol creatinine)	7.7 ± 3.6

Table 2: Genotype frequencies of PPARG gene SNPs.

rs12497191	**AA**	**GA**	**GG**
N (%)	31(60.8)	18 (35.3)	2 (3,9)
Pro12Ala	**CC**	**GC**	**GG**
N (%)	34 (66.7)	17 (33.3)	0 (0.0)
His477His	**CC**	**TC**	**CC**
N (%)	38 (74.5)	12 (23.5)	1 (2.0)

Carriers of rs12497191 GA+GG genotype had significantly greater increase of BMD-ls after one year of alendronate treatment (P=0.024) (Fig. 1), suggesting that rs12497191 is associated with responsiveness to alendronate treatment in postmenopausal osteoporosis. G allele was associated with decreased transcriptional activity *in vitro* (4). Decreased transcription of *PPARG* gene could lead to decreased adipogenesis, which could in turn increase osteoblastogenesis. This is in concordance with the greater BMD-ls change in G allele carriers in our study. No associations of rs12497191 with BMD-th or biochemical markers of bone turnover were found.

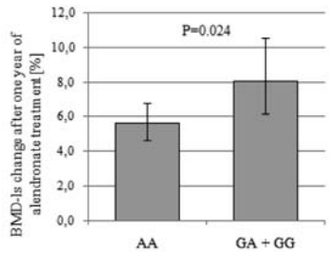

Fig. 1: Influence of rs12497191 genotype on BMD-ls change. Values are geometric means with 95% confidence intervals.

There were no associations between the Pro12Ala or His477His SNPs and changes in BMD or biochemical markers of bone turnover after one year of alendronate treatment, suggesting that Pro12Ala and His477His do not influence alendronate treatment.

CONCLUSIONS

Our preliminary results suggest that the rs12497191 SNP is associated with responsiveness to alendronate treatment in postmenopausal osteoporosis. Our findings need to be confirmed in larger cohorts.

REFERENCES

1. Assessment of fracture risk and its application to screening for postmenopausal osteoporosis. Report of a WHO Study Group. World Health Organ. Tech. Rep. Ser. 1994;843:1-129.
2. Duque G, Rivas D. Alendronate has an anabolic effect on bone through the differentiation of mesenchymal stem cells. J. Bone Miner. Res. 2007; 22 :1603-11
3. Gimble JM, Zvonic S, Floyd ZE, Kassem M. Playing with bone and fat. J. Cell. Biochem. 2006; 98: 251-266
4. Muller YL, Bogardus C, Beamer BA, Shuldiner AR, Baier LJ. A functional variant in the peroxisome proliferator-activated receptor gamma2 promoter is associated with predictors of obesity and type 2 diabetes in Pima Indians. Diabetes. 2003;52:1864-1871.

IMPACT OF LIVE HIGH – TRAIN MIDDLE/LOW TRAINING METHOD ON EPO – SERUM IN ATHLETES

J. Vodičar[1*], M. Vodičar[2], J. Osredkar[3]

[1] Faculty of Sport, Institute of Sport, University of Ljubljana, Gortanova 22, 1000 Ljubljana, Slovenia; [2] University Medical Centre Ljubljana, Orthopaedic clinic, Zaloška cesta 9, 1000 Ljubljana, Slovenia; [3] University Medical Centre Ljubljana, Institute of Clinical Chemistry and Biochemistry, Zaloška cesta 7, 1000 Ljubljana, Slovenia

INTRODUCTION

Many authors have dealt with the effect of high altitude training on athletes' performance. (1) While the results of the studies remain somewhat controversial the current protocol of choice in hypoxic training is live high-train low (2). Question either artificial or natural hypoxia should be the mainstay has also been raised. Artificial hypoxia exerts no atmospheric influences that could lead to different results (3). Our study investigates the impact of a live high – train middle to low training protocol on serum erythropoietin (EPO) levels. We used artificial hypoxia.

MATERIALS AND METHODS

We compared serum concentrations in a group of Slovene cross-country skiers. Upon the protocol they were divided in two groups, first (G2400) slept on the high attitude – 2400 m above see level, while the second group (G1600) slept on 1600 m above see level. Both groups performed the same training protocol of heightened character. Results have been obtained between 8th June 2010 and 6th August 2010. In the G2400 there were 5 competitors with average age 22.0 years; SD=2.35, while in the G1600 group there were 6 competitors aged 20.8; SD=3.19. Determination of serum EPO was performed with ELISA method.

RESULTS AND DISCUSSION

We show a change of EPO levels for seven training sessions for both groups. Comparably, the EPO levels in the group G2400 were higher than in the group G1600 throughout all seven sessions of the training period. In the group G1600 the EPO concentrations have even decreased throughout the training period in all seven training sessions.

Table 1: EPO serum concentrations in the training period for group G1600

G1600	training 1	training 2	training 3	training 4	training 5	training 6	training 7
comp. 1	23,8	15,2	14,5	20,5	17,7	13,3	12,2
comp. 2		24,7	16,9	13,5	17,6	14,1	
comp. 3	25,4	19,8	14,2	16,3	9,2	20,1	13,5
comp. 4	18,3	14,5	17,9	14,1	11,4	15,9	11,8
comp. 5	26,4	17,7	20,5	20,9	14,4	15,0	16,3
comp. 6	30,2	24,5	22,3	28,6	17,6	22,3	15,4
average	24,8	19,4	17,7	19,0	14,6	16,8	13,8
min	18,3	14,5	14,2	13,5	9,2	13,3	11,8
max	30,2	24,7	22,3	28,6	17,7	22,3	16,3
STD	4,3	4,4	3,2	5,6	3,7	3,6	2,0

Table 2: EPO serum concentrations in the training period for group G2400

G2400	training 1	training 2	training 3	training 4	training 5	training 6	training 7
comp. 1	22,7	34,3	23,3	16,0	9,7	17,1	15,0
comp. 2	34,0	35,3	26,3	27,1	13,7	27,8	24,6
comp. 3	18,3	11,4	32,6	12,9	4,8		11,3
comp. 4	16,2		17,7	9,5	4,4	10,6	12,8
comp. 5	24,1	25,7	23,4	29,3	30,4	23,7	18,2
average	23,1	26,7	24,7	19,0	12,6	19,8	16,4
min	16,2	11,4	17,7	9,5	4,4	10,6	11,3
max	34,0	35,3	32,6	29,3	30,4	27,8	24,6
STD	6,9	11,1	5,4	8,8	10,7	7,6	5,3

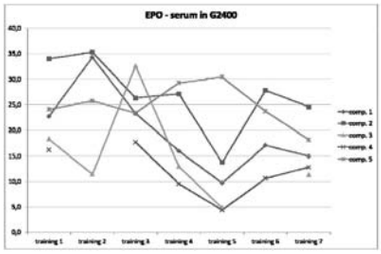

Fig. 1: EPO serum concentrations in the training period for group G2400

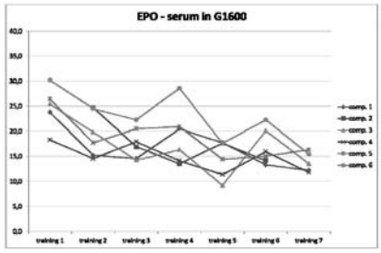

Fig. 2: EPO serum concentrations in the training period for group G1600

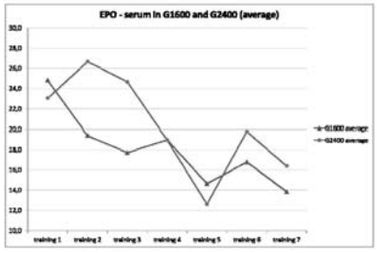

Fig. 3: Comparison of average EPO serum concentrations between the two groups

CONCLUSIONS

EPO concentrations rose at the beginning of training and later by increasing the intensity of training and time of training gradually declined. All measured values were higher in the group G2400 than in the group G1600. The increments of EPO serum concentration are very individual. These conclusions lead toward a need for more detailed protocols on different altitudes and individualization of protocols to be athletes' fit.

REFERENCES

1. de Paula P, Niebauer J, Effects of high altitude training on exercise capacity: fact or myth, Sleep Breath. 2010 Nov 26.
2. Stray-Gundersen J, Chapman RF, Levine BD, "Living high-training low" altitude training improves sea level performance in male and female elite runners, J Appl Physiol, 2001 Sep;91(3):1113-20.
3. Levine BD, Stray-Gundersen J, Dose-response of altitude training: how much altitude is enough?, Adv Exp Med Biol, 2006;588:233-47.

THE +4845G>T AND +12534G>A IN IL1A GENE ARE IN COMPLETE LINKAGE DISEQULIBRIUM IN SLOVENIAN POPULATION AND NOT ASSOCIATED WITH INCREASED EXPRESSION OF IL1A GENE IN OSTEOPOROSIS

J. Zupan[1*], F. Vindišar[2], R. Komadina[2], J. Preželj[3], J. Marc[1]

[1] University of Ljubljana, Faculty of Pharmacy, Aškerčeva cesta 7, 1000 Ljubljana, Slovenia; [2] General hospital Celje, Department of Traumatology, Oblakova 5, 1000 Ljubljana, Slovenia; [3] University Medical Centre Ljubljana, Department of Endocrinology and Metabolic Diseases, Zaloška 7, 1000 Ljubljana, Slovenia

INTRODUCTION

With the advantage of the new field of osteoimmunology, evidence on the role of inflammation in pathogenesis of osteoporosis (OP) is increasing. Various pro-inflammatory cytokines have been classified as either osteoclastogenic or anti-osteoclastogenic, regarding their stimulatory or inhibitory effect on bone resorbing cells, osteoclasts.

Among osteoclastogenic cytokines, interleukin 1α (IL-1α) has been proposed in the pathogenesis of OP. Clinical studies, performed on peripheral blood cells have led to contradictory results, indicating that production of IL-1α occurs in bone microenvironment (1). Studies on the influence of various genetic variants in IL-1α gene IL1A on decreased bone mineral density (BMD) in OP and rheumatiod arthritis have produced opposing outcomes (2, 3). Our results in human OP and osteoarthritic (OA) human bone tissue have shown almost 5-fold higher expression of IL1A in OP (submitted for publication), which is in accordance with inversely related BMD phenotype observed in this two bone diseases.

Based on these findings, the aim of our current study was to find out, whether two single nucleotide polymorphisms, +4845G>T (rs17561) located in exon 5 and +12534G>A (rs2071375) in intron 6 of the IL1A, influence the expression of IL-1α gene, BMD and the risk of OP fractures in Slovenian patients.

SUBJECTS AND METHODS

Patients

72 elderly Slovenian people, 53 women and 19 men from General Hospital Celje were included. OP group consisted of 49 patients with medically confirmed OP fracture. In the OA group, 23 patients undergoing hemi or total hip arthroplasty, because of OA were included.

BMD measurement

BMD at the lumbar spine (L2-L4) BMD-ls, total hip BMD-hip and femoral neck BMD-fn were measured by dual-energy X-ray absorptiometry (DXA) (QDR-4500, Hologic, Inc., Waltham, MA, USA).

+4845G>T and +12534G>A genotyping

Both SNPs were genotyped using real-time polymerase chain reaction (PCR) in combination with TaqMan allele discrimination assays (C__9546471_10 and C__1839911_10, Applied BioSystems Foster, CA, USA). The PCR reaction mix of 6.0 µL comprised of 10 ng of DNA sample, 1.2 µL of 5x HOT FIREPol Probe qPCR Mix Plus no ROX (Solis BioDyne, Tartu, Estonia), 0.15 µL of 40x TaqMan® assay and 3.65 µL of highly purified water. Real-time PCR was carried out using standard protocol on the LightCycler 480 (Hoffmann-La Roche, Basel, Switzerland) and endpoint genotyping program was used to call genotypes.

Statistical analysis

Hardy-Weinberg equilibrium was calculated. The genotype, haplotype and allele frequencies between OP and OA patients were compared using chi-square or Fisher's exact probability test. The degree of linkage disequilibrium (LD) was calculated using EMLD (4). PHASE was used to estimate haplotypes (5). The effect of genotypes and haplotypes on gene expression and BMD was evaluated by Kruskal-Wallis test, while the presence of specific allele (one or two copies versus none) on these variables was assessed with Mann-Whitney U tests. The effect of SNPs on fracture risk was examined by logistic regression analysis. Models included alleles (no allele or combined group of one or two alleles under the study), age (in years) and body mass index (BMI, in kg/m^2) as variables. The significance threshold was set at 0.05. For the statistical analysis SPSS 18.0 (IBM, Chicago, IL, USA) was used.

RESULTS AND DISCUSSION

Characteristics of the patients and the results of genotyping analysis are shown in Table 1 and Table 2, respectively.

The genotype frequency distributions for both SNPs were in Hardy-Weinberg equilibrium. There were no differences in genotype, haplotype or allele distribution between men and women and between OP and OA patients.

Table 1: Patients' characteristics. Values are medians (25th;75th percentile).*p < 0.05.

	OP N = 49	**OA N = 23**
Age (years)	70 (76;78)	72 (71;75)
Sex (women/men)	35/14	18/5
Body mass index (kg/m^2)	**24.9 (23.4 ; 28.4)**	**27.6 (26.6 ; 30.1)***
BMD-hip (g/cm^2)	**0.703 (0.644 ; 0.764)**	**0.852 (0.779 ; 0.987)***
BMD-fn (g/cm^2)	**0.621 (0.574 ; 0.677)**	**0.742 (0.637 ; 0.832)***
BMD-ls (g/cm^2)	**0.871 (0.776 ; 0.945)**	**0.952 (0.795 ; 1.137)***

In Slovenian population, evidence of strong LD between both polymorphisms (D' = 0.99, r^2 = 0.99) was confirmed. PHASE analysis disclosed TA and GG as haplotypes with the highest frequencies (0.24 and 0.76, respectively).

Table 2: Frequency distributions of +4845G>T and +12534G>A.

		OP N = 49	**OA N = 23**
+4845G>T +12534G>A	**GG/GG**	27 (55.1)	13 (56.5)
	GT/GA	20 (40.8)	9 (39.1)
	TT/AA	2 (4.1)	1 (4.3)
Haplotype GG/TA (%)	**no GG/two TA**	2 (4.1)	1 (4.3)
	one GG/TA	20 (40.8)	9 (39.1)
	two GG/no TA	27 (55.1)	13 (56.5)
Allele GG (%)	**no allele GG**	2 (4.1)	1 (4.3)
	one or both allele GG	47 (95.9)	22 (95.7)
Allele TA (%)	**no allele TA**	27 (55.1)	13 (56.5)
	one or both allele TA	22 (44.9)	10 (43.5)

For assessing the influence of the studied SNPs on expression of IL1A, data on IL1A gene expression in 23 OP and 31 OA human bone tissue, from our previous study was used. No significant associations with IL1A gene expression and consequently BMD and the risk of OP fractures were found. Our results thus indicate that genetic variants +4845G>T and +12534G>A in IL1A gene are not responsible for higher expression of IL1A in OP bone tissue.

As limitations of our study include relatively small groups of patients and comparisons with OA patients, the replication of the study analyzing only one of the studied SNPs in larger groups, including healthy controls is suggested.

REFERENCES

1. Khosla S, Peterson JM, Egan K, Jones JD, Riggs BL. Circulating cytokine levels in osteoporotic and normal women. J Clin Endocrinol Metab 1994;79(3):707-711.
2. Knudsen S, Harslof T, Husted LB, Carstens M, Stenkjaer L, Langdahl BL. The effect of interleukin-1alpha polymorphisms on bone mineral density and the risk of vertebral fractures. Calcif Tissue Int 2007;80(1):21-30.
3. Kobayashi T, Ito S, Kuroda T, Yamamoto K, Sugita N, Narita I, Sumida T, Gejyo F, Yoshie H. The interleukin-1 and Fcgamma receptor gene polymorphisms in Japanese patients with rheumatoid arthritis and periodontitis. J Periodontol 2007;78(12):2311-2318.
4. https://cge.mdanderson.org/~qhuang/Software/pub.htm Access date: May 2011.
5. Stephens M, Smith NJ, Donnelly P. A new statistical method for haplotype reconstruction from population data. Am J Hum Genet 2001;68(4):978-989.

ACQUIRED POLYSPECIFICITY AND AUTOIMMUNE REACTIVITY OF HUMAN IMMUNOGLOBULINS DURING PURIFICATION PROCEDURE

J. Omersel[1*], U. Žager[2], T. Kveder[2], B. Božič[1,2]

[1] University of Ljubljana, Faculty of Pharmacy, Aškerčeva cesta 7, 1000 Ljubljana, Slovenia; [2] University Medical Centre, Division of Internal Medicine, Vodnikova 62, 1000 Ljubljana, Slovenia

INTRODUCTION

The complexity of antibody production and purification methods remains demanding task not only for large scale monoclonal production but as well for basic research of antibody molecule characteristics and laboratory sample handling (1). Many studies report the heterogeneous effect of solvents, especially acidic pH, on immunoglobulin structure, usually associated with partial denaturation, increased accessibility of hydrophobic amino acids and alternative folding states (2). Acidic environment, usually in affinity chromatography approach, seems to be related to specific structural modification, affecting antibody's biological activity through altered effector functions or binding characteristics (3,4).

The aim of the study was to compare the immunoglobulin yield after various column desorbing conditions and to analyze the influence of acidic pH on IgG fraction reactivity towards autoantigens, involved in autoimmune diseases - β_2-glycoprotein I, cardiolipin and cyclic citrullinated peptide.

MATERIALS AND METHODS

Materials

Seven sera samples were tested on a spectrum of autoimmune reactivities. Five samples confirmed to be negative on anti-cardiolipin (aCL), anti-β_2-glycoprotein I (aβ_2-GPI), antinuclear antibody and to anti-cyclic citrullinated peptide reactivity (aCCP). Two sera were diagnosed as low positive in aCL titre.

Time Dependent Influence of Low pH on Serum Specificity

Sera were exposed to acetic acid at pH=2.4, 3.3, 5.2 for 1, 2, 5, 10, and 15 min. Before sampling and analyzing, neutralization was done with 1M Tris.

IgG Isolation

50 polyclonal IgG fractions were isolated out of 7 sera by affinity chromatography following the original protocol or using different elution conditions: a) With ImmunoPure (G) IgG Purification Kit (Pierce Biotechnology, IL) IgG fraction was desorbed from the column with original elution buffer (pH=2.8) or acetic acid buffer pH=2.4, 3.0, and 3.5 and immediately adjusted to the physiological pH by neutralization with 1M Tris. b) Using MabTrapTM Kit (Amersham, GE Healthcare, UK), IgG fraction was desorbed with glycine-HCl (pH=2.7) and neutralized as before. All fractions were desalted to PBS (150 mM, pH=7.4).

Total protein Estimation

The amount of recovered IgGs was determined with Camspec M501 Single Beam UV/VIS Spectrophotometer, (Camspec Ltd., UK), using the extinction coefficient of 14.0 for 1% IgG solution.

Electrophoresis

The purity and integrity of desalted IgGs were assessed by sodium dodecyl sulfate-polyacrylamide gel electrophoresis (7.5%) (SDS-PAGE).

Analysis of Autoantibody Specificity

Non-treated sera, acid treated sera, and isolated IgG fractions eluted at different pHs were tested by aCL (˝in house˝), aβ_2-GPI (˝in house˝), and commercial aCCP (Euro-Diagnostica Am, Sweden) ELISA methods.

RESULTS AND DISCUSSION

IgG fractions desorbed from the column with various pH showed high and comparable antibody purity, confirmed by an intensive band at 150 kDa on SDS-PAGE gel, indicating the presence of polyclonal IgGs (5).

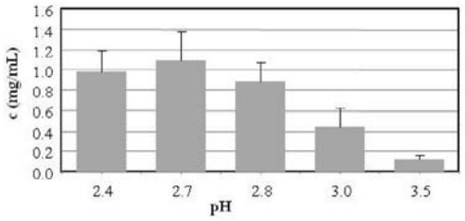

Fig. 1: The influence of elution pH on the amount of recovered IgGs. Data are presented as average concentration of recovered IgGs ±SD.

The highest yield was obtained by low pH elution (2.4-2.8) (Fig 1) which provided sufficient disruption of charged and polar interactions between protein G and antibody's Fc region. However, compared to glycine-HCl buffer, acidic acid buffer (pH=2.4) significantly altered immunoreactivity of IgG fraction, isolated from healthy blood donors.

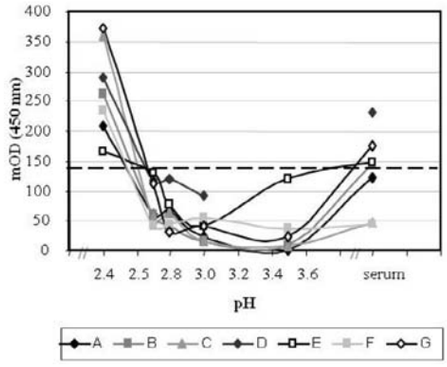

Fig. 2: Effect of the elution buffer's pH on changes in immunoreactivity of IgG fractions in aCL ELISA compared to their original sera. Dashed line indicates minimal mOD (mili Optical Density) for positive samples.

Increased reactivity resulted in clinically significant titers on aCL and aCCP ELISA (Fig 2), indicating on presence of antibodies with specificities towards autoantigens.

Similar results, pH and incubation time dependant increase of immunoreactivity on aCL, were observed also after incubation of whole serum with acetic acid buffer (Fig 3).

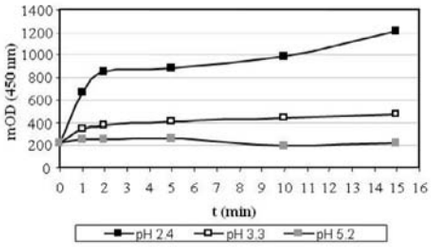

Fig. 3: Time dependent immunoreactivity alterations after exposure of sera to different pH of acetic acid.

CONCLUSIONS

Polyreactivity, manifested by the affinity purification procedure as a result of low pH, could therefore be presented as an expected consequence of a limited immunoglobulin denaturation during production/purification methods.

Or, it may be an additional explanation for uncontrolled alteration of antibody specificity *in vivo,* at locally established denaturating (acidic) microenvironment.

REFERENCES

1. Sharma VK, Chih HN, Lu P, An Z, Chin CN. The Formulation and Delivery of Monoclonal Antibodies, In: An Z (Ed.), Therapeutic Monoclonal Antibodies: From Bench to Clinic, 2009, Jon Wiley&Sons, Inc., Hoboken, New Yersey, pp. 675-710.
2. Buchner J, Renner M, Lilie H, Hinz HJ, Jaenicke R et al. Alternatively folded states of an immunoglobulin. Biochemistry. 1991; 30(28): 6922-6929.
3. Narhi LO, Caughey DJ, Horan T, Kita Y, Chang D et al. Effect of three elution buffers on the recovery and structure of monoclonal antibodies. Anal Biochem. 1997; 253(2): 236-245.
4. Bergmann-Leitner E, Mease RM, Duncan EH, Khan F, Waitumbi J et al. Evaluation of immunoglobulin purification methods and their impact on quality and yield of antigen-specific antibodies. Malaria Journal 2008; 7(1):129.
5. Omersel J, Žager U, Kveder T, Božič B. Alteration of antibody specificity during isolation and storage. J. Immunoass. Immunochem. 2010; 1(31):45-59.

EVALUATION OF ARSENIC TRIOXIDE-INDUCED APOPTOSIS IN PRIMARY MULTIPLE MYELOMA CELLS

K. Reberšek*, U. Turnšek, P. Černelč, H. Podgornik

University Medical Centre Ljubljana, Zaloška cesta 2, 1000 Ljubljana

INTRODUCTION

Multiple myeloma (MM) is a clonal B-cell malignancy characterized by clonal expansion of plasma cells in the bone marrow. The uncontrolled growth of myeloma cells has many consequences, including skeletal destruction due to uncoupled bone metabolism, bone marrow failure, suppression of normal immunoglobulin production, and renal insufficiency (1). Due to heterogeneous pattern of bone marrow plasma cell infiltration in MM, an alternative to conventional morphology for quantification and detection of abnormal plasma cells is multiparameter flow cytometry. Basic panel of antibodies directed against CD38, CD138, CD45, CD56, CD19 for the detection of abnormal plasma cells can be upgraded with antibodies directed against CD20, CD117 and CD28 (2). MM cells are characterized by a profound genetic instability resulting in a complex set of numerical and structural chromosomal abnormalities, e.g. partial deletions of 13q, 17p, 1p and 6q, chromosomal translocations involving the immunoglobulin heavy chain locus (14q32), and amplifications of 1q and 15q (3). MM which accounts for approximately 10% of all hematologic cancers remains incurable disease. Advances in treatment are only effective in palliating the disease and prolonging survival. Therefore, it is essential to provide patients with additional therapeutic options. Arsenic trioxide (ATO) is effective in the treatment of patients with acute promyelocytic leukaemia (1). In addition, ATO shows promising results in MM cell lines (4). In this study, the extent of apoptosis induced by ATO in 27 primary MM samples was measured and analysed. Comparison of the extent of apoptosis and cytogenetics, and immunophenotype was analyzed.

MATERIALS AND METHODS

Bone marrow specimens from newly diagnosed MM patients were obtained after informed consent. Cells were incubated with 2 μM or 5 μM ATO for 24 hours. Cells incubated with camptothecin, a known inductor of apoptosis (5), represented a positive control, while those cells with nothing added served as a negative control. Erythrocytes in primary bone marrow samples were lysed using a solution of NH_4Cl. The cells were then incubated with CD38 and CD138 antibodies. The extent of apoptosis was evaluated by flow cytometry using annexin V and propidium iodide (PI). Both subpopulations, annexin V^+/PI^- and annexin V^+/PI^+ were considered as apoptotic, as described previously (1). Statistical evaluation of the extent of apoptosis was conducted using one-way RM ANOVA. The extent of apoptosis was compared with cytogenetics, and immunophenotype using two-way ANOVA. Results were considered statistically significant if the p value was less than 0.05.

RESULTS AND DISCUSSION

In attempt to measure the extent of apoptosis specifically on MM plasma cells antibodies against CD38 and CD138 were applied. Furthermore, as cell debris attaches antibodies as well, a specific gating strategy was applied, i.e. the annexin/propidium iodide histogram was gated on that part of CD38/CD138-positive population (population A, Figure 1a) that did not include cell debris (population I, Figure 1b); A and not I (Figure 1c).

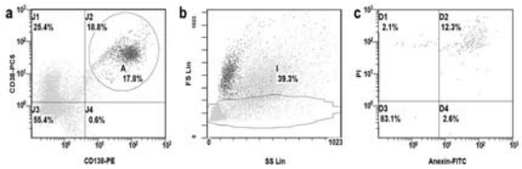

Fig. 1: Specific gating strategy. CD38/CD138-positive population (population A, Figure 1a). Cell debris (population I, Figure 1b). The annexin/propidium iodide histogram gated on CD38/CD138-positive population excluding cell debris (Figure 1c); A and not I.

Using such modified approach, the extent of apoptosis was measured in 27 newly diagnosed MM patients. The extent of apoptosis for 2 μM ATO was above the control in most of the cases studied (19 out of 27), but the difference did not reach statistical significance. In contrast, the extent of apoptosis for 5 μM ATO, and camptothecin was significantly higher than the control ($p<0.05$), and the value for 2 μM ATO ($p<0.05$). The extent of apoptosis for camptothecin was higher than the extent of apoptosis for 5 μM ATO in most of the studied cases (21 out of 27), but did not reach statistical significance. The extent of necrosis for 2 μM ATO was significantly higher than the extent of necrosis for 5 μM ATO. The extent of necrosis did not reach statistical significance for other treatment groups. Since cell debris was excluded from the analysis, it is possible that 5 μM ATO and camptothecin caused higher extent of necrosis in comparison to 2 μM ATO, and that the process of necrosis was completed before our detection. Furthermore, results demonstrated that in cases with low extent of apoptosis, the extent of necrosis was present in greater extent. There are two possible explanations. The simple one is that the process of apoptosis has already completed before our detection. According second, functional explanation we can speculate that patients' response to ATO treatment can differ. The apoptosis is the leading process in some of patients while in others necrosis is the leading process. It should be stressed that in 27 diagnostic cases studied we did not find non-responders to ATO treatment.

Comparison of the extent of apoptosis with cytogenetics, and MM cell immunophenotype showed significantly higher extent of apoptosis for CD28-negative cases in comparison to CD28-positive cases for 5 μM ATO (p=0,041). Furthermore, significantly higher extent of apoptosis for del(13)-positive cases in comparison to del(13)-negative cases for camptothecin was observed (p=0,005). Comparison of other groups did not show statistical significance.

CONCLUSIONS

This study demonstrates that ATO is effective apoptosis inductor in MM plasma cells obtained directly from MM patients. This suggests a potential role of ATO in therapeutic management of MM patients. In addition, we can conclude that aberrant expression of CD28 on MM plasma cells has influence on susceptibility of MM plasma cells to ATO-induced apoptosis.

REFERENCES

1. Ge F, Lu XP, Zeng HL, He QY, Xiong S et al. Proteomic and functional analysis reveal a dual molecular mechanism underlying arsenic-induced apoptosis in human multiple myeloma cells. J. Proteome Res. 2009; 8: 3006-3019.
2. Rawstron AC, Orfao A, Beksac M, Bezdickova L, Broolmans RA et al. Report of the European Myeloma Network on multiparametric flow cytometry in multiple myeloma and related disorders. Haematologica 2008: 93: 431-438.
3. Mohamed AN, Bentley G, Bonnett ML, Zonder J, Al-Katib A. Chromosome aberrations in a series of 120 multiple myeloma cases with abnormal karyotypes. Am. J. Hematol. 2007; 82: 1080-1087.
4. Hayashi T, Hideshima T, Akiyama M, Richardson P, Schlossman RL et al. Arsenic trioxide inhibits growth of human multiple myeloma cells in the bone marrow microenvironment. Mol. Cancer Ther. 2002; 1: 851-860.
5. Smolewski P, Grabarek J, Lee BW, Johnson GL, Darzynkiewicz Z. Kinetics of HL-60 cell entry to apoptosis during treatment with TNF-α or camptothecin assayed by the stathmo-apoptosis method. Cytometry 2002; 47: 143-149.

HIGH CONCENTRATIONS PROTEIN S100B IN SERUM PREDICTS MORTALITY AFTER TRAUMATIC BRAIN INJURY

L. Krnjak[1*], P. Gradišek[2], S. Herman[3], M. Koršič[4], J. Osredkar[1]

[1] Clinical Institute of Clinical Chemistry and Clinical Biochemistry, University Medical Centre, Ljubljana, Slovenia; [2] 2Clinical Department of Anaesthesiology and Intensive Therapy, Centre for Intensive Therapy, Surgery Division, University Medical Centre, Ljubljana, Slovenia, [3] Department of Traumatology, Surgery Division, University Medical Centre, Ljubljana, Slovenia, [4] Department of Neurosurgery, Surgery Division, University Medical Centre, Ljubljana, Slovenia

INTRODUCTION

The number of brain injuries is increasing year after year. Every year 1.5 million people die worldwide, while millions of victims seek emergency aid following accidental brain injury (1). Brain injury ranks third as the cause of death in Slovenia. Slovenia's 2006 Statistical Yearbook puts the incidence of all accidental injuries in Slovenia at around 322 per 100,000 people (2). Mortality from mild head injury is low (between 0.04 and 0.29%) and occurs as a result of internal bleeding (3). Mortality following severe accidental head injury is estimated from 20 to 30%, and survivor disability at 50% (4). The S100B protein is a sensitive biochemical marker for brain damage. The literature indicates that the separate analysis of the S100A1B and S100BB subunits does not have any advantages compared to measuring total S100B (5). In our study, we attempted to determine what time is the best predictor of death following accidental head injury by measuring the concentrations of the S100B protein and its subunit S100BB.

MATERIALS AND METHODS

A prospective, longitudinal, observational clinical study was conducted on 70 head injury patients. The study included 30 patients with severe head injury, 2 patients with moderate head injury and 38 patients with mild head injury. The confidentiality of personal data was protected in accordance with the law governing personal data protection. The study proposal was also approved by the Medical Ethics Commission at the Ministry of Health. Blood samples were taken immediately on admission and 6 hours, 12 hours, 24 hours, 48 hours and 72 hours following injury.

RESULTS AND DISCUSSION

In the injury victims that did not survive, we monitored the dynamics of S100B concentrations following head injury from admission to hospital until 72 hours. In the 12 non-survivors the concentration of S100B protein was 2.0 μg/L at admission, 4.86 μg/L after 6 hours, 5.92 μg/L after 12 hours and 6.48 μg/L after 24 hours ($p < 0.05$). After 48 and 72 hours, the concentrations were still above 2 μg/L, but these values cannot be taken into account as we did not have data for all those that died. In the 12 non-survivors, the protein S100B concentrations peaked 24 hours after the injury. The increase in the concentration of S100B in the first 24 hours was greater in the non-survivors. In monitoring the dynamics of S100BB concentrations in those that did not survive head injury from admission to 72 hours, we observed that the concentrations increased until 24 hours. The subsequent S100BB values cannot be taken into account because we had insufficient data for S100BB. Elevated concentrations of S100B and S100BB were observed in both survivors and non-survivors. The higher the concentration of S100B, the lower the rate of survival (Figure 1).

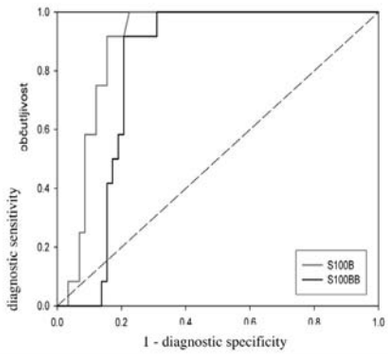

Fig. 1: ROC survival curve for the S100B and S100BB values at admission.

By contrast, the higher the concentration of S100BB, the higher rate of survival. S10BB evidently has a greater protective effect than S100B, or it is possible that S100BB acts protectively.

In our study, 12 patients died, including 2 patients with mild head injury and 10 patients with severe brain injury. In the patients that did not survive, the S100B concentrations were 3 times as high as in the patients who survived. The S100B concentrations in the patients who did not survive were marginally statistically significant when compared with the concentrations in the surviving patients ($p = 0.056$). Our results show that a higher concentration of S100B indicates lower survival (Figure 1). By contrast, a higher concentration of S100BB means higher survival. We observed higher concentrations in the surviving patients than in the non-survivors. Perhaps a subunit of S100BB has a protective effect on the cell (Table 1).

Table 1: S100B and S100BB concentrations at admission in the surviving and non-surviving patients

	S100B (μg/L)	SE	S100B (μg/L)	SE	N
Survivors	0.73	0.23	0.68	0.29	58
Non-survivors	2.05	0.53	0.20	0.06	12

Values: Mean value and SE (standard error), N-number of patients

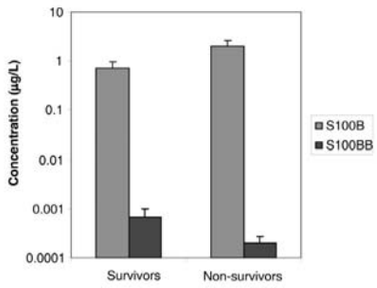

Fig. 2: S100B and S100BB concentrations at admission in the survivors and non-survivors

A broader study is needed to confirm its usefulness for the prognosis of survival.

REFERENCES

1. Fleminger S, Ponsford J. Long term outcome after traumatic brain injury. BMJ. 2005; 331:1419–20. doi: 10.1136/bmj.331.7530.1419.
2. 2006 Medical Statistical Yearbook of Slovenia (Zdravstveni statistični letopis, Slovenija 2006.) Ljubljana: National Institute of Public Health; 2008.
3. Klauber MR, Marshall LF, Luerssen TG et al. determinants of head injury mortality: importance of the low risk patient. Neurosurgery 1989; 24:31–36.
4. Traumatic brain injury in the United States: an epidemiologic overview. Mt Sinai J Med 2009; 76: 105–10.
5. Nylén K, Ost M, Csajbok LZ, Nilsson I, Hall C, Blennow K, Nellgård B, Rosengren L. Serum levels of S100B, S100A1B and S100BB are all related to outcome after severe traumatic brain injury. Acta Neurochir (Wien). 2008;150:221–7.

EXPRESSION OF PITUITARY TUMOR TRANSFORMING GENE 1 (PTTG1) IN MULTIPLE MYELOMA PATIENTS

M. J. Mandelc Mazaj*, P. Černelč, H. Podgornik

University Medical Centre Ljubljana, Zaloška 7, 1000 Ljubljana, Slovenia

INTRODUCTION

Multiple myeloma (MM) is a B-cell malignancy characterized by a clonal proliferation of plasma cells in the bone marrow. A significant prognostic factor in MM is cytogenetics. The most frequent chromosomal abnormalities are loss of chromosome 13, IgH translocations, deletion 17p13 (the locus for the tumor suppressor gene p53), chromosome 1 abnormalities (1p deletion and 1q amplification), 15q abnormalities, 12p deletions and hyperdiploidy. Generally, almost all chromosomal abnormalities, particularly IgH translocations are associated with more aggressive clinical features and shorter survival. The exception is t(11;14) and hyperdiploidy which are associated with a favorable outcome (1). Besides genetics, different new prognostic factors have been tested to better predict treatment outcome.

Recently, a study have focused on expression of human pituitary tumor transforming gene 1 (*PTTG1)* in multiple myeloma cells. *PTTG1* is a protooncogene and a potential cancer biomarker, which was first described by Pei and Melmed in 1997 (2,3). *PTTG1* is located on chromosome 5 and encodes a 22-kDa securin protein. It is highly expressed in various tumors including pituitary, thyroid, colon, ovary, testis, lung, and breast (4). It has been shown to play an important control role in mitosis. PTTG1 regulates sister chromatide separation by binding to separase, and preventing cohesin cleavage. Overexpression of PTTG1 leads to chromosome instability and aneuploidy.

PTTG1 is also involved in cell cycle regulation, DNA repair and transactivation. It regulates bFGF secretion, promotes tumor angiogenesis, and inhibits p53 transcriptional activity. p53 stabilization is also uncoupled by loss of PTTG1 (5).

The aim of this study was to investigate the expression of PTTG1 by immunofluorescence in plasmocytoma cells from multiple myeloma patients.

MATERIALS AND METHODS

Samples

Bone marrow cells of 17 MM patients were short time cultivated (24 h) in complete Marrowmax growth medium (Gibco). After cell's harvesting (1 x 10^7 cells) cytospin slides were prepared using a centrifuge. Dehydrated slides were stored at -20°C. Bone marrow samples containing less than 2% of plasma cells used as a negative control.

Immunofluorescence staining

Cytospin slides were thawed, rehydrated in ethanoles of decreasing concentration and washed by phosphate-buffered saline (PBS). Cells were fixed in 2% formaldehyde, permeabilized with 0.1% Triton X-100, and blocked in blocking buffer (5% normal goat serum in PBS). Cells were then incubated with primary antibody rabbit anti-PTTG-1 ((1:100), Invitrogen) in 1 % normal goat serum in PBS for 1 h at 37°C in a humidified chamber. After washing a secondary antibody Alexa Fluor goat anti-rabbit IgG (H+L) with green fluorescence ((1:500), Invitrogen) was applied for 1 h at 37°C. After PBS washing nuclei were counterstained with 4',6-diamidino-2-phenylindole (DAPI). Slides were evaluated using a fluorescence microscope.

RESULTS AND DISCUSSION

Figure 1A shows representative bone marrow sample of multiple myeloma patient after PTTG1 immunostaining. A high cytoplasmic expression of PTTG1 was observed in MM cells while there was no expression of PTTG1 in other bone marrow cells. Cytomorphology of the stained cells corresponded well to plasmocytoma cells considering the size and position of nucleus (eccentric) and abundant cytoplasm. Immunostaining of bone marrow without infiltration with plasma cells (control) didn't give any flourescence (1B).

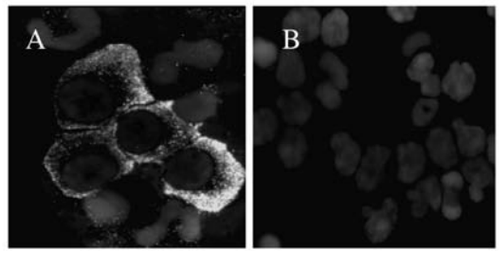

Fig. 1: A) Expression of PTTG1 (green) in cytoplasm of multiple myeloma cells. B) PTTG1 staining of bone marrow cells from a control group (autofluorescence is shown in red colour).

Samples differed in intensity as well as in localization of PTTG1 antibody fluorescence. Regarding intensity, we evaluated slides semi quantitatively as absent (Figure 1B), weak (Figure 2B), moderate (Figure 2C), or intensive (Figure 2A). In cases of intensive fluorescence it was mainly located in cytoplasm (Figure 1A, 2A). In some cases, fluorescence was concentrated on the cell membrane (Figure 2B).

Preliminary data suggest that the difference in intensity and localization of PTTG1 expression may be due to different MM cells cytogenetics (Fig. 2). PTTG1 expression in patients with different cytogenetic abnormalities should be analysed in future.

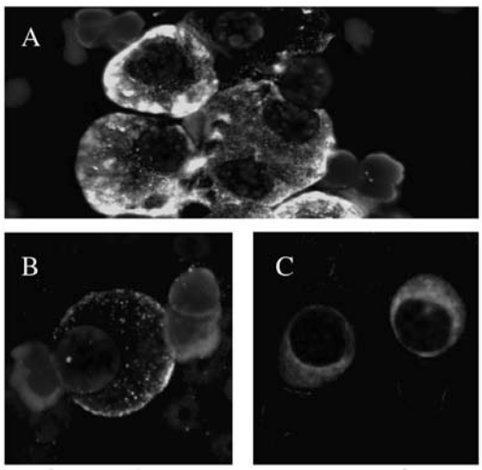

Fig. 2: Expression of PTTG1 in MM cells of multiple myeloma patient A) Intensive cytoplasmic expression in MM cells with del(13). B) Membrane expression in MM cell with del(6q). C) Nuclear membrane expression in MM patient with del(13) and amplified signals for MAF.

CONCLUSIONS

Our data confirmed expression of PTTG1 in cytoplasm, on cell membrane and also on nuclear membrane of MM cells. PTTG1 expression in bone marrow was limited to multiple myeloma cells.

PTTG1 expression was different regarding its intensity and localization in samples of different MM patients. Since we assume that intensity of expression of PTTG1 correlates with tumour invasiveness, we intend to compare a specific PTTG1 expression with one of the most important prognostic factor, namely cytogenetics.

REFERENCES

1. R Fonseca, PL Bergsagel, et al. International Myeloma Working Group molecular classification of multiple myeloma: spotlight review. Leukemia. 2009; 23: 2210–2221.
2. F. Salehi, K. Kovacs et al. Pituitary tumor-transforming gene in endocrine and other neoplasms: a review and update. Endocrine-Related Cancer. 2008; 15: 721–743.
3. Y. Tong, S. Melmed. PTTG1 as a biomarker for cancer treatment, U.S. Patent US 2011/0009473A1, 13, 2011.
4. M. Chiriva-Internati, R. Ferrari, et al. The pituitary tumor transforming gene 1 (PTTG-1): An immunological target for multiple myeloma. J Translat Med 2008, 6: 15.
5. G. Vlotides, T. Eigler et al. Pituitary Tumor-Transforming Gene: Physiology and Implications for Tumorigenesis. Endocrine Rev. 2007; 28:165–186.

SERUM BIOMARKERS IN ISCHEMIC NEUROLOGICAL COMPLICATIONS

M. Skitek*, A. Jerin

Institute of Clinical Chemistry and Biochemistry, University Medical Centre Ljubljana, Slovenia

INTRODUCTION

During the last few years several biomarkers have been proposed to predict and diagnose brain injury (1). Ischemic stroke is associated with variety pathophysiological changes affecting glial and neuronal brain changes (2). Several recently published reports have described tissue-protective nonhematological effects of recombinant human erythropoietin (rHuEpo) that could have potential protective effects on ischemia-induced tissue damage in several organs (3).

The goal of present study was to determine whether molecular brain biomarkers could identify an acute ischemic brain injury following cardiopulmonary bypass (CPB) in patients treated with rHuEpo versus control, and whether molecular biomarkers are consistent with magnetic resonance imaging (MRI) findings.

MATERIALS AND METHODS

20 consecutive patients were divided in two groups: group of 10 patients received rHuEpo and control group. Neurological complications were monitoring by measuring serum concentrations of N-methil-D-aspartate (NMDA) receptors antibodies (NR2Ab), protein S100B and neuron-specific enolase (NSE) before and in the first 5 days after surgery, comparing neurological outcome with MRI.

Concentration of protein S100B and NSE was measured using automated immunoassay with luminometric detection (reagents and analyser Liaison, DiaSorin, Saluggia, Italy). NR2Ab concentrations were determined by ELISA (reagent Gold Dot-1, CIS-Biotech Inc, GA, USA; instrument Personal Lab™, Adaltis, Italy). All samples were measured in one batch.

Lower level of detection was 0.02 µg/L (S-100B), 0.04 µg/L (NSE) and 0.5 AU (NR2Ab). Reference value was set at 0.2 for S100B, 18.3 for NSE and 2.0 µg/L (1.4 AU) for NR2Ab according to 95 percentile of the "healthy" population and declaration of manufacturer.

RESULTS AND DISCUSSION

The erythropoietin-treated and control group was comparable with respect to serum NR2Ab, S100B (before and after operation) and NSE (before operation) according to comparable study clinical outcome such as coronary artery bypass grafts, operative time, transfusion volume and blood pressure values at all stages of operation. The significant difference is shown for the postoperative NSE (p=0.026), but all levels were bellow reference value of 18.3 µg/L (Table 1).

Table 1: Comparison of serum preoperative (pre) and postoperative (post) median concentrations of biomarkers of the erythropoietin-treated (Epo) and control group by Mann-Whitney test (10 patients of each group).

Parameter (µg/L)	Epo	Control	p
pre S100B	0.090	0.085	0.362
Q1- Q3	0.065 – 0.108	0.065 – 0.095	
post S100B	0.290	0.310	0.773
Q1- Q3	0.200 – 0.405	0.215 – 0.345	
pre NSE	8.00	8.75	0.934
Q1- Q3	7.025 - 9.63	6.25 – 9.60	
post NSE	**16.20**	**11.00**	**0.026**
Q1- Q3	**10.70 – 19.23**	**9.15 – 14.00**	
pre NR2Ab	1.99	2.34	0.364
Q1- Q3	1.53 – 2.73	1.74 – 4.32	
post NR2Ab	1.36	1.67	0.563
Q1- Q3	1.24 – 2.40	1.30 – 2.74	

The comparison between MRI results, neurological outcome and brain ischemia/injury biomarkers proved interesting finding especially regarding nontreated control group, where we observed postoperative fresh ischemic lesions in 4 of 10 patients without rHuEpo therapy. Two of them had lesions larger than 5 mm and experienced delirium (cerebrovascular insult). In both patients the preNR2Ab levels were above 6.0 µg/L (3 times reference value of 2.0 µg/L). Comparison of serum concentrations of biomarkers of 16 patients without brain ischemia and 4 patients with acute ischemia regardless erythropoietin therapy proved significant difference for postoperative NR2Ab (p=0.016) and near significant difference for preoperative NR2Ab (p=0.057). Both concentrations of NR2Ab (pre&post) were in average about 2 times higher in ischemic patients (Table 2).

Table 2: Comparison of serum preoperative (pre) and postoperative (post) median concentrations of biomarkers of 4 patients with (ISCH) and 16 patients without brain ischemia (NOISCH) regardless erythropoietin therapy.

Parameter	(µg/L)	NOISCH	ISCH p
pre S100B	0.090	0.085	0.547
Q1- Q3	0.063 – 0.100	0.065 – 0.095	
post S100B	0.290	0.310	0.803
Q1- Q3	0.200 -0.388	0.230 – 0.335	
pre NSE	8.00	8.75	0.764
Q1- Q3	6.48 – 9.88	7.30 – 9.55	
post NSE	15.00	12.85	0.424
Q1- Q3	10.03 – 18.48	10.80 – 14.00	
pre NR2Ab	1.99	4.32	0.057
Q1- Q3	1.52 – 2.36	2.20 – 6.37	
post NR2Ab	**1.36**	**2.74**	**0.016**
Q1- Q3	**1.16 – 2.19**	**2.18 – 2.88**	

Diagnostic accuracy proved high sensitivity, specificity and negative predictive value for the pre&post NR2Ab serum concentrations (Table 3).

Table 3: Sensitivity (sens) and specificity (spec) in optimal cut-off values of NR2Ab serum preoperative (pre) and postoperative (post) concentrations (> 2.38 µg/L and > 2.51 µg/L) of 4 patients with and 16 patients without brain ischemia.

	Sens	Spec	+LR	-LR	+PV	-PV
pre NR2Ab	75.0	80.0	3.75	0.31	48.4	92.8
post NR2Ab	75.0	93.3	11.2	0.27	73.8	93.7

The use of brain biomarkers is helpful because it can show injury that cannot otherwise be appreciated by imaging (4). The results reported here suggest the possibility of a neuroprotective effect of rHuEpo when administered to patient in the perioperative period of cardiac surgery. Whereas NR2Ab may be a marker of cerebral ischemia, S100B and NSE are considered the markers of blood-brain barrier (BBB) dysfunction. Ischemic stroke is usually accompanied with BBB dysfunction, but BBB dysfunction is not necessarily indicative of cerebral ischemia.

The erythropoietin-treated and control group was comparable with respect to serum biomarkers, the significant difference is shown only for the postoperative NSE. Comparison of 16 patients without and 4 patients with acute brain ischemia regardless erythropoietin therapy proved significant difference only for the postoperative NR2Ab.

CONCLUSIONS

Our results regarding diagnostic value of pre- and postoperative NR2Ab levels and brain protection with rHuEpo are very promising. Patients known to be at increased risk pre- and postoperatively may benefit from medical intervention. The analysis of serum concentrations of glial-neuronal tissue derived proteins might be promising strategy to monitor acute ischemic brain injury. Evaluation of alternative molecular biomarkers to reliably identify ischemic brain injury in this population would be useful (5).

REFERENCES

1. Maas MB, Furie KL. Molecular biomarkers in stroke diagnosis and prognosis. Biomark Med. 2009;3:363-383.
2. Herrmann M, Ehrenreich H. Brain derived proteins as markers of acute stroke: their relation to pathophysiology outcome prediction and neuroprotective drug monitoring. Restor Neurol and Neurosci. 2003;3-4:177-190.
3. Xiong Y, chopp M, Lee CP. Erythropoietin improves brain mitochondrial function in rats after traumatic brain injury. Neurol Res. 2009;31:496-502.
4. Laskowitz DT, Kasner SE, Saver J, Remmel KS, Jauch EC. Clinical usefulness of a biomarker-based diagnostic test for acute stroke the biomarker rapid assessment in ischemic injury (BRAIN) study. Stroke. 2009;40:77-85
5. Saenger AK, Christenson RH. Stroke Biomarkers: Progress and challenges for diagnosis, prognosis, differentiation, and treatment. Clin Chem. 2010; 56:21-33.

ESTIMATING RENAL FUNCTION FOR DRUG DOSING ADJUSTMENTS

P. Meško Brguljan[1*], M. Sabotin[1,2], A. Mrhar[2]

[1] University Clinic for respiratory Diseases and Allergy Golnik, Clinical Chemistry Department, Golnik 36, 4204 Golnik Slovenia; [2] Faculty of Pharmacy, Aškerčeva 5, 1000 Ljubljana, Slovenia

INTRODUCTION

For many drugs is adviced to adjust the dose for patients with reduced renal function. A simplistic model would indicate that if drug is removed from the body by renal filtration and the GFR is reduced, then the drug may accumulate in the blood producing a greater chance of toxicity. There are however many other changes that occour in kidney disease other than reduced GFR which can affect drug clearance (1). In order to adjust the dose of renally excreted drugs, it is necessary to estimate glomerular filtration rate (GFR) of the patient. Usually this has been done by the measurement of creatinine clearance (ECC), but the inconvenience of a timed urine collection, failure to collect the entire specimen and the wide within-subject variability, restrict the usefulness of this method (2). The National Kidney Foundation Disease Outocomes Quality Initiative (K-DOQI) recommended use of estimates of GFR calculated from prediction equations based on plasma or serum creatinine (3). Usually Cockroft and Gault (C&G) equation (4) have been used. C&G equation has many limitations, among them also the requirement for weight and height, which restricted the possibilities to report the estimates by the laboratory (2).

The aim of this study was to check the usefulness of the new quantitative formulas for estimation of GFR in drug dosage adjustment. Among them the MDRD (Modification of Diet in Renal Disease) estimates of GFR has become available on clinical chemistry laboratory reports in Slovenia (5), together with ordered examination of creatinine in serum.

MATERIALS AND METHODS

Data were collected prospectively. eGFR values were calculated for patients admitted to hospital using abbreviated MDRD equation. Severely malnourished patients, amputees, patients with muscle dystrophy or incontinence were excluded from the study. Creatinine clearance measurements (ECC) from 24-hour collected urine was performed in the case of eGFR < 60 mL/min/1,73 m^2 and when possible. Unappropriatelly collected daily urine samples have been excluded from the study. Data from 72 patients (M(38); F(34); age=74±10) were used in statistic analyses. Drug dosing regimen before, during and after hospitalization were followed. The study was focused on main renally cleared drugs. Reference values for drug dosage adjustment were took from Summary of Product Characteristics.

Serum creatinine determinations have been performed using kinetic Jaffe reaction, rate-blanked and compensated on a Roche/Hitachi 912 analyzer (Roche Diagnostics). The method is standardized to Isotope Dilution Mass Spectrometry (IDMS) method. Urine creatinine determinations have been performed on the Roche/Hitachi 912 analyzer using the same method and calibrator as in serum.

Table 1: Calculation formulas used in the study (S, U-$_{Cr}$- creatinine in serum or urine (µmol/L); LBM – lean body mass (kg), BSA – body size area (m^2), t – time of urine collection (min), V_{dU} volume of collected urine (ml)).

ECC (mL/min)=$(U_{Cr} \times V_{dU})/(S_{Cr\text{-}2} \times t)$
GFR (MDRD) (mL/min) = $175 \times (S_{Cr} / 88{,}4)^{-1{,}154} \times (age)^{-0{,}203} \times (0{,}742$ if female)× BSA/1,73 m^2
Cl_{cr} C&G (mL/min) = $((140 - age) \times BM)/(0{,}814 \times S_{Cr}) \times (0{,}85$ if female)
Cl_{cr} C&G(LBM) (mL/min) = $((140 - age) \times LBM)/(0{,}814 \times S_{Cr}) \times (0{,}85$ if female)
eGFR (mL/min/1,73 m^2) = result (mL/min) × 1,73 m^2/BSA

Statistical analyses were performed using SPSS 15.0 and Microsoft Office Excell.

RESULTS AND DISCUSSION

Reciprocal values of S_{cr} showed the lowest correlation with ECC (0,714). Equation based GFR estimations showed high correlations with ECC (C&G (0,786), MDRD (0,829), C&G(LBM) (0,833); p<0,01). Fisher's z-test of correlation coefficients comparison between different eGFR determinations and ECC shown that no equation is superior.

Distributions of patients into two GFR intervals (>60 mL/min, <60 mL/min) showed no statistically significant difference comparing ECC distribution with distribution according to MDRD and C&G equation (p(MDRD)=0,18; p(C&G)=0,38; α=0,05). The difference was statistically significant comparing ECC with C&G(LBM) distribution ($p=4,4*10^{-6}$; α=0,05). Frequency of necessity of drug dosage adjustment according to 4 different GFR determinations was: ECC(10), C&G(9), MDRD(7).

CONCLUSIONS

There is need to estimate GFR for drug adjustment dosage. Recognition of renal function as a prescribing issue is more important than the precision of different estimates of renal function. When drug product information for prescribers includes dosing advice for renal impairment, it is important to know the method of renal impairment determination in the particular case of product information if a patient's dose has to be reviewed (8). The most practical is the use of estimates of GFR according to MDRD formula, reported from the laboratories, but this has limitations in use. There is need to use BSA adjustments in the case of some patients. The NKDEP recommend in 2010 to utilise either an eCrCl or an eGFR with BSA normalisation removed as acceptable in drug dosing in chronic kidney disease (6). The usefulness of the new estimation equation eGFR-CKD-EPI (7) has to be evaluate for dug dosage adjustments in our population of patients.

REFERENCES

1. Jones GRD. Estimating renal function for drug dosing decisions. Clin. Biochem. Rev. 2011; 32: 81–88.
2. Florkowski CM, Chew-Harris JSC. Clin. Biochem. Rev. 2011; 32: 75-79.
3. National Kidney Foundation Guidelines. http://www.kidney.org/professionals/kdoqi/guidelines.cfm (Accessed 10 June 2011).
4. Cockcroft DW, Gault MH. Prediction of creatinine clearance from serum creatinine. Nephron 1976; 16:31-41.
5. Hojs R, Gorenjak M, Krsnik M, Lainščak M, Lindič J, Meško Brguljan P, Možina B, Zaletel Vrtovec J. Presejalne metode za kronično ledvično bolezen: ocean glomerulne filtracije. ISIS 2009; 3: 44-46.
6. Chronic Kidney Diseases and Drug Dosing: Information for Providers. http://www.nkdep.nih.gov/professionals/drug-dosing-information.htm (Accessed 5 January 2011)
7. Levey AS, Stevens LA, Schmid CH, Zhang YL, Castro AF 3rd, FeldmanHI, et al. A new equation to estimate glomerular filtration rate. Ann. Intern. Med. 2009; 150: 604-612.
8. Doogue MP, Polasek TM. Drug dosing in renal disease. Clin. Biochem. Rev. 2011; 32: 69-73.

CLINICAL ROLE OF ALPHA FETOPROTEIN DETERMINATION IN HEPATOCELLULAR CARCINOMA WITH DIFFERENT ETIOLOGY

J. Osredkar[1], R. Janša[2*]

[1] University Medical Centre Ljubljana, Clinical institute of Clinical Chemistry and biochemistry, Zaloška cesta 2, 1000 Ljubljana; [2] University Medical Centre Ljubljana, Division of Internal Medicine, Department of Gastroenterology, Zaloška cesta 2, 1000 Ljubljana

BACKGROUND

The most common primary liver tumour is hepatocellular cancer (HCC). It is the cause of high rate of death and poor prognosis, especially because the diagnosing is difficult and treatment options are limited. Many years have been spent in discussing the role of alpha fetoprotein (AFP) determination in the management of HCC.

METHODS

We enrolled 48 HCC patients, collected in Internal Clinic for gastroenterology. When the diagnosis was made, tumour size was determined with ultrasound (the largest diameter of tumour was measured), and biochemical, haematological and liver function tests were performed by standard laboratory procedures. AFP levels were measured by chemiluminiscence immunoassay technique. We stratified collected data with respect to tumour stage, AFP level and Child-Pugh score.

RESULTS

AFP showed 83,3% sensitivity and 72% specificity in the management of HCC. We found weak correlation between AFP level and tumour size in patients where AFP didn't exceed 400 µg/l (R= 0,578) and in those with Child B (R = 0,447) and Child C (R = 0,397).

CONCLUSIONS

Higher AFP level is suggesting major damage of the hepatocytes in patients with AFP level > 8 mg/l and in those with Child C cirrhosis.

CHARACTERIZATION OF CLINICALLY RELEVANT ANTIBODIES AGAINST β2-GLYCOPROTEIN I

U. Žager[1,2*], M. Lunder[2], V. Hodnik[3], G. Anderluh[3], S. Čučnik[1], T. Kveder[1], B. Rozman[1], B. Božič[1,2]

[1] University Medical Centre Ljubljana, Division of Internal Medicine, Vodnikova cesta 62, 1000 Ljubljana, Slovenia; [2] University of Ljubljana, Faculty of Pharmacy, Aškerčeva cesta 7, 1000 Ljubljana, Slovenia; [3] University of Ljubljana, Biotechnical Faculty, Jamnikarjeva ulica 101, 1000 Ljubljana, Slovenia

INTRODUCTION

Antibodies against β_2-glycoprotein I (anti-β_2-GPI) represent one of the laboratory criteria of antiphospholipid syndrome (APS), a complex clinical syndrome characterized by recurrent vascular thrombosis, pregnancy morbidity and thrombocytopenia (1). There is a great heterogeneity that exists among samples in terms of anti-β_2-GPI' avidity and epitopic specificity (2, 3). Clinical significance of anti-β_2-GPI' avidity has been demonstrated by associating the high avidity anti-β_2GPI with thrombotic events in APS patients (4, 5). According to the latter the determination of high avidity anti-β_2GPI could improve clinical risk assessment in APS.

The aim of this study was to determine the unique immunochemical and epitope characteristics of polyclonal high avidity anti-β_2-GPI (in comparison with low avidity anti-β_2-GPI) that could be useful for the development of improved diagnostic tests.

MATERIALS AND METHODS

Samples

High and low avidity polyclonal anti-β_2-GPI were isolated from plasma of APS patients by affinity chromatography using gradient salt elution.

Binding of anti-β_2-GPI to native β_2-GPI in solution

The binding of high and low avidity anti-β_2-GPI to native β_2-GPI in solution was evaluated by incubating both anti-β_2-GPI fractions with various concentrations of β_2-GPI in solution. The amount of unbound anti-β_2-GPI was determined by enzyme-linked immunosorbent assay (ELISA) and the results were expressed as percentage of inhibition.

Influence of solid bound β_2-GPI density on anti-β_2-GPI binding

The influence of β_2-GPI density on the binding of high and low avidity anti-β_2-GPI was evaluated by ELISA and surface plasmon resonance (SPR). Both

anti-β2-GPI fractions were applied to decreasing densities of β_2-GPI immobilized on microtitre plates. By SPR the binding of both fractions was evaluated on β_2-GPI density lower than in ELISA.

Determination of anti-β_2-GPI fine specificity by phage display

Fine specificities of monoclonal (HCAL), high and low avidity anti-β_2-GPI were determined by screening each anti-β_2-GPI subgroup with a linear heptamer phage display library (New England BioLabs, Ipswich, MA, USA). Single-stranded DNA from amplified selected phage clones was isolated and sequenced (MWG Biotech, Munich, Germany). Binding affinity and inhibition ability of selected clones were confirmed by ELISA.

RESULTS AND DISCUSSION

Influence of solid bound β_2-GPI density on anti-β_2-GPI binding

On high density β_2-GPI (10 ng/mm^2) both anti-β_2-GPI fractions exhibited comparable level of binding (Figure 1, left). On low density β_2-GPI (1 ng/mm^2) the binding of high avidity anti-β_2-GPI was diminished to some degree due to a lower amount of β_2-GPI, while binding of low avidity fraction was abolished (Figure 1, right). The lesser influence of β_2-GPI density on binding of high avidity anti-β_2-GPI suggests that their binding is predominately monovalent, while the binding of low avidity anti-β_2-GPI is predominately bivalent.

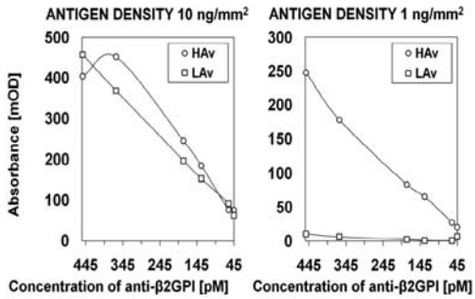

Fig. 1: Binding profiles of high and low anti-β_2-GPI bound to high (left) and low (right) β_2-GPI density.

Binding of anti-β_2-GPI to native β_2-GPI in solution

Binding of high and low avidity anti-β_2-GPI in ELISA was inhibited in a concentration dependent manner by β_2-GPI in solution. For notable decrease in ELISA signal of low avidity anti-β_2-GPI, 5-10 times higher concentrations of β_2-GPI were required than for high avidity anti-β_2-GPI, indicating significantly higher affinity of the latter toward native β_2-GPI in solution (Figure 2).

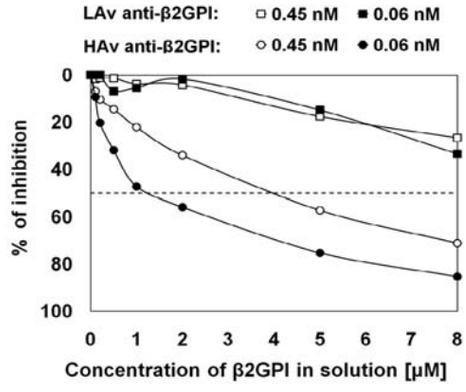

Fig. 2: Inhibition of binding of anti-β_2GPI to immobilized β_2GPI in ELISA by β^2GPI in solution.

Fine specificity of anti-β_2-GPI

The peptide sequences presenting putative epitopes of anti-β_2-GPI exhibited high affinity toward corresponding anti-β_2-GPI subgroups and various degrees of inhibition ability. Prevalence of polar residues suggests the importance of hydrogen and electrostatic bonds for antibody-antigen interactions (Table 1).

Tab. 1: Heptapeptide sequences presenting putative epitopes of anti-β2-GPI.

ANTI-β_2-GPI SUBGROUP	HEPTAPEPTIDE SEQUENCES
HCAL	S L D S D R S
HIGH AVIDITY ANTI-β_2-GPI	F N P Y W Y V Q G P A H S K
LOW AVIDITY ANTI-β_2-GPI	K M D G N H P

With the decreasing content of hydroxyl residues in the selected peptides the antibody avidity decreases, supporting the significance of hydrogen bonds for high affinity binding.

CONCLUSIONS

High avidity anti-β_2GPI (i) possess higher capacity for binding the antigen in solution, (ii) are less dependent to solid-bound antigen density and (iii) express high(er) affinity through hydrogen bonds.

REFERENCES

1. van Os GM, Urbanus RT, Agar C, Meijers JC, de Groot PG. Antiphospholipid syndrome. Current insights into laboratory diagnosis and pathophysiology. Hamostaseologie. 2010; 30: 139-143.
2. Čučnik S, Kveder T, Rozman B, Božič B. Binding of high avidity anti-b2-glycoprotein I antibodies. Rheumatology (Oxford) 2004; 43: 1353-1356.
3. Giles IP, Isenberg DA, Latchman DS, Rahman A. How do antiphospholipid antibodies bind beta2-glycoprotein I? Arthritis Rheum. 2003; 48: 2111-2121.
4. Cucnik S, Kveder T, Ulcova Gallova Z, Swadzba J, Jacek M, Valesini G, Avcin T, Rozman B, Bozic B. Avidity of anti-beta2-glycoprotein I antibodies in patients with or without antiphospholipid syndrome. A collaborative study in the frame of the European forum on antiphospholipid antibodies. Lupus. 2011; (in press)
5. de Laat B, Dersken RH, de Groot PG. High-avidity anti-β2-glycoprotein I antibodies highly correlate with thrombosis in contrast to low-avidity anti-β2-glycoprotein I antibodies. J. Throm. Haemost. 2006; 4: 161916-21.

IMPACT OF THIOPURINE S-METHILTRANSFERASE OVEREXPRESSION ON CELL REDOX CAPACITY IN HepG2 CELLS

M. Milek, A. Šmid*, I. Mlinarič-Raščan

University of Ljubljana, Faculty of Pharmacy, Aškerčeva cesta 7, 1000 Ljubljana, Slovenia

INTRODUCTION

Thiopurine S-methyltransferase (TPMT) is a genetically polymorphic enzyme which deactivates thiopurine drugs such as 6-mercaptopurine (6-MP) (1). Although TPMT is widely expressed in human tissues and its role in metabolism of thiopurines well established, its endogenous substrate remains unknown (2). As an S-adenosylmethionine (SAM) dependent methyltransferase, TPMT is closely connected to L-methionine (Met) recycling, folate metabolism, trans-sulfuration and glutathione (GSH) synthesis (3) and, as such, might play an important role in the regulation of cell methylation as well as in redox homeostasis. Aberrations in methylation and redox homeostasis have been implicated in several liver pathologies. We aimed to define the function of TPMT in oxidative stress conditions and found that TPMT over-expression increased the cell vulnerability to oxidative damage due to lower GSH levels, indicating that TPMT acts as a pro-oxidative protein that is directly or indirectly involved in cellular control of antioxidant capacity.

MATERIALS AND METHODS

Materials

All reagents were from Sigma-Aldrich (St. Louis, MO, USA) unless stated otherwise.

Cell culture

For routine culturing HepG2 cells (ATCC, LGC Promochem, Wesel, Germany) were grown in Dulbecco's modified Eagle's medium containing 200 µM Met (Met+ DMEM), supplemented with 10% FBS (Gibco, Carlsbad, CA, USA), 2 mM L-glutamine and 100 U/ml penicillin/streptomycin.

Stable transfection

HepG2 cells stably expressing the N-terminal EGFP-TPMT fusion protein (TPMT+) were prepared and characterized as described (4).

Cell proliferation and viability

Metabolic activity, as an indication of cell proliferation, was determined by the CellTiter Aqueous One Proliferation Assay, while ATP content, as an indication of cell viability, was determined by the CellTiter Glo Luminescent Cell Viability Assay (both from Promega, Madison, WI, USA) on an automated plate reader (Tecan Safire2, Zürich, Switzerland) as described (5).

Enzyme activity and autophagy

Caspase-3 activity was determined in cell lysates with a kinetic assay using the fluorigenic N-Acetyl-Asp-Glu-Val-Asp-7-amido-4 trifluoromethyl-coumarin substrate as described (5).

Staining and microscopy

To detect lipid vesicles, HepG2 cells were stained with Oil Red O dye, and transmission images were acquired on a CKX41 microscope using C-7070 camera (Olympus).

RESULTS AND DISCUSSION

To determine whether differential expression of wild-type TPMT (TPMT*1) modulates cell proliferation and viability on the induction of oxidative stress, we screened the effects of various substances with known mechanisms of toxicity on HepG2 cells stably transfected with a pEGFP-TPMT construct (TPMT+) (4). Incubation with identical concentrations of oxidative stress inducers (e.g. 1 mM H_2O_2, 20 µM NEM) resulted in higher toxicity in TPMT+ cells relative to untransfected (UT) cells (Fig. 1A, B).

No differential response between TPMT+ and UT cells was observed when apoptosis inducers (TPCK, DMSO) were tested (not shown). This indicates that TPMT plays an important role in oxidative stress response by antagonizing cell detoxification mechanisms. In addition, increased numbers of Oil Red O-stained lipid vesicles and necrotic morphology were observed in TPMT+ H_2O_2-treated cells compared to UT cells treated with the same amount of H_2O_2 (Fig. 2).

No differences in caspase-3 activity or autophagic vacuole formation were observed in H_2O_2-treated UT or TPMT+ cells (not shown), supporting the interpretation that necrosis was the main mechanism of cell death.

To determine whether TPMT influences cell survival by modulating synthesis of the major cellular antioxidant, GSH, cells were pre-incubated with NAC, a precursor of cysteine and GSH. Compared to UT cells, significantly higher NAC concentrations were required in TPMT+ cells to prevent cell death induced by NEM, a GSH-depleting agent (not shown). This led us to hypothesize that high cellular TPMT may decrease the SAM flux through the Met cycle and consequently limit GSH synthesis. In order to confirm that TPMT modulates cell redox capacity, total intracellular GSH concentrations were measured in untreated, H_2O_2- and NEM-treated untransfected or TPMT+ cells. Significantly lower GSH levels were observed in TPMT+ cells than in UT cells in untreated, as well as in H_2O_2- and NEM-treated, cells (not shown).

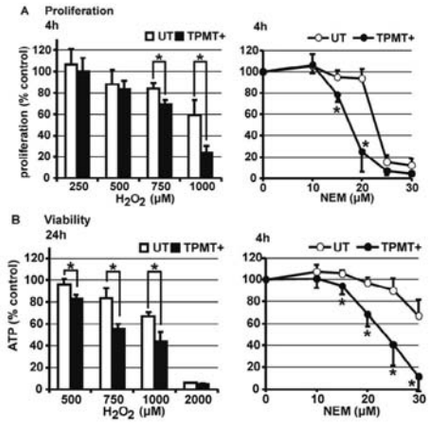

Fig. 1: Overexpression of TPMT results in higher sensitivity to oxidative stress inducers due to decreased redox capacity. (A, B) Untransfected (UT) or TPMT+ HepG2 cells were incubated for the indicated time periods in the presence of increasing concentrations of H2O2 or NEM, followed by determination of cell proliferation (A) and viability (B).

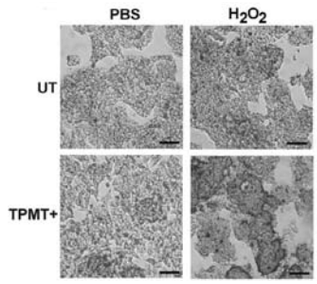

Fig. 2: After incubation in FBS-free Met+ medium for 48 h, UT and TPMT+ cells were incubated with PBS or H2O2 (5 mM) for 4 h, followed by fixing and lipid staining with Oil red O. Representative transmission images are shown. Magnification, 20×; scale bar, 50 µm.

CONCLUSIONS

The results presented above show that, on the induction of oxidative stress, cell death depends on TPMT status, such that high activity correlates with more rapid GSH depletion, which has an impact on cell redox capacity and antioxidant response in hepatocellular carcinoma cells.

REFERENCES

1. Panetta JC, Evans WE, Cheok MH. Mechanistic mathematical modelling of mercaptopurine effects on cell cycle of human acute lymphoblastic leukaemia cells. Br J Cancer 2006; 94 (1): 93-100.
2. Weinshilboum R. Thiopurine pharmacogenetics: clinical and molecular studies of thiopurine methyltransferase. Drug Metab Dispos 2001; 29 (4 Pt 2): 601-5.
3. Chiang PK, Gordon RK, Tal J, et al. S-Adenosylmethionine and methylation. FASEB J 1996; 10 (4): 471-80.
4. Egle R, Milek M, Mlinaric-Rascan I, et al. A novel gene delivery system for stable transfection of thiopurine-S-methyltransferase gene in versatile cell types. Eur J Pharm Biopharm 2008; 69 (1): 23-30.
5. Milek M, Karas Kuzelicki N, Smid A, et al. S-adenosylmethionine regulates thiopurine methyltransferase activity and decreases 6-mercaptopurine cytotoxicity in MOLT lymphoblasts. Biochem Pharmacol 2009; 77 (12): 1845-53.

SOLID-PHASE EXTRACTION AS PREATRETMENT TECHNIQUE FOR PREPARATION OF BIOLOGICAL SAMPLES: APPLICATION IN HPLC DETERMINATION OF VALPROIC ACID IN SALIVA

A. Haxhiu[1*], J. T. Ribarska[2], S. T. Jolevska[2]

1 Department of Pharmacy, Medical Sciences Faculty, "State University of Tetova", Str. Ilinden nn, 1200 Tetova, Macedonia; 2 Faculty of Pharmacy, University "Ss Cyril and Methodius", Vodnjanska 17, 1000 Skopje, Macedonia

INTRODUCTION

There are three major objectives of sample preparation of biological samples prior to chromatographic separation: the dissolution of analyte in suitable solvent, removal of interfering compound as possible and preconcentration of the analyte (1).Solid –phase extraction(SPE) is the most important technique used in sample pre-treatment for HPLC analysis. SPE is more efficient separation process than liquid-liquid extraction (LLE) and has a number of potential advantages compared to LLE: more complete extraction of the analyte, more efficient separation of interferences from analytes, reduced organic solvent consumption, easier collection of the total analyte fraction, more convenient manual procedures, removal of particulates, more easy automated,it is easier to obtain a higher recovery of the analyte (2).

The aim of our study was to establish a rapid, precise and reliable SPE procedure followed by RP-HPLC with UV detection for determination of the antiepileptic drug -valproic acid (VPA) in human saliva. The method was validated according to the EMA Guideline on validation of bioanalytical methods (3) .

MATERIALS AND METHODS

Chemicals and reagents

Valproic acid sodium salt and octanoic acid (internal standard, IS), were purchased from Sigma-Aldrich Inc., St. Louis, USA. Methanol and acetonitrile -HPLC grade, potassium dihydrogen phosphate and phosphoric acid were purchased from Merck (Darmstadt, Germany). For all analysis, HPLC grade water was used. SampliQ OPT cartridges (30mg/1mL) used for sample preparation were procured from Agilent Technologies, USA.

Chromatographic conditions

The assay was performed on Agilent 1200 series HPLC with Zorbax Eclipse XDB (150 x 4.6mm; 5µm) column with a mobile phase of acetonitrile - phosphate buffer (pH 3.0; 0.02M) (40:60, v/v). Detection was made at 210 nm.

Preparation of standards and quality control standards

Stock standard solutions of VPA (500 µg/ml) and IS (364 µg/ml) were prepared by accurately weighed the required amounts into separate volumetric flasks and dissolving in methanol. Working solutions were obtained by serial dilutions of stock solution of VPA with purified water.Four levels of quality control (QC) samples were prepared by spiking the blank saliva aliquots with appropriate volume of the working solutions of VPA and 10% H_3PO_4, giving the final concentration of 1.0 µg/mL (lower limit of quantitation), 5.0 µg/mL (low QC sample), 10.0 µg mL^{-1} (medium QC sample) and 20.0 µg/mL (high QC sample).Each spiked saliva were vortex-mixed for 30s and loaded into SampliQ OPT cartridges previously conditioned according to the following steps: a) conditioning with 1ml methanol; b) equilibration with 1 ml water; c)loading of 1ml saliva sample; d) washing twice with 1ml water and 1ml 10% methanol; e) elution with 90% methanol. The eluent was transferred to microvials and autosampler was programmed to inject 100 µl into the HPLC system.

RESULTS AND DISCUSSION

During the optimization of solid phase extraction procedure, two different types of SPE columns (SampliQ OPT and SampliQ C18 cartridges) and different steps of washing and elution were evaluated. In order to find the best elution solvent, several trials were made. At first, an elution with 1ml acetonitrile was tested; valproic acid was completely retained by the cartridge. Similar results, with low recovery, were obtained using pure methanol or an acetonitrile-methanol (50:50,v/v) mixture. Also, different steps of washing were tested, first with water and then with 5% methanol or only with 5% methanol. The best results of recovery 99.4 % and 97.9 % for valproic acid and IS, respectively, were obtained using SampliQ OPT cartridges and the SPE procedure described on the sample preparation.Through the parameters of validation has been proven that sample pretreatment by the proposed SPE procedure was yielded very good results .

The chromathograms for blank saliva, blank saliva spiked with VPA and octanoic acid are presented in Fig 1.

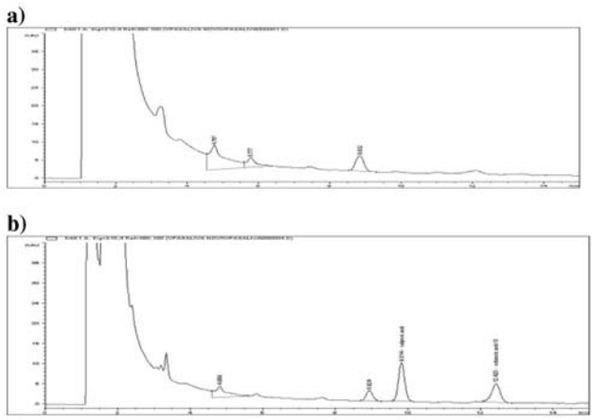

Fig. 1: RP-HPLC chromatograms obtained from (a) a blank saliva (drug free saliva) and (b) blank saliva spiked with valproic acid (50µg/mL) and octanoic acid (36.2µg/ mL), after the SPE procedure

Retention times of VPA and IS were 9.8 min and 12.4 min, respectively. No interfering peaks were observed in the retention times of analyte or IS.

Recovery of VPA and IS in the extraction procedure was determined by comparing the peak area of the analyte or IS from an SPE extracted sample to the peak area of the analyte from a post-extracted spiked sample representing the 100% recovery (4). The recoveries of VPA at four concentration levels (1.0, 5.0, 10.0 and 20.0 µg/mL) were in the range 96.8% - 99.4% (Table 1), and the recovery of IS was 97.9%. These results indicate good recoveries for valproic acid and IS which means that the proposed SPE procedure could be applied to the determination of valproic acid in saliva.

Table 1: Recoveries of valproic acid from saliva (n=5)

Concentration (µg/ml)	Recovery (%)
1.0	98.2
5.0	96.8
10.0	99.4
20.0	98.6

CONCLUSION

A rapid, precise and reliable method for solid - phase extraction (SPE) has been developed for HPLC determination of VPA in human saliva. The method allows determination of VPA at low concentration without need prior derivatization.

REFERENCES

1. P.Wal, B.Kumar, A.Bhandari, A.K. Rai, A.Wal, Bioanalytical Method Development – Determination of Drugs in Biological Fluids, J. Pharm. Sci. Tech. 2 (2010) 333-347
2. R.Lloyd,J.Joseph,Introduction to modern chromatography-3rd ed.pp.757-789
3. Guideline on validation of bioanalytical methods, European Medicines Agency, Committee for Medicinal Products for Human Use (CHMP), 2009,
4. A guide to effective method development in bioanalysis, Waters, The science of what's possible, 2008, www.waters.com/bioanalysis

OVERCOMING POOR IMMUNOGENICITY OF GLUTEN PEPTIDES USING MULTIPLE ANTIGEN PEPTIDE

T. Šuligoj[1,2], S.C. Donnelly[1], B. Božič[2*], P.J. Ciclitira[1], H.J. Ellis[1]

1 Kings College London, Diabetes and Nutritional Sciences Division, Gastroenterology, Rayne Institute, St. Thomas' Hospital London SE1 7EH, United Kingdom; [2] Faculty for Pharmacy, University of Ljubljana, Aškerčeva 7, 1000 Ljubljana, Slovenia

INTRODUCTION

Gluten-specific monoclonal antibodies (mAbs) have been used to quantify gluten content in food to identify safe foodstuffs for individuals with coeliac disease (CD). Currently available assays quantify only one out of two groups of gluten proteins (gliadin as opposed to gliadin and glutenins), therefore extrapolation to full gluten content may be inaccurate. Additional mAbs, detecting other peptides triggering CD, are needed. The production of a mAb of desired specificity and reactivity relies on a number of key stages: immunisation, screening, characterisation and the nature of an immunogen used. In our attempt to produce mAbs to selected gluten peptides two forms of immunogen are used: (i) peptide conjugated to carrier proteins and (ii) multiple antigen peptides (MAPs). The later eliminate the need for a carrier protein, multiple copies of peptides being attached to a poly-lysine core (1).

MATERIALS AND METHODS

Selection of antigens

(i) Two gluten peptides involved in the pathogenesis of coeliac disease: a) DQ8 peptide found in A-gliadin 203-220 (2) corresponding to amino acid sequence QYPSGQGSFQPSQQNPQA and b) HMWG peptide found in high molecular weight glutenins (3) corresponding to amino acid sequence PGQGQQGY-YPTSPQQSGQGQ. DQ8 and HMWG peptides were conjugated to tuberculin purified protein derivative (PPD). Neither DQ8-PPD nor HMWG-PPD conjugates caused successful immunisation of mice. (ii) Therefore sequences of these two peptides were used in MAP formats: Initially shorter peptides were selected for MAP generation (DQ8i-MAP and HMWGi-MAP) for reasons of cost; following failure to generate immune responses to these, longer peptides were utilised (DQ8-MAP and HMWGii-MAP).

Immunisations and sera screening

BALB/c mice on a gluten-free diet were primed subcutaneously with 0.1 ml BCG vaccine and two weeks later immunised with 100 µg PPD-conjugated gluten peptide emulsified in Complete Freund's Adjuvant (CFA). Where immunogen used was MAP mice were immunised subcutaneously with 100 or 300 µg MAPs emulsified in CFA. Mice were immunised 4 weeks later as above, but with the conjugate emulsified in Incomplete Freund's Adjuvant (IFA). Tail bleeds were drawn two weeks later and serum titres of IgG antibody to gluten (gliadin or glutenin as appropriate) tested with ELISA. If the animals had serum IgG titre greater than 1:10,000 they were given an intravenous injection of 100 µg immunogen and culled 3-5 days later to proceed with further experiments for hybridoma production.

Production of hybridomas

Splenocytes of immunised mice were fused with murine myeloma cells (P3X63/Ag8.653) using standard techniques. Hybridomas culture supernatants were investigated for the IgG or IgM antibody production with ELISA.

RESULTS AND DISCUSSION

Previously we have successfully developed a panel of mAbs to known celiac toxic gluten sequences using peptides conjugated to PPD as immunogens. However serological response of mice injected with DQ8- or HMWG-PPD conjugates were not suggestive of successful immunizations (Table 1).

Table 1: Sera responses of mice injected with peptides in conjugate and MAP formats at different amounts of injected antigen (100 or 300 µg) as assessed by ELISA

Gluten peptide sequence Format of injected antigen	Titres of sera responses	
	to 100 µg antigen	to 300 µg antigen
a) Sequences of DQ8 peptide		
QYP**SGQGSFQPSQQNP**QA (DQ8) DQ8-PPD conjugate	+ + +	nd nd nd
PSGQGSFQPSQQNP (DQ8i) DQ8i-MAP	- - -	nd nd nd
QYP**SGQGSFQPSQQNP**QA (DQ8) DQ8-MAP	+ + +	+ + *
b) Sequences of HMWG peptide		
PG**QGQQGYYPTSPQ**QSGQGC (HMWG) HMWG-PPD conjugate	- - -	nd nd nd
QGQQGYYPTSPQ (HMWGi) HMWGi-MAP	- - +	nd nd nd
QPG**QGQQGYYPTSPQ** (HMWGii) MWGii-MAP	+++ + nd	+++ +++ +++

- no response, + low response (titre <3200), +++ high response (titre>10000), * a mouse that died during the course of immunisations, nd not done

In an attempt to overcome poor immunogenicity of these two peptide conjugates, MAP format of antigens were used for further immunisations. Neither the shorter DQ8i derived peptide sequences nor longer DQ8 sequence in a MAP format resulted in desired serum response in any of the mice injected with these antigens regardless of the amount of antigen. Interestingly, the above does not fully apply to the HMWG derived sequences used in the MAP format. The shorter HMWG derived sequence in a MAP format (HMWGi-MAP) did not trigger the desired immune response in any of the three mice. However, the longer HMWGii peptide sequence in a MAP format (HMWGii-MAP) injected at 100 µg per immunisation resulted in positive serum response in one out of two mice. For this reason later immunisations with HMWGii-MAP were undertaken with greater amount of injected antigen (300 µg per immunisation). Sera response of all three mice were positive resulting in IgG titre greater 1:10,000. Spleens of two immunised mice from the later HMWGii-MAP immunisations were used for further fusion experiments for production of mAbs. One fusion of spleen with myeloma cells resulted in growth of 15 hybridomas and the other fusion in 2 hybridomas. However, none of the hybridoma supernatants showed good reactivity as ascertained by very low IgG and IgM titres in ELISA against HMWG glutenins. For this reason further experiments for production of mAbs were not undertaken.

CONCLUSIONS

DQ8 and HMWG-PPD conjugates did not evoke immune responses, as previously demonstrated for some other peptide conjugates (4). Multimerization of a HMWGii peptide in the MAP design resulted in desired serum response, as seen in other studies where MAP format overcame the ineffectiveness of a linear peptide in obtaining antiserum (1). However, this immunisation strategy may yield weakly reactive mAbs inadequate for application to gluten measurement in food.

REFERENCES

1. Tam JP. Recent advances in multiple antigen peptides. J. Immunol. Methods. 1996; 196: 17-32.
2. van de Wal Y, Kooy YMC, van Veelen PA, Peña SA, Mearin LM et al. Small intestinal T cells of celiac disease patients recognize a natural pepsin fragment of gliadin. Proc. Natl. Acad. Sci. USA.1998; 95: 10050–10054.
3. van de Wal Y, Kooy YMC, van Veelen P, Vader W, August SA et al. Glutenin is involved in the gluten-driven mucosal T cell response. Eur. J. Immunol.1999; 29: 3133–3139.
4. Waldron EE, Murray P, Kolar Z, Young L, Brown C et al. Reactivity and Isotype Profiling of Monoclonal Antibodies using Multiple Antigenic Peptides. Hybrid Hybridomics. 2002; 21: 393-398.

TRACE ANALYSIS OF PHENOLIC XENOESTROGENS IN WATER SAMPLES BY MEANS OF STIR BAR SORPTIWVE EXTRACTION AND GAS CHROMATOGRAPHY

I. Rykowska*, W. Wasiak, R. Wawrzyniak

Adam Mickiewicz University, Faculty of Chemistry, Grunwaldzka 6, 60-780 Poznań, POLAND

INTRODUCTION

A technique of sorptive extraction with a magnetic stir bar covered with extraction medium SBSE (Stir Bar Sorptive Extraction) is an example of a widely applied micro-extraction technique. This technique was introduced in 1999 by Baltussen et al. (1) for a determination of organic micro-pollutants in water solutions. The technique has been applied successfully to trace analysis in environmental, biomedical and food applications, with a possibility to obtain extremely low detection limits.

Among several groups of components to be determined by means of SBSE, particular attention should be put to estrogens – steroid sexual hormones, fitoestrogens – plant hormones, and xenoestrogens – chemical compounds artificially produced by the industry and further disposed to the water environment (such as alkilophenols and bisphenol A). It is continuously proven that the above mentioned third group of components, as well as estrogens and fitoestrogens, are responsible for so called "estrogenic effect", that in turn lead to the feminization and hermaphroditism of the water organisms, and further humans [2].

In this work an approach is presented of an optimized method of the preconcentration of xenoestrogens on a mobile sorptive element, to determine such compounds as 4-nonylphenol, 4-tert-octylphenol, and 2,2-bis-(4-hydroxyphenyl)-propane in real samples (fresh and cleaned sewage).

MATERIALS AND METHODS

Materials

4-nonylphenol (4NP), 4-tert-octylphenol (4tOP), and 2,2-bis-(4-hydroxyphenyl)-propane (BPA) were purchased from Sigma–Aldrich (Poznań, Poland). The chemical structures and mass spectra are shown in Fig. 1. Methanol was purchased from Merck.

Instrumentation

Stir bars coated with a 0.5 mm-thick layer of PDMS (twister: a magnetic stirring rod is placed a glass jacket and coated with PDMS) were obtained from Gerstel (Műlheim un der Ruhr, Germany). GC-MS was performed using an VARIAN GC CP-3380 MS 4000 equipped with mass spectrometric detector (MS). A J&W Scientific VF - 5 ms (30 m x 0,25 mm; DF=0,39 µm) capillary column was used. Helium was the carrier gas. All the work was carried out in a constant flow mode set at 1 mlµmin^{-1}. The oven temperature was programmed to increase from 80°C to 260°C (held for 2 minutes) at 15°Cµmin^{-1}. The transfer line to the mass spectrometer was set at 300°C. The dwell time was set at 80 ms and the multiplier potential was equal to 450 V. Full-scan mass spectra between 35 and 200 m/z were acquired once every second. For SIM (selected ion monitoring) were monitored m/z = 135, m/z = 107, m/z = 177 for OP and NP, and m/z = 213, m/z = 270 for BPA.

Sample preparation

Water sample (25 mL; pH = 7)) was poured into a 30 ml glass vial. The stir bar was stirred in the sample for 120 min at room temperature. Next, the stir bar was placed into a 3 ml glass vial with 1 ml MeOH for liquid desorption under ultrasonic treatment for 60 min (25°C). After back extraction, the stir bar was removed by means of magnetic rod, the extract was evaporated and followed by reconstitution with 100 µl of MeOH.

RESULTS AND DISCUSSION

Phenolic xenoestrogens in two water samples (fresh and cleaned effluent) collected from sewage plants were analyzed using stir bar sorptive extraction and gas chromatography. The detection limits of the proposed method ranged from 1.0 to 5.0 ng·mL^{-1}. In addition, the presented method showed good linearity and correlation coefficients using surrogate standards. The recovery rates of the analytes for water samples from sewage plants spiked with standards at 50 ng·mL^{-1} ranged from 70.2 to 75.0 % (4tOP), 62.5- 68.5% (BPA) and 61.5-67.4% (4NP), while spiked with standards at 100 ng/ml – 80.4-86.3 % (4tOP), 85.2-91.2% (BPA), and 70.4-74.8% (4NP), respectively. This simple, accurate and highly sensitive method is expected to have potential applications in various aquatic samples.

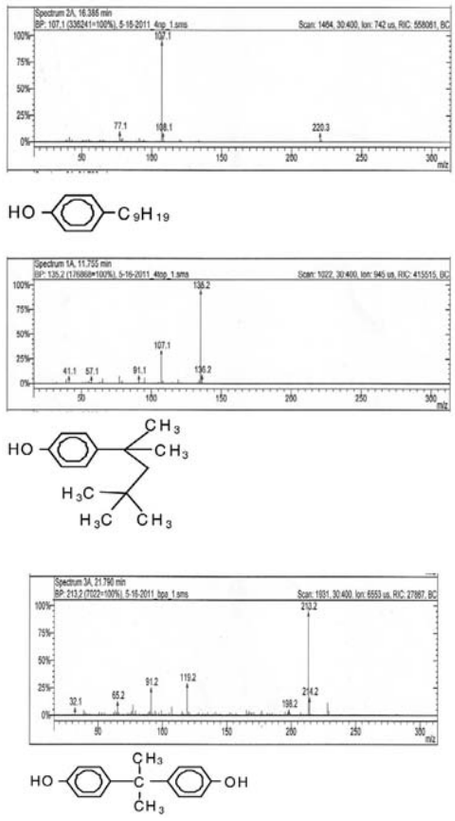

Fig. 1: The structure and mass spectra of a) 4NP, b) 4tOP, and c) BPA

ACKNOWLEDGMENT

This work was partially funded by the KBN grant N N204 214340.

REFERENCES

1. E. Baltussen, P., Sandra, et al. Stir bar sorptive extraction (SBSE), a novel extraction technique for aqueous samples: Theory and principles. J. Microcolumn Separations, 1999; 11: 737-747.
2. B I. Rykowska, W. Wasiak Properties, threats, and analysis methods of bisphenol A and its derivatives. Acta Chromatographica 16 (2006) 7-27.

MODULATION OF ABCC1 PROTEIN TRANSPORT ACTIVITY BY NATURAL AND SYNTHETICALLY MODIFIED FLAVONOIDS

J. Maniewska[1,3*], A. B. Hendrich[2,3]

[1] Department of Chemistry of Drugs, Wrocław Medical University, Tamka 1, 50-137 Wrocław, Poland; [2]Department of Biology and Medical Parasitology, Wrocław Medical University, J. Mikulicza-Radeckiego 9, 50-367 Wrocław, Poland; [3]Department of Biophysics, Wrocław Medical University, Chałubińskiego 10, 50-368 Wrocław, Poland

INTRODUCTION

Overexpression of multidrug resistance-associated protein (ABCC1) confers multidrug resistance (MDR) on tumor cells, that is defined as the ability of a living cell to show the resistance to a wide variety of structurally and functionally unrelated compounds. The widespread occurrence of MDR in tumor cells represents a major impediment to successful cancer chemotherapy. Among many multidrug resistance mechanisms the ATP-driven efflux of anticancer drug leading to the reduction of its intracellular concentration inside the cells is most effectual. Herein we present the results of studies on two natural flavonoids – quercetin and genistein – and two synthetically modified genistein derivatives, which all are putative MDR modulators (1). We were looking for the optimal chemical modification in genistein molecule to create more effective ABCC1 modulators to avoid frequent chemotherapy failures in future.

MATERIALS AND METHODS

Materials

Genistein and quercetin were purchased from Sigma-Aldrich. The genistein derivatives were synthesized by prof. W. Szeja in the Department of Organic, Bioorganic Chemistry and Biotechnology of Silesian Technical University, Gliwice, Poland. Their purity was checked by HPLC and NMR. Chemical structures and abbreviations of flavonoids used in the present paper are shown in Figure 1.

Since these flavonoids were almost insoluble in water, their DMSO solutions were used for the experiments. The fluorescent probe, BCECF – 2',7'-*bis*-(3-carboxyethyl)-5-(and-6)-carboxyfluorescein – was purchased from Molecular Probes (Eugene, OR).

Methods

The influence of different flavonoids on transport activity of multidrug resistance-associated protein (ABCC1) was studied using a BCECF assay developed by Rychlik et al (2). Human erythrocytes were used as a cell model expressing ABCC1 protein in their plasma membrane. The fluorescent probe, BCECF, was applied as a substrate for multidrug resistance transporter (ABCC1).

RESULTS AND DISCUSSION

In the present work, by means of functional fluorescence assay we have shown that ABCC1-mediated efflux of BCECF out of human erythrocytes is inhibited by quercetin, genistein and it's synthetically modified derivatives. Genistein inhibited studied transport to lesser extent than quercetin, while Lak-3 and Ram-3 were more potent ABCC1 inhibitors then genistein (Fig. 2).

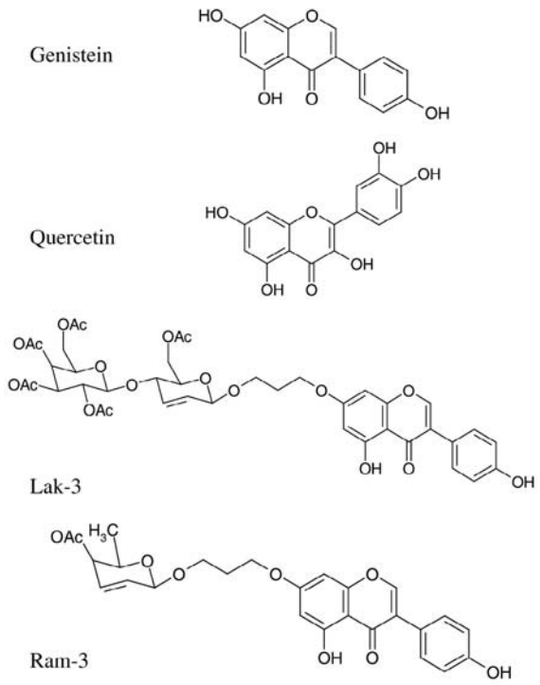

Fig. 1: Studied flavonoids

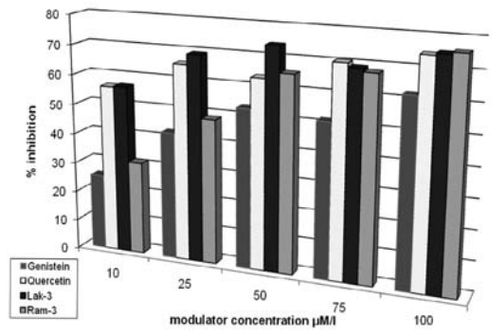

Fig. 2: The inhibition of ABCC1-mediated BCECF efflux from erythrocytes induced by studied flavonoids

CONCLUSIONS

The studied flavonoids showed the inhibitory influence on transport carried out by multidrug resistance-associated protein. Since ABCC1 inhibition could be caused either by direct interaction of studied chemicals with protein or by indirect perturbation of membrane properties, some further investigations are necessary to explain the molecular mechanism underlying the inhibitory activity of genistein and it's derivatives.

REFERENCES

1. Hendrich A.B, Flavonoid-membrane interactions: possible consequences for biological efects of some polyphenolic compounds. ActaPharmacologica Sinica. 2006; 27(1): 27–40.
2. Rychlik B, Balcerczyk A, Klimczak A, Bartosz G, The role of multidrug resistance protein 1 (MRP1) in transport of fluorescent anions across the human erythrocyte membrane. J. Membrane Biol. 2003; 193: 79–90.

THERAPEUTIC USE EXEMPTIONS ISSUED TO SLOVENIAN ATHLETES BETWEEN 2008 AND 2010

J. Osredkar

University Medical Centre Ljubljana, Clinical institute of Clinical Chemistry and biochemistry, Zaloška cesta 2, 1000 Ljubljana

BACKGROUND

»Doping« refers to an athlete's use of prohibited drugs or methods to improve training and sporting results. Athletes, like all others, may have illnesses or conditions that require them to take particular medications. If the medication an athlete is required to take to treat an illness or condition happens to fall under the prohibited list, a Therapeutic Use Exemption (TUE) may, under certain well-defined and restricted conditions, give that athlete the authorization to take the needed medicine.

METHODS

Slovenian Therapeutic Use Exemption Committee has been authorized to issue such certificates. We examined all granted TUE to Slovenian athletes in the three years period. TUEs are issued by the competent authority in accordance with the International Standard for TUE, which is obligatory followed by all signatories of the World Anti-Doping Code.

RESULTS

The analysis of approved TUE found that in 2008 we issued 17 TUE, in 2009 31 TUE and 33 TUE in 2010. TUE percentage approved for the treatment of asthma in 2008 was 82%, in 2009 84% and in 2010 73 %. TUEs have been granted also for substances which were used for the treatment of other diseases. TUE were approved in 23 different sports. The highest number of granted TUE is in swimming, cross country skiing, cycling and athletics.

CONCLUSIONS

Taking in account rules in force, medical information to support the decisions of TUE committee and the prescribed treatment, it could be concluded that the treatment was in compliance with regulations and recommendations of World Anti-Doping Agency.

MEASUREMENT OF PROCOAGULANT AND PROINFLAMMMATORY RESPONSE OF HUMAN CORONARY ARTERY ENDOTHELIAL CELLS BY ENDOTHELIAL MICROPARTICLES

M Frank[1], J Trček[1], AN Kopitar[2], A Bedina-Zavec[3,4], K Mrak-Poljšak[1], K Lakota[1*], A Ihan[2], V Kralj-Iglic[4], B Rozman[1], S Sodin-Šemrl[1]

[1] Department of Rheumatology, University Medical Centre Ljubljana, Vodnikova 62, Ljubljana, Slovenia; [2] Institute of Microbiology and Immunology, Faculty of Medicine, University of Ljubljana, Korytkova 2, Ljubljana, Slovenia; [3] Laboratory of Biosynthesis and Biotransformation, National Institute of Chemistry, Hajdrihova 19, Ljubljana, Slovenia; [4] Laboratory of Clinical Biophysics, Institute of Biophysics, Faculty of Medicine, University of Ljubljana, Lipičeva 2, Ljubljana, Slovenia

INTRODUCTION

Elevated plasma levels of serum amyloid A (SAA), an acute phase reactant and systemic inflammatory marker, are strongly associated with increased cardiovascular risk, correlate with endothelial dysfunction in coronary artery disease and independently predict future cardiovascular events and worse prognosis of coronary artery disease (1,2). Endothelial microparticles, membrane-coated vesicles released from activated or apoptotic endothelial cells, serve as biomarkers of endothelial injury or dysfunction in coronary artery disease and other cardiovascular diseases. Increased plasma levels of endothelial microparticles associate with high-risk angiographic lesions in coronary artery disease and were shown to independently predict future cardiovascular events in high risk patients (3-8).

The aim of the present study was to investigate the role of SAA in generation of endothelial microparticles in cultured human coronary artery endothelial cells (HCAEC) and define if endothelial microparticles could reflect SAA-induced procoagulant and proinflammatory responses in HCAEC.

MATERIALS AND METHODS

HCAEC were stimulated with recombinant human SAA (1000nM) for 4, 8, 16 and 24h. Endothelial microparticles were isolated from cell culture supernatants by differential centrifugation. The number of endothelial microparticles, binding of Annexin V and the expression of surface endothelial markers (CD31, CD62E) and tissue factor on endothelial microparticles were analyzed by flow cytometry. The expression of tissue factor, CD62E, IL-6 and IL-8 mRNAs in HCAEC was determined by quantitative PCR using beta actin as an endogenous control. Tissue factor activity was measured in cell lysates using Actichrome TF Activity Assay. IL-6 and IL-8 protein levels in culture supernatants were determined by ELISA.

RESULTS AND DISCUSSION

SAA induced the release of significantly increased numbers of Annexin V and CD31 positive endothelial microparticles from HCAEC. Time-dependent rise in the number of SAA-induced Annexin V positive endothelial microparticles highly correlated with IL-6 and IL-8 levels in cell culture supernatants ($p<0.01$). CD62E antigen was expressed only on endothelial microparticles from SAA-stimulated HCAEC and reflected time-dependent changes in CD62E mRNA levels in HCAEC, indicating cell activation. Tissue factor mRNA expression, tissue factor surface exposure and activity in HCAEC peaked at 4h following SAA stimulation and were accompanied by tissue factor surface exposure and activity on endothelial microparticles. Later during SAA stimulation tissue factor expression and activity progressively decreased in SAA-induced HCAEC and endothelial microparticles, suggesting tight regulation of tissue factor.

CONCLUSIONS

We showed for the first time that SAA can induce the release of endothelial microparticles from primary human coronary artery endothelial cells. SAA-induced endothelial microparticles reflected early procoagulant and late proinflammatory responses of human coronary artery endothelial cells and may serve as surrogate biomarkers and/or mediators of SAA-induced changes of endothelial function in cardiovascular diseases.

REFERENCES

1. Johnson BD, Kip KE, Marroquin OC, et al. Serum amyloid A as a predictor of coronary artery disease and cardiovascular outcome in women: the National Heart, Lung, and Blood Institute-Sponsored Women's Ischemia Syndrome Evaluation (WISE). Circulation. 2004;109(6):726-32.
2. Ogasawara K, Mashiba S, Wada Y, et al. A serum amyloid A and LDL complex as a new prognostic marker in stable coronary artery disease. Atherosclerosis. 2004;174(2):349-56.
3. Sinning JM, Losch J, Walenta K, et al. Circulating CD31+/Annexin V+ microparticles correlate with cardiovascular outcomes. Eur. Heart J. 2010
4. Nozaki T, Sugiyama S, Koga H, et al. Significance of a multiple biomarkers strategy including endothelial dysfunction to improve risk stratification for cardiovascular events in patients at high risk for coronary heart disease. J. Am. Coll. Cardiol. 2009;54(7):601-8.
5. Philippova M, Suter Y, Toggweiler S, et al. T-cadherin is present on endothelial microparticles and is elevated in plasma in early atherosclerosis. Eur. Heart J. 2011;32(6):760-71.
6. Morel O, Pereira B, Averous G, et al. Increased levels of procoagulant tissue factor-bearing microparticles within the occluded coronary artery of patients with ST-segment elevation myocardial infarction: role of endothelial damage and leukocyte activation. Atherosclerosis. 2009;204(2):636-41
7. Morel O, Jesel L, Freyssinet JM, Toti F. Cellular mechanisms underlying the formation of circulating microparticles. Arterioscler. Thromb. Vasc. Biol. 2011; 31(1):15-26.
8. Amabile N, Rautou PE, Tedgui A, Boulanger CM. Microparticles: key protagonists in cardiovascular disorders. Semin. Thromb. Hemost. 2010;36(8):907-16.

EP4 RECEPTOR IS A POTENT MODULATOR OF BCR INDUCED CYTOKINE RELEASE IN MATURE B LYMPHOCYTES

M. Prijatelj*, T. Čelhar, M. Gobec, I. Mlinarič-Raščan

University of Ljubljana, Faculty of Pharmacy, Aškerčeva cesta 7, 1000 Ljubljana, Slovenia

INTRODUCTION

B cell receptor (BCR) induces apoptosis of immature and proliferation of mature B lymphocytes. In an otherwise complex transcriptional program that is triggered by the BCR, one of the recognized decision-making genes, between apoptosis and clonal expansion of B lymphocytes, was also Ptger4, coding for the EP4 receptor [1]. The EP4 receptor is one of the four prostaglandin E (EP) receptors (EP1, EP2, EP3, and EP4) that recognize prostaglandin E2 (PGE2) as its natural binding ligand [2]. PGE2 is emerging as an important co-modulator of B cell responses [3]. We confirmed this notion, showing that PGE2 enhances BCR-induced cell death of immature B cells by binding to the EP4 receptor [4]. Similarly, PGE2-EP4 signaling prevents the BCR-induced proliferation of mature B lymphocytes [5]. In this study we addressed involmend of EP4 receptor signaling in the modulation of cytokine release from mature B cells, using A20 cell line as a model.

First we report EP4 receptor is up-regulated upon BCR crosslinking on A20 cells, and that it conways growth inhibitory signals on mature B cell proliferation. Moreover it can inhibit BCR induced production of TNF-alfa, IL-10 and IL-12.

MATERIALS AND METHODS

Reagents

PGE1-OH and PGE2 were from Cayman Chemical (Ann Arbor, MI, USA), anti-IgG was from Jackson ImmunoResearch Laboratories (West Grove, PA, USA).

Cell culture

A20 cells were maintained as described [4].

Metabolic activity assay

As a direct measure of proliferation, trypan blue dye exclusion assay (Sigma-Aldrich) was performed as described [4].

Metabolic activity of A20 cells was assessed using the CellTiter 96® Aqueous One Solution Cell Proliferation Assay (Promega, Madison, WI, USA), according to the manufacturer's instructions.

Quantative PCR

RNA extractiona and quantative PCR was preformed as previously described [4]. The mRNA level of the analyzed gene was quantified using specific Taqman Gene Expression assays (AssayIDs; *Ptger4:* Mm00436053_m1) relative to the expression of eukaryotic 18S rRNA endogenous control (P/N: 4352930E, Applied Biosystems).

Fluorescence microscopy

EP4 receptor expression was determined by fluorescence microscopy of A20 cells stimulated with anti-IgG (10 µg/mL) or vehicle (PBS) for 24 h as previously described [4].

Cytokine production

To measure the release of cytokines (IL-6, TNF-alfa, IL-10 and IL-12) the BD Mouse Inflammation Cytokine CBA kit (Becton-Dickinson) was used. A20 cells (0,5*10/6 cells/mL) were cultured in duplicates. The assay was performed according to manufacturer's instruction with supernatants form anti-IgG (10 µg/mL) and/or Pge1-OH (10 µM) stimulated A20 cells, collected at indicated time points.

RESULTS AND DISCUSSION

The expression of the Ptger4 gene in A20 mature B cells after BCR receptor triggering, was evaluated using quantitative PCR. Significantly increased *Ptger4* mRNA levels were observed with a 6-fold maximum increase at 8h post BCR-crosslinking (Fig 1A). Increased transcriptional levels of the *Ptger4* gene correspond to upregulation of the EP4 receptor on the A20 cell surface, as determined by fluorescence microscopy at 24h post stimulation (Fig 1B).

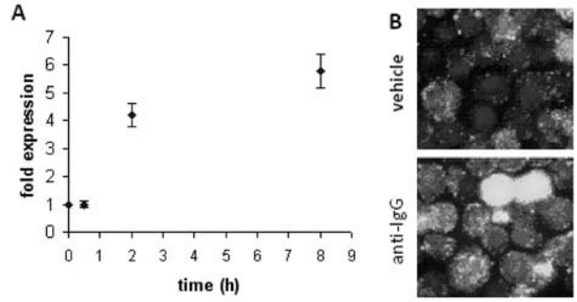

Fig. 1: Triggering of BCR up-regulates EP4 receptor
(A) qPCR analysis of A20 cells stimulated with 10 µg/mL anti-IgG for the indicated periods of time. *Ptger4* expression was normalized to the expression level of the reference gene for 18S rRNA. (C) Expression of EP4 receptor on A20 cells as determined by fluorescence microcopy.

We used PGE2 and PGE1-OH, an selective EP4 receptor agonist (5), to evaluate the growth inhibitory effect of EP4 receptor transduced signals on A20 cells.

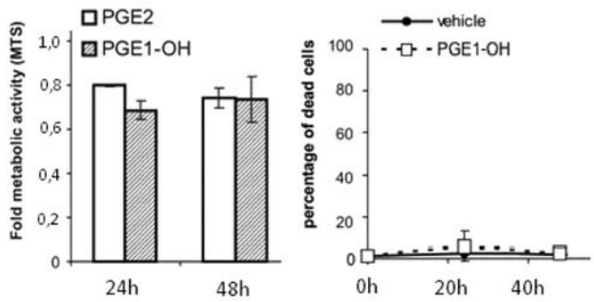

Fig. 2: PGE1-OH and PGE2 inhibit proliferation of A20 cells.
(A) WEHI 231 cells were incubated with 10 µM PGE2 or 10 µM Pge1-OH for indicated periods of time. MTS test was used to assess the metabolic activity at indicated periods of time. (B) A20 cells were incubated with 10 µ PGE1-OH or vehicle for 24 and 48 hours. After the indicated times trypan blue dye exclusion assay was performed.

PGE2 and PGE1-OH caused growth suppression of A20 cells (Figure 2A) and not cell death, which was proven with the trypan blue dye exclusion test, where we could observe an overall decrease in cell numbers, but no significant increase in the percentage of dead cells (Figure 2B).

To further explore the inhibitory action of EP4 agonist, we investigated a possible EP4-mediated suppression of BCR-induced IL-6, IL-12, IL-10 and TNFα cytokine production in mature B cells. BCR crosslinking on mature B cells results in increased levels of IL-12, IL-10 and TNFα (no changes in IL-6 were detected). EP4 agonist Pge1-OH was able to significantly inhibit BCR-induced cytokine expression of above mentioned cytokines (Figure 3).

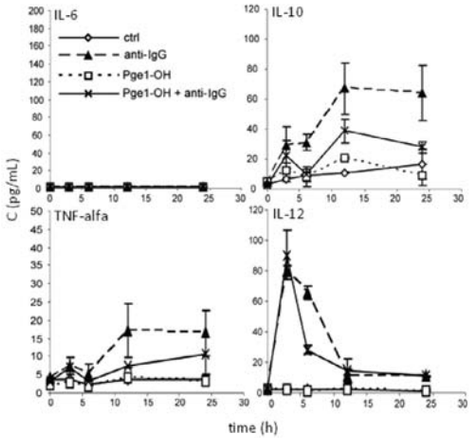

Fig. 3: Kinetic analyses of cytokine secretion by BCR activated A20 cells. Determination of IL-6, TNF-alfa, IL-10 and IL-12 concentrations in media of BCR activated A20 cells with or without EP4 receptor co-stimulation, using cytometric bead array.

CONCLUSION

Our results show that EP4 receptor is up-regulated in BCR activated mature B cells and that EP4 receptor agonists could be used to modulate BCR induced cytokine production in various pathological conditions.

REFERENCE

1. Murn J, Mlinaric-Rascan I, et al. A Myc-regulated transcriptional network controls B-cell fate in response to BCR triggering. BMC Genomics 2009; 10:323.
2. Narumiya S, Sugimoto Y, et al. Prostanoid Receptors: Structures, Properties, and Functions. Physiological Reviews 1999; 79:1193-1226.
3. Rocca B, FitzGerald G.A. Cyclooxygenases and prostaglandins: shaping up the immune response. Int Immunopharmacol 2002; 2:603-630.
4. Prijatelj M, Celhar T, et al. Prostaglandin EP4 receptor enhances BCR-induced apoptosis of immature B cells. Prostaglandins and other lipid mediators. In press.
5. Murn,J, Alibert O, et al. Prostaglandin E2 regulates B cell proliferation through a candidate tumor suppressor, Ptger4. J Exp Med 2008; 205:3091-3103.

OPTIMIZATION OF HILIC METHOD FOR SIMULTANEOUS DETERMINATION OF ROCURONIUM AND 17-DESACETYLROCURONIUM IN INJECTION USING MULTIVARIATE EXPERIMENTAL DESIGN APPROACH

N. Nakov*, R. Petkovksa, L. Ugrinova, S. Trajkovic-Jolevska, A. Dimitrovska

University "Ss.Cyril and Methodius", Faculty of Pharmacy, Center of drug quality control, Vodnjanska 17, 1000 Skopje, Macedonia

INTRODUCTION

Rocuronium bromide (Roc) is a new quaternary aminosteroidal neuromuscular blocking agent which produces rapid muscle relaxation. In the market, rocuronium bromide is only avaible as a solution intended for intravenous or intramuscular injection (1).

Rocuronium is polar (log P 0.5), basic compound and is insufficiently retained on clasical RP-HPLC columns. USP-34 recommends determination of Roc substance and its related compounds by RP-HPLC with ion-pair mobile phase. Hydrophilic interaction liquid chromatography (HILIC) is viable alternative technique for analysis of this kind of hydrophilic compounds (2,3). The HILIC method has overcome the drawbacks of the ion-pair chromatography: long equilibration time, disturbance of eqiulibration by an injection, column cannot be used anymore for other ion-pair reagents, etc (4,5). The literature search has shown that there is no reported HILIC method for determination of Roc substance and its related compounds. The purpose of this work is to optimize HILIC method for simultaneous determination of Roc and its decomposition product 17-desacetylrocuronium (impurity C) in pharmaceutical dosage forms using multivariate experimental design approach.

MATERIALS AND METHODS

Materials

Standard solution of Roc was degradated for one hour at 105°C in oven, in aim to produce impurity C.

Rocuronium bromide 1 mg/ml solution for injection was used as a test solution. The working concentration of the solutions was 1 mg/ml. Mixture of acetonitrile:water in ratio 9:1 (*v/v*, %) was used as a solvent.

Chromatographic conditions

Separation was performed on Agilent Rapid Resolution HPLC System 1200 Series, using Purospher STAR Si 150 x 4,6mm, 5µm partical size column at 30°C. All measurements were made with flow rate 2.0 ml/min, 10µl injection volume and UV detection at 210 nm.

Experimental design

Central Composite Face Centered (CCF) Design was used for method optimization. The MODE 8.0 software was used for generation and evaluation of the experimental design.

RESULTS AND DISCUSSION

In our preliminary investigation, we have studied the influence of three factors: acetonitrile content in the mobile phase (70, 80, 90 *v/v*, %), ionic strenght of the mobile phase (20mM, 50mM and 90mM ammonium formate) and pH of the buffer (4.0, 5.5 and 7.0). The conducted experiments shown that ACN content and the ionic strength of the mobile phase had the largest influence on resolution (Rs) between Roc and impurity C. The pH value of the mobile phase had the lowest influence on separation, so in further experiments it was kept constant (pH= 7.0)
(Fig 1).

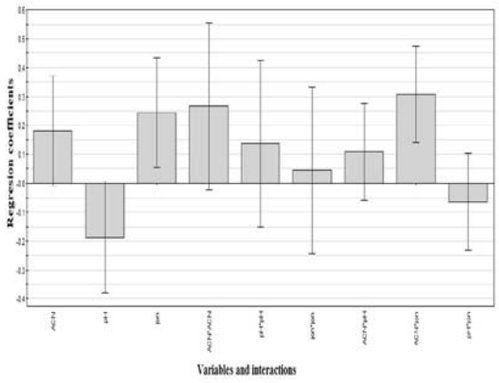

Fig. 1: Regression coefficient plot

In order to define the optimum separation conditions further optimization of the method was performed using the same experimental design (CCF). Two factors were optimized: acetonitrile content in the mobile phase in the range from 85 to 95 (*v/v* %) and ionic strength of the mobile phase in the range from 95 mM to 118 mM ammonium formate at pH 7.0. The experimental design shown that Rs >1.5 can be obtained in the range of ACN content from 89 to 92 (*v/v* %) and ionic strength of the mobile phase from 105 mM to 108 mM ammonium formate at pH 7.0
(Fig 2).

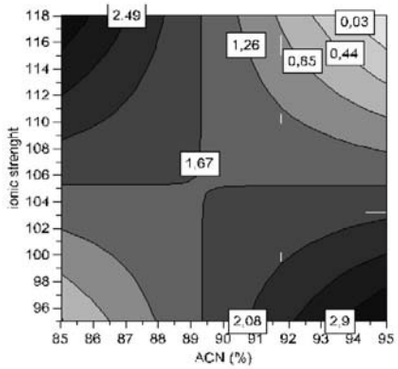

Fig. 2: A contour diagram of the *Rs* as a function of ACN content (*v* %) and ionic strenght (mM)

The best result, which corresponds to high values of the Rs was obtained using mobile phase composition of ACN : 108 mM ammonium formate pH 7.0 (91:9 *v/v* %) The representative chromatogram of the degradeted standard solution obtained under optimized conditions is presented in Fig. 3.

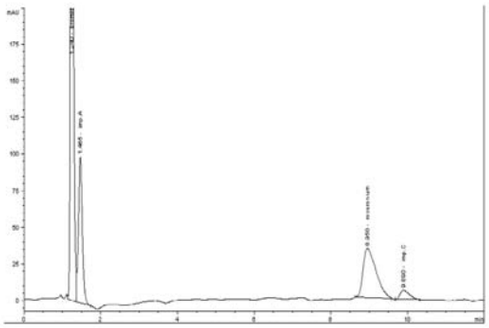

Fig. 3: Standard Rocuronium bromide degradeted 1h at 105˚C

CONCLUSION

The developed HILIC method allows simultaneous determination of Roc and its main impurity C in the drug substance and in the pharmaceutical dosage form due to good separation and resolution of the chromatographic peaks. The multivariate experimental design represents an efficient and easily accomplishable approach in resolving the problem of searching for optimum HILIC conditions.

REFERENCES

1. M.L.A.D. Lestari, G.Indrayanto, Rocuronium Bromide in: Profiles of Drug substances,Excipients, and Related Methodology, Vol.35, 2010, pp.286-308.
2. D.V.McCalley. The challenges of the analysis of basic compounds by high performance liquid chromatography: some possible approaches for improved separation. J.Chrom.A. 2010;1217: 858-880.
3. P.Hemstrom, K.Ingum. Hydrophilic interaction chromatography. J.Sep.Sci. 2006; 29:1784-1821
4. B.Dejaegher, Y Vander Heyden. HILIC methods in pharmaceutical analysis. J.Sep.Sci. 2010; 33: 698-715
5. L.R.Snyder, J.J.Kirkland, J.W.Dolan Intoduction to modern liduid chromatography 3th edition, Jonh Wiley & Sons, Inc., Hoboken, New Jersey, 2010, pp. 347-349.

HIGH-PERFORMANCE LIQUID CHROMATOGRAPYH METHOD FOR SIMULTANEOUS DETERMINATION OF FOUR SECOND GENERATION ANTIEPILEPTIC DRUGS IN PLASMA

T. Vovk*, B. Martinc, I. Grabnar

University of Ljubljana, Faculty of Pharmacy, Aškerčeva cesta 7, 1000 Ljubljana, Slovenia

INTRODUCTION

Clinical experience has clearly demonstrated that individualized dose adjustment by the aid of therapeutic drug monitoring (TDM) can significantly improve treatment with older antiepileptic drugs (AED). In case of newer AEDs, drug concentrations are yet not routinely monitored, since the relationship between plasma concentrations and effects is still largely unknown. Nevertheless, to effectively optimise the treatment outcome and reduce side effects, drug doses and schedule of some newer AED should be personalized by the help of TDM (1, 2).

The aim of our study was to develop a new, sensitive method for the simultaneous determination of the four recent antiepileptic drugs pregabalin (PGB), gabapentin (GBP), vigabatrin (VGA) and topiramate (TOP) in human plasma. This is the first report of simultaneous determination of selected four AED.

MATERIALS AND METHODS

Standard sample preparation

Stock solutions (1 mg/ml) of VGA, TOP, PGB, GBP, and p-fluoro-DL-phenylalanine as internal standard (IS) were prepared in water. Standards for method validation were prepared by spiking 500 µl of plasma sample with 20 µl of analytes and 30 µl of IS solution to provide appropriate concentration ranges.

Extraction procedure

Plasma standards were mixed with 1 ml of 0.1 M HCl solution and loaded to the preconditioned (2 × 2 ml MeOH, 2 × 2 ml H_2O) Oasis MCX 60 mg/mL solid phase extraction (SPE) cartridges. After loading the samples the cartdiges were washed (2 × 1 ml 0.1 M HCl; 2 × 1 ml 50 mM KH_2PO_4 pH 5.0; 1 ml H_2O), dried, and samples eluted with 2 ml of 2M NH_3 in MeOH.

Derivatization procedure

To the dry extracted samples 200 µl of 5 mg/ml of 4-chloro-7-nitrobenzofurazan (NBD-Cl) in methanol:acetonitrile solution (1:1 vol/vol) and 25 µl of 250 mM H_3BO_3 pH 10.5 were added. The samples were derivatized at 60°C for 15 minutes.

Chromatographic conditions

The analyses were performed on HPLC system Agilent 1100/1200 series (Agilent Techologies Inc.). The chromatographic separation was obtained with a reversed-phase column (Agilent, Eclipse Plus C18, 150 × 4.6 mm, 5 µm) that was connected to the same type of precolumn. The mobile phase consisted of 57% of 50 mM KH_2PO_4 pH 4.90) and 43 % of methanol. The flow rate of the mobile phase was 1.5 mL/min, and the volume of injected samples was 5 µl. The derivatized samples were kept at 5°C in autosampler and detected with fluorescence detector set at excitation and emission wavelengths of 470 and 530 nm, respectively.

RESULTS AND DISCUSSION

The extraction of analytes from plasma samples was developed using SPE procedures. The SPE method using mixed mode reversed-phase strong cation exchanged was found suitable for extraction of all four analytes (Table 1).

As PGB, GBP, VGB and TOP have no significant ultraviolet or visible absorption, we chose derivatization procedure using NBD-Cl. This reagent enables derivatization of primary amines. We confirmed the reaction products by indentifying appropriate m/z of derivatives (Figure 1) using electrospray ionization tandem mass spectrometer operating in negative mode.

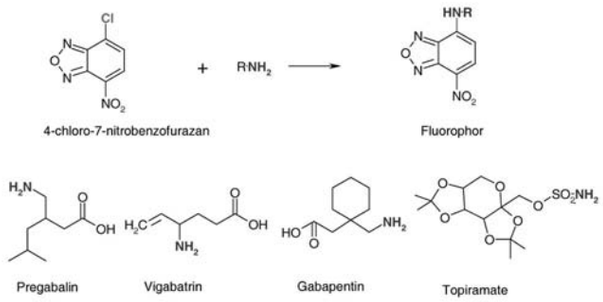

Fig. 1: Reaction scheme of 4-chloro-7-nitrobenzofurazan with amine group of pregabalin, vigabatrin, gabapentin and sulfamate group of topiramate.

The derivatization conditions in means of buffer concentration (50 - 250 mM) and pH (9-11), organic solution (methanol, acetonitrile and dichloromethane) were investigated. The optimal derivatization conditions required 250 mM borate buffer pH 10.5 and organic mixture with methanol and acetonitrile.

Developed reverse phase C18 chromatographic method is simple and suitable for routine TDM as it requires only common HPLC system configuration. The representative chromatograms of plasma samples are shown in Figure 2.

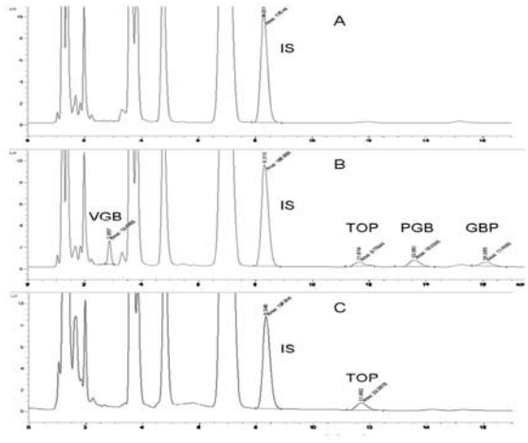

Fig. 2: Chromatograms of plasma blank (A), low quality control (B) and sample of patient receiving 25 mg of topiramate daily (C).

The method was validated according to FDA Guidance for Industry Bioanalytical Method Validation. It was found that it meet the criteria for intraday accuracy and precision and interday precision. The extraction recovery was higher than 82%, and limit of quantification was at least 0.5 µg/L for all four analytes. The linear ranges of analytes enable antiepileptic quantification in reported reference ranges (1).

Table 1: Summary of method validation parameters.

Validation parameter		VGB	TOP	PGB	GBP
Intraday accuracy and precision (RSD) in %; n=5	QC_l	104.5 (2.1)	111.5 (3.5)	100.7 (2.4)	100.1 (1.3)
	QC_m	103.7 (2.1)	101.8 (1.6)	100.8 (1.2)	99.9 (1.3)
	QC_h	105.8 (2.4)	103.1 (5.8)	101.7 (1.1)	101.6 (1.2)
Interday precision (RSD) in %; n=5	QC_l	9,8	7,1	2,5	4,9
	QC_m	9,7	3,9	6,1	6,0
	QC_h	9,2	9,8	4,8	4,3
Extraction recovery (%)		84.1	94.9	82.1	85.7
Lim. of quant. (µg/L)		0.5	0.5	0.375	0.375
Linear range (µg/L)		0.5 – 30	0.5 – 20	0.375 – 30	0.375 – 30

RSD- relative standard deviation; QC_l, QC_m, QC_h - low, medium, and high quality control plasma samples; Lim. of quant. - limit of quantification.

CONCLUSIONS

The developed method for determination of VGB, TOP, PGB, and GBP in plasma samples meets the validation criteria and it is appropriate for use in routine TDM. Moreover, this is the first reported method which employs simultaneous quantification of all four antiepileptic drugs.

REFERENCES

1. Patsalos PN, Berry DJ, Bourgeois BF, Cloyd JC, Glauser TA et al. Antiepileptic drugs—best practice guidelines for therapeutic drug monitoring: a position paper by the subcommission on therapeutic drug monitoring, ILAE Commission on Therapeutic Strategies. Epilepsia. 2008; 49: 1239-76.
2. Vovk T, Jakovljević MB, Kos MK, Janković SM, Mrhar A te al. A nonlinear mixed effects modelling analysis of topiramate pharmacokinetics in patients with epilepsy. Biol. Pharm. Bull. 2010; 33:1176-82.

LIPOPROTEIN ASSOCIATED PHOSPHOLIPASE A_2 AND ATHEROTHROMBOTIC RISK FACTORS RESPONSE TO COMBINED LIPID LOWERING THERAPY IN PATIENTS WITH CORONARY ARTERY DISEASE

Z. Fras[1,*], J. Osredkar[2], C. Rezar[2], D. Latifić Jasnić[3], N. Ružič Medvešček[3], M. Mulej[4], M. F. Kenda[3]

[1] UMC Ljubljana, Division of Internal Medicine, Dpt of Vascular Medicine, Zaloška 7, SI-1525 Ljubljana, Slovenia, [2] UMC Ljubljana, Institute for Clinical Chemistry and Biochemistry, Njegoševa 4, SI-1525 Ljubljana, Slovenia, [3] UMC Ljubljana, Division of Internal Medicine, Dpt of Cardiology, Zaloška 7, SI-1525 Ljubljana, Slovenia, [4] General Hospital Jesenice, Dpt for Internal Medicine, Jesenice, Slovenia

INTRODUCTION

Lipoprotein-associated phospholipase A_2 (PLA_2) is a proinflammatory enzyme secreted by macrophages that is primarily bound to LDL-C in the circulation (1). It plays a crucial role in a number of diverse cellular responses, since it hydrolyzes oxidized phospholipids to lysophospha-tidylcholine and oxidized fatty acids, which have proinflammatory properties, and its activity is increased in small, dense LDL (2). PLA_2 is found in both LDL and HDL particles. The release of LDL-associated oxidative products by PLA_2 may potentially worsen atherosclerotic lesions, while overexpression of PLA_2 in HDL particles may potentially reduce CHD risk (3). Human studies have suggested that Lp-PLA_2 is a risk factor for coronary artery disease (CAD) (4). Atorvastatin has been shown to preferentially reduce LDL-associated Lp- PLA2, presumably through the reduction in LDL-C levels, while HDL-associated Lp-PLA2 did not appear to be affected (5, 6). This represents one potential mechanism of action explaining the reduction in CAD events with statins. Combined lipid lowering drug therapy, e.g. with statins and/or fibrates - with comple-

mentary mechanisms of action - has been proposed not only as a means of improving lipid-modifying efficacy but also with some other potential anti-atherothrombotic effects, including the modification of hemostatic factors, as well as the inhibition of inflammatory mediators involved in atherogenesis (6). Animal studies have demonstrated that inhibition of Lp-PLA2 may be anti-atherogenic and thus, inhibitors of this enzyme may represent novel therapies that specifically target the atherosclerotic processes in the arterial wall (1, 4). Anyhow, the human clinical implications of these potential positive therapeutic effects remain to be established.

AIM OF THE STUDY

The main aim of the present study was to elucidate the separated and joint effects of the long-term (12 months) treatment with statins and/or fibrates on various athero-thrombotic risk factors in a prospective, randomised, open and intention-to-treat study in high-risk patients with various types of CAD.

MATERIALS AND METHODS

109 consecutive CAD patients (mean age 59,5 (±10,4) years were randomly allo-cated into two treatment groups, receiving either fenofibrate (250 mg/day) or simvastatin (20 mg/per day). At the first follow-up visit (at 12 weeks) the groups were further halved randomly - till the end of the study (52nd week) patients received either fenofibrate (250-500 mg/d) (group F), fenofibrate (250 mg/d) + simvastatin (10 mg/d) (group F+S), simvastatin (20 mg/d) (group S) or simvastatin (10 mg/d) + fenofibrate (250 mg/d) (group S+F). Plasma lipid and fibrinogen levels were measured by standard methods , and PLA_2 by a colorimetric assay using sPhospholipase A Assay Kit (IBL, Immuno-Biological Laboratories, Hamburg, Germany).

RESULTS

Simvastatin alone decreased total cholesterol (TC) significantly more than fenofibrate (-18,3 % vs. -8,9 %), while it was decreased by -20,9% and -21,2 % in combined therapy groups. Fenofibrate increased HDL-C significantly more than simvastatin (by +9,6% vs. +1,7%), while in statin-fibrate group it increased by +7,7 – 8,3%. The mean baseline fibrinogen levels (4,85±1.34 mg/l) decreased on average significantly more by fenofibrate alone, -34 % (group F), while there were no significant differences betwen the rest of the three treatment groups, -23,7% (group S), -25,4% (group F+S), and -22% (group S+F). During 12 months of therapy the serum PLA_2 activity decreased significantly more using the statin therapy alone (-16,6%), while significant increases were established in patients treated with fibrates alone (+12,1%) or combination of statins and fibrates (+17,1%) ($p<0,005$). Significant correlations of serum PLA_2 were observed with decreased TC, total triglyceride, and LDL-C. The absence of a correlation with HDL-C suggests that the PLA_2 activity of HDL is not related to its total concentration, but rather to an as yet undetermined functional or structural property of HDL particles, possibly associated with TC or triglyceride levels.

CONCLUSIONS

The simvastatin-fenofibrate lipid lowering combination has a highly beneficial and more prominent effect than monotherapy on all lipid parameters by which it significantly improves overall patient's risk status. From the results of the present study it can also be concluded that besides its effects on blood lipids, the benefical alterations in other atherothrombotic / proinflammatory atherosclerotic markers were exerted by combined statin-fibrate treatment. The trend of increasing activity of serum PLA_2 during one year of combined lipolytic therapy could be explained as a manifestation of antiatherogenic role of $sPLA_2$ (6). If its changes induced with lipid lowering drugs are related to the reduction in clinically manifest events observed in clinical trials, then it can be defined as the novel target for therapy to reduce cardiovascular risk (7). Future studies should determine whether selective inhibition of PLA_2 reduces ischemic cardiovascular events and whether statins and/or fibrates are more effective for their prevention in patients with elevated levels of PLA_2(8).

REFERENCES

1. Hurt-Camejo E, Camejo G, Peilot H, Öörni K, Kovanen P. Phospholipase A2 in Vascular Disease. Circ Res 2001; 289-298.
2. Mallat Z, Benessiano J, Simon T, et al. Circulating Secretory Phospholipase A2 Activity Events in Healthy Men and Women. Arterioscler Thromb Vasc Biol 2007;27:1177-1183.
3. Virani SS, Nambi V. The Role of Lipoprotein-associated Phospholipase A2 As a Marker for Atherosclerosis. Curr Atheroscl Rep 2007;9:97-103.
4. Nambi V, Ballantyne MC. Lipoprotein-associated Phospholipase A2: Pathogenic Mechanisms and Clinical Utility for Predicting Cardiovascular Events. Curr Ather Rep 2006;8:374-81.
5. Papathanasiou AI, Lourida ES, Tsironis LD, Goudevenos JA, Tselepis AD. Short- and long-term elevation of autoantibody titers against oxidized LDL in patients with acute coronary syndromes. Role of lipoprotein-associated phospholipase A2 and the effect of atorvastatin treatment. Atherosclerosis. 2008;196:289-97.
6. Saougos VG, Tambaki AP, Kalogirou M, et al. Differential Effect of Hypolipidemic Drugs on Lipoprotein-Associated Phospholipase A2. Arterioscler Thromb Vasc Biol 2007;27:2236-43.
7. Robins SJ, Collins D, Nelson JJ, Bloomfield HE, Asztalos BF. Cardiovascular Events With Increased Lipoprotein-Associated Phospholipase A2 and Low High-Density Lipoprotein-Cholesterol. The Veterans Affairs HDL Intervention Trial. Arterioscler Thromb Vasc Biol 2008;28:1172-78.
8. Anderson JL. Lipoprotein-Associated Phospholipase A2: An Indipedend Predictor of Coronary Artery Disease Events in Primary and Secondary Prevention. Am J Cardiol 2008; 101:23-33.

PERFORMANCE EVALUATION OF DIFFERENT HPLC COLUMNS IN SILDENAFIL AND TADALAFIL ANALYSIS

Z. Poposka*, M. Shishovska, Z. Arsova–Sarafinovska, D. Doneva, K. Starkoska, Z. Mustafa

Institute for Public Health of the Republic of Macedonia, 50 Divizija 6, 1000 Skopje, Republic of Macedonia

INTRODUCTION

Sildenafil and tadalafil are oral drugs used to treat male sexual function problems (impotence or erectile dysfunction) by blocking an enzyme 5-phosphodiesterase in the body. However, there is no analytical method for determination of these two active compounds in pharmaceutical preparations in the current European and US Pharmacopoeia. The aim of this study was to evaluate performance of the various HPLC columns in sildenafil and tadalafil analysis using validated HPLC method.

MATERIALS AND METHODS

The following columns were compared: LiChrospher® 100 RP-18 (250 x 4 mm i.d., 5 µm); Hypersil BDS-C18 (125 x 4 mm i.d., 5 µm) and Chromolith® Performance RP-18e (100 x 4.6 mm i.d., monolithic rod). The performance evaluation was done by comparison of the following parameters: resolution (*Rs*), back-pressure (Δ*P*, bar), and theoretical plate height (*ΔH*, µm) in correlation with flow-rate (*u*, mL/min).

HPLC analyses were performed using a Schimadzu LC-2010 chromatographic system (Schimadzu, Kyoto, Japan) consisting of a LC-20AT Prominence liquid chromatograph pump with DGU-20A5 Prominence degasser, a SPD-M20A Prominence Diode Array Detector, RF 10AXI fluorescence detector and a SIL-20 AC Prominence auto sampler. Data analyses were done using Class VP 7.3 Software. The mobile phase consisted of a phosphate buffer (20 mM, pH 2.8)-acetonitrile (71:29, *V/V*) at controlled temperature (25ºC) and autosamler temperature at 4 ºC. Detection of sildenafil and tadalafil was carried out at 285 nm.

RESULTS AND DISCUSSION

Chromatographic peak resolution data (*Rs*) obtained are acceptable for all three tested columns with values higher then the limit given in Ph.Eur. (>1.5) (Fig. 1). The best peak resolution data showed the longest column, as it was expected.

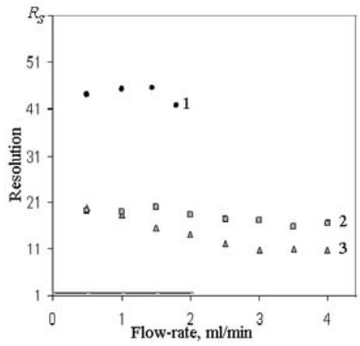

Fig. 1: Correlation between flow-rate and resolution: LiChrospher® 100 RP-18 (1); Hypersil BDS-C18 (2) and Chromolith® Performance RP-18e (3).

There is a significant difference between column back-pressure using different flow-rate. Thus, the longest column was tested only at flow-rate up to 2 ml/min because its high back-pressure induced by increasing flow-rate. The other two columns were tested up to flow-rate of 4 ml/min. The monolithic rod column generates fourfold lower back-pressure in comparison with the longest column, and nearly twice lower back-pressure then the other column.

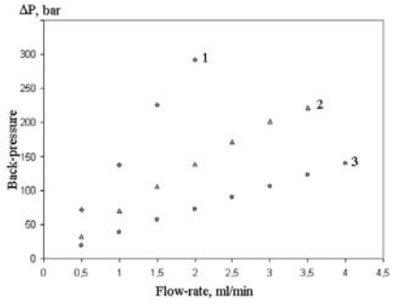

Fig. 2: Correlation between flow-rate and back-pressure: LiChrospher® 100 RP-18 (1); Hypersil BDS-C18 (2) and Chromolith® Performance RP-18e (3).

The efficiency of the columns is presented by the van Deemter plots. According to the results, the most efficient column is the longest column packed with particles, but the flow-rate which might be used is limited at maximum 2 ml/min. The shorter column packed with particles showed the worst efficiency in comparison with other tested columns. This column has acceptable efficiency only up to flow-rate of 1 ml/min. With increasing flow-rate its efficiency dramatically decreases. The van Deemter plot of the monolithic rod column demonstrates clearly that separation efficiency does not decrease significantly when the flow-rate is increased, as it is the case with particulate columns. Therefore it is possible to operate with this type of columns at higher flow-rate without loss of peak resolution. The same conclusion for efficiency of the columns is obtained for the both tested compounds, but the results obtained for tadalafil are better in comparison with those for sildenafil.

CONCLUSIONS

According to all experimental results obtained, the monolithic rod column is a column of choice for tadalafil and sildenafil analysis. Using this column means shorter analysis time (for factor 3.6) in comparison with the longest column. Additionally, it is important to be mentioned that decreased consumption of organic solvent considerably reduces the laboratory expenses.

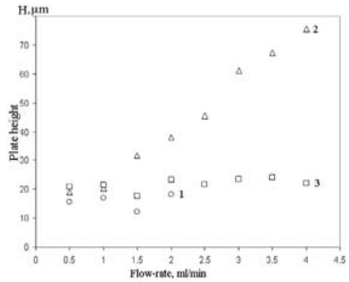

Fig. 3: Correlation between flow-rate and plate height obtained for sildenafil: LiChrospher® 100 RP-18 (1); Hypersil BDS-C18 (2) and Chromolith® Performance RP-18e (3).

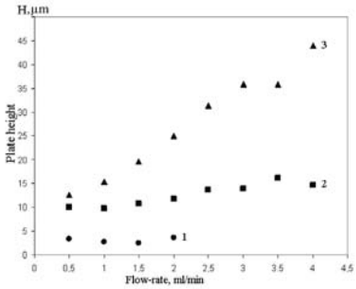

Fig. 4: Correlation between flow-rate and plate height obtained for tadalafil: LiChrospher® 100 RP-18 (1); Hypersil BDS-C18 (2) and Chromolith® Performance RP-18e (3).

REFERENCES

1. Rabbaa-Khabbaz L, Abi Daoud R. A Sensitive and Simple High Performance Liquid Chromatographic Method for Quantification of Tadalafil in Human Serum. J App Res. 2006;6(1): 170-5.
2. Pomerol JM, Rabasseda X. Tadalafil, a further innovation in the treatment of sexual dysfunction. Drugs Today (Barc). 2003;39:103-13.
3. Francis SH, Morris GZ, Corbin JD. Molecular mechanisms that could contribute to prolonged effectiveness of PDE5 inhibitors to improve erectile function. Int J Impot Res. 2008 Jul-Aug;20(4):333-42.
4. Daugan A, Grondin P, Ruault C, Le Monnier de Gouville AC, Coste H, Kirilovsky J, Hyafil F, Labaudinière R. The discovery of tadalafil: a novel and highly selective PDE5 inhibitor. 1: 5,6,11,11a-tetrahydro-1H imidazo[1',5':1,6]pyrido[3,4-b]indole-1,3(2H)-dione analogues. J Med Chem. 2003 Oct 9;46(21):4525-32.

OPTIMATION OF AIR VOLUME IN TABLET COATING PROCESS WITH SCALE DOWN METHOD

P. Kása[1*], T. Sovány[1], A. Kiss[2], K. Pintye-Hódi[1]

[1] University of Szeged, Department of Pharmaceutical Technology, H-6720, Eötvös u. 6. Szeged, Hungary; [2]Béres Pharmaceuticals Ltd., H-5000, Nagysándor József u. 39., Szolnok, Hungary

INTRODUCTION

In the pharmaceutical industry the coating process of the solid preparations needs almost the highest energy and cost. One of the main aim of the formulators, to prepare the best preparation with a most economic way. To ensure the clear and filtered air during coating is very expensive because of the length of the coating procedure. The applied volume of the air depends on the size and the geometric parameters of the coating pan. The coater manufacturers develop different equipment with a different drum size and geometry, which causes a difficulty in the process adoption from one to another equipment. If the process conditions including the equipment parameters are well known the procedure transfer or scaling up or down is most simple and cost effective.

MATERIALS AND METHODS

Materials

There were four different tablet preparations with different size and geometry which was used for the optimization (T1, T2, T3, and T4), and four different coating materials.

Methods

To optimize the process parameters a laboratory scale perforated coating pan was used (Formate 4M8 Pro-C-epT, Belgium). Before the optimization it was necessary to compare the geometric parameters and the applied air volume of the different equipment. For the comparison the following equation was used:

$$V_{drum} = R\Pi l + 2\frac{k\Pi(R^2 + Rr + r^2)}{3}$$

where V_{drum} = the volume of the drum, R = radius of the drum, r = the radius of the drum throat, *l* = the breadth of the perforated part, and k = the height of the truncated cone.

The used volume of the air was calculated by the next formula:

$$\frac{V_1}{A_1} = \frac{V_2}{A_2}$$

where V_1 and V_2 are the volumes of the drums, A_2 and A_2 are the volumes of the air.

The results was compared with two industrial scale coating equipment Accelacota 350 and CSI Technicota. Both equipment has a horizontal perforated drum with different volume, size, and shape.

RESULTS AND DISCUSSION

The first important step was to compare the technical data of the drums (Table 1.)

The investigations were prepared with a 4M8 Pro-C-epT lab scale equipment which has a same layout perforated drum. The process data was recorded, and collected by a built in computer (Fig. 1).

Table 1: Technical data of the different coaters

Param	Unit	Accelacota	Technicota	Pro-C-epT
D	mm	1530	1220	203
L	mm	1400	970	145
d	mm	600	380	145
D/L		0.91	0.79	0.71
V	m^3	1.897	1.358	0.0042
A	m^2	1.514	0.837	0.021
Nozzle	num	5	3	1
Nozzle	mm	1.2	1.2	0.75
NDis	mm	250-300	250-300	50-55

D=drum diameter; L=drum deep; d=drum throat; V=drum volume; A=effective surface; NDis=nozzle distance from the core.

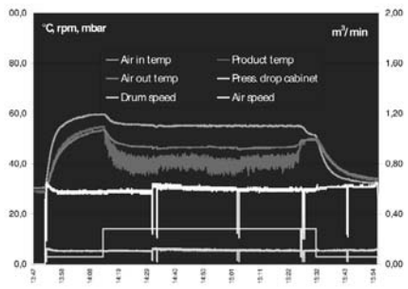

Fig. 1: Recorded data from Pro-C-epT equipment during preparation process

Before the investigations there was necessary to convert the required amount of the air volume and the liquid addition speed from the originally used coaters to the lab scale equipment.

In the case of T1 sample the air volume was decreased to the minimum capacity of the Pro-C-epT equipment and the liquid addition speed was increased three times faster than the original was. In all runs the properties of the coated film was sufficient.

To prepare an appropriate film on the T2 sample the air volume was decreased with 20% and the liquid addition was increased about two times more than the original process.

To prepare an appropriate film on the tablet surface in the case of T3 sample there was necessary to increase the amount of the air with 17%, but the speed of the coating liquid addition was possible to increase more than double than the initial was.

In the case of the T4 sample the necessity of the air volume for the correct coating formation was 20% more than the initial, but there was possible to increase the liquid addition more than 100% which decrease the coating process time.

CONCLUSIONS

It can be concluded that after the final calculation the necessity of the clear and filtered air can be decreased in all cases which results a more economic coating process (Table 2).

Table 2: Amount of the air volume after optimation

	Air volume		
	original	optimated	difference
T1	1	0.40	-60%
T2	1	0.56	-44%
T3	1	0.86	-14%
T4	1	0.80	-20%

The total savings of the air volume is more than 30% which assure a significantly economic coating process.

ACKNOWLEDGEMENT

The Project named „TÁMOP-4.2.1/B-09/1/KONV-2010-0005 – Creating the Center of Excellence at the University of Szeged" is supported by the European Union and co-financed by the European Regional Development Fund.
www.nfu.hu, www.esza.hu

REFERENCES

1. R. Turton, X.X. Cheng: The scale-up of spray coating processes for granular solids and tablets, Powder Techn. 150 (2005) 78–85
2. R. Mueller, P. Kleinebudde: Influence of scale-up on the abrasion of tablets in a pan coater, Eur.J.Pharm.Biopharm. 64 (2006) 388–392
3. P. Pandey et all: Scale-up of a Pan-Coating Process, AAPS PharmSciTech 2006; 7 (4) Article 102

COMPARISON OF CRYSTALLINE AND DIRECTLY COMPRESSIBLE IBUPROFEN FOR PREPARATION OF BI-LAYER TABLETS

T. Sovány[1*], K. Papós[1], P. Kása Jr.[2], I. Ilić[2], S. Srčič[2], K. Pintye-Hódi[1]

[1] University of Szeged, Faculty of Pharmacy, Department of Pharmaceutical Technology, H-6720, Eötvös utca 6, Szeged, Hungary; [2] University of Ljubljana, Faculty of Pharmacy, Department of Pharmaceutical Technology, 1000, Aškerčeva cesta 7, Ljubljana, Slovenia

INTRODUCTION

The use of combination preparations has advantages in the medication treatment. The patient compliance can be significantly improved with reduction of the number of necessary preparations. A fixed combination of multiple agents will therefore provide enhanced therapeutic effect (1). However, a number of problems, such as chemical incompatibility or the need of different dissolution profiles for each drug can occur. These problems can be potentially solved by the formulation of bi-layer tablets. Small contact surface between the two layers reduces the possibility of chemical interactions, and separate dissolution profiles for each layer can be provided as well. Nevertheless, the formulation of such dosage form has considerable challenges, such as propagation of lamination. This necessitates better understanding how the physicochemical properties of materials and their interactions influence the mechanical behaviour of the bi-layer tablets, which can show considerable differences from single layer tablets (2).

MATERIALS AND METHODS

Materials

Drotaverine HCl (Sanofi-Aventis-Chinoin, Budapest Hungary), crystalline ibuprofen (Sanofi-Aventis-Chinoin, Hungary), ibuprofen DC 85 (BASF, Germany), microcrystalline cellulose (Vivapur 102, J. Rettenmeier & Söhne, Germany), modified maize starch (Starch 1500, Colorcon, UK), agglomerated lactose (Tablettose, Meggle Pharma, Germany).

Methods

The surface free energies of the materials were determined with a Dataphysics OCA 20 contact angle tester, with use of sessile drop method. The method is based on the measurement of equilibrium contact angle, the value of which is determined by the interfacial energies of the solid, liquid and vapour phases, as described by the Young equation. Disperse and polar components of the solid materials surface energies were calculated by using the Wu equation and by considering the polar and nonpolar parts of test liquids (water and diiodomethane) surface tensions. The contact angles were determined on comprimates prepared with a Specac hydraulic press (Specac Inc, UK) at a pressure of 4 tons.

The plasticities of the materials and their mixtures were established via force-displacement measurements with a computer-connected Korsch EK0 eccentric tablet press (E. Korsch Machienenfabrik, Germany), instrumented with strain gauges on both punches and a displacement transducer. The materials were filled into the die and compressed manually (to ensure similar conditions for a well and poorly compressible material) in the compression force range from 1 to 30 kN.

The bi-layer tablets were prepared using an instrumented eccentric tablet press Killian SP 300 (IMA Kilian, Germany).

The hardness of tablets was measured with VK 200 (Varian, USA) tablet hardness tester. A slide clipper (MIB Messzeuge GmbH., Germany) was used for the measurement of the tablet's geometric parameters.

The rate of drug dissolution was determined with Erweka DT 700 (Erweka GmbH, Germany) dissolution tester. The samples were collected automatically, and the concentrations were measured by using a Unicam Helios α UV-VIS spectrophotometer (Unicam, UK).

RESULTS AND DISCUSSION

It was found in the preliminary experiments, when pure materials were compressed into the bi-layer tablets, that one of the main causes of lamination was the difference between the cohesive forces inside a layer and the adhesive forces between the two layers. In this case an extensive difference between the hardness of these layers was observed as well. The data showed that tablets prepared with different types of ibuprofen exhibited considerable difference in their mechanical properties. This different behaviour cannot be explained only by different cohesiveness, as added hydrophilic excipients changed the surface free energy of DC ibuprofen minimally compared to the crystalline one. However, there was a considerable difference in their compressibility behaviour.

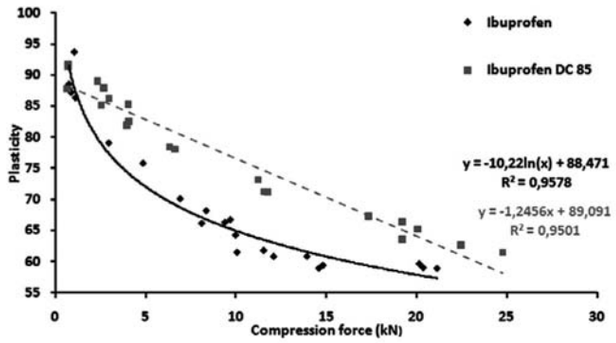

Fig. 1: Plasticity vs. compression force of two different types of ibuprofen.

The directly compressible (DC) ibuprofen has significantly better plasticity (Fig. 1), which results in considerably higher tablet hardness. This significantly improves the mechanical properties of tablets and has an essential role in the reduction of the lamination of the bi-layer tablets. Nevertheless, the addition of hydrophilic excipients did have favourable effect not only on the mechanical properties; however, it significantly improved the dissolution rate of the drug as well (Fig 2).

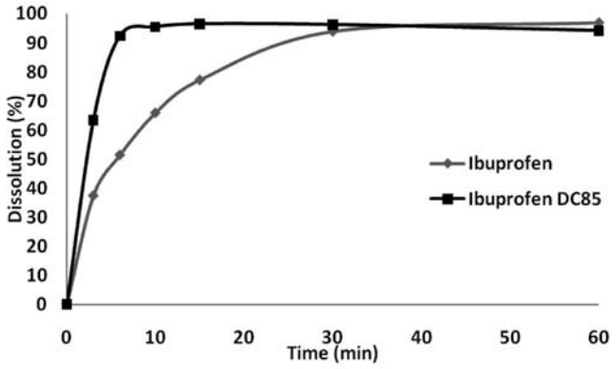

Fig. 2: Dissolution profiles of the two ibuprofen formulations.

CONCLUSIONS

Understanding the relationship between physicochemical properties of materials (both APIs and excipients) and mechanical properties of tablets enables elimination of the problems during the tabletting and optimization of the bi-layer tablets mechanical properties.

ACKNOWLEDGEMENT

The Project named „TÁMOP-4.2.1/B-09/1/KONV-2010-0005 – Creating the Center of Excellence at the University of Szeged" is supported by the European Union and co-financed by the European Regional Fund.
www.nfu.hu

REFERENCES

1. Rosenthal T, Gavras I. Fixed-Drug Combinations as First-Line Treatment for Hypertension Prog. Cardiovasc. Dis. 2006; 48:416-425.
2. Belda PM, Mielck JB. Considerations about the theoretically expected crushing strength of tablets from binary powder mixtures: Double layer tablets versus arithmetic additivity rule. Eur. J. Pharm. Biopharm. 2006; 64:343–350.

COEFFICIENT OF RESTITUTION OF SELECTED NEUTRAL AND COMMERCIAL PELLETS

R. Šibanc*, R. Dreu

University of Ljubljana, Faculty of Pharmacy, Aškerčeva cesta 7, 1000 Ljubljana, Slovenia

INTRODUCTION

Coefficient of restitution (COR) is an impact property defined as the ratio of rebound and impact velocity (1). It is an important parameter that is used in computer simulations, such as computational fluid dynamics (CFD) and discrete element method (DEM). CFD and DEM can be used to analyze process equipment and processes, study operating conditions such as the effect of particle size and the design of new equipment (2). Simulations provide additional information to experiments; however care must be taken to validate simulation results using experimental data. In order to obtain correct simulation results appropriate models must be chosen, as well as correct material properties and process boundary conditions. Material properties of pellets that are important for CFD and/or DEM simulations are: distribution of particle size, density, coefficient of friction, coefficient of restitution and others. The aim of this study was to obtain COR for wide range of neutral pellet cores and commercial pellets.

MATERIALS AND METHODS

Materials

Microcrystalline cellulose neutral pellets (Cellets 700, Harke Pharma, Germany) and neutral sugar spheres (Pharm-a-spheres, 710-850 µm, Hanns G. Werner GmbH, Germany) were used in experiments. Cellets 700 were sieved using sieves 900 and 1000 in order to obtain narrow particle distribution. Alventa, Asasantin, Bazetham, Effectin, Lanzul S, Naklofen Duo, Olfen, Olicard, Ortanol S, Sporanox, Tanyz and Teotard capsules filled with pellets were obtained from local pharmacy. Glass spheres (SiLibeads type GZ, Sigmund Linder, Germany) were for comparison.

Determination of COR

Pellets were released onto a steel plate from five different heights using a nozzle connected to a vacuum system. These five heights correspond to impact velocity of 300, 500, 1000, 2000 and 3000 mm/s. Each impact was recorded with a high speed camera Casio Exilim EX-F1 equipped with Raynox DCR-150 macro conversion lens. Macro lens enabled shallow depth of field, which helped to determine movement in and out of focus plane. Recordings were done at 600 frames per second using shutter speed of 1/8000, aperture value of F/2.8 and ISO 400. Samples were released from each height until 20 valid measurements were obtained. Measurements in which significant particle rotation or movement perpendicular to focus plane was observed were considered invalid. Data points were fitted to equation using Wolfram Mathematica for each pellet type, where e is COR and v_i is impact velocity.

RESULTS AND DISCUSSION

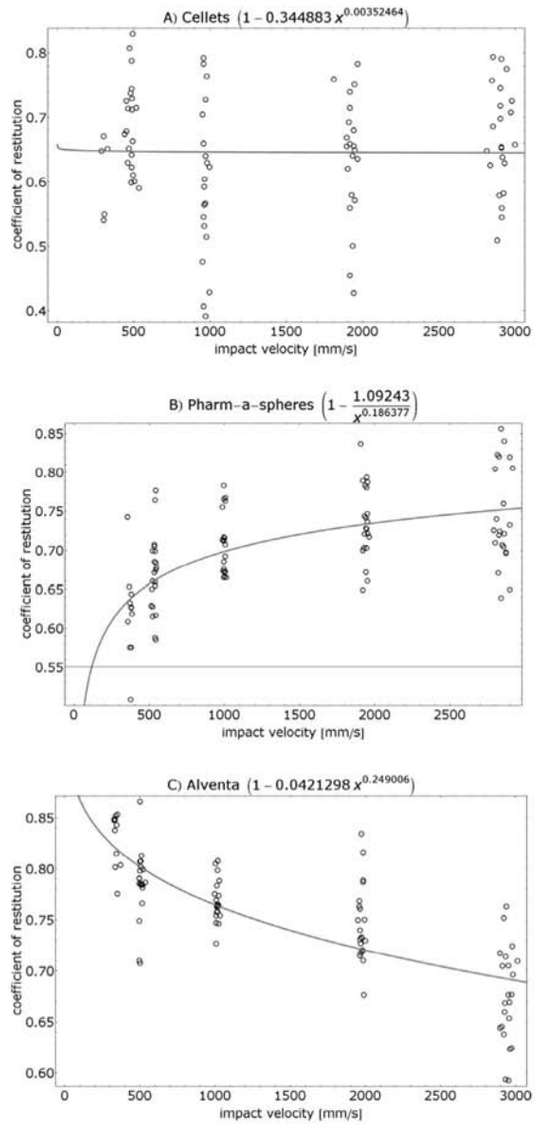

Fig. 1: Coefficient of restitution data and fitted equations as a function of impact velocity for A) Cellets B) Pharm-a-spheres C) Alventa

Values of COR between pellets and steel plate are mostly in the range of 0.5 to 0.9, with average about 0.7. The results of COR measurements can be put into three distinct groups: a) COR does not vary significantly with impact velocity b) COR increases with impact velocity c) COR decreases with impact velocity. Two pellets sample can be put into the first group: Cellets (Fig 1 A) and Asasantin and two pellets sample can be put into second group: Pharm-a-spehres (Fig 1 B) and Olicard. According to patient information leaflet Olicard pellets contain sugar and we can assume that this sugar is the core of this pellets and therefore the results of Pharm-a-spheres and Olicard pellets are very similar. All other tested pellets as well as glass spheres show decrease of COR with increase of impact velocity (Fig 1 C), which is normal behaviour for viscoelastic materials and is expected for pellets with polymer coatings.

All average COR values for all pellets and each tested velocity are collected in the Table 1. Results show that glass beads have higher COR in impact

with steel than any tested pellets, ranging from 0.960 at the lowest impact velocity (300 mm/s) and to 0.824 at the highest tested impact velocity (3000 mm/s). Interestingly the lowest two values of COR at the lowest impact velocity were for both neutral cores – 0.619 for sugar and 0,667 for microcrystalline pellets. The highest COR of pellets at lowest velocity was 0.843 and at the highest velocity the values of COR of pellets were between 0.568 and 0.760.

Table 1: Coefficient of restitution for all tested pellets measured with steel plate

Impact velocity sample	300 mm/s	500 mm/s	1000 mm/s	2000 mm/s	3000 mm/s
Alventa	0,830	0,785	0,768	0,746	0,675
Asasantin	0,750	0,600	0,710	0,691	0,630
Bazetham	0,802	0,799	0,764	0,758	0,722
Cellets	0,667	0,689	0,597	0,638	0,667
Efectin	0,822	0,769	0,754	0,702	0,705
Lanzul S	0,802	0,790	0,783	0,765	0,726
Naklofen Duo	0,772	0,748	0,704	0,680	0,687
Olfen	0,721	0,677	0,619	0,609	0,607
Olicard	0,710	0,713	0,735	0,738	0,749
Ortanol S	0,843	0,797	0,780	0,758	0,776
Sporanox	0,791	0,771	0,768	0,735	0,728
Pharm-a-spheres	0,619	0,668	0,709	0,735	0,744
Tanyz	0,810	0,749	0,759	0,698	0,760
Teotard	0,697	0,662	0,597	0,594	0,568
Glass	0,960	0,943	0,925	0,856	0,824

REFERENCES

1. Mangwandi C, Cheong YS, Adams MJ, Hounslow MJ, Salman AD. The coefficient of restitution of different representative types of granules. Chem Eng Sci. 2007 Jan;62(1-2):437-450.
2. Kremer DM, Hancock BC. Process simulation in the pharmaceutical industry: A review of some basic physical models. J Pharm Sci. 2006;95(3):517-529.

INFLUENCE OF CURING CONDITIONS ON DRUG RELEASE FROM CONTROLLED RELEASE PELLETS

K. Kristan, M. Horvat*

Lek Pharmaceuticals, d.d., Sandoz Development Center Slovenia, Verovškova 57, 1000 Ljubljana, Slovenia

INTRODUCTION

The curing process of a release controlling coating is one of the critical formulation and process steps in the development of oral modified release drug products (1, 2). To control the variability of drug release rates from latex polymer coated pellets we have studied the effect of humidity and curing time on the curing of the rate-controlling polymer film. Thirteen pellet samples were prepared according to an experimental design. The pellets underwent different curing condition and the respective dissolution results were used for establishing a process Design Space (3) for consistently achieving target dissolution.

MATERIALS AND METHODS

Preparation of controlled release pellets

The pellet cores containing microcrystalline cellulose and 3% of a representative BCS class 1 drug were manufactured by high-shear wet granulation (Collete Gral 150 PRO) and subsequent extrusion-spheronization (Gabler DE120 twin-screw extruder/Gabler R400 spheronizer, 0.8 mm die plate). The pellets were coated in a fluid bed coating system (Hüttlin HKC-50-DJ). The coating dispersion consisted of a mixture of plasticized ethylcellulose latex dispersion and hydroxypropyl methylcellulose pore former in mass ratio of 8:1. Pellets were additionally coated in a laboratory fluid bed system (HKC-05-TJ) with aqueous solution of hydroxypropyl methylcellulose, dried to LOD <3% and underwent curing in a tray drier at 60 °C. The samples were cured at different (controlled) air humidity and curing times:

PARAMETER	LEVEL SETTINGS
Humidity	15, 25, 35 g/kg
Time	1, 2, 3, 4 h
Temperature	60 °C

The studied conditions were chosen from a mixed-level full-factorial design with repetition of the center point (3×4+1).

Drug release from controlled release pellets

Dissolution testing was performed at 37 °C in 0.05 M phosphate buffer, pH 6.8 and specific hydrodynamic parameters which represent biorelevant conditions for the drug product under study. The samples were collected at predetermined times (1, 2, 3 and 4 h), filtrated and analyzed for API content using an Acquity UPLC System (Waters, MA, USA) equipped with a binary solvent manager, autosampler, column oven and PDA detector.

RESULTS AND DISCUSSION

Drug release studies

Release of API from pellets that underwent different curing conditions differ substantially (Fig. 1).

It is evident that air humidity has the most important effect; however, sufficient curing time is also important to achieve satisfactory dissolution (Fig. 2). Generally, higher moisture and longer times result in slower dissolution. However, significant interactions are clearly observed.

The dissolution profile of uncured pellets is shown for visual comparison.

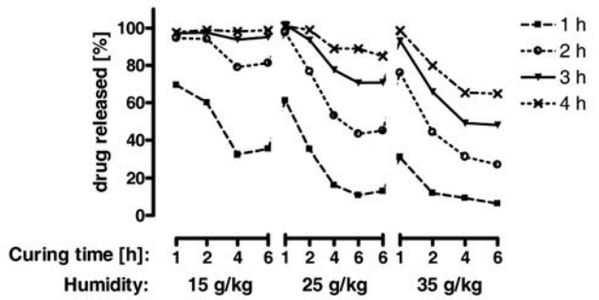

Fig. 1: The % of drug released from individual pellet samples at 1, 2, 3 and 4 hours.

Each selected dissolution time point was modeled as a function of curing process parameters. A parameterized non-linear model equation was found to be valid for all dissolution times. The obtained model shows good correlation to the experimental data (Fig. 3), with $R^2 = 0.98$, SD = 3.9%.

The obtained process Design Space (the multidimensional combination and interaction of input variables (e.g. material attributes) and process parameters that have been demonstrated to provide assurance of quality) is presented in Fig. 4, along with the most robust process point suggested. Curing time and humidity were both shown to have a significant effect on dissolution.

The systematic evaluation of curing process condition employing experimental design and modeling methodology allowed establishment of a curing process Design Space within limited time and resources. Using traditional approaches this would be difficult to achieve with same amount of resources due to significant nonlinearities and interactions.

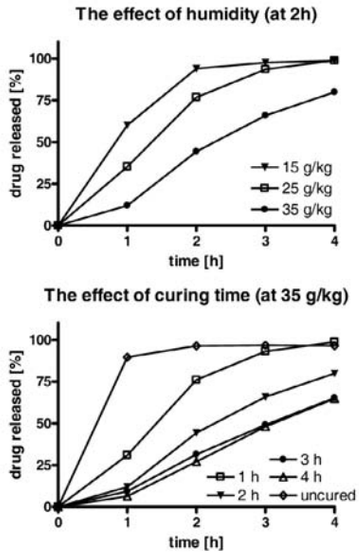

Fig. 2: The effect of humidity (above) and curing time (below) on drug release from control released pellets.

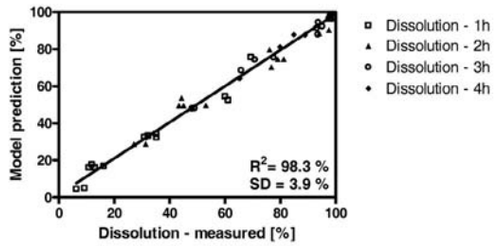

Fig. 3: Correlation between dissolution results and mode prediction at 1, 2, 3 and 4 hour time points.

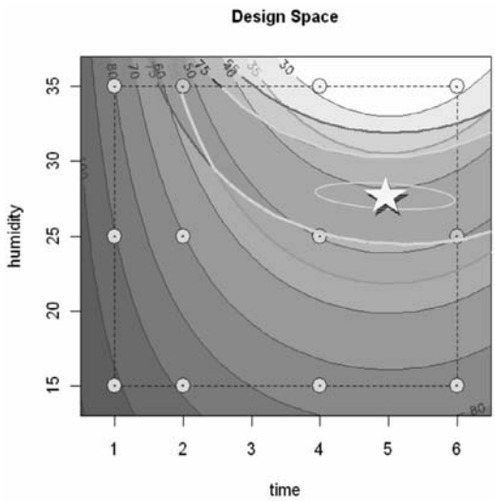

Fig. 4: Modified release pellets curing process Design Space region. Green shaded region represents the robust conditions, the yellow star indicating the most optimum point.

REFERENCES

1. Amighi K, Moes AJ. Influence of curing conditions on the drug release rate from Eudragit NE30D film coated sustained-release theophylline pellets. S.T.P. PHARMA SCIENCES. 1997; 7(2): 141–147.
2. Lee WP, Routh AF. Time evolution of transition points in drying latex films. JCT RESEARCH, 2006; 3(4); 301-306.
3. Guidance for industry: ICH Q8(R2) Pharmaceutical development, Federal Register, November 2009, Vol. 71, No. 98

EFFECTS OF PHYSICAL CHARACTERISTICS OF ACTIVE INGREDIENT ON ATORVASTATIN CALCIUM TABLETS

M.Vehabović*, N.Hodžić

Bosnalijek d.d., Jukićeva 53, 71000 Sarajevo, Bosnia and Herzegovina

INTRODUCTION

Equipment

Atorvastatin is a poorely soluble substance and a number of approaches have been developed in order to enhance dissolution rate and solubility. Particle size reduction and surface increase is one of them (1).

The objective of this study was to test the characteristics of the active substance by various manufacturers, as well as to define the factors which can influence the formulation and technology of producing film-coated tablets similar to the reference drug, more precisely selecting the formulation which can be used for further *in vivo* studies (bioequivalence)

MATERIALS AND METHODS

Materials

Raw materials of atorvastatin calcium from various manufacturers (A1- Ind Swift Lab. India, A2 - Biocon India, A3 - Teva Israel, A4 - Jubilant India, and A5 - Ranbaxy India) were used for preformulation tests. Formulation tests have been performed on tablets (core) and film-coated tablets, as well as samples of reference products (Zarator film-coated tablets 20mg, Pfizer, Portugal; Sortis film-coated tablets 20mg, Pfizer, Germany; Lipitor film-coated tablets 20mg, Pfizer Nederland.).

Using atorvastatin calcium, from three manufacturers (A1; A2; A5), tablet samples were prepared with a direct compression method. Samples of tablets and film-coated tablets 20mg were marked as P04, P05 and P06. The following excipients were also used: calcium carbonate DC, sodium laurylsulphate, lactose monohydrate, croscarmellose sodium, anhydrous silicon, talc, magnesium stearate and opadry II white.

Olympus BX51 was used for morphological characterization of API; Mastersizer 2000 for testing particle size, Van Kel 7025 for determining assay of atorvastatin in raw material samples, system for dissolution Cary VK7010 Van Kel and fraction collector VK8000 were used for determining dissolution of atorvastatin in the samples (tablets, film-coated tablets). For quantitative determination of atorvastatin assay in the samples, we used HPLC Shimadzu with PDA detector. From production equipment: a sifting machine with oscillator, type FREWITT MG 336, mixer Drum Blender, rotation press–CourtoyD Module S7, tablet coating machine Manesty, Accelacota XLlab01.

Morphological characterisation

The enlargement of 100 and 500X was used for the purpose of determining particle size, as well as similarity and difference between the raw materials of different manufacturers.

Particle size determination

Wet and dry methods were used for determining particle size of atorvastatin calcium. The specified particle size for atorvastatin calcium is d(0,9)<20µm.

Testing solubility of API

Phosphate buffer pH 6.8 was used as a solvent. The measurements were carried out at a wave length of 241 nm with UV spectrophotometry.

Dissolution of active ingredient, tablets and film-coated tablets

The method was done in accordance with method for dissolution of atorvastatin calcium from the tablet (2).

Comparing of dissolution profiles

Comparison of dissolution profiles helps in determining similarity between the products (3).

The mathematic model for comparing dissolution profile is calculated as follows:

$$f_2 = 50 \cdot \log_{10}\left\{\left[1+\frac{1}{n}\sum_{t=1}^{n}(R_t - T_t)^2\right]^{-0.5} \cdot 100\right\}$$

Where: f2 - similarity factor, n-number of points at a time, Rt- reference product dissolution values at time t, Tt – dissolution value of the test product at time t. f2 value between 50 – 100 confirms similarities between the two compared products. The samplings were done in the following time intervals: 5, 10, 15, 20, 25, 30 minutes.

RESULTS AND DISCUSSION

It was determined with microscopic tests that all the samples have particles having prism-shape and stick shape, and they do not differ much. Raw material A4 with d(0.9)<34.51 µm and with an expressive agglomeration (jumbled clusters), as well as bad solubility, was appraised as inconvenient for the production process. The raw material A3 with d(0.9)<364.91µm and the worst dissolution of the active ingredient, has been appraised as inconvenient for further processing. The remaining three raw materials have been proven to have a satisfactory distribution of the particle size (micronisation), better solubility and better dissolution. As such, they were evaluated as good candidates for production of tablets (core) and film-coated tablets with direct compression process.

With the same formulation and technological process, the obtained tablets (core) had similar dissolution profiles (from over 67% in 5th minute, to above 90% in 30th minute). Upon application of the film-coating, there was an insignificant reduction in the volume of dissolution (from 60% in 5th minute to 87% in 30th minute). Moreover, the tested dissolution profiles of the reference medications have shown similar results (from more than 70% in 5th minute to around 90% in the 30th minute). Cross-testing of similarity factor (f2) between the test samples (P04, P05, P06) and reference medicines, has given satisfactory results (Tables 1, 2 and 3.).

Table 1: Overview of similarity factor (f2) for test sample P04 and reference samples

Test sample	Reference sample	f2
P04	Zarator	f2=62,46
	Sortis	f2=58,95
	Lipitor	f2=62,43

Table 2: Overview of similarity factor (f2) for test sample P05 and reference samples

Test sample	Reference sample	f2
P05	Zarator	f2=78,09
	Sortis	f2=72,16
	Lipitor	f2=79,17

Table 3: Overview of similarity factor (f2) for test sample P06 and reference samples

Test sample	Reference sample	f2
P06	Zarator	f2=65,55
	Sortis	f2=69,52
	Lipitor	f2=62,61

CONCLUSIONS

In view of the above, it can be concluded that all three active ingredients can be used in the production process of atorvastatin film-coated tablets 20mg, noting that the best results were obtained with raw material A2 that was used for producing sample P05. At the same time, the raw material A2 had the best solubility and dissolution.

REFERENCES

1. Shargel L, Kanfer I, Generic Drug Development - Solid Oral Dosage Forms, Informa Healthcare 2004.
2. The United States Pharmacopoeia, USP 34-NF 29
3. Shah V.P, Tsong Y,. Sathe P, In vitro dissolution profile comparison - statistics and analysis of the similarity factor, f2. Pharm. Res. 1998; 15: 889-896.

UTILIZATION OF DISTRIBUTION LAMELLAS WITHIN FBD COATER AND THEIR INFLUENCE ON COATING UNIFORMITY AND PRESSURE DROP FLUCTUATIONS WITHIN THE DRAFT TUBE

M. Luštrik[1, 2*], M. Perpar[3], R. Dreu[1], S. Srčič[1], I. Žun[3]

[1] Faculty of Pharmacy, University of Ljubljana, Aškerčeva 7, 1000 Ljubljana, Slovenia; [2] Brinox d.o.o. Process systems, Sora 21, 1215 Medvode, Slovenia; [3] Faculty of Mechanical Engineering, University of Ljubljana, Aškerčeva 6, 1000 Ljubljana, Slovenia

INTRODUCTION

The goal of the fluid-bed coating process is to prepare particles with a well controlled thickness and even coating layer, especially when applying functional coatings. Numerous passes of particles through the spraying zone, result in a sufficient mass and thickness of coating layer. The amount of coating applied per-particle varies from the constructional design. It is connected with the number of particle passes through the spraying zone and sheltering effect. They are correlated with the volume fraction of particles inside the draft tube (1), motion of particles in the annular region (2) and inside the draft tube (3). The influence of special distribution lamellas in the annular region around the bottom part of the draft tube has been studied with regard to the hydrodynamics of two phase system and consequently on the pressure drop fluctuations within the draft tube and particle coating uniformity.

MATERIALS AND METHODS

Materials

Pellets (Cellets®, HARKE, and Germany) of a narrow size fraction (710-800µm) were used in each coating experiment. Coating polymer dispersion was comprised of 8.00% of hydroxypropyl methyl cellulose (Pharmacoat 606, Shin-Etsu, Japan), 1.00% of polyethylene glycol (PEG 6000, Fluka, Switzerland) and 1.09 % of coloring agent (Tartrazine, Sigma-Aldrich, Germany).

Methods

Set of coating experiments was conducted in a process chamber equipped with a swirl airflow generator and set of 30 lamellas, positioned radially between the outer wall of the draft and the wall of the process chamber. Reference measurements were performed in a swirl Wurster coating chamber without the lamellas at the bottom part.

Process parameters, i.e. inlet air flow (Φ) and draft tube height (H) (Fig. 1), were varied between coating experiments.

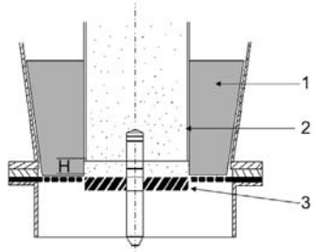

Fig. 1: Schematic diagram of lower part of coating chamber: 1- position of the lamellas, 2-draft tube, 3- swirl generator.

In each experiment 980 g of polymer dispersion was sprayed onto the pellet batches of 1000 g, using the binary nozzle. Pressure difference between the upper and lower edge of the draft tube were measured every 10 minutes of coating process for period of 60 seconds (Fig. 2.). Average of relative standard deviations of pressure drops, calculated from 60 seconds intervals of data logging (ΔP RSD), are listed in the table 1.
Spectrophotometric evaluation of the coloring agent distribution was carried out for sets of pellet samples, obtained from each coating procedure (3).

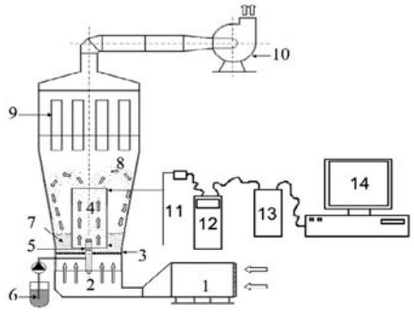

Fig. 2: Schematic diagram of experimental set up: 1-air preparation unit, 2-fluidizing air intake, 3- distribution plate 4-draft tube, 5-spray nozzle, 6-coating dispersion, 7- product, 8-particle motion, 9-filters, 10-exhaust fan, 11-pressure measuring points, 12-pressure sensor, 13-data logging unit, 14-computer.

RESULTS AND DISCUSSION

The results clearly indicate the influence of the hydrodynamics in the annular region to the flow inside the draft tube. When using the lamellas, lower ΔP RSD values were noticed in every experiment compared to the reference experiment. This is most probably the result of the reduced bubble formation in the annular region (Table 1). The formation of the bubble is hindered due to small distance between walls of the lamellas.
It can also be noticed that coating variation was higher in the experiments conducted in a chamber equipped with lamellas. The phenomena can be explained by reduced mixing of particles, due to reduced bubble formation in the annular region, before entering the draft tube. This presumably promotes the particles located closer to the wall of the draft tube to enter the spraying zone more often than the particles located in the vicinity of the wall of the chamber. As a result more coating is received.
Additionally, it is probable that some particles dwell for a longer period of time in the corner of the chamber wall and distribution plate when modified coater with lamellas is used.
Results surprisingly show that larger pressure drop fluctuations lead to more uniformly coated product as one would expect. The assumption that the homogenous flow of particles without disturbances would be the condition for homogenous coating is oversimplification of the phenomena.

Table 1: Coating chamber type (SW- swirl Wurster, SWL –swirl Wurster equipped with lamellas, Inlet flow Φ (m3/h), draft tube height H (mm), RSD of the pressure difference ΔP RSD (%) and coating variation (%).

Type	Φ (m3/h)	H (mm)	ΔP RSD (%)	Coating variation (%)
SW	105	10	17,22	6,42
SWL	105	10	15,66	7,73
SW	105	20	30,94	6,26
SWL	105	20	25,69	6,98
SW	156	10	18,38	5,10
SWL	156	10	16,01	5,35
SW	156	20	39,36	4,31
SWL	156	20	28,67	6,62

CONCLUSIONS

Use of lamellas reduces the mixing of particles in the annular region of the chamber, leading to more heterogeneously coated pellets. The effect of lamellas is observed and confirmed by the measurement of the relative standard deviation of the pressure drop within the draft tube. Included lamellas led to lower pressure fluctuations due to reduced bubble formation in the annular region, which resulted in higher coating thickness variations.

REFERENCES

1. Cheng XX, Turton R. The prediction of variability occurring in fluidized bed coating equipment. II. The role of nonuniform particle coverage as particles pass through the spray zone. *Pharm Dev Tech*, 2005, (3), 323-32.
2. Wang LK, Heng PWS, Liew CV. Classification of annular bed flow patterns and investigation on their influence on the bottom spray fluid bed coating process. *Pharm Res*, 2010, 27(5), 756-66.
3. Luštrik M, Dreu R, Šibanc R, Srčič S. Comparative study of the uniformity of coating thickness of pellets coated with a conventional Wurster chamber and a swirl generator-equipped Wurster chamber. *Pharm Dev Tech*, 2010, DOI: 10.3109/10837450.2010.531740.

A COMPARATIVE STUDY OF THE IMPACT OF GRANULATION METHOD ONTO THE COMPACTIBILITY OF COMPRESSION MIXTURES

Maja Šantl[1,*], Ilija Ilić[2], Franc Vrečer[1,2], Saša Baumgartner[2]

[1] Krka d.d., Šmarješka cesta 6, 8501 Novo Mesto, Slovenia; [2] Faculty of Pharmacy, Aškerčeva 7, 1000Ljubljana, Slovenia

INTRODUCTION

Compactibility is the ability of powder to form mechanically strong compacts (1). It can be quantified in several different ways; most often it is expressed as the relationship between tensile strength and compression pressure (compactibility profile).
The purpose of this study was to investigate the influence of various powder agglomeration processes on compactibility, friability and disintegration of the tablets produced. Four different granulation methods of the same model placebo formulation were produced at a semi-industrial scale: wet granulation (fluid-bed = FBG and high-shear = HSG) and dry granulation (slugging = DGS and roller compaction = DGRC). The properties of the mixtures were compared to those of the directly compressed mixture (DC).

MATERIALS AND METHODS

Materials

The model placebo mixture consisted of lactose monohydrate (filler, Pharmatose DCL15, DMV International GMBH), 65.42% (w/w); microcrystalline cellulose (filler/dry binder, Avicel PH 102, FMC International), 25.01% (w/w); sodium starch glycolate (disintegrating agent, Primojel, DMV International GMBH), 5.18% (w/w); polyvinylpyrrolidone (binder, Povidone K25, BASF SE), 3.31% (w/w); colloidal silica (lubricant, Aerosil 200, Evonik Degussa GMBH), 0.36% (w/w); and magnesium stearate (antiadhesive agent, FACI SPA), 0.72% (w/w).

Compactibility

Tablets were compressed at five different compression pressures (50, 100, 150, 200, 250 MPa) using an instrumented single-punch tableting press (Kilian SP300, IMA, Germany). The slopes of compactibility profiles (C_p) were estimated using the linear regression from the plot of tablet radial tensile strength, σ_t (N/mm^2) versus compression force, P (kN). The data was statistically treated as reported in previous studies (2). The tablet crushing strength (H) was evaluated using a hardness tester VK200 (Varian, USA). The radial tensile strength (σ_t) was calculated using equation by Fell (3).

Friability and disintegration

Tablet friability and disintegration time were determined according to Ph. Eur. 6th Ed. (2.9.7. Friability of uncoated tablets; 2.9.1. Disintegration of tablets and capsules) using a friability apparatus (Erweka TAR200, Erweka, Germany) and disintegration tester (Erweka ZT 72, Erweka, Germany).

RESULTS AND DISCUSSION

Compactibility

Tableting mixture's compactibility is especially important with respect to tablet hardness and friability. Poorly compactible powders form weak bonds between the particles and extensive elastic relaxation may further decrease tablet tensile strength and induce or increase capping tendencies. Higher tensile strength of tablets often means that the tablets are less friable and have longer disintegration time (4).

The compactibility results are shown in Table 1. The FBG mixture has highest compactibility, however, its compactibility does not significantly ($p = 0.148$) differ from the DGRC mixture. The differences among all other mixtures are statistically significant. By far the least compactible is the DGS mixture.

Table 1: The compactibility of the studied tableting mixtures, where C_p represents the compactibility.

Tableting mixture	$Cp \times 10^2$	RSE (%)	R^2
FBG	10.03 [9.91-10.15]	0.59	0.996
HSG	8.58 [8.47–8.69]	0.65	0.995
DC	8.87 [8.75–9.00]	0.70	0.994
DGRC	9.83 [9.59–10.07]	1.26	0.982
DGS	5.83 [5.68–5.99]	1.38	0.978

RSE is the relative standard error of slope ($N = 120$). The two-sided 95% confidence interval is given in parentheses.

The median particle size of HSG, FBG and DGS mixtures is between 250 and 350 µm. From these three mixtures, DGS shows poorest bonding properties. We partly attribute this to lower granule porosity of DGS mixture. This may be especially important during tableting of fragmentable materials, such as our agglomerated lactose based formulation. The reduction of bonding properties of dry granulated mixtures is most commonly associated with work hardening (5), which was confirmed for DGS mixture. The DC and DGRC mixture have considerably lower median particle size of 90–100 µm. Contrary to our expectations, the DGRC mixture, despite double particle processing, shows a high degree of compactibility. This is attributed to the much smaller particle size and high amount of fines compared to other mixtures, therefore the DGRC mixture is able to form more bonds during tablet production. DC mixture does not show superior compactibility, despite no pretreatment and small particle size. The main difference between DC and wet granulated mixtures is likely in binder distribution, where a more uniform distribution is expected for both wet granulated mixtures.

Friability and disintegration

The friability of tablets made from all mixtures decreases and the disintegration time becomes longer as compression pressure increases (data not shown). The comparison of the friability and disintegration time of tablets compressed from different compression mixtures are shown in Table 2.

The most friable tablets are the ones produced from the both dry granulated mixtures (DGRC, DGS), confirming their poor bonding properties observed from compactibility results. Tablets produced from the DC mixture have the quickest disintegration due to the optimal choice of excipients for direct compression in this formulation. Slower disintegration was observed for wet granulated mixtures compared to dry granulated.

Table 2: Friability (F) (%) and disintegration time (D) (min) of tablets produced at 150 MPa.

Tableting mixture	F (%)	D (min)
FBG	0.03	5.3 ± 0.6
HSG	0.05	5.4 ± 0.9
DGRC	0.39	3.9 ± 0.6
DGS	0.31	3.1 ± 0.3
DC	0.02	2.3 ± 0.1

CONCLUSION

Mechanical properties of tablets produced from dry granulated mixtures are inferior to wet granulated and direct compression mixture, which show similar compactibility and friability. DC mixture produces tablets with fastest disintegration.

REFERENCES

1. Leuenberger H. The compressibility and compactibility of powder systems. Int. J. Pharm. 1982; 12: 41–55.
2. Ilić I, Kása Jr P, Dreu R, Pintye-Hódi K, Srčič S. The compressibility and compactibility of different types of lactose. Drug Dev. Ind. Pharm. 2009; 35(10):1271–1280.
3. Fell JT, Newton JM. Determination of tablet strength by the diametral compression test. J. Pharm. Sci. 1970; 59: 688–691.
4. Zupančič BD, Dreu R, Vrečer F. Influence of dry granulation on compactibility and capping tendency of macrolide antibiotic formulation. Int. J. Pharm. 2008; 357: 44–54.
5. Malkowska S, Khan KA.. Effect of re-compression on the properties of tablets prepared by dry granulation. Drug Dev. Ind. Pharm. 1983; 9(3): 331–347.

PHYSICOCHEMICAL INVESTIGATION OF A MULTIPARTICULATE DRUG DELIVERY SYSTEM

K. Nikowitz[1,*], M. Wirges[2], K. Knop[2], P. Kleinebudde[2], K. Pintye-Hódi[1], G. Regdon jr.[1]

[1] Department of Pharmaceutical Technology, University of Szeged, Eötvös utca 6, H-6720 Szeged, Hungary; [2] Institute of Pharmaceutics and Biopharmaceutics, Heinrich-Heine-University, Universitaetsstr 1, 40225 Düsseldorf, Germany

INTRODUCTION

Raman spectroscopy is an increasingly popular analytical method in solid state characterisation. Its main advantages beside its versatility are its speed, non-destructiveness and lack of sample preparation requirements (1). The measuring of layered pellets poses challenges such as uneven surface and low signal intensity (2).

In our work we evaluated the use of Raman spectroscopy in the characterisation of a multiparticulate system prepared with solution layering technique.

MATERIALS AND METHODS

Materials

Piridoxin hydrochloride (Ph. Eur.) was used as a model drug. Cellet 500 (Shin-Etsu Chemical Co., Ltd., Tokyo, Japan) was used as non-pareil core material. Pharmacoat 606 (BASF, Ludwigshafen, Germany) was applied as a binder. Acryl-EZE (Colorcon, Dartford Kent, UK), a fully formulated enteric coating dispersion was used as coating material.

Layering of diltiazem hydrochloride

The pellet samples were prepared in a Strea-1 (Niro Aeromatic, Bubendorf, Switzerland) fluid bed Wurster chamber.

A solution of piridoxin hydrochloride and Pharmacoat 606 in 5:2 mass ratio with a total solid content of 12.28% was sprayed onto 200 g nonpareil cores until 175 g dry material was applied. The loading parameters were: inlet temperature 50°C, outlet temperature 43°C, spray rate of 4 ml/min, air volume 75 m^3/h and nozzle diameter 1 mm. The pellets were dried in the spray coater for 10 minutes.

Coating of layered pellets
Acryl-EZE dispersion was prepared and applied following the guidelines provided by the manufacturer as 20% aqueous dispersion. Only a small amount (0.1%) of dimeticone was added to prevent foaming during the process. Samples were prepared with different coating levels.

Measurement of layer thickness
An image analysis method (Leica Quantimet 500 MC, Leica Cambride Ltd, Cambridge, UK) was used to determine the thickness of the film layer on the pellets. The mean thicknesses were calculated using the mean diameters of the particles which were calculated by measuring 300 particles of each batch using a stereomicro-scope (Zeiss, Oberkochen, Germany).

Raman spectrometry
A Raman RXN2 analyzer of Kaiser Optical Systems (Ann Arbor, USA) with a laser wavelength of 785 nm was used. The spectrometer was equipped with a non-contact optic sampling device (PhAT probe with 6mm diameter).

Dissolution of piridoxin hydrochloride from pellets
Dissolution studies were done according to Ph. Eur. standards with a rotating basket (Erweka DT 700, Erweka GmbH, Heusenstramm, Germany). Concentration was measured using a spectrophotometer (Unicam Helios α, Thermo Fisher Scientific Inc., Waltham, USA) at 325 nm wavelength.

Thermal analysis
Thermoanalytical examinations were carried out with a Mettler TGA/DSC1 (Mettler–Toledo GmbH, Switzerland) instrument. Curves were evaluated with STARe Software. The starting and final temperatures were 25°C and 400°C and heating rate was 10°C/min.

RESULTS AND DISCUSSION

Measurement of layer thickness
Film thickness corresponded well with the amount of coating dispersion used. The uncoated API-layered pellets exhibited mixed results in roundness with roundnesses varying between 1.04 and 1.70 (largest SD=3.36) but this parameter has improved due to the coating to 1.04-1.36 (largest SD=0.35).

Raman spectrometry
Acryl-EZE exhibits three Raman peaks. Only the one at 638.7 cm^{-1} does not overlap with peaks in the API's spectrum so only this peak was used in further examinations. The correlation between the peak integral and the film thickness can be seen in Fig. 1.

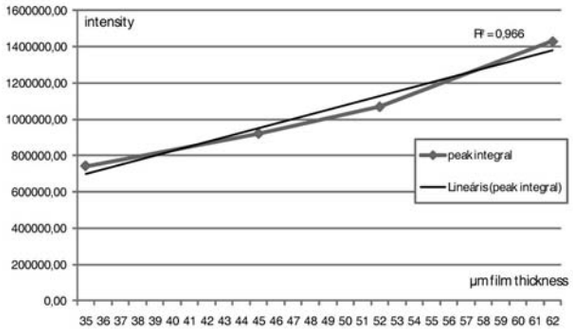

Fig. 1: Correlation between film thickness and Raman peak integral measured offline

Dissolution of piridoxin hydrochloride from pellets
As expected, the dissolution profiles of the samples with a higher coating level meet the requirements better. Samples showed satisfactory dissolution profile above approx. 45 mm coating thickness (Fig. 2.).

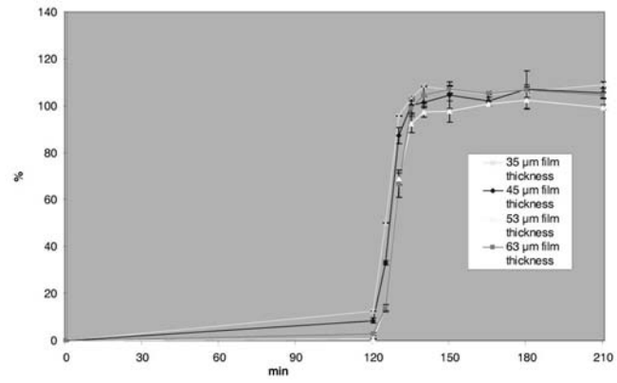

Fig. 2: Dissolution profiles of the pellets; the first 120 minutes were performed in simulated gastric acid, then pellets were transferred to simulated intestinal fluid

Thermal analysis
Both film coating and API transitions can be clearly seen on the curves (Fig. 3.). TG examinations showed that the decline in mass was slower in coated samples.

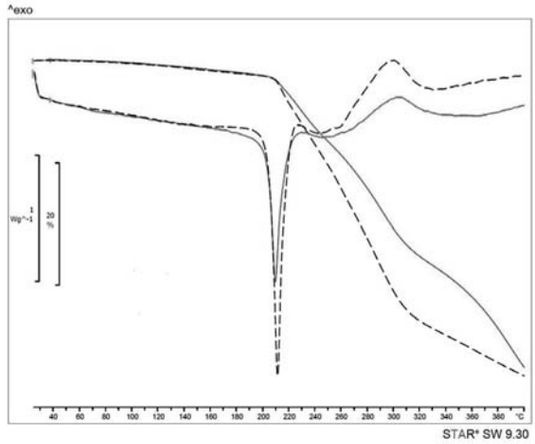

Fig. 3: TG and DSC curves of a coated (full red curves) and an uncoated (broken line) sample

When film thickness is the main determining factor of the dissolution profile non-destructive methods might be used to predict dissolution trends in coated samples.

ACKNOWLEDGEMENTS
This project has been supported by the DAAD (Project PPP Ungarn 50430305) and by the European Union ("TÁMOP-4.2.1/B-09/1/KONV-2010-0005 – creating the Center of Excellence at the University of Szeged"), co-financed by the European Regional Fund.

REFERENCES

1. Strachan CJ, Rades T, Gordon KC, Rantanen J, Raman spectroscopy for quantitative analysis of pharmaceutical solids. J. Pharm. Pharmacol. 2007 :59 :179-192.
2. Sovány T, Nikowitz K, Regdon G jr, Kása P jr, Pintye-Hódi-K, Raman spectroscopic investigation of film thickness. Polym. Test. 2009:28:770-772

FLUDIZED HOT MELT GRANULATION: IN SITU VS. SPRAY-ON PROCEDURE

I. Mašić[1,*], I. Ilić[2], J. Parojčić[1], Z. Đurić[1], S. Srčič[2]

[1] Department of Pharmaceutical Technology and Cosmetology, Faculty of Pharmacy, University of Belgrade, Vojvode Stepe 450, 11000 Belgrade, Serbia; [2] Department of Pharmaceutical Technology, Faculty of Pharmacy, University of Ljubljana, Aškerčeva cesta 7, 1000 Ljubljana, Slovenia

INTRODUCTION

Fluidized hot melt granulation (FHMG) is recognized as promising technique due to the significant advantages over conventional granulation methods (1, 2). FHMG involves the use of meltable binders which can be added either in the form of molten liquid (spray-on procedure) or as discrete particles that melt during the process (*in situ* procedure) (3). In contrast to intensive studies on melt granulation in high-shear mixers, the interest on FHMG is more recent and there is still a lack of knowledge with regard to predictability and mechanism of melt agglomeration in fluid bed processors.

The aim of the present study was to investigate the influence of binder concentration and binder addition method on granule characteristics and mechanism of agglomerate growth.

MATERIALS AND METHODS

Materials

Starting materials were: paracetamol (Acros Organics, Belgium), lactose monohydrate (Carlo Erba Reagents, Italy). Gelucire 50/13 (Gattefosse, France) was used as meltable binder.

Characterization of starting materials

The particle size distribution of lactose and paracetamol was determined by sieve analysis. Median particle diameter (d_{50}) was calculated by linear interpolation of the cumulative percentage frequency curve. The span (S_{75-25}) is defined as a quotient of difference between the agglomerate sizes corresponding to the quartile points at 75% and 25% and mass median diameter.

Granule preparation

Granulation process was performed in Mycrolab fluid bed processor, OYSTAR Hüttlin. Two different binder particle size fractions were used for the *in situ* FHMG. Binder pellets were ground, using a mortar and pestle, to give a mass mean particle size of ≈ 655 µm. Smaller binder particles (mass mean particle size ≈ 94 µm) were prepared by spray congealing technique (Büchi Mini Spray Dryer B-290, Switzerland). All the ingredients were filled into the fluid bed chamber, fluidized and preheated to product temperature of 55°C. The inlet air flow rate was 35 m^3/h. Ten minutes after the product temperature reached 55°C the inlet air heating was switched off. When spray-on procedure was applied, the tube, which delivers the melted binder, was electrically heated to 70°C. Both components of the compressed air (spray air and microclimate) were also electrically heated to 80°C. The addition of melted binder (feed rate - 8 or 16 g/min) was started when product temperature reached 60°C. The spray air pressure was 0.6 bar and microclimate pressure was 0.2 bar. The inlet air flow rate was 25 m^3/h. After the binder addition heating was switched off, and the inlet air flow rate increased to 30 m^3/h.

Granulates were prepared with 14 or 18% binder and 20% paracetamol.

Granule characterization

The granule size distribution was evaluated by sieve analysis, and median particle diameter and span were calculated. Bulk and tapped densities were measured and Carr index (CI) calculated. The granule shape was examined using Olympus BX50 microscope coupled with a Sony DXC-950P digital camera and image processing software AnalySIS® (Soft Imaging System GmbH, Germany). The following shape parameters were calculated: aspect ratio (AR), projection sphericity (PS) and circularity (C). The morphology of the agglomerates was investigated by SEM (Supra 35VP, Carl Zeiss, Germany) with an acceleration voltage of 1 kV and a secondary detector.

RESULTS AND DISCUSSION

Material properties

Paracetamol median particle diameter was found to be 190.96 µm, and the span was 0.35. Lactose median particle diameter and span were found to be 57.80 µm and 0.27, respectively.

Granule characteristics

The results of granule shape and size analysis and Carr index values are given in Table 1.

Table 1: Granule properties.

Granulate			d_{50} (µm)	S_{75-25}	CI	AR	PS	C
In situ FHMG	14% binder	binder particle size ≈ 94 µm	252.06	0.37	13.10	1.36	0.56	0.70
		binder particle size ≈ 655 µm	720.91	1.19	13.85	1.16	0.76	0.95
	18% binder	binder particle size ≈ 94 µm	631.45	0.30	6.76	1.33	0.58	0.78
		binder particle size ≈ 655 µm	1141.12	0.52	8.06	1.21	0.71	0.91
Spray-on FHMG	14% binder	binder feed rate - 8 g/min	332.12	0.74	13.33	1.25	0.67	0.87
		binder feed rate - 16 g/min	270.79	0.91	12.82	1.22	0.69	0.92
	18% binder	binder feed rate - 8 g/min	421.19	0.56	8.57	1.27	0.65	0.89
		binder feed rate - 16 g/min	462.33	0.72	8.70	1.22	0.70	0.91

In situ FHMG resulted in narrow particle size distribution. Exception was granulate prepared with larger binder particles and lower binder content. Larger binder particles and/or higher binder content resulted in larger agglomerates. When spray-on procedure was applied, larger agglomerates were obtained with higher binder content. Higher binder feed rate resulted in higher span values.

The results obtained indicated the influence of agglomeration mechanism on granule sphericity. SEM revealed the presence of the hollow core in the samples prepared with larger binder particles (Fig. 1), which indicates that immersion and layering was dominant agglomeration mechanism. When *in situ* procedure with smaller binder particles was applied distribution and coalescence occurred resulting in lower degree of granule sphericity. Formation of hollow core granules was also observed for spray-on FHMG at higher binder feed rate.

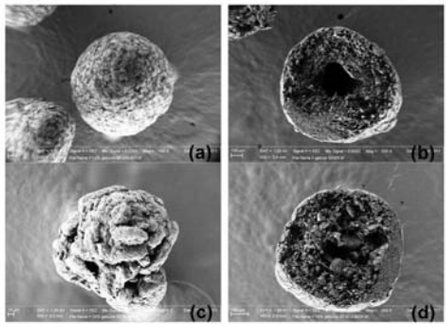

Fig. 1: SEM micrographs of granulates with 14% Gelucire 50/13: (a) a single granule and (b) cross section of granule prepared by *in situ* procedure with larger binder particles; (c) a single granule prepared by *in situ* procedure with smaller binder particles; (d) a cross section of granule prepared by spray-on procedure at higher binder feed rate.

CONCLUSIONS

Both spray-on and *in situ* procedures can be used for production of granules with high sphericity and uniform particle size distribution. Further investigations are needed for thorough process understanding.

ACKNOWLEDGMENT

This work was done under the project TR-34007 supported by the Ministry of Education and Science, Republic of Serbia.

REFERENCES

1. Heng PWS, Wong TW, Melt process for Oral Solid Dosage Forms, in: Swabrick J (Ed.), Encyclopedia of Pharmaceutical Technology, 3rd ed., Informa Healthcare, New York, 2006, pp. 2257-2261.
2. Andrews GP. Advances in solid dosage form manufacturing technology. Philos. Trans. R. Soc. Lond. A. 2007; 365: 2935-2949.
3. Abberger T. Influence of binder properties, method of addition, powder type and operating conditions on fluid-bed melt granulation and resulting tablet properties. Pharmazie 2001; 56: 949–952.

IMPACT OF WET AND DRY GRANULATION ON COMPRESSIBILITY

I. Ilić[1,*], M. Šantl[2], F. Vrečer[1,2], S. Baumgartner[1]

[1] Faculty of Pharmacy, University of Ljubljana, Aškerčeva 7, 1000 Ljubljana, Slovenia;
[2] Krka d.d., Šmarješka cesta 6, 8501 Novo Mesto, Slovenia

INTRODUCTION

Compressibility is the powder's ability to deform under pressure (1). It is most often described by the change in the relationship between porosity or volume and applied compression pressure represented by the Heckel (2) and Walker (3) models.

The aim of this study was to determine the influence of wet and dry granulation on compressibility. Four different granulation methods (wet: fluid-bed = FBD and high-shear = HSG; dry: slugging = DGS and roller compaction = DGRC) of the same model placebo formulation were used to prepare the granules and the results were compared to directly compressed mixture (DC).

MATERIALS AND METHODS

Materials

The model placebo mixture consisted of lactose monohydrate (filler, Pharmatose DCL15, DMV International GMBH), 65.42% (w/w); microcrystalline cellulose (filler/dry binder, Avicel PH 102, FMC International), 25.01% (w/w); sodium starch glycolate (disintegrating agent, Primojel, DMV International GMBH), 5.18% (w/w); polyvinylpyrrolidone (binder, Povidone K25, BASF SE), 3.31% (w/w); colloidal silica (lubricant, Aerosil 200, Evonik Degussa GMBH), 0.36% (w/w); and magnesium stearate (antiadhesive agent, FACI SPA), 0.72% (w/w).

Compressibility

Compressibility was determined using "out-die" Heckel (2) and Walker (3) models and force-displacement measurements. The tablets were compressed at five different compression pressures (50, 100, 150, 200, 250 MPa) using an instrumented single-punch tableting press (Kilian SP300, IMA). Round, flat-faced punches with diameter of 12 mm were used to compress tablets with nominal mass 600 mg at tableting speed of 30 tbl/min. At each compression pressure 24 tablets were evaluated 24 hours after compression. Tablet dimensions were measured using a slide caliper (MIB Messzeuge). The data was statistically treated as reported in previous studies (4). True density was determined using Helium pycnometer (AccuPyc 1330, Micromeritics). Using force-displacement measurements, the hysteresis between compression and decompression curve was used as a measurement of material's compressibility or plasticity (5).

RESULTS AND DISCUSSION

The results of the Heckel analysis are presented in Table 1. Higher values of K (slope) and lower values of P_y (yield pressure, reciprocal value of K) are typical for more compressible materials and vice-versa. Differences in compressibility between mixtures are statistically significant, except in case of HSG and DC mixture, which exhibit equal compressibility ($p = 0.815$). The results show a clear general trend, that both dry granulated mixtures are noticeably less compressible than two wet granulated and DC mixture. The latter shows good compressibility due to choice of input raw materials, that are themselves already suitable (pregranulated lactose DCL15) for direct tableting.

Poorer compressibility of dry granulated mixtures is partially attributed to double particle processing and work hardening phenomenon. Both dry granulated mixtures also have lower initial powder height during compression, which leads to reduced contact time, allowing shorter time for deformation.

Table 1: Compressibility results of Heckel analysis.

Tbl mixture	$K \times 10^3$ (MPa^{-1})*	Py (MPa)	R^2
FBG	5.62 [5.50–5.74]	178	0.987
HSG	5.14 [5.01–5.26]	195	0.983
DC	5.11 [4.99–5.24]	196	0.984
DGRC	4.25 [4.15–4.35]	235	0.985
DSG	3.80 [3.73–3.86]	264	0.991

*The two-sided 95% confidence interval is given in parentheses ($N = 120$).

The results of Walker model are shown in Table 2. The data fits the Walker model slightly better compared to Heckel model. This is noticed in slightly higher R^2 values and narrower confidence intervals. High values of w correspond to excellent compressibility and vice-versa. The results confirm compressibility determined by the Heckel model and a positive correlation between them is observed. Walker model is more discriminative shown by the wider range between most and least compressible mixture.

Table 2: Compressibility results of Walker analysis.

Tbl mixture	$w' \times 100$ (%)*	R^2
FBG	35.0 [34.3–35.8]	0.986
HSG	31.8 [31.2–32.4]	0.988
DC	32.2 [31.5–32.8]	0.988
DGRC	27.0 [26.7–27.4]	0.994
DSG	21.0 [20.8–21.2]	0.997

*The two-sided 95% confidence interval is given in parentheses ($N = 120$).

Compressibility was also determined using force-displacement measurements. Area of hysteresis between compression and decompression curve represents specific net work (W_{net}) of compression. The values of W_{net} represent energy used for irreversible processes during compression (mainly plastic deformation, but also friction and fragmentation) and may be related to compressibility of tableting mixture. A comparison between W_{net}, Heckel (K) and Walker (w) coefficient is shown in Figure 1.

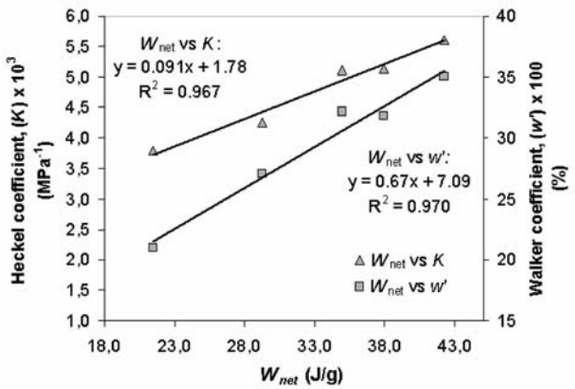

Fig. 1: Relationship between W_{net} at 250 MPa, Heckel and Walker coefficients.

The W_{net} results are in agreement with Heckel and Walker model. The established correlation is strong and confirms the compressibility results obtained by Heckel and Walker models.

CONCLUSIONS

Most compressible tableting mixture can be produced using fluid-bed wet granulation process. The compressibility of both dry granulated mixtures is inferior to wet granulated ones. Direct compression mixture has comparable compressibility to HSG. The results of force-displacement show accurate estimate of material's compressibility. This procedure requires compression of only one tablet at one compression pressure, perhaps allowing easier and faster determination of tableting mixture's mechanical properties.

REFERENCES

1. Leuenberger H. The compressibility and compactibility of powder systems. Int. J. Pharm. 1982; 12:41–55.
2. Heckel RW. Density-pressure relationships in powder compaction. Trans. Metall. Soc. AIME 1961; 221:671–675.
3. Walker EE. The properties of powders VI: The compressibility of powders. Trans. Faraday Soc. 1923; 19:73–82.
4. Ilić I, Kása Jr P, Dreu R, Pintye-Hódi K, Srčič S. The compressibility and compactibility of different types of lactose. Drug Dev. Ind. Pharm. 2009; 35(10):1271–1280.
5. Stamm A, Mathis C. Verpressbarkeit von festen Hilfsstoffen fuer Direkttablettierung. Acta Pharm. Technol. 1976; 22:7–16.

OPTIMIZATION OF SUSTAINED RELEASE PELLET CURING PROCESS

G. Hudovornik[1,*], F. Vrečer[1,2]

[1] KRKA d.d., Novo mesto, Šmarješka cesta 6, 8501 Novo mesto, Slovenia; [2] University of Ljubljana, Faculty of Pharmacy, Aškerčeva cesta 7, 1000 Ljubljana, Slovenia

INTRODUCTION

Coated pellets as a multiparticulate system offer many advantages over monolithic matrix systems in terms of in-vivo behavior and are often used when sustained release of active ingredient(s) is required (1, 2).

Polymethacrylates are frequently used in modified release coatings where Eudragit® RS and RL are two types that are most commonly used. By mixing both polymers that have different water permeability a variety of dissolution profiles can be obtained.

Eudragit® RS and RL films even when properly plasticized require curing after coating to complete the film forming process. The most common used technique for curing process is tray drying, whereas time, temperature and drying air relative humidity are the most important factors that influence curing process (3, 4).

The aim of the present work was to investigate the influence of these factors on curing process of Eudragit® RS and RL coated pellets using design of experiments.

MATERIALS AND METHODS

Materials

Drug coated pellets of Diclofenac sodium (Krka, Novo mesto, Slovenia) were used as a basis for film coating. Eudragit® RS and RL 30 D dispersion (Evonik GmbH, Germany), Talc (Luzenac Val Chicone SPA, Italy) and Triethylcitrate (Vertellus Performance Materials Inc., USA) were used as dry components of coating dispersion.

Preparation of coated pellets

Coated pellets were prepared in Glatt GPCG-3 Fluid bed coater using bottom spray insert (Glatt GmbH, Germany).

Design of experiments

Experiments were made according to a Central Composite Design (CCD) which was designed and analyzed using Unscrambler X software ver. 10.1 (Camo Software).

Curing of the coated pellets

Curing of the coated pellets was performed in a tray oven at different temperatures and under different relative humidity which was achieved using saturated solutions of different salts.

Drug release studies

Drug release studies were performed in phosphate buffer at pH 6.8. The studies were performed using dissolution apparatus Apparatus I,1000 mL, 50 rpm, 37°C±0.5 °C. Samples were UV analysed at 277 nm.

RESULTS AND DISCUSSION

Three factors were studied in the range which is commonly used for tray oven curing (Table 1).

Table 1: Factor levels

Factor	Low	Med.	High
Temperature	40°C	50°C	60°C
Relative Humidity	~15%	~50%	~75 %
Time	4 h	14 h	24 h

Dissolution of diclofenac sodium in Phosphate buffer with pH 6.8 at 180 minutes was chosen as a response. Different dissolution profiles were obtained ranging from 18 %-45 % of the dissolved diclofenac sodium after 180 minutes. The amount of dissolved diclofenac sodium for uncured pellets was 60 % (5).

After statistical evaluation of responses a model with p-value of 0,0962 was obtained. Significant factor was found to be Humidity (p-value: 0,0378) and all two factor interactions. Temperature and time did not significantly influence the model.

Response surfaces were modelled at all three levels of temperature for factors Time and R. Humidity and response Dissolution at 180 min (Fig. 1-Fig. 3)

It can be seen from the above figures that the influence of air relative humidity and time is different at different temperatures. At 40°C lower dissolution profiles can be achieved when curing time was close to 24 hours and medium relative humidity was maintained in the range between 20-50 %.

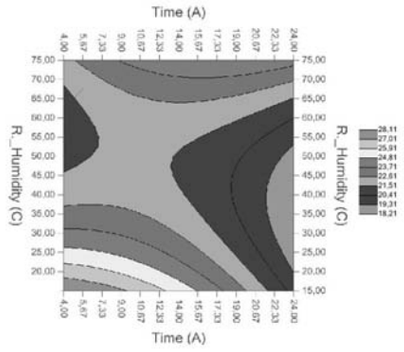

Fig. 1: Response surface at 40°C

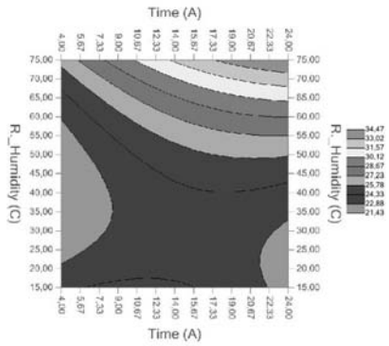

Fig. 2: Response surface at 50°C

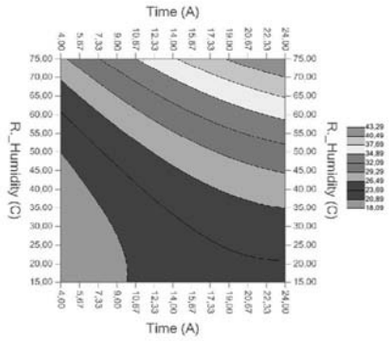

Fig. 3: Response surface at 60°CAt 50°C lower dissolution profiles can be achieved ether with low relative humidity and longer curing time (24 hours) or with medium relative humidity (20-50% RH) and short curing time (4-8 hours) (Fig. 2). We also observed that when using high humidity and long curing time the dissolution rate of the drug increases.

This effect is even more pronounced at 60°C (Fig. 3) where low dissolution profile can only be obtained at lower humidity (15-50 %) range and short curing time up to 8 hours. At the extreme point with 24 hours curing at 75 % RH the dissolution raises to 45% after 180 minutes. We concluded that the reason for this phenomenon was extensive softening of the film coating and penetration of the drug layer into the coating which was confirmed by the results of scanning electron image analysis.

CONCLUSIONS

Design of experiments was successfully used to study and optimize the curing process of polymethacrylate film coating. The optimal conditions for pellet curing were found to be 40°C, 24 hours and 40% RH.

ACKNOWLEDGMENTS

The authors would like to thank KRKA d.d., Novo mesto for providing support in performing the study.

REFERENCES

1. Swarbrick J, Boylan JC. Encyclopedia of Pharmaceutical Technology. Marcel Dekker, New York 1995; 11: 151-154;369-374
2. McGinity JW, Felton AL. Aqueous polymeric coating for pharmaceutical dosage forms. 3rd Ed., New York: 64-65, 237-268
3. A. Kramar, S. Turk and F. Vrečer, Statistical optimization of diclofenac sustained release pellets coated with polymethacrylic films, Int. J. Pharm, 2003, vol. 256, no. 1-2, str. 43-52
4. Eudragit® Application Guidelines. 2009, 11th Ed., Evonik Industries
5. Ivanušič M. The study of influence of curing on properties of prolonged release film coated pellets. B. S. Thesis. Ljubljana, 2011

STUDY THE BIOAVAILABILITY OF ATENOLOL WITH ALKALIZING COMPONENT IN RATS

E. I. Hamedelniel[1], P. Kása Jr.[1], K. Pintye-Hódi[1], I. Zupkó[2]

[1] Department of Pharmaceutical Technology, University of Szeged, Eötvös u. 6, H-6720 Szeged, Hungary; [2] Department of Pharmacodynamics and Biopharmacy, University of Szeged, Eötvös u. 6, H-6720 Szeged, Hungary

INTRODUCTION

Atenolol is a potent cardio-selective β-adrenoreceptor blocking agent applied for the treatment of hypertension. The absorption of the drug in humans and most laboratory animal species is rapid, but incomplete (50-60%). Atenolol is well absorbed at pH >7.5 (1), especially in the dog, in which the pH of the ileum is >8, and in which absorption from the gut is therefore almost complete: 98% of the total dose (2). Preparation of a multiparticulate matrix system with an alkalizing component is a reasonable way to ensure an appropriately alkaline micromilieu (3). The aim of the present work was the formulation of a multiparticulate system containing Atenolol with a view to increasing its bioavailability. The delayed release was ensured by coating with a gastroresistant polymer.

MATERIALS AND METHODS

Materials

Atenolol (Ariane Organochem Private Ltd., Mumbai, India), EC (Ethocel standard 10 premium,Colorcon Ltd. Dartford, England) and MCC (Vivapur 103, Rettenmaier& Söhne GmbH, Rosenberg, Germany). Na_3PO_4 $12H_2O$ (VWR International, Belgium), Opadry clear (HPMC) and Acryl EZE MP (Colorcon Ltd., Dartford, England), (Eudragit L100-55)® Dimethicone (Silfar E 1049, Wacker Chemie AG, supplier: Brenntag Hungaria Kereskedelmi Kft, Hungary) and Ariavit sunset yellow CI 15985 (Sensient Food Colors Hungary Kft, Hungary).

Preparation of pellets

Three types of coated pellets were prepared: containing Atenolol with alkalizing component and matrix former (B1), without alkalizing component (B2) and without both alkalizing component and matrix former which was substituted by lactose (B3). Wetting was performed in a high-shear mixer (ProCepT 4M8 granulator, ProCepT nv, Zelzate, Belgium). The wet mass was extruded by a mini screw (Caleva Ltd., Sturminster Newton, Dorset, UK) and spheronized at a time, on a spheronizer 12 cm in diameter (Model-120, G.B. Caleva Ltd., Sturminster Newton, Dorset, UK).

Coating of pellet cores

Pellet cores were coated in a fluidized bed coater equipped with a Wurster insert (Strea 1; Aeromatic-Fielder, Bubendorf, Switzerland) with Opadry solution 3% (w/w) and Acryl EZE MP dispersed system 17 % (w/w) respectively.

Morphological study
The particle size and the shape of the pellet surface were studied by using a system consisting of a stereomicroscope (Zeiss Stemi 2000-C, Carl Zeiss GmbH, Vienna, Austria).

In vitro drug release
Pellets (100 mg) were filled into HPMC capsules, which were placed into the basket of a dissolution tester (Erweka DT 700, Heusenstamm, Germany). The investigation conditions: (pH=1.2). HCL phosphate buffer (pH=6.8), 37 °C and 100 rpm.

In vivo experiment
Male SPRD rats (190-210g) were fasted for 16 hours and then pellet-filled capsules were orally administered representing 30mg/kg Atenolol. After 2, 4, 6 and 8 hour animals were sacrificed and serum samples were prepared for analysis by HPLC.

RESULTS AND DISCUSSION

Table 1 reveals that the all types of the pellets before coating were close to spherical, with an aspect ratio close to 1. This means that these samples are suitable for coating.
Acryl EZE MP aqueous dispersion was used as gastroretentive polymer. But in the case of pellets containing alkalizing component (B1) a protective polymer layer was developed before this functional film coating, to prevent direct contact between the alkalizing layer and the Acryl EZE (4).
Fig.1 illustrates the cross-section of *B1*. The spherical form and a relative large pore in the middle of the pellet can be observed, but around the pore the matrix is rather compact. The coating layer is clearly visible and the two polymer layers are distinguishable.
The *in vitro* dissolution test (Fig. 2) generally for each sample, revealed a tendency to delayed release profiles displayed a sigmoid shape, which is characteristic of sustained release preparations from coated pellets, there is no release in acidic pH.

Table 1: Shape of the pellets

Sample	Aspect ratio	Breadth (mm)	Length (mm)
B1	1.1±0.04	1.78±0.14	1.95±0.15
B2	1.07±0.03	1.72±0.09	1.87±0.12
B3	1.07±0.0	1.71±0.12	1.84±0.14

It can be concluded, that in *in vitro* dissolution experiments the *B2* and *B3* pellets showed a perfect dissolution during 240 min. The dissolved drug value is a little smaller in the case of *B1* sample because of the double coating layer. It should be mentioned, that in the in vitro experiments we can test only the dissolution rate of the drug from the dosage form, which based on the solubility of the API. In this experiment is not possible to know the degree of absorption of the Atenolol. It can be reflect only in the *iv vivo* experiment (Fig 2.). In these results can be seen the signal peak of Atenolol at 4 min in the sample *B1*, which was not detected for both *B2* and *B3*.

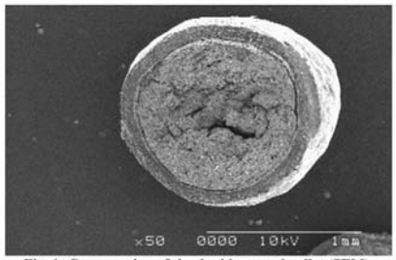

Fig. 1: Cross-section of the double-coated pellet (SEM).
Magn.: 50x

Fig. 1: Cross-section of the double-coated pellet (SEM). Magn.: 50x

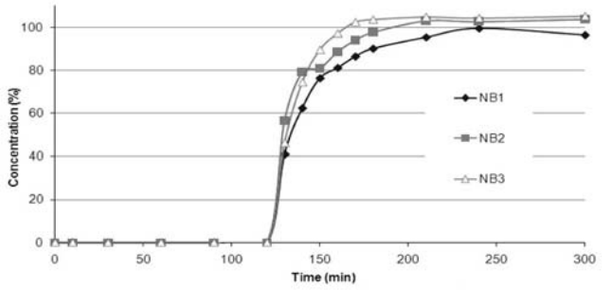

Fig. 2: Dissolution profile of Atenolol in acidic 1.2 pH and buffer 6.8 pH from coated pellet together of subcoating.

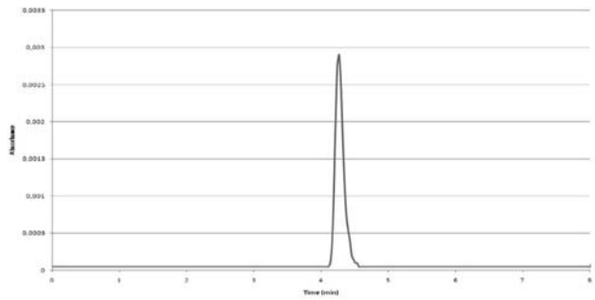

Fig. 3: HPLC determination of Atenolol from pellet sample (B1)

CONCLUSIONS

The pellets the three samples, prepared by extrusion and spheronization were spherical and had high strength. The dissolution test generally for each sample, revealed a tendency to sustained release profiles displayed a sigmoid shape, which is characteristic of sustained release of At at pH=6.8, HPLC showed signal peak for *B1* only.

REFERENCES

1. Tabacova, S.A., Kimmel, C.A., 2002, Atenolol: pharmacokinetic/dynamic aspects of comparative developmental toxicity. Reprod. Toxicol.16: 1-7.
2. Reeves, P.R., Barnfield, D.J., Longshaw, S., et al., 1978, Disposition and metabolism of atenolol in animals. Xenobiotica 8:305–11.
3. Hamedelniel, E.I, Bajdik, J, Pintye-Hódi, K. 2010a, Optimization of preparation of matrix pellets containing ethylcellulose. Chem. Eng. Process 49:120–124.
4. Bozdag, S., Calis, S., Sumnu, M., 1999, Formulation and stability evaluation of entericcoated omeprazole formulations. STP Pharma Sci. 9: 321–327

TWO STEP GRANULATION – PIOGLITAZON/METFORMIN CASE STUDY

R. Starič*, T. S. Ljubin, S. Skubin

Lek Pharmaceuticals, d.d., SDC Slovenia , Verovškova 57, SI-1526 Ljubljana, Slovenia

INTRODUCTION

Many new pharmaceutical products are combination of two active ingredients. Some of them can have major differences in their chemical and especially physical characteristics. Different approaches for formulating such combinations are known: bi-layer tablet, separate granulate preparation, etc. Herein described is a method of preparing combination of Pioglitazon and Metformin, substances which are very different in their physical properties with respect to particle size, dose and solubility. High portion of Metformin is the reason that substance has poor compactation properties and needs to be modified to assure good tablet physical properties. As Pioglitazon is a typical BCS 2 class compound formulation and process must provide dissolution which is comparable with reference product.

MATERIALS AND METHODS

Tablets were prepared by many different techniques such as dry mixture, high-shear granulation, combination of separate high shear - fluid bed granulation and two-step granulation were performed. For two-step granulation first both APIs were granulated with small amount of water in high shear granulator, dried and further granulated in fluid bed apparatus in second step.

Granulate was finally blended with microcrystalline cellulose and glidants and compressed into 1090 mg tablets.

Prepared tablets were tested on hardness, prolonged friability, disintegration and dissolution. Also pictures were taken using light microscope to study granulate structure. To detect granulate structure 0.09 % of total tablet mass of black pigment was added to Pioglitazone before sample preparation.

RESULTS AND DISCUSSION

Sample prepared from dry mixture had very poor physical properties (hardness 20N) and tablet cores did not meet acceptance criteria for film coating. Sample prepared only with high shear technology had much betters physical properties (hardness 100-200N) however technology was not acceptable for industrial production as Metformin formed conglomerate during high-shear mixing which was very difficult to dry and also Pioglitazon segregation was observed during tablet compression. Sample prepared with separate and two-step granulation gave tablets with good physical properties (hardness 150-250N), however dissolution of Pioglitazon from separate granulation sample was poor. Two step granulation sample had good Pioglitazon dissolution and also tablets had appropriate physical properties.

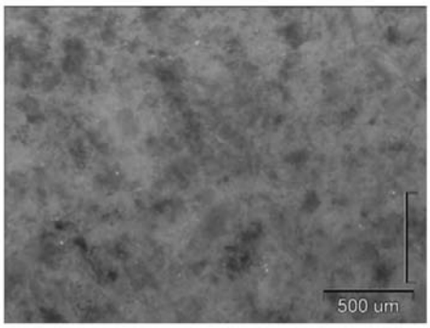

Fig.1: Two-step granulation sample tablet morphology

CONCLUSIONS

During the first step of granulation only slight bonding of particles in granulate is achieved, that is strong enough to prevent air segregation and improves dissolution of Pioglitazon. In second step stronger bonding of particles is achieved, and particles can be compressed into tablet cores suitable for film coating.

LIGNIN AND LIGNOCELLULOSES - POTENTIAL FUTURE EXCIPIENTS IN PHARMACEUTICAL SOLID DOSAGE MANUFACTURING

J. Heinämäki[1,*], M. Hakola[2], U. Paaver[1], S. Vuorinen[2], K. Kirsimäe[3], K. Kogermann[1], O. Antikainen[4], P. Veski[1], J. Yliruusi[4], T. Repo[2]

[1] Department of Pharmacy, Faculty of Medicine, University of Tartu, Nooruse 1, 50411 Tartu, Estonia; [2] Laboratory of Inorganic Chemistry, Department of Chemistry, Faculty of Science, PL 55 (A. I. Virtasen aukio 1), 00014 University of Helsinki, Finland; [3] Institute of Ecology and Earth Sciences, University of Tartu, Ravila 14a, 50411 Tartu, Estonia; [4] Division of Pharmaceutical Technology, Faculty of Pharmacy, PL 56 (Viikinkaari 5E), 00014 University of Helsinki, Finland

INTRODUCTION

The design and synthesis of new biomaterials for excipients in pharmaceutical and biomedical systems have created much interest in recent years (1-3). Lignin and lignocelluloses are side-products in the pulp manufacturing process (4), and they are readily available and cheap but have not been investigated as excipients in pharmaceutical applications. It is evident that these materials could provide many advantages associated with e.g. dry and wet granulation, pelletisation, tablet compression, film coating and controlled release applications. To date, very little is known about e.g. compaction properties of lignin and lignocelluloses as direct compression materials.

In the present study, physical material properties of lignin and lignocelluloses relevance to manufacturing and perform-ance of pharmaceutical oral solid dosage forms, were investigated. The physical material characterisation included solid-state properties, particle size, size distribution and shape, morphology, flowability, densification and tablet compression properties. The biomaterials studied were isolated from the pine wood (*Pinus sylvestris*) pulp mass produced by pulp industry with a new procedure (5). Using the present technique and by varying conditions of isolation process, chemical purity, physical material and powder properties as well as solubility of lignin and lignocelluloses can be modified.

MATERIALS AND METHODS

Materials

Lignin and lignocellulose from pine soft wood (*Pinus sylvestris*) were obtained using a new isolation technique based on catalytic oxidation and subsequent acid precipitation (Fig. 1). Industrial kraft softwood lignin (Indulin AT), hardwood lignin (PC-1369) and microcrystalline cellulose, MCC (Avicel^{O} PH 102, FMC Biopolymer, USA) were used as reference materials.

Methods

Solid-state properties of pine lignin and lignocellulose were studied by means of X-ray powder diffractometer (XRPD) (D8 Advance, Bruker AXS GmbH, Germany). The particle size and morphology were

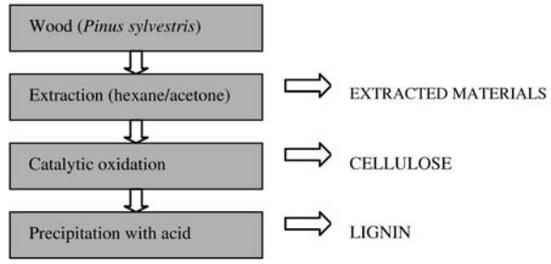

Fig. 1: Schematic diagram of the isolation of lignin and lingo-celluloses from from pine soft wood (*Pinus sylvestris*).

investigated with a Scanning Electron Microscope (SEM) (Helios NanoLab 600, FEI Company). Tablets were compressed by direct compression in an instrumented single-punch tablet machine (Korsch EK-O, Berlin, Germany) equipped with 9-mm flat-faced punches.

RESULTS AND DISCUSSION

The XRPD patterns of softwood lignin obtained with a new catalytic isolation technique and two reference lignins (Indulin AT and PC-1369 obtained from softwood and hardwood, respectively), showed amorphous structure (Fig. 2).

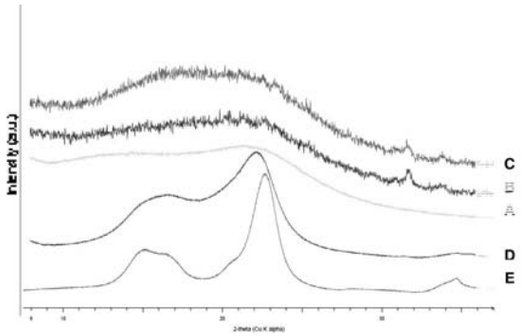

Fig. 2: Representative XRPD patterns of the softwood pine lignin (A) vs industrial reference samples Indulin AT (B) and PC-1369 (C), and pine cellulose (D) vs. MCC (E).

Scanning electron micrographs (SEMs) on the lignins and softwood pine cellulose are shown in Figs 3 and 4, respectively.

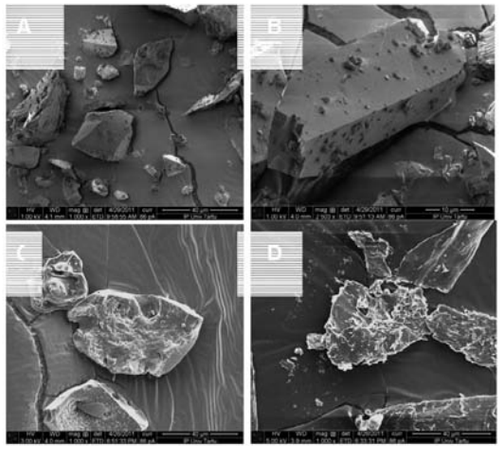

Fig. 3: Scanning electron micrographs (SEMs) of the softwood pine lignin (A,B) vs industrial reference lignin samples Indulin AT (C) and PC-1369 (D).

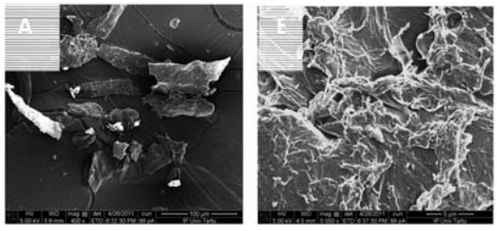

Fig. 4: Scanning electron micrographs (SEMs) of softwood pine cellulose. Magnification 400 x (A) and 5000 x (B).

Both softwood and hardwood lignins exhibited particles with a relatively round but irregular shape, and particle size ranged from 30 mm to 100 mm. Softwood pine cellulose exhibited larger particles with an elongated or fiber-like shape. Softwood pine lignin and cellulose were found to have a tendency to plastic deformation, and the pine cellulose showed a good compression behaviour compared with other direct compression excipients.

CONCLUSIONS

It can be concluded that softwood pine lignin and lignocellulose exhibit particle and powder properties (including flowing and densification) suitable for e.g. a filler-binder excipient for tablet compression applications

ACKNOWLEDGEMENTS

This research was supported by European Social Fund's Doctoral Studies and Internationalisation Programme DoRa. Mr. J. Aruväli (X-ray laboratory of Institute of Ecology and Earth Sciences, University of Tartu) and Prof. V. Sammelselg (Institute of Physics, University of Tartu) are acknowledged for the XRPD and SEM experiments, respectively.

REFERENCES

1. Jayakumar R., New N., Tokura S., Tamura H. Sulfated chitin and chitosan as novel biomaterials. Int. J. Biol. Macromolecules 2007; 40 (3): 175-181.
2. Rinaudo M. Main properties and current applications of some polysaccharides as biomaterials. Polymer Int. 2008; 57 (3): 397-430.
3. Prabaharan M. Chitosan derivatives as promising materials for controlled drug delivery. J.Biomater.Appl. 2008; 23 (1): 5-36.
4. Chakar F.S., Ragauskas A.J. Review of current and future softwood kraft lignin process chemistry. Industrial Crops and Products 2004; 20 (2): 131-141. 6th International Lignin Institute conference.
5. Hakola M., Kallioinen A., Kemell M., Lahtinen P., Lankinen E., Leskelä M., Repo T., Riekkola T., Siika-aho M., Uusitalo J., Vuorela S., von Weymarn N. Liberation of cellulose from the lignin cage: A catalytic pretreatment method for the production of cellulosic ethanol. ChemSusChem 2010; 3 (10): 1142-1145.

MACROGOLS EFFECT ON STABILITY PERFORMANCE OF DRUG PRODUCT

M. T. Jaklič*, R. Jurečič, A. Bastarda, R. Grahek

Lek Pharmaceuticals,d.d., Sandoz Development Center Slovenia, Verovškova 57, 1526 Ljubljana, Slovenia

INTRODUCTION

Macrogols are a known source of numerous issues in formulation stability. They readily decompose under presence of oxygen to form peroxides which in turn react with APIs and other excipients (1). Nonetheless, macrogols still find widespread use in formulations as an effective plasticizer, ointment and suppository base, and gaining in importance trough new uses as a solubilizing agent, solid solution carrier (2).

MATERIALS AND METHODS

A case is presented where macrogols (PEG 6000) is present as a plasticizer at usual levels (about 6% w/w) in a hypromellose based separating layer. Pellet formulation consists of neutral pellet cores, API layer, macrogols containing separating layer and gastric layer.

RESULTS AND DISCUSSION

Two incompatibilities were detected during stability testing of thus prepared product. First, presence of macrogols in separating layer reduces the performance of gastric polymer i.e. causing the reduced resistance of coated pellets to acidic media. It is suggested that macrogols oxidation leads to cleavage of hypromellose phthalate thus reducing the gastric resistance of polymer. The second observed effect was a marked increase in an API impurity formed through formic acid-formaldehyde methylation of a secondary amine (3). The proposed mechanism for this interaction is

through formation of formaldehyde as a degradation product of the macrogols, which is able to diffuse freely within the formulation and thus react with the API, forming the methylated product. The formation of formaldehyde from macrogols and its capability to react with the API was also confirmed experimentally.

Both effects are much more pronounced at accelerated stability conditions which is consistent with literature reports (2) on oxidation of macrogols during storage at elevated temperatures (above 50 C).

CONCLUSION

In conclusion macrogols are a ready source of instability. As shown in present case instability is not limited to API only, but can influence performance of excipients as well.

REFERENCES

1. McGinity et al. J. Pharm. Sci., Vol.64, No. 2, 1975, 356-357.
2. Rowe CR (Ed). Polyethylene Glycol. In: Pharmaceutical Excipients. London: Pharmaceutical Press. Electronic version, 2011.
3. Pine et al. J. Org. Chem., Vol.36, No. 6, 1971, 829-832.

VISCOELASTIC PROPERTIES OF AQUEOUS SOLUTIONS OF DIFFERENT SUBSTITUTION TYPES OF HYDROXYPROPYL METHYLCELLULOSE (HPMC)

S. Devjak Novak[1*], V. Kuhelj[1], F. Vrečer[1,2], S. Baumgartner[2]

[1] Krka, d.d., Novo mesto, Šmarješka cesta 6, 8501 Novo mesto, Slovenia; [2] University of Ljubljana, Faculty of Pharmacy, 1000 Ljubljana, Slovenia

INTRODUCTION

HPMC is one of the most frequently used drug carrier materials in hydrophilic matrix tablets. Four different degrees of substitution (DS) and many viscosity grades are approved according to Ph. Eur. and USP. Drug release from HPMC tablets occurs by water absorption, matrix swelling and forming gel layer around the tablet core (1). The behaviour of the gel layer is of the major importance for the drug release profiles. Rheological properties of hydrated polymer are related to gel structure, inter-chain interactions, erosion and diffusion processes. Therefore it is important to investigate rheological behaviour of HPMC by visco-elasticity measurements (2). The aim of the study was to characterize the viscoelastic properties of HPMC solutions under dynamic conditions of non-destructive oscillatory tests and correlate them with the drug release from HPMC tablets.

MATERIALS AND METHODS

Materials

HPMC polymers used are listed in Table 1. Samples A, B and E were supplied by Colorcon (Dow Chemical Co., USA) and samples C and D by Harke Pharma (ShinEtsu, Japan). Samples were of the same viscosity grade (4000mPas), but different DS: USP2208 (A,B,C), USP2910 (D) and USP2909 (E).

Preparation of HPMC aqueous solutions

Water was heated to 80°C. HPMC was added to obtained the 6%(w/w) solutions. The stirring was continued at a temperature bellow 10°C for another 40min. The solution was adjusted with water to 500g and then centrifuge for 3min at 3000rpm.

Rheological studies

Viscoelastic properties of 6%(w/w) solutions were determined with Anton Paar Physica MCR 301Rheometer at 20 ±0.5°C. Elastic (G`), viscous (G``) moduli, tangent of the phase angle (tanδ) and complex viscosity (η*), were obtained at the frequency range from 0,1 to 100Hz.

Table 1: HPMC samples and their properties. Methoxyl and hydroxypropyl contents were supplied by suppliers.

HPMC saples	Grade	Hydroxy propyl content (%)	Methoxyl content (%)
A	K4M	7.5	23.4
B	K4M	7.6	22.1
C	SH90-4000	9.3	22.9
D	SH60-4000	9.3	29.1
E	F4M	6.7	28.1

Preparation of tablets by direct compression

Composition of tablets: 90mg HPMC-A or B, 104mg Lactose monohydrate, 6 mg magnesium stearat and 100mg of diclofenac sodium. Tablets were made by direct compression (Killian Pressima), 2r=10mm, 15±0.5kN, m=300±15mg.

Dissolution testing

Drug release studies were performed on a dissolution apparatus using paddle method (VanKel 7025), 50rpm, 900mL of phosphat buffer solution (pH=6.8) at 37°C±0.5°C. Filtered samples were analyzed spectrophotometrically at 276nm.

RESULT AND DISCUSSION

From Fig. 1 it can be observed that G` and G`` are strongly frequency dependent for all samples. Bellow the crossover point G`` is higher than G` and above this point the situation is opposite. The reason is that at low frequency the chains have enough time to follow the changes and systems indicate liquid-like behaviour where polymers are conformational disordered. When the frequency is higher the chains cannot follow the changes and the system behaves more rigid. It can be assumed that more concentrated solutions would indicate a weak gel structure.

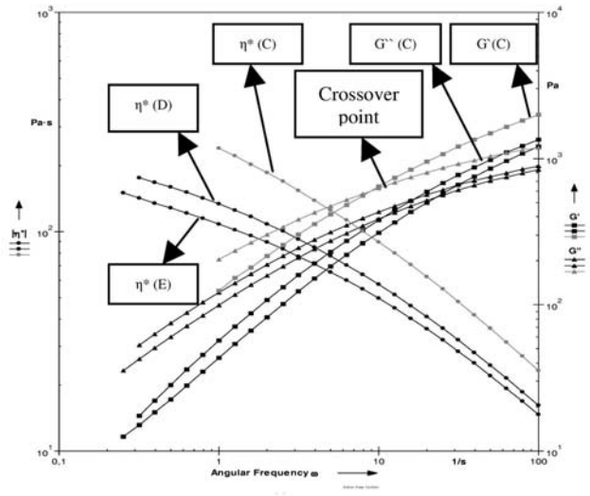

Fig. 1: G`, G``, η* for different HPMC substitution type: samples C, D and E. G`, G``, η* for D and E are very similar.

The values G`, G``, tan δ and η* were compared at frequency of 1Hz (Table 2). From results it can be concluded that sample B has significantly lower G`, G`` and η* in comparison to A and C. Sample B has also higher tanδ than A and C what indicate dominating viscous behaviour. That was rather unexpected because all three samples were of the same viscosity and substitution type. This finding was attributed to batch-to-batch variability between batches A, B and C. That is interesting because A and B are from the same manufacturer and show bigger differences in comparison to C, which is from another manufacturer. Samples D and E have the highest tanδ

and the lowest η*. Those observations indicate higher viscous behaviour and much weaker structure of systems, what can be explained with their chemical structure. Namely, batches D and E are highly substituted HPMC type. From presented results we can also conclude that DS have impact on visco-elastic behaviour. From results it can be seen that A and B have almost identical DS, but have significantly different η*, although both samples are from the same manufacturer.

Table 2: G`, G``, tanδ, η*of all batches at a frequency of 1Hz.

HPMC samples	G` (Pa)	G`` (Pa)	tan δ	Complex viscosity η* (Pas)
A	132.0	209.0	1.59	247
B	75.5	136.0	1.80	156
C	125.0	205.0	1.64	240
D	56.9	121.0	2.13	134
E	43.4	99.4	2.29	108

From Fig. 2 it is seen that both HPMC tablets enable prolonged drug release, but there are some diffrences. HPMC-B tablets are completely eroded within 20 hours, while HPMC-A tablets are still observed after that time. The release from HPMC-A is slower compared to HPMC-B. This can be explained by the differences in η* of solutions of both samples: HPMC-A has higher η*, compared to HPMC-B. The dissolution of HPMC-A is thus slower, gel layer thicker and drug release slower.

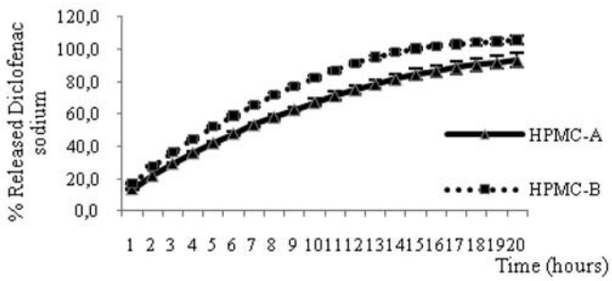

Fig. 2: Comparison of dissolution of diclofenac sodium from tablets of HPMC-A and HPMC-B.

CONCLUSION

Oscillatory tests provide us useful information about behaviour of polymer chains in highly-concentrated HPMC solutions. All samples indicate liquid-like behaviour, where G` and G`` are strongly dependent on frequency. Different η* was determined as a consequence of different chemical structure irrespective to the same nominal viscosity of all batches. It can also be concluded that viscosity is one of the key parameter influencing formation of hydrogel layer around the HPMC tablets and regulating drug release rate.

REFERENCES

1. Baumgartner S, Lahajnar G, Sepe A, Kristl J. Quantitative evaluation of polymer concentration profile during swelling of hydrophilic matrix tablets using 1H NMR and MRI methods. Eur. J. of Pharm. and Biopharm.2005; 59: 299-306
2. Michailova V, Titeva S, Kotsilkova R, Krusteva E, Minkov E. Influence of aqueous medium on viscoelastic properties of carboxymethylcellulose sodium,hydroxypropylmethyl cellulose and thermaly pregelatinized starch gels.Colloids and Surfaces A: Physicochemical and Engineering Aspects 1999; 149: 515-520

EFFECT OF FORMULATION CHARACTERISTICS TO FLOWABILITY OF RAMIPRIL GRANULES

B. Aksu[1], A.Yıldız[2,*], E.Cevher[2]

[1] Santa Farma Pharmaceuticals, Okmeydanı, Istanbul, Turkey; [2] Istanbul University, Faculty of Pharmacy, Department of Pharmaceutical Technology, Istanbul-Turkey

INTRODUCTION

Granulation is a process by which fine powders are agglomerated into larger particles using a liquid binder. Flow properties of granules are of critical importance in fabrication of reproducible tablet formulations (1). An optimum flow of granules should be achieved to ensure uniform feed from funnel into dies to obtain tablet formulations with acceptable content uniformity, weight variation and physical consistency (2). In our study, therefore, with an eye to developing optimum tablet formulations of ramipril which is an angiotensin-converting enzyme inhibitor, granule formulations were fabricated by wet granulation technique and the effect of some parameters such as granule size, type and amount of lubricants on their flow characteristics were investigated.

MATERIAL AND METHODS

Materials

Ramipril was purchased from Santa Farma Pharmaceutical Company; Hydroxypropyl methyl cellulose (HPMC), Collorcon; Magnesium stearate, Faci; Sodium stearyl fumarate, JRS Pharma. All the other excipients were pharmaceutical grade.

Fabrication of granule formulations

Ramipril (5 mg) and other additives (Lactose monohydrate, pregelatinised starch, Ac-Di-Sol, sodium hydrogen carbonate, ferrum oxide) were granulated in high shear granulator (ProCept, Belgium) by using HPMC solution and passed through an oscillating granulator fitted with 0.250 mm screen, and dried in a hot-air oven at 50°C. After re-sieving using 0.80 mm and 1.25 mm screens, the granules were blended with different amount of two distinct lubricants (magnesium stearate and sodium stearyl fumarate) for 5 min (Table 1).

Table 1: Formulation parameters of ramipril granule formulations

Formulation	Sieve mesh size (mm)	Amount of Lubricant (%)	
		Magnesium stearate	Sodium stearyl fumarate
F1	0.8	-	-
F2	0.8	0.75	-
F3	0.8	1.00	-
F4	0.8	-	0.60
F5	0.8	-	1.20
F6	1.2	-	-
F7	1.2	0.75	-
F8	1.2	1.00	-
F9	1.2	-	0.60
F10	1.2	-	1.20

Determination of granule flow characteristics

Granule characterization was performed on unlubricated and lubricated granules using Powder reometer (TA-XT*Plus*, Stable Micro Systems, UK). The instrument was calibrated for force and distance measurements. A cylindrical vessel was partly filled (140 mL) with each granule formulation and set on the platform of the apparatus. A helical blade which moves into the granule bed was used to probe and to measure *a)* the cohesion (*Cohesion test*), *b)* the caking (*Caking test*) and *c)* the changes on granule

flow properties due to the increasing and decreasing flow speeds (P*owder flow speed dependence test).*

RESULTS AND DISCUSSION

Cohesion is tendency for particles of granules to cling together. *Cohesion test* results showed that the addition of both lubricants decreased the cohesiveness of granule formulations. Whereas the concentration of lubricants did not significantly change the cohesiveness of the granules. Granules which were sieved 0.8 mm and 1.2 mm screen and lubricated with 1.2 % sodium stearly fumarate had lowest caking strength (Figure 1).

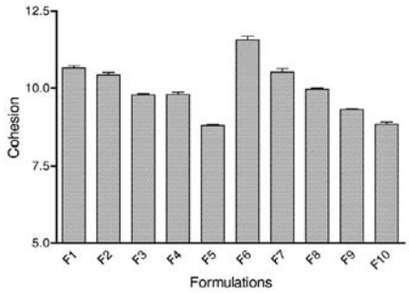

Fig.1: Cohesion test result of unlubricated and lubricated granule formulations.

Caking is defined the tendency of granules to form larger agglomerates during storage and transportation. *Caking test* indicated that the caking strength decreased with addition of both lubricants. However, concentration of the lubricants and screen size (0.8mm and 1.2mm) did not significantly change the caking-strength of the granules. Granules which were lubricated with magnesium stearate showed less caking characteristics than sodium stearly fumarate due to their lowest caking strength (Figure 2).

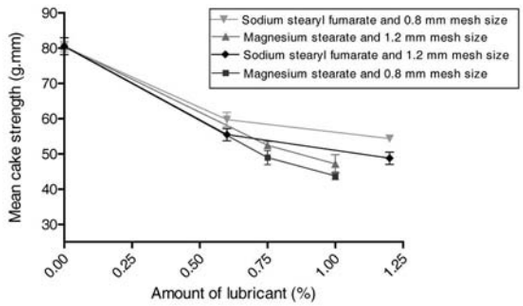

Fig. 2: Effect of lubricant type and amount on cake strength of granule formulations

Granule flow properties may change with increasing and decreasing flow speeds. Powders/granules may become more resistant to flow as it is forced to flow faster or indeed it may become more free flowing as the flow speed increases. While marginal or no change of the compaction coefficient with flow speed would show that the granule is flow speed independent, an increase or decrease in the compaction coefficient as the test speed dependence may result inadequate feed from bulk container into dies during tablet preparation. Flow stability also gives important information about the flow resistance of the granules. In this study, lubricated granules flow stability values were found to be very close to 1.00. On the other hand, the lubricant concentration and screen size did not significantly change the flow stability of granules. Flow stability result results show that granules sieved through 0.8 mm and 1.25 mm screen size and lubricated with both concentration of sodium stearly fumarate (0.6 and 1.2 %) had the best flow stability (Figure 3).

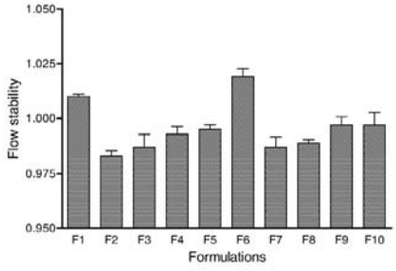

Fig. 3: Flow stability values of unlubricated and lubricated granule formulations.

CONCLUSION

As a conclusion, sodium stearyl fumarate was found to be the effective lubricant for ramipril granule formulations.

REFERENCES

1. Kani T, Suzuki T, Tsukada M, Kamiya H. Influence of surface-adhered nanoparticles and nanoporous structure on bulk flowability of silica Powder Technology, 176, 108-113, 2007.
2. Navaneethan CV, Missaghi S, Fassihi R. Application of Powder Rheometer to Determine Powder Flow Properties and Lubrication Efficiency of Pharmaceutical Particulate Systems. AAPS PharmSciTech, 6(3), Article 49, 2005.
3. Aksu B, Yıldız A, Özer Ö, Güneri T. Optimisation studies for making free-flowing compactable powder and granule containing ramipril with high concentration of HPMC at 60ºC and 0,5-1,0 % humidity. Controlled Release Society 37th Annual Meeting and Exposition, July 10-14, 2010. Portland Oregon, USA.

OPTIMIZATION OF ALFUZOSIN HCL TABLET FORMULATIONS USING ARTIFICIAL NEURAL NETWORK

B. Mesut[1*], B. Aksu[2], Y. Özsoy[1]

[1] Istanbul University, Faculty of Pharmacy, 34116, Beyazıt, İstanbul, Turkey; [2] Santa Farma Ilaç San. ve Tic. A.Ş., Okmeydanı Boruçiçeği Sok. No:16, 34382, Şişli, İstanbul, Turkey

INTRODUCTION

In terms of content, pharmaceutical product development knowledge is very intensive and product development process is quite complex and long. Different softwares based on mathematical models have been developed In order to ease the completion of the product development process. Recent developments in mathematics and computer science resulted in new programs based on artificial neural networks (ANN) techniques. These programs have been employed in development and formulation of pharmaceutical dosage forms (1).

In our study, Alfuzosin HCl was used as a model drug and formulations of modified release tablet forms were designed with the application of a program based on ANN technique.

MATERIALS AND METHODS

Materials

Alfuzosin was purchased from Generica Pharmaceutical Company; hydoxypropyl methyl cellulose (HPMC), Colorcon; Xanthan gum (XG), Sigma Aldrich Chemie; Magnesium stearate, Faci. All the other excipients were of analytical grade.

Preparation of modified release tablets

Briefly, Alfuzosin (10 mg) and the additives (Microcrystalline cellulose 101, lactose monohydrate, polyvinyl pyrrolidone and HPMC/XG) were blended for 10 min and sieved through 0.75mm screen. Magnesium stearate was added into this mixture and blended for an additional 5 min. Formulation parameters and pressure forces of alfuzosin tablets are shown in Table 1.

Table 1: Formulation parameters of alfuzosin tablet formulations

Formulation	Binder type	Binder (%)	Lubricant (Magnesium stearate) (%)	Pressure force (psi)
F1	HPMC	65	0.5	1000
F2	HPMC	65	0.5	2000
F3	HPMC	65	1.0	1000
F4	HPMC	65	1.0	2000
F5	HPMC	75	0.5	1000
F6	HPMC	75	0.5	2000
F7	HPMC	75	1.0	1000
F8	HPMC	75	1.0	2000
F9	XG	45	0.5	1000
F10	XG	45	0.5	2000
F11	XG	45	1.0	1000
F12	XG	45	1.0	2000
F13	XG	55	0.5	1000
F14	XG	55	0.5	2000
F15	XG	55	1.0	1000
F16	XG	55	1.0	2000

Drug release from tablets

In vitro dissolution studies of alfuzosin tablets were performed using USP paddle method (Apparatus II, Sotax, Switzerland). Dissolution medium was 900 ml of 0.01 N HCl (37°C±0.5) and stirred at 100 rpm (2). The test was continued for 24 hours and samples of 5 ml were withdrawn at predetermined time intervals. The withdrawn volume was replenished immediately with the same volume of the dissolution medium. The drug content was analyzed at 244 nm by UV spectrophotometer (Schimadzu, Japan). Comparision was made to Xalfu XL 10 mg tablet (Generica Pharmaceutical Company). The effect of polymer type, polymer and lubricant concentration and pressure force on in vitro dissolution of alfuzosin were investigated.

ANN training parameters

The program used in this study was Form Rules V3.32 data mining package. Having five model criteria, the program is based on neurofuzzy logic technique and has been developed by Intelligensys Ltd. "Structure Risk Minimization" (SRM) model of the program was used and it was trained accordingly.

RESULTS AND DISCUSSION

Drug dissolution profiles

The dissolution profiles of all formulations of all formulations (F1-F16) are shown in Figure 1.

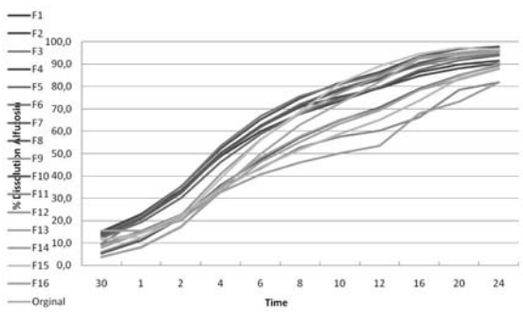

Fig. 1: Drug dissolution profiles

Evaluation of the training data

The variable parameters used at drug dissolution intervals are evaluated with SRM program and the number of r^2 values complying with the training data of the model was obtained (Table 2).

Table 2: Test data example of 4th hour

Dis. Time	r^2	Formules
4 h	IF	mer type is LOW THEN D-4h is HIGH
0,9	Poly	IF Polymer type is HIGH THEN D-4h is LOW

The evaluation of the points which are affected from a couple of parameters is also supported with submodels of the program.

According to our results, the formulation F16 including XG 0.55% as polymer showed the highest similarity to the original formulation containing HPMC (Table 3).

Table 3: Best Match Table

	%Match	Polymer type	Polymer conc(%)	Lubricant Conc(%)	Pressure Force
F1	0	HPMC	0,65	0,5	1000
F2	42,9871	HPMC	0,65	0,5	2000
F3	1,44336	HPMC	0,65	1,0	1000
F4	50,8001	HPMC	0,65	1,0	2000
F5	52,6514	HPMC	0,75	0,5	1000
F6	27,1101	HPMC	0,75	0,5	2000
F7	29,1183	HPMC	0,75	1,0	1000
F8	27,267	HPMC	0,75	1,0	2000
F9	45,6542	XG	0,45	0,5	1000
F10	94,1638	XG	0,45	0,5	2000
F11	94,8855	XG	0,45	1,0	1000
F12	85,786	XG	0,45	1,0	2000
F13	61,7509	XG	0,55	0,5	1000
F14	94,0697	XG	0,55	0,5	2000
F15	29,6517	XG	0,55	1,0	1000
F16	95,262	XG	0,55	1,0	2000

CONCLUSIONS

It is very important for the generic pharmaceutical manufactures to select the formulation of a drug product with a highest level of similarity of in-vitro release profile in comparison to the original one. As a conclusion, by using Form Rules V3.32 data mining program it was possible to optimize in short time and with reduced cost.

REFERENCES

1. Colbourn E, Rowe C R, Modelling and Optimization of a Tablet Formulation Using Neural Networks and Genetic Algorithms. Pharm. Tech.Eur. 1996, 8:46-55.
2. FDA dissolution data base; www.accessdata.fda.gov/scripts/cder/dissolution/

INFLUENCE OF SUPERDISINTEGRANT SELECTION ON THE RATE AND EXTENT OF DISSOLUTION OF POORLY SOLUBLE DRUGS

T. Vágó[1*], J. Fitzpatrick[2], T. Bee[3]

[1] ISP Representation Office, 1137 Budapest, Szt. István park 18., Hungary; [2] ISP Global Technologies Deutschland GmbH, Emil-Hoffmann-Str. 1a, 50996 Köln, Germany; [3] International Specialty Products, 1361 Alps Road, Wayne, NJ 07470, USA

INTRODUCTION

Dissolution of a drug is essential for its absorption through the biological membranes into systemic circulation for therapeutic efficacy. In many solid dosage forms, disintegration occurs prior to dissolution. But the correlation between tablet disintegration and drug dissolution is not always observable. It is well documented that superdisintegrants facilitate the rate and extent of tablet disintegration. However, the selection of superdisintegrant can also influence the rate of drug dissolution.

In this study, the effect of the three commonly used superdisintegrants on the respective rates and extent of dissolution of 13 poorly soluble drug actives whose aqueous solubilities ranged from 2 to 2,300 micrograms per milliliter was evaluated.

MATERIALS AND METHODS

Superdisintegrants

The superdisintegrants studied were: crospovidone Type A (Polyplasdone® XL, International Specialty Products (ISP)); crospovidone Type B (Polyplasdone XL-10, ISP); croscarmellose sodium (Ac-Di-Sol®, FMC Biopolymer); and sodium starch glycolate (GLYCOLYS®, Roquette).

Active Pharmaceutical Ingredients (APIs)

Table I lists the 13 poorly soluble APIs tested.

Table I: APIs Studied

API	Supplier
Piroxicam	ACE Chemicals, India
Acyclovir	Int'l Group Hua Tai Imp and Exp Co.,Ltd
Terbinafine HCl	Panchseel Organic Limited, India
Nevirapine	Aurbindo Pharma Ltd, India
Atorvastatin	Aurbindo Pharma Ltd, India
Clopidogrel bisulfate	Glochem Industries Limited, India
Carbamazepine	Benzo chem Life Sciences, India
Ketoconazole	Glochem Industries Limited, India
Efavirenz	Aurbindo Pharma Ltd, India
Ezetimibe	Glenmark Pharma Ltd, India
Simvastatin	Artemis Biotech, India
Loratadine	Cadila Pharmaceutical Sciences, India
Raloxifene HCl	Glochem Industries Limited, India

Tablet Preparation

Tablets were prepared at the highest market dose using a direct compression or wet granulation process as considered appropriate through a review of the ingredients listed in the Physician's Desk Reference (PDR) and patent literature.

Tablets were compressed using appropriate tooling on a 16-station, instrumented, rotary compression machine (Cadmach). Advanced Instrumentation Monitor (AIM) software (Metropolitan Computing Corporation, USA) was used with the tablet press to determine the compression force required to yield tablets of approximately equal breaking force for the various drugs used in the study.

Tablet Evaluation

The respective breaking forces of the prepared tablets were determined 24 hours after compression using ERWEKA TBH 310 MD hardness tester (ERWEKA, Germany). Ten tablets from each batch of prepared were tested for tablet breaking force, and the mean and standard deviation were calculated.

Respective disintegration times of the prepared tablets were measured in 900 ml of purified water with disks at 37ºC using ERWEKA TAR series tester. Disintegration times of six individual tablets were recorded.

The dissolution studies of the prepared tablets were carried out using USP Apparatus 2 (Vankel VK). Dissolution profiling was performed with the USP or US FDA recommended medium for the respective drug. Dissolution profiling was also carried out in a medium developed in-house and derived from the recommended media, capable of better discrimination between the formulations.

The time required to achieve 80% drug release (t_{80}) was determined by fitting the dissolution data to a four-parametric logistic model using the Marquardt–Levenberg algorithm (Sigmaplot 9.0 SPSS Inc., Chicago, IL).

RESULTS AND DISCUSSION

With the 13 poorly soluble drugs evaluated, no significant differences were observed in the breaking force and disintegration times of the tablets prepared using the various superdisintegrants for a given drug studied.

The time required to achieve 80% drug release (t_{80}) was considered for comparing dissolution results. The t_{80} results in the recommended media showed crospovidone provided the fastest t_{80} for 12 of the 13 drugs studied and crospovidone, Type B provided the fastest t_{80} for 10 of the 13 drugs studied. In the discriminating media, crospovidone Type B provided the fastest release for 12 of 12 drugs. A discriminating medium for raloxifene HCl tablets was not developed as the recommended medium was sufficiently discriminating; hence only 12 drugs were evaluated in a discriminatory medium.

For the most poorly soluble drugs, crospovidone Type B was often the only superdisintegrant to yield a formulation achieving 80% drug release in the discriminating media.

CONCLUSIONS

The results show that crospovidone Type B is more effective in enhancing the dissolution rate of poorly soluble drugs. The results also clearly show that selecting a superdisintegrant should extend beyond consideration simply of its tablet-disintegration capability and take into account its ability to influence the rate of drug dissolution.

ACKNOWLEDGMENTS

The authors wish to acknowledge the support and contributions of ISP's pharmaceutical research and development and analytical scientists in Hyderabad, India, and Wayne, New Jersey, USA.

RAPID SCREENING OF DRUG SUPERSATURATION AND ENHANCED SOLUBILITY OF BCS CLASS II COMPOUND IN THE PRESENCE OF EXCIPIENTS

M. Petrusevska, M. Homar, L.Peternel

Lek Pharmaceuticals d.d. Verovskova 57, Ljubljana, Slovenia

INTRODUCTION

Supersaturation presents a thermodynamic unstable state where compounds stay in solution at a concentration above their equilibrium solubility (1). Induction and/or maintenance of this state represent an attractive strategy toward improvement of intestinal absorption (1,2). Supersaturation can be obtained by using different salt forms of the drug, using surfactants, solid dispersions, and nanoparticles (3,4). Therefore, one of the key aims is to prevent/retard drug precipitation.

The aim of the present study was to determine the impact of selected excipients on investigative BCS class II LK compound, which can be increased by taking advantage of drug supersaturation state.

LK compound does not contain any ioniazable functional groups and is practically insoluble in water. Its solubility was determined to be 2.6 µg/ml. *In vitro* 96 – well drug supersaturation method was developed to rapidly evaluate which excipients may be best suited to provide enhanced solubility i.e. drug supersaturation state.

MATERIALS AND METHODS

Materials

Poloxamer 188, Polysorbate 80, PVP K25 and HPMC, were chosen as possible inductors of LK compound supersaturation state.

%(v/v) Polysorbate 80							
t(h)	1	0.5	0.1	0.05	0.01	0.001	C
SI mean with SEM (n=4) in parenthesis							
2	109 (3)	106 (3)	79 (4)	76 (3)	71 (2)	11 (1)	0.95 (0.1)
4	90 (0.5)	88 (2)	68 (4)	57 (6)	59 (3)	6 (0.4)	1.5 (0.1)
24	58 (2)	59 (1)	42 (6)	24 (2)	8 (1)	4 (1)	1
DS mean with SEM (n=4) in parenthesis							
2	2.0 (0.1)	1.8 (0.1)	1.9 (0.1)	4.4 (1.1)	8.2 (1)	2.1 (0.2)	0.95 (0.1)
4	1.6 (0.1)	1.5 (0.04)	1.6 (0.1)	3.0 (0.5)	7.8 (1)	2.0 (0.6)	1.5 (0.1)
% (v/v) Poloxamer 188							
SI mean with SEM (n=4) in parenthesis							
2	101 (5)	103 (5)	89 (0.5)	88 (2)	21 (2)	8 (1)	0.95 (0.1)
4	83 (4)	85 (2)	68 (3)	65 (3)	12 (1.5)	10 (4)	1.5 (0.1)
24	71 (4)	59 (4)	13 (0.5)	7 (2)	6 (1)	6 (0.5)	1
DS mean with SEM (n=4) in parenthesis							
2	2.8 (1.3)	1.4 (0.4)	7.1 (0.2)	7.6 (2.4)	4.0 (0.7)	1.4 (0.2)	0.95 (0.1)
4	2.6 (1.4)	1.1 (0.4)	5.5 (0.2)	5.8 (1.9)	2.2 (0.5)	1.7 (0.8)	1.5 (0.1)
% (v/v) HPMC							
t(h)	10	5	1	0.1	0.01	0.001	C
SI mean with SEM (n=4) in parenthesis							
2	147 (6)	162 (11)	21 (3)	54 (10)	34 (4)	40 (8)	0.95 (0.1)
4	80 (7)	101 (5)	25 (3)	16 (2)	24 (5)	21 (2)	1.5 (0.1)
24	60 (3)	152 (12)	10 (0.2)	7 (0.1)	6 (0.2)	7 (0.4)	1
DS mean with SEM (n=4) in parenthesis							
2	2.5 (0.1)	1.1 (0.1)	2.3 (0.4)	8 (1.5)	5.5 (1)	6 (1)	0.95 (0.1)
4	1.5 (0.2)	0.64 (0.6)	2.7 (0.3)	4 (2)	3.3 (1)	3.3 (0.5)	1.5 (0.1)
% (v/v) PVP K 25							
SI mean with SEM (n=4) in parenthesis							
2	44 (3)	33 (5)	36 (6)	13 (6)	23 (1)	7 (0.6)	0.95 (0.1)
4	31 (2)	19 (0.7)	13 (1)	19 (8)	13 (1.5)	7.5 (0.8)	1.5 (0.1)
24	20 (1)	16 (0.3)	8 (0.3)	9 (0.6)	8 (0.2)	6 (0.3)	1
DS mean with SEM (n=4) in parenthesis							
2	2.2 (0.1)	2.1 (0.3)	3.6 (0.7)	1.4 (0.4)	3.1 (0.2)	1.0 (0.1)	0.95 (0.1)
4	1.6 (0.1)	1.3 (0.1)	1.6 (0.5)	2.2 (0.7)	1.7 (0.1)	1.1 (0.1)	1.5 (0.1)

Table1: Solubility index (SI) and degree of supersaturation (DS) of LK compound in the presence of excipients at 6 different concentrations, in time intervals of 2, 4 and 24 h. Two-way ANOVA, grey fields $p<0.05$, C (control)

Experimental method

LK compound (10mM in DMSO) was dispensed into each well of the polypropylene microtiter plate (MTP), followed by 50-times dilution with excipient solutions in phosphate buffer pH=6.8. MTP's were immediately sealed followed by incubation (37^{0}C, 550 rpm). The final DMSO content in the tested media was 2% (v/v). Samples were taken at appropriate time intervals, and centrifuged, followed by supernatant dilution (10-times) with mobile phase. LC analysis was performed on Acquity UPLC, using C18 analytical column, absorbance was measured at 278 nm with PDA. The solubility enhancement index (SI) was defined as the ratio of the drug concentration at particular time point in the excipient present media with the solubility at 24 h in phosphate buffer pH 6.8. The degree of supersaturation (DS) was calculated by dividing the concentration measured at particular time point by the equilibrium solubility in exactly the same medium.

RESULTS AND DISCUSSION

We have tested four excipients including two polymers and two non-ionic surfactants, at six different concentrations. As shown in Table 1, all of the tested excipients enhanced the solubility of LK compound in the concentration-dependent manner in the following order: HPMC > Tween80 = Poloxamer188 > PVPK 25. Surfactants showed initial increase of dissolved drug concentration at the beginning of the experiment, followed by time-dependent decrease without reaching an asymptote value. On the other hand, the drug concentration levelled off in the experiments where polymers were used suggesting a significant inhibition of LK compound precipitation for longer period and possible stabilization of this state. The measured equilibrium LK compound solubility in the excipient solution was lower than the solubility measured at earlier time points, indicating that different degrees of LK compound supersaturation was achieved (Tab.1). Lower DS value in the case of Polysorbate 80 1% and 0.1% is a result of prolonged enhancement of LK solubility. The ability of PVP K25 to enhance the duration of supersaturation, rather than the degree of supersaturation suggests inhibition through retardation of crystal growth (2). One of the causes for precipitation inhibition of LK might be a result of the hydrophobic interactions (polypropylene oxide segment in Polaxamer 188), hydrogen bonding (HPMC, PVP K 25) and micellization (Polaxamer 188, Polysorbate 80) between the drug molecule and the polymers.

CONCLUSIONS

A rapid assay was developed to identify excipients that can efficiently improve solubility and/or induce the supersaturation of poorly water soluble LK compound. HPMC was most effective in increasing LK compound solubility and promoting drug supersaturation over the time tested period. In addition, Poloxamer 188 and Polysorbate 80 provided increased drug solubility. Information gained from the presented high throughput method can be usefully applied in decision making in designing of drug formulation, assuring successful exploitation of the supersaturation and solubility enhancement *in vivo*.

REFERENCES

1. Browers J, Brewster M, Augustinjs P. Supersaturating drug delivery systems: The answer to solubility limited oral bioavailability? J. Pharm. Sci. 2008; 98:2549-2572
2. Warren BD, Benameur H, Porter CJH, Pouton CW. Using polymeric precipitation inhibitors to improve the absorption of poorly water-soluble drugs: a mechanistic basis for utility. J.Drug Target. 2010; 18:704-731
3. Dai WG, Dong LC, Shi X, Nguyen J, Evans J, Xu Y, Creasey AA. Evaluation of drug precipitation of solubility enhancing liquid formulations using milligram quantities of new molecular entity. J. Pharm. Sci. 2006; 96:2957-2969
4. Bagchi S, Mukherjee T, Plakoguannis F. Re-evaluation of in vitro dissolution techniques for supersaturating delivery systems. Pharm. Dev. Technol. 2011, 1-6, Early Online.

THERMOPLASTIC AGGLOMERATION AS A METHOD OF SOLUBILISATION OF POORLY SOLUBLE ACTIVE PHARMACEUTICAL INGREDIENTS

T. German[1,*], K. Pintye-Hódi[2], F. Vrečer[1,3]

[1] KRKA d.d., Novo mesto, Šmarješka cesta 6, 8501 Novo mesto, Slovenia; [2] University of Szeged, Faculty of Pharmacy, Eötvös u. 6, 6720 Szeged, Hungary; [3]University of Ljubljana, Faculty of Pharmacy, Aškerčeva cesta 7, 1000 Ljubljana, Slovenia

INTRODUCTION

Thermoplastic agglomeration is an alternative to classical technological processes which offers a number of advantages. The process does not require the use of solvents and is therefore suitable for the formulation of moisture-sensitive active ingredients. Additionally the drying phase is eliminated and consequently the process is shorter and more economical. A further advantage of this process is the availability of a wide range of meltable binders with different chemical and physical characteristics, which can be used to prepare controlled release granules or to enhance the dissolution rate of poorly soluble drugs (1,2).

Hydrophilic binders such as macrogol (PEG), gelucire and poloxamer have been shown to successfully enhance the dissolution of poorly soluble drugs using hot melt technology (3). Sugar esters (SE), non-ionic surface-active agents consisting of sucrose as hydrophilic moiety and fatty acids as lipophilic groups have also been applied in hot melt technology, but information available on these carriers is limited (4).

The aim of present study was to investigate the effect of different binders on dissolution of a poorly soluble model drug nitrendipine from solid dosage form prepared via thermoplastic agglomeration process.

MATERIALS AND METHODS

Materials

Nitrendipine (Krka, Novo mesto, Slovenia) was used as a model drug with poor water solubility. The following binders were used: sugar esters D-1816, D-1616 and D-1616 (SE, Surfhope® SE Pharma, Japan), Macrogol 6000 (PEG 6000, Clariant Vertrieb, Germany), Gelucire® 44/14 (Gattefossé, France) and Poloxamer 188 (Lutrol® F68, BASF, Germany), lactose monohydrate was used as a diluent (DMV, The Nederland).

Preparation of granules

Granules were prepared by hot melt granulation in a ProCept Mi-Pro high-shear mixer equipped with a double jacket for heating/cooling and a six-bladed impeller, with a bowl capacity of 250g. Six different granulates were prepared, each with different binder but the same quantitative composition: 20% Binder, 20% Nitrendipine and 60% Lactose monohydrate.

Drug release studies

For drug release studies 0.3% solution of Sodium lauryl sulphate in purified water was used. The studies were performed in dissolution apparatus, paddle method (Apparatus II, VanKel 7010), 1000 mL, 50 rpm, 37°C±0.5 °C. Samples were UV analysed at 358 nm (Agilent 8453).

Measurement of contact angle

Contact angle (θ) was measured on comprimates weighing 250 mg obtained by compression (compression force 550N) of granulates or physical mixtures using demineralised water as a liquid (volume 0.5 µL) on apparatus Contact Angle Meter KRÜSS.

X-ray powder diffraction studies.

XRPD profiles were taken with a Philips X`Pert Pro MPD. The scanning angle ranged from 3°–32.5° of 2θ, the steps were 0.033° of 2θ, integration time was 100s.

RESULTS AND DISCUSSION

The results showed that both dissolution rate and extent could be modified by the choice of different binders and the use of melt granulation technology (Fig 1). No increase in dissolution rate of nitrendipine from granules prepared with PEG 6000 and only limited increase form granules with Gelucire 44/14 was observed. However there was an observable increase in dissolution of nitrendipine from the granules containing sugar esters and notable increase form granules containing Lutrol F68. There were only minor differences in the dissolution profiles of nitrendipine from samples of granulate containing different sugar esters with various HLB values.

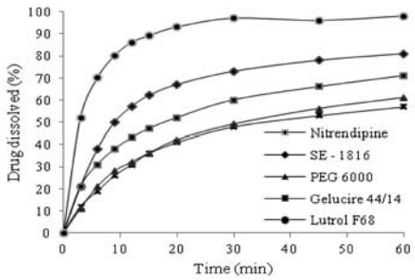

Fig. 1: Dissolution profiles of pure nitrendipine and granules containing different binders and nitrendipine (5).

Contact angle measurements showed that wetting properties of pure drug, physical mixtures and granules were different. The highest contact angle was measured for pure drug, which showed the lowest dissolution rate, and the lowest contact angle was measured for granules containing Lutrol F68 (Fig 2).

The wetting properties were improved for granules prepared by melt granulation compared to physical mixture for all tested binders with the exception of Gelucire 44/14, where unusually low contact angle was observed for physical mixture. This could be attributed to waxy properties of Gelucire and consequently possible low homogeneity of physical mixture.

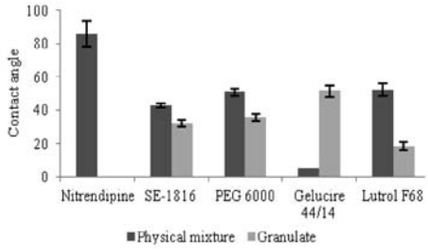

Fig. 2: Contact angle (θ) of pure nitrendipine and, physical mixture and granules (5).

Powder X-ray difractograms of pure nitrendipine and samples of granulates with different binders clearly show that the drug is present in crystalline form. Somewhat lower intensities of diffraction lines in granulates were observed and were attributed to lower drug content due to dilution of nitrendipine in the granules

CONCLUSIONS

The results of this study show that thermoplastic agglomeration is an effective technology for increasing the dissolution of poorly soluble drug. All the binders with the exception of PEG6000, increased the dissolution of nitrendipine, and Lutrol F68 proved to have the highest effect. The increase was not due to formation of amorphous nitrendipine, but a consequence of improved wettability of granules.

ACKNOWLEDGEMENT

The authors would like thank Harke Pharma GmbH for donation of samples of sugar esthers and KRKA, d.d., Novo mesto for the support in performing the study.

REFERENCES

1. Royce A, Suryawanshi J, Shah U, Vishnupad K. Alternative Granulation Technique: Melt Granulation. Drug. Dev. Ind. Pharm. 1996; 22(9&10): 917-924.
2. Passerini N, Calogera G, Albertini B, Rodriguez L. Melt granulation of pharmaceutical powders: A comparison of high-shear mixer and fluidised bed processes. Int. J. Pharm. 2010; 391: 177–186.
3. Krošelj V, Pišek R, Večer F. Production and characterization of immediate release lansoprazole pellets produced by melt pelletization. Pharm. Ind. 2008; 70 (1): 147-155.
4. Szuts A, Makai Z, Rajkó R, Szabó-Révész P. Study of the effects of drugs on the structures of sucrose esters and the effects of solid-state interactions on drug release. J. Pharm. Biomed. Anal. 2008; 48 (4): 1136-42.
5. Barbo M. Solubilization studies of nitrendipine with melt granulation process. B.S. Thesis, University of Ljubljana, Faculty of Pharmacy. Ljubljana, 2011

BIORELEVANT DISSOLUTION METHOD FOR EXTENDED RELEASE PRODUCT

S. Berglez*, I. Legen

Sandoz Development Centre Slovenia, Lek Pharmaceuticals, Verovškova 57, 1526 Ljubljana, Slovenia

INTRODUCTION

During development of generic product similar safety and efficacy as reference product is usually proven in bioequivalence study. Due to high cost and time consuming of bioequivalence study establishing IVIVC or IVIVR is a strong tool in formulation development. Biorelevant dissolution testing can to guide formulation development towards bioequivalent product.

The aim of our study was to find the biorelevant method using available in vivo results. In vivo data obtained from two sets of bioequivalence studies was used as a basis for finding in vitro dissolution method that simulates in vivo dissolution. In each set of bioequivalence study reference product with different controlled release formulation was used. Dissolution testing was performed with different apparatus, media and agitation. Some conventional methods using Apparatus 2 as well as some lees convention methods with Apparatus 3 (Bio-Dis) were used.

This biorelevant method will serve as a tool for further development of generic product and will reduce the number of bioequivalence studies needed.

METHODS

Data from two sets of bioequivalence studies (fast, fed, ss condition) were obtained. In first set reference product had HPMC in formulation (Reference 1) and in second reference formulation had alginate (Reference 2) as release control polymer. Test product was in both cases the same formulation with HPMC as release control polymer.

Dissolution studies were conducted using Apparatus 2, paddle method, and Apparatus 3, bio dis method. Several tests were performed with different dissolution media and different agitation parameters. Results of three tested methods that are presented here have following testing conditions:

1. Method (Figure 1):
   - Apparatus 2,
   - 900 ml phosphate buffer pH 6.8, 75 rpm;
2. Method (Figure 2):
   - Apparatus 2,
   - 500 ml Fassif, 75 rpm
3. Method (Figure 3):
   - Apparatus 3,
   - three rows with 250 ml phosphate buffer pH 6.8; 10, 20 and 30 dpm;

Next to these methods others methods were tested and are not presented here due to abstract limitation and lower importance.

RESULTS AND DISCUSSION

Summary of bioequivalence results with ratio of test and reference Cmax is presented in Table 1.

Table 1: Bioequivalence results

Study	BE results - Cmax Reference 1 - HPMC formulation	BE results - Cmax Reference 2 - alginate formulation
fast	93,31 (84,12-103,50) CV=28%	60,36 (54,71-66,59) CV=28,3%
fed	116,12 (104,66-128,84) CV=28%	78,65 (71,67-86,30) CV=26,3%
ss	125,29 (109,60-143,23) CV=37%	86,24 (79,54-93,51) CV=23,1%

Mean values of percent dissolved from both reference products and Test product are graphically presented in Figures 1, 2 and 3. In Figure 1 results obtained with first method are presented. The fastest release profile has Reference 1, followed by Reference 2 and Test product. This method has shown no correlations with in vivo results.

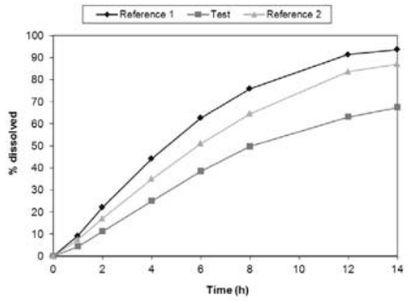

Fig. 1: Dissolution profiles of investigated formulations with method 1 (USP II, 900 ml phosphate buffer pH 6.8, 75 rpm).

In method 2 Fassif was used as commercially available biorelevant dissolution medium (figure 2). Again, no correlation with in vivo data was found. The fastest dissolution profile was from Test product; both reference products had similar and lower dissolution profile. Changing the dissolution media to more biorelevant one did not contribute to higher correlation with in vivo data.

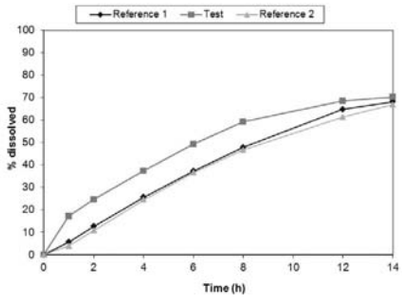

Fig. 2: Dissolution profiles of investigated formulations with method 2 (USP II, 500 ml Fassif; 75 rpm).

In method 3 same media (phosphate buffer pH 6.8) as in method 1 was used. Test was made on Apparatus 3 were tablets are exposed to different agitation condition and hydrodynamic environment. Media volume was reduced to 250 ml in each vessel and three rows with different dipping

speed were used. Dissolution results obtained with this method are in correlation with Cmax values from bioequivalence studies. In both cases the fastest substance release was from Reference 2, then Reference 1 and the slowest from Test product.

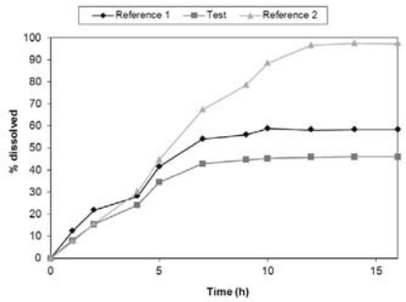

Fig. 3: Dissolution profiles of investigated formulations with method 3 (USP III, three rows, 250 ml phosphate buffer pH 6.8; 10, 20, 30 dpm).

Reducing volume of dissolution media is a step towards in vivo conditions as well as change in hydrodynamic achieved with replacing Apparatus 2 with Apparatus 3. Relevance of this method suggests that not only the releases of substance from matrix but also substance parameters like solubility are important. Especially the low release of Test and Reference 1 in a third row of dissolution test suggests that the environment inside matrix strongly differs among these formulations. This should be further investigated.

CONCLUSIONS

With our studies we were able to find dissolution method that correlates with in vivo results and can be used to support pharmaceutical development of this product. As shown, Apparatus 3 (Bio-Dis) can serve as a strong tool in development of controlled release formulations. Additional testing needs to be performed to optimize this method as well as final validation on next bioequivalence study.

REFERENCES

1. Q. Wang, N. Fotaki, Y. Mao: Biorelevant dissolution: methodology and application in drug development DissolutiontechVolume 16, Issue 3: Aug 2009

OPTIMIZATION OF DISSOLUTION METHOD FOR NIMESULUIDE TABLETS USING RESPONSE SURFACE METHODOLOGY

D. Kostovski[1], J. Petrovic[2], S. Jordanoska[1], M. Arsova[1], S.Ugarkovic[1], S. Ibric[2]

[1] Institute for research and development, Alkaloid AD-Skopje, bul. Aleksandar Makedonski 12, 1000 Skopje, Macedonia; [2] Faculty of Pharmacy, Institute of Pharmaceutical Technology and Cosmetology, University of Belgrade, Vojvode Stepe 450, 11221 Belgrade, Serbia

INTRODUCTION

Dissolution testing is a key technique in pharmaceutical development laboratories. Methods are described in various pharmacopoeias, along with the calibration of the testing apparatus (1). Measuring the drug release rate with dissolution testing method is a crucial factor for solid oral dosage forms evaluation, since a product must be in solution to be absorbed (2). There are several guidances, EP and USP general chapters devoted to dissolution and in vitro release testing (3-5). None describes a method for dissolution testing of Nimesulide tablets. This study describes the optimization of dissolution method variables for Nimesulide tablets 100 mg, using the application of statistical experimental design. The goal of this design of experiments is to obtain a set of in vitro dissolution parameters (i.e. volume of the medium, paddle rotational speed and surfactant concentration) that will derive a dissolution profile of 75 % dissolved Nimesulde at 5 min. time period, and 90 % or more at 15 min. time mark. Since second condition is achieved more easilly, we will concentrate on optimizing the parameters for the first requirement.

MATERIALS AND METHODS

All procedures were performed in the facility for R&D, Alkaloid AD-Skopje. For the purpose, Nimesulide tablets 100 mg were used (research laboratory trials from Alkaloid AD-Skopje). Common ingredients were used for formulating the tablets. Quantity of 25% of micronized Nimesulide per tablet was incorporated in the formulation. Dissolution testing was performed on a standard USP dissolution apparatus 2 (Varian VK 7050 Varian Inc, USA). Dissolution medium was varied between 500 – 900 ml, paddle speed between 50 – 100 rpm/min and Tween 80 concentration between 0.1% - 1%, at constant pH 7.4. The concentration of the drug dissolved was determined using HPLC method (Hitachi apparatus linked to UV-VIS detector). Generation and evaluation of the statistical design was performed on Design Expert software, release 7.00 (Stat-Ease Inc. 2021 E. Hennepin Avenue, Minneapolis).

RESULTS AND DISCUSSION

Three-factor, three level, face centered cubic design was used. This variety requires 3 levels of each factor. Total of 20 runs, 14 for the factorial points and 6 for the replicated center points were made. After taking only the parameters that are statistically significant, the model was postulated:

$$y = \beta_0 + \beta_1 x_1 + \beta_2 x_2 + \beta_3 x_3 + \beta_{11} x_1^2 + \beta_{22} x_2^2 + \beta_{33} x_3^2 + \beta_{13} x_{13} + \beta_{23} x_{23} + \beta_{22,3} x_2^2 x_3 + \varepsilon$$

Different variable combinations ranged yield from 38.785 % (for all lower values) to 92.72 % (for all upper values). The values for the center points ranged from 75.97 % to 80.69 % with an average value of 78.25 % and standard deviation of 1.55. Yield represents the percentage of Nimesulide dissolved in dissolution media in time period of 5 minutes.

In order to estimate the significance of the model used, an analysis of variance (ANOVA) was applied. Calculated p-value for the model, R^2 value and Lack of fit value can provide assurance for significance of the results.

Table 1: ANOVA of the Regression: Central Composite Face Centered Design

Source	Degrees of freedom	Sum of squares	Mean square	F value	Probabilit y > F
Model	9	4515.28	501.7	163.21	<.0001*
Pure Error	5	12.10	2.42		
Lack of Fit	5	18.64	3.73	1.54	0.3233
C.Total	19	4546.02			
R^2 = 0.993	R_{adj}^2 = 0.987				

Three dimensional (3-D) response surface plots illustrating the relationship between the independent variables and the response are illustrated throughout several Figures.

CONCLUSION

After generating the model, the process was optimized for the requested responce. The optimum set of parameters to achieve dissolution of Nimesulide of 75 % in time period of 5 minutes will be 750 ml of Dissolution Volume, 75 rpm of paddle speed and 0.5 % of surfactant (Tween 80).

Table 3: Observed and predicted responce

No.	Observed responce	Observed responce-Mean	Predicted responce
1	74,34%	75.38%	74,02 ± 1,54 %
2	76,41%		74,02 ± 1,54 %

At the end, in order to confirm the validity of the calculated set of parameters, a duplicate of runs were made. Using the predetermined set of parameters, the goal was dissolution of 75 % of Nimesulide in period of 5 minutes. The predicted and observed responses are presented in Table 3.

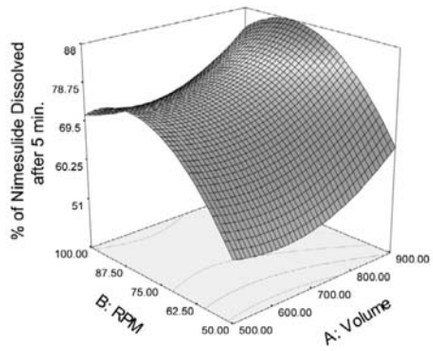

Fig. 1: Effect of factors Dissolution Volume (ml) (X_1) and Paddle Speed (RPM) (X_2) on nimesulide dissolved in 5 minutes of dissolution testing

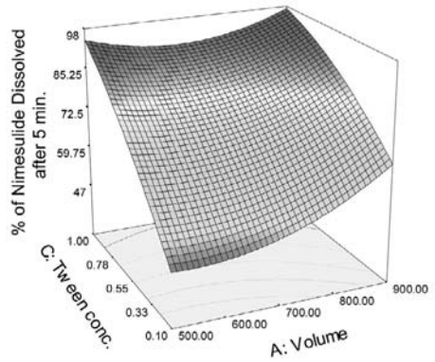

Fig. 2: Effect of factors Dissolution Volume (X_1) and Tween concentration (X_3) on nimesulide dissolved in 5 minutes of dissolution testing

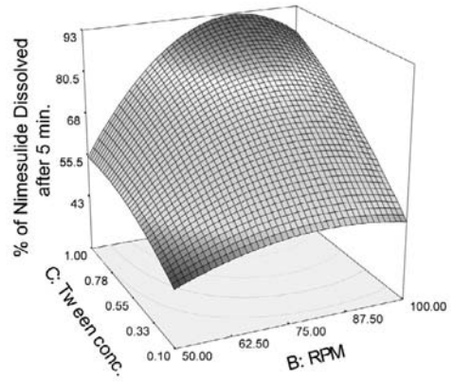

Fig. 3: Effect of factors Tween concentration (X_3) and Paddle Speed (X_2) on nimesulide dissolved in 5 minutes of dissolution testing

REFERENCES

1. Pharmaceutical Experimental Design, G.A. Lewis, D. Mathieu, and R. Phan-Tan-Lu, Marcel Dekker, Inc., New York, 1999
2. Formulation and Analytical Development for Low-Dose Oral Drug Products. Zheng J editor, John Wiley & Sons, 2009
3. EMEA 2010. Guideline on the Investigation of Bioequivalence. CPMP/EWP/QWP/1401 /98 Rev.1
4. EMEA 2007. Concept Paper on BCS-Based Biowaiver. /CHMP/EWP/213035/2007
5. FDA, CDER 1997. Guidance for Industry: Dissolution Testing of Immediate Release Solid Oral Dosage Forms

EFFECT OF SOLID STATE TO THE DISSOLUTION BEHAVIOUR OF PIROXICAM IN ARTIFICIAL GASTRIC FLUID

Lust*, M. Palo, P. Veski, K. Kogermann

University of Tartu, Faculty of Medicine, Department of Pharmacy, Nooruse 1, 50411 Tartu, Estonia.

INTRODUCTION

Piroxicam (PRX) is a known non-steroidal anti-inflammatory drug. PRX has two pKa values: pKa_1=1.86 and pKa_2 = 5.46 (1). Since it has low aqueous solubility and high permeability, it belongs to Class II in Biopharmaceutical Classification System(2).

PRX has four different crystal forms: I, II, III and monohydrate (3). Also, it can be obtained in amorphous form. All these solid state forms may have different physico-chemical properties and consequently result in different dissolution rate and bioavailability characteristics.

The aim of this study was to compare the dissolution behaviour of PRX solid state forms (PRX anhydrate I *vs* PRX monohydrate *vs* amorphous PRX in solid dispersion) *in vitro* in artificial gastric fluid (pH 1,2) and reveal the possible solid state changes.

MATERIALS AND METHODS

Materials

PRX anhydrate I (PRXAH) was purchased from Letco Medical, Inc., USA. Soluplus® was kindly gifted from BASF group. PRX monohydrate (PRXMH) was obtained by recrystallisation from hot water. Physical mixture of PRXAH and Soluplus® 1:4 (PRXPM) were obtained by mixing them in a mortar with pestle using geometric dilution. Solid dispersion of PRXAH and Soluplus® 1:4 (PRXSD) was prepared using solvent method. Soluplus® and PRX were dissolved in acetone. After evaporating the solvent at 40°C, the resulting solid dispersion was gently ground using a mortar and pestle.

All of the PRX samples were passed through a sieve with gauge of 150 µm. Size nuber 3 hard cell gelatin capsules (Posilock™, Elanco) were used for dissolution tests.

Solid state characterisation

All solid state forms were verified with Raman spectroscopy (BWS415 i-Raman Miniature Raman Spectrometer (B&W TEK inc., USA)) and X-ray powder diffractiometry (XRPD, D8 Advance XRPD, Bruker AXS GmbH, Germany).

Dissolution studies

Dissolution profiles from capsules were obtained using USP XXVIII method I, in 900 ml buffer solution (pH 1.2) at 50rpm and 37±0,5°C. Each capsule was filled with 20 mg of PRXAH/PRXMH or equivalent amount of PRX mixtures, keeping PRX amount as constant. Dissolution studies were carried out with Distek Dissolution system 2100B, samples were taken automatically with minipuls 3 peristaltic pump (Gilson) and analysed in line with Uvikon spectrophotometer 922 (Kontron instruments) at 354nm. Buffer solution pH was checked before the experiment with pH meter (Hanna instruments, H19024, Microcomputer pH meter).

Slurry experiments

In order to determine the possible phase transformations of PRX in artificial gastric fluid during dissolution testing, slurry tests were performed. 2 g of anhydrous PRX sample (PRXAH/PRXPM/PRXSD) was suspended in 5 ml artificial gastric fluid (pH 1,2). Continuous mixing was performed and on-line Raman spectra collected.

RESULTS AND DISCUSSION

Solid state characterisation

Raman spectroscopy and XRPD confirmed the solid state forms of PRX. XRPD patterns of PRXMH and PRXAH matched the theoretical XRPD patterns obtained from CSD (Fig 1.). XRPD pattern of PRXSD showed characteristic halo and verified the presence of amorphous PRX (Fig 1.).

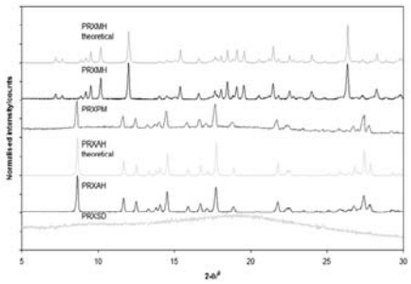

Fig. 1: XRPD patterns of PRXAH, PRXMH, PRXPM and PRXSD.

Different solid forms of PRX exhibit differences in Raman spectra (Fig. 2), and enable their identification.

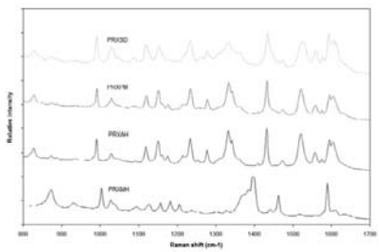

Fig. 2: Raman spectra of PRXAH, PRXMH, PRXPM and PRXSD.

Dissolution studies

PRXSD showed the fastest dissolution rate compared to other PRX samples (Fig. 3). This is probably due to the fact that PRX exists in amorphous form in PRXSD. The slowest dissolution rate was seen with PRXMH samples. which is the most stable form of PRX in given conditions, and therefore is least soluble (Fig. 3).

Experiment with PRXPM was performed to confirm that increase in dissolution rate of PRX from solid dispersion compared to anhydrous form was caused by its amorphous form and not only by solubilisating properties of Soluplus® (Fig. 3). It was seen, that both PRXSD and PRXPM increased the total amount of dissolved PRX.

Slurry tests

All anhydrous PRX samples converted to PRXMH in different time-scales. PRXAH converted to PRXMH after 220 min of mixing, explaining the slowdown in dissolution rate in the middle of dissolution testing. PRXSD coverted to PRXMH after 10 minutes of mixing (Fig. 4).

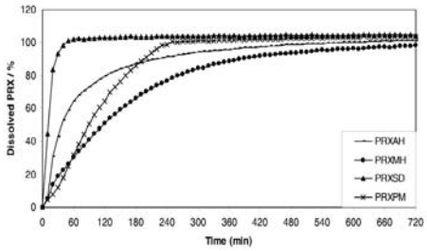

Fig. 3: Dissolution behaviour of PRX solid state forms from capsules in artificial gastric fluid (pH 1,2).

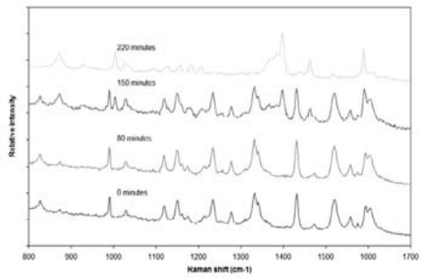

Fig 4: PRXAH converting to PRXMH during slurry test monitored by Raman spectroscopy.

ACKNOWLEDGEMENTS

Dr Jaan Aruväli (X-ray laboratory of Institute of Ecology and Earth Sciences, University of Tartu) is acknowledged for the XRPD experiments. This work is part of ETF grant no ETF7980 and targeted financing project no SF0180042s09. The Estonian Science Foundation and the Estonian Ministry of Education and Research are acknowledged for financial support.

REFERENCES

1. Jinno J, Oh D-M, Crinson J R, Amidon G L. Dissolution of Ionizable Water-Insoluble Drugs: The Combined Effect of pH and Surfactant. J. Pharm. Sci. 89 (2000): 268–274
2. Amidon G L, Lennernäs H, Shah V P, Crison J R. A Theoretical Basis for a Biopharmaceutic Drug Classification: The Correlation of in Vitro Drug Product Dissolution and in Vivo Bioavailability. Pharm. Res. 12 (1995): 413–420.
3. Vrečer F, Vrbinc M, Meden A. Characterization of piroxicam crystal modifications. International Journal of Pharmaceutics 256 (2003): 3–15.

USE OF PHYSIOLOGICALLY BASED PHARMACOKINETIC (PBPK) MODELS FOR ESTABLISHING IN VIVO IN VITRO CORRELATION FOR EXTENDED RELEASE FORMULATION

I. Legen

Sandoz Development Center Slovenia, Lek Pharmaceuticals, Verovškova 57, 1526 Ljubljana, Slovenia

INTRODUCTION

During formulation development setting the right targets is crucial with respect of the speed and efficacy of the development. One of these targets are dissolution requirements which would provide bioequivalent formulation through relevant *In Vivo In Vitro* Correlation (IVIVC). For modified release formulations a deconvolution method is typically used to calculate oral absorption profile from the plasma profile. Using classical deconvolution methods such as Wagner- Nelson (1-compartment) and Loo-Riegelman (2- or 3-compartment) the absorption profile is correlated to *in vitro* dissolution profile to establish level A IVIVC. This approach is valid for drugs with high permeability and comparable absorption through entire gastrointestinal tract (GIT), because in this case the absorption profile is practically superimposed to dissolution profile in the GIT (1). In case of low permeability drugs and/or drugs with unequal absorption along the GIT the absorption profile is different to dissolution profile, therefore classical deconvolution methods might not be appropriate and other alternative methods are necessary.

The aim of the present study was to evaluate physiologically based pharmacokinetic (PBPK) modelling for establishing level A IVIVC for modified release enteric coated mini-tablet (in capsule) formulation.

METHODS

The advanced compartmental absorption and transit model implemented in GastroPlus™ software (version 7.1, Simulations Plus, Inc., Lancaster, CA, USA) was used for PBPK simulations in the present study (2). Loo-Riegelman method was performed with IVIVCPlus™ module, fitting of plasma profiles to one, two and three compartment model was performed with PKPlus™ module; both modules are incorporated in GastroPlus™ software.
pH solubility profile of the drug, pKa value (2.9, acidic), logP (0.23 at pH 7.4), molecular weight, plasma profiles of two formulations (formulation A and formulation B), dissolution profiles – only buffer stage (Fig. 1) and absolute bioavailability were obtained from publicly available database (3). CR integral tablet was used for dosage form input. Permeability coefficient was fitted to reach the measured absolute bioavailability. For all other parameters default values were used.

RESULTS AND DISCUSSION

A two compartment model was found to best describe the pharmacokinetic behaviour of the investigated drug. Therefore, Loo-Riegelman deconvolution method was first used to calculate the absorption profile. The absorption profile was correlated to dissolution data, but very poor correlation was observed, because absorption is much slower than dissolution (Fig. 2). It is possible that permeability also limits the absorption and/or that permeability in different regions of the intestinal tract is different, which is in agreement with the acidic nature of the drug. For acidic drugs absorption is dependent on the pH, with higher permeability at lower pH values (i.e. upper small intestine) (4).

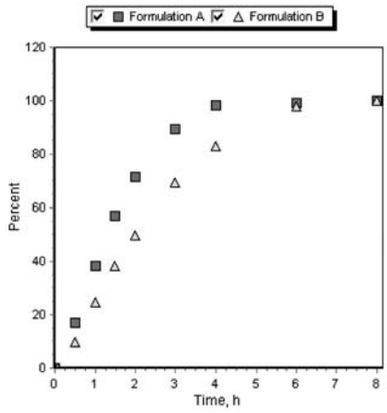

Fig. 1: Dissolution profiles of investigated formulations.

Therefore, PBPK model, which include also permeability characteristics of the drug, was used to establish level A IVIVC.

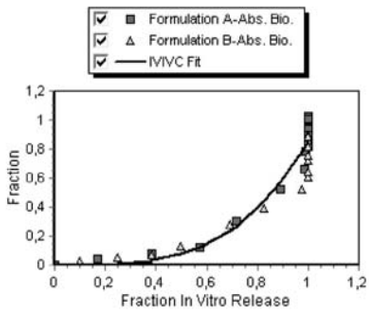

Fig. 2: IVIVC using Loo-Riegelman deconvolution method (power function, R2=0.92, AIC=-30.4)

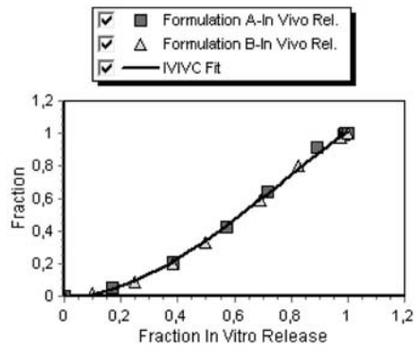

Fig. 3: IVIVC using PBPK model (GastroPlus, deconvolute then correlate with single weibull procedure (3rd order polynomial function, R2=0.99, AIC=-94.9)

Deconvolute then correlate procedure was used with parameters of single weibull function fitted to give an in *vivo release* profile that results in the best match for the plasma profiles.

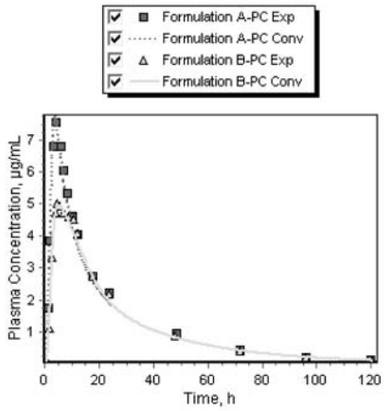

Fig. 4: Fitted versus observed plasma profiles using IVIVC based on PBPK model (GastroPlus).

A much better level A IVIVC (Fig. 3), with much better internal predictability was observed for PBPK modelling compared to conventional procedure (Fig. 4, Table 1).

Table 1: Comparison of internal predictability between IVIVCs for Loo-Riegelman and PBPK (GastroPlus) deconvolution methods.

	Cmax (µg/ml) - observed	Cmax - prediction error (%)	
		Loo-Riegelman	PBPK modelling
Formulation A	7.53	-25.2	-2.7
Formulation B	5.01	-88.3	1.3

CONCLUSIONS

Physiologically based pharmacokinetic modelling can be used as alternative to conventional deconvolution methods for establishing level A IVIVC for oral modified release formulations.

REFERENCES

1. Hwang SS, Bayne W, Theeuwes F. In Vivo evaluation of controlled release products. J. Pharm. Sci. 1993; 82:1145-1150.
2. Lukacova V, Woltosz WS, Bolger MB. Prediction of Modified Release Pharmacokinetics and Pharmacodynamics from In Vitro, Immediate Release, and Intravenous Data. AAPS J. 2009; 11:323-334.
3. http://www.accessdata.fda.gov/scripts/cder/drugsatfda/
4. Legen I, Kristl A. pH and energy dependent transport of ketoprofen across rat jejunum in vitro. Eur. J. Pharm. Biopharm. 2003; 56:87-94.

DIFFERENT MECHANICAL INFLUENCES ON DRUG RELEASE FROM MATRIX TABLETS OF DIFFERENT COMPOSITION

N. Nagelj Kovačič*, A. Mrhar, M. Bogataj

University of Ljubljana, Faculty of Pharmacy, Aškerčeva cesta 7, 1000 Ljubljana, Slovenia

INTRODUCTION

The forecasting of the behaviour of dosage forms in vivo by in vitro drug release testing is frequently used (1, 2). When physico-chemical properties of the gastrointestinal (GI) fluids and also GI motility parameters are considered in the in vitro drug release testing it is expected in vivo behaviour to be the most accurately predicted (3, 4).

Recently, a new flow-through dissolution system with glass beads was designed at Faculty of Pharmacy, University of Ljubljana (5). As the contact between tablet and glassy beads represents the gentle contact between the tablet and the GI mucosa it might be appropriate dissolution system to forecast the influence of mechanical stress implied to tablets after oral administration.

The performance of the dosage form in the GI tract is dependent on physiological conditions of the GI tract as well as on the composition of the dosage form investigated. Various polymers are used for matrix tablets. Amongst the most common is HPMC of different substitution grades, and viscosities.

The aim of this work was to investigate the influence of tablet composition on mechanical susceptibility of the tablets. Matrix tablets containing different types of HPMC and methylcellulose were tested.

MATERIALS AND METHODS

Materials

Different HPMC substitution grades and viscosities were used. Methocel K4M was kindly donated by Colorcon, whereas Metolose 60SH (50cP), 65SH (50, 4000cP), 90SH-SR (100, 4000, 100000 cP), and methylcellulose Metolose SM-4000 were supplied by Shin Etsu (Harke Pharma GmbH). Model drug was paracetamol for all tablets purchased from Sigma-Aldrich. Dissolution medium was 0.01M hydrochloric acid prepared from 1M Titrisol (Merck) solution.

Preparation of matrix tablets

Homogenous mixtures were directly compressed (SP 300, Kilian&co., Cologne) to form tablets of hardness 100N±10N (VanKel VK200), except tablet H3 that had hardness of 50N. Tablets were prepared by using round 12mm, flat punch. The weight of tablets was 400mg. Table 1 shows tablets characteristics.

Table 1: HPMC tablets characteristics.

tablet	HPMC substitution grade		HPMC viscosity (cP)	% of drug	tablet hardness (N)
H1	2208	*K4	4000	25	100
H2		M		50	100
H3				50	50
H4		90SH	100	50	100
H5		-SR	4000*	50	100
H6			100000	50	100
H7	2906	65SH	50	50	100
H8			4000	50	100
H9	2910	60SH	50	50	100
H10		SM	4000	50	100

Drug release from matrix tablets

Dissolution studies were performed in a conventional dissolution apparatus [USP: paddle method (Apparatus II, Vankel VK7000), 1000ml, 100rpm] and newly developed dissolution system with glassy beads [volume of 40ml, 25g of glass beads, flow of 2ml/min, 50rpm] (shown in Fig. 1). Dissolution medium was 0.01M hydrochloric acid at 37°C. Samples were analyzed at 243nm spectrophotometrically (HP diode array UV spectrophotometer, Agilent 8453).

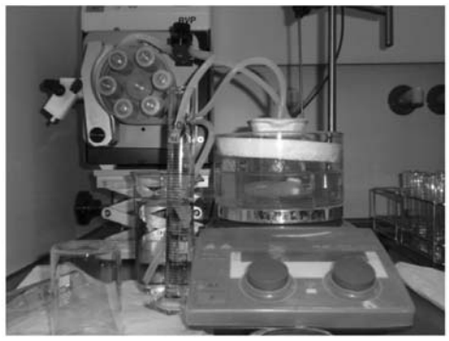

Fig. 1: Photography of dissolution system with glass beads developed at Faculty of Pharmacy, University of Ljubljana.

RESULTS AND DISCUSSION

HPMC is a hydrophilic polymer that is often used in controlled release matrices. It swells after the contact with water and forms a gel layer around the tablet that controls the drug release.

HPMC matrices, that were tested in USP and our dissolution system, showed no or a slight difference in drug release between two dissolution systems for all HPMC tablets. Typical profile comparison is shown in Fig. 2.

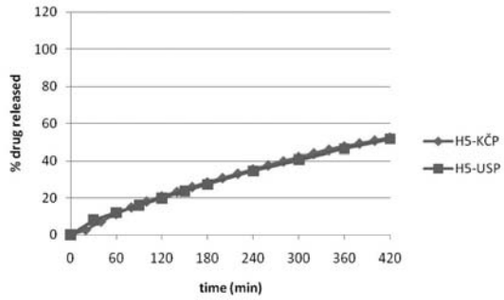

Fig. 2: Drug release profiles from HPMC 90SH-4000SR matrix (H5).

Methylcellulose is another water-soluble semi-synthetic derivative of cellulose. Fig. 3 shows the difference in the drug release between two dissolution apparatuses indicating the matrix is susceptible to different conditions of dissolution testing. However, different mechanical stress, hydrodynamics, and volume of dissolution medium might be the reason. When comparing the drug release between HPMC and methylcellulose matrices, accelerated drug release from the latter is observed.

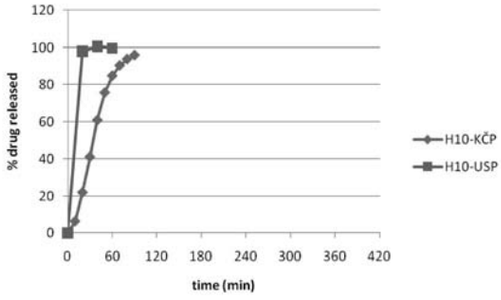

Fig. 3: Drug release profiles from methylcellulose matrix (H10).

CONCLUSIONS

These results clearly show the difference in drug release rate between HPMC and methylcellulose matrices. Differences between two dissolution apparatuses in drug release are noticed in case of methylcellulose matrices, while HPMC matrices are rather unaffected by apparatus at these conditions. There might be different reasons for this observation. Firstly, greater mechanical impact of the dissolution apparatus might have the influence on removing or weakening of the hydrogel layer in case of swellable matrices. This is not the case for HPMC matrices. Secondly, mechanical stress could cause faster erosion of the erodible matrices However, when mechanical influence is strong enough it might be reflected in the drug release.

REFERENCES

1. Galia, E., Nicolaides E., Hörter D., et al. Evaluation of various dissolution media for predicting in vivo performance of class I and II drugs. Pharm. Res. 1998; 15(5): 698-705.
2. Jantratid, E., Janssen N., Reppas C. Dressman J.B. Dissolution media simulating conditions in the proximal human gastrointestinal tract: an update. Pharm. Res. 2008; 25(7): 1663-1676.
3. Dressman, J.B., Amidon G.L., Reppas C., Shah V.P. Dissolution testing as a prognostic tool for oral drug absorption: immediate release dosage forms. Pharm. Res. 1998; 15(1): 11-22.
4. Klein, S. The use of biorelevant dissolution media to forecast the in vivo performance of a drug. AAPS J 2010; 12(3): 397-406.
5. Bogataj, M., Cof G., Mrhar A. Peristaltic movement simulating stirring device for dissolution testing. PCT, WO 2010/014046 A1 (2010).

GASTROINTESTINAL SIMULATION: THE POTENTIAL OF DISSOLUTION TO PREDICT BIOEQUIVALENCE OF GLIMEPIRIDE IR TABLETS

S. Grbic[1], I. Homsek[2], A. Spasic[2], M. Dacevic[2*], Z. Djuric[1]

[1] University of Belgrade, Faculty of Pharmacy, Vojvode Stepe 450, 11221 Belgrade, Serbia; [2] Galenika a.d., R&D Institute, Batajnički drum bb, 11080 Belgrade, Serbia

INTRODUCTION

With the introduction of Biopharmaceutics Drug Classification System (BCS) and BCS-based biowaivers, it has been generally accepted that bioequivalence (BE) between generic and reference drug formulations may be demonstrated solely on the basis of *in vitro* dissolution data. At present, biowaivers are adopted for IR drug products containing BSC Class I drugs, but some suggestions point out that biowaiver concept could be extended to some BCS class II and III drugs (1). It has been demonstrated that gastrointestinal simulation technology (GIST) is a promising tool to justify biowaivers (2, 3). However, in order to achieve accurate simulation of drug pharmacokinetic (PK) profile on the basis of dissolution data, *in vitro* conditions need to be carefully evaluated and defined.

The objective of this study was to assess the ability of GIST to predict the oral absorption of BCS class II drug glimepiride (GLM) on the basis of *in vitro* dissolution data, in order to identify biorelevant drug release methodology.

MATERIALS AND METHODS

In vivo study

An open-label, randomized, single dose, two-way cross-over BE study of GLM IR tablets was performed on 24 healthy subjects, using Amaryl, Sanofi-Aventis as a reference product. Each volunteer received a 6 mg GLM dose (two 3 mg IR tablets). Drug concentration in the blood samples, collected during 48 hours, was determined by a validated HPLC method.

In vitro studies

Dissolution studies of 3 mg GLM IR tablets were carried out in a rotating paddle apparatus (Erweka DT 70, Germany) at 37±0.5°C and rotational speed of 75 rpm, using 900 ml of USP phosphate buffer pH 6.8 without/with the addition of 1 % sucrose-laurate (D1216) as a surfactant. Samples were analyzed by a validated HPLC method.

Gastrointestinal simulation

GastroPlus™ software (version 6.1.0003, Simulations Plus, Inc., Lancaster, CA, USA) was used for computer simulations. The required input parameters related to GLM physicochemical and PK properties are shown in Table 1. Virtual trials were based on a group of 24 volunteers, assuming log-normal distributions of physiological and PK variables.

Table 1: Summary of the GIST input parameters.

Parameter	Value
molecular weight	490.62 g/mol
logP (pH 7.4)[a]	1.8
pKa[b]	7.26
human jejunal permeability[c]	$4.22 \cdot 10^{-4}$ cm/s
dose; dose volume	6 mg; 200 ml
solubility (pH 4,5)[b]	2.12 µg/ml
mean precipitation time[d]	900 s
diffusion coefficient[e]	$0.59 \cdot 10^{-5}$ cm^2/s
drug particle density[d]	1,2 g/ml
effective particle radius	5 µm
body weight	78.1 kg
unbound percent in plasma[f]	0.6 %
clearance[g]	1.56 L/h
volume of distribution[g]	0.05 L/kg
elimination half-life	10.85 h
distribution rate constants, K_{12}, K_{21}[g]	0.45 1/h, 0.16 1/h
peripheral volume	0.15 L/kg
simulation time	48 h

[a]value taken from ref [4]; [b]experimental values; [c]calculated on the basis of *in vitro* measured permeability (Caco-2 cell line) [4] using permeability converter utility integrated in GastroPlus™; [d]default GastroPlus™; [e]GastroPlus™ predicted; [f]value taken from ref [5]; [g]calculated from *in vivo* data

RESULTS AND DISCUSSION

In vivo data

Statistical analysis of the *in vivo* observed data demonstrated bioequivalence between the test and reference GLM preparations. The obtained results are summarized in Fig 1 and Table 2.

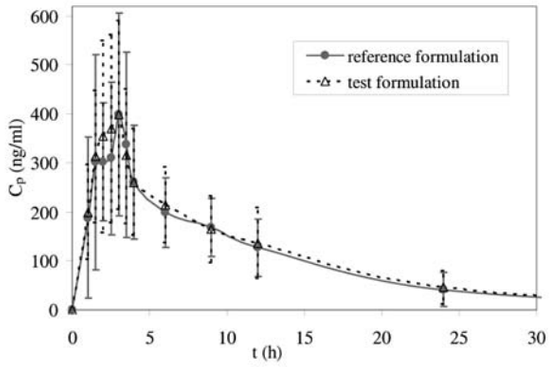

Fig. 1: Plasma concentrations (arithmetic means ± SD) of GLM observed in the *in vivo* BE study (n = 24).

Table 2: PK parameters calculated from the mean plasma concentration-time profiles.

parameter	reference formulation	test formulation
C_{max} (ng/ml)	399.3	398.2
t_{max} (h)	3.0	3.0
$AUC_{0-\infty}$ (ng h/ml)	3900.8	4141.1

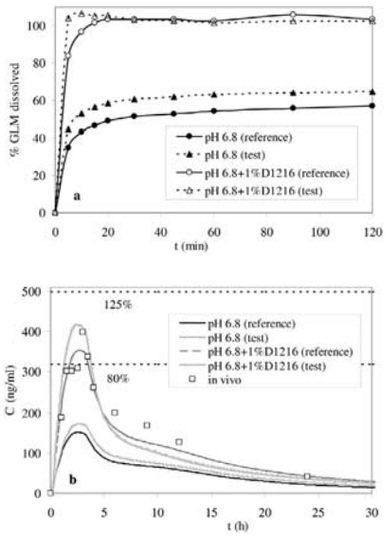

Fig. 2: GLM IR tablets dissolution profiles in various dissolution media (a), and the corresponding simulated in vivo profiles, along with the actual *in vivo* data for the reference product; dotted lines represent 80-125% BE limits (b).

Influence of drug dissolution on virtual trial GIST simulation

Dissolution data, used as the input function for virtual trial GIST simulation, are presented in Fig 2a. Considering the time discrepancies between the *in vitro* and *in vivo* release profiles, time scaling factor was taken into account. The simulation results are presented in Fig 2b and Table 3.

In medium pH 6.8, GLM dissolution was incomplete, and the resultant prediction values were outside of the BE limits. On the other hand, with the release rates in the presence of 1% D1216 (complying with the "very rapid" dissolution), simulation results gave good prediction of GLM oral absorption.

CONCLUSION

The obtained results indicate that "very rapid dissolution" in the presence of surfactant appears to simulate the *in vivo* GLM profile better than „incomplete dissolution" in simple buffer. These findings suggest that biorelevant dissolution medium for GLM IR tablets should combine the effects of pH and surfactant.

Table 3: Comparison of PK parameters between simulated and in vivo observed data for GLM after oral administration of 6 mg IR tablets.

Parameter	Cmax (ng/ml)		AUC0-∞ (ng h/ml)	
	simulated	PE (%)	simulated	PE (%)
pH 6.8 (reference)	153.9	-159.5	1842.0	-111.8
pH 6.8 (test)	175.7	-127.2	2194.4	-77.8
pH 6.8+1%D1216 (reference)	357.4	-11.7	3773.7	-3.4
pH 6.8+1%D1216 (test)	425.0	6.0	3686.8	-5.8
observed values: C_{max} = 399.3 ng/ml; AUC = 3900.8 ng h/ml				

REFERENCES

1. Yu LX, Amidon GL, et al. Biopharmaceutics classification system: the scientific basis for biowaiver extensions. Pharm. Res. 2002;19: 921–925.
2. Kovacevic I, Parojcic J, et al. Justification of biowaiver for carbamazepine, a low soluble high permeable compound, in solid dosage forms based on IVIVC and gastrointestinal simulation. Mol. Pharm. 2008; 6: 40–47.
3. Okumu A, DiMaso M, Löbenberg R. Computer simulations using GastroPlusTM to justify a biowaiver for etoricoxib solid oral drug products. Eur. J. Pharm. Biopharm. 2009; 72: 91–98.
4. Frick A, Möller H, Wirbitzki E. Biopharmaceutical characterization of oral immediate release drug products. In vitro/in vivo comparison of phenoxymethylpenicillin potassium, glimepiride and levofloxacin. Eur. J. Pharm. Biopharm. 1998; 46: 305-311.
5. Malerczyk V, Badian M, et al. Dose linearity assessment of glimepiride (Amaryl®) tablets in healthy volunteers. Drug Metab. Drug Interact. 1994; 11: 341-357.

CURCUMIN: ANTICARCINOGEN FOR VAGINAL DELIVERY?

K. Berginc[1*], P. Basnet[2], N. Škalko-Basnet[2], A. Kristl[1]

[1] Faculty of Pharmacy, University of Ljubljana, Aškerčeva 7, 1000 Ljubljana, Slovenia; [2]Department of Pharmacy, Faculty of Health Sciences, University of Tromsø, Universitetsveinen 57, N-9037 Tromsø, Norway

INTRODUCTION

Polyphenolic compound curcumin is the main active ingredient of herbal remedy and spice turmeric, isolated from the *Curcuma longa* and with a long history of use in traditional Indian medicines (1). The extensive *in vitro* research indicates that this phytochemical exerts antioxidant, anticancer, anti-inflammatory and antiviral activities, making curcumin an attractive candidate for human use and therapy (2). However, its oral administration is rather limited, due to its low bioavailability, owing to extremely low water solubility, instability and co-ordinately regulated alliance between intestinal efflux transporters (Pgp, MRP1 and MRP2) and enzymes (CYP3A4, SULT1A1 and 1A3, GST), acting in tandem to limit its absorption (2). In spite of all efforts to formulate curcumin as per oral drug delivery system, optimal bioavailability has not been achieved yet. Clinical studies have shown that curcumin in oral doses of up to 8-12 g daily are well tolerated and pose no toxicological issues to the patients (3). Similarly, high curcumin doses applied locally to prevent progression of malignancies in colorectal cancer patients have yielded favourable results (4) and are believed to be useful also for the treatment of conditions outside the gastrointestinal (GIT) tract (2).

The aim of this study was thus to investigate the possibility of vaginal curcumin delivery targeting the management of vaginal conditions (i.e. fungal-, viral-infections, malignancies). The delivery of curcumin to the vaginal mucosa was investigated both for curcumin in a form of solution and for liposomal curcumin (made of phospatidylcholine). Permeability data across intestinal membrane were compared to data obtained for vaginal mucosa.

The reasons for low intestinal permeability after per oral administration were further explored.

MATERIALS AND METHODS

Materials

Curcumin, transporter inhibitors (PSC for Pgp, MK571 for MRPs, estrone-3-sulfate (E3S) for OATP), ingredients for cell cultivation and salts for incubation saline were purchased from Sigma, Germany, Phosphatidylcholine (S-100) was a generous gift from Lipoid, Germany. were from Sigma. All chemicals used were of the highest analytical grade.

Methods

In vitro experiments with rat intestine and Caco-2 cells were performed in side-by-side diffusion chambers as already described elsewhere (5). Vaginal tissue (cow) was obtained directly after the slaughter. The vaginal mucosa was isolated, mounted in Franz diffusion chambers to determine the apparent permeability (P_{app}) of curcumin. For the vaginal transport studies simulated vaginal fluid pH 4.5 (6) was used on the apical and Williams Medium E pH 7.4 on the basolateral side. The permeated curcumin was analyzed by LC/MS/MS. Liposomes were prepared by the modified film method, followed by sonication, and characterized for particle size, polydispersity and encapsulation efficiency (7).

RESULTS AND DISCUSSION

Low solubility, instability in GIT lumen and avid pre-systemic metabolism are considered main causatives for curcumin plasma concentrations to be below the LC/MS/MS detection limit in human plasma (4). We investigated the influence of the intestinal transporters on low curcumin absorption in Caco-2 cells. Results indicated a modest curcumin efflux from cells back to the apical

side (Fig. 1 – R_{ex} values ca 2). Although transporters involved in curcumin secretion have been at least partially identified (Pgp, MRP1, MRP2) (2), none of the applied specific inhibitors succeeded to diminish the efflux of this phytochemical at tested concentrations (saturated 100 mM solution), which are significantly below clinically recommended per oral doses (Fig. 1). The absorption of curcumin was not mediated by the absorptive OATP transporter either, since estrone-3-sulfate failed to exert any influence on the efflux ratio.

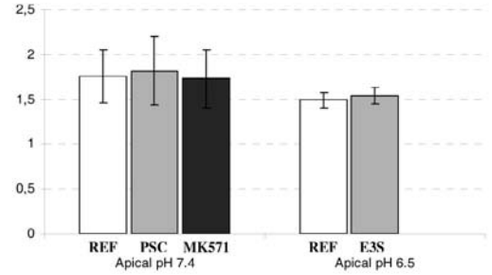

Fig. 1: The *in vitro* influence of efflux (Apical pH 7.4) and influx (Apical pH 6.5) transporters on the curcumin permeability through Caco-2 cell monolayers, expressed as R_{ex} values (the ratio between BL-AP and AP-BL permeabilities).

Besides solubility, transporter-enzyme interplay and instability, we also identified low intestinal permeability (Table 1) as another important reason for low plasma level of curcumin. Namely, the intestinal permeability was substantially below the permeability limit of highly permeable FDA standards (1×10^{-5} cm/s). However, its vaginal permeability from solution was significantly higher than that in the intestine ($p<0.05$). The permeability of curcumin entrapped in multilamelar liposomes (d = 1mm) was significantly lower than from solution but similar to the intestinal permeability.

Table 1: The *in vitro* absorptive permeability of curcumin (P*app*) through intestinal and vaginal mucosa determined for different formulations (solution; multilamelar vesicles – MLV) at physiological pH values.

	Formulation	pH gradient	Papp (×10-7 cm/s)
Intestinal mucosa	100 mM solution	6.5-7.4	2.3 ± 0.2
Vaginal mucosa	50 mM solution	4.5-7.4	18.2 ± 5.1
	50 mM MLV	4.5-7.4	6.9 ± 2.6

CONCLUSIONS

Low intestinal permeability combined with poor solubility and stability will curtail curcumin absorption from GIT at clinically relevant doses. As the permeability of curcumin through vaginal mucosa was much higher, its local delivery has potentials in (pre)malignant conditions. Liposomes appeared as appropriate drug delivery system for curcumin. Namely, they increase the stability of curcumin and simultaneously ensure lower permeability of this polyphenol through vaginal mucosa, assuring higher drug concentration on administration site.

REFERENCES

1. Wahlang B, Pawar YB, Bansal AK. Identification of permeability-related hurdles in oral delivery of curcumin using the Caco-2 cell model. Eur. J. Pharm. Biopharm. 2011; 77: 275–282.
2. Hatcher H, Planalp R, Cho J, Torti FM, Torti SV. Curcumin: from ancient medicine to current clinical trials. Cell. Mol. Life Sci. 2008;65: 1631-1652.
3. Dhillon N, Aggarwal BB, Newman RA, Wolff RA, Kunnumakkara AB, et al. Phase II trial of curcumin in patients with advanced pancreatic cancer. Clin. Cancer Res. 2008; 14: 4491-4499.
4. Sharma RA, Euden SA, Platton SL, Cooke DN, Shafayat A, et al. Phase I clinical trial of oral curcumin: biomarkers of systemic activity and compliance. Clin. Cancer Res. 2004; 10; 6847-6854.
5. Berginc K, Žakelj S, Kristl A. In vitro interactions between aged garlic extract and drugs used for the treatment of cardiovascular and diabetic patients. Eur. J. Nutr. 2010; 49: 373-384.
6. Pavelić Ž, Škalko-Basnet N, Filipović-Grčić J, Martinac A, Jalšenjak I. Development and in vitro evaluation of a liposomal vaginal delivery system for acyclovir. J. Control. Release 2005; 106: 34-43.
7. di Cagno, M., Styskala J., Hlaváč, J., Brandl, M., Bauer-Brandl, A., Skalko-Basnet, N. Liposomal solubilization of new 3-hydroxy-quinolinone derivatives with promising anticancer activity: a screening method to identify maximum incorporation capacity. J. Liposome Res., 2011, early online

THE INFLUENCE OF FITC-LABELED CHITOSAN ON THE PERMEABILITY OF PIG URINARY BLADDER WALL

M. Kerec Kos

Faculty of Pharmacy, University of Ljubljana, Aškerčeva 7, 1000 Ljubljana, Slovenia

INTRODUCTION

Fluorescently labeled chitosan is used to study mucoadhesive interactions of the polymer with a tissue as well as biodegradation and distribution of drug delivery systems with chitosan (1-3).

In our previous studies chitosan increased the permeability of pig urinary bladder wall in a time and concentration dependent manner (4). The aim of the present study is to determine whether fluorescently labeled chitosan influences the permeability of the urinary bladder wall in the same manner as unmodified chitosan.

MATERIALS AND METHODS

Materials

Chitosan hydrochloride (CH) Protasan UP CL 213 (86% of deacetylation, apparent viscosity of 1% w/v aqueous dispersion 76mPa·s) was purchased from FMC BioPolymer/NovaMatrix, Norway. Moxifloxacin (MOX) was kindly provided by Bayer AG, Germany. Fluorescein isothiocyanate (FITC) was purchased from Sigma. All other chemical used were of analytical grade.

Methods

The synthesis of FITC-labeled chitosan (FITC-CH)

100 ml of methanol was mixed with 1% w/v dispersion of CH in 0.1M acetic acid (100 ml). In the next step 50 ml of FITC, dissolved in methanol (2 mg/ml), was slowly added. After 3 hours of reaction in the dark at ambient temperature, FITC-CH was precipitated in 0.2M NaOH. The precipitate was first extensively washed with deionised water and then dialyzed in the dark against water for at least 3 days. At the end the FITC-CH was freeze-dried (1, 3).

Permeability experiments

Pig urinary bladders were obtained from a local slaughterhouse. Until used in the experiments they were kept in phosphate buffer saline cooled to 5°C. The bladder corpus was cut into pieces (approximately 25 x 25 mm), which were mounted into diffusion cells, developed at the Faculty of Pharmacy, Ljubljana, Slovenia (5). Luminal side of the bladder wall was exposed for 1 hour to a solution of MOX, a dispersion of CH with MOX or a dispersion of FITC-CH with MOX. 0.005, 0.05 and 0.25% w/v concentrations of CH and FITC-CH were tested. In all experiments the concentration of MOX was 0.4 mM. All solutions were prepared in phosphate buffer (0.472 g Na_2HPO_4, 0.095 g KH_2PO_4 and 1.6 g NaCl in 1L of deionised water) and their pH was adjusted to 4.5. The experiments were performed at ambient temperature.

Determination of MOX in the tissue

At the end of the permeability experiments the tissue was washed with phosphate buffer and frozen with liquid nitrogen. Tissue was then sectioned by cryostat (Leica CM 1850, Germany) in sections of 20µm thickness parallel to luminal surface up to 1.2 mm of the tissue depth. Three consecutive sections were pooled and mobile phase (0.2% trichloroacetic acid/methanol/ acetonitrile, volume ratio 67/4/29) was added to each sample. After extraction and centrifugation of the samples the concentration of MOX in the supernatant was determined by HPLC (PRP-1 column, Hamilton, USA). Fluorescence detection at an excitation wavelength 296 nm and an emission wavelength 500 nm was applied.

Statistics

The influence of CH and FITC-CH on cumulative amounts of MOX that permeated into the bladder wall was analyzed by one-way ANOVA (IBM

SPSS Statistics, Version 19). For pairwise comparisons of means Bonferroni post hoc test (a=0.05) was applied.

RESULTS AND DISCUSSION

The tissue amounts of MOX decreased with increasing tissue depth under all the tested conditions (Fig. 1).

All tested concentrations of CH significantly increased the cumulative amounts of MOX that permeated into the urinary bladder wall (Fig. 2). There were no significant differences in the tissue permeability when 0.005, 0.05 or 0.25% w/v CH was used. This is in accordance with our previous results (4) where already 0.0005% w/v CH significantly enhanced the permeability of the bladder wall and at 0.001% w/v concentration the maximal effect on the tissue permeability was achieved.

Fluorescent labeling of CH decreases the amount of primary amino groups, which are important for interactions of CH with a tissue. However, in our study fluorescent labeling of CH did not significantly influence the polymer ability to increase the permeation of MOX in the urinary bladder wall at any concentration tested (Fig. 2). Moreover, it was published that characteristics of fluorescently labeled and unmodified CH nanoparticles are very similar (2, 3).

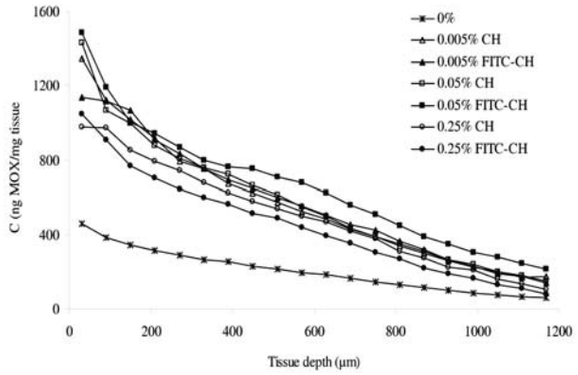

Fig. 1: The amounts of MOX that permeated into the urinary bladder wall as a function of the tissue depth (mean, n=5-6). The tissue was exposed for 1 hour to solution of MOX, a dispersion of CH with MOX or a dispersion of FITC-CH with MOX. The concentrations of CH and FITC-CH are labeled.

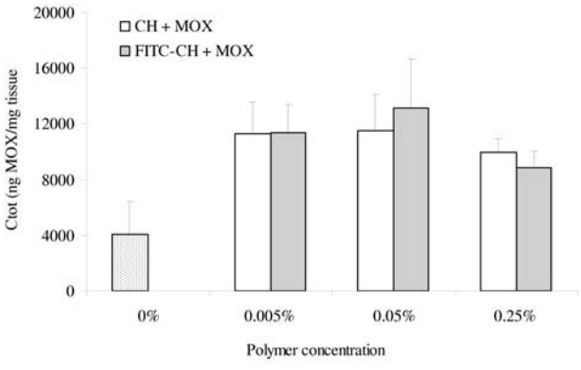

Fig. 2: The cumulative amounts of MOX that permeated into the urinary bladder wall when the tissue was exposed for 1 hour to the solution of MOX, a dispersion of CH with MOX or a dispersion of FITC-CH with MOX (mean ± S.D., n=5-6). The concentrations of CH and FITC-CH are labeled.

CONCLUSIONS

Fluorescently labeled CH influences permeability of the urinary bladder wall in a similar manner as unlabeled CH. The advantage of FITC-CH is that enables the visualization of CH interactions with a tissue.

REFERENCES

1. Qaqish RB, Amiji MM. Synthesis of a fluorescent chitosan derivative and its application for the study of chitosan-mucin interactions. Carbohydr. Polym. 1999; 38: 99-107.
2. de Campos AM, Diebold Y, Carvalho EL, Sánchez A, Alonso MJ. Chitosan nanoparticles as new ocular drug delivery systems: in vitro stability, in vivo fate, and cellular toxicity. Pharm. Res. 2004; 21(5): 803-810.
3. Ma Z, Lim TM, Lim LY. Pharmacological activity of peroral chitosan-insulin nanoparticles in diabetic rats. Int. J. Pharm. 2005; 293(1-2): 271-280.
4. Kos MK, Bogataj M, Veranic P, Mrhar A. Permeability of pig urinary bladder wall: time and concentration dependent effect of chitosan. Biol. Pharm. Bull. 2006; 29: 1685-1691.
5. Kerec M, Bogataj M, Veranic P, Mrhar A. Permeability of pig urinary bladder wall: the effect of chitosan and the role of calcium. Eur. J. Pharm. Sci. 2005; 25: 113-121.

ENHANCING ORAL BIOAVAILABILITY OF VINPOCETINE THROUGH MECHANOCHEMICAL CITRATE SALT FORMATION

D. Hasa[1], D. Voinovich[1], B. Perissutti[1*], M. Grassi[1], S. Bhardwaj[2], M. R. Chierotti[3], R. Gobetto[3]

[1] University of Trieste, P. le Europa 1, I-34127 Trieste, Italy; [2] TASC-IOM-CNR AREA Science Park, S.S.14, Km. 163 Basovizza, I-34149 Trieste, Italy; [3] University of Torino, Laboratory of NMR Spectroscopy, Via P. Giuria 7, I-10125 Turin, Italy; [3]University of Padova, via F. Marzolo 5, I-35131 Padova, Italy

INTRODUCTION

Vinpocetine (VIN), a vincamine derivative, presents a series of very interesting pharmacological properties in relation to cerebral circulation, acting on vascular resistance, particularly in the area of blood vessels (1). However, due to its low aqueous solubility and wettability, and extensive metabolism during first pass, VIN suffers from reduced oral bioavailability (~6.7%) (2). So there is a need to enhance its poor aqueous solubility to increase its oral absorption.

With this aim in this research the formation of the VIN water-soluble citrate was investigated. The transformation of the parent drug in the salt form has been reported to permit rapid absorption with unaltered pharmacological actions (3). The salt was prepared through a solid state reaction conducted with the aid of the mechanical energy. VIN was coground in a planetary mill bowl with citric acid as a reactant, and crosslinked polymer (micronized crospovidone) as a processing aid. The shearing forces resulting from the rolling of ball elements on the wall of the planetary mill bowl were employed for the dry synthesis of VIN citrate. Thus, such an approach represents a solvent-free green technology in alternative to patented synthesis (3) involving the use of solvents.

MATERIALS AND METHODS

Materials

VIN (Linnea SA, Riazzino-Locarno, CH), Oxopocetine®-VIN citrate (Covex s.a., Madrid, E). Citric acid (Sigma-Aldrich, Milano, Italy). Micronized crospovidone (BASF, Ludwigshafen, D). All other chemicals and solvents of HPLC grade, were from Carlo Erba (Milan, Italy).

Methods

Preparation of coground mixtures

Drug and citric acid were coground in different drug-to-citric acid (1:0.55, 1:1.1) weight ratios in presence of crospovidone in several drug-to-polymer weight ratios (1:2, 1:4, 1:7), using different milling times (15, 30, 60 min) in a planetary mill Fritsch P5 (Pulverisette, Contardi Fritsch, Milan, Italy) .

Physico-chemical characterization of the samples

The impact of formulation and process variables (amount of polymer and citric acid, and milling time) on vinpocetine solubilization kinetics from the coground was studied through an experimental design. The best performing samples were characterized by means of Differential scanning calorimetry, X-ray diffraction, Raman imaging/spectroscopy, X-ray photoelectron spectroscopy, solid-state NMR spectroscopy and porosimetry to ascertain the salt formation and to study their solid state characteristics.

Bioavailability studies

The best performing sample was orally administered to 4 rats and its oral bioavailability was compared to that of the corresponding PM and commercial vinpocetine citrate salt (Oxopocetine®).

RESULTS AND DISCUSSION

The analyses attested that the mechanochemical process is a viable way to obtain in absence of solvents vinpocetine citrate salt in an amorphous state. The combination of analytical techniques, such as Raman, XPS (Fig. 1) and ^{15}N CPMAS SS NMR spectroscopies, allowed the ternary coground to be assigned as a VIN citrate in the same solid form as in the commercial salt, Oxopocetine®. The acid-base salt was obtained in absence of solvents in only 30 min of cogrinding in the planetary mill, in presence of micronised crospovidone.

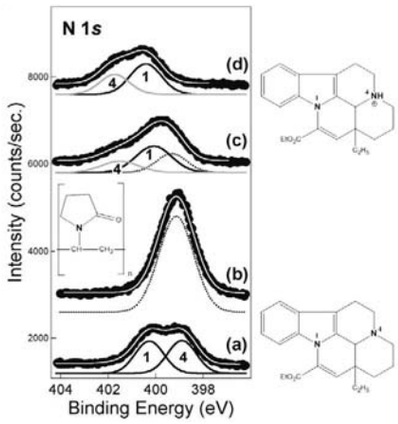

Fig. 1: XPS N 1s spectra of a) pure VIN, b) PVP-CL, c) 1:1.1:2 coground system, and d) Oxopocetine® commercial salt.

The resulting amorphous citrate salt of VIN readily dissolved in g.i. fluids, and was rapidly and highly absorbed by oral administration.

In fact, from the *in vivo* studies on rats (Fig. 2) the obtained salt resulted to be 4 times more bioavailable than its physical mixture and bioequivalent to the commercial salt produced by traditional synthetic process involving the use of solvent.

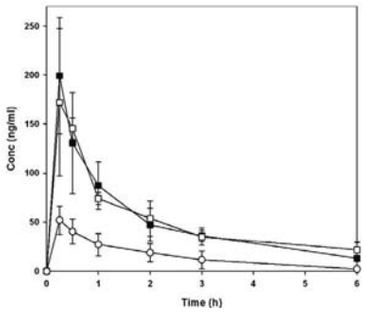

Fig. 2: Mean plasma levels (± S.D.) of VIN obtained after single dose (11mg/kg): in 1:1.1:2 coground system (□), 1:1.1:2 PM (○) and Oxopocetine® commercial salt (■).

CONCLUSIONS

The need to improve the VIN poor aqueous solubility to increase its oral bioavailability has been fully achieved by means of a solvent-free solid state mechanochemical process that has induced physical and chemical changes on the original VIN. The final product is bioequivalent to the commercial salt produced by conventional synthetic process implying the use of solvent.

ACKNOWLEDGMENTS

B. P. thanks University of Trieste for founding (FRA 2009).

REFERENCES

1. Bencsath P., Debrczeni L., Takács L.. Effect of ethyl apovincaminate on cerebral circulation of dogs under normal conditions and in arterial hypoxia. Arzneim.-Forsch /Drug Res. 1976; 26: 1920-1923.
2. Grandt R., Beitinger R., Schateltenbrand R., Braun W.. Vinpocetine pharmacokinetics in elderly subjects. Arzneimittelforschung/Drug Res. 1989; 39:1599-1602.
3. Calvo F. and Manresa M.T., U.S. patent 4749707, Spain , Covex S.A. , 1988.

HIGH SHEAR AND FLUID BED MELT GRANULATION TO IMPROVE THE DISSOLUTION RATE OF CARVEDILOL

S. Kukec[1*], R. Dreu[2], F. Vrečer[1,2]

[1] Krka, d.d., Novo mesto, Research and Development Division, Šmarješka cesta 6, SI-8501 Novo mesto, Slovenia; [2] University of Ljubljana, Faculty of Pharmacy, Aškerčeva 7, SI-1000 Ljubljana, Slovenia

INTRODUCTION

Melt granulation is a process by which pharmaceutical powders are efficiently agglomerated using binders which melts at relatively low temperature (50-80 ˚C). Low melting binders can be added to the powders either in the form of a solid that melts during the process (in situ melt granulation or melt-in procedure) or in the form of a molten liquid (spray-on procedure) (1). Many advantages of hot melt processes are described in the literature (2).

Recently, some authors have described melt granulation technique as an effective method to improve the dissolution rate of poorly water soluble drugs (3-4).

The aim of this study was to prepare a granulated poorly soluble drug carvedilol using high shear (HS) and fluid bed (FB) melt granulation with melt-in or spray-on procedure monitored by PAT probes. Prepared granules were characterized in terms of physical characterization and dissolution rate of carvedilol (CAR).

MATERIALS AND METHODS

Materials

Carvedilol (CAR, Krka, Novo mesto, Slovenia) was used as a poorly soluble drug. Lactose NF mesh 200 and microcrystalline cellulose (MCC) (Avicel PH 101) were used as fillers and starting materials. Polyethylene glycol (PEG) 4000 and Poloxamer 188 (P188) were used as meltable binders.

Methods

The batch size was 1200 g (1000 g of fillers: lactose and MCC in mass ratio 4:1, 150 g of meltable binder: PEG 4000 or P188 and 50 g of drug: CAR).

• HS melt granulation

The granules were prepared in a laboratory scale HS mixer (Collette Gral 10, Belgium), equipped with hot water heated double jacket.

Binder addition by melt-in procedure: The jacket temperature was set up to 75 ˚C. The product temperature was raised up to 55 ˚C and 60 ˚C for P188 and PEG 4000 formulation, respectively. Binder addition by spray-on procedure: The jacket temperature was set up to 45˚C. Melted binder (temp.: 85 ˚C) with homogeneously dispersed drug was added to the powder by use of spraying nozzle.

• FB melt granulation

The granules were prepared in a laboratory scale FB granulator (Brinox BX CGD 1, Slovenia).

Binder addition by melt-in procedure: The fluidizing inlet air temperature was set to 80 ˚C. The product temperature was raised up to 57 ˚C and 60 ˚C for P188 and PEG 4000 formulation, respectively. Binder addition by spray-on procedure: Melted binder (temp.: 85 ˚C) with homogeneously dispersed drug was fed to the atomizing nozzle and sprayed at 1.5 bar over the powders.

Focused beam reflectance measurement (FBRM) and Parsum probes were used for real time in-line particle size analysis during the FB and HS granulation.

• Sample characterization

Physical characteristics of granulate were determined: flowability and angle of repose (θ); bulk (V_B) and tapped (V_T) volume; particle size distribution of granules by sieve analysis.

In vitro dissolution tests were performed using the USP Apparatus 2 rotating at 50 rpm. As dissolution media, 900 mL of phosphate buffer solution (pH 6.8) were used. Samples equivalent to 25 mg of CAR were added to the dissolution medium.

RESULTS AND DISCUSSION

Tables 1 and 2 report the technological properties of the obtained granules. Particle size distribution of P188 and PEG granules are shown in Fig. 1 and 2. These results confirmed that HS and FB processes enabled the production of granules having appropriate technological properties.

Table 1: Physical characteristics of PX 188 granules.

Parameter	HS*	HS**	FB*	FB**
Flowability [s/100g]	17,9	19,8	32,6	29,4
θ [˚]	33,3	34,1	30,5	31,0
V_B [ml/g]	1,74	1,84	1,80	2,06
V_T [ml/g]	1,42	1,48	1,54	1,84

*melt-in procedure; **spray-on procedure

Table 2: Physical characteristics of PEG 4000 granules.

Parameter	HS*	HS**	FB*	FB**
Flowability [s/100g]	16,5	18,3	13,0	13,9
θ [˚]	35,2	34,7	29,0	32,5
V_B [ml/g]	1,88	1,90	1,80	2,20
V_T [ml/g]	1,58	1,56	1,52	1,94

*melt-in procedure; **spray-on procedure

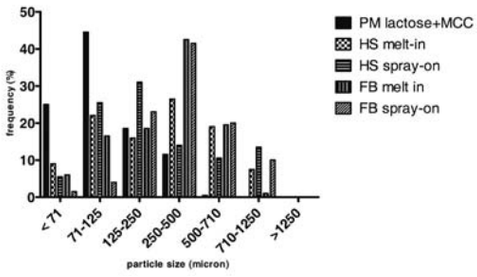

Fig. 1: Particle size distribution of P188 granules.

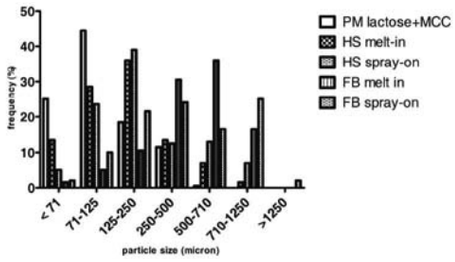

Fig. 2: Particle size distribution of PEG 4000 granules.

Dissolution of CAR formulations produced by melt granulation showed significantly higher dissolution rate compared to pure CAR and physical mixture (PM) of CAR and P188 or PEG 4000. A significant difference has been observed in dissolution of granulate prepared by spray-on in comparison to melt-in procedure (Fig. 3).

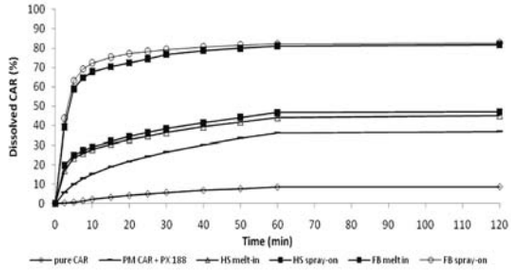

Fig. 3: Dissolution profiles of CAR, PM and P188 granules.

Faster initial dissolution of CAR was obtained in P188 formulations compared to PEG 4000 formulations (Fig. 4).

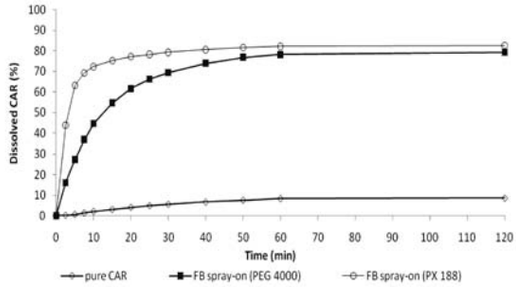

Fig. 4: Dissolution profiles of FB spray-on PEG and P188 granulate.

CONCLUSIONS

The results of this study show that melt granulation can be successfully performed in both HS and FB granulators. Melt granulation, especially spray-on procedure, is an effective method to improve dissolution rate of poorly water soluble drugs.

ACKNOWLEDGEMENTS

The authors would like to thank KRKA, d.d., Novo mesto for supporting this study.

REFERENCES

1. Wong TW, Cheong WS, Heng WS. Melt granulation and pelletization, in: Parikh DM (Ed.), Handbook of Pharmaceutical Granulation Technology, Synthon Pharmaceutical Inc., North Carolina, pp. 385-406.
2. Heng PWS, Wong TW. Melt processes for oral solid dosage forms . Encyclopedia of pharmaceutical technology Vol 4. Informa Healthcare USA. New York 2007: 2257-2261.
3. Passerini N, Albertini B, Gonzales-Rodriguez ML, Cacallari C, Rodriguez L. Preparation and characterisation of ibuprofen-poloksamer 188 granules obtained by melt granulation. Eur J Pharm Sci 2002; 15: 71-78.
4. Perissutti B, Rubessa F, Moneghini M, Voinovich D. formulation design of carbamzepine fast –release tablets prepared by melt granulation technique. Int J Pharm 2003; 256: 53-63.

INFLUENCE OF GENETIC VARIATIONS IN ORGANIC CATION TRANSPORTER 1 AND 2 AND MATE1 ON EFFICIENCY AND SAFETY OF ANTIDIABETIC PERORAL DRUG METFORMIN THERAPY

L. Tarasova[1*], I. Kalnina[1], A. Bumbure[2], K. Geldnere[2], R. Ritenberga[2], L. Nikitina-Zake[1], I. Vaivade[1], V. Pirags[2], J. Klovins[1]

[1] Biomedical Research and Study Centre, University of Latvia, Ratsupites 1, LV 1067, Riga, Latvia; [2] University of Latvia and Department of Endocrinology, Pauls Stradins Clinical University Hospital

INTRODUCTION

One of the most widely used medicaments for treating type 2 diabetes (T2D) is a peroral antidiabetic drug metformin. Despite its overall efficiency in T2D treatment metformin shows significant proportion of patients suffering from number of side effects (1). Metformin is not metabolised in human body, therefore a great role in metformin pharmacokinetics plays coordinated activity of drug transportiers in the liver and kindney. So far number of polymorphisms (mainly in genes coding for various metformin transporter proteins) has been described in association with metformin efficiency
(2-4). However no information exists whether genetic variations in metformin transporters genes influence tolerability of metformin therapy. OCT1, OCT2 and MATE1 transporters are involved in pharmacokinetics of metformin. In this study, we assessed whether 5 SNP and 2 indel polymorphisms are associated with metformin side effects in patients with T2D. In this study we report an investigation of the 7 polymorphisms from OCT1, OCT2 and MATE1 gene loci in association with metformin intolerance in the cohort of 310 patients with T2D and history of metformin use.

MATERIALS AND METHODS

We used information from Genome Database of Latvian Population (LGDB) and METFOGENE study to identify all metformin users and their response to metformin intake. Polymorphisms in SLC22A1 - rs12208357, rs34059508, rs628031; rs36056065 and rs72552763; SLC22A2 - rs316019; SLC47A1 - rs2289669 were compared between 74 T2D patients with metformin intolerance and 236 metformin users without symptoms of metformin intolerance.

Materials

All subjects selected for this case-control study were acquired from Genome Database of Latvian Population (LGDB), a governmentally funded biobank. All participants of LGDB have to be over 18 years old, information about their health status was affirmed by physicians using ICD-10 codes (International Classification of Diseases), data about anthropometric measurements (including weight and stature) were obtained by direct measurement, ethnic, social, environmental information and familial health status were obtained in the questionnaire based interview. All metformin users, using 0.5 and more grams of metformin per day with clearly registered metformin tolerance status were further selected for study, resulting in a group of 236 T2D patients without side-effects of metformin therapy. Metformin intolerance group (n=74) was defined as having one or more of the following symptoms: diarrhea, nausea, meteorism and abdominal pain. The Biobank protocol was approved by the Central Medical Ethics Committee of Latvia (Protocols Nr. A-30, 2005 and A-7, 2007). This study was conducted in accordance with the Declaration of Helsinki and was approved by the Central Medical Ethics Committee of Latvia. All subjects gave their written informed consents.

RESULTS AND DISCUSSION

Genotyping of SNPs was carried out using Applied Biosystems TaqMan SNP Genotyping assay with modified protocol using 4.75 µl TaqMan Genotyping Mix (Applied Biosystems, USA), 0.25 µl SNP genotyping assay (Applied Biosystems, USA) and 5 µl Millipore H_2O on 7500 Real-Time PCR system (Applied Biosystems). AutoCaller 1.1 (Applied Biosystems) software was used to assign genotype calls for all samples simultaneously. Genotyping of *indel* rs72552763 was performed by direct sequencing of PCR products. PCR was performed using the following primers: 5'-GCA TTC TAA ACC CAG TGA T-'3 and 5' - CAT TCC AGA GGC TTA TCA A-'3. Following PCR reaction setup was used: 1mM DB buffer, 2,5mM $MgCl_2$, 0, 5 units Hot FirePol, 0,2mM dNTP mix (SolisBioDyne, Estonia), 0,3mM primers and 28ng template DNA. PCR temperatures were 95^0C – 5min, 40 cycles – 95^0C – 30sec, 55^0C – 30sec, 72^0C – 1min, and 5min at 72^0C for final extension and the PCR was carried out on Veriti96ThermalCycler (Applied Biosystems, USA). The PCR product was confirmed by agarose gel electrophoresis and dephosphorylation of remaining dNTPs was done with shrimp alkaline phosphatase (Fermentas, Lithuania) according to manufacturer's protocol.
Statistical analyses were performed with the PLINK 1.06 software (5). Deviation from the Hardy–Weinberg equilibrium was assessed by the exact test. Logistic regression assuming an additive, dominant, or recessive mode of inheritance was used to test the difference between cases and controls to adjust the analysis for other non-genetic factors. Sex, age and body mass index (BMI) were included in the logistic regression models as cofactors.
Waist, BMI and HbA1c levels displayed normal distribution and were further used in linear regression analysis using the sex, age and metformin tolerance status as cofactors. In order to adjust the analysis for multiple testing we performed a permutation with 100,000 permutations for each analysis and EMP2 p-values were used. We found a statistically significant association between A allele of rs628031 (p=0.007353, OR=0.5744, CI 95% [0.3819-0.8639])) as well as 8 bp insertion (rs36056065) (p=0.007819, OR=0.582, CI 95% [0.3899-0.8686]) and presence of metformin intolerance. Additionally carriers of rs2289669 A allele (SLC47A1) displayed significantly lower (p=0.004894) mean BMI (33.32 kg/m^2) compared to wt GG genotype (36.87 kg/m^2) among regular metformin users.

CONCLUSIONS

Genetic variation in OCT1 encoded by SLC22A1 may predispose to increased incidence of metformin intolerance in patients with T2D. Our results may also suggest that rs2289669 located in SLC47A1 gene coding for MATE1 transporter may be associated with increased efficiency of metformin effect on the weight lowering.

REFERENCES

1. Kirpichnikov, D., S.I. McFarlane, and J.R. Sowers, Metformin: an update. Ann Intern Med, 2002. 137(1): p. 25-33.
2. Tzvetkov, M.V., et al., The effects of genetic polymorphisms in the organic cation transporters OCT1, OCT2, and OCT3 on the renal clearance of metformin. Clin Pharmacol Ther, 2009. 86(3): p. 299-306.
3. Shikata, E., et al., Human organic cation transporter (OCT1 and OCT2) gene polymorphisms and therapeutic effects of metformin. J Hum Genet, 2007. 52(2): p. 117-22.
4. Becker, M.L., et al., Genetic variation in the multidrug and toxin extrusion 1 transporter protein influences the glucose-lowering effect of metformin in patients with diabetes: a preliminary study. Diabetes, 2009. 58(3): p. 745-9.
5. Purcell, S., et al., PLINK: a tool set for whole-genome association and population-based linkage analyses. Am J Hum Genet, 2007. 81(3): p. 559-75.

INVESTIGATION OF RANDOMLY METHYLATED BETA-CYCLODEXTRIN PERMEABILITY ON CACO-2 CELL MONOLAYER

F. Fenyvesi[1*], K. Réti-Nagy[1], Zs. Bacsó[2], É. Fenyvesi[3], L. Szente[3], J. Váradi[1], I. Bácskay[1], G. Szabó[2], M. Vecsernyés[1]

[1] University of Debrecen, Department of Pharmaceutical Technology, PO Box 78, H-4010 Debrecen, Hungary; [2] University of Debrecen, Department of Biophysics and Cell Biology Egyetem tér 1. Debrecen, 4032 Hungary; [3] Cyclolab Cyclodextrin R&D Laboratory Ltd., PO Box 435, H-1097 Budapest, Hungary

INTRODUCTION

Cyclodextrins are widely used excipients for increasing water solubility and delivery of lipophilic drugs (1). They are considered hydrophilic, non-cell membrane permeating agents with high cholesterol inclusion capacity. In cell biology methyl-β-cyclodextrins are applied for the modification of cholesterol content of cell membranes and to study the role of cholesterol on cellular functions (2). Recently hydroxylpropyl-β-cyclodextrin was found to be able to enter the cells and reduce intracellular cholesterol accumulation (3). In the present study our aim was to investigate the interaction of Caco-2 colon cells with the fluorescent labelled randomly methylated β-cyclodextrin (Fitc-Rameb) and measure the amount of cyclodextrins permeated through the monolayers. We also focused on the possible cell membrane penetration of Fitc-Rameb.

MATERIALS AND METHODS

Materials

Rameb was purchased from Wacker Chemie (Munich, Germany), Fitc-Rameb was the product of Cyclolab Ltd., while all other reagents purchased from Sigma.

Methods

Caco-2 cells were cultured in Dulbecco's modified Eagle's medium containing 1% non-essential amino acids at 37 °C in 5 % CO_2 atmosphere. The effect of cyclodextrins on cell viability was evaluated by MTT-test. For permeability measurements cells were seeded on Transwell® inserts. Monolayers were incubated with 5mM Rameb containing 0.05 mM Fitc-Rameb for 2 hours at 37 °C and the permeated amount of cyclodextrin was determined by FLUOstar Optima microplate reader (BMG LABTECH) at 492 nm excitation and 520 nm emission wavelength. The monolayer integrity was checked with transepithelial electric resistance (TEER) measurements.

RESULTS AND DISCUSSION

Cell viability

Viable cell number did not decrease after 5 mM cyclodextrin treatment compared to the untreated control.

Monolayer integrity

TEER values decreased significantly after cyclodextrin treatment, from 2381±205 Ω×cm^2 to 1888±197 Ω×cm^2 (p=0.001, n=6). This indicates the cyclodextrin's effect on membrane structure, but the value remained high and monolayers kept their integrity.

Rameb permeation measurements

The amount of Rameb permeated through Caco-2 monolayer was very low. Only 0.069 % of the initial cyclodextrin appeared in the basal chamber. This rate can be interpreted as Caco-2 monolayer is practically impermeable to Rameb and it is not available from the intestine. It is in agreement with previous data which revealed the very limited intestinal absorption of β-cyclodextrin (4), but in the other hand it also highlights that cyclodextrins are able to overcome the cellular barrier somehow. We also measured a comparable amount of Rameb bound to the cell monolayer. At the end of the experiments, after several washing steps, 0.062 % of the initial cyclodextrin proved to be located in the cells. Considering the volume of the apical chamber, cyclodextrin concentration and the small volume of the cell layer, cyclodextrin uptake of the Caco-2 cells was significant. As Rameb is a hydrophilic molecule this is an unexpected and new observation. These results were confirmed also by flow-cytometry and fluorescent microscopy.

CONCLUSIONS

The low amount of Rameb permeated through the Caco-2 cell monolayer is related to the cyclodextrin-cell interactions and these results could support new aspects of cyclodextrin research and drug delivery.

REFERENCES

1. Szejtli J. Medical applications of cyclodextrins. Med. Res. Rev. 1994; 14: 353-386.
2. Fenyvesi F, Fenyvesi É, Szente L, et al. P-glycoprotein inhibition by membrane cholesterol modulation. Eur. J. Pharm. Sci. 2008; 34(4-5): 236-242.
3. Rossenbaum AI, Zhang G, Warren JD, Maxfield FR. Endocytosis of beta-cyclodextrins is responsible for cholesterol reduction in Niemann-Pick type C mutant cells. Proc. Natl. Acad. Sci. 2010; 107(12): 5477-5482.
4. Gerlóczy A, Fónagy A, Keresztes P, Perlaky L, Szejtli J. Absorption, distribution, excretion and metabolism of orally administered 14C-beta-cyclodextrin in rat. Arzneimittelforschung, 1985; 35(7): 1042-47.

APPLICATION OF GASTROINTESTINAL SIMULATION FOR DEVELOPMENT OF IN VITRO-IN VIVO CORRELATION FOR LEVOTHYROXINE SODIUM IMMEDIATE-RELEASE TABLETS

I. Kocic[1*], I. Homsek[1], M. Dacevic[1], S. Grbic[2], J. Parojcic[2], B. Miljkovic[2]

[1] Galenika a.d, Batajnicki drum bb, 11000 Belgrade, Serbia; [2] University of Belgrade, Faculty of Pharmacy, Vojvode Stepe 450, 11000 Belgrade, Serbia

INTRODUCTION

Levothyroxine sodium (LT4) is a drug used as the replacement therapy in primary hypothyroidism (1). Its absorption profile is difficult to interpret because the endogenous LT4 level must be taken into account. Since *in vivo* drug disposition may be affected by drug dissolution rate from the dosage form, the influence of the *in vitro* conditions has to be carefully evaluated in order to achieve accurate simulation of the pharmacokinetic profile. Dissolution data can be used to establish *in vitro-in vivo* correlation (IVIVC) with clinically observed plasma concentration-time curves and to identify biorelevant dissolution specifications (2). The aim of this study was to develop a drug-specific absorption model for LT4 using gastrointestinal simulation technology and to evaluate the influence of different *in vitro* drug dissolution kinetics on *in vivo* performance of LT4 immediate-release (IR) tablets.

MATERIALS AND METHODS

Gastrointestinal Simulation

Gastrointestinal simulation based on the advanced compartmental absorption and transit model (GastroPlus™ version 6.1.0003, Simulations Plus, Inc., Lancaster, USA) was used. The input parameters required for the simulation were experimentally determined, *in silico* predicted and/or taken from the literature.

***In vitro* data**

Dissolution studies of LT4 tablets were performed in the USP apparatus 2 (Erweka DT 70, Germany), according to the USP 34 monograph for LT4 tablets (3), in 0.01 M HCl with 0.2% SLS at 50 rpm, and according to the USP 24 monograph for LT4 tablets (4), in phosphate buffer pH 7.4 at 100 rpm. The percent of LT4 dissolved was determined by validated HPLC method. Virtual *in vitro* profiles were generated to reflect the situation where more

than 70% of the drug is dissolved in 45 minutes (USP 34 dissolution test requirement, *profile a*) and where more than 55% of the drug is dissolved in 80 minutes (USP 24 dissolution test requirement, *profile b*).

RESULTS AND DISCUSSION

Drug absorption simulation

Gastrointestinal simulation results for LT4 IR tablets are presented in Fig. 1, together with the *in vivo* observed data (*in-house* data on file). The calculated percent prediction errors were less than 10% for all pharmacokinetic parameters, indicating that the generated absorption model gave good prediction of LT4 oral absorption.

Dissolution profiles of LT4 IR tablets, obtained under USP 34 and USP 24 conditions, as well as virtual profiles representing both pharmacopoeial dissolution specification limits are presented in Fig 2a. The simulated *in vivo* profiles are presented in Fig. 2b. The predicted pharmacokinetic profiles based on experimental results were in a good agreement with the *in vivo* observed data.

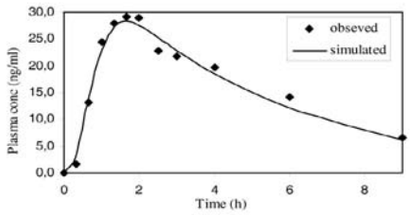

Fig. 1: Predicted and observed mean LT4 C_{p-t} profiles following administration of a single 600 µg dose.

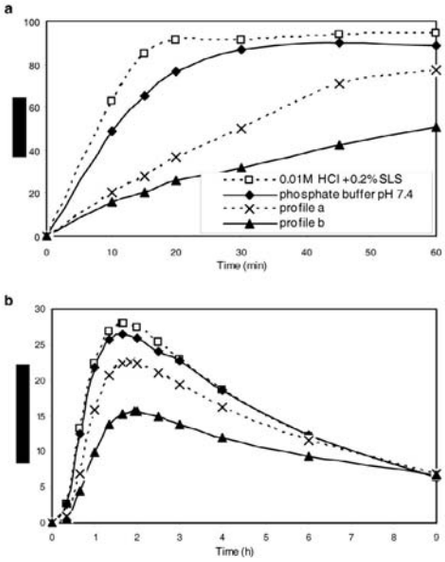

Fig. 2: LT4 tablets experimental and virtual dissolution profiles (a) and the corresponding simulated *in vivo* profiles (b).

In vitro – in vivo correlation

The predicted plasma concentration–time profiles for experimental and virtual input dissolution data, estimated on the basis of the generated LT4-specific absorption model, were plotted against the *in vivo* observed data in order to develop a level A IVIVC (Fig. 3). High level of correlation was observed for the profiles simulated on the basis of experimental *in vitro* data ($r = 0.989$ for USP 34 dissolution profile and $r = 0.958$ for USP 24 dissolution profile). Lower levels of correlation were obtained for profiles representing pharmacopoeial dissolution limits ($r = 0.505$ for *profile a* and $r = 0.770$ for *profile b*). The study showed that proposed USP 34 and USP 24 dissolution test specifications for LT4 IR tablets cannot be considered biorelevant. Additional simulations, based on virtual dissolution profiles representing different release kinetics should be done in order to set the biorelevant dissolution acceptance criteria.

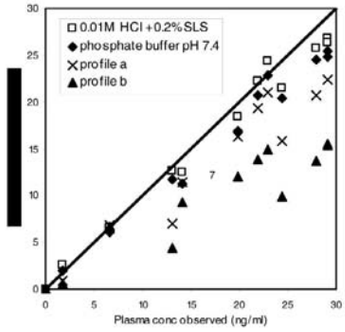

Fig. 3: IVIVC plots for LT4 tablets.

CONCLUSIONS

The presented data demonstrate that gastrointestinal simulation technology can be successfully used to predict levothyroxine absorption profile. The obtained results of gastrointestinal simulation and IVIVC modeling indicate that dissolution requirements given in USP 34 and USP 24 monographs cannot be considered as biorelevant dissolution specification criteria for LT4 IR tablets.

REFERENCES

1. Blakesley VA. Current methodology to assess bioequivalence of levothyroxine sodium products is inadequate. AAPS J. 2005; 7: E42-E46.
2. Grbic S, Parojcic J, Ibric S, Djuric Z. In vitro-in vivo correlation for gliclazide immediate-release tablets based on mechanistic absorption simulation. AAPS PharmSci Tech. 2011; 12: 165-171.
3. USP 34, The United States Pharmacopoeia 34th ed. Rockville, MD: The United States Pharmacopoeial Convention, Inc; 2010, p. 3304.
4. USP 24, The United States Pharmacopoeia 24th ed. Rockville, MD: The United States Pharmacopoeial Convention, Inc; 2000, p. 969.

^{14}N NQR LINEWIDTH DEPENDENCE ON DEFFECTS AND RESIDUAL STRESS IN COMPACTS OF PARACETAMOL AND FAMOTIDINE

Z. Lavrič[1*], J. Lužnik[2], Z. Trontelj[2], S. Srčič[1]

[1] University of Ljubljana, Faculty of Pharmacy, Aškerčeva cesta 7, 1000 Ljubljana, Slovenia; [2] Institute of Mathematics, Physics and Mechanics, Jadranska cesta 19, 1000 Ljubljana, Slovenia

INTRODUCTION

^{14}N NQR method has certain characteristics that make it a very attractive analytical tool for the broader pharmaceutical field.

The method is based on coupling of electric field gradient tensor (EFG) with ^{14}N quadrupolar nuclei which are present in most active pharmaceutical ingredients (API) (1). Since EFG is a result of ordering of molecules in solid matter, the method was proved to be highly suitable for the study of APIs polymorphism (2).

Furthermore any external influence that would change the internal ordering of solid substances would also be amenable to ^{14}N NQR measurements.

In the presented work ^{14}N NQR technique was employed to study compacts of famotidine and paracetamol. When compressed, particles are subjected to fracture, plastic and elastic deformation. These mechanisms are theoretically bound to influence ^{14}N NQR signal through residual stress and

defects. These effects influence the crystal structure of a studied substance and thus modify its EFG at the position of resonating quadrupolar ^{14}N nuclei. As a result the ^{14}N NQR spectra of studied substances are modified relative to uncompressed samples.

Previously only papers concerning reversible pressure dependent line shifts were published (3). With the decrease in pressure, these spectra reverse to normal. There are no reports of utilization of NQR to the study of changes still present when the pressure is removed as is the case of tableting.

Our work therefore provided a new analytical tool on how to obtain new insights into the properties of solid substances when subject to compression procedure.

MATERIALS AND METHODS

Materials

Pure paracetamol I and famotidine B crystal forms were obtained on the market.

Methods

Compacts of pure API weighing around 0,6g were prepared. Instrumented eccentric tablet press (IMA Killian SP300) fit with 12mm flat faced punches was used for compression with forces of 1-30kN. For forces above and up to 150kN a hydraulic press (Specac) was used. Compacts of paracetamol laminated heavily as expected, since they have a very unsuitable compactibility characteristic.

Paracetamol samples were measured with NQR spectrometer tuned at 1921 and 2564 kHz, and famotidine samples at 2848 kHz. Additionally the time of sustained force of compaction was varied (0.1s, 15s and 60s). Once the compacts were made, the reversibility of linewidth broadening was probed with milling in a ball mill, intended to relieve internal residual stresses.

RESULTS AND DISCUSSION

Dependence of ^{14}N NQR spectral linewidth on the compaction force

As is seen from Fig. 1 there is a substantial linewidth broadening with increase in force of compaction. This increase seems to have a plateau at the highest forces used.

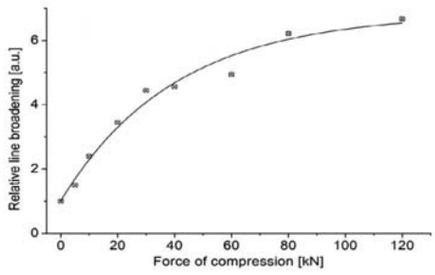

Fig. 1: Dependance of ^{14}N NQR spectral linewidth increase on compaction force for compacts of paracetamol. Measured with NQR spectrometer tuned at 1921kHz.

One possibility to explain this behaviour would be a high ratio of plastic deformation and fracture (creating defects in crystalline matter) in relation to elastic deformation. Once the force has increased to the maximal values used, the data suggest that the magnitudes of plastic deformation and fracture of particles reach a plateau. This would imply that deformation at the molecular level is now governed by elastic deformation only. These results show the direct effects of compression on the crystal lattice of API on a molecular level, since EFG is dependent on local molecular surroundings. Graph similar to Fig. 1 was obtained with ^{14}N NQR measurements of famotidine at 2848 kHz.

Dependence of spectral linewidth on duration of compaction of paracetamol

When time of sustained maximum force of compression was increased from ≈0,1s to 15s and then 60s, there was also an increase in linewidth of resulting spectral peaks (Fig 2). The increase was less pronounced with increase in time of compression than it was with increasing force of compression. Additionally the time has a measurable influence only in the first 15s of compression. These results could be connected with the viscoelastic properties of compressed material.

Influence of milling on the compacts of paracetamol

When compacts of paracetamol prepared with the compaction force of 150 kN were subject to the milling in a ball mill, the linewidth of ^{14}N NQR spectral peaks at 1921 was only slightly decreased. This could be explained by the relaxation of internal residual stress thereby causing the crystal structure to only partially relax to its normal state.

CONCLUSIONS

^{14}N NQR can be successfully applied to the study of compaction of pharmaceutical materials as shown by the work presented. For paracetamol and famotidine compacts there seems to be a plateau to the extent of plastic deformation and fracture when the maximal values of compaction force were used. Elastic deformation is then probably the dominating component of deformation. Compaction time also increases linewidth but less significantly than the compaction force. Milling only partially decreased linewidth. Effects of compression force on the deformation at molecular level were evident and the information gathered provided a new insight into the deformation process.

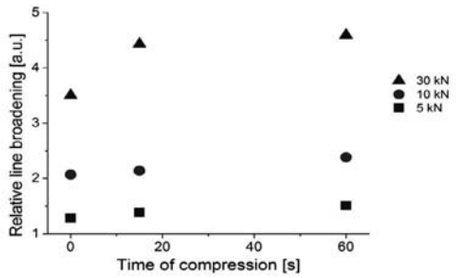

Fig. 2: Dependance of ^{14}N NQR spectral linewidth increase on time and compaction force for compacts of paracetamol. Measured with NQR spectrometer tuned at 1921kHz.

REFERENCES

1. Pérez S C, Cerioni L, Wolfenson A E, Faudone S, Cuffini S L. Utilization of pure nuclear quadrupole resonance spectroscopy for the study of pharmaceutical crystal forms. Int. J. Pharm. 2005; 298: 143-152.
2. Lavric Z, Pirnat J, Luznik J, Seliger J, Zagar V, Trontelj Z, Srcic S. Application of 14N NQR to the Study of Piroxicam Polymorphism. J. Pharm. Sci. 2010; 99: 4857-4865.
3. Brown RJC. Pressure dependence of NQR frequencies in molecular crystals. J. Mol. Struct. 1980; 58: 85-88

AFM NANOINDENDATION TECHNIQUE FOR ASSESING MECHANICAL PROPERTIES OF CLARYTHROMYCIN CRYSTALS

B. Govedarica*, O. Planinšek, S. Srčič

University of Ljubljana, Faculty of Pharmacy, Aškerčeva 7, 1000 Ljubljana, Slovenia

INTRODUCTION

Crystal engineering is generally considered as a design of crystalline molecular solids with the aim of impacting material attributes such as physical, chemical and mechanical. The crystallization technique can influence different crystal properties such as habit, size and type of the polymorph. Even in isomorphic forms, crystals can have different outer appearance which can affect processing properties such as flowability, blending and mixing as well as compressibility. The effect of crystal habit on tabletting behaviour can be linked to the relative orientation of the crystals in the tablet die and their mechanical properties such as elasticity and plasticity [1]. The elasticity of the crystals is indicated by the Young's modulus while the plasticity can be described by the indentation hardness. Recently, nanoindentation has become a practical tool for investigation of material's mechanical properties in small dimensions and it can be performed by atomic force microscope (AFM) and nano/microindenters.

Nanoindentation involves the approaching and retracting of the AFM tip or indenter into a surface and measuring of load and depth of penetration, which is related to deformation of the material [2].

The aim of the current paper was to reveal the differences in mechanical properties of isomorphic form of clarithromycin exhibited different habits.

MATERIALS AND METHODS

Preparation of clarithromycin form II

A suspension of clarithromycin in two separated solvents (acetone and ethanol) was heated at reflux for 15 minutes. The solid fraction was separated from the hot solution by filtering. Furthermore, the filter flask was rinsed with acetone. Combination of the filtrate and rinse were warmed on reflux and acetone or ethanol was added to dissolve any remaining solid. The solution was cooled to ambient temperature and then in an ice-water. The resulting solid was filtered and dried overnight in a vacuum oven to give form II [3]. Obtained crystals from the ethanol were rectangular in shape (Fig. 1A) while hexagonal form was crystallized from the acetone (Fig. 1B).

For the characterization of the Form II, DSC measurements were performed.

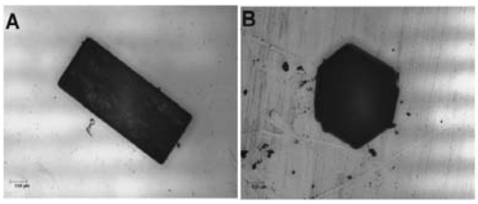

Fig. 1: Clarithromycin crystals from ethanol (A) and acetone (B).

Nanoindentation measurements

AFM force spectroscopy was carried out on NanoScope IIIa (Veeco, Santa Barbara, CA, USA) AFM, using diamond coated cantilevers with pyramidal tips (PPP-FM, Nanosensors, Wetzler, Germany, nominal spring constant 29 N/m).

The indentation experiments of clarithromycin crystals were performed on the largest crystalline plane. Measurements involved collecting of the individual force curves on different locations at the scanned surface. Smaller areas (~ 500 nm) were focused before performing the nanoindentation experiments. The linear region of the force-deformation curves was used to calculate the Young's modulus following the Hertz equation (Eq. 1):

$$F = \frac{4\sqrt{Rc}}{3} \frac{E}{1-r^2} \delta^{3/2} \qquad \textit{Eq. 1}$$

Here, F is the loading force, δ is the deformation, R_c is the probe's radius of the curvature, E is the Young's modulus and ν is Poisson ratio of the elastic solid. The Poisson ratio of 0.3 was used in calculation. At least 50 force curves were collected on each investigated sample.

Breaking Force measurements

Crystals of clarythromycin from both solvents were disposed in a height-adjustable sample holder. Breaking force was measured on CSM Micro Indentation Tester (MHT). Maximum applied force during measurements was 10 N.

RESULTS AND DISCUSSION

Nanoindentation measurements performed on predominant face of clarithromycin crystals confirmed differences in their mechanical properties (Fig. 2).

According to the Young's moduli more stiffer structure exhibited rectangular crystals of clarithromycin (E = 7.38 ± 1.12 GPa) in comparison to hexagonal (E = 0.18 ± 0.09 GPa).

Larger variations in Young's moduli of hexagonal crystals can be explained with anisotropy involved in bonding of the crystals plains or possible defects in crystal structure.

On the other hand, reliableness of the AFM nanoindentation results was confirmed by measuring the breaking force of crystals on microindenter (Fig. 3). The results support stiffer mechanical properties of rectangular crystals ($F_{breaking}$ = 3.97 ± 1.47 N) of clarithromycin in comparison to hexagonal ($F_{breaking}$ = 0.26 ± 0.05 N).

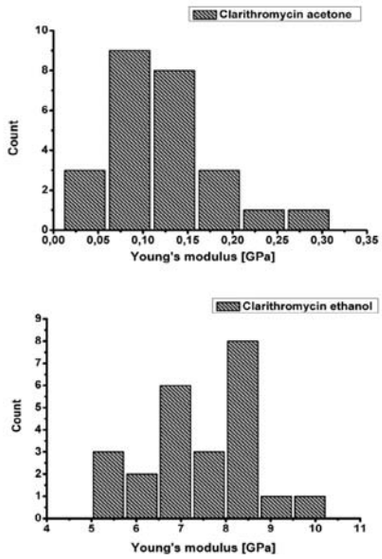

Fig. 2: Young's modulus of clarithromycin crystals from ethanol and acetone.

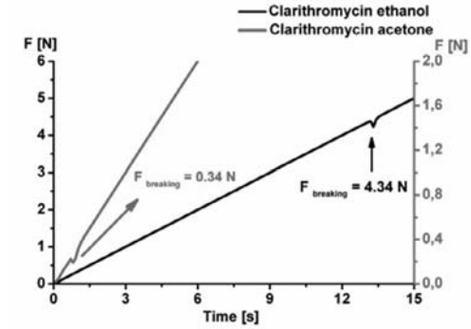

Fig. 3: Breaking Forces of clarithromycin crystals from ethanol and acetone.

CONCLUSIONS

Two isomorphic forms of clarithromycin crystals with different habits exhibit distinct mechanical properties. AFM nanoindentation results strongly confirmed brittle attributes of rectangular crystals in comparison to more ductile behaviour of hexagonal ones.

REFERENCES

1. Rasenack N, Muller W B. Crystal habit and tableting behavior. Int. J. Pharm. 2002; 244: 45-57
2. Feng Y, Grant J D. Influence of crystal structure on the compaction properties of n-Alkzl 4-Hydroxybenzoate Esters. Pharm. Res. 2006; 23: 1608-1616.
3. Sohn Y, Rhee J, Im W. Polymorphism of clarithromycin. Arch. Pharm. Res. 2000; 4: 381-384.

INVESTIGATION OF CRYSTALLIZATION PROCESSES USING IN-LINE RAMAN SPECTROSCOPY

H. Pataki*, B. Vajna, Zs. K. Nagy, Gy. Marosi

Budapest University of Technology and Economics, Department of Organic Chemistry and Technology, Budapest, Budafoki Street 8. 1111, Hungary

INTRODUCTION

Polymorphism is defined as the ability of a substance to exist as two or more crystalline phases that have different arrangements. The identification of polymorphism in the pharmaceutical industry is critical, as unexpected drug changes of a drug substance can affect solubility, physical stability, morphology and bioavailability. Raman spectroscopy affords a non-destructive, fast quantitve measurement of the solid state of pharmaceutical ingredient. One of the advantages of the method is that it can be used for real-time monitoring during solid pharmaceutical elaboration processes. Several applications of the Raman spectroscopy can be published within pharmaceutical processes (1), but this study focused on in-situ monitoring of dynamic processes for instance solvent mediated polymorphic transitions (2), or crystallizations under different conditions.

Solvent-mediated polymorphic transformation could be determined in the case of progesteron, where the achievements have allowed reseraches to define processing parameters required to control the morphology of crystalline progesteron (3).

The transformation between anhydrous and dihydrated carbamazepine in ethanol-water mixtures was studied using a fiber optic Raman probe as well (4). The experiments confirmed, that transformation rate depends on both solvent composition and temperature.

In this study in-line Raman spectroscopy was used for in situ monitoring of cooling crystallizations and polymorphic transitions of a model pharmaceutical ingredient, so as to be able to examine both the formation and transformation of polymorphs.

MATERIAL AND METHODS

Materials

Carvedilol drug (which exists in different forms) has six polymorphs and two solvates), and ethyl acetate (water content < 0,2n/n%) were used for all experiments.

Experimental setup

A 0,5L jacketed glass reactor with a stirrer was applied for crystallizations. The temperature controlling was carried out with a Julabo thermostat. Raman spectroscopy (produced by Jobin Yvon) was used for in-line monitoring phase changes in the reactor, where a fiber optic Raman probe was immersed into the crystallizer (Fig 1).

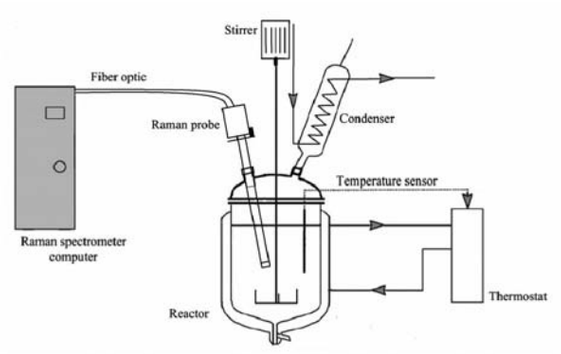

Fig. 1: Experimental set-up for in-line Raman application

Solvent-mediated polymorphic transition, crystallization

Carvedilol Form II -kinetically preferred- polymorph of the drug was suspended in EtOAc solvent at different temperature (25, 50, 60°C), then seeded 1w/w% thermodinamically stable polymorph Form I. Form II was dissolved in EtOAc at different drug concentrations (2.9; 9; 16w/w%) by 0,32°C/min cooling rate.

Analytical tools

In situ measurements were performed using a Raman spectroscope and equipped with a fiber optic coupled probe, using a 400mW, 785nm laser source and air cooled CCD detector. The quantitve evaluation was performed with CLS method (classical least square).

RESULTS AND DISCUSSION

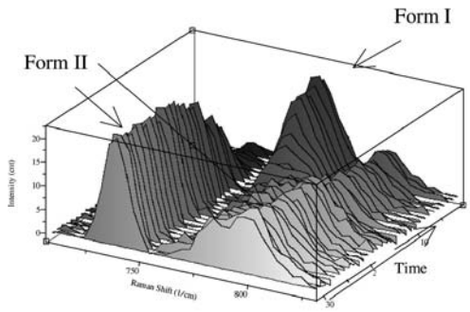

Fig. 2: 3D Raman spectra of polymorphic transition from Form II to Form

Raman peaks at 727cm^{-1}, and at 768cm^{-1} were used for in situ quantification of the polymorphic fraction of Form II, moreover Form I is characterized by a single peak at 757cm^{-1}. In suspensions solvent mediated polymorphic transformations could be determined from the metastable (Form II) to the thermodinamically stable (Form I) polymorph (Fig 2). The speed of transformation is largely dependent on temperature values (Fig 3). As a function of increasing temperature a significant growing could be appeared in the period of the transformations.

Cooling crystallization was executed in three different concentrations (16w/w%, 9w/w%, 2,9w/w%). In the case of one group (16, 9 w/w% solutions) cooling crystallization results in each experiment the formation of metastable Form II, while at lower concentration rate (2,9w/w%) solvate formation could be obtained. During the crystallization of 16w/w% solution, the dissolution has been complete at 69°C, and crystallization has started at 45°C respectively. Both processes took place extremely rapidly (Fig 4).

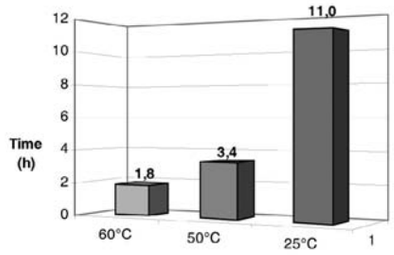

Fig. 3: Period of solvent mediated polymorphic transformations at different temperatures

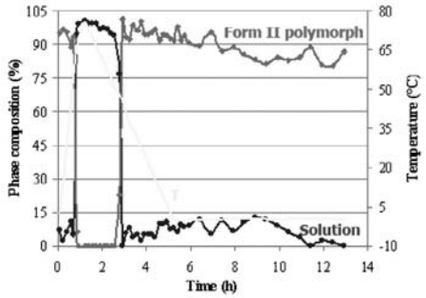

Fig. 4: Evaluation of cooling crystallization at 16 w/w% concentration

CONCLUSIONS

These results show the potential of Raman spectroscopy for process optimization and control, besides, it is a promising technique to understand the relationships between the process parameters and the final crystal properties.

REFERENCES

1. Starbuck C, Spartalis A, Wai L, Wang J, Fernandez P, Lindemann CM,Zhou GX, Ge Z, Process optimization of complex pharmaceutical polymorphic Polymorphic System via In Situ Raman Spectroscopy. Cryst. Growth. Des. 2002; 2: 515-522.
2. Jiang S, ter Horst JH, Jansens PJ, Concomitant Polymorphism of o-Aminobenzoic Acid in Antisolvent Crystallization. Cryst. Growth. Des. 2008; 8: 37-43.
3. Wang F, Wachter JA, Antosz FJ, Berglund KA, An Investigation of Solvent-Mediated Polymorphic Transformation of Progesterone Using in Situ Raman Spectroscopy. Org. Proc. Res. Dev. 2000; 4: 391-395.
4. Qu H, Louhi-Kultanen M, Rantanen J, Kallas J, Solvent-mediated phase transformation Kinetics of an Anhydrate/Hydrate System. Crys. Growth. Des. 2006; 6: 2053-2060.

PHARMACOPOEIAL QUALITY OF NON-EXPIRED AND EXPIRED NIFEDIPINE FORMULATIONS FROM ESTONIAN AND RUSSIAN FEDERATION MEDICINAL PRODUCTS MARKET

K.Teder[1,2*], A. Pepeloshev[1], V. Matto[1], A. Meos[1]

[1] Department of Pharmacy University of Tartu, Nooruse 1, Tartu 50411, Estonia;
[2] Tartu University Hospital Pharmacy, Puusepa 8, Tartu 51014, Estonia

INTRODUCTION

Nifedipine (NIF; ATC code: C08CA05) is a relatively safe and well tolerable dihydropyridine-like calcium channel blocker, mainly administered by mouth as the extended release (ER) formulations (1-3). Since NIF is a light sensitive and well degradable compound (4), the appropriate pharmaceutical procedures for the manufacture and the subsequent optimal storage conditions must be strictly followed.

The aim of this study was to evaluate the pharmacopoeial quality of non-expired and expired NIF tablets of the same batches purchased from the Estonian and Russian Federation medicinal products market.

MATERIALS AND METHODS

The non-expired NIF formulations were evaluated from January to April 2006. The remained tablets were stored in their original package at ambient temperature (22±2°C) in a dark storage cabinet and after expiration the formulations were tested in June to September 2010.

Quality and quantity of API

The API was identified using the Shimadzu IR-spectrometer FTIR-8400S with GoldenGate ATR interface.

The quality and quantity of NIF and the related substances were studied according to the HPLC method described in NIF monograph of the 5th EP. The same HPLC method was used to exclude any interference of the NIF degradation products with the dissolution test results (dissolution medium was analyzed immediately after test completion).

Table 1: List of tested nifedipine formulations

Formulation	*Manufacturer/ holder of marketing authorization*
Adalat retard, 10mg	Bayer HealthCare AG, Germany
Cordipin retard, 20mg	KRKA, d.d., Slovenia
Cordipin XL, 40mg	KRKA, d.d., Slovenia
Corinfar retard, 20mg	AWD pharma GmbH & Co.KG, Germany
Corinfar, 10mg	AWD pharma GmbH & Co.KG, Germany
Nifedipin retard-ratiopharm, 20mg	Merckle GmbH, Germany
NifeHEXAL retard, 20mg	Salutas Pharma GmbH Member of Hexal Group, Germany
Nycopin, 40mg	Nycomed SEFA AS, Estonia
Vero-nifedipine, 0.01g*	ZAO "Verofarm", Russian Federation
Nifedipine-Shtshelkovsky, 0.01g*	OAO " Shtshelkovsky vitaminnyi zavod, Russian Federation
Nifedipine-Farkos, 0.01g*	OOO NPF "Farkos", Russian Federation
Fenigidin, 0.01g*	OOO Farmacevticheskaya kompanuya „Zdarov'ye", Ukraine

*formulations registered and sold in Russian Federation

Table 2: Dissolution tests results. The percent of released nifedipine after 3rd and 12th hour.

Formulation	Released API %			
	Non-expired		Expired	
	3h	12h	3h	12h
Adalat retard, 10mg	60±4	93±3	80±2	95±1
Cordipin retard, 20mg	53±2	92±2	66±3	89±2
Cordipin XL, 40mg	32±3	69±4	40±4	81±2
Corinfar retard, 20mg	40±2	80±2	75±2	81±3
Corinfar, 10mg	80±5	87±2	60±5	87±3
Nifedipin retard- ratiopharm, 20mg	63±4	83±4	80±2	93±1
NifeHEXAL retard, 20mg	51±2	80±2	67±4	93±3
Nycopin, 40mg	28±2	69±2	33±4	90±3
Vero-nifedipine, 0.01g *	70±2	81±2	n.a.	n.a.
Nifedipine-Shtshelkovsky, 0.01g *	71±2	83±2	91±4	93±4
Nifedipine-Farkos, 0.01g *	77±4	87±4	92±3	93±3
Fenigidin, 0.01g *	74±3	84±2	82±3	91±3

*formulations registered and sold in Russian Federation

Dissolution test

Dissolution tests were performed using the Sotax AT-7 multi-bath dissolution test system coupled to the Ultrospec III (Pharmacia LKB) spectrophotometer, fed by the peristaltic pump (Watson-Marlow 202 U/AA). The system was driven by the custom-adapted software.

The 28th USP *Nifedipine Extended-Release Tablets* monograph test 2 was implied (apparatus 2; 50rpm; +37±0.5°C; test medium (pH=6.8) contained

11.25ml of phosphate buffer concentrate, 90ml of 10% sodium lauryl sulphate solution and water (ad 900ml)).
The dissolution test lasted for 12h; the samples were measured every 15min (at 238nm). To prevent photodegradation of the NIF, the whole test system was covered with dark, nontransparent cover.

RESULTS AND DISCUSSION

All tested formulations contained high quality NIF as the API and by this aspect the Russian registered NIF formulations are comparable with the European competitors.
There was no information about the type of the dosage form of the Russian formulations, but they were treated as conventional, since according to the attached PIL, the recommended administration frequency (2 to 3 times daily) for the Russian formulations was similar to the Corinfar 10mg (the only European conventional dosage form).
Although, there were differences in excipiences in Russian formulations (the Vero-nifedipine tablets contained more advanced excipients and the list resembled to the European ER tablets), the releasing characteristics of the API were almost identical: at least 2/3 of the NIF was released within 3 hours. Though in the non-expired Russian NIF tablets the initial release of API was fast, it was still constantly sustained during the first 3 hours. The expired Russian tablets released the API abruptly and the dissolution curve resembled that of the conventional tablets. Accelerated release of API could be observed also in expired European NIF tablets but the release was not as rapid as in Russian formulations.
As a limitation, one has to keep in mind that the NIF release from the ER formulations is very method-sensitive (5), thus our dissolution test results have to be considered only in the frame of the present test conditions.
Though NIF is a photosensitive compound (4) it is notable that the NIF degradation products in the dissolution medium did not exceed the trace level. Therefore, apart of the fact that the dissolution tests were performed appropriately, this finding also confirms that there was no significant NIF degradation in the expired tablets.

CONCLUSIONS

Our present study unveiled that the NIF of the ER tablets as the API preserves well beyond the expiration date regardless of the country of origin of the formulations, however, the expired NIF tablets tend to release the API faster than the non-expired tablets.
Consequently, one can say that though the API is well preserved in the expired tablets, the API release may be quick and thus there exists a risk of accelerated NIF absorption. The latter should be considered as a medical threat and therefore the use of the expired NIF tablets should be discouraged.

REFERENCES

1. Dolezal T, Nemecek K, Krsiak M. Trends in consumption of calcium channel blockers in the Czech Republic during 1993-1999 and comparison with selected countries: drug utilization study. Eur J Clin Pharmacol. 2002; 58: 477-478
2. Kiivet RA, Bergman U, Rootslane L, Rägo L, Sjöqvist F. Drug use in Estonia in 1994-1995: a follow-up from 1989 and comparison with two Nordic countries. Eur J Clin Pharmacol. 1998; 54: 119-124
3. Pontremoli R, Leoncini G, Parodi A. Use of nifedipine in the treatment of hypertension. Expert Rev Cardiovasc Ther. 2005; 3: 43-50
4. Kawabe Y, Nakamura H, Hino E, Suzuki S. Photochemical stabilities of some dihydropyridine calcium-channel blockers in powdered pharmaceutical tablets. J Pharm Biomed Anal. 2++8; 47: 618-624
5. Garbacz G, Golke B, Wedemeyer RS, Axell M, Söderlind E, Abrahamsson B, Weitschies W. Comparison of dissolution profiles obtained from nifedipine extended release once a day products using different dissolution test apparatuses Eur J Pharm Sci. 2009; 38: 147-155

ICH Q8 IMPLEMENTATION BY A GENERIC PHARMACEUTICAL INDUSTRY – CRITICAL VIEW

Lj. Karanakov[1*], J. Tonic-Ribarska[2], S. Trajkovic-Jolevska[2]

[1] Replek Farm Ltd, Kozle 188, 1000 Skopje, Macedonia; [2] Faculty of Pharmacy, University "Ss Cyril and Methodius", Vodnjanska 17, 1000 Skopje, Macedonia

INTRODUCTION

Generic industry goal is to satisfy the patients' expectation, by obtaining safe, efficient, high quality medicines. The ICH Q8 -Pharmaceutical development gives guidance for: optimization of medicine quality through its life cycle, presentation of science based data in CTD Module 3 and meaning of transfer from finished product inspection to build in quality and real time release testing.
The aim of this paper is to present a brief overview of the guideline, realize and give a critical point of view for implementation of Quality by Design (QbD) and Process Analytical Technology (PAT), by generic pharmaceutical industry.

METHODOLOGY

Description and analyses of Q8, focused on determination and implementation of QbD and PAT, pointing out the contrast of the life cycle, concluded from generic industry aspect.

QbD/ PAT IMPLEMENTATION

ICH Q8 core guideline provides guidance on the minimal contents approach of section CTD 3.2.P.2 - Pharmaceutical Development. This document points out the section parts where knowledge gained from scientific - risk based development approaches and comprehensive product and processes understanding should be presented. QbD can enhance achieving the desired product quality, science and risk based regulatory approaches and better understanding of the company strategy. (1)
QbD is a systematic approach to development that begins with predefined objectives and emphasizes product and process understanding and process control, based on sound science and quality risk management (1). QbD means 'building in quality from the development phase and throughout a product's life cycle' or 'designing and developing a product and associated manufacturing processes that will be used during product development to ensure that the product consistently attains predefined quality at the end of the manufacturing process'(2). Quality by design elements:
1. Defined Quality Target Product Profile
2. Critical Quality Attributes
3. Design space
4. Control strategy

PAT is defined as a system for analyzing and controlling manufacturing during processing, of critical quality and performance attributes of raw and in-process materials and processes, with the goal of ensuring final product quality (3). The goal of PAT is to expand the process understanding, focusing on enhanced control during processing, optimizing the process efficiency. (4) PAT encompasses a variety of technologies, methodologies and tools designed to shift the pharmaceutical industry's quality focus from post-production inspection to building quality into its products by design (5). Empirical approach based on predefined specification for compliance, where variable at a time is tested may end up with OOS results. Production process is fixed including repeated controls after each cycle, without possibility of unauthorized changes, and validation is based on minimum three pilot batches manufactured at industrial facilities. Control strategy is testing and inspection, focused on repeatability and optimization of processes in compliance with approved specification. Retrospective quality assurance and corrective measures, based on in-process and finished product analysis are used, where opportunities for statistical and basic

problem cause analysis are limited. Deferring from the empirical approach, QBD/PAT implementation represents a systematic, multidimensional, CQAs determination within design space. Defining design space depends on QTPP and available resources, using prior scientific knowledge and design of multivariable experiments, to better understanding of input materials and process qualitative attributes. Product quality is reflected in the approved design space. Safety and efficacy data in this phase are obtained by performing in vitro studies and IV/IVC correlations. Specification in compliance with regulatory requirements and risk assessment of CQA, results in: determination of CQAs should be tested and PAT tools should be used. Production processes and scale up to industrial facilitates are flexible, easier and faster. QbD product almost never fails the bioequivalence study and transfer to commercial manufacturing is predictable. Ongoing quality management leads to processes validation through the life cycle. This approach focuses on robust processes and determination of scientific and risk based control strategy. PAT enables statistical analysis and quality monitoring at real time, as a base for proactive quality management. Quality performances are improved through the life cycle using QbD/PAT.

DISSCUSION

Major focus of the generic industry is components selection, formulation, manufacturing process and control strategy development, for easier and faster commercialization of consistent quality product. There are no strict requirements for QbD/PAT application. Depending on needs and possibilities for built in quality, QbD implementation should be optimized. Robust processes and understanding of variables justifies the shift of control. QbD/PAT Implementation is innovative challenge for generic industry with great opportunities for cost reduction, lowered rate of batch failures and science based regulatory assessment.

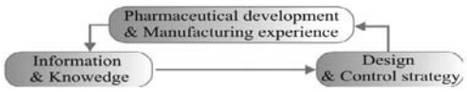

Fig. 1: QbD (ICHQ8)

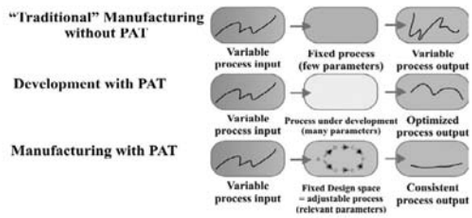

Fig. 2: PAT, source: adopted from K. Ho, CHMP Biologics Working Party, EMA, presentation

CONCLUSIONS

Implementation of QbD/PAT is challenge and opportunity for the generic industry in manner of technological, financial and quality improvement.Investment in the development enables better understanding of product and processes leading to: easier improvement of the built in quality, faster and easier regulatory assessment. Due to economic competition, wider design space leads to faster commercialization and reduced post-approval variations. QbD as systemic approach to pharmaceutical development supported with PAT tools is cost and time benefit for generic industry.

REFERENCES

1. ICH, Guideline Q8 (R2) – Pharmaceutical Development, Step 5, November 2008, http://www.ich.org
2. FDA.(2006) FDA Guidance for Industry: Quality System Approach to Pharmaceutical cGMP Regulations, US Department of Health and Human service Rockville, MD: FDA.
3. EMA: European Medicine Agency – Human Medicines – EMA Pre Submission Procedural Advice – Questions and Answers, EMA Website
4. Varu, R. K.; Khanna A. 2010, Opportunities and Challenges to Implementing Quality by Design Approach in Generic Drug Development. Journal of Generic Medicines, 7, (1), pp. 60–73
5. Lo, S.; Venkatesh, K.; Foster, G. 2006, Benefits and Challenges of PAT Implementation in Generic Pharmaceutical Manufacturing. American Pharmaceutical Review, 3, (1), pp. 13-18.

INFLUENCE OF FORMULATION VARIABLES ON SURVIVAL OF L. CASEI LOADED IN CHITOSAN-Ca-ALGINATE MICROPARTICLES PREPARED BY SPRAY-DRYING

T. P. Ivanovska[1*], L. P. Tozi[1], K. Smilkov[2], E. Popovski[3], T. Stafilov[3], A. Grozdanov[4], N. Geskovski[1], R. Petkovska[1], K. Mladenovska[1]

[1] University "Ss Cyril and Methodius", Faculty of Pharmacy, Vodnjanska 17, 1000 Skopje, Macedonia; [2]University "Goce Delcev", Faculty of Medical Sciences – Pharmacy, Krste Misirkov bb, 2000 Stip, Macedonia; [3] University "Ss Cyril and Methodius", Faculty of Natural Sciences and Mathematics, Arhimedova 5, 1000 Skopje, Macedonia; [4] University "Ss Cyril and Methodius", Faculty of Technology and Metallurgy, Ruger Boskovic 16, 1000 Skopje, Macedonia

INTRODUCTION

Few methods of microencapsulation are widely used to enhance the viability of probiotics in pharmaceutical and food products and during the passage in the GIT (1). Functional properties of microparticles for effective colon delivery of viable cells depend to great extent on the type of the encapsulating materials. Although different protective materials are applied during the microencapsulation process (2), natural biopolymers alginate and chitosan are of continuous interest due to their biocompatibility, potential for effective preservation of probiotics and targeted release of viable cells in the colon (3, 4).

The aim of this study was to evaluate the effect of encapsulating materials in given ranges of concentrations on viability of probiotic *L. casei* in simulated *in vivo* conditions using polynomial regression model at 2nd level.

MATERIALS AND METHODS

Materials

Freeze-dried probiotic culture of *Lactobacillus casei* was purchased from Chr. Hansen, Denmark. Prebiotic fructo- oligosaccharide (FOS) was supplied from Sigma-Aldrich, USA. As encapsulating agent, alginate-LF 10/60 (Protanal, FMC Biopolymers, UK) was used. For additional coating of spray-dried microparticles, chitosan (Chitine, France) and for cross-linking procedure, $CaCl_2$ (Merck, Germany) were used.

Preparation of microparticles and determination of physicochemical properties

The microparticles were prepared by modified spray-drying method, previously used for microencapsulation of drugs (5) and for the first time for micro-encapsulation of probiotic cells. An aqueous dispersion of alginate, FOS and *L. casei* was spray-dried (nozzle diameter 0.7 mm, aspirator pressure 90%, flow rate 6 ml/min, inlet and outlet temperature, 120 °C and 60 °C, Büchi Mini Spray Dryer B-290, SW) to obtain microparticles, which were subsequently cross-linked and coated in solution of $CaCl_2$ and chitosan in 1% *w/w* acetic acid. Prepared microparticles were cured for 3 h, separated and freeze-dried (-50 °C, 0.070 mbar, 24 h, Freeze-Dryer, Labconco, USA). Following physicochemical properties were determined: particles size (Master-sizer Hydro-2000S, Malvern Instruments Ltd., UK), Ca-content (AES-ICP, Varian, USA), zeta-potential (Zeta-sizer Nano ZS, Malvern Instruments Ltd., UK) and cell viability into the microparticles (plate-count method).

Experimental modelling

The cross-linking procedure and poly- electrolyte complexation were carried out at concentration limits of alginate (1% and 4% *w/w*), chitosan (0.1 and 0.5% *w/w*) and $CaCl_2$ (0.5 and 5% *w/w*). The cell load in the feed suspension was ca. 11-12 log_{10} cfu/g. The plan matrix included 11 batches.

Viability of microencapsulated *L. casei* in simulated *in vivo* conditions

To determine the viability of encapsulated probiotic, experiments were performed in simulated gastric juice for 3 h (0.08 M HCl with 0.2% NaCl, pH 1.5), bile salts solution for additional 3 h (0.05 M KH_2PO_4 with 1% bile salt, pH 6.8) and in colonic pH 7.4 (0.1 M KH_2PO_4) up to 24 h.

RESULTS AND DISCUSSION

Microparticles with d_{vs} ranging from 6.7 to 12.5 µm, zeta-potential -22.6 to 30.3 mV, Ca-content 3.5 to 12.5% and survival rates of probiotic within the particles from 6.91 to 11.43 log_{10} cfu/g were obtained. Viability of microencapsulated *L. casei* in simulated GI conditions is presented in Fig.1.

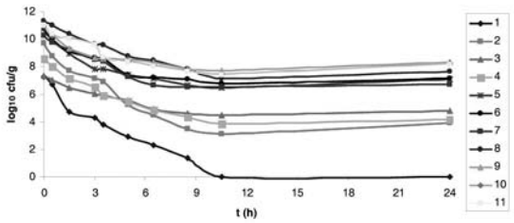

Fig.1: Viability of microencapsulated *L. casei* (log_{10} cfu/g) in simulated GI conditions in different series generated with experimental design

Overall effects of the formulation variables pointed to the dominant influence of the concentration of $CaCl_2$ on survival rate of the microencapsulated cells of *L. casei* in all pH media tested. Higher content of Ca^{2+} in the microparticles resulted in increased viability of *L. casei*. The relationships between variable factors and responses were plotted by holding constant one of the three variables. Chitosan concentrations produced only minor influence on probiotic's viability in simulated gastric and intestinal conditions and by fixing its value, survival rate of probiotic cells increased with increased alginate concentration. At constant level of chitosan, the viability of microencapsulated probiotic cells would increase to 9.1 log_{10} cfu/g or higher and 7.35 log_{10} cfu/g or higher, for alginate concentrations of 2.64-4% and 1-4% (*w/w*) and for $CaCl_2$ in range of 4.64-5% and 3.58-5% (*w/w*) in gastric juice and bile salts solution, respectively (Fig 2).

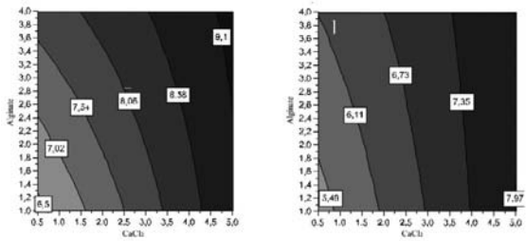

Fig.2: Response surface plot for viability of microencapsulated *L. casei* (log_{10} cfu/g) showing the effects of alginate and CaCl2 for constant level of chitosan, 0.5% (w/v); a) pH 1.5; b) pH 6.8

Considering the influence of the formulation variables on the physico-chemical properties of the microparticles and on the viability of *L. casei* in simulated GI conditions, an optimal formulation was prepared, with 4% alginate, 0.5% chitosan and 5% $CaCl_2$. The data for the viability of *L.casei* confirmed the predicted values, 9.62 log_{10} cfu/g in pH 1.2, 8.46 log_{10} cfu/g in pH 6.8 and 7.67 log_{10} cfu/g in pH 7.4.

In conclusion, the prepared microparticles showed potential for effective colon delivery of live probiotic cells.

REFERENCES

1. Kailasapathy K. Microencapsulation of probiotic bacteria: technology and potential applications. Curr. Issues Intest. Microbiol. 2002; 3:39-48.
2. Anal AK, and Singh H. Recent advances in microencapsulation of probiotics for industrial applications and targeted delivery. Trends Food Sci. Technol. 2007; 18:240-251.
3. Sandoval-Castilla O, Lobato-Calleros C, Garcia Galindo HS, Alvarez-Ramirez J, Vernon-Carter EJ. Textural properties of alginate-pectin beads and survivability of entrapped Lb. casei in simulated gastrointestinal conditions and in yoghurt. Food Res. Int. 2010; 43:111-117.
4. Chavarri M, Maranon A, Ares R, Ibanez FC, Marzo F, del Carmen Villaran M. Microencapsulation of a probiotic and prebiotic in alginate-chitosan capsules improves survival in simulated gastro-intestinal conditions. Int. J. Food Microbiol. 2010; 142:185-189.
5. Mladenovska K, Raicki RS, Janevik EI, Ristoski T., Pavlova MJ, Kavrakovski Z, Dodov MG, Goracinova K. Colon-specific delivery of 5-aminosalicylic acid from chitosan-Ca-alginate microparticles. Int. J. Pharm. 2007; 342(1-2):124-136.

THE INFLUENCE OF SHELL FORMING PHASE ON EFFICIENCY OF SMES ENCAPSULATION INTO POLYMERIC MATRIX

A. Zvonar*, K. Bolko, M. Gašperlin

Faculty of Pharmacy, University of Ljubljana, Aškerčeva 7, 1000 Ljubljana, Slovenia

INTRODUCTION

The ability to develop an effective oral dosage form is crucial for the successful launch of a new active pharmaceutical ingredient (API) in the marketplace. One of formulation strategies recently employed for APIs with poor biopharmaceutical properties are self-microemulsifying drug delivery systems (SMES) (1). In our previous study (2,3) liquid SMES was successfully transformed to solid microcapsules by technique of liquid jet co-extrusion by vibrating nozzle technology. Obtained microcapsules merge the advantages of SMES with those of a solid dosage forms, and thus provide a promising alternative to ensure successful oral delivery of drugs with poor biopharmaceutical properties.

Key steps for the successful encapsulation of the furosemide-loaded SMES by above mentioned technology are to prevent mixing between the core (SMES) and the shell forming phase (polymer solution with additives) during microcapsules production and drying process. The main scope of the current study was therefore to optimize the properties of shell forming phase with respect to encapsulation efficiency and microcapsules morphology.

MATERIALS AND METHODS

SMES was prepared by blending 88 % of the Labrasol® and Plurol oleique® (2:1) mixture (both from Gattefosse, France) with 12 % of Mygliol 812® (Hüls, Germany). Afterwards 0.5 % of $CaCl_2$ was added to promote shell hardening from the inside out as soon as the capsules are formed. Finally, SMES was loaded with 5 % furosemide and thickened with 4 % of colloidal silica (Aerosil 200, Degussa, Germany) (3).

Shell forming phase was prepared by mixing 2 % Na-alginate solution (Low viscosity Na-alginate, Sigma, Germany) with 2 % pectin solution (Genu® pectin type LM-104 AS-Z, CP Kelco, Denmark) in 3:1 ratio (4). Afterwards 5-20 % of hydrophilic filling agent (lactose, trechalose, mannitol, or sorbitol) was added to the aqueous solution of polymers.

SMES was microencapsulated within the polymeric shell by coextrusion of liquid jet by using an Inotech IE-50R encapsulator (Inotech, Switzerland). Microcapsules were than hardened according to different procedures: (a) 15 min incubation in 0.5M $CaCl_2$ (*$CaCl_2$*) followed by (b) 5 min incubation in 1mg/ml chitosan solution (*$CaCl_2$+C-LV*) or (c) 1mg/ml chitosan solution with 0.5M $CaCl_2$ (*$CaCl_2$+C-LV with $CaCl_2$*) to apply additional chitosan coating;

alternatively, microcapsules were simultaneously incubated (15 min) in 1mg/ml chitosan solution with 0.5M $CaCl_2$ (*C-LV with $CaCl_2$*). Hardened microcapsules with SMES in the core that were coated with chitosan (low, medium or high viscosity chitosan, Fluka, Germany) were dried in a fluid bed system.

The efficiency of encapsulation (EE) was calculated according to Eq. (1) for cross-linked (non-dried) and Eq. (2) for dried microcapsules:

$$EE = \frac{\text{mass of drug in crosslinked microcapsules x 100}}{\text{mass of drug in non-crosslinked microcapsules}} \quad (1)$$

$$EE = \frac{\text{mass of drug in dried microcapsules x 100}}{\text{mass of drug in non-crosslinked microcapsules}} \quad (2)$$

RESULTS AND DISCUSSION

The main challenge in production of microcapsules by technique of liquid jet co-extrusion by vibrating nozzle technology is to prevent the undesired mixing of the self-microemulsifying core with the aqueous shell forming phase, which results in core leakage and decreased encapsulation efficiency. Beside modification of the core phase (3), and alginate/pectin ratio in the shell forming phase (4), the microencapsulation efficiency is also affected by the hydrophilic filling agents added to the shell forming phase (Table 1) and hardening procedure of microcapsules, applied prior to the drying process (Fig. 1).

Table 1: The dependence of encapsulation efficiency of drug - loaded SMES into polymeric matrix on filling agent added to the shell – forming phase.

Filling agent	Encapsulation efficiency [%]	
	Raw MC	Dried MC
No additives	82,6 ± 11,5	40,5 ± 5,5
10 % mannitol	54,0 ± 0,7	51,0 ± 2,0
10% sorbitol	70,5 ± 18,0	61,0 ± 7,3
10 % trechalose	64,8 ± 10,3	58,4 ± 11,0
10 % lactose	81,1 ± 9,2	74,2 ± 0,5
5 % lactose	67,6 ± 21,8	56,3 ± 18,1
15 % lactose	71,5 ± 10,1	35,3 ± 8,4
20 % lactose	27,7 ± 17,3	22,9 ± 6,3

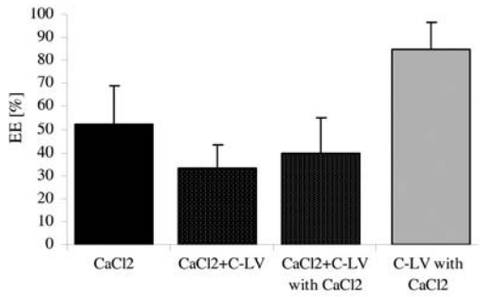

Fig. 1: The influence of hardening process on encapsulation efficiency [EE] of drug-loaded SMES into polymeric matrix; C-LV: low viscosity chitosan solution.

A shell forming phase consisting solely of 2% alginate/pectin solution shows leakage of core phase during drying of cross-linked microcapsules. In order to reduce core leakage different hydrophilic filling agents were added to the shell phase. As shown in Table 1 lactose exhibited highest influence on core phase retention during drying process among all filling agents tested (mannitol, sorbitol, trechalose, and lactose). To determine the optimal amount of lactose in the shell forming phase the dependence of core phase retention on lactose content (5-20 %) was studied. In both, raw (non-dried) and fluid bed dried microcapsules highest encapsulation efficiency was observed when lactose was added in 10 % ratio as tested initially.

The encapsulation efficiency results for microcapsules cross-linked according to different procedures are presented on Fig. 1. Enhanced core phase retention was observed when microcapsules were hardened in one step process, which included 15 min incubation in either 0,5 M $CaCl_2$ (~ 52 %), or 1% chitosan solution containing 0,5 M $CaCl_2$ (~ 84 %). The later was selected as optimal hardening process when considering also the encapsulation efficiency results obtained in dried microcapsules (data not shown).

Encapsulation efficiency of core phase was least influenced by the viscosity of applied chitosan coating. Yet, considering also the microcapsules morphology, low viscosity chitosan was chosen as the most appropriate coating.

CONCLUSIONS

Best shaped microcapsules with highest encapsulation efficiency were obtained from the shell forming phase with the alginate/pectin ratio of 1:3 containing 10 % lactose, which were hardened by one-step process and coated with low-viscosity chitosan.

REFERENCES

1. Haus DJ (Eds.) Oral Lipid-Based Formulaitons, Informa Healthcare Inc., New York, USA (2007).
2. Homar M., Šuligoj D., Gašperlin M. Preparation of microcapsules with self microemulsifying core by a vibrating nozzle method. J Microencapsulation 2007; 24(1): 72-81.
3. Zvonar A, Berginc K, Kristl A, Gašperlin M. Microencapsulation of self-microemulsifying systems: improving solubility and permeability of furosemide. Int J Pharm. 2010; 388: 151–158.
4. Zvonar A, Gašperlin M. Microcapsules with self-microemulsifying core: optimization of shell-forming phase. Pharmazie. 2010; 65: 390–391.

EVALUATION OF ACIDO-RESISTANCE AND DRUG RELEASE FROM ALGINATE MICROSPHERES FORMULATED USING DIFFERENT DISPERSION METHODS

D. Grizić[1*], E. Vranić[1], O. Planinšek[2], S. Srčič[2], D. Planinšek[3]

[1]Department of Pharmaceutical Technology, Faculty of Pharmacy, University of Sarajevo, Čekaluša 90, 71 000 Sarajevo, Bosnia and Herzegovina; [2] Department of Pharmaceutical Technology, Faculty of Pharmacy, University of Ljubljana, Aškerčeva 7, SI-1 000 Ljubljana, Slovenia; [3] Agency for medicinal products and medical devices, Ptujska 21, SI-1000 Ljubljana, Slovenia

INTRODUCTION

Acido-resistance and controlled drug release are properties usually linked with modern drug delivery systems. Microspheres obtained using alginate as a cross-linked polymer exhibit these properties. The term "Ionotropic gelation" is referred to the formation of alginate hydrogels (1), and it describes the linkage of multivalent cations (Ca^{2+}, Ba^{2+}, Zn^{2+}) on the carboxylic anions of alginate. Since alginate is an environmental-sensitive polymer, the produced microspheres will have similar properties, which gives them their controlled drug delivery properties (2). These microspheres are pH-sensitive; very stable in acidic medium (3) that gives them the acido-resistant properties, as well, but fast disintegrating in basic medium. One aim of this study is the comparison of the microspherical acido-resistance prepared using different procedures. The drug release from microspheres is often influenced by the particle size of the active substance. The anti-solvent crystallization method can be a useful technique for the dispersion and size-reduction (4) of water-insoluble active substances. Because of this fact, different particle sizes can be obtained, using different dispersion methods. These different particle sizes often have direct influence on the

drug release. The evaluation of the drug release can be achieved using *in vitro* dissolution tests (5). Therefore, the second aim of our sudy is the dissolution profile investigation of microspheres prepared using different formulation procedures.

MATERIALS AND METHODS

Materials

Ibuprofen (B.P., BASF Chemtrade GmbH, Burgbernheim, Germany) was a gift from Belupo (Koprivnica, Croatia). Sodium alginate (3 Pas, 2 %), Calcium chloride dihydrate p.a., Ethanol and Hydrochloric acid (37%) were purchased from Semikem (Sarajevo, B&H). Potassium dihydrogen phosphate p.a., and Sodium hydroxide p.a. were purchased from Merck (Darmstadt, Germany). All other reagents used were of analytical grade.

Preparation of microspheres

Two formulations (named F_1 and F_2) containing fixed quantity of ibuprofen (2%), sodium alginate (1%), calcium chloride (2%), were prepared. Curing time for both formulations was 30 minutes. F_1 formulation was prepared as follows: ibuprofen was added in previously prepared sodium alginate solution and dispersed by magnetic stirrer. Each dispersion was transferred into injection syringe containing needle (21 G) and by dropping (velocity 10 ml/min) added into calcium chloride solution. After 30 minutes (curing time) the microspheres were filtered using funnel with Whatman #4 qualitative filter paper and washed out twice with distilled water and dried at room temperature for 24^h. F_2 formulation was prepared by anti-solvent crystallization technique under following conditions: ibuprofen was dissolved in ethanol (6% solution obtained). This solution was added dropwise in a continuously stirred sodium alginate solution (2%). Further steps in microsphere preparation were as it was already described for F_1 formulation.

Acido-resistance investigation

The acido-resistance analysis was performed using an Erweka DT 700 dissolution tester (Erweka GmbH, Heusenstamm, Germany). Six samples for both methods of preparation (F_1 and F_2) were used. The test was performed on a USP rotating basket apparatus at 37±0.5 °C, 100 rpm during 2h in 0.1M HCl. The aliquots were filtered trough a 0.45µm nylon membrane filter, and quantified on a UV/VIS spectrosphotometer at 260 nm.

Drug release studies

The drug release was performed on an Erweka DT 700 dissolution tester (Erweka GmbH, Heusenstamm, Germany) for both formulations (F_1 and F_2) in hexaplicate using USP rotating basket apparatus. The samples were dropped into 500 mL of phosphate buffer pH 7.4 maintained at a temperature of 37°C ± 0.5°C and stirred at a speed of 100 rpm for 2h. A 10 mL aliquot of the sample was withdrawn every 20 minutes and the volume was replaced with an equivalent amount of phosphate buffer medium kept at 37°C. The collected samples were filtered through a 0.45µm nylon membrane filter and analyzed at 260 nm using a UV/VIS spectrophotometer.

RESULTS AND DISCUSSION

Acido-resistance investigation

Fig. 1 shows the low drug release in acidic medium for both samples (F_1 and F_2). Because the percentage of release for both samples is below 10%, both samples can be declared as acido-resistant (in accordance with Ph. Eur. 7.0.)

Drug release

As shown in Fig. 2., the sample F_1 shows slower release than sample F_2, which is a very significant difference between the samples.

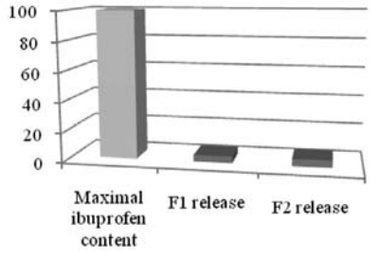

Fig. 1: Acido-resistance of F_1 and F_2 microspheres

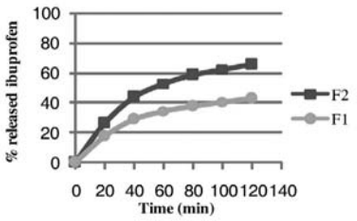

Fig. 2: Dissolution profiles of F_1 and F_2 microspheres

CONCLUSION

It is evident that both samples express satisfactory acido-resistance and different release rates of ibuprofen. These properties can be very useful for the formulation of controlled drug delivery systems.

REFERENCES

1. Das M., Senapati P. Evaluation of furosemide-loaded alginate microspheres prepared by ionotropic external gelation technique. Acta Pol. Pharm. 2007; 64(3): 253-262
2. Pandey R., Khuller G., Alginate as a drug delivery carrier. In: Handbook of carbohydrate engineering. First edition. Ed: Yarema K. CRC Press, 2005: pp. 799-814
3. Patil J.S., Kamalapur M.V., Marapur S.C., Kadam D.V. Ionotropic gelation and polyelectrolyte complexation: The novel techniques to design hydrogel particulate sustained, modulated drug delivery system. Digest J. Nanomaterials and Biostructures, 2010; 5(1): 241-248
4. Li C., Li C., Le Y., Chen J. Formation of bicalutamide nanodispersion for dissolution rate enhancement. Int. J. Pharm., 2011; 404(1): 257-263
5. Lee S., Raw A., Yu L. Dissolution testing. In: Biopharmaceutics applications in drug development. First edition. Ed: Krishna R., Yu L. Springer, UK, 2007: pp. 47-74

MICROSCOPICAL EVALUATION OF THE ANTI-SOLVENT CRYSTALLIZATION METHOD INFLUENCE ON THE MATRIX ARCHITECTURE OF ALGINATE MICROSPHERES

E. Vranić[1*], D. Grizić[1], O. Planinšek[2], D. Planinšek[3], S. Srčič[2]

[1] Department of Pharmaceutical Technology, Faculty of Pharmacy, University of Sarajevo, Čekaluša 90, 71 000 Sarajevo, Bosnia and Herzegovina; [2] Department of Pharmaceutical Technology, Faculty of Pharmacy, University of Ljubljana, Aškerčeva 7, SI-1 000 Ljubljana, Slovenia; [3] Agency for medicinal products and medical devices, Ptujska 21, SI-1000 Ljubljana, Slovenia

INTRODUCTION

Alginate is a linear polysaccharide, obtained from marine brown algae (*Phaeophyceae*) or certain species of bacteria. It forms hydrogels by ionotropic gelation process (1). During this process, a reticulated structure is formed, which is cross-linked by divalent cations (Ca^{2+}, Ba^{2+}, Zn^{2+}) to carboxylic anions of manuronic and guluronic acid. If the extrusion of alginate solution was performed by dropping of a drug-loaded polymeric solution into an aqueous solution of divalent cations, microspheres of different sizes (2) and properties could be produced depending of their composition. The preparation of microspheres is a multi-step process. The most important step is the dispersion of an active substance into the

microspheric matrix, especially if the active substance is poorly soluble in water (BCS - Class II). Additionally, it is also very important to choose the appropriate method of incorporation of substances (3) into alginate microspheres. Anti-solvent crystallization method is an advanced technique that can be used for the incorporation of poorly soluble active substances in polymeric hydrogels. This process is used in order to obtain smaller particles, which occur due to differences in solubility of active substances in various solvents (4). The aim of our study was to: perform *in situ* coating of ibuprofen crystals, using high viscosity anti-solvent (5) (aqueous solution of sodium alginate), and to evaluate the anti-solvent crystallization method influence on the matrix architecture of alginate microspheres.

MATERIALS AND METHODS

Materials

Ibuprofen (B.P., BASF Chemtrade GmbH, Burgbernheim, Germany) was a gift from Belupo (Koprivnica, Croatia). Sodium alginate (3 Pas, 2 %), Calcium chloride dihydrate p.a., and Ethanol were purchased from Semikem (Sarajevo, B&H). All other reagents used were of analytical grade.

Preparation of microspheres

The microspheres were prepared by the extrusion/external ionotropic gelation technique using sodium alginate and calcium chloride solutions. Two formulations (named F_1 and F_2) containing fixed quantity of ibuprofen (2%), sodium alginate (1%), calcium chloride (2%), were prepared. Curing time for both formulations was 30 minutes. F_1 formulation was prepared as follows: ibuprofen was added in previously prepared sodium alginate solution and dispersed by magnetic stirrer. Dispersions were transferred into injection syringe containing needle (21 G) and by dropping (velocity 10 ml/min) added into calcium chloride solution. After 30 minutes (curing time) the microspheres were filtered, washed out twice with distilled water and kept in distilled water until analysed. F_2 formulation was prepared by anti-solvent crystallization technique under following conditions: ibuprofen was dissolved in ethanol (6% solution obtained). This solution was added drop-wise in a continuously stirred sodium alginate solution (2%). As a result of this procedure, a white suspension was formed containing small particles of ibuprofen. Further steps in microspheres preparation were as it was already described for F_1 formulation.

Sample preparation and micro-scoping

The morphology and appearance of microspheres were examined by microscopy (Olympus 500 Ultrazoom U-TV1X-2 microscope + integrated camera), after fixation at -25ºC for 24 hours (cryo-fixation). Cross-sections of both microspheres were prepared. Ibuprofen crystals obtained by previously described methods were also analysed. Microscopic evaluation of each sample was performed at 10X, and 40X magnification.

RESULTS AND DISCUSSION

Ibuprofen crystal sizes

As illustrated in Fig. 1, the anti-solvent crystallization technique has a direct influence on the ibuprofen crystals size. Ibuprofen crystals that are not prepared by this method, are bigger in size (around 55 µm). Using anti-solvent crystallization technique, a larger number of small crystals were obtained. Their length varies around 10 µm.

Microsphere matrix homogeneity

Fig. 2 clearly illustrates differences between the microspheres produced by different methods of dispersion. Sample F_1 consists of small ibuprofen crystals, that are, due to their size, homogeneously distributed. Sample F_2 shows inhomogeneity of matrix architecture due to larger ibuprofen crystal sizes. This fact proves that the dispersion method is directly related to the ibuprofen crystal size, and to the microspherical matrix architecture.

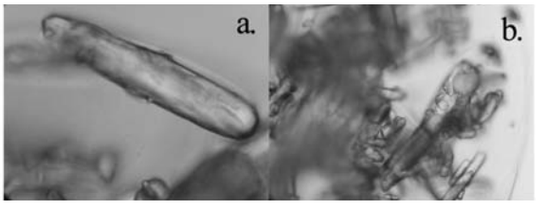

Fig. 1: Photomicrographs of ibuprofen crystals: before (a.) and after (b.) anti-solvent crystallization procedure, magnification 40X.

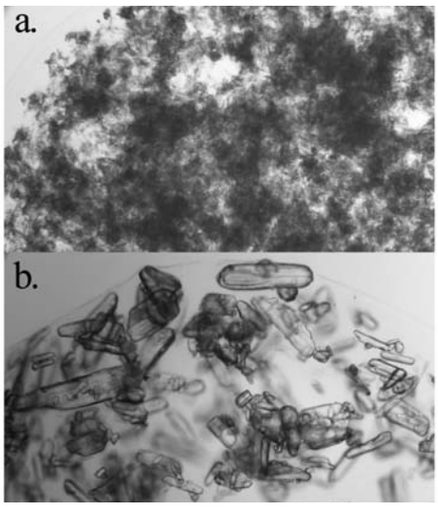

Fig. 2: Photomicrographs of F_1 (a.) and F_2 (b.) microspherical cross sections, magnification 10X.

CONCLUSION

F_1 sample shows greater matrix homogeneity, what indicates that the method of choice for dispersion of ibuprofen in alginate matrix, would be the anti-solvent crystallization method.

REFERENCES

1. Patil J.S., Kamalapur M.V., Marapur S.C., Kadam D.V. Ionotropic gelation and polyelectrolyte complexation: The novel techniques to design hydrogel particulate sustained, modulated drug delivery system. Digest J. Nanomaterials and Biostructures, 2010; 5(1): 241-248
2. Diane J. Burgess, Anthony J. Hickey. Microsphere technology and application. In: Encyclopedia of Pharmaceutical Technology. Third edition. Ed: Swarbrick J. Taylor & Francis group, Abingdon, Oxford, UK, 2006: 2328-2351
3. Cook J., Addick W., Wu Y. H. Application of the biopharmaceutical clasiffication system in clinical drug development – an industrial view. AAPS j., 2008; 10(2): 306-310
4. Grosso M, Galan O, Baratti R, Romagnoli J.A. A Stochastic formulation for the description of the crystal size distribution in antisolvent crystallization processes. AIChE J., 2010: 56(8), 2077-2087
5. Xiao X., Hong Z. Firstborn microcrystallization method to prepare nanocapsules containing artesunate. Int. J. Nanomedicine, 2010; 58: 483-486

IN VIVO EVALUATION OF LOW MOLECULAR WEIGHT HEPARIN-ALGINATE BEADS

F. Acarturk[1*], C. İskenderoğlu[2]

[1] Department of Pharmaceutical Technology, Gazi University, Faculty of Pharmacy, 06330, Etiler, Ankara, Turkey, facar@tr.net; [2] Refik Saydam Hygiene Center, 06100, Ankara / Turkey

INTRODUCTION

Low molecular weight heparin (LMWH) and heparin are widely used as anticoagulants for the treatment and prevention of deep vein thrombosis and pulmonary embolism (1). LMWH and heparin preparations are currently available to patients only by parenteral administration, because of its poor oral bioavailability.

Oral route is the most convenient and preferred route of drug administration. Various studies have been carried out to develop an oral delivery system of LMWH (2,3). Alginate beads have the advantages of being non-toxic orally and having high biocompatibility.

The aim of this study is to develop a formulation for the oral administration of LMWH. For this purpose, LMWH-alginate beads were prepared. After oral administration of LMWH-alginate beads to rabbits, the time course of anticoagulant activity was evaluated measuring the anti-Xa activity and the bioavailability was also calculated.

MATERIALS AND METHODS

Materials

Low molecular weight heparin (LMWH) was purchased from Fluka (U.S.A.). Sodium alginate (Protonal LF120M) was kindly supplied by FMC Biopolymer (U.S.A.). Anti-Xa assay kits (STA-Rotachrom) were purchased from Diagnostica Stago (France).

Preparation and Characterization of Alginate Beads

Alginate beads were prepared based on the 2^3 factorial design. The preparation method was reported in the previous study (4). The formulation consisting of 1:2 drug/alginate ratio and cured using 0.5 M $CaCl_2$ for 15 minutes gave the best result in terms of encapsulation efficiency and $t_{50\%}$. Drug encapsulation efficiency, swelling ratio, particle size measurements and drug release studies were carried out. Surface morphology of the beads was examined using scanning electron microscopy (SEM).

In Vivo Studies

Male adult New Zealand White rabbits (2.5-3 kg) were used after an overnight fast for at least 12 h in the study. Alginate beads carrying LMWH (LMWHAB) (5000 IU/kg) were administered to rabbits by oral route. A solution of LMWH (LMWHS), administered either intravenously (ear vein, 100 IU/kg, bolus) or orally (5000 IU/kg, oral gavages), as well as drug–free beads (AB) administered by oral route. The anti-Xa activity was measured in blood plasma at 0, 0.5, 1, 2, 3, 4 and 6 h after administration of each dosage form. Blood samples (1 mL) were withdrawn from the ear vein into a vial containing sodium citrate and centrifugated for 10 min at 3000 g. Plasma was stored at -80°C until analysis.

RESULTS AND DISCUSSION

The encapsulation efficiency of the beads was determined to be 85.4%. The particle size of the beads was found to be 1496±10 μm. The swelling ratio of formulations varied with pH. The swelling ratio of beads at pH 6.8 was more than that of pH 1.2. Beads rapidly swelled and broke apart at pH 6.8. The SEM photographs of alginate beads are shown in Figure 1. Almost spherical particles were obtained.

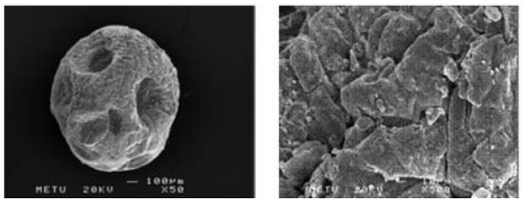

Fig. 1: The SEM photographs of LMWH loaded alginate beads.

Figure 2 depicts the release profiles of the LMWH-alginate beads. About 62 % of the drug was released at pH 1.2 within two hours. After the medium was replaced with pH 6.8 buffer solution, the beads completely dissolved within half an hour.

The anti-Xa activity of the orally administered formulations and as well as the IV solution are shown in Figures 3 and 4.

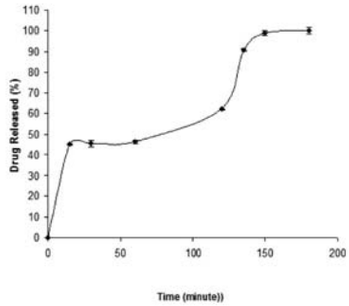

Fig. 2: Drug release profile of the LMWH-alginate beads

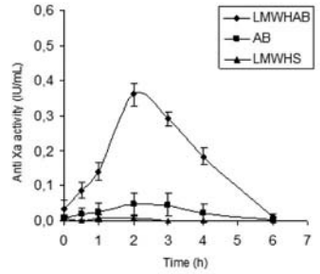

Fig. 3: The anti-Xa activity of LMWH-alginate bead, drug-free alginate bead and LMWH solution after oral administration.

The indication of effectiveness is achieved when anti-Xa activity reach a minimum of 0.2 IU/mL value. After the oral administration of alginate beads containing LMWH (5000 IU/kg) to rabbits, the level of anti-Xa activity reached 0.360 IU/mL and an anticoagulant effect was achieved (>0.2 IU/mL). AUC and C_{max} values are shown in Table 1. It was observed that the bioavailability of alginate beads containing LMWH was enhanced 69.3 times compare to that of LMWH solution.

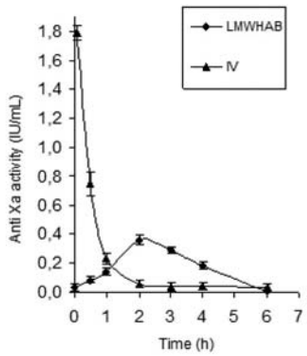

Fig. 4: The Anti Xa activity of LMWH-alginate bead and IV solution.

Table 1: The AUC and Cmax values of the oral and IV administered formulations.

FORMULATION	$AUC_{0-\infty}$	C_{max} (IU/mL)
IV[a]	1.16±0.12	1.79±0.05
LMWH-solution	0.0176±0.0102	0.009±0.007
LMWH-alginate bead[a]	1.22±0.19	0.360±0.032
Alginate bead	0.166±0.124	0.0468±0.0324

[a]p <0.05 compare to LMWH-solution and alginate bead

The LMWH solution was administered IV at a dosage of 100 IU/kg and the absolute bioavailability was calculated. Absolute and relative bioavailabilities of the LMWH-alginate beads were found to be 2.10 and 6930 %, respectively. The absolute bioavailability of the oral solution was 0.0303 %.

CONCLUSION

In conclusion, anticoagulant effectiveness was achieved using alginate beads containing LMWH after oral administration to rabbits.

ACKNOWLEDGMENTS

This study was supported by a grant from Gazi University (02/2004-24). We wish to thank S. Kirazlı for anti-Xa activity measurements and FMC Biopolymer for supplying alginate samples.

REFERENCES

1. Bick RL, Proficient and cost effective approaches for the prevention and treatment of venous thrombosis and thromboembolism. Drugs 2000; 60: 575-595.
2. Hoffart V, Lamprecht A, Maincent P, Lecompte T, Vigneron C, Ubrich NJ, Oral bioavailability of low molecular weight heparin using a polymeric delivery system J. Control. Rel. 2006; 113: 38-42.
3. Lee D, Lee J, Lee S, Kim S, Byun YJ, Liphophilic complexation of heparin based on bile acid for oral delivery. J.Control. Rel. 2007;123: 39-45.
4. Iskenderoğlu C, Acartürk F, Preparation and in vitro evaluation of low molecular weight heparin-alginate icroparticles 33th Annual Meeting& Exposition of the Controlled Release Society, 22-26 July 2006, Viena, Austria.

PREPARATION AND CHARACTERIZATION OF DRUG FORMULATIONS OF ORDERED AND NONORDERED MESOPOROUS SILICA MICROPARTICLES

T. Limnell[1], E. MäKilä[2], T. Heikkilä[2], J. Salonen[2], D.Y. Murzin[3], N. Kumar[3], T. Laaksonen[1], L. Peltonen[1], J. Hirvonen, H.A. Santos[1*]

[1] Division of Pharmaceutical Technology, Faculty of Pharmacy, University of Helsinki, FI-00014, Finland; [2] Laboratory of Industrial Physics, Department of Physics and Astronomy, University of Turku, FI-20014, Finland; [3] Laboratory of Industrial Chemistry, Process Chemistry Centre, FIN-20500 Abo Akademi, Turku, Finland

INTRODUCTION

One major challenge in the pharmaceutical industry is the poor bioavailability of drug formulations, which is a result of the poor solubility/permeability of the drugs (1). In order to overcome the abovementioned problems extensive research has been focused on mesoporous silica-based materials (1–4). Despite the extensive research on mesoporous materials, there is still lack of direct comparison between ordered and nonordered porous silica materials.

In this study, commercial silica-gel Syloid 244 and ordered mesoporous silica, MCM-41, were used as carriers for indomethacin (IMC). IMC was loaded into the mesoporous silica particles using a rotavapor and fluid bed methods. The loaded mesoporous silica particles were also formulated and compressed into tablets using common pharmaceutical excipients.

MATERIALS AND METHODS

Materials

IMC was used as received (Hawkins Inc., USA) and Syloid 244 (Syloid) was kindly provided by Grace Davison (Grace GmbH, Germany). Synthesis of MCM-41 was carried as described elsewhere (4).

Loading of IMC

IMC was first loaded with an immersion method as described elsewhere (4). A rotavapor (Hei-VAP Advantage; Germany) loading method was also used at drug–particle ratio of 1:2.3 (30% IMC and 70% silica), and the solvent (ethanol) was evaporated under reduced pressure at 45-50 °C for 15 min. Finally, a fluid bed (Glatt GmbH, Germany) loading method was also tested for the loading of IMC at drug–particle ratio of 1:2.3. The solvent was evaporated by spraying the suspension at pressure of 0.8 bar and at 90 °C.

Tablet formulations

Avicel PH 102 and Ac–Di–Sol (FMC BioPolymer, Ireland), Aerosil 200 (Evonik Degussa GmbH, Germany), Kollidon 30 (BASF, Germany), Pharmatose 200M (DMV International GmbH, Netherlands), and magnesium stearate (Orion Pharma, Finland) were used as excipients in tablet formulations. The tablets were compressed manually (Korsch EK0, Germany) using round flatfaced punches (d=5 mm). The compression forces were 4.6 ± 2.4 kN.

Drug dissolution and release

The dissolution experiments were performed using the Ph. Eur. paddle dissolution method (Sotax AT7, Switzerland) at 100 rpm with 500 mL of buffer (pH 5.5) at 37 °C. IMC was quantified by HPLC (Agilent 1100 Series, Germany) using acetonitrile and 0.2% phosphoric acid pH 2.0 (60:40 %, v/v), a Luna 100 Å C18 column, at a flow rate of 1.5 mL/min and injection volumes of 20 µL.

RESULTS AND DISCUSSION

Loading methods

IMC loaded into the silica particles with both the rotavapor and fluid bed methods proved to be effective, yielding loading degrees of 24–29 w-%. No crystalline fractions of IMC on the particles' surface were observed after loading. In the rotavapor loading method, the IMC concentration in the loading solution increases slowly as the solvent is evaporated, whereas in the fluid bed the solvent evaporates fast as the suspension is sprayed into the product chamber. Solvent evaporation, and particles' pore diameter and morphology were crucial parameters to obtain an efficient loading.

Tablet formulations

The amount of drug-loaded silica particles in the formulation was kept constant at 25%. The weight of the tablets was ca. 50 mg, the crushing strengths were 60-80 N. Syloid tablets disintegrated remarkably slower (6.8–11.6 min) than the MCM-41 tablets (0.8–3.5 min). The thickness of the tablets was ca. 1.94 mm. The mesoporous structure of the particles was intact even after tableting.

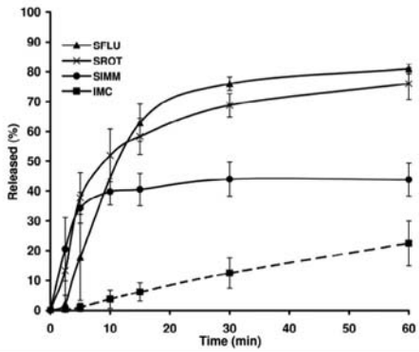

Fig. 1: Release profiles of IMC from encapsulated Syloid particles loaded by the different methods at pH 5.5 and 37 °C. SIMM, SROT, and SFLU are Syloid particles loaded with the immersion, rotavapor, and fluid bed methods, respectively. Bulk IMC is included as a reference (dashed lines).

Release of IMC

The IMC release was not affected by the loading method, rotavapor vs. fluid bed, as shown in Fig 1 for Syloid particles. Similar results were obtained with MCM-41 (not shown). The IMC release from the encapsulated particles was faster from Syloid than from MCM-41 (see MFLU vs. SFLU in Fig. 2). When the excipients were added to the MFLU capsule (named MFLUE), the dissolution of IMC from the formulation was remarkably improved and slightly faster than from SFLU (Fig 2).

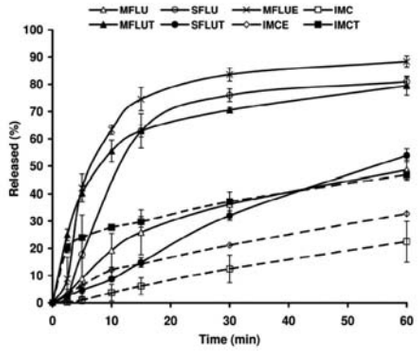

Fig. 2: Release profiles of IMC from Syloid (SFLU) and MCM-41 (MFLU) particles loaded by the fluid bed method (solid lines) at pH 5.5 and 37 °C. Comparison of the loaded particles/IMC as such or with excipients in capsule (MFLUE and IMCE) and tablet formulations (MFLUT, SFLUT, and IMCT). Bulk IMC is included as a reference (dashed lines).

CONCLUSIONS

Rotavapor and fluid bed methods were used to load IMC into mesoporous silica particles. No excess amount of drug was needed, which is an advantage of those methods over commonly used loading methods. IMC was released faster from Syloid 244 than from MCM-41, due to larger pore size and smaller particle size. IMC-loaded particles were also compressed without problems into tablets. The porous structures of the particles remained unchangeable after compression. Finally, the IMC dissolution rate was enhanced even after tableting.

REFERENCES

1. Wang S. Ordered mesoporous materials for drug delivery. Micropor. Mesopor. Mat. 2009; 117: 1–9.
2. Vallet-Regí M, Rámila A, del Real RP, Pérez-Pariente J. A new property of MCM-41: Drug delivery system. Chem. Mater. 2001; 13: 308–311.
3. Heikkilä T, Salonen J, Tuura J, Kumar N, Salmi T et al. Evaluation of mesoporous TCPSi, MCM-41, SBA-15, and TUD-1 materials as API carriers for oral drug delivery. Drug Delivery 2007; 14: 337–347.
4. Limnell T, Riikonen J, Salonen J, Kaukonen AM, Laitinen L et al. Surface chemistry and pore size affect carrier properties of mesoporous silicon microparticles. Int. J. Pharm. 2007; 343: 141–147.

PROBIOTIC MICROORGANISMS WITH IMPROVED STRESS-TOLERANCE FOR DEVELOPMENT OF ADVANCED FORMULATIONS

H. Viernstein*, S. Stummer, S. Salar-Behzadi

Department of Pharmaceutical Technology and Biopharmaceutics, University of Vienna, Althanstraße 14, 1090 Vienna, Austria

INTRODUCTION

In recent years the interest in probiotic products has been growing due to the health-promoting activities associated with their use. During the development of such products, probiotic microorganisms have to withstand different kinds of stress including high temperatures (1, 2, 3). The aim of this study was to investigate the effect of heat stress on the culturability and the cellular properties of the probiotic microorganism *Enterococcus faecium* M74. Afterwards, the tolerance of this microorganism to heat stress was improved, facilitating the development of pharmaceutical and nutraceutical formulations containing this microorganism.

MATERIALS AND METHODS

E. faecium M74 was obtained from Medipharm (Sweden). Fluorescent dyes were purchased from Sigma-Aldrich (Austria); other chemicals and culture media were obtained from Merck (Germany).

Effect of heat stress

Freshly harvested *E. faecium* M74 were suspended in phosphate buffer (pH 6.8) and stressed by heating them for certain durations at predefined temperatures. Unstressed bacteria were used as controls.

After each heating process the cell culturability was determined by spreading the cells onto kanamycin esculin azide agar plates and calculating the number of colony forming units (CFU). The cell membrane damage, the esterase activity, and the change in hydrogen peroxide production of the cells was investigated by exposing them to the fluorescent dyes propidium iodide (PI), fluorescein diacetate (FDA), and dihydrorhodamine 123 (DHR 123), respectively. The fluorescence measurements were done using a microplate reader Infinite®200.

Improvement of heat tolerance

Freshly harvested *E. faecium* M74 (1st generation) were suspended in phosphate buffer (pH 6.8) and stressed by heating. After heat stress of either 80°C for 1 min (moderate stress) or 80°C for 90 sec (severe stress) the cells were stressed a second time at 90°C for 1 min to observe any changes in heat tolerance. The only once stressed cells were inoculated into MRS-broth, incubated for 24 hours at 37°C, and harvested (2nd generation). The process described above was repeated until the 5th generation was reached. For each bacterial generation the cell culturability as well as the cellular properties were determined.

RESULTS AND DISCUSSION

Effect of heat stress

Figure 1 shows that all temperature conditions used, except 50°C, reduced the number of colony forming units and thus had a negative effect on the culturability of *E. faecium* M74. It can be seen that the higher the temperature the earlier a severe decrease in CFU occured.

Figure 2 indicates the impact of different heating temperatures on the membrane permeability of *E. faecium* M74. PI represents the status of the cell membrane – the higher the value the higher the membrane damage. The obtained data correlate with the results depicted in Figure 1. The results of the alterations in PI intensity were furthermore confirmed by the results obtained by using FDA or DHR 123.

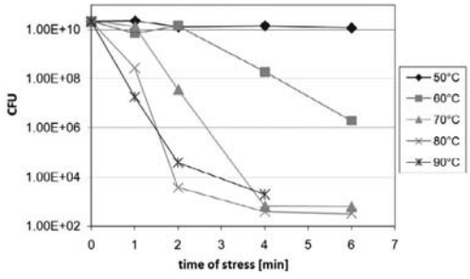

Fig. 1: Effect of heat on the culturability of E. faecium M74.

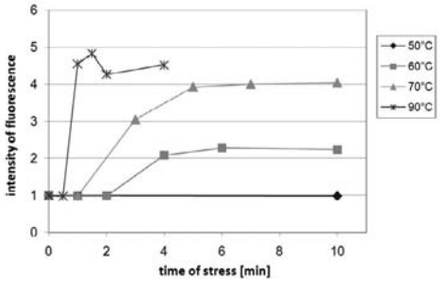

Fig. 2: Effect of heat on the relative PI intensity of E. faecium M74.

Improvement of heat tolerance

Figure 3 shows that the cells heat stressed at 80°C for 90 sec have an increased heat tolerance in the 3rd generation.

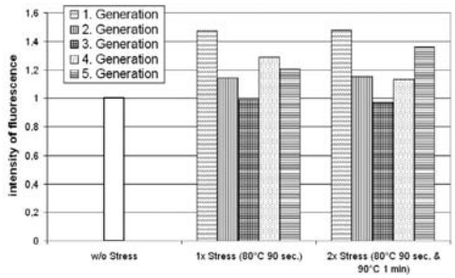

Fig. 3: Effect of multiple heat stress on the relative PI intensity of E. faecium M74.

A moderate temperature stress of 80°C for 1 minute was not sufficient to cause changes in the heat tolerance of *E. faecium* M74.

CONCLUSIONS

The results indicate that the higher the temperature applied, the faster the CFU were reduced. These results correlate with those obtained by the fluorescence measurements., which show that the more intense the applied heat, the sooner the alterations in cellular properties.

Concerning the increase of heat tolerance it was observed that *E. faecium* M74 stressed at 90 sec with 80°C were more resistant to heat in the 3rd generation. Therefore, when the 3rd generation is used for the development of probiotic formulations using a heat requiring production process, it is very likely that the number of living microorganisms in the product will be higher than that obtained employing unstressed bacteria.

REFERENCES

1. Golowczyc MA, Silva J, Teixeira P, De Antoni GL, Abraham AG, Cellular injuries of spray-dried Lactobacillus spp. isolated from kefir and their impact on probiotic properties. Int. J. Food Microbiol. 2011; 144: 556-560.
2. Baatout S, De Boever P, Mergeay M, Temperature-induced changes in bacterial physiology as determined by flow cytometry. Annals of Microbiology. 2005; 55 (1): 73-80.
3. Desmond C, Stanton C, Fitzgerald GF, Collins K, Ross RP, Environmental adaptation of probiotic lactobacilli toward improvement of performance during spray drying. Int. Dairy J. 2001; 11: 801-808.

MICROCAPSULES WITH FUROSEMIDE LOADED SMES: THE INFLUENCE OF SHELL COMPOSITION ON DRUG RELEASE

K. Bolko*, A. Zvonar, M. Gašperlin

University of Ljubljana, Faculty of Pharmacy, Aškerčeva cesta 7, 1000 Ljubljana, Slovenia

INTRODUCTION

Selfmicroemulsifying systems (SMES), among other lipid based systems, offer an efficient way of improving bioavailability of drugs with poor biopharmaceutical properties. Due to nature of lipids and surfactants, SMES are usually prepared as liquids, which are inconvenient to use. They are often filled in soft gelatin capsules, however, incompatibility issues are usual (1). The aim of our work was therefore to develop SMES loaded Ca-pectinate/alginate microcapsules containing furosemide as BCS class IV drug. Aqueous solution of pectin/alginate (3:1) was used as shell forming phase with addition of different filling agents and their influence on drug release profile was examined.

MATERIALS AND METHODS

Materials

SMES was composed and microcapsuled within the Ca-pectinate/alginate polymeric shell by a vibrating nozzle method using an Inotech IE-50R encapsulator (Inotech, Switzerland) as previously described by Zvonar et al (2). Pectin (Genu® pectin type LM-104 AS-Z; CP Kelco, Denmark) and low viscosity sodium alginate (Sigma, Germany) were used as polymer matrix. Low-, medium- and high-viscosity chitosane was used as an additional coating polymer (Fluka, Germany). Furosemide as model drug and lactose monohydrate (mesh 200) as shell phase additive were kindly provided by Lek Pharmaceuticals d.d. Other shell phase additives studied were mannitol, sorbitol (Merck, Germany) and trechalose (Calbiochem, USA).

In vitro dissolution test

The drug release studies were conducted using USP dissolution rate test apparatus (Apparatus II, 75 rpm, 37 ± 0.5°C) (VK7000, VanKel, USA) for 4 h in pH 3 hydrochloric acid aqueous solution and pH 6.8 phosphate buffer (900 ml). At the predetermined intervals (0 min, 15 min, 30 min, 45 min, 1h, 2h and 4h) 10 ml sample aliquots were withdrawn, filtered through a 0.45 µm membrane filter and assayed by HPLC method. Cumulative percentages of the drug dissolved from the products were calculated and plotted vs. time.

RESULTS AND DISCUSSION

Due to nature of pectin and alginate, all microcapsules exhibited fast drug release in pH 6.8 phosphate buffer, whereas results obtained in pH 3 buffer were more discriminatory. We will focus on drug release results in the latter. Lactose, trechalose, mannitol and sorbitol are small hydrophilic molecules, expected to dissolve fast in release media and thus behave as pore inducers during drug release process. Due to formation of pores in the surface and channels in the matrix of the microcapsules the penetration of water into the matrix as well as release of liquid core out of the matrix are enhanced. As seen in Fig. 1, our results confirm enhanced drug release with added 10 % sorbitol and 10 % trechalose to the shell forming phase. On the contrary, addition of both 10 % lactose and 10 % mannitol resulted in decreased drug release. This is probably due to their lower and slower solubitily in water in comparison to trechalose and sorbitol (results not shown).

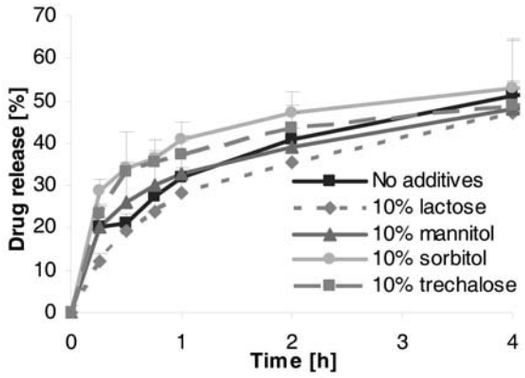

Fig. 1: Effect of different shell additives on drug release from SMES loaded microcapsules in pH 3 buffer.

In addition, the influence of shell additive ratio on drug release was studied on the example of lactose (Fig. 2).

As expected, pore forming effect is more pronounced with increased lactose content. In agreement to this the slowest drug release would be expected for microcapsules with lowest lactose content due to formation of smaller pores or channels in the polymer matrix. Yet, furosemide was

released less rapidly from microcapsules with 10 % lactose, whereas microcapsules with 5 % lactose exhibited surprisingly rapid release profile. We propose that drug release from microcapsules containing different amount of lactose was controlled not only by its pore inducing effect but also by the formation of hydrated viscous layer around the capsules, which acted as a barrier to drug release. This was confirmed by swelling and erosion study (results not shown).

Lastly, we discovered that drug release from SMES loaded microcapsules can also be modified using coating of different viscosity chitosan (Fig. 3).

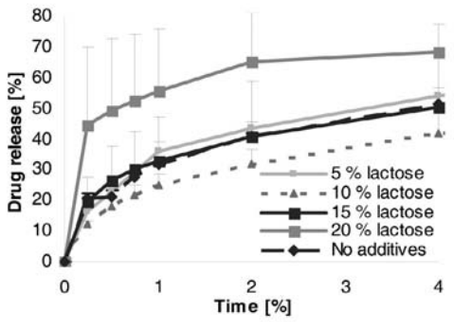

Fig. 2: Influence of lactose weight ratio in shell forming phase on drug release from microcapsules in pH 3 buffer.

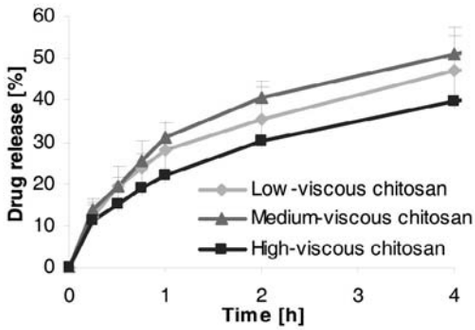

Fig. 3: Drug release from microcapsules with low-, medium- and high-viscous chitosan coating in pH 3 buffer.

High-viscous chitosan forms the thickest coat around the beads, resulting in the slowest drug release in pH 3 buffer. Medium-viscous chitosan coating was the least efficient in modifying drug release, as was in preventing core leakage (results not shown).

CONCLUSIONS

Hydrophilic filling agents in the shell forming phase can be used to modify drug release profile from SMES loaded Ca- pectinate/alginate microcapsules. Addition of 10 % sorbitol enhanced drug release the most, while 10 % lactose inhibited drug release in comparison to results obtained with microcapsules with no added filling agents. Furthermore, drug release could also be varied by the amount of filling agents added to the shell forming phase or using coating of different viscosity chitosan.

REFERENCES

1. Tuleu C, Newton M, Rose J, et al. Comparative bioavailability study in dogs of a self-emulsifying formulation of progesterone presented in a pellet and liquid form compared with an aqueous suspension of progesterone. J. Pharm. Sci. 2004; 93: 1495-502.
2. Zvonar A, Berginc K, Kristl A, Gašperlin M. Microencapsulation of self-microemulsifying system: improving solubility and permeability of furosemide. Int. j. pharm. 2010; 388 :151-158

EFFECTS OF FORMULATION VARIABLES ON VIABILITY OF L. CASEI LOADED IN WHEY PROTEIN-Ca-ALGINATE MICROPARTICLES IN SIMULATED IN VIVO CONDITIONS

K. Smilkov[1*], L. P. Tozi[2], T. P. Ivanovska[2], N. Geskovski[2], R. Petkovska[2], M. G. Dodov[2], K. Baceva[3], D. Dimitrovski[4], K. Mladenovska[2]

[1] University "Goce Delcev", Faculty of Medical Sciences, dept. Pharmacy, Krste Misirkov bb, 2000 Stip, Macedonia; [2]University "Ss Cyril and Methodius", Faculty of Pharmacy, Vodnjanska 17, 1000 Skopje, Macedonia; [3]University "Ss Cyril and Methodius", Faculty of Natural Sciences and Mathematics, Arhimedova 5, 1000 Skopje, Macedonia; [4] University "Ss Cyril and Methodius", Faculty of Technology and Metallurgy, Ruger Boskovic 16, 1000 Skopje, Macedonia

INTRODUCTION

Since the establishment of the probiotic concept by Metchnikoff there has been continuing rise of interest in the field of probiotics (1). Most of the beneficial effects of probiotics depend on their viability and activity on-site. It is known that *Lactobacillus spp.* lack the ability to survive the harsh environment in the human gastrointestinal tract (2). To improve the viability and survival of probiotics after oral administration, various polymer substances and various coating methods have been used (3). Among the biopolymers used as coating agents, alginate and whey proteins appear as potential candidates since they are entirely biodegradable and used in many types of food (4, 5). The objective of this work was to assess the influence of formulation variables of *L. casei* loaded whey protein-Ca-alginate microparticles on probiotic survival under different conditions, representing simulated *in vivo* environment.

MATERIALS AND METHODS

Materials

The probiotic culture, *Lactobacillus casei 01*, freeze-dried, was purchased from Chr. Hansen, Denmark. As encapsulating agent, alginate-LF 10/60 (Protanal, FMC Biopolymers, UK) was used. For the emulsion method of microencapsulation, olive oil (Sigma Aldrich, USA) containing 0.2% Tween 80 (Merck, Germany) was used. The cross-linking of the microparticles was performed by $CaCl_2$ solution. For coating of the microparticles, native solution of commercially available 100% hydrolyzed whey protein isolate (Dymatize Nutrition, USA) was used. Pepsin, bile salt and pancreatin (Sigma, USA) were used for the study of probiotic viability in simulated *in vivo* conditions.

Preparation of microparticles and determination of physicochemical properties

Emulsion technique was applied to aqueous dispersion of alginate and *L. casei* (10ml) in olive oil (40ml), in order to obtain spherical particles, which were then cross-linked in $CaCl_2$ solution. Microparticles were subsequently coated with hydrated native whey protein, collected, washed and freeze-dried (-50°C, 0.070 mbar, 24 h, Freeze-Dryer, Labconco, USA). Microparticles with d_{vs} ranging from 41.53 to 186.85μm (Mastersizer Hydro-2000S, Malvern Instruments Ltd., UK), zeta potential from -36.23 to -21.07*mV* (Zeta-sizer Nano ZS, Malvern Instruments Ltd., UK), calcium content from 2.96 to 4.72% (AES-ICP, Varian, USA) and survival rate of the probiotic between 9.30 and 10.78 $\log_{10}$cfu/g (plate-count method on MRS agar) were obtained, meeting the criterion of a minimum therapeutic dose per day i.e. 10^7–10^9 cells.

Experimental modelling

To deduce the influence of formulation variables, polynomial regression model at 2nd level was used with the experimental matrix of 11 batches. Concentration limits of three variables were alginate (1 and 4%*w/w*), whey protein (1 and 3%*w/w*) and $CaCl_2$ (1 and 5%*w/w*). The cell load in the initial suspension was ca. 10-11 $\log_{10}$cfu/g.

Viability of microencapsulated *L. casei* in simulated *in vivo* conditions

The viability of microencapsulated *L. casei* was examined in simulated gastric juice (SGJ) (0.08M HCl with 0.2% NaCl and 3g/l pepsin, pH 1.5) for 3 h, followed by simulated intestinal juice (SIJ) (0.05M KH_2PO_4 containing 0.6% bile salt and 10g/l pancreatin, pH 6.8) for 3.5 h and in colonic pH 7.4 (0.1M KH_2PO_4) up to 24 h. The viability of the cells was assessed after beads dissolution in 0.05M PBS, pH 6.5 (4).

RESULTS AND DISCUSSION

The survival of microencapsulated *L. casei* for different series in simulated GI conditions is presented in Fig.1.

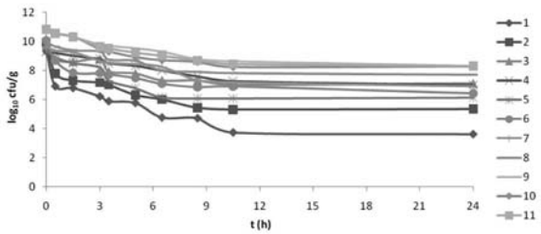

Fig.1: Viability of microencapsulated *L. casei* in simulated GI conditions

Overall effects of the formulation variables pointed to the dominant influence of the concentration of whey protein on survival rate of the microencapsulated cells of *L. casei* in all simulated *in vivo* conditions. Higher concentration of whey protein in the coating medium resulted in increased viability of *L. casei*. The lowest influence for the concentration of $CaCl_2$ was observed (Fig. 2).

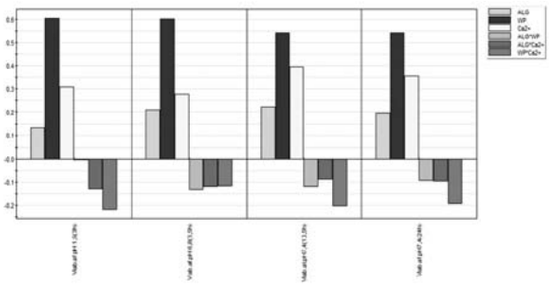

Fig. 2: Effect of the experimental variables on survival of *L. casei* loaded in whey protein-Ca-alginate microparticles.

At constant level of $CaCl_2$ at 3 %*w/v*, with alginate ranging from 2.5-4%*w/v* and whey protein ranging from 2.8-3%*w/v*, the viability of microencapsulated *L. casei* would be ≈ 9 $\log_{10}$cfu/g in SGJ and ≈ 8 $\log_{10}$cfu/g in SIJ (Fig. 3).

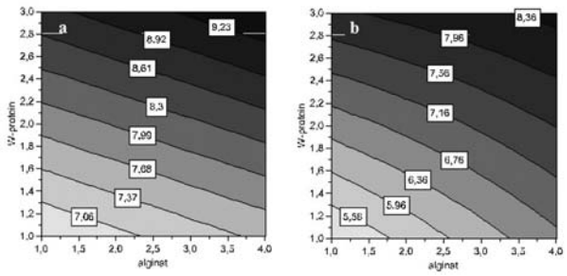

Fig. 3: Response surface plot for viability of microencapsulated *L. casei* showing the effects of alginate and whey protein for constant level of $CaCl_2$, 3%*w/v*; a) pH 1.5; b) pH 6.8

The above-mentioned results pointed to the optimal formulation for preparing *L. casei* loaded microparticles, including 2.5%*w/v* sodium alginate, 3%*w/v* whey protein and 3%*w/v* $CaCl_2$, with potential for effective colon delivery of live probiotic cells.

REFERENCES

1. Vasiljevic, T., Shah, N. P.: Probiotics-From Metchnikoff to bioactives, Int. Dairy J. 2008; 18: 714-728.
2. Mandal, S., Puniya, A. K., Singh, K.: Effect of alginate concentration on survival of microencapsulated Lactobacillus casei NCDC-298, Int. Dairy J. 2006; 16: 1190-1195
3. Krasaekoopt, W., Bhandari, B., Deeth, H.: Evaluation of encapsulation techniques of ptobiotics for yoghurt, Int. Dairy J. 2003; 13: 3-13
4. Gbassi, G. K., Vandamme, T., Ennahar, S., Marchioni, E.: Microencapsulation of Lactobacillus plantarum spp in an alginate matrix coated with whey proteins, Int. J. Food Microbiol 2009; 129: 103-105.
5. Kitabatake, N., Kinekawa, Y.I.,. Digestibility of bovine milk whey protein and β-lactoglobulin in vitro and in vivo. J. Agric. Food Chem. 1998; 46 (12): 4917–4923.

MESOPOROUS SILICON PARTICLES AS BIOCOMPATIBLE DRUG DELIVERY AGENTS

L. M. Bimbo[1*], M. Sarparanta[2], E. Mäkilä[3], T. Laaksonen[1], L. Peltonen[1], V-P Lehto[4], A. J. Airaksinen[2], J. Salonen[3], J. Hirvonen[1], H.A. Santos[1]

[1] Division of Pharmaceutical Technology, Faculty of Pharmacy, University of Helsinki, FI-00014, Finland; [2] Laboratory of Radiochemistry, Department of Chemistry, University of Helsinki, FI-00014 Finland; [3] Laboratory of Industrial Physics, Department of Physics, University of Turku, FI-20014 Finland; [3] Department of Physics and Mathematics, University of Eastern Finland, FI-70211 Kuopio, Finland

INTRODUCTION

Porous silicon (PSi) possesses several properties that make it an attractive material for controlled release and drug delivery applications (1). PSi shows distinctive advantages when compared with other materials, such as the possibility to stabilize loaded drugs or peptides within its pores and easy surface modification for imaging purposes (2). Several studies have already been published about the biological interaction of mesoporous silicon particles at a micro- and nanoscale which further support the claim of its biocompatibility (3). In the present study, the behavior of different sizes of porous silicon interacting with Caco-2 cells and RAW 264.7 macrophages was investigated regarding cell viability. Confocal microscopy images of the nanoparticle association in RAW 264.7 macrophages were made and drug permeation studies from the nanoparticles at pH 5.5 were also conducted.

MATERIALS AND METHODS

PSi nanoparticle production and characterization

Free standing multilayer PSi films were fabricated from monocrystalline <100> p^+ silicon wafers (Cemat Silicon S.A.) by electrochemical anodization in a 1:1 (v/v) hydrofluoric acid (38%) ethanol solution. The particles were subsequently loaded with griseofulvin and the drug permeation rate was assessed at pH 5.5.

Cell viability and drug permeation

The cells were maintained in DMEM and were seeded in 96-well plates and allowed to attach overnight. The medium was then aspirated and 100 µL of Psi nanoparticle suspensions with concentrations of 250, 100, 50 and 15 µg/mL were added to the wells. After 24 h, 100 µL of the CellTiter-Glo™ reagent (Promega Corporation) was added to each well according to the manufacturer's instructions. For the permeation experiments, a differentiated Caco-2 cell monolayer was grown in 12-Transwell cell culture inserts (Corning Inc. Life Sciences) for 21-28 days and transport experiments were made with griseofulvin loaded nanoparticles and bulk griseofulvin, inserted into the apical compartment.

Confocal Microscopy

Cells were seeded in 8-well chambered no. 1.0 borosilicate coverglass system plates (Lab-Tek Nunc) and allowed to attach overnight. After that, FITC labeled nanoparticles suspensions were added to the wells for a final concentration of 15 and 50 µg/mL and incubated for 3 h. The particles were then removed and the wells washed three times with HBSS. Prior to measurements, the cells were fixed with 4% paraformaldehyde (PFA, Fluka) in PBS for 20 min. Confocal pictures were taken with a Leica SP2 inverted confocal microscope, equipped with argon (488 nm) and DPSS (561 nm) lasers, and using a HCX Plan Apochromat 63/1.2 water immersion objective (Leica Microsystems).

RESULTS AND DISCUSSION

Cell viability

Cell viability of different sized Psi micro- and nanoparticles were assessed at 24h. Both Caco-2 and RAW 264.7 macrophage cells incubated with nanoparticles with a size of 164 nm showed a higher viability than the cells incubated with particles with a 1-10µm size (Fig. 1A and 1B).

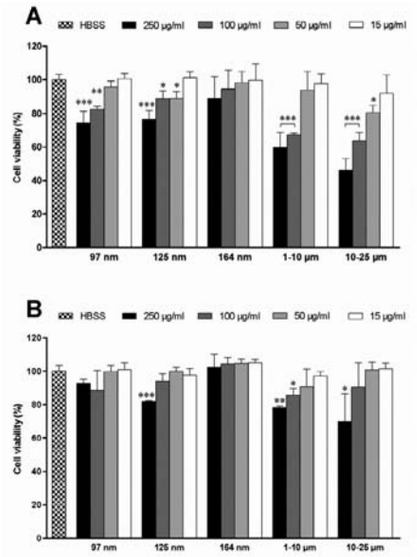

Fig. 1: Cell viability of Caco-2 (A) and RAW 264.7 macrophages when incubated with Psi particles

In order to investigate the cellular interaction of the FITC-labeled 164 nm particles with RAW 264.7 macrophages, confocal images were taken. It is visible the interaction of the nanoparticles with the cell membrane of the macrophages without the occurrence of extensive internalization by the RAW 264.7 macrophages (Fig. 2).

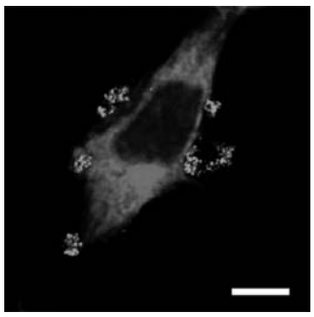

Fig. 2: Confocal microscope images of FITC-labelled nanoparticles (green) with the cellular membrane of RAW 264.7 macrophages (orange). Scale bar = 5 µm.

Drug permeation experiments

The nanoparticles loaded with griseofulvin showed a significantly faster drug release than the bulk drug over a period of 6h (Fig. 3).

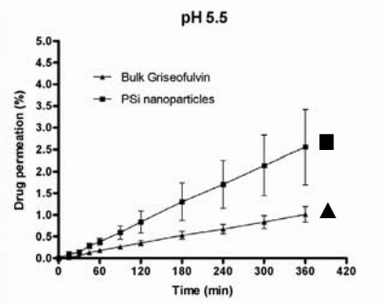

Fig. 3A: Permeation of bulk griseofulvin (▲) and griseofulvin loaded PSi nanoparticles (■) across a differentiated Caco-2 cell monolayer at apical pH of 5.5.

CONCLUSIONS

The PSi nanoparticles used in this study showed excellent compatibility, very low cell internalization and faster drug permeation profile, demonstrating great potential as drug delivery carriers.

REFERENCES

1. Salonen J, Kaukonen AM, Hirvonen J, Lehto VP. Mesoporous Silicon in Drug Delivery Applications. J. Pharm. Sci. 2008; 97: 632–653.
2. Bimbo LM, Sarparanta M, Santos HA, Airaksinen AJ, Makila E et al. Biocompatibility of thermally hydrocarbonized porous silicon nanoparticles and their biodistribution in rats. ACS Nano 2010;4(6):3023–3032.
3. Bimbo LM, Makila E, Laaksonen T,. Lehto VP, Salonen J et al. Drug permeation across intestinal epithelial cells using porous silicon nanoparticles. Biomaterials 2011; 32:2625-2633.

SELECTION OF SHELL PHASE FOR THE PREPARATION OF MICROCAPSULES WITH LIQUID SELF-MICROEMULSIFYING CORE

M. Homar*, J. Kerč

Lek Pharmaceuticals,d.d., Sandoz Development Center Slovenia, Verovškova 57, 1526 Ljubljana, Slovenia

INTRODUCTION

Microcapsules are micrometer-sized particles (20-2000 µm), outwardly similar to microspheres, but with distinguishable core and shell. The vibrating nozzle method is often used for preparation of microspheres, since it allows an efficient production of uniform sized beads with mean diameters in the range from 200 to 2000 µm.

Self-microemulsifying systems (SMES) are system consisting of lipophylic component(s) and surfactant(s) which spontaneously form microemulsions when in contact with aqueous media. They offer several advantages for the formulation of poorly soluble drugs, such as enhanced solubility, dissolution rate, permeability and consequently bioavailability. The application of SMES is currently limited to liquid formulations and soft gelatin capsules, therefore incorporation of these systems into a solid dosage form would offer an important advantage from the view of patient compliance as well as dosage form design.

The aim of our work was to evaluate and select the most appropriate alginate composition of the shell phase for preparation of microcapsules with liquid SMES core.

MATERIALS AND METHODS

Materials

Self-microemulsifying system was prepared using Miglyol 812® (Condea Chemie GmbH, Germany) as lipophilic phase, Labrasol® as emulsifier and Plurol oleique® (Gattefosse, France) as co-emulsifier. Sodium alginate of four different viscosities was used: Type 1: ≥ 2000 mPa*s, 2 % solution at 25°C; type 2: 250 mPa*s, 2 % solution at 25°C (Type 2) were from Sigma (Germany) while type 3: 70-150 mPa*s, 1 % solution at 25°C and type 4: 20-70 mPa*s, 1 % solution at 25°C were from FMC (Norway). Lactose was purchased from Fonterra excipients (Germany). All other chemicals were of laboratory grade.

Methods

Self-microemulsifying systems were prepared by mixing the excipients and saturated by $CaCl_2$ as described elsewhere (1).

An Inotech IE-50 R encapsulator (Inotech, Switzerland) equipped with a 500 µm / 750 µm concentric nozzle, a 50 ml syringe and an air pressure solution delivery system was used to prepare microcapsules. Water solutions of alginates with different concentrations was used as the shell forming phase. Lactose was added in some cases to further reduce core leaking as described earlier (2). Flow rates of both phases were adjusted for each alginate solution. Microcapsules were incubated in 0.5 M $CaCl_2$ solution for 5 minutes and dried on trays at room conditions.

The suitability of the process was assessed according to the physical appearance of the microcapsules and the turbidity of the incubation media (higher turbidity indicating higher core leaking).

RESULTS AND DISCUSSION

Composition of shell phase was varied in terms of alginate type and concentration to prepare microcapsules with suitable physical properties and to reduce the core leakage during preparation. Lactose was added in some cases to further reduce core leaking. Viscosity of all tested alginate solutions was measured at 23 °C by Vibro SV-10 viscometer (AND, Japan) (Table 1).

Table 1: Composition and viscosity of shell phase used for the preparation of microcapsules.

Sample	Alginate type	Alginate / lactose concentration in shell phase (m/m %)	Viscosity (mPa*s)
1	Type 1	2,0 / 0,0	601,95
2	Type 2	3,0 / 0,0	406,67
3	Type 2	2,5 / 0,0	249,32
4	Type 2	2,5 / 10,0	277,12
5	Type 2	2,0 / 0,0	134,36
6	Type 2	2,0 / 10,0	166,33
7	Type 3	2,5 / 0,0	485,90
8	Type 4	3,0 / 0,0	380,88
9	Type 4	2,5 / 0,0	227,10
10	Type 4	2,5 / 10,0	280,10
11	Type 4	2,0 / 0,0	128,54

Preparation of samples with alginate concentration of 2,0 and 2,5 % for type 1 and 3, respectively, was problematic due to the high viscosities of the solutions, which prevented continuous flow of the shell phase and caused nozzle blockage (Table 2). Viscosity of the solutions can be decreased to processable levels by reducing the concentration of the alginate, but unfortunately the porosity of the shell and core leakage are consequently increased and ultimately the shell fails to solidify. High viscosity grades of alginate were therefore proved unsuitable for the preparation of microcapsules with SMES core.

Higher concentrations (3%) of alginate type 2 and 4 exhibited high viscosity and posed similar processability problems as the higher viscosity alginate grades. On the other hand, 2% concentration of both low viscosity grades of alginate failed to form a solid shell, probably due to too low alginate concentration. The only concentration of alginate that enabled the preparation of suitable microcapsules was 2,5% for both low viscosity alginate types. As expected, the addition of lactose reduced the core leakage and did not have a significant impact on the processability, as can be seen from Table 2.

Table 2: Physical appearance, processability and turbidity of the incubation liquids for tested shell phases listed in table 1.

Sample	Physical appearance / processing remarks	Turbidity
1	No capsules / viscosity too high, nozzle blockage	High
2	No capsules / viscosity too high, nozzle blockage	High
3	Capsules formed / no problems	Medium
4	Capsules formed / no problems	Low
5	No capsules / shell not formed	High
6	No capsules / shell not formed	High
7	No capsules / viscosity too high, nozzle blockage	High
8	No capsules / viscosity too high, nozzle blockage	High
9	Capsules formed / no problems	Medium
10	Capsules formed / no problems	Low
11	No capsules / shell not formed	High

CONCLUSIONS

Alginate concentration in the shell forming phase should be as high as possible to enable the formation of a solid shell. However, this concentration is limited by the increasing viscosity of the solution, since higher viscosities cause inconsistent flow rates and nozzle blockage. The optimal viscosity of the alginate shell phase is in the range of 200-300 mPa*s, which translates to the maximum concentration of 2,5 %. The addition of lactose in the shell reduces core leakage during preparation.

REFERENCES

1. Homar M, Dreu R, Kerč J, Gašperlin M.. Preparation and evaluation of celecoxib-loaded microcapsules with self-microemulsifying core. J Microencap. 2009; 26: 479-484.
2. Homar M, Šuligoj D, Gašperlin M. Preparation of microcapsules with self-microemulsifying core by a vibrating nozzle method. J Microencap. 2007; 24: 72-81.

STABILITY STUDIES OF ITRACONAZOLE-LOADED MESOPOROUS SILICON AND NON-ORDERED MESOPOROUS SILICA MICROPARTICLES

P. Kinnari[1*], E. Mäkilä[2], T. Heikkilä[2], J. Salonen[2], J. Hirvonen[1], H.A. Santos[2]

[1] Division of Pharmaceutical Technology, Faculty of Pharmacy, University of Helsinki, FI-00014, Finland; [2] Laboratory of Industrial Physics, Department of Physics and Astronomy, University of Turku, FI-20014, Finland

INTRODUCTION

In the last decades mesoporous materials have impacted tremendously the research on biomedical applications, in particular in the field of oral drug delivery (1,2).

In spite of the extensive research on porous materials and their potential applications in the drug delivery field, there is still lack of data for direct comparison between porous silicon (PSi) and non-ordered mesoporous silica materials. Several properties of the mesoporous materials may affect the loading degree and release rate of the drug, such as the surface area, pore size, total pore volume, pore geometry and surface chemistry (3–5).

In this study we investigated the dissolution behaviour of itraconazole (ITZ)-loaded mesoporous materials before and after 3 months of storage. For this purposes, thermally oxidized-PSi (TOPSi), thermally carbonized-PSi (TCPSi), and non-ordered mesoporous silica (Syloid AL-1 and 244) materials were tested and compared.

MATERIALS AND METHODS

Materials

Syloid 244 and Syloid AL-1 microparticles were kindly provided by Grace Davison (Grace GmbH, Germany). The PSi microparticles were fabricated as described in detail elsewhere (1,3–5). ITZ was used as received (Apotecnia, Spain).

ITZ loading and storage

The drug loading was performed by an immersion method in dichloromethane. For stability studies the ITZ-loaded particles were stored for 3 months under stressed conditions (40 °C and 70% RH).

Characterization of the microparticles

DSC (Mettler Toledo, Columbus, OH) with a heating range of 25-220 ºC was used to study the state of the loaded drug (crystalline or amorphous).

Drug dissolution and release

The ITZ release from the microparticles and dissolution of pure ITZ were carried out with the Ph. Eur. paddle apparatus method (Sotax AT7, Switzerland) at 250 rpm with 500 ml of pH 1.2 medium at 37 °C. The total amount of ITZ loaded and/or released was quantified by HPLC (Agilent 1100, Germany) using a Gemini C18 column, a mobile phase of acetonitrile and 0.1% trifluoroacetic acid pH 2.0 (55:45 %, v/v) with a flow rate of 1 ml/min, and 20 µl injection volumes. The loading degrees, for the calculation of percentage-released drug amounts, were determined by extracting the particles in methanol and quantifying the drug concentrations with HPLC.

RESULTS AND DISCUSSION

Characterization of the mesoporous materials

Fig 1 shows an example of the DSC thermograms of the PSi microparticles studied. The ITZ melting point was at 168 °C. No ITZ melting point was detected for the loaded mesoporous particles, which indicates that the drug loaded was in an amorphous form after the loading.

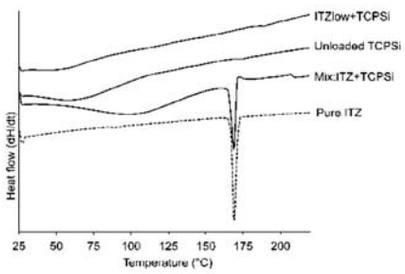

Fig. 1: DSC thermograms of loaded (ITZlow+TCPSi) and unloaded TCPSi particles. DSC thermograms of pure ITZ and physical mixtures of ITZ and TCPSi particles (Mix:ITZ+TCPSi) are also presented as reference. Endothermic signals are pointed downwards.

Drug release studies

The ITZ release from all the loaded mesoporous microparticles was faster than the dissolution of pure ITZ at pH 1.2 (Fig 2a). This is explained by the amorphous state of ITZ inside the pores of the particles after loading. An amorphous drug has higher dissolution rate compared to the relative crystalline drug.

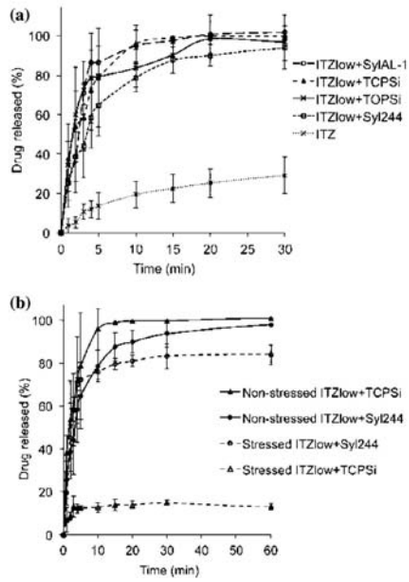

Fig. 2: Comparison of the release profiles of ITZ from silica and silicon microparticles, loaded at low drug concentrations (ITZlow), at pH 1.2 and 37 °C before (a) and after (b) storage at 40 °C and 70% RH. The dissolution curves of bulk ITZ are also presented as reference.

After 3 months of storage under stressed conditions only a slight decrease in the amount of drug released from the Syloids compared to the non-stressed samples was observed (Fig 2b). In contrast, a significant decrease in the release profiles of ITZ was observed from the stressed PSi particles when compared with the non-stressed samples (Fig 2b). This is explained due to the almost complete chemical degradation of ITZ in the PSi particles after storage (Fig 3).

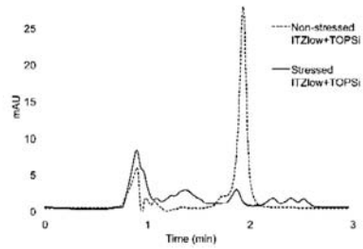

Fig. 3: HPLC chromatograms of stressed (3 months, 40 °C and 70% RH) ITZlow+TOPSi and non-stressed ITZlow+TOPSi particles.

CONCLUSIONS

The release of ITZ at pH 1.2 from TCPSi and Syloid AL-1 microparticles was faster than from TOPSi and Syloid 244 particles due to the smaller pore size of Syloid AL-1 compared to Syloid 244, and of the more favorable surface chemistry of TCPSi compared to TOPSi. Interestingly, the drug release kinetics was not affected by the particle size. Large amounts of silanol groups on the particle's surface and small particle sizes revealed to be advantageous properties for the efficient loading of ITZ. Storage of ITZ-loaded PSi particles after 3 months revealed to be inefficient to protect ITZ from chemical degradation.

REFERENCES

1. Salonen J, Kaukonen AM, Hirvonen J, Lehto V-P. Mesoporous silicon in drug delivery applications. J. Pharm. Sci. 2008; 97: 632–653.
2. Vallet-Regí M, Balas F, Arcos D. Mesoporous Materials for Drug Delivery. Angew. Chem. Int. Ed. 2007; 46: 7548–7558.
3. Heikkilä T, Salonen J, Tuura J, Kumar N, Salmi T et al. Evaluation of mesoporous TCPSi, MCM-41, SBA-15, and TUD-1 materials as API carriers for oral drug delivery. Drug Delivery 2007; 14: 337–347.

4. Limnell T, Riikonen J, Salonen J, Kaukonen AM, Laitinen L et al. Surface chemistry and pore size affect carrier properties of mesoporous silicon microparticles. Int. J. Pharm. 2007; 343: 141–147.
5. Limnell T, Riikonen J, Salonen J, Kaukonen AM, Laitinen L et al. Surface chemistry and pore size affect carrier properties of mesoporous silicon microparticles. Int. J. Pharm. 2007; 343: 141–147.

COMPARISON OF IBUPROFEN-LOADED ALGINATE MICROSPHERES FORMULATED USING DIFFERENT INCORPORATING METHODS

E. Vranić[1], D. Grizić[1], S. Srčič[2*], D. Planinšek[3], O. Planinšek[2]

[1] Department of Pharmaceutical Technology, Faculty of Pharmacy, University of Sarajevo, Čekaluša 90, 71 000 Sarajevo, Bosnia and Herzegovina; [2] Department of Pharmaceutical Technology, Faculty of Pharmacy, University of Ljubljana, Aškerčeva 7, SI-1 000 Ljubljana, Slovenia; [3] Agency for medicinal products and medical devices, Ptujska 21, SI-1000 Ljubljana, Slovenia

INTRODUCTION

Microencapsulation has become a common technique for the production of controlled release dosage forms. Many results have been reported, concerning the use of alginate beads as controlled release drug formulations. Alginate has a unique gel-forming property in the presence of multivalent cations (1). One approach for controlled release formulation is the production of polymeric gel beads that serve as the solid substrate on which the drug is coated or encapsulated in the core of the beads. Beads can provide controlled release properties and uniform distribution of drug. Furthermore, bioavailability of drugs formulated in beads has been enhanced. Ibuprofen is an excellent analgesic and antipyretic, non-steroidal anti-inflammatory agent with a high therapeutic index. Formulation of ibuprofen in beads could reduce its gastric ulcerogenicity (2). Anti-solvent crystallization method is a technique of forming dispersion, used for the incorporation of poorly soluble substances in polymeric hydrogel (3). One of the important data is that the alginate microspheres after drying, can re-hydrate (4). Re-hydration depends on the type of medium used for the process (5). The aim of our study was to examine the influence of the dispersion method and swelling profile of microspheres in different media. FTIR spectra analyses of sodium and calcium alginate have been provided.

MATERIALS AND METHODS

Materials

Ibuprofen (B.P., BASF Chemtrade GmbH, Burgbernheim, Germany) was a gift from Belupo (Koprivnica, Croatia). Sodium alginate (3 Pas, 2 %), Calcium chloride dihydrate p.a., and Ethanol were purchased from Semikem (Sarajevo, B&H). Potassium dihydrogen phosphate p.a., and Sodium hydroxide p.a. were purchased from Merck (Darmstadt, Germany). Potassium bromide FT-IR grade >99% was obtained from Sigma-Aldrich chemie GmbH (Göttingen, Germany). All other reagents used were of analytical grade.

Preparation of microspheres

Two formulations (named F_1 and F_2) containing fixed quantity of ibuprofen (2%), sodium alginate (1%), calcium chloride (2%), were prepared. Curing time for both formulations was 30 minutes. F_1 formulation was prepared as follows: ibuprofen was added in previously prepared sodium alginate solution and dispersed by magnetic stirrer. Each dispersion was transferred into injection syringe containing needle (21 G) and by dropping (velocity 10 ml/min) added into calcium chloride solution. After 30 minutes (curing time) the microspheres were filtered using funnel with Whatman #4 qualitative filter paper, washed out twice with distilled water and dried at room temperature for 24h. F_2 formulation was prepared by anti-solvent crystallization technique under following conditions: ibuprofen was dissolved in ethanol (6% solution obtained). This solution was added dropwise in a continuously stirred sodium alginate solution (2%). As a result of this procedure, a white suspension was formed containing small particles of ibuprofen. Further steps in microsphere preparation were as it was already described for F_1 formulation.

Swelling rate profile

The swelling behavior of the microspheres was studied at room temperature using a vernier, after exposure to: phosphate buffer (pH 7.4) for 30 minutes and distilled water for 90 minutes. The swelling rate was calculated using the following equation (Eq.1):

$$SR = \frac{R_e - R_o}{R_o} \times 100 \qquad \text{(Eq.1):}$$

SR - swelling rate
Re - size of miscrosphere at equilibrium swelling degree
R_0 - size of miscrosphere before swelling

FTIR analysis

The FTIR spectra were recorded over the wavelength range of 4500–146 cm^{-1} using FTIR (FTIR-8400S spectrometer (Shimadzu, Kyoto, Japan). Samples were prepared in KBr disks and analyzed. The resolution was 4 cm^{-1}.

RESULTS AND DISCUSSION

Swelling rate profile

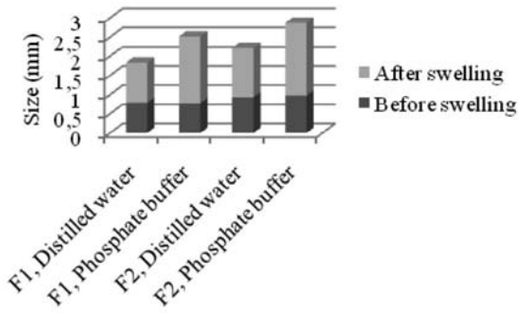

Fig. 1: Swelling profiles of F1 and F2 microspheres in distilled water and phosphate buffer

As shown in Fig. 1, differences in swelling profiles in distilled water and in phosphate buffer were observed. Swelling rates for F_1 and F_2 microspheres were as follows:

- 31.14%, in water and 124.22% in phosphate buffer (F_1 microspheres),
- 37.83 %, in water and 94.26 % in phosphate buffer (F_2 microspheres), respectively.

FTIR analysis

Fig. 2 shows the IR spectra of sodium and calcium alginate, with major peaks at 3500 cm^{-1},1600 cm^{-1} and 1035 cm^{-1}. At 1425 cm^{-1}, the absence of a peak was observed at the calcium alginate spectrum, as a result of calcium (Ca^{2+}) to carboxyl group complexation.

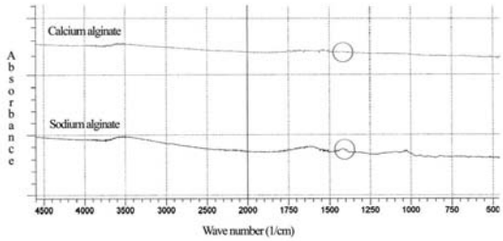

Fig. 2: Sodium and calcium alginate spectra

CONCLUSION

According to the results obtained, it could be concluded that F_1 microspheres expressed better swelling ability in phosphate buffer, while F_2 microspheres expressed better swelling ability in distilled water. Additionally, the FTIR analysis revealed the binding between calcium ions and the anionic residues of alginate.

REFERENCES

1. Gomez G., Malinconico M., Laurienzo P. Marine derived polysaccharides for biomedical applications: Chemical modification approaches. Molecules, 2008; 13: 2069-2106
2. Khazaeli P., Pardakhty A., Hassanzadeh F. Formulation of ibuprofen beads by ionotropic gelation. Iranian J. Pharm. Res., 2008; 7 (3): 163-170
3. Grosso M, Galan O, Baratti R, Romagnoli J.A. A Stochastic formulation for the description of the crystal size distribution in antisolvent crystallization processes. AIChE J., 2010: 56(8), 2077-2087
4. Vreeker R., Li L., Fang Y., Appelqvist I., Mendes E. Drying and rehydratation of calcium alginate gels. Food Biophysics, 2008; 3: 361-369
5. Torres L., Velasquez A., Brito-Arias M. Ca-alginate spheres behavior in presence of some solvents and water-solvent mixtures. Adv. Biosci. Biotechnol., 2011; 2: 8-12

FORMULATION STUDIES OF SYLIBUM MARIANUM SEED EXTRACS

Z. Ujhelyi[1*], F. Fenyvesi[1], T. Kiss[1], P. Fehér[1], M. Pétervári[1], G. Tajti[1], S. Kéki[2], M. Zsuga[2], M. Vecsernyés[1], I. Bácskay[1]

[1] University of Debrecen, Department of Pharmaceutical Technology, PO Box 78, H-4010 Debrecen, Hungary; [2] University of Debrecen, Department of Applied Chemistry, Egyetem tér 1, H-4032 Debrecen, Hungary

INTRODUCTION

Sylimarin, the active substance of Sylibum Marianum has a well-known hepatoprotective effect (1). The result of extraction process of the Sylibum Marianum seed were 25% oil and a dry, water insoluble sylimarin extract. The aim of the study was to prepare sylimarin formulations with high bioavailability for the treatment of acut hepatotoxicity. Water miscible self micro emulsifying drug delivery systems (SMEDDS) (2) of the oil and water soluble formulations of sylimarin were produced which are suitable for further *in vitro* and *in vivo* examinations.

MATERIALS AND METHODS

Materials

Sylibum Marianum seed oil and sylimarin were originated from Sylibum Marianum seeds. Hydroxylpropyl-β-cyclodextrin (HPBCD), randomly methylated β-cyclodextrin (RAMEB) and 2,6-di-O-methyl β-cyclodextrin (DIMEB) were the product of Cyclolab Ltd. (Hungary), Labrasol® was a kind gift of Gattefosse (France), while all other reagents purchased from Sigma.

Methods

Sylibum Marianum seed oil was incorporated into SMEDDS, using Labrasol. Cyclodextrin-sylimarin complexes were produced by kneading method (3). The weight ratio of cylodextrins and sylimarin was 10:1 in the mixtures. The UV-spectra of the solutions were recorded by Shimadzu UV-1601 spectrofotometer.

RESULTS AND DISCUSSION

To increase the bioavailability of Sylibum Marianum seed oil we produced different SMEEDS compositions. The emulsifying agent (Labrasol) content and the oil content of SMEEDS varied between 60-80% and 10-30% respectively. Each system remained stable in 10, 100 and 1000 times dilutions in water. The diameter of the dispersed oil phase was in micrometer range as confirmed by microscopic investigation.

Excess amount of cyclodextrin-sylimarin mixtures were dissolved in water until equilibrium is reached between the unsolved and dissolved phases and the UV-spectra of the filtered solutions were recorded. All of the cyclodextrins (HPBCD, RAMEB and DIMEB) were able to solubilise sylimarin, but DIMEB had the greatest ability for the complexation (Fig. 1.)

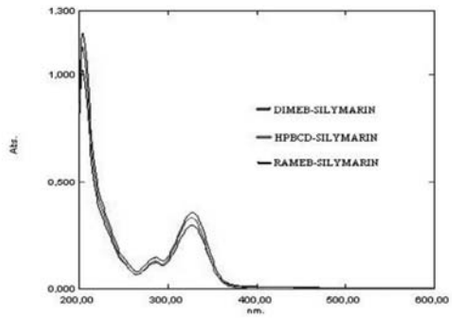

Fig. 1: UV-spectra of different cyclodextrin-sylimarin complexes.

CONCLUSIONS

Stable Sylibum Marianum seed oil SMEDDS; HPBCD, RAMEB and DIMEB water soluble sylimarin complexes were produced. The products are suitable for further safety and effectiveness examinations.

ACKNOWLEDGEMENTS

This work was financially supported by the Hungary-Romania Cross-Border Co-operation Programme 2007-2013 (HURO/0901/058/2.2.2.).

REFERENCES

1. Pradhan S.C, Girish C. Hepatoprotective herbal drug, silymarin from experimental pharmacology to clinical medicine. Indian J. Med. Res. 2006; 124: 491-504.
2. Pouton C.W. Lipid formulations for oral administration of drugs: non.emulsifying, self-emulsifying, and self-micro emulsifying drug delivery systems. Eur. J. Pharm. Sci. 2000; Suppl. 2: 93-98.
3. Ascenso A, Guedes R, Bernardino R, et al. Complexation and full characterization of the tretionin and dimethyl-β-cyclodextrin complex. AAPS Pharm. Sci. Tech. 2011; DOI:10.1208/s12249-011-9612-3.

FORMULATION AND CHARACTERIZATION OF CHITOSAN/HEPARIN NANOPARTICLES

P. Ahlin Grabnar*, J. Kristl

University of Ljubljana, Faculty of Pharmacy, Aškerčeva 7, 1000 Ljubljana, Slovenia

INTRODUCTION

Polyelectrolyte complexes (PECs), which represent new possibilities in drug formulation, are the association complexes formed between oppositely charged substances (polymer–polymer, polymer –drug and polymer–drug–polymer). These are formed due to electrostatic interaction between oppositely charged polyions. Many different polyanions, such as alginate (1), pectin (2), carrageenan, dextran sulphate, carboxymethyl cellulose, xanthan gum, chondroitin sulphate, enoxaparin (3), have been used to form polyelectrolyte complexes with chitosan and appeared promising as an oral drug delivery system.

Heparins are the standards of anticoagulants used in the prophylaxis and the treatment of deep vein trombosis and pulmunary embolism. The prophylactic therapy is recommended for at least 10 to 14 days after surgery and represents a huge pharmaceutical market worldwide. One of the drawbacks of heparin is a lack of oral absorption, presumably because of its negative charge and/or molecular size. Heparin is a polyanionic mucopoly-saccharide with a mean molecular weight of 15 kDa. Since it is highly negatively charged molecule, it is expected to be able to interact with chitosan very efficiently. Chitosan is a polycationic, nontoxic, mucoadhesive polysaccharide, which has been extensively exploited as promising oral drug delivery vehicles to increase the transport of drugs across intestinal epithelium.

The object of this study was to prepare nanoparticles (NP) composed of chitosan and heparin and examined their physicochemical characteristics. Such NP could enhance the paracellular permeability of heparin.

MATERIALS AND METHODS

Materials

Chitosan hydrochloride (Protasan UP CL 212; MW 270000, degree of deacetylation 70%) was obtained from Pronova (Norway) and heparin (50 mg/ml) from Krka (Novo mesto, Slovenia).

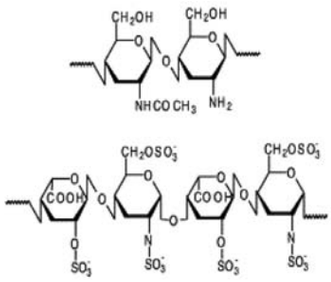

Fig. 1: Chemical structures of chitosan and heparin.

Preparation of chitosan/heparin NP

The NP were prepared by an ionic gelation method with magnetic stirring at room temperature. In brief, aqueous heparin (1.0 mg/mL, 4 mL, pH 7.4) was added with a pipette tip into aqueous chitosan at various concentrations (0.2, 0.6, 0.9 or 1.2 mg/mL, 20 mL). Dispersions were magnetically stirred for an hour.

Size and zeta potential measurements

The mean particle size and polydispersity index were estimated by a photon correlation spectroscopy and zeta potential by laser Doppler electrophoresis using a Zetasizer Nano ZS (Malvern, UK). The autotitration of chitosan solution (0.6 mg/ml, 10 ml) with heparin solution (1 mg/ml) was performed by Malvern Multi Purpose Titrator (MPT 2). The option of additive linear titration was used.

RESULTS AND DISCUSSION

NP were formed by electrostatic interaction between the chitosan and heparin. The final pH of dispersion was 5.5, which is in the pKa interval of the two polymers (pKa (heparin) = 3.1 and pKa (chitosan) = 6.5). At this pH chitosan is positively charged due to the protonation of the amino groups and heparin is negatively charged. Dynamic light scattering analysis was performed to examine the effect of various weight ratios between heparin and chitosan on the size and zeta potential of NP.

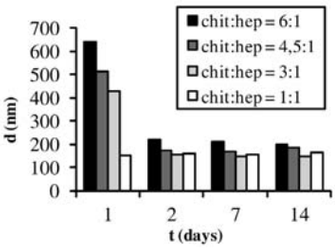

Fig. 1: The mean diameter of NP with different chitosan:heparin ratio determined after preparation, 2, 7 and 14 days.

The mean particle size of various NP with different chitosan:heparin ratio were determined after preparation, after 2, 7 and 14 days and are presented in Fig. 1. After preparation the size of NP was in the range 150-650 nm. It can be seen that the mean particle size increase with increasing chitosan concentration. After 2 days the NP size decreased (except at chitosan/heparin=1:1) and was in the range 150-210 nm. It is assumed that it takes time for chitosan and heparin chains to entangle and new interactions between amino groups of chitosan and negatively charged groups of heparin are formed. NP dispersions were physically stable at least 14 days.

Zeta potentials of NP depend on the weight ratio between chitosan and heparin. The autotitration of chitosan solution with heparin solution (Fig. 2) has shown that the zeta potential of particles was inverted from positive to negative values at heparin:chitosan ratio of 0.52. This indicates that there is a balance between positive and negative charges and therefore the physical stability of dispersion is low. NP which are formed at heparin:chitosan ratio < 0.5 have positive charge and NP which are formed at heparin:chitosan ratio > 0.6 have negative charge.

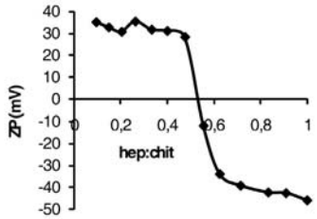

Fig. 2: Zeta potential of NP with different heparin:chitosan weight ratios.

CONCLUSIONS

A novel nanoparticle system composed of chitosan and heparin was successfully prepared using a simple ionic gelation method under mild aqueous-based conditions. The smallest NP diameter was achieved at mass ratio chitosan:heparin 1:1.

REFERENCES

1. Sarmento B, Ribeiro A, Veiga F, Sampaio P, Neufeld R, Ferreira D. Alginate/chitosan nanoparticles are effective for oral insulin delivery. Pharm Res. 2007; 24: 2198-206
2. Ahlin Grabnar P, Kristl J, Physicochemical characterization of protein-loaded pectin-chitosan nanoparticles prepared by polyelectrolyte complexation. Pharmazie. 2010; 65: 851-2.
3. Sun W, Mao S, Mei D, Kissel T, Self-assembled polyelectrolyte nanocomplexes between chitosan derivatives and enoxaparin. Eur J Pharm Biopharm. 2008, 69: 417-25.

EFFECT OF THE INCLUSION OF CHITOSAN INTO POLY-EPSILON-CAPROLACTONE PARTICLES ON ADSORPTION EFFICACY OF 4 DIFFERENT MODEL ANTIGENS

S. Jesus[1,2*], G. Borchard[3], O. Borges[1,2]

[1] Center for Neuroscience and Cell Biology, University of Coimbra, 3000 Coimbra, Portugal; [2] Faculty of Pharmacy, University of Coimbra, Pólo das Ciências da Saúde Azinhaga de Santa Comba 3000-548, Coimbra, Portugal; [3] School of Pharmaceutical Sciences, University of Geneva, University of Lausanne, Quai Ernest Ansermet 30, 1211 Geneva, Switzerland

INTRODUCTION

The design of particulate delivery systems for mucosal vaccination has achieved an increase interest in the last years (1). Among several antigen loading procedures, the adsorption on particle surface has been appointed as one of the most suitable for vaccines. The main reason is because is an easy and mild process, normally achieved by the simple incubation of the antigens with a suspension of the particles. Moreover, a second hypothetical advantage of the adsorption process of the antigens is that the particles could present multiple copies of the antigen on its surface, an effect which has been shown to be optimal for B-cell activation (2).

Therefore in order to have a better understand of the effect of the inclusion of a hydrophilic polymer into poly-epsilon-caprolactone particles, adsorption studies with 4 different model antigens were performed and presented.

MATERIALS AND METHODS

Materials

Chitosan was purchased from Primex BioChemicals AS (ChitoClearTM, Avaldsnes, Norway). Polycaprolactone (PCL) was purchased from Sigma-Aldrich. All other chemicals and reagents were analytical grade.

Production of chitosan-PCL (CHI-PCL) and PCL nanoparticles

To prepare CHI-PCL nanoparticles (NP), an acetonic solution of PCL was added dropwise to an acetic acid solution containing chitosan and Tween 80, during high speed homogenization. After a brief maturation process under magnetic stirring, the final nanoparticle suspension was obtained upon evaporation of acetone under a nitrogen flux. For PCL NP, the same procedure was accomplished, excluding chitosan from the solutions. Nanoparticles were isolated by ultracentrifugation at 16000 g during 75 min at 20 ºC, with a glycerol bed to prevent particle aggregation.

Size, Zeta Potential

Nanoparticles size and zeta potential were measured on Beckman Coulter - Delsa™ Nano C, Particle Size Analyzer.

Loading efficacy

Nanoparticles were ressuspended on phosphate buffer (PB) pH 7.4 to the following average concentrations: 7.1 x 10^{-4} g/mL (CHI-PCL NP) and 6.5 x 10^{-4} g/mL (PCL NP). Then, incubation of NP suspensions with different proteins was accessed by mixing 300 µL of the suspension with a protein solution, so that the final protein concentration was 500 µg/mL. Several times of incubation were tested (5, 10, 20, 30, 60, 120 and 180 minutes), followed by a centrifugation at 16000 g to collect the supernatants and non-adsorbed protein was measured using the BCA protein assay.

MTT cell viability assay

Using sterile 96-well tissue culture plates,
100 µL of splenocyte suspension from three C57BL/6 mice were plated individually, in quadruplicate along with 100 µL of a nanoparticle suspension and incubated (37 ºC, 95 % relative humidity, 5 % CO2) for 24 h. Several concentrations were used for the CHI-PCL and PCL NP. Cytotoxicity was evaluated by measuring the reduction of MTT by the mitochondrial dehydrogenase of living cells as an indication of cell viability.

RESULTS AND DISCUSSION

Nanoparticle characterization

Medium of size of CHI-PCL nanoparticles measured after ressuspension in PB pH 7.42 was 416.1 nm, which was higher than the PCL nanoparticles (146.7 nm). Zeta potential was positive on the CHI-PCL NP and negative on the PCL NP, supporting the fact that chitosan is coating PCL NP.

Loading efficacy (%LE)

Proteins were efficiently adsorbed on CHI-PCL NP surface (Fig 1) and in a greater extent than on the PCL NP (Fig 2). These results were more evident for ovalbumin, α-casein, lactalbumin and albumin (BSA) as they have a low isoelectric point (IP) promoting the electrostatic interaction of the proteins to the positively charged CHI-PCL NP. % LE of mioglobin on both NP was found to be similar, as mioglobin IP (7.2) on PB favours its neutrality.

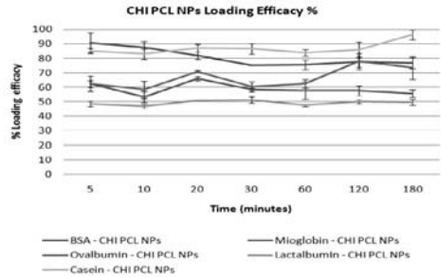

Fig. 1: Loading efficacy of different proteins on CHI-PCL NPs.

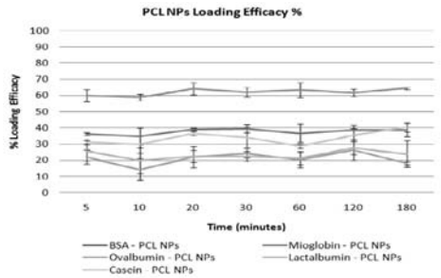

Fig. 2: Loading efficacy of different proteins on PCL NPs.

Cytotoxicity

No significant cytotoxicity was found on the tested concentrations of CHI-PCL NP and also of PCL NP. Nevertheless, particularly PCL NP were found to decrease viability rates with concentrations higher than 60 µg/mL.

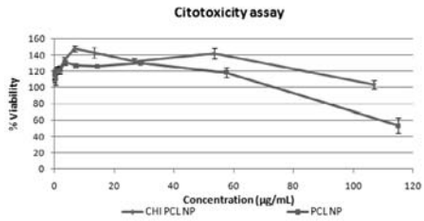

Fig. 3: Cytotoxicity of CHI-PCL and PCL NP on spleen cells.

CONCLUSIONS

Preliminary results obtained so far, showed attractive characteristics on both systems and some important differences on CHI-PCL NP compared to PCL NP, namely the increased adsorption ability. Further studies will be performed to fully characterize this system as a promissory mucosal antigen delivery system.

ACKNOWLEDGEMENTS

This work was supported by the FCT project PTDC/SAU-FAR/115044/ 2009.

REFERENCES

1. J. Holmgren, C. Czerkinsky, K. Eriksson, A. Mharandi, Mucosal immunisation and adjuvants: a brief overview of recent advances and challenges, Vaccine 21 (Supp l 2) (20 03) S 89–S95.
2. Bachmann MF, Rohrer UH, Kundig TM, Burki K, Hengartner H, Zinkernagel RM. The influence of antigen organization on B cell responsiveness. Science 1993;262 (5138):1448–51

NANOPARTICULATE CARRIERS FOR DRUG DELIVERY TO THE BRAIN

É. Molnár, C.F. Lien, D.C. Górecki, J. Tsibouklis, E. Barbu*

School of Pharmacy and Biomedical Sciences, University of Portsmouth, White Swan Rd., PO1 2DT, Portsmouth, UK

INTRODUCTION

The blood-brain barrier (BBB) is a regulated interface between the peripheral circulation and the central nervous system that plays an important role in the maintenance of normal brain functions (1); however, while it protects the brain, the BBB impedes at the same time the access of a large number of CNS-active therapeutic agents (2). Here we present results of our investigations into nanoparticulate delivery systems that combine the BBB-penetration properties of amphiphilic short chain alkylglycerols (shown to influence the arrangement of the membrane lipids of the BBB (3)) with the transport capabilities of biocompatible and biodegradable carriers based on materials of natural origin such as chitosan.

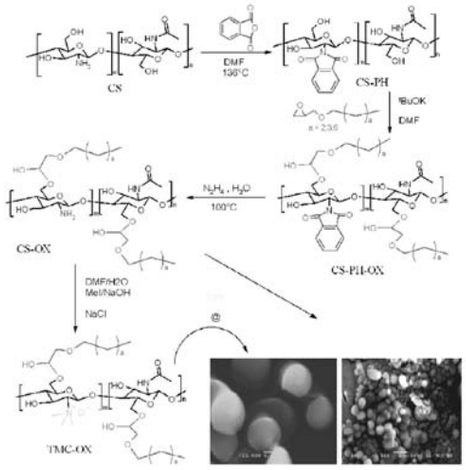

Fig. 1: Synthetic steps for the preparation of alkylglyceryl-modified chitosans and SEM images (7,500×; 33,000×) of TPP-formulated NPs.

MATERIALS AND METHODS

The selective attachment of alkylglyceryl chains was achieved by *N*-phthaloylation followed by treatment with oxirane and subsequent deprotection with hydrazine (Fig.1). Further reaction with CH_3I afforded quaternised alkylglyceryl-modified chitosans. Nanoparticles (NP) were prepared by ionotropic gelation using pentasodium tripolyphosphate (TPP) and were loaded with markers such as Evans Blue (EB). NP characterisation was performed by SEM and dynamic light scattering. The interactions between NPs and mouse brain capillary endothelial cells (bEnd3) were investigated using confocal microscopy; the cytotoxicity of the nanoparticles was evaluated using MTT assays.

RESULTS AND DISCUSSION

Materials with different degrees of substitution (3 - 200 %) were obtained with good overall yields (67 – 82 %) by varying the oxirane/chitosan ratio. Studies of the influence of pH upon the NP size and zeta potential revealed that partial quaternisation improves stability (Fig. 2).

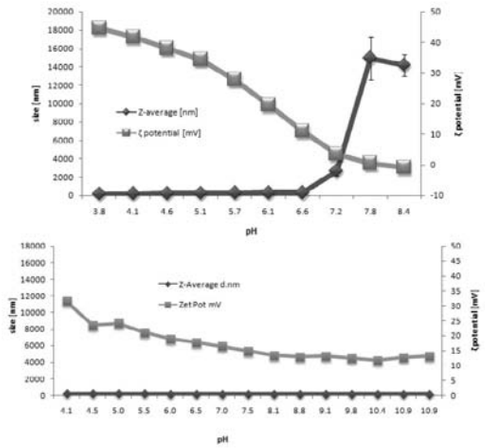

Fig. 2: The influence of pH on the hydrodynamic volume and zeta potential of nanoparticles prepared from alkylglycerol-modified chitosan/TPP (CS-OX/TPP) and trimethyl alkylglycerol-modified chitosan (TMC-OX/TPP).

Confocal microscopy demonstrated an efficient uptake of EB-loaded NPs (*red* as EB fluorescence) into the cytoplasm of the bEnd3 cells, whereas Evans Blue in solution (negative control) was not taken up by the cells (Fig. 3). Further studies indicated that the alkylglyceryl-modified NPs affected the tight junction protein arrangements while the unmodified chitosan nanoparticles had no effect.

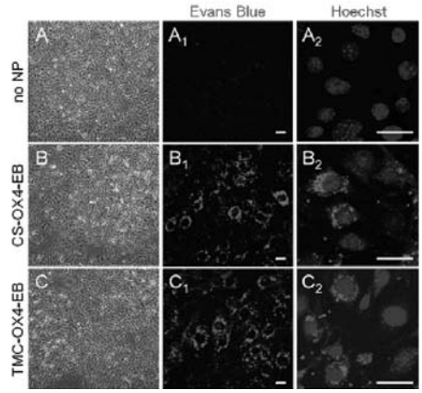

Fig. 3: Uptake and intracellular distribution of NPs in bEnd3 cells. Bright-field images of bEnd3 cells 24-hr after addition of: (A) Evans Blue solution; NPs (B) CS-OX4-EB/TPP; (C) TMC-OX4-EB/TPP. Cells nuclei with Hoechst counterstain (blue). Scale bar = 20 µm.

CONCLUSIONS

The attachment of alkylglyceryl groups (butyl, pentyl, octyl) to chitosan have not introduced significant changes in the particle size and the zeta potential of the particles formulated from these materials compared to particles formulated in the same way from normal chitosan. However, the investigations of their stability found an increase in the hydrodynamic diameter and a corresponding decrease of their zeta potential as the pH increases in the range 4 to 7.4. It has also been found that partial quaternisation introduces a stabilizing effect on the nanoparticles in the pH range of 4 - 8. Cytotoxicity studies showed that NPs prepared from alkylglyceryl-modified chitosans are non-toxic, though quaternisation somewhat lowered the viability of the bEnd3 cells. I*n vitro* experiments using bEnd3 cells indicated a time-dependent cell uptake of Evans Blue-loaded nanoparticles prepared from both butylglyceryl chitosan and butylglyceryl *N,N,N*-trimethyl chitosan.

ACKNOWLEDGMENTS

The authors would like to thank BBSRC (Grant no: BB/F011865/1) and IBBS for financial support.

REFERENCES

1. Ricci M. et al., Curr Med Chem. 2006; 13, 1757.
2. Pardridge W.M. Drug Discov Today. 2007; 12, 54.
3. Erdlenbruch B. et al., Brit J Pharmacol. 2003; 140, 1201.

DEVELOPMENT AND CHARACTERIZATION OF IL-2 LOADED CHITOSAN-TPP NANOGELS

C. Aslan[1], N. Çelebi[1*], I.T. Degim[1], A. Atak[2], L.A. Aral[2]

[1] Gazi University, Faculty of Pharmacy, Department of Pharmaceutical Technology, Etiler 06330 Ankara/TURKEY; [2]Gazi University, Faculty of Medicine, Department of Immunology, Beşevler 06510 Ankara/TURKEY

INTRODUCTION

Nanogels are swellable drug delivery systems that composed of nanometer size gel molecules in polymer matrix and can be prepared by linking of specific poly-anions with cationic polymers or cross-linking of polymer molecules. Some advantages of nanogels (high loading capacity, high stability … etc.) are quite significant for especially pharmaceutical uses. It has been also known that peptides and proteins can be delivered by nanogels.

IL-2 is a cytokine which is effective on the immune system. Studies on IL-2 loaded drug delivery systems were generally subjected to cancer treatments besides other studies because of its immune system related effects. As a result of literature reviews, we did not come across to any study dealing with IL-2 loaded nanogels. Furthermore, efficacy of IL-2 is thought to be increased by loading IL-2 into the nanometer size nanogels and precise targeting can also be achieved. Therefore human IL-2 was selected as an active substance.

MATERIALS AND METHODS

Materials

As chitosan, Protasan UP G 213 (Novamatrix, Norway) was used. TPP was supplied from Sigma, USA. Active substance IL-2 was supplied from Novartis, England. ELISA studies conducted with Human IL-2 ELISA kit (Bender MedSystems Australia).

Preparation of chitosan-TPP Nanogel

In this study, ionic gelation method was used to prepare chitosan-TPP nanogel formulation (1). According to this method, basic TPP solution was dropped into the chitosan acidic solution which was stirred on a magnetic stirrer at a constant rate. Selected chitosan-TPP nanogel formulations were loaded with IL-2 by simple incubation. Table 1 shows the contents of formulations.

Characterization of chitosan-TPP nanogel

Characterization of unloaded and IL-2 loaded nanogels was also performed by measuring particle size and distribution, zeta potential, polydispersity index and imaging by TEM, SEM and AFM. IL-2 loading capacity measurements were performed on IL-2 loaded chitosan-TPP nanogels. IL-2 content was measured using ELISA.

In vitro release studies

In vitro release studies were performed with Franz diffusion cells at 37°C and pH 7.4 phosphate buffer saline (PBS) was used as in vitro release medium. PBS samples were withdrawn from receptor compartment at predetermined time intervals and replenished with fresh solution. IL-2 assay of samples was determined with ELISA method.

Table 1: Contents of chitosan-TPP formulations

Formulation code	Chitosan % (g/mL)	TPP % (g/mL)	Stirring rate(rpm)
NG1	0.15	0.8	250
NG2*	0.15	0.8	500
NG3	0.15	1.6	250
NG4	0.15	1.6	500
NG5	0.30	0.8	250
NG6	0.30	0.8	500
NG7	0.30	1.6	250
NG8*	0.30	1.6	50
NG9	0.20	0.8	250
NG10*	0.20	0.8	500
NG11	0.20	1.6	250
NG12	0.20	1.6	500

* Selected chitosan-TPP nanogel formulations (IL-2 loaded nanogel formulations)

RESULTS AND DISCUSSION

In pre-formulation studies, studied concentrations of chitosan and TPP found to be suitable for ionic gelation (Table 1). It was observed that stirring rate was also an important parameter for ionic gelation of chitosan and TPP. It was also noticed that more homogenous dispersion of nanogels can be formed when 500 rpm was used for stirring. IL-2 loading capacity value of chitosan-TPP nanogel was found to be 100 %±0.010 (±SEM, n=3). IL-2 was detected in filtrate of IL-2 loaded chitosan-TPP nanogels but IL-2 content of the filtrate was negligible. Calculated IL-2 loading capacity was found to be notably successful.

Particle size was decreased with increased stirring rate. It was thought that unloaded NG3, NG5 and NG6 formulations represented quite large particles due to agglomeration. Standard deviation values of particle size of chitosan-TPP formulations were found to be high. The mean particle size of three replicates of IL-2 loaded NG2, NG8 and NG10 formulations were found to be 317 ± 338 nm, 1201 ± 650 nm and 1007± 796 nm respectively. Polydispersity index of unloaded chitosan-TPP nanogels was found to be in a range of 0.427 ± 0.074 to 1.00 ± 0.00. Polydispersity index of IL-2 loaded NG2, NG8 and NG10 formulations were determined 0.974 ± 0.047, 0.795 ± 0.224 and 0.763 ± 0.328 respectively (n=3). Polydispersity index values of unloaded and IL-2 loaded nanogels were found between 0-1 and this was suitable for biological use. If polydispersity index values were smaller than 0.2, particles of these system are accepted as homogenously dispersed (2). Zeta potential of unloaded chitosan-TPP was found to be between -3.39 ± 5.81 mV to 0.752 ± 0.460 mV and zeta potential values of IL-2 loaded NG2, NG8 and NG10 formulations were 0.431 ± 0.033, -1.38 ± 1.72 mV and 0.645 ± 0.185 mV respectively (n=3). Chitosan-TPP nanogels were also found to be dispersed homogenously according to TEM, SEM and AFM imaging study results.

According to in vitro release studies, IL-2 was released slowly following a fast release (burst effect) (Fig. 1).

CONCLUSIONS

Chitosan-TPP nanogel was prepared successfully and particle size of chitosan-TPP nanogel was decreased when high stirring rate was used. IL-2 was finally loaded to selected three chitosan-TPP nanogels (NG2, NG8, NG10). Those formulations were selected according to their particle size and distributions. IL-2 loading capacities of chitosan-TPP nanogels were found to be 100 %. IL-2 was released slowly after burst effect in first 1 to 2 hours. Chitosan-TPP nanogel was found to be homogenously dispersed according to observed TEM, SEM and AFM analysis. The morphological structure was not found to be changed too much after IL-2 loading.

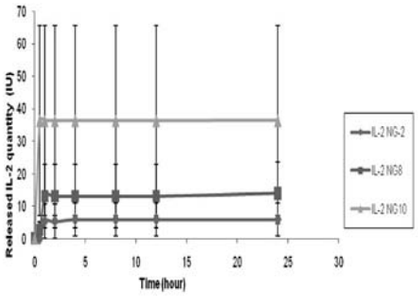

Fig. 1: In vitro release profiles of IL-2 loaded NG2, NG8 and NG10 formulations (n=3, SE).

REFERENCES

1. Lopez-Leon T, Carvalho ELS, Seijo B, Ortega- Vinuesa JL, Bartos-Gonzalez D. Physicochemical characterization of chitosan nanoparticles: electrokinetic and stability behaviour. J. Colloid. Interface Sci. 2005; 283: 344-351.
2. Juno Y, Srinivasan S, Chung-Kil S, Dae-Duk K, Han-Gon C, Chul-Soon Y, Jong-Soo W, Bong Kyu Y. Skin penetration and retention of L-Ascorbic acid 2-phosphate using multilamellar vesicles. Arch. Pharm. Res. 2008; 31: 1652-1658.

DEVELOPMENT OF CHITOSAN NANOPARTICLE-DNA COMPLEXES FOR NASAL IMMUNIZATION AGAINST HEPATITIS B

F. Lebre [1,2*], G. Borchard[3], H. Faneca[1,4], M. C. Pedroso de Lima[1,4], O. Borges[1,2]

[1] Center for Neuroscience and Cell Biology, University of Coimbra, 3000 Coimbra, Portugal; [2] Faculty of Pharmacy, University of Coimbra, Pólo das Ciências da Saúde Azinhaga de Santa Comba 3000-548, Coimbra, Portugal; [3] School of Pharmaceutical Sciences, University of Geneva, University of Lausanne, Quai Ernest Ansermet 30, 1211 Geneva, Switzerland; [4] Department of Life Sciences, FCTUC, University of Coimbra, 3004-517 Coimbra, Portugal.

INTRODUCTION

New generation of Hepatitis B vaccines are needed in order to overcome the limitations of HBV injectable vaccines. DNA vaccines can induce both humoral and cell-mediated immune responses and constitute one of the most exciting developments in vaccinology. An ideal delivery system for DNA needs to be able to protect it while within the body and to efficiently deliver it to the cell nucleus. One of the major drawbacks of DNA loaded chitosan (CH) particles is their low transfection efficiency. Albumin may promote transgene expression, as previously reported (1) and decrease DNA-chitosan interaction, thus facilitating cytoplasmic release of DNA. Therefore, to improve transfection, bovine serum albumin (BSA) was incorporated into the chitosan nanoparticles prior to the addition of DNA.

MATERIALS AND METHODS

Materials

Chitosan (ChitoClear™ - 95% DD) was purchased from Primex Bio-Chemicals AS (Avaldsnes, Norway). BSA was obtained from Sigma-Aldrich Corp. (USA). Plasmid pCMVluc was purified using QIAGEN Plasmid Giga Kit (QIAGEN, Hiden, Germany). All other chemicals and reagents were analytical grade.

Preparation of the delivery systems

Particles were prepared according to methods previously described (2) with some modifications. Briefly, equal volumes of a chitosan solution and an aluminum solution, with- or without BSA, were mixed under high speed vortexing for 20 seconds and let to rest for 1 hour for complete nanoparticle formation.

Complex formation was achieved simply by adding nanoparticles (NPs) to a DNA solution.

Characterization of the delivery system

Size and zeta potential were measured by dynamic light scattering with a Delsa™ Nano C (Beckman Coulter).

Particle morphology was evaluated by scanning electron microscopy (SEM) (JSM-700 1FA, JEOL, Tokyo, Japan).

Aluminum quantification was determined based on a reaction with eriochrome cyanine.

DNase I protection assay

The capacity of the complexes to protect DNA from nuclease degradation was studied by agarose gel electrophoresis. Complexes were submitted to DNase I action (2 DNase I units/µl), for 15 minutes at 37 ºC, followed by enzyme inactivation upon incubation with 0.5 M EDTA. Samples were analyzed in a 1% agarose gel containing 0.5 µg/ml of ethidium bromide at a constant voltage of 100 V. The DNA bands were visualized using a UV-transilluminator.

Cellular viability studies

Cellular viability was evaluated by the MTT assay. Studies were performed with splenocytes obtained from 7-week old female C57BL/6 mice. 100 µl of the cell suspension ($1x10^7$) were seeded together with equal volumes of the chitosan formulation. Different concentrations of the nanoparticles were tested for 24 hours.

RESULTS AND DISCUSSION

Delivery system characterization

Size of the prepared NPs was found to be 268.1 ± 14.2 nm (without albumin) and 193.2 ± 25.4 nm (with albumin) and the respective zeta potential was +30.1 ± 1,9 mV and +30.9 ± 1.1 mV (measured in sodium acetate buffer). However, scanning electron microscopy (SEM) images revealed the presence of smaller nanoparticles (around 100 nm).

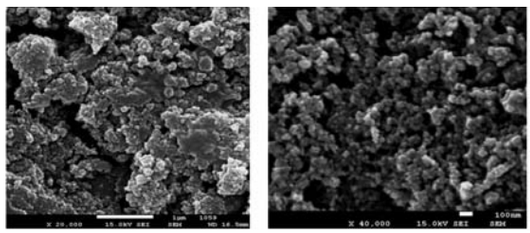

Fig. 1: SEM images of chitosan nanoparticles (left) and chitosan-albumin nanoparticles (right)

Complexes were prepared at different NP:DNA ratios (20:1; 10:1; 5:1). The average diameter of the complexes was higher as compared to the NPs alone.

Aluminum quantification revealed that 55% of the aluminum added for nanoparticle formation remained incorporated.

DNase I protection assay

For all NP:DNA ratios chitosan nanoparticles could fully complex the DNA and protect it against degradation by DNase I. DNA was still protected by the nanoparticles after incubation with 1 U DNase I/ µg DNA, which represents a 10 000 x higher degree of protection as compared to naked DNA.

Cellular viability studies

CH NPs showed no cytotoxic effects for concentrations below 1000 ug/mL, which is the maximum concentration used to prepare the complexes. CH-albumin NPs seem to be more cytotoxic and further studies are needed to fully

evaluate the causes for this decrease in viability. The aluminum compound used as cross-link revealed no cytotoxicity over the same range of concentrations.

CONCLUSIONS

Data collected so far revealed some attractive features concerning CH NP-DNA complexes. Two delivery systems were developed and optimized. The strong mucoadhesive property of CH and is immune-stimulating activity makes it an attractive polymer for nasal vaccination. In addition, the incorporation of aluminum, which is a well known vaccine adjuvant, and albumin in the formulation further enhances the potential of the generated delivery system. Transfection studies are currently being undertaken to fully assess the potential of the complexes before proceeding to *in vivo* studies.

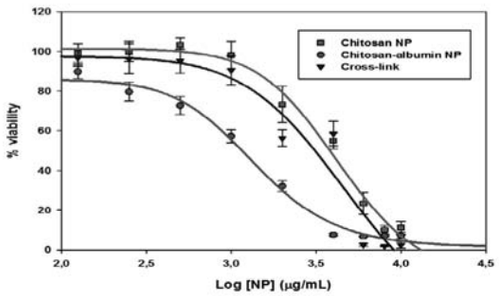

Fig. 2: Viability of splenocytes incubated with chitosan-NP (■), chitosan-albumin NP (●) and aluminium solution (▼).

This work was supported by a grant from the Portuguese Ministry of Science and Technology (SFRH/BD/64046/2009) and by GlaxoSmithKline Portuguese Foundation.

REFERENCES

1. Faneca H, Simoes S, Pedroso de Lima MC. Association of albumin or protamine to lipoplexes: enhancement of transfection and resistance to serum. J Gene Med 2004;6(6):681-92
2. Roy K, Mao HQ, Huang SK, Leong KW. Oral gene delivery with chitosan—DNA nanoparticles generates immunologic protection in a murine model of peanut allergy. Nat Med 1999;5(4):387-91

MODIFIED NANOPRECIPITATION METHOD FOR INCORPORATION OF HYDROPHILIC DRUG SUBSTANCES INTO AMPHIPHILIC PLGA NANOCARRIERS

M. Simonoska Crcarevska[1], M. Glavas Dodov[1], S. Calis[2], N. Geskovski[1], K. Goracinova[1]

[1] Faculty of Pharmacy, University of Ss Cyril and Methodius, Vodnjanska 17, 1000 Skopje, Macedonia ; [2] Faculty of Pharmacy, Haccetepe University, 06100 Ankara, Turkey

INTRODUCTION

Commonly utilized techniques for nanoparticle preparation usually do not provide conditions for good encapsulation efficiency of hydrophilic anticancer drugs because of the rapid partitioning of the drug into the external aqueous phase. However, there are only few attempts through the literature to establish modification of nanoprecipitation method for production of hydrophilic drug loaded particles, but with even less success compared to the emulsification diffusion methods. Formation of submicrone particles during the nanoprecipitation method depends on the differences in the surface tension between the solvents, which leads to interfacial turbulence resulting with breaking up the organic phase and dispersing it as a drops in the aqueous phase (1). These droplets continuously brake down into smaller submicrone droplets due to the interfacial convective flow which contributes to renewing the interfacial surface increasing the mass-exchange rate between the phases. During the diffusion of the organic solvent into the water dissolved polymer chains are also dragged into the water medium which is followed by aggregation and nanoparticle formation. In the standard procedure the organic phase containing the polymer that will form the nanoparticles (NP) is poured into the aqueous phase under slight magnetic stirring. Logical approach to improve hydrophilic drug loading might be rapid micromixing to induce faster supersaturation, polymer agregation and particle formation and at the same time to prevent fast diffusion of drug into the outer water phase. Having this in mind, we hypothesized that dispersing the drug solution into the organic polymer solution (nonsolvent for the drug substance (API)) prior nanoprecipitation, might delay the hydrophilic drug partitioning into the outer water phase during nanopricipitation (2). For this reason, we developed modified nanoprecipitation method for hydrophilic drug loading into amphiphilic PLGA nanocarriers. The particles were prepared using PLGA and polyethylene oxide tri-block copolymer Pluronic® F127 (F127). As model hydrophilic drug, irinotecan hydrochlorid (IR-HCl) was used.

The aim of this study was to test the influence of physicochemical properties of the solvents used for dissolution of API and consequent dispersion into the organic polymer solution (acetone, nonsolvent for API) prior nanoprecipitation, on the efficicay of encapsulation of IR-HCl. All API solvents are characterized with good miscibility with acetone. Also the influence of production process on the NP properties was evaluated.

MATERIALS AND METHODS

Materials

PLGA (lactate/glycolate ratio 85/15) was purchased from Sigma, Germany, while F127 was generous gift from BASF, Germany. IR-HCl was obtained from Biotech Co., China. All other chemicals were of analytical grade.

Preparation and characterization

NP with IR-HCl were prepared using modified nanoprecipitation method (2). In order, to test the hypothesis enunciated above, we choose 4 different solvents for IR-HCl (water (W-NP), ethanol (E-NP), acetonitrile (A-NP) and PEG 200 (P-NP) with different physicochemical properties (Table 1). The solution of IR-HCl (1.5mg/ml) was added to PLGA and F127 acetone solution (PLGA : F127 ratio =1:1,77) under rapid micromixing (6500 rpm, Ultra-turrax T-18, IKA, Germany). Nanoprecipitation was carried out in water under the identical operating conditions.

Table 1: Physicochemical properties of solvents

	Surface tension (mN/m)	Density (g/ml)
water	71.99	1.0
PEG 200	43.50	1.12
Acetonitrile	28.34	0,786
Ethanol (96%)	21.80	0.789
Acetone	22.73	0.792

NP were characterized in terms of morphology (Jeol-SEM 6400, Japan), particle size, polydispersity index (PDI) and zeta potential (Zetasizer Nano Series, Nano-ZS, Malvern Instruments Ltd., UK). Encapsulation efficiency (EE) was determined, after separation by size-exclusion chromatography (Sephadex G-25 column), with validated HPLC method.

RESULTS AND DISCUSSION

Modified nanoprecipitation was robust and reproducible production process resulting in NP with acceptable spherical morphology and smooth surface (Fig. 1). Particle size, PDI and encapsulation efficiency are presented in Table 2, Fig. 2.

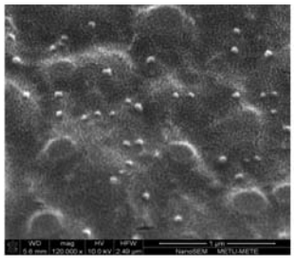

Fig. 1: SEM image of prepared NP (formulation W-NP)

Table 2: Particle size, PDI and EE of prepared formulations

	Z-Average (nm)± SD	PDI±SD	EE%
W-NP	124±0.02	0.108±0.004	52±3
P-NP	135±0.05	0.250±0.014	35±2
A-NP	116±0.03	0.110±0.002	18,5±1
E-NP	123±0.02	0.104±0.016	6,82±1

Zeta potential of prepared NP was in a range from -1 to -5 mV. Compared to the EE of NP prepared using non modified nanoprecipitation (less than 5% IR-HCl), EE in the batches prepared by modified nanopericipitation method was in range of 6 to 60%, depending of the API solvent used in the procedure.

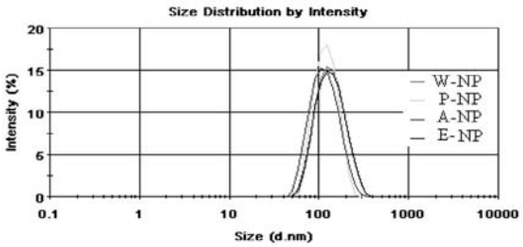

Fig. 2: PDI of different NP loaded with IR-HCl

Improved EE is probably due to faster aggregation and particle formation as well as slower diffusion of IR-HCl into the outer water phase. The EE of IR-HCl increased in the following order E-NP<A-NP<P-NP<W-NP. Having in mind that solubility of IR-HCl in selected API solvents as well as solvent miscibility with acetone polymer solution are quite similar, most likely, differences in EE could be related to differences in surface tensions between IR-HCl solutions and acetone polymer solution, thus influencing the dispersing manner of the phases and mass exchange rate, consequently.

CONCLUSIONS

EE of hydrophilic drug was markedly improved by simple surface-tension related modification of the drug partitioning into the outer water phase. Larger surface tension difference among the API solvent and polymer solvent resulted in higher EE.

REFERENCES

1. Mora-Huertas CE, Fessi H, Elaissari A, Influence of process and formulation parameters on the formation of submicron particles by solvent displacement and emulsification-diffusion methods Critical comparison, Adv. Colloid. Interface. Scin. 2011; 163 (2): 90-122.
2 Glavas M, Calis S, Simonoska M, Geskovski N, Goracinova K, Colloidal carriers for anticancer drug delivery formulation aspects, Abstraktbook of International Symposium on Drug Research & Development, Antalya, Turkey, 2011.

POLYSACCHARIDE-BASED NANOPARTICLES FOR PERORAL DELIVERY OF BIOPHARMACEUTICALS

M Cegnar[1,*], A Miklavžin[2] and J Kerč[1,2]

[1] Lek Pharmaceuticals, d.d., Sandoz Development Center Slovenia, Verovškova 57, SI-1526 Ljubljana, Slovenia; [2] Faculty of Pharmacy, University of Ljubljana, Aškerčeva 7, SI-1000 Ljubljana, Slovenia

INTRODUCTION

Peroral administration is the most preferred route of drug administration but is extremely difficult for proteins due to their low bioavailability. Although peroral delivery of proteins has often been considered an unattainable goal, the efforts to develop peroral protein formulation continue to be numerous. One of the most promising strategies to improve protein peroral delivery relies on its association in nanoparticles (NPs). Development of NPs with protein fundamentally differs from that for classical low molecular weight drugs. Key factors in developing such system are composition and production processes of NPs, which should results in the formation of small particle size with preferably high association efficiency of protein and preserved biological activity, good penetration properties and desired biopharmaceutical properties including protection against enzymatic degradation in gut, relatively fast protein release in the intestine to achieve desired concentration gradients for absorption but retained release in the acidic gastric milieu when passing through the stomach.

NPs for delivery of model protein drug albumin were formulated by mild method of polyelectrolyte complexation using water soluble polymers, which are able to spontaneously associate with protein in NPs under gentle stirring (1, 2). Polysaccharides, alginate and chitosan, were used as polymer carriers having opposite charge, mucoadhesive and permeation enhancing properties, the latter applies especially to chitosan (2). In this study we focused on evaluation of biorelevant parameters of NPs during their passage through the GI tract, e.g. enzymatic degradation and protein release in different sections of the GI tract of different pH.

METHODS

Alginate/chitosan NPs associating albumin were prepared by polyelectrolyte complexation. NPs (alginate/albumin/chitosan, 1:1:0.1 w/w) had size 280 nm, zeta potential -40 mV and protein association efficiency of app. 80% (3). The release of protein from NPs was performed on freeze-dried NPs (containing sucrose and mannitol as cryoprotectants) after incubation in buffers with different pH and ionic strength (phosphate buffer saline (PBS, 0.15M, pH 7.4), water (pH 4.0), 0.9% NaCl solution (pH 4.0) and an acidic saline solution (0.1M HCl, 0.9% NaCl, adjusted to pH 3.0) raised to pH 6.8 after 2h incubation). At specific time points, the amount of released protein was determined in the supernatant after ultracentrifugation using HPLC method.

Resistance of NPs against enzymatic degradation was assessed by proteolytic assay with pepsin, after incubating albumin either free or associated in NPs with specific amount of pepsin for different time periods. A degree of proteolysis was determined by visual analysis of SDS-PAGE gel after staining with Coomassie Brilliant Blue.

RESULTS AND DISCUSSION

Protein release

Approximately 90% of albumin was released in PBS, pH 7.4. The release was lower in water and 0.9% NaCl solution (both dispersion had pH 4.0) reaching the value of 40% and 60%, respectively. These release profiles are characterized by initial burst release, which is common with the nanometer size particles since the rate of protein diffusion is proportional to the particle's surface area.

The differences in the release profiles suggest that the release of albumin from NPs is mostly dependent on the pH of the medium, and that the presence of electrolytes contributes to the higher release. The pH of the medium primarily

affects the charges of polyelectrolytes and hence their attraction or repulsion forces. At pH 7.4, which is above the pI of albumin (pI 4.7), repulsion forces between both negatively charged polyelectrolytes (albumin and alginate) took place. CS minimally influenced protein release due to its low content in NP composition. The release was lower in media with pH 4.0, where some interactions between polyelectrolytes were still present. However, the release was substantially higher in 0.9% NaCl solution, indicating that salts weakened the attraction between oppositely charged polyelectrolytes.

Under acidic saline solution, pH 3.0, the release of albumin was retained although containing salts. But when the pH was increased to pH 6.8, albumin immediately released from NPs reaching the value of app 70%. Retained release in low pH could be a consequence of even more stronger attraction between albumin and alginate. It is also possible that some of carboxylic groups on alginate molecules became protonated at pH 3.0; which could form sort of a network that captured protein (4). By increasing the pH, repulsion between polyelectrolytes took place. At higher pH, alginate also became ionized and more soluble what contributed to albumin release.

Proteolysis assay

A protective property of NPs against degradation of albumin with pepsin relative to the free albumin solution is presented in Fig. 1. NPs were able to protect albumin from pepsin degradation up to 1 h of incubation.

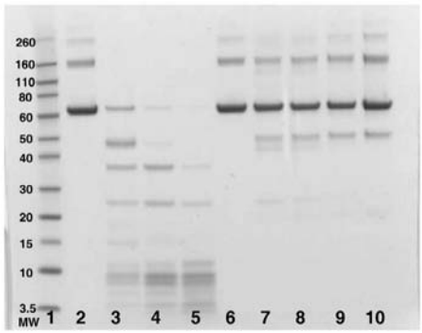

Fig. 1: SDS-PAGE results after proteolytic degradation of albumin (66.4 kDa, 0.1 mg/ml), either free or in NPs, with pepsin (34 kDa) at pH 4.0 (albumin/pepsin mass ratio, 20/1). Lane 1, MW standards. Lane 2, untreated free albumin. Lane 3, 4 and 5, free albumin treated with pepsin for 5, 15 and 30 min, respectively. Lane 6, untreated albumin-loaded NPs. Lane 7, 8, 9 and 10, albumin-loaded NPs treated with pepsin for 5, 15, 30 and 60 min, respectively.

Strong staining could be observed for the band of albumin-associated with NPs. On the contrary, free albumin progressively degraded already after 15 min of incubation with pepsin, and after 30 min no staining could be observed for the band of albumin, indicating complete degradation of free albumin. Also degradation products with lower MW could be observed for free albumin.

CONCLUSIONS

NPs prepared by mild method of polyelectrolyte complexation represent promising delivery systems for peroral delivery of proteins. Small particle size and specific polymers used could provide good mucoadhesion and permeation properties; partial protection against pepsin degradation and retained release in acidic pH may protect the protein in the harsh conditions in the stomach, whereas burst release at higher pH may have a favorable effect on locally increased concentration gradient that is necessary for absorption.

REFERENCES

1 Hartig SM et al. Pharm Res, 24 (2007)
2. Fuente M. Nanomedicine, 3 (2008)
3. Cegnar M et al. Acta Chim Slo, 57 (2010)
4. Sarmento et al. J Nanosci Nanotechnol 7 (2007)

INCORPORATION OF A MAST CELL ACTIVATOR IN CHITOSAN BASED DELIVERY SYSTEMS FOR MUCOSAL IMMUNIZATION

D. Bento[1,2*], G. Borchard[3], O. Borges[1,2]

1 Center for Neuroscience and Cell Biology, University of Coimbra, Rua Larga 3004-504 Coimbra, Portugal; 2 Faculty of Pharmacy, University of Coimbra, Pólo das Ciências da Saúde Azinhaga de Santa Comba, 3000-548 Coimbra, Portugal; [3] School of Pharmaceutical Sciences, University of Geneva, University of Lausanne, Quai Ernest Ansermet 30, 1211 Geneva, Switzerland

INTRODUCTION

Mucosal vaccines have been suggested as substitute to parenteral immunization with the advantage to induce both systemic and mucosal immunity. However, its progress has been delayed, largely due to the lack of effective mucosal adjuvants.

It was recently showed that the mast cell activators may act as adjuvants by inducing dendritic cell migration to draining lymph nodes via a mechanism that required mast cells (MCs) and MC derived TNF (1). The same authors showed that nasal immunization of mice with the MC activator compound 48/80 (C48/80) and PA (protective antigen) resulted in higher mucosal and systemic immune responses compared to PA alone (1). These results make C48/80 a promising adjuvant for mucosal immunization. Chitosan (Chi), a polysaccharide with immunostimulating and bioadhesive properties, is also considered to be very promising on the design of antigen delivery systems for mucosal surfaces. This work describes the optimization of particle preparation methods and characterization of a new chitosan based delivery system with C48/80 incorporated.

MATERIALS AND METHODS

Materials

LMW Chitosan was purchased from Primex BioChemicals AS (Avaldsnes, Norway). Alginate (MANUCOL LB®) was kindly donated by ISP Technologies Inc. (Surrey, UK). Compound 48/80 was from Sigma-Aldrich.

Preparation of particles

Chitosan/alginate (Chi/Alg) particles were prepared using a method modified from Rajaonarivony et al (2). Briefly, a $CaCl_2$ solution is added to a sodium alginate solution while stirring in order to prepare a pre-gel. The particles are formed upon mixing pre-gel and Chi solution during high-speed vortexing. Chitosan nanoparticles (Chi NPs) were prepared adding dropwise a Na_2SO_4 solution to a chitosan solution. C48/80 loaded Chi/Alg and Chi particles were obtained by addition of the compound to chitosan and Na_2SO_4 solutions of each preparation method, respectively.

Characterization of particles

Particles size and zeta potential were analyzed by dynamic light scattering using a Delsa™ Nano C (Beckman Coulter).

Loading Efficacy

C48/80 on particles supernatant was determined based on a reaction of secondary amines with sodium nitroprusside and acetaldehyde (3) and the loading efficacy (LE) of particles calculated using the following equation:

$$LE(\%) = \frac{\text{total C48/80} - \text{C48/80 free}}{\text{total C48/80}} \times 100$$

***In vitro* cytotoxicity studies**

The cytotoxicity of loaded and blank particles was assessed using MTT viability assay after 24h of incubation with spleen cells from female C57BL/6 mice.

RESULTS AND DISCUSSION

Characterization of particles

The mean size of Chi/Alg particles is dependent on Chi concentration of the solutions used during preparation of the particles. Lower values lead to higher diameters and larger aggregates (not shown).

Loaded and blank Chi NPs have a mean size of 465 and 389 nm, respectively, and PI < 0.200. Zeta potential is 28.9 mV for loaded and 27.9 mV for blank NPs.

Loading Efficacy

The C48/80 LE in Chi/Alg particles is affected by the Chi amount, the lower the concentration, the higher the LE (Fig.1). This can be explained by competition between Chi and C48/80 amino groups for acidic groups of alginate. LE of 48 % in Chi NPs indicates a more balanced competition for sulfate between the amino groups.

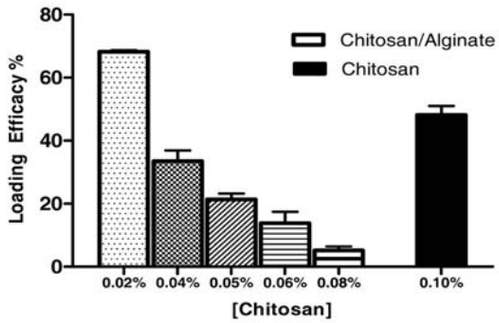

Fig.1: Loading Efficacy of C48/80 in different particles.

***In vitro* cytotoxicity studies**

Blank and C48/80 loaded Chi NPs showed no cytotoxicity for concentrations bellow 1 mg/mL (Fig.2). Concerning the cell viability in the presence of C48/80, it was found that is higher when the C48/80 is associated with Chi particles (Fig. 3) but similar when associated with Chi/Alg (not shown), when comparing with compound in solution. This indicates that most probably C48/80 is on surface of Chi/Alg particles.

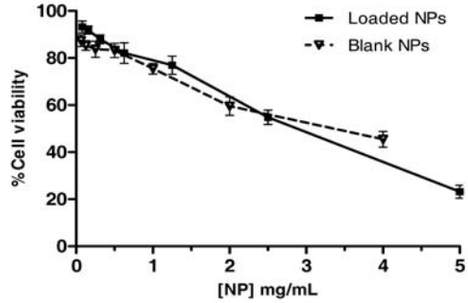

Fig. 2: Cytotoxicity of blank and C48/80 loaded Chi NPs.

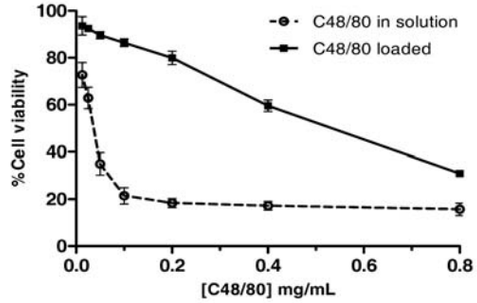

Fig. 3: Cytotoxicity of C48/80 in solution and loaded in Chi NPs.

CONCLUSIONS

C48/80 can efficiently be incorporated into Chi based particles. C48/80 cytotoxic effects are described in literature. On this work we demonstrated that the cytotoxicity can be diminished by the incorporation of the compound into chitosan particles. Further studies have to be done in order to assess the capability of the C48/80 loaded particles to activate mast cells.

ACKNOWLEDGEMENTS:

Work financially supported by Portuguese Foundation for Science and Technology (grant SFRH/BD/65141/2009 and project PTDC/SAL-FAR/115044/2009).

REFERENCES

1. McLachlan JB, et al. Mast cell activators: a new class of highly effective vaccine adjuvants. Nature Medicine. 2008; 14(5): 536-541.
2. Rajaonarivony M, et al. Development of a new drug carrier made from alginate. J Pharm. Sci 1993; 82(9): 912-917.
3. Cullis CF, Waddington DJ. The colorimetric determination of secondary amines, Analytica Chimica Acta. 1956: 15(C): 158-163.

ACCOMPANYING OF NANOPARTICLES' DISTRIBUTION WITHIN THE CELLS

J. Kristl[1*], K. Teskač Plajnšek[1], S. Pečar[1,2], S. Pajk[1], M. Erdani Kreft[3]

[1] University of Ljubljana, Faculty of Pharmacy, Aškerčeva 7, 1000 Ljubljana, Slovenia; [2] Institute Jožef Stefan, Jamova 39, 1000 Ljubljana, Slovenia; [3] University of Ljubljana, Faculty of Medicine, Cell Biology Institute, Ljubljana, Slovenia

INTRODUCTION

Following the uptake of nanoparticles (NPs) (e.g. solid lipid nanoparticles; SLN) and their trafficking in the cells are imperative to fully explore their usage as efficient intracellular drug delivery system for the range of therapeutic targets (1). To realize that, we synthesize a novel fluorescent probe, tetradecyl diethylamino coumarin amid, named 14-DACA, which is retained in SLN due to the long lipophilic chain. It enables superior imaging without suffering from fluorescence quenching is enabled. Contrary, 6-coumarin, a fluorescent probe with the same fluorophore as 14-DACA but lower lipophilicity, is quickly released from NPs' core and consequently makes visualization of SLN in the cell culture indistinctly (Fig. 1) (2).

The aim of this work was to examine the pathways of fluorescently-labeled SLN in live or fixed cell' environment.

METHODS

SLN preparation and characterization

Fluorescently-labeled SLN were prepared by the melt-emulsification process, where lipid Compritol 888 ATO, Phospholipon 90H, fluorescent probe 14-DACA and Lutrol were stirred with a rotor-stator homogenizer (Omni Int., USA) for 10 min at 15000 rpm. Obtained SLN were characterized for size, surface charge and topography by using Zetasizer nano-ZS (Malvern Instrument, UK).

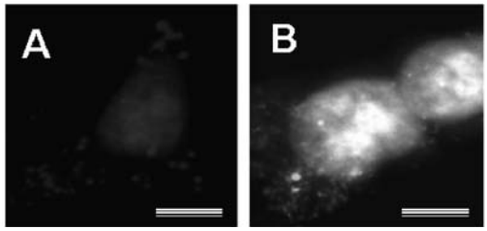

Fig. 1: (A) Distinct intracellular visualization of SLN, labeled by fluorescent probe 14-DACA. Red are seen nuclei, stained by propidium iodide. (B) SLN, labeled by 6-coumarin, can not be clearly intracellular distinguished. Due the covering of absorption spectrum of 6-coumarin and propidium iodide, the nuclei are seen yellow. Bar is 10 µm.

Localization of SLN in the cells

Traffic of SLN in cell culture (human keratinocytes NCTC2544) was monitored by live-cell imaging immediately after addition of SLN in cell culture.

Intracellular monitoring of SLN was established by preparing fixed-slides of cells following 24-h incubation with 100 µg/ml SLN and stained for nuclei with propidium iodide (red) or with Hoechst 33342 (blue), for actin filaments with Phalloidin-FITC (green) and for mitochondria with Mitotracker (red). Cell- images were processed with Cell^R Software of Olympus IX 81 fluorescence microscope using co-localization technique, profiles of fluorescence intensity and "pseudo filter".

RESULTS AND DISCUSSION

Fluorescently labeled SLN were approx. 120 nm in diameter, spherical shape and repulsed due to the high zeta potential.

Real-time live cell imaging showed rapid internalization of SLN and were trafficked to the distinct compartments within the cell very dynamically. Majority of SLN were moving from the cell-periphery toward the nuclear-proximity (Fig. 2).

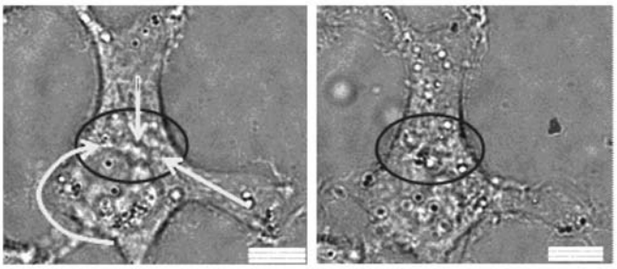

Fig. 2: Intracellular traffic of SLN (blue dots) mostly toward perinuclear location (marked with circle). Bar is 10 µm.

Next, 'pseudo' three-dimensional display of Fig. 3A' is showing SLN, seen as particles, positioned mostly close to the hatched circle, which represents nucleus (Fig. 3A").

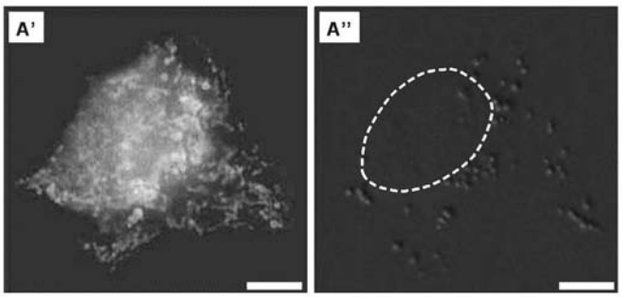

Fig. 3: "Pseudo filter" exposed SLN as intense blue particles mostly surrounding yellow hatched circle, marking nucleus (A"). Originally, cell was stained for mitochondria (red, Mitotracker) and nucleus (blue, Hoechst 33342) (A'). Bar is 10 µm.

Using co-localization technique and profiles of fluorescence intensity enable to proof the location of SLN regarding nuclei.

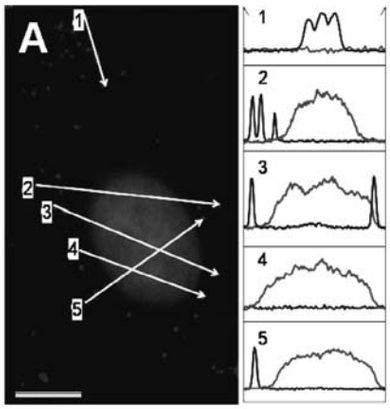

Fig. 4: Intracellular localization of SLN. Graphs represent relative fluorescence intensity of nanoparticles (blue curves) and nucleus (red curves) regarding the arrows marked on the fluorescence images next to the graph on the left. Bar is 10 µm.

According Fig. 4, majority of peaks of blue fluorescence, marking SLN, are close to the increased red fluorescence, representing nucleus, what provide evidence perinuclear localization of SLN.

Finally, visualization of fixed cells, stained for actin fibres (green) and nuclei (red), indicated SLN (blue dots) distributed over whole intracellular space and mostly surrounding nuclei (Fig. 5). This is case of effective multicolor imaging, where any spectrum' interferences among fluorescent probes appear, as it is seen in Fig. 1 using 6-coumarin.

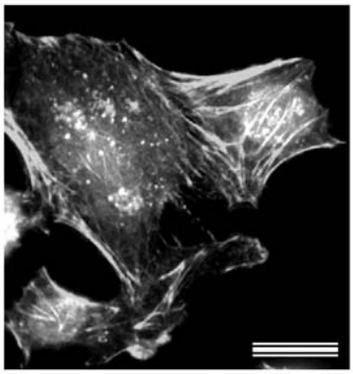

Fig. 5: Imaging the intracellular localization of SLN after fixed-slides' preparation. Legend: red – nuclei stained with propidium iodide; blue – SLN, stained with DACA-14; green – actin, stained with phalloidin-FITC. Bar is 20 µm.

CONCLUSIONS

To sum up, by using case-designed fluorescent dye, 14-DACA, we adequately and certainly elucidated the intracellular fate of SLN, what is an excellent progress on the area of drug delivery on site of action.

REFERENCES

1. Watson P, Jones AT, Stephens DJ, Intracellular trafficking pathways and drug delivery: fluorescence imaging of living and fixed cells. Adv. Drug Deliv. Rev. 2005; 57: 43-61.
2. Teskac K., Kristl J. The evidence for solid lipid nanoparticles mediated cell uptake of resveratrol. Int. J. Pharm. 390, 2010, 61-69.
3. Teskač Plajnšek K,, et al., A novel fluorescent probe for more effective monitoring of nanosized drug delivery systems within the cells.Int J Pharm, 2011.

A COMPARATIVE STUDY ON PROPERTIES OF DIFFERENT COLLOIDAL FORMULATIONS OF BETAMETHASONE VALERATE

T. Senyigit*, I. Ozcan, M. Ozyazici, O. Ozer

Ege University, Faculty of Pharmacy, Department of Pharmaceutical Technology, 35100, Bornova-İzmir

INTRODUCTION

Topical corticosteroids (TCs) are the most frequently used drugs in dermatological practice. Despite their demonstrated benefit in the therapy of psoriasis and atopic dermatitis, TCs are associated with number of side effects that limit their use. Betamethasone-17-valerate (BMV) is the gold standard of these agents and serves as a reference in the clinical studies for the registration of new TCs [1]. It is a medium potency TCs, lacking mineralocorticoid properties, currently available in four topical dosage forms: cream, ointment, lotion and foam with a strength of 0.1 % w/w. Colloidal drug carrier systems such as nanoparticles, liposomes and ethosomes appear to be promising for the targeting of TCs to the viable epidermis where the inflammatory reactions take place [2]. The aim of this study was to prepare and to compare the physical properties of nanoparticular, liposomal and ethosomal formulations containing BMV for topical delivery.

MATERIALS AND METHODS

Materials

BMV was a kind gift from GlaxoSmithKline, Turkey. Lecithin (Lipoid S45), Phosholipon 90 G, Lipoid S 100 and chitosan (MW 140 KDa) were purchased from Lipoid AG (Ludwigshafen, Germany) and Primex (Haugesund, Norway), respectively. All other materials were of analytical grade.

Methods

Preparation of nanoparticular formulation

Nanoparticles (F1) were obtained by rapidly injecting 4 ml of the lecithin ethanolic solution through a glass pipette under mechanic stirring (Ultra-Turrax IKA-T25), into 46 ml of a chitosan solution obtained by diluting with distilled water 0.5 ml of 1% (w/v) chitosan solution in 0.275 N HCl [3]. In the colloidal suspension, lecithin/chitosan was present in ratio 20:1 (w/w).

Preparation of liposomal formulations

The thin film hydration method was used to prepare the liposomal suspensions (F2 and F3) [4]. Phospholipids (Phosholipon 90 G and Lipoid S 100), cholesterol and BMV were dissolved in chloroform, and organic solvent was evaporated (IKA RV 10 rotary evaporator) to form a thin film. Subsequently, the resulting thin film was hydrated in distilled water. Finally the liposomal suspension was homogenized with a sonicator for 15 min (Bandelin Sonopuls HD 2070).

Preparation of ethosomal formulations

Ethosomal formulations (F4 and F5) were prepared according to the method reported by Touitou [5]. These were composed of 2% phospholipid, 40% ethanol, 0.1% BMV and water to 100% w/w. For preparation of ethosomes, phospholipids (Phosholipon 90 G and Lipoid S 100) and BMV were dissolved in ethanol. Water was added slowly to the lipid mixture with constant stirring at 700 rpm and the system was kept at 30°C. The resulting vesicle suspension was homogenized at 13.000 rpm for 15 min (Ultra-Turrax IKA-T25).
In all formulations the concentration of BMV was kept constant as 0.1 % (w/w).

Characterization of Formulations

The average particle size and polydispersity index (PI) of the colloidal formulations were determined by dynamic laser light scattering method (Nanosizer Coulter N4 Plus®, Malvern Instruments). The zeta potential values of formulations were measured in aqueous dispersion with a Zetasizer 4 (Malvern Instruments) at 25 °C. Experimental values were reported the average of six different formulations. The vesicles were visualized to confirm particle sizes and distribution using TEM (Philips) by negative staining method.

RESULTS AND DISCUSSION

BMV loaded colloidal formulations were characterized in terms of size, zeta potential and size distribution. Table 1 shows the characteristics of formulations.

Table 1: Physicochemical properties of colloidal formulations

	Particle size (nm)	Zeta potential (mV)	Polydispersity index (PI)
F1	274.6 ± 14	40.8 ± 2.80	0.241 ± 0.02
[a]F2	123.7 ± 2	-27.4 ± 0.50	0.485 ± 0.03
[b]F3	764.6 ± 11	-34.5 ± 0.64	0.547 ± 0.02
[a]F4	286.0 ± 12	-12.0 ± 0.85	0.212 ± 0.08
[b]F5	346.0 ± 16	- 8.4 ± 0.06	0.322 ± 0.12

[a]prepared with Phosholipon 90 G
[b]prepared with Lipoid S 100

As it was shown in Table 1, colloidal nanoparticles were characterized by relatively small size and high positive surface charge attributed to the presence of chitosan chains on the particle surface.
Liposomal and ethosomal formulations prepared with Phospholipon 90G showed smaller particle size than that made of Lipoid S100. The negative charge of the formulations could be explained by the presence of phospholipids on the surface. The higher negative charge of liposomal formulations compared with ethosomes could be result in better stability of the formulations.
In this study, the size distribution was narrow and PI value of nanoparticle dispersion was below 0.25. These data confirmed the homogeneity of nanoparticle dispersion of BMV (Figure 1).

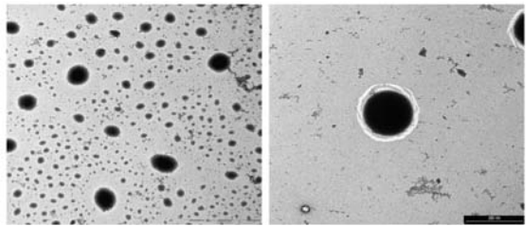

Fig. 1: TEM images of F1

Similar to nanoparticles, ethosomal formulations exhibited small PI values which indicate the homogeneity of formulations. Although liposomes have higher PI values in comparison to other formulations, the PI around 0.5 might be assumed as homogeneous systems.

CONCLUSIONS

In conclusion, novel BMV loaded colloidal formulations were successfully prepared with good physical characteristics for topical use. Nanoparticles and formulations prepared with Phospholipon 90G would be used for further studies to increase accumulating capacity of BMV depending on their better physical properties.

ACKNOWLEDGEMENTS

This work was supported by The Scientific and Technological Research Council of Turkey (Project number: 109S433).

REFERENCES

1. Sivaramakrishnan, R., Nakamura, C., Mehnert, W., J Control Release, 97, 493-502, 2004.
2. Santos Maia, C., Mehnert, W., Schaller, M., J Drug Target, 10, 489-495, 2002.
3. Senyigit, T., Sonvico, F., Barbieri, S., J Control Release, 142, 368-373, 2010.
4. Yu, H.Y., Liao, H.M., Int J Pharm, 127, 1–7, 1996.
5. Touitou E., J Control Relaese, 65, 403-418, 2000.

DRUG DELIVERY OF SYNTHETIC ANTISENSE-DNA "BIOCONJUGATES" FOR ANTICANCER THERAPY

L. Basile*[1], V. Greco[2], C. B. M. Platania[3], C. La Rosa[2], D. Milardi[4], S. Sciuto[2], S. Guccione[3]

[1] Etnalead s.r.l., c/o Etna Building -Scuola Superiore di Catania –Via S. Nullo 5/i I-95124 Catania, Italy; [2] Department of Chemical Sciences - University of Catania- V.le A.Doria 6 Ed. 3 Città Universitaria, I-95125 Catania, Italy; [3] Department of Drug Sciences - University of Catania- V.le A.Doria 6 Ed. 2 Città Universitaria , I-95125 Catania, Italy; [4] Istituto CNR di Biostrutture e Bioimmagini - Sezione di Catania- Department of Chemical Sciences, V.le Andrea Doria 6 Ed. 3 Città Universitaria , I-95125 Catania, Italy.

INTRODUCTION

Angiogenesis is the process of blood vessel formation from the pre-existent ones. It is a crucial event in the transition from dormant to malignant tumors. The stoppage of blood provision in cancer cells leads to the inhibition of their growth, thus this strategy has been applied in cancer treatment. Our antiangiogenetic approach aims to silence the expression of mRNA encoding the VEGF (Vascular Endothelial Growth Factor) using a modified oligonucleotide (ODNs), targeted to the 261-275 codifying region common to all splicing isoforms of VEGF [1-2]. We have recently synthesized [3] some 5'-*O*-phosphatidyl-tetradecanucleotides, differing in the fatty acid composition of the phosphatidyl moiety and showing a nucleotide sequence complementary to the above mentioned VEGF (Fig. 1).

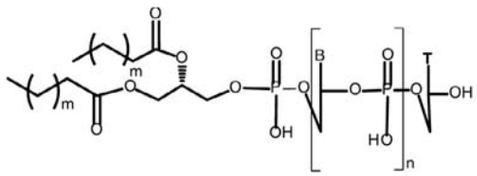

m =14,16,18. n= 14.

Fig. 1: General structure of modified antisense ODNs

These amphiphilic compounds which have potential in the gene therapy of cancer, have shown a tendency to self-aggregate at micromolar concentration (UV-DSC). The ability to introduce
genetic material into cells (i.e., transfection) to either overexpress or inhibit protein expression has boosted developments of nanotechnology applied to gene therapy, since the use of viral-vectors has limits as delivery system [3-6]. With the aim to increase the delivery of our novel antisense pro-drug to malignant target cells, we are developing high biocompatible nanoparticles such as stealth [7] and no-stealth liposomes [8]. DSC studies involving LUVs-antisense bioconjugates were carried out to qualitatively and quantitatively evaluate the grafting of the pro-drug on the nanoparticle surface. Stealth liposomes will be prepared and characterized for *in vivo* studies.

METHODS

Lipo-antisense bioconjugates were synthesized, on solid phase, using a synthetic methodology which allows to avoid the final treatment with ammonium hydroxide commonly used to detach and deprotect the oligo. In this way oligonucleotides conjugated to base-labile moieties may be obtained.

The synthetic pathway was applied aiming to obtain antisense phosphatidyloligonucleotides differing each other either in their phosphatidyl moiety (consisting of different fatty acids) and/or in their sequence.

LUV preparations: Lipid dispersions were prepared by dissolving the required amounts of DPPC and PEG–DSPE lipids in chloroform. The solvent was evaporated in a nitrogen gas stream and then kept under *vacuum* overnight. The dried lipid samples were fully hydrated with PBS at pH 7.4 by heating at 60°C and periodically vortexing for 40 min until homogeneous lipid dispersions were obtained. Three preparations were produced for each sample. To obtain LUVs, MLV (Multi Lamellar Vesicles) prepared by film hydratation were extruded through polycarbonate membrane (mesh 2500 Å).

DSC (Differential Scanning Calorimetry) was used for the assessment of the thermotropic parameters of the nanoparticles.

A VP-DSC micro-calorimeter was used to assess the Tm (melting temperature) of the DNA hybrid duplexes. DSC was used for assessment of thermotropic parameters of nanoparticles.

MD (Molecular Dynamics): The CMC of our phosphatidyl-antisense has been determined by means of long-term MD all-atom simulations, using different number of replies. These simulation might be useful to predict the structure of aggregates.

RESULTS AND DISCUSSION

DSC was used to analyzed the thermal stability of the sense-antisense duplex. The 5'-O-[1,2-Di-O-miristoyl-sn-glycero-3-phosphoryl]-tetradecamer showed a typical ODN melting-, with a Tm value higher than the control (Fig. 2) suggesting potential use of those bioconjugates as mRNA-silencing pro-drugs realized by eincapsulating into colloidal carriers. The insertion of acylic chains at the level of LUV membranes as a consequence of the Phophatidyl Antisense ODNs amphiphylic nature was confirmed .

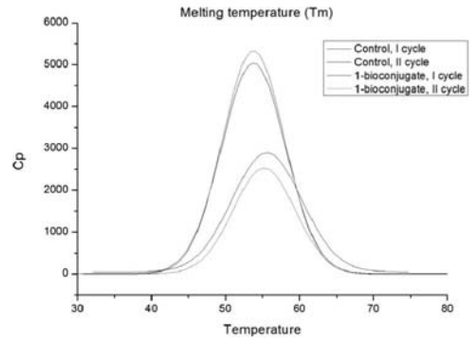

Fig. 2: DSC scan cycles; Transition temperature of DNA duplex unfolding. Control: unmodified antisense (5'-TGGCTTGAAGATGT-3') and sense.

REFERENCES

1. Mongerard-Coulanges M, Migianu-Griffoni E, Lecouvey M, Jolles B. Impact of alendronate and VEGF-antisense combined treatment on highly VEGF-expressing A431 cells. Biochemical Pharmacology. 2009; 77, 1580–1585.
2. Rizwan Masood, Jie Cai et al. Vascular endothelial growth factor/vascular permeability factor is an autocrine growth factor for AIDS-Kaposi sarcoma. Medical Sciences Proc. Natl. Acad. Sci. USA. 1997; 94: 979–984.
3. Chillemi R, Greco V, Sciuto S, XXIII National Meeting of SCI. Sorrento 5-10 July 2009 (Italy).
4. Anand V, Duffy B, Yang Z, Dejneka NS, Maguire AM, Bennett. A deviant immune response to viral proteins and transgene product is generated on subretinal administration of adenovirus and adeno-associated virus. J Mol. Ther. 2002; 5(2): 125–132.
5. Caminade AM, Majoral JP. Nanomaterials based on phosphorus dendrimers. Acc. Chem. Res. 2004; 37(6); 341–348.
6. Caminade AM, Turrin CO, Majoral JP. Dendrimers and DNA: combinations of two special topologies for nanomaterials and biology Chemistry. 2008; 14(25): 7422–7432.
7. Liu XX, Rocchi P, Qu FQ et al. PAMAM dendrimers mediate siRNA delivery to target Hsp27 and produce potent antiproliferative effects on prostate cancer cells. Chem. Med.Chem. 2009; 4(8): 1302–1310.
8. Pappalardo M et al. Journal of Thermal Analysis and Calorimetry. 2005; 80: 413-418.
9. Gonçalves E et al. The effect of liposome size on the final lipid/DNA ratio of cationic lipoplexes. Biophysics Journal. 2004; 86: 1554-1563.

IN-SITU PREPAPARATION OF ZnO AND ZnO/ SILICA PARTICLES ON DIFFERENT FIBERS

Dajana Japić[1], Tina Maver[2,3], Karin Stana-Kleinschek[2,3], Zorica Crnjak Orel[1,3*]

[1] National Institute of Chemistry, Hajdrihova 19, 1000 Ljubljana, Slovenia; [2] University of Maribor, Faculty of mechanical engineering, Smetanova ul. 17, 2000 Maribor, Slovenia; [3] Centre of excellence Polimat, Tehnološki park 24, 1000 Ljubljana, Slovenia

INTRODUCTION

Wound treatment is very profitable and therefore one of the largest markets in the world. One of most important aspect to consider is the limitation of infections (1). In the past few decades ZnO has attracted greater attentions because of its interesting physical and chemical properties. Our group already published different ways of preparation of ZnO from nano to micro size (2, 3). ZnO is a metal oxide, which is very stable and has a longer life than organic-based antimicrobial agents (4). This is especially important for harsh conditions as high pressure and temperature occurring during product manufacturing (5). In this study we evaluate the new approach of in-situ synthesis of zinc oxide (ZnO) nanoparticles and ZnO with silica on different polysaccharides based materials, already used in wound treatment. Materials coated with ZnO nanostructures show an excellent antimicrobial activity against *Escherichia coli* bacteria. The problem of ZnO nanoparticles toxicity was considered and was avoided by use of larger nanoparticles.

MATERIALS AND METHODS

As a starting material for synthesis $Zn(NO_3)_2x6H_2O$ (Sigma-Aldrich), LiOH (Sigma –Aldrich), MQ water, etylenglycol (Sigma-Aldrich) absolute EtOH (Sigma-Aldrich), ammonia solution 25% (Merck), tetraethyl ortosilicate (TEOS) (Sigma-Aldrich), and different fibres (cotton, washed viscose, two times washed viscose, and alginate) were used.

In-situ preparation of ZnO and ZnO /silica on different fibres

Zinc nitrate (0,1M) and LiOH (0,1M) were dispersed in the solvent mixture, ethylene glycol/MQ water at volume ratio (1:5). In some samples TEOS ($9{,}78x10^{-4}$M) was added. For in-situ preparation method we added fibres in already prepared solutions in order to cover fibres with ZnO and ZnO/silica particles. For each deposition of ZnO or ZnO/TEOS we weight the quantity of fibre to control the ratio of deposited ZnO or ZnO/TEOS on them. Synthesis was carried out in the glass bottle without stirring, for 2 hours at temperature 100 ˚C. After synthesis, fibres were washed with MQ water, filtered and dried at the room temperature.

SEM microscopy

Products were characterized by scanning field emission electron microscopy (FE-SEM, Zeiss Supra 35 VP).

IR spectroscopy

FTIR spectrometer, (Perkin Elmer 2000) was used for obtain IR spectra. The KBr pellet technique was used for the sample preparation.

Antimicrobial testing

Modified AATCC standard method (AATCC Test Method 100-1999) was used in order to test material's antimicrobial activity. Test organism was *E. coli*, while Trypticase Soy Agar (TSA); pH = 7.2 ±0.1 was used as culture medium.

RESULTS AND DISCUSSION

SEM images presented in (Fig 1.) shows structure of pure fibre (a, d, g), after covering with pure ZnO (b, e, h) and after covering ZnO/silica (c, f, i). The particles of ZnO are nicely visible on the fibres. It is obvious that after addition of TEOS the ZnO particles more homogenously covered the surface of the fibres. In some cases (washed viscose and alginate) the quantity of materials on fibres (Table 1) is higher after addition of TEOS.

Table 1: Quantity of ZnO on fibres material (g ZnO/g fibre). Samples 1, 3, 5 and 7 were prepared with addition of TEOS.

Sample	Type of fibre	g ZnO/g fibre
1	washed viscose	0.1650
2	washed viscose	0.1096
3	cotton	0.2191
4	cotton	0.2586
5	2 times washed viscose	0.1436
6	2 times washed viscose	0.1520
7	alginate	1.1837
8	alginate	0.3927

Based on SEM images and results shown in table (Fig. 1), we decided to reduce the concentration of ZnO particles on the fibres, because we wanted to achieve the highest antimicrobial effectiveness at the lowest concentration of ZnO. The loaded concentration of ZnO particles on fibres (samples 1 and 2) are presented in (Table 2) on which we performed antimicrobial tests for the bacterium *Escherichia coli* .

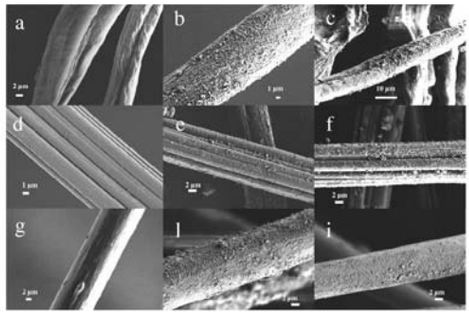

Fig. 1: SEM images for different fibres with ZnO and ZnO /TEOS: a) cotton, b) sample 3 c) sample 4 d) washed viscose, e) sample 5, f) sample 6 g) alginate, h) sample 7, i) sample 8.

All IR spectra (Fig. 3), of all prepared samples confirmed the formation of ZnO due to presence of stretching mode in the range from 600 up to 370 cm^{-1}.

Table 2: Antimicrobial efficiency of tested material with incorporated ZnO nanoparticles.

Sample	Concentration (g ZnO/g viscose)	% of reduction *E. coli*
washed viscose	0	no reduction
Sample1	0.1096	99.3 %
Sample2	0.1650	99.6 %

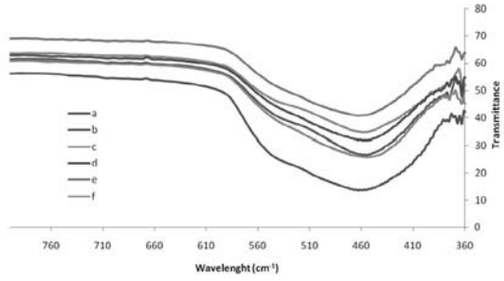

Fig 3: IR spectra of samples prepared from precursors (0,1M $Zn(NO_3)_2x6H_2O$ and LiOH) on a) cotton, b) washed viscose, c) alginate and precursor with addition of TEOS on d) cotton, e) washed viscose, f) alginate.

Obtained results as presented in (Table 2) with the lowest concentration of ZnO on washed viscose fibres were tested for antimicrobial efficiency and they confirmed very good percent of reduction of *Escherichia coli* which was more than 99%.

CONCLUSIONS

Presented material (sample 1, 2, 3, 4, 5, 6, 7, 8) was very well covered with ZnO, and ZnO/silica. The excellent percent of reduction of *Escherichia coli* were confirmed for samples of washed viscose.

ACKNOWLEDGMENT

We acknowledge the financial support from the Ministry of Higher Education, Science and Technology of the Republic of Slovenia through the contract No. 3211-10-000057 (Centre of Excellence for Polymer Materials and Technologies).

REFERENCES

1. Yudanova TN, Reshetov IV. Modern wound dressings: manufacturing and properties. Pharm. Chem. J. 2006; 40; 24 – 31.
2. BITENC, Marko, PODBRŠČEK, Peter, CRNJAK OREL, Zorica, CLEVELAND, Michael A., PARAMO, Jorge Antonio, PETERS, Raul M., STRZHEMECHNY, Yuri M. Correlation between morphology and defect luminescence in precipitated ZnO nanorod powders. Cryst. growth des., 2009, vol. 9, no. 2, str. 997-1001.
3. BITENC, Marko, DRAŽIĆ, Goran, CRNJAK OREL, Zorica. Characterization of crystalline zinc oxide in the form of hexagonal bipods. Cryst. growth des., 2010, vol. 10, no. 2, str. 830-837
4. Zhang L, Jiang Y, Ding Y, Daskalakis N, Jeuken L, Povey M, O'Neill A, York D. Mechanistic investigation into antibacterial behaviour of suspensions of ZnO nanoparticles against E.coli. J. Nanopart. Res. 2010; 12; 1625 – 1636.
5. Sawai J. Quantitative evaluation of antibacterial activities of metallic oxide powders (ZnO, MgO and CaO) by conductimetric assay. J. Microbiol. Methods. 2003; 54; 177 – 182.

ELECTROSPUN NANOFIBERS FOR TOPICAL DRUG DELIVERY

I. Wagner[1,*], H. Pataki[1], A. Balogh[1], Zs. K. Nagy[1], A. H. Harasztos[2], Á. Suhajda[2], Gy. Marosi[1]

[1] Budapest University of Technology and Economics, Department of Organic Chemistry and Technology, Budafoki út 8. 1111, Hungary; [2] Budapest University of Technology and Economics, Department of Applied Biotechnology and Food Science, Műegyetem rkp. 3. 1111, Hungary

INTRODUCTION

In the beginning of the XXI[st] century, which is the great period of biotechnology, one of the largest challenges in the field of pharmaceutical technology is the formulation of biopharmaceuticals, which are generally very sensitive to the physical and chemical properties of their environment. After the biotechnological process biodrugs are in aqueous medium, where many of them have low stability, what can lead low stability in the product as well (1). Therefore it might be very advantageous to design solid forms what provides good stability of biodrugs and easy administration. However, the available techniques, such as freeze drying, have several drawbacks. Another very challenging field for pharmaceutical technologists is formulation of poorly water soluble drugs (2). Recently the number of drug candidates of low water solubility increases continuously due to the applied screening and test methods and due to the limited patentability of molecules with low molecular weight. Preparation of nanofibers by electrostatic spinning has been introduced recently and used successfully in various scientific fields such as composites, filters, tissue engineering and pharmaceutical technology as well (3,4,5). In this work an antiviral protein, a probiotic bacteria and Carvedilol with poor water solubility were used as model drugs to investigate the capabilities of electrospun materials to improve the stability of biodrugs and the dissolution rate of Carvedilol. Besides using this technology the topical drug delivery (creating an orally dissolving web (ODW) for instance) can be feasible.

MATERIALS AND METHODS

Materials

Polyvinyl-pyrrolidone (PVP) (molecular weight: PVP K30: ~ 50000 Da) was kindly provided by BASF (Ludwigshafen, Germany). Carvedilol was originated from Sigma-Aldrich (Budapest, Hungary).

Electrostatic spinning process

The electrostatic spinner used for the experiments was equipped with NT-35 High Voltage DC Supply. The utilized electrical potential on the spinneret electrode was between 10–35 kV which was adjusted during the experiments. A grounded steel plate covered with teflon was used as collector. Polymer solutions were dosed by SEP-10S Plus syringe pump. The experiments were performed at ambient temperature (25°C).

Dissolution test followed by UV-VIS

Dissolution of the Carvedilol from the electrospun mats were performed by Erweka DT6 dissolution tester. Concentrations of the collected samples were measured by Hewlett Packard 8452A type UV spectrophotometer.

Protein analysis

Protein analysis was carried out by Lab-on-a-chip (Laboratory on a chip (LOC)) technique (Agilent bioanalyzer 2100) what performs micro system capillary electrophoresis.

RESULTS AND DISCUSSION

Carvedilol dissolution results

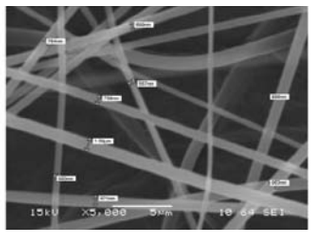

Fig. 1: SEM image of the Carvedilol (12%) loaded PVP nanofibers

SEM image (Fig. 1) confirms that nanofibers were formed with huge surface area which is very promising from the dissolution point of view.

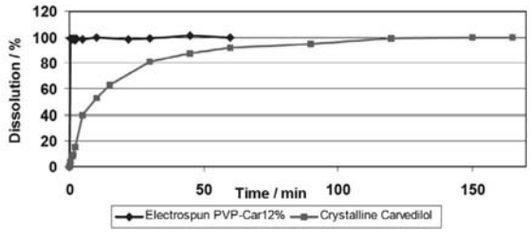

Fig. 2: Dissolution of the Carvedilol samples, Blue: electrospun PVP-Carvedilol (12%), Violet: crystalline Carvedilol

The electrospun mats were dissolved in water immediately as they were immersed in the dissolution media. It means that the drug release was instant (~2 sec.) and the dissolution of Carvedilol was decreased from 2 hours down to few seconds by electrospun nanofibers (Fig. 2).

Protein encapsulation

Generally the biggest challenge during the formulation of proteins is the avoidance of the aggregation. According to our measurements the protein did not aggregate during the electrospinning process. It can be ascribed probably to the gentle treatment and to the protecting action of the PVP

macromolecules. This result means that the formulation of sensitive proteins can be solved this way with avoidance of the aggregation.

Probiotic bacteria encapsulation

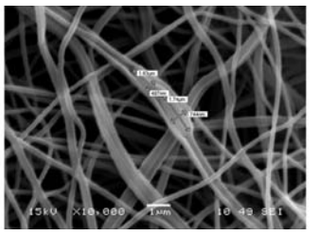

Fig. 3: SEM image of probiotic bacteria embedded in polymer nanofibers

SEM image (Fig. 3) enabled to see how the polymer fiber gets thicker and encompasses two rod-shaped bacterium adhered to each other. It made clear that polymer coating was formed around bacteria during the process. The size of bacteria is similar to their original form (width: ~0.5-0.9 µm length: ~1.3-2 µm). Viable testing showed the nanofibers contain a huge amount of living bacteria. These results demonstrate that electrospinning is a capable technique to encapsulate living probiotic bacteria into polymer nanofibers forming a biohybrid nanoweb.

REFERENCES

1. Dave A. Parkins, Ulla T. Lashmar, The formulation of biopharmaceutical products. Pharmaceutical Science & Technology Today 2000, 129-137
2. Patyi G., Bódis A., Antal I., Vajna B., Nagy ZK., Marosi G. 2010. Thermal and spectroscopic analysis of inclusion complex of spironolactone prepared by evaporation and hot melt methods. Journal of Thermal Analysis and Calorimetry 102: 349-355.
3. Kostakova E., Meszaros L., Gregr J. 2009. Composite nanofibers produced by modified needleless electrospinning. Materials Letters 63: 2419-2422.
4. Verreck G., Chun I., Peeters J., Rosenblatt J., Brewster M.E., 2003. Preparation and characterization of nanofibers containing amorphous drug dispersions generated by electrostatic spinning. Pharmaceutical research 20: 810-817.
5. Nagy, ZK., Nyúl K., Wagner I., Molnár K., Marosi G., 2010. Electrospun water soluble polymer mat for ultrafast release of Donepezil HCl. Express Polymer Letters 4: 763–772.

INVESTIGATION OF PHYSICAL METHODS FOR EFFECTIVE STABILIZATION OF PVA NANOFIBERS

R. Rošic*, J. Pelipenko, P. Kocbek, S. Baumgartner, J. Kristl

University of Ljubljana, Faculty of Pharmacy, Aškerčeva cesta 7, 1000 Ljubljana, Slovenia

INTRODUCTION

Electrospun nanofibers are one of the most modern forms of nanocomposite systems and have been widely studied in recent years due to their ease of formulation and unique characteristics, among which their ability to mimic the fundamental elements of the natural extracellular matrix outstands (1). Therefore, nanofibers are promising candidates for many biomedical applications, such as wound dressings, drug delivery and scaffolds for tissue engineering (2). A promising functional material for nanofiber preparation has been polyvinyl alcohol (PVA) due to its good chemical stability, hydrophilicity, biocompatibility, nontoxicity and excellent electrospinnability. However, its water solubility limits it's extended application in biomedical field (3).

The aim of this study was to design biomimetic PVA nanofibers with low water solubility or improved water resis- tance. To achieve that, nanofibers were pared by electrospinning and further stabilized by different physical methods. Our goal was to increase stability and avoid use of any toxic cross–linking agent.

MATERIALS AND METHODS

Preparation of the solution

PVA solution (8 % w/w) was prepared from PVA powder (Mowiol 20-98, M_w 125 000 g/mol, Sigma-Aldrich) by dissolving the weighted amount of the polymer in distilled water at 90°C for 2 hours.

Electrospinning

The solution was placed in a 20 ml syringe with a 0.8 mm needle on which the high voltage supply of 15 kV was connected. The grounded planar collector covered with aluminium foil was located at a distance of 15 cm from the needle tip and flow rate was set to 0.707 ml/h.

Characterization of nanofibers

Morphology of electrospun nanofibers was examined using a scanning electron microscope (SEM, 235 Supra 35VP-24-13, Carl Zeiss, Germany) operated at an accelerating voltage of 1 kV, with a secondary detector without coating with any conductive layer before imaging.

Stabilization of nanofibers

Different approaches for physical cross linking of obtained nanofibers were used. Nanofibers were soaked in two non-solvents, ethanol and methanol respectively, for 24 hours. Additionally, nanofibers were heat treated at 160° C for 10 min. The hydratation of the stabilized nanofibers in physiological environment was studied by immersion in phosphate buffer (pH 7.4) (PBS) and weighting the samples at regular time interval.

RESULTS AND DISCUSSION

Figure 1a shows SEM image of electrospun PVA nanofibers at 5000 x magnification. It can be seen that the matrix is consisted of a very uniform fibers with diameters of 150 ± 29 nm and smooth surface. However, when the PBS was purred onto white PVA network, it instantly became transparent and has completely dissolved. Thus the unique nanofibrous structure was lost. Therefore, the stabilization of PVA nanofibers is essential in order to successfully use them in physiological environment.

The stabilization of PVA fibers against water can be accomplished using various physical and chemical cross linking methods. Chemical cross linking demands usage of reactive species that can remain in the sample and can compromise biocompatibility. Therefore, the physical stabilization by soaking in non-solvent (methanol and ethanol, respectively) and heat treatment were chosen.

Fig. 1b-c shows SEM images of nanofibers after stabilization. It can be clearly seen that there are no visible changes in nanofiber morphology after heat treatment, whereas nanofiber network stabilized in alcohol has changed, but the fibrous structure was still preserved.

As mentioned before, un-stabilized PVA nanofibers dissolve in PBS instantly. On the other hand all physically stabilized nanofibers retain they integrity for more than 96 h (Fig. 2). Moreover, our results show that stabilization method does not have a significance impact on the hydratation.

The main reason for prolonged water resistance of stabilized PVA is increased degree of cristallinity, which acts as physical cross links and stabilize the nano-fibers. This may occur by removal of residual water within the nanofibers by the alcohol or increased temperature, allowing PVA-water hydrogen bonding to be replaced by intermolecular polymer hydrogen bonding resulting in additional crystallization (4). Since such mechanism is present in all three stabilization methods, this is probably the reason why there is no observed major difference in behaviour of nanofibers in physiological environment.

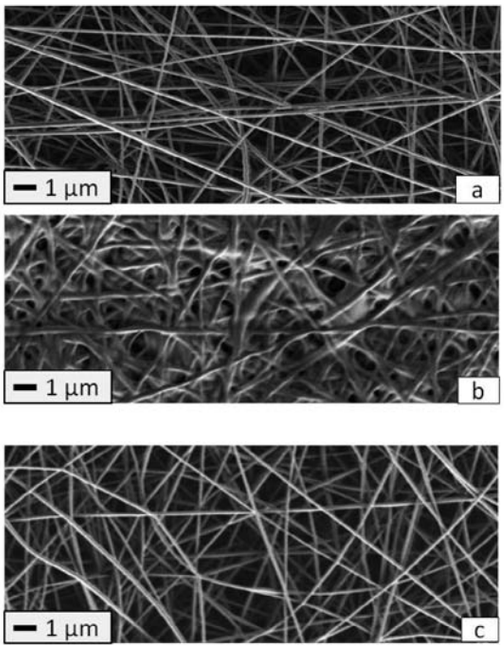

Fig. 1: Representative SEM images of a) untreated PVA nanofibers, b) PVA nanofibers after soaking in non-solvent for 24h and c) PVA nanofibers after heat treatment (160° C 10 min)

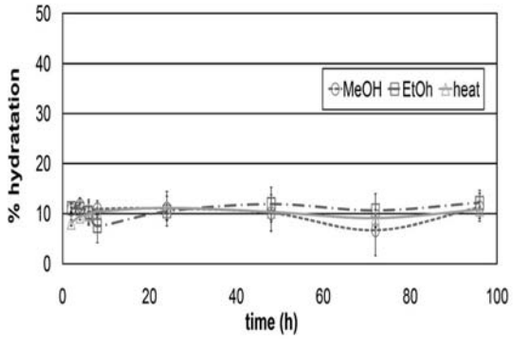

Fig. 2: Degree of hydratation (%) of nanofibers stabilized with methanol, ethanol and heat, respectively.

CONCLUSIONS

The electrospun PVA nanofibers were successfully stabilized against disintegration in physiological environment by a simple soak in non-solvent or heat treatment. Regardless physical method used all stabilized nanofibers gain their resistance in physiological environment for longer period of time. Hence, incorporation of active substances into stabilized PVA nanofibers could be undoubtedly used as biocompatible and biomimetic drug delivery systems with prolonged release.

REFERENCES

1. Rošic R, Kocbek P, Baumgartner S, Kristl J. Electrospun hydroxyethyl cellulose nanofibers: the relationship between structure and process. J. Drug Del. Sci. Tech. 2011; In Press
2. Beachley V, Wen X. Polymer nanofibrous structures: fabrication, biofunctionalization, and cell interactions. Progress in Polym. Sci. 2010 ; 35: 868-892
3. Cao S, Liu Z, Hu B, Liu H. Stabilization of electrospun PVA nanofibrous mats in aqueos solutions. Chin. J. Polym. Sci. 2010; 28 (5): 781-788
4. Yao L. at al. Electrospinning and stabilization of fully hydrolyzed PVA fibers. Chem.. Mater. 2003; 15:1860-1864

NOVEL METHOD FOR PREPARATION OF AMORPHOUS COMPOSITE NANO-FIBERS OF PIROXICAM

U. Paaver[1,*], I. Laidmäe[1], J. Kozlova[2], J. Heinämäki[1], K. Kogermann[1], P. Veski[1]

[1] University of Tartu, Department of Pharmacy, Nooruse 1, Tartu 50411, Estonia;
[2] University of Tartu, Institute of Physics, Riia 142, Tartu 51014, Estonia

INTRODUCTION

Many poorly water-soluble crystalline active pharmaceutical ingredients (APIs) can exist in different polymorphic or solvated crystal forms, and also in amorphous state. The amorphous form has an enhanced dissolution and bioavailability compared to the crystalline state, but being physically unstable it has a tendency to spontaneously crystallise back to the crystalline state (1). Piroxicam (PRX) is a poorly water-soluble polymorphic API which belongs to Class II (high permeability, low solubility) in the Biopharmaceutical Classification System. Amorphous state of PRX can be obtained only by ball-milling at low temperature and it is very unstable (2). Electrospinning is an effective and simple method to fabricate polymer nanofibers with a diameter from a few nanometers to several micrometers and a large surface area (3). Electrospinning could be a novel approach for stabilising APIs in amorphous state, and consequently, improving their dissolution rate. For poorly water-soluble APIs, enlarging of surface area and/or modification of solid state form may offer a convenient way to improve their dissolution rate.

The aim of the present study was to investigate electrospinning as a technique for fabricating amorphous composite fibers of API and polymer. Special attention was paid on the effects of a hydrophilic polymer and solvent system on solid-state properties and stability of the composite fibers.

MATERIALS AND METHODS

Materials

PRX (Letco Medical, Inc. USA) was used as a model API. Different grades of hydroxypropyl methylcellulose, HPMC (Methocel K100M premium CR; K4M premium CR; K100 premium LV) were kindly gifted from Colorcon Ltd (England). The primary solvents, 1,1,1,3,3,3-Hexafluoro-2-propanol (HFIP) (≥99,0%) and methanol, were purchased from Sigma-Aldrich Chemical Company and the other solvents (acetone, ethanol, 2-propanol) were from Lach-Ner, s.r.o., (Czech Republic). All these materials were used as received without further purification.

Methods

A schematic diagram of the electrospinning process is shown in Fig. 1. The high voltage power supply Gamma High Voltage Research (Model No. ES3OP-10W/DAM, USA) was used for electrospinning. The voltage applied was 7 kV. The distance between the spinneret and the fiber collector was 8 cm. The automatic syringe pump KdScientific (Model No: KDS-250-CE, Geneq Inc, USA) was used with a pumping speed of 1 ml/h.

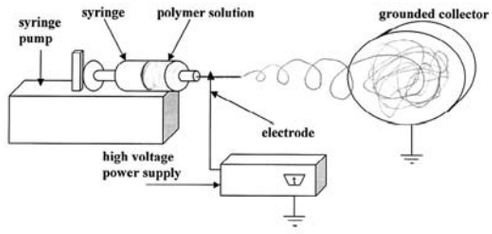

Fig. 1: Schematic diagram of the electrospinning equipment.

Solid-state properties of starting materials and electrospun composite fibers were studied by means of X-ray powder diffractometer (XRPD) (D8 Advance, Bruker AXS GmbH, Germany) and Raman spectroscopy (B&W TEK inc., USA). The morphology of fibers was investigated with a Scanning Electron Microscope (SEM) (Helios NanoLab 600, FEI Company). The electrospun nanofibers were investigated immediately after the preparation and after 1 week short-term aging at 0%RH and low temperature (6°C).

RESULTS AND DISCUSSION

The XRPD patterns of crystalline PRX forms (PRX monohydrate, PRX anhydrate forms I and II), and electrospun composite nanofibers revealing amorphous PRX are shown in Fig. 2. In order to fabricate electrospun nanofibers with a large surface area, the quick solvent evaporation is important. The best polymer-solvent combination for electrospinning was found to be a 0.8 % solution of Methocel K100M premium CR in HFIP. The present nano-fibers contained PRX in amorphous form immediately after fabrication and after a one week aging period, indicating the improved stability of amorphous PRX (Fig. 2).

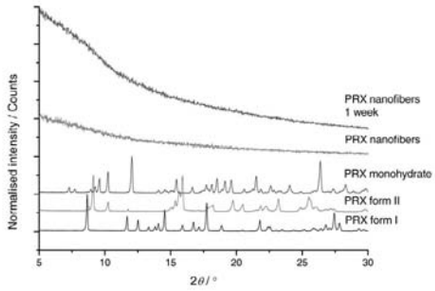

Fig. 2: XRPD patterns of crystalline PRX forms and nanocomposite fibers consisting amorphous PRX on 0 day, and after 1 week of storage. All data are normalised.

Scanning electron micrographs (SEMs) on the electrospun nanofibers are shown in Fig. 3. The thickness of the composite nano-fibers are slightly larger (ranging from 400 to 600 nm) than that of the reference electrospun fibers fabricated from the pure polymer-solvent system (200 - 400 nm). In addition, pure nanofibers without PRX show more uniform structure and smooth surface.

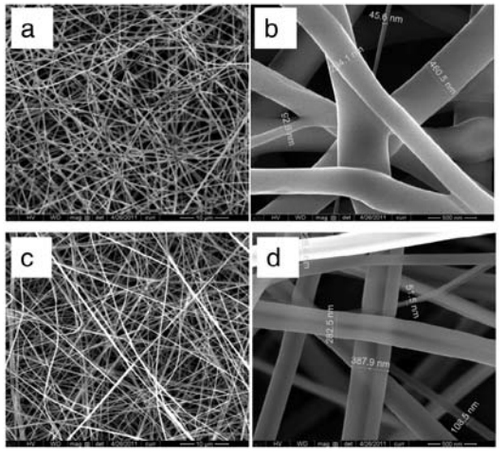

Fig. 3: SEM micrographs of electrospun nanofibers with PRX a) magnification x5000, b) x50000, and without PRX c) magnification x5000 and d) x50000.

CONCLUSIONS

Electrospinning process can be used to fabricate amorphous HPMC and PRX composite nanofibers. It seems that amorphous state of PRX exists also after a short-term aging at low temperature. Physical stability of amorphous PRX can be improved by electrospinning it together with HPMC.

ACKNOWLEDGEMENTS

This work is part of the targeted financing project no SF0180042s09 and ETF grant project no ETF7980. Estonian Minister of Education and Research is acknowledged for financial support. Mr. J. Aruväli (X-ray laboratory of Institute of Ecology and Earth Sciences, University of Tartu) and Prof. V.Sammelselg (Institute of Physics, University of Tartu) are acknowledged for the XRPD and SEM experiments, respectively.

REFERENCES

1. Hancock BC, Zografi G, Characteristics and Significance of the Amorphous State in Pharmaceutical Systems. Journal of Pharmaceutical Sciences, 1997; Vol. 86, No. 1:1-12.
2. Vrečer F, Vrbinc M, Meden A, Characterization of piroxicam crystal modifications. Int. J. Pharm. 2003; 256: 3-15.
3. Agarwal S, Wendorff JH, Greiner A, Use of electrospinning technique for biomedical applications. Polymer, 2008; 49: 5603-5621.

RHEOLOGICAL PROPERTIES OF PVA SOLUTION INFLUENCING ITS ABILITY TO ELECTROSPIN

J. Pelipenko*, R. Rošic, S. Baumgartner, J. Kristl

University of Ljubljana, Faculty of Pharmacy, 1000 Ljubljana, Slovenia

INTRODUCTION

Nanofibers are solid fibers with diameter in nanometer scale and theoretically unlimited length. In recent years the interest in nanofibers has greatly increased their potential use in different biomedical fields, especially in those where high surface to volume ratio and high porosity of nanocomposite systems is needed (1).

Moreover, polymer nanofibers have appropriate structure for the development of tissue substitutes, since their physical and chemical properties are able to mimic natural extracellular matrix and thus accelerate tissue regeneration (2).

Modern, versatile and widely used method for nanofiber prepararion is electrospinning. Previous studies have shown that efficiency of electrospinning process and morphology of nanofibers strongly depend on both, solution and process parameters (3).

The aim of our study was to investigate the rheological properties of poly-(vinyl alcohol) (PVA) solutions and determine the correlation between rheological properties and ability to electrospin.

MATERIALS AND METHODS

Preparation of polymeric solutions

PVA solutions in concentration range 7% - 12% were prepared by dissolving the weighted amount of powder (Mowiol 20-98, MW=125.000g/mol, Clariant, Frankfurt, Germany) in distilled water at 90 °C for 2 hours. Solutions were stirred on magnetic stirrer for another 24 hours.

Rheological characterisation

Before electrospinning the viscosity, elastic modulus (G') and plastic modulus (G") of prepared polymeric solutions were determined by cone-plate system (diameter: 49,961 mm, angle 2,001°) of rheometer Physica (model MCR 301, Anton Paar, Austria) at 25 °C.

Electrospinning

Polymer solution was placed in a plastic syringe with metal needle and inner diameter 0,8 mm. The syringe was mount in the pump (model R-99E,

RazelTM) that maintained steady flow rate. A high voltage on the needle was achieved by connection to a voltage generator (model HVG-P60-R-EU, Linari Engineering s.rl. Italy). Planar collector covered with aluminium folium was placed 15 cm from the needle, flow rate was set on 0,7070 ml/h and applied voltage was 15 kV.

SEM characterisation of nanofibers

Nanofibers were characterised with SEM, 235 Supra 35VP-24-13, Carl Zeiss, Germany, operated at an accelerating voltage of 1 kV.

RESULTS AND DISCUSSION

Our results show that by increasing the concentration of PVA the viscosity increase, as well as elastic and plastic modulus (Fig. 1). The increase in viscosity is due to greater numbers of chain entanglements, which is also the reason for more homogenous and beads-free nanofiber morphology (Fig. 2). Therefore, the sufficient number of entanglements between chains is crutial for stabilization of electrospun jet (3). From Fig. 2 it can be observed that only concentrations above 8% (viscosity values above 0,27 Pas) posses sufficient number of entanglements for stabilisation and beads free nanofibers formation.

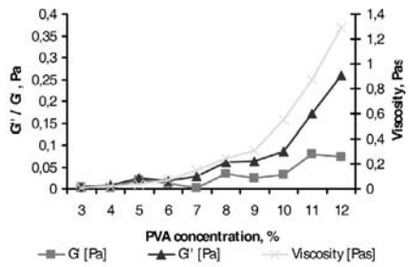

Fig. 1: Loss modulus, storage modulus and viscosity as function of polymer concentration

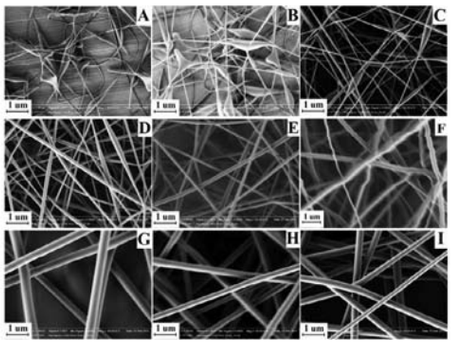

Fig. 2: SEM images of electrospun nanofibers; A-4% PVA, B-5% PVA, C-6% PVA, D-7% PVA, E-8% PVA, F-9% PVA, G-10% PVA, H-11% PVA, I-12% PVA, at 15 kV, flow rate 0,7070 ml/h and collector to needle distance 15 cm

Additionally we found out that increased polymer concentration resulted in thicker fiber diameter (Fig. 3). This can also be explained by increased number of entanglements between molecules, which reduce the thinning of the jet under the influence of applied voltage.

We also studied the correlation between elastic and plastic modulus and stabilization of the electrospun jet. Plastic modulus is a fraction of the energy that will be lost during loading system, while the elastic modulus represents the fraction of energy that will be stored. Measurements showed that both modulus increased with increased polymer concentration. It was determined that for efficient stabilization of the jet a considerable value of elastic module is needed, which ensures that the entanglements between the chains are maintained during the flight of electrospun jet to the collector. Fig. 1 and 2 show that the sufficient values of G' for beaded free nanofibers formation are above 0,02 Pa. As a result of lover values of G' beaded nanofibers are formed. Additionally, in our opinion interfacial rheological properties of polymeric solutions have an essential role for nanofibres formation, what will be discussed further.

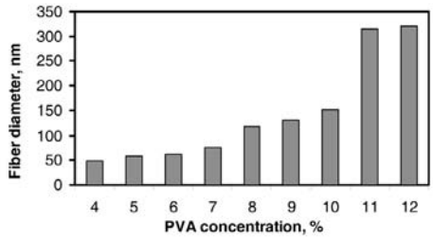

Fig. 3: Fiber diameter as a function of polymer concentration

CONCLUSIONS

It can be concluded that understanding the viscosity and elastic modulus can partially predict the successfulness of electrospinning. Our results show that at concentrations above 10 % viscosity begins to rise vigorously as well as the diameter of nanofiber.

The results enable the integration of chemical and physical aspects of polymer solutions and have a powerful impact on the rational design of suitable nanofibers for tissue engineering applications.

REFERENCES

1. Rošic R, Kocbek P, Baumgartner S, Kristl J. Electrospun hydroxyethyl cellulose nanofibers: the relationship between structure and process. J. Drug Del. Sci. Tech. 2011; In PressAli SL,
2. Beachley V, Wen X, Polymer nanofibrous structures: Fabrication, biofunctionalisation and cell interactions. Progress in Polymer Science, 35; 2010: 868-892
3. Gupta P, Elkins C, Long T, Garth L. Wilkes: Electrospinning of linear homopolymers of poly(methyl methacrylate): exploring relationships between fiber formation, viscosity, molecular weight and concentration in a good solvent, Polymer 2005; 46,4799–4810

NANOFIBROUS DRUG DELIVERY SYSTEMS FOR ENHANCED DISSOLUTION PREPARED BY ELECTROSPINNING

Z. K. Nagy[1*], A. Balogh[1], I. Wagner[1], P. Sóti[1], H. Pataki[1], K. Molnár[2], G. Marosi[1]

[1] Budapest University of Technology and Economics, Department of Organic Chemistry and Technology, 1111 Budapest Budafoki út 8, Hungary; [2] Budapest University of Technology and Economics, Department of Polymer Engineering, 1111 Budapest Műegyetem rkp 3, Hungary

INTRODUCTION

One of the largest challenges in the field of pharmaceutical technology is the enhancement of drug release from orally taken solid dosage forms as most of recently developed APIs are poorly soluble in water (1). Electrostatic spinning is a remarkably simple and efficient technique to generate water soluble polymeric fibers in submicron scale from polymer solutions (or melts) applying high electric voltage (2). Co-solution of polymer and API can be electrospun as well. This process, resulting in very fast drying, is advantageous from the formulation point of view of sensitive drugs. Generally the drying step is faster than 0.1 sec owing to the huge surface area formed during the spinning process and that it works in ambient temperature. Because of the ultra-fast drying there is no time for agglomeration or arrangement (recrystallization) of API molecules, thus, amorphous material is collected embedded in amorphous water soluble

polymer (PVP, PVA, PEG). Huge surface, amorphous physical state and water soluble polymer matrix are very promising to achieve adequate dissolution of poorly water soluble drugs (3). Bioavailability of drugs or drug candidates with good permeability and low water solubility (BCS II) is mainly dependent on the speed of dissolution step, thus, dissolution enhancement is often required (4). The aim of this work was to investigate solvent electrospinning and melt electrospinning techniques for improvement of the dissolution of drugs with poor water solubility. Electrospinning techniques were compared to melt-extrusion method. Isodymensional micro- and nanoparticles were also prepared using solvent-based electrospinning method. To map the industrial feasibility of electrospinning different types of solvent and melt electrospinning scaling-up capabilities were examined.

MATERIALS AND METHODS

Materials

Polyvinyl alcohol (PVA), purchased from Fluka (Buchs, Switzerland, molecular weight: 31000 Da), polyvinyl pyrrolidone (PVP) with two different chain lengths (molecular weight: PVP K12: 2500 Da, PVP K30: 50000 Da), kindly provided by BASF (Ludwigshafen, Germany) and Eudragit EPO was supplied by Evonik (Essen, Germany). Spironolactone was used as model drug and it was originated from Sigma-Aldrich (Budapest, Hungary).

Electrostatic spinning process

The electrostatic spinner used for the experiments was equipped with NT-35 High Voltage DC Supply (MA2000, Nagykanizsa, Hungary). The electrical potential applied on the spinneret electrode was adjusted during the experiments between 10-35 kV. Distance of the spinneret and the collector was 15 cm and the experiments were performed at room temperature (25 °C). Polymer solutions were dosed by SEP-10S Plus type syringe pump (Aitecs, Vilnius, Lithuania).

In vitro dissolution

The dissolution studies were performed by Erweka DT6 dissolution tester (Erweka, Heusenstamm, Germany). Concentrations of the collected samples were measured by Hewlett Packard 8452A type UV spectrophotometer.

RESULTS AND DISCUSSION

Morphology studies

According to microscopic investigations diameters of fibers were mainly in the submicron range (300-700 nm) in the case of Eudragit E-ethanol system (Fig 1). However, diameters of some thicker fibers were around 1 µm.

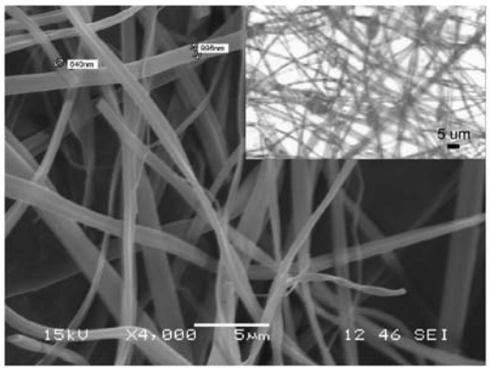

Fig. 1: SEM and optical microscopic images of EudragitE nanofibers loaded with 20 w/w % API

Fibers obtained by electrospinning of PVP-ethanol based systems had similar diameter distribution. In the case of melt electrospinning diameters of the fibers were significantly thicker (few microns).

Physical state of the API in the fibers and in the extrudates was examined by X-ray diffractometer (PANalytical X'pert Pro MDP).

Fig. 2 shows that successful amorphization of spironolactone was achieved using PVPK12 as a polymer matrix. Similar to PVPK12 XRD results amorphous systems were formed using the other polymers in all cases.

Raman map of electrospun Eudragit E - spironolactone (20 %) fibers acquired by Raman-microscope (Horiba Jobin Yvon, LabRam) showed practically perfect distribution of spironolactone forming a solid solution which was confirm by differential scanning calorimetric results. Spironolactone acted as a plasticizer since it lowered the glass transition temperature of Eudragit E.

Dissolution of spironolactone from the prepared solid forms were significantly faster owing to the successful amorphization of spironolactone, the increased wetting of spironolactone caused by polymer matrix and the formed huge surface area in the case of the electrospun ultrathin fibers.

Nanofibrous mat based orally dissolving web (ODW) technology was also successfully utilized for topical delivery. Scaling-up ideas of electrospinning applied in the textile industry are very promising for pharmaceutical applications as well.

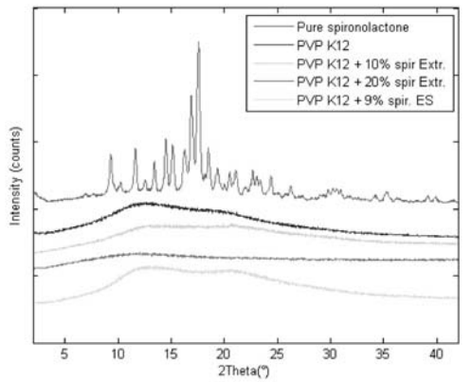

Fig. 2: X-ray diffractograms of PVPK12 based samples

ACKNOWLEDGEMENTS

This research was supported by OTKA Research Fund (code K76346), ERA Chemistry (code NN 82426) and New Hungary Development Plan (Project ID: TÁMOP-4.2.1/B-09/1/KMR-2010-0002).

REFERENCES

1. Keserű GM, Makara GM. The influence of lead discovery strategies on the properties of drug candidates. Nature Reviews Drug Discovery, 2009; 8: 203-212.
2. Nagy, ZK., Nyúl K., Wagner I., Molnár K., Marosi G., Electrospun water soluble polymer mat for ultrafast release of Donepezil HCl. Express Polymer Letters, 2010; 4: 763–772.
3. Nagy ZK., Sauceau M., Nyúl K., Rodier E., Vajna B., Marosi G., Fages J. Use of supercritical CO2-aided and conventional melt extrusion for enhancing the dissolution rate of an active pharmaceutical ingredient. Polymers for Advanced Technologies. 2011; Article in Press, doi: 10.1002/pat.1991
4. Patyi G., Bódis A., Antal I., Vajna B., Nagy Z., Marosi G., Thermal and spectroscopic analysis of inclusion complex of spironolactone prepared by evaporation and hot melt methods. Journal of Thermal Analysis and Calorimetry, 2010; 102: 349-355.

IN VITRO BIOCOMPATIBILITY OF ELECTROSPUN CHITOSAN-BASED NANOFIBERS

P. Kocbek[1,*], R. Rošic[1], A. Arranja[1,2], A. Fortuna[1], S. Baumgartner[1], J. Kristl[1]

[1] University of Ljubljana, Faculty of Pharmacy, Aškerčeva cesta 7, 1000 Ljubljana, Slovenia; [2] University of Lisbon, Faculty of Pharmacy, Av. Prof. Gama Pinto, 1649-003 Lisbon, Portugal

INTRODUCTION

The electrospun nanofibers show great potential in the management of wound healing and tissue regeneration, since their nanotopography resembles structure of extracellular matrix and may promote cell attachment and proliferation. However, electrospinning is very complex process affected by solution properties (viscosity, surface tension, conductivity) as well as process parameters (applied electric field, needle-to-collector distance, flow rate, type of the collector). The interplay among all these parameters governs the electrospining process and determines the final product (1). In current study chitosan (CS) was selected as a biocompatible, and biodegradable material for nanofiber formation, since it has been widely investigated for various biomedical applications, due to its haemostatic activity, promotion of normal tissue regeneration, bacteriostatic and fungistatic effects (2, 3). To improve its spinnability CS solution was supplemented with polyethylene oxide (PEO) as a spinnable carrier, Triton X-100 as a nonionic surfactant and dimethylsulphoxide (DMSO) as a cosolvent. The aim of the research was firstly to prepare and characterize CS/PEO blended solutions, then to produce electrospun nanofibers and finally to evaluate their biocompatibility using a keratinocyte cell line.

MATERIALS AND METHODS

Materials

CS with 75-85% degree of deacetylation (50-190 kD), PEO (900 kD), Triton X-100, and DMSO were all obtained from Sigma-Aldrich. Glacial acetic acid was from Merck. All other reagents used were of analytical grade. For cell culture experiments human keratinocyte cell line NCTC2544 was used (ICLC, Italy).

Blended polymer solutions

CS/PEO blended solutions were prepared by mixing 2% (w/v) CS solution with 3% (w/v) PEO solution in 30% aqueous acetic acid. The solutions were mixed in various CS/PEO ratios (v/v) (90/10, 80/20, 70/30, 60/40) and stirred on a magnetic stirrer for 5 h, then 0.3% (w/v) Triton X-100^{TM} and 10% (v/v) DMSO were added. Solutions were continuously stirred and their viscosity was measured before electrospinning using a modular compact rheometer (Physica MCR 301, Anton Paar) with a 50 mm measuring cone at 25.0±0.1°C.

Electrospinning

Horizontally set up electrospinning device consisted of 20 ml disposable syringe fitted with a metal needle (0.8 mm), a syringe pump (Model R-99E, RazelTM) to feed constant flow rate, a grounded collector covered with aluminium foil with or without fixed cover slips and a high voltage power supply (Model-P60-R-EU, Linari Engineering s.r.l., Italy). The electrospinning conditions were adjusted and the nanofibers were typically obtained at 20-22 kV, with 18 cm distance between the needle tip and the collector, and the flow rate set to 0.70 ml/h.

Washing of nanofibers

Obtained nanofibers were washed several times with 75% ethanol, water and PBS in order to remove residual solvent and to evaluate the effect of washing on the fiber structure.

SEM imaging

The dry samples were fixed onto metallic studs with double-sided conductive tape and analyzed using Supra 35 VP (Oberkochen, Zeiss, Germany) scanning electron microscope with an acceleration voltage of 1.00 kV and a secondary detector. The images were analyzed using software ImageJ 1.44p (NIH, USA) and the average nanofiber diameter was determined.

Cell attachment and growth

Keratinocytes were seeded (2x10^4 cell/cm^2) on cover slips with electrospun nanofibers. Inverted optical microscopy (Olympus CKX41, Japan) was used to investigate the cell attachment and growth, and fixed-slide samples were prepared to evaluate the architecture of actin filaments. The cells were fixed with 4% paraformaldehyde permeabilized with 0.1% Triton X-100 and finally stained using phalloidin–tetramethylrhodamine B isothiocyanate. Fluorescence microscopy was performed using Olympus IX 81 fluorescence microscope.

RESULTS AND DISCUSSION

The viscosity of blended solutions decreased with increasing amount of CS in the mixture, which correlated well with the number of beads in the electrospun product (Fig. 1A, B). Addition of PEO disrupted self-association of CS chains resulting in improved spinnability of the polymer solution. Therefore, a progressive transformation from a bead-like to a fibrous structure was observed, as well as an increase in the average fiber diameter (from 20 to 50 nm). Furthermore, the fiber nanotopography was better preserved after washing if nanofibers contained more PEO (Fig. 1C, D). Keratinocytes attached to nanofiber regardless to their composition, however, the cell morphology was mostly changed (Fig. 2). Cells in contact with nanofibers adopted rounded shape in contrast to extended, asymmetrical shape of control cells. Furthermore, the cell growth in form of rounded clusters was typically observed. Staining of actin revealed besides more spherical cell shape also absence of visible actin filaments compared to the control (Fig. 3).

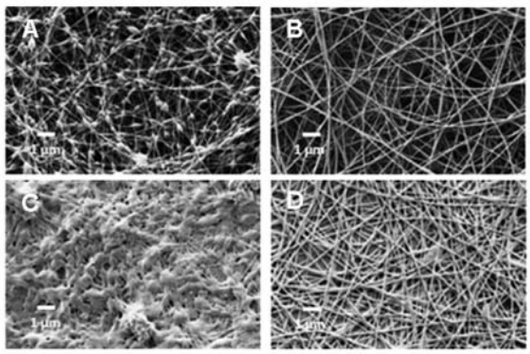

Fig. 1: SEM images of representative electrospun nanofibers prepared from blended CS/PEO solutions (A) CS/PEO 90/10 and (B) CS/PEO 40/10. The morphology of the same samples after washing is shown on (C) (CS/PEO 90/10) and (D) (CS/PEO 60/40).

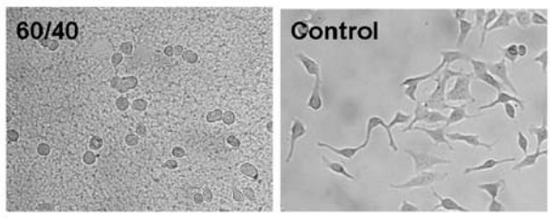

Fig. 2: Keratinocytes 24 h after seeding on CS/PEO 60/40 nanofibers.

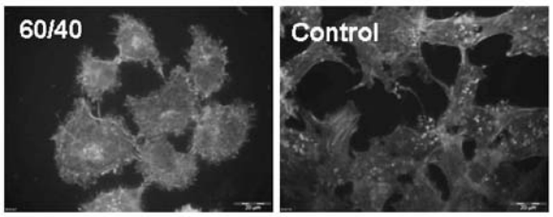

Fig. 3: Actin filaments in control cells and cell grown for 3 days on CS/PEO (60/40) nanofibers.

To conclude, the results show a significant effect of nanofibers on keratinocyte growth *in vitro,* but further studies are needed to better understand the cell behaviour on CS/PEO nanofibrous surfaces.

REFERENCES

1. R. Rošic, P. Kocbek, S. Baumgartner, J. Kristl. Electrospun hydroxyethil cellulose nanofibres: the relationship between structure and proces. J Drug Del Sci Tech 2011, in press
2. J.P. Chen, G.Y. Changb, J.K. Chen. Electrospun collagen/chitosan nanofibrous membrane as wound dressing. Physicochem. Eng. Aspects. 2008; 183–188
3. N. Bhattarai, D. Edmondson, O. Veiseh, F.A. Matsen, M. Zhang. Electrospun chitosan-based nanofibers and their cellular compatibility. Biomaterials. 2005; 26: 6176–6184

IN VITRO EVALUATION OF VANCOMYCIN MICROSPHERES IN SERRATIOPEPTIDASE LOADED THERMOSENSITIVE GEL FOR THE TREATMENT OF BACTERIAL BIOFILM

Y. Cirpanli[1], S. Bozdag-Pehlivan[1], M. Ekizoglu[1], E. Bodur[3], M. Ozalp[2], S. Calis[1,*]

[1] Hacettepe University, Faculty of Pharmacy, Department of Pharmaceutical Technology Ankara Turkey; [2] Hacettepe University, Faculty of Pharmacy, Department of Pharmaceutical Microbiology Ankara Turkey; [3] Hacettepe University, Faculty of Medicine, Department of Biochemistry, Ankara Turkey

INTRODUCTION

Vancomycin HCl, is a glycopeptide antibiotic often used to treat gram-positive pathogens and is the agent of choice for infections with meticillin-resistant Staphylococcus aureus (MRSA) (1). Biofilms cause the administrated antibiotic be ineffective, using a proteolytic enzyme such as serratiopeptidase is one of the approach for degrading the biofilm (2). In this study, formulation and evaluation of Vancomycin HCl loaded PLGA (50:50) (Mw: 40.000-75.000 D) microspheres and serratiopeptidase loaded Pluronic® F127 thermosensitive gel were realized.

MATERIALS AND METHODS

Materials

Vancomycin HCl was a gift from Sandoz Pharm. Co. (Turkey). Serratiopeptidase was supplied as a gift from Specialty Enzymes and Biochemicals Co. (USA). Pluronic® F127 and PLGA 50:50 were purchased from Sigma Aldrich (St. Louis, USA). All other reagents were of HPLC grade.

Preparation of PLGA (50:50) Microspheres

Microspheres containing Vancomycin HCl were prepared by water-in-oil-in-water (w/o/w) technique. For this purpose, polymer and drug solution was injected into aqueous PVA solution (4 %). Then transferred into PVA solution (0.35 %) and stirred continuously (2000 rpm) at room temperature for 2 h until the evaporation of dichloromethane was completed. Finally, the resulting microspheres were collected by centrifugation at 15 000 rpm for 15 min, washed with water and lyophilized.

Particle Size Analysis

Mean particle size (diameter, nm ± S.D.) and polydispersity index of the microspheres were determined by Malvern Hydro 2000S (Malvern Instruments, Malvern, UK) in triplicate.

Scanning Electron Microscope (SEM) Analysis

A scanning electron microscope (Jeol-SEM ASID-10. Device in 80 KV, Japan) was used to evaluate surface characteristics of microspheres. Microspheres were mounted on the metal stubs with conductive silver paint and then sputted with a 150A° thick layer of gold in a Bio-Rad apparatus.

Drug Encapsulation Efficiency

Loaded drug quantity was determined according to the following procedure: Vancomycin HCl loaded microspheres (10 mg) was dissolved in dichloromethane, and then drug extracted to distilled water. The sample was filtered and analyzed by HPLC.

HPLC Analysis

The analysis of Vancomycin HCl was performed using HP Agilent 1200, USA. It was equipped with a C18 column (20µm, 300X3.9 mm, µBondapak, Waters, UK). The HPLC conditions used were similar to those reported by US Pharmacopoeia 30-NF25 (3). Validation of the method used was realized by determination of linearity, accuracy, precision, sensitivity and specificity (r^2=0.9999).

In Vitro Drug Release from Microspheres

Release profile of Vancomycin HCl from microsphere formulation was determined in 50 mL of isotonic PBS (pH 7.4) providing sink conditions in a thermostated shaker bath system (Memmert, Schwabach, Germany) at 37°C with the dialysis technique (Spectra/Por Cellulose Ester Membrane MWCO:100,000 Da, Spectrum Labs, Rancho Dominguez, CA). At predetermined time intervals, 1 mL samples were withdrawn from the system and replaced with equal volume of fresh release medium maintained at the same temperature. The released amount of drug was analysed by HPLC.

Preparation and Characterization of Pluronic® F127 Gel

Pluronic® F127 gel was prepared according to the cold method. Pluronic® F127 (20 %) were dissolved with gentle mixing overnight at 4°C. In order to prepare gel formulation; the drug, serratiopeptidase and drug loaded microspheres were stirred magnetically for 1 h. The flow curves of blank and drug loaded microspheres were determined using Brookfield Model DV-II Viscometer (Essex, UK) fitted wth CP-52 spindle (the cone/plate geometry). In vitro drug release from the gel was determined.

Antimicrobial Activity of Drug Released from Thermoreversible Gel

The antimicrobial effectiveness of drug released from thermoreversible gel was assessed by microbiological evaluation using broth microdilution method.

The Enzyme Activity of Serratiopeptidase Released from Thermoreversible Gel

It was determined as the method reported in the Food Chemical Codex which is based on proteolytic hydrolysis of casein at 37°C.

RESULTS AND DISCUSSION

Vancomycin HCl loaded PLGA microspheres were characterized in vitro by particle size measurements. Particle size of microspheres was 124±13 µm and polydispersity indices and standard deviations of formulation were very low indicating unimodal monodisperse particle size distributions.

Examination of SEM photograph of the microspheres revealed that the surface was smooth and spherical. SEM image of the microspheres is presented in Figure 1.

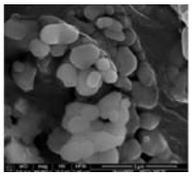

Fig. 1: SEM photograph of the PLGA microspheres

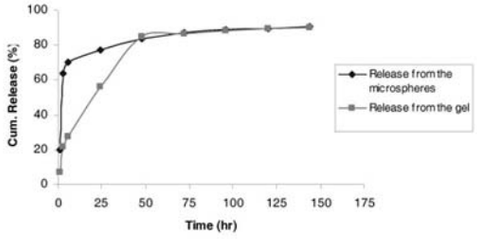

Fig. 2: In vitro release profile of Vancomycin HCl from microspheres

The encapsulation efficiency was about 50.6%. In vitro release profile of Vancomycin HCl from the microspheres is seen in Figure 2. Microspheres release drug within 150 hours completely.
The results showed that, the antimicrobial activity of drug and the enzyme activity serratiopeptidase were remained during the in vitro release study.

CONCLUSIONS

In this study, a promising microparticulate delivery system for Vancomycin HCl has been designed and evaluated for the treatment of bacterial biofilm. We preferred the preparation of a thermosensitive gel formulation because of their injectability advantage. In the light of these findings, it can be concluded that Pluronic® F127 gel formulations was demonstrated to be safe and effective for theis stage of our studies.

REFERENCES

1. Sayin, B., Calis, S., Atilla, B., Marangoz, S., Hincal, A.A. "In Vitro–In Vivo Characterization of Vancomycin–Impregnated and Vancomycin-Loaded Microspheres Blended With Human / Rabbit Bone Grafts", J. Microencapsulation, 2006; 23(5), 553-566.
2. Cheung, R.P.H., Dipiro, J.T. Vancomycin: an update. Pharmacotherapy 1986; 6(4): 153-169.
3. US Pharmacopoeia 30 -NF25. The United States Pharmacopoeial Convention, USA, (2007).

A NOVEL LONG ACTING INTRA-ARTICULAR DELIVERY SYSTEM FOR OSTEOARTHRITIS: STABILITY AND NANOPARTICLE RELEASE

M. Freddi[1,*], S. Stolnik-Trenkic[1], T. Woolley[2], S. Cruwys[2], MC. Garnett[1]

[1] University of Nottingham, School of Pharmacy, Boots Science Building, University Park, Nottingham, UK; [2] AstraZeneca R&D Charnwood, Discovery BioScience, Bakewell Road, Loughborough, UK.

INTRODUCTION

Osteoarthritis (OA) is a common degenerative disease characterised by loss of articular cartilage from the joint. Despite its prevalence there is no established cure and current treatments for OA act to provide symptomatic relief.
Intra-articular injection is used as a delivery route for OA as this disease only affects individual joints, and so local administration can be used to target affected joints reducing systemic side effects. However rapid clearance occurs from the synovial cavity leading to a short activity for these therapies (1).
To increase the length of action a delivery system is proposed consisting of nanoparticles held within an injectable hydrogel, Fig 1. The hydrogels are polyelectrolyte complexes between hyaluronic acid (HA) and chitosan (Ch). A modified HA (HAM) has been used to incorporate cross-links to further enhance the complex properties. These complexes have been found to form more rapidly with the modified HA, and to be able to incorporate high levels of nanoparticles.

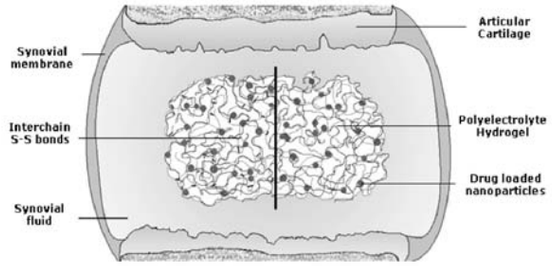

Fig. 1: Diagram of delivery system with and without interchain cross-links

MATERIALS AND METHODS

Materials

HBSS and Bovine Serum were supplied by Invitrogen. HA sodium salt was supplied by Optima Chemicals. Chitosan chloride salt was supplied by Novamatrix Biopolymers. Poly(glycerol) adipate (PGA) polymer and nanoparticles were prepared as previously reported (2,3). All other chemicals were supplied by Sigma-Aldrich. Modified hyaluronic acid (HAM) was prepared through cysteamine substitution of HA catalysed by 1-ethyl-3-(3-dimethylaminopropyl) carbodiimide.

Complex Preparation

Chitosan and HA or HAM solutions were thoroughly mixed and incubated at 37°C for 60 minutes. Suspension of fluorescently labelled nanoparticles (NP) was included where indicated.

Mass Degradation

Polyelectrolyte complexes were incubated at 37°C in buffer (5mls, replaced 3 times per week). Complexes were extracted at each time point, dried and weighed. HBSS used as basis for artificial synovial fluid (ASF), ASFP includes 33% (v/v) bovine serum.

Nanoparticle Release from complexes

Nanoparticle loaded complexes were incubated in 5mls buffer at 37°C, at each time point fluorescence was measured and fresh medium added. Bovine testicular hyaluronidase was used in 0.1M formate buffer (pH 4.5) at 0.6U/ml.

RESULTS AND DISCUSSION

These complexes are stable when incubated in buffer for 56 days, with over 60% remaining in all cases (Fig 2). Both the presence of modified HA and nanoparticles slow the degradation, with a significant reduction in degradation seen in these samples at certain time points. However the degradation in all cases reaches a common plateau level at around 70%.

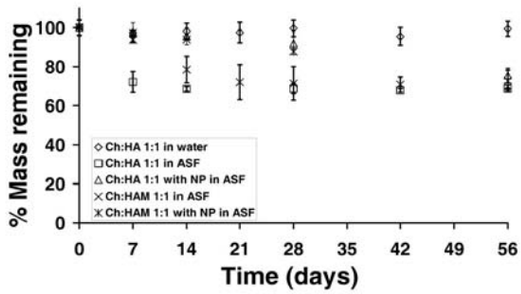

Fig. 2: Mass degradation of complexes in buffer

The release of particles from these complexes (Fig 3) occurs at a much slower rate than the level of degradation seen in the mass degradation study (Fig 2). The presence of protein in the buffer promotes the release of particles; however it still occurs at a low level after an initial burst release. This shows that the complexes are able to hold and retain particles. This is important in allowing a gradual drug release to occur as any released particles would rapidly escape from the joint.

The modified HA protects the complexes from degradation by hyaluronidase (Fig 4), with a significant decrease in particle release seen over the period from 16 to 30 days. The complexes show the presence of a resistant core which retains around 30% of particles which remains even after 56 days. However the susceptibility of these complexes to hyaluronidase degradation shows that these complexes will degrade within the body and so are biocompatible. However the enzyme activity used here is higher than has been found in the joint and was also at the optimal pH for this enzyme (4) rather than the physiological pH of synovial fluid.

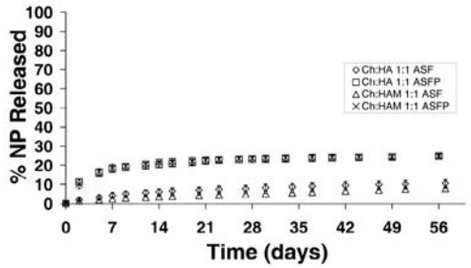

Fig. 3: Nanoparticle release from complexes in buffer

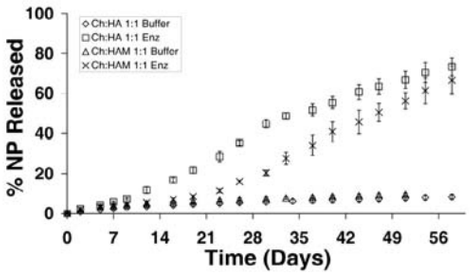

Fig. 4: Hyaluronidase degradation of complexes

CONCLUSIONS

The stability of these complexes in buffer and the presence of enzymes, as well as their ability to hold and retain nanoparticles shows that these complexes would be stable in the joint environment and be able to provide a sustained drug release.

REFERENCES

1. Butoescu N, Jordan O, Doelker E. Intra-articular drug delivery systems for the treatment of rheumatic diseases: a review of the factors influencing their performance. Eur J Pharm Biopharm. 2009; 73: 205–218.
2. Puri S, Kallinteri P, Higgins S, Hutcheon GA, Garnett MC. Drug incorporation and release of water soluble drugs from novel functionalised poly(glycerol adipate) nanoparticles. J Control Release. 2008; 125: 59–67.
3. Meng W, Parker TL, Kallinteri P, Walker DA, Higgins S, Hutcheon GA, Garnett MC. Uptake and metabolism of novel biodegradable poly(glycerol-adipate) nanoparticles in DAOY monolayer. J Control Release. 2006; 116: 314–321.
4. Nagaya H, Ymagata T, Ymagata S, Iyoda K, Ito H, Hasegawa Y, Iwata H. Examination of synovial fluid and serum hyaluronidase activity as a joint marker in rheumatoid arthritis and osteoarthritis patients (by zymography). Ann Rheum Dis. 1999; 58: 186-188.

POTENTIAL CYTOTOXICITY OF LYOTROPIC LIQUID CRYSTALS: EVALUATION ON KERATINOCYTES

M. Gosenca*, B. Govedarica, S. Srčič, M. Gašperlin

University of Ljubljana, Faculty of Pharmacy, Aškerčeva cesta 7, 1000 Ljubljana, Slovenia

INTRODUCTION

Lyotropic liquid crystals (LLC) are used as delivery systems for different pharmaceutical applications due to high solubilisation capacity, thermodynamic stability and easy preparation. LLC with lamellar structure are particularly suitable for dermal application due to special skin-similarity structure and ideal consistency (1).

LLC are formed by particular surfactants in the presence of water and/or oil phase. In order to formulate skin biocompatible LLC with lamellar structure, adequate surfactants regarding their chemical structure and skin acceptability should be used (2). According to this, lecithin and Tween 80 were chosen; lecithin is an integral part of cell membranes and thus highly biocompatible while Tween 80 is a non-ionic surfactant tends to cause minor skin irritation. In addition, isopropyl myristate (IPM), a non-toxic ester, was used as an oily phase.

The aim of this study was to evaluate influence of LLC with different composition on human keratinocyte cell line. Potential cytotoxicity was tested by evaluating keratinocyte viability, while atomic force microscopy (AFM) was used for visualization of cell's morphological alterations.

MATERIALS AND METHODS

Materials and cell culture

LLC were composed of IPM, Tween 80® (both from Fluka, Germany), lecithin (Lipoid S-100®) (Lipoid GmbH, Germany) and bidistilled water (Table 1).

Human keratinocyte cell line (cell line NCTC 2544, ICLC, Univeristy of Genova) were grown in supplemented Eagle's minimum essential medium (Sigma, Germany & Gibco, Invitrogen, USA).

Table 1: Composition of tested LLC (m/m %).

LLC	lecithin	Tween 80	IPM	water
Ia	26,35	26,35	22,55	24,75
IIa	22,50	22,50	30,00	25,00
IIIa	23,65	23,65	15,70	37,00
Ib	17,55	35,10	22,50	24,75
IIb	15,00	30,00	30,00	25,00
IIIb	15,75	31,5o	15,75	37,00

a indicating mass ratio lecithin : Tween = 1:1;
b indicating mass ratio lecithin : Tween = 1:2

Preparation of test formulations

Test formulations were prepared by diluting LLC and sodium dodecyl sulphate (SDS) in medium to final concentrations of 0.45, 0.90 and 4.5 mg/ml. Cells were treated for 4h and subsequently evaluated on viability (MTS assay) and morphological changes (AFM).

MTS assay

Cell viability was determined using the MTS assay (Promega, Madison, WI). Cells were seeded at a density of 0.5×10^4 cells per well in 96-well plates. The absorbance of formazan was measured at 492 nm using a Safire2TM microplate reader (Tecan, Switzerland). The results were expressed as the absorbance ratio of treated to control cells.

AFM imaging of cells

For AFM investigations cells were plated on glass cover slips in 6-well plates at a density of 1×10^4 cells per well. Prior to AFM imaging cells were fixed with ice cold 4% paraformaldehyde in PBS pH 7.4 for 10 min. AFM study

was performed in contact mode in air at room temperature using silicon-nitride pyramid tip (PPP-ContAu, Nanosenors, Germany; nominal force constant 0.02-0.77 N/m). Scan speed was set at 2.0 line/s. Topography, deflection and friction images were collected simultaneously and stored in 512 × 512 pixel format.

RESULTS AND DISCUSSION

LLC effect of on cell viability

A viability assay was performed at different LLC concentrations. At 0.45 mg/ml there was no significant effect on cell viability (~ 100 % for all LLC systems) whereas it was slightly decreased at 0.9 mg/ml (ranging from ~ 81 % for IIb to 95 % for IIIa). At 4.5 mg/ml, the cell viability was reduced with respect to LLC composition; significantly higher viability was observed for LLC with the highest water content (IIIa & IIIb) and at mass ratio lecithin : Tween 80 = 1:1 (Ia-IIIa). In addition, cell viability was significantly higher at all concentrations of tested systems compared to SDS that is used as a positive control in skin irritation testing (3).

LLC effect on cell morphology

Cell viability assay is not able to determine potential structural damages at not-cytotoxic dose (4). Therefore, AFM was used as a complementary technique to estimate cell surface modifications induced by non-cytotoxic exposure of LLC (IIIa at 0.45 mg/ml based on MTS assay). Control cells had round or polygonal shape with height of 1.36 ± 0.29 µm, defined nuclei and cytoplasm, the cell surface was smooth and lacking of roughness and holes (Fig. 1). For treated cells morphological changes were observed in forms of defined pseudopodia spreading out in different directions, decentralised position of the nucleus and a large and flat lamelilipodium. The cells were flattened (height: 0.93 ± 0.24 µm) if compared to control with evident heterogeneous surface (Fig. 1). In addition, hole-like depressions were distributed on the whole membrane surface.

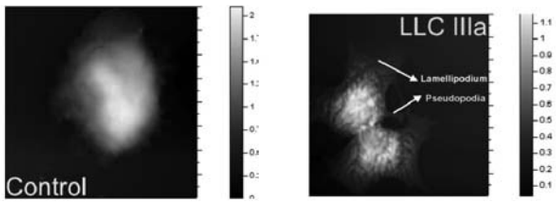

Fig. 1: 2D topography.

The lower roughness of treated cell (Ra 0.079 ± 0.02 µm; Rq 0.099 ± 0.03 µm) compared to control (Ra 0.122 ± 0.05 µm; Rq 0.176 ± 0.08 µm) implies on higher density of citoskeletal fibers goverened by cell activation (Fig. 2) (5).

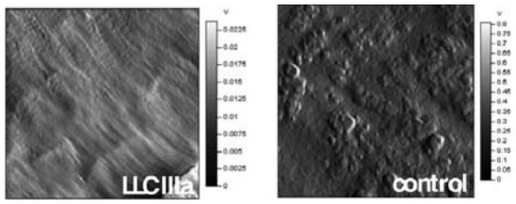

Fig. 2: Deflection images of cell membrane: fibrilar cell structure (LLC IIIa) compared to control.

CONCLUSIONS

In the present work, LLC effect on cell viability, regarding their concentration and composition, as well as cellular topography characterization is reported. The viability was high at 0.45 and 0.9 mg/ml but decreased considerably at 4.5 mg/ml, being higher for LLC with higher water content and with lecithin : Tween 80 = 1:1. AFM results revealed morphological alternations of cell membrane when exposed to LLC at non-cytotoxic concentration. Eventually, the study provides important data for further interpretation of relationship between morphological changes of cell membrane in respect to concentration and composition of LLC.

REFERENCES

1. Makai M, Csányi E, Németh ZS, Pálinkás J, Erős I. Structure and drug release of lamellar liquid crystals containing glycerol. Int. J. Pharm. 2003; 256: 95-107.
2. Moreno MA, Ballesteros MP, Frutos P. Lecithin-Based Oil-inWater Microemulsions for Parenteral Use: Pseudoternary Phase Diagrams, Characterization and Toxicity Studies. J. Pharm. Sci. 2003; 7: 1428-1437.
3. Effendy I, Maibach HI: Detergent and skin irritation. Clinics in Dermatology 1996; 14: 15-21.
4. Lastella M, Lasalvia M, Perna G, Biagi PF, Capozzi V. Atomic force microscopy study on human keratinocytes treated with HgCl2. J. Phys: Conf. Ser. 2007; 61: 920-925.
5. Berdyyeva TK, Woodworth CD, Sokolov I. Human epitelial cells increase their rigidity with ageing in vitro: direct measurments. Phys. Med. Biol. 2005; 50: 81-92.

TRANSDERMAL IONTOPHORETIC DELIVERY OF ONDANSETRON HYDOCHLORIDE IN VITRO: INFLUENCE OF VEHICLE COMPOSITION

D. Ozdin, and S. Gungor*

Department of Pharmaceutical Technology, Faculty of Pharmacy, Istanbul University, 34116, Istanbul, Turkey

INTRODUCTION

Ondansetron hydrochloride (OND) is a selective antagonist at 5-HT3 receptors. It is indicated for the prevention of nausea and vomiting associated with emetogenic cancer chemotherapy and cytotoxic radiotherapy (1).

Iontophoresis delivers drugs across the skin via two main transport mechanisms called as electromigration and electro-osmosis. While electromigration refers the direct interaction of the charged molecules and applied electrical field, electro-osmosis is convective solvent flow which occurs depending on the perm-selective characteristics of the skin (2). The skin is negatively charged and it is a cation-permselective membrane at pH 7.4 (3). However, lipophilic cations can associated with the skin negative charge and alter its permselectivity, consequently decrease or even reverse the electro-osmosis (3, 4).

The aim of the present study was to characterize the principal electro-transport mechanisms of OND across skin depending on the composition of vehicle.

MATERIALS AND METHODS

Materials

Dematomed pig skin (750 µm) was clamped between two comportment side-by-side diffusion cells. Ag/AgCl electrodes were and connected to a power supply.

Iontophoretic delivery protocol

Anodal iontophoresis of OND was performed. The electrodes were isolated from both donor and receptor solutions via salt bridges to prevent drug adsorption on the surface of electrodes. The salt bridges comprised 3% agarose in solution of 100mM Trizma®HCl. The receptor compartment was 154mM NaCl solution. Some experiments were done in the presence of an electro-osmotic marker in donor to quantify electro-osmosis. Passive control experiments were also performed in each case.

(a) Effect of competition ions (presence / absence): The donor consisted of aqueous solutions of 20mM and 50mM OND as single-ion situation or buffered solutions in the presence of 25mM Trizma®HCl as background electrolyte.

(b) Effect of competition ions (type): 25mM Trizma®HCl or 25mM NaCl were used as background electrolyte. The experiment was run at 5mM OND concentration in donor.
(c) *Effect of pH:* 0.5mM OND in buffered 25mM Tris-Trizma®HCl solutions at pH≈5.2 or pH≈6.4 were used as donor.
(d) *Effect of donor concentration:* 0.5, 1, 5, 20 and 50mM OND in donor were examined in the presence of 25mM Trizma®HCl.

RESULTS AND DISCUSSION

The results indicated that there was no statistical difference between iontophoretic fluxes obtained in the presence or absence of background electrolyte with donor solutions an 20 mM OND concentration ($P > 0.05$). It can be elucidated by two reason: (a) pH of donor solutions were ≈4.99 and ≈5.39 for aqueous solution and buffered drug solution with 25mM Trizma®HCl, respectively. Therefore, there is stronger possibility and sooner occurring electro-osmosis in reverse direction in the case of single-ion situation. (b) Less probable leakage of salt-bridge causes contamination in donor solution resulting in more similar condition in donor.
Although, it was expected to obtain higher iontophoretic drug flux with donor having Trizma®HCl due to its bigger structure and, consequently less competition capability in carrying the charge, there was no statistical difference in OND electro- transport efficiency in the presence of Trizma®HCl or NaCl. This might be also due to the difference in pH of the solutions which was measured as ≈5.18 and ≈5.40 for donor solutions in presence of Trizma®HCl and NaCl, respectively.
While the electro-osmotic transport of marker was higher in donor solutions at pH 6.5 (Fig.1), there was no statistical difference in the total iontophoretic OND flux with its donor solutions at pH 5.2 and 6.5 (Fig.2) at the 8 hours. It indicated that the dominant transport mechanism of OND is electromigration.

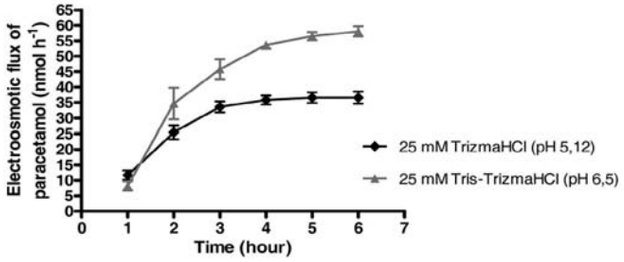

Fig. 1: Electro-osmotic flux of marker in the presence of 0.5mM OND at different pHs donor solutions.

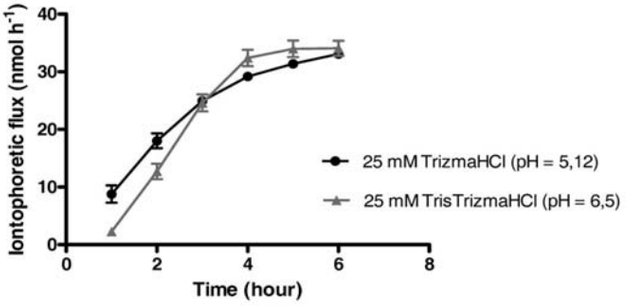

Fig. 2: Total iontophoretic fluxes of OND in donors at different pHs donor solutions.

OND electro-transport increased about 2-fold when the drug concentration was raised from 0.5 mM to 1.0 mM, but it did not increase linearly with increasing its concentration in donor above 5mM and finally there was a reverse relationship between concentration and drug flux above 20mM (Fig.3). This transport behaviour can be explained by the fact that the association and accumulation of the positively-charged drug with fixed negative charge on the skin. Thus, in prior electro-osmotic flux can be decreased with increasing drug concentration and then it reversed in cathodal direction. This phenomenon has been observed in the transdermal iontophoresis of cationic lipophilic drugs (5).

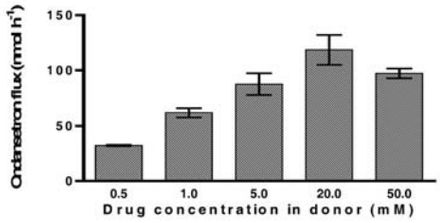

Fig. 3: Total iontophoretic flux of OND at different donor concentrations in the presence of background electrolyte.

CONCLUSIONS

Electromigration is the dominant transport mechanism of transdermal iontophoretic delivery of OND, but the role of electro-osmosis is quite sufficient to be considered in the optimization of formulation. The obvious difference in behaviour of electro-osmosis in pH changes, the lack of strong relationship between iontophoretic flux with both type and absence/presence of competition ions- in contrast with our expectation- the non-linear relationship between flux and donor concentration above specific concentration prove this interpretation. As a result, the composition of vehicle in iontophoretic procedure will influence electro-transport of OND, when they cause apparent modification on its electro-osmotic flow.

REFERENCES

1. Wilde MI, Markham A. Ondansetron. Drugs. 1996; 52: 773–794.
2. Marro D, Guy RH, Delgado-Charro MB. Characterization of the iontophoretic permselectivity properties of human and pig skin. J. Control. Rel. 2001; 70: 213-217.
3. Marro D, Kalia YN, Delgado-Charro MB, Guy RH. Contributions of electromigration and electroosmosis to iontophoretic drug delivery. Pharm. Res. 2001; 18: 1701– 1708.
4. Delgado-Charro MB, Rodriguez-Bayon AM, Guy RH. Iontophoresis of nafarelin: effects of current density and concentrationon electrotransport in vitro. J. Control. Rel. 1995; 35: 35–40.

MICROEMULSIONS OF NAFTIFINE HYDROCHLORIDE: CHARACTERIZATION OF IMPACT ON STRATUM CORNEUM PERMEABILITY WITH ATR-FTIR SPECTROSCOPY

M.S. Erdal*, S. Güngör, Y. Özsoy

Department of Pharmaceutical Technology, Faculty of Pharmacy, Istanbul University, 34116 Istanbul, Turkiye

INTRODUCTION

The solubility potential of microemulsions may be an important factor in increasing skin delivery of drugs as the cutaneous delivery rate is generally related to the concentration gradient of the drug towards skin (1). A considerable amount of *in vitro* as well as some *in vivo* studies indicated that drugs incorporated into microemulsions penetrate efficiently into the skin (2). The purpose of this study is to investigate the effect of microemulsion type colloidal carriers of a lipophilic antifungal agent, Naftifine HCl (NFT), on the skin by ATR-FTIR Spectroscopy. The key components of the microemulsion system considered (in addition to water) were oleic acid (OL) (oil phase), Cremophor EL (CREL) or Cremophor RH (CRRH) (surfactant) and Transcutol (TC) (cosurfactant).

MATERIALS AND METHODS

Materials

CREL and CRRH were obtained as gift sample from BASF. TC was a kind gift from Gattefossé. NFT was provided from Eczacıbaşı Pharmaceuticals. High purity deionized water was used throughout the experiments. All other chemicals were of analytical grade and used without further purification.

Preparation of NFT Loaded Microemulsions

1% of NFT (w/v) was dissolved in the mixture of oil (OL), surfactant (CREL or CRRH) and co-surfactant (TC). An appropriate amount of water was added to the mixture drop by drop under moderate magnetic stirring. The composition of microemulsions is presented in Table 1.

Table 1: Composition of microemulsions

Formulation Components	ME1 (% w/w)	ME2 (% w/w)
OL	8	8.7
CREL:TC (1:2)	-	52.2
CRRH:TC (1:2)	56	-
Water	34.4	39.13
NFT	1	1

Measurement of Droplet Size

Droplet size distribution and the polydispersity index (PI) of NFT loaded microemulsions were determined by dynamic light scattering measurements (Malvern Zetasizer, Malvern, UK).

ATR-FTIR Studies

Dermatomed porcine skin (750 µm) was used by the ATR-FTIR experiments. The surface of 4cm^2 pieces of skin was treated with 300 µl of either CREL, CRRH, TC, OL, ME1 and ME2 for 3h. At the end of treatment period skin was patted dry with a paper towel and placed *stratum corneum* (SC) side down onto the ATR crystal and reproducible contact between the sample and the crystal was ensured. Spectra were recorded as the average of 40 scans with a spectral resolution of 4cm^{-1} in the 4000-650 cm^{-1} range using a Perkin Elmer Spectrum 100 FTIR spectrometer (UK) equipped with a ZnSe ATR crystal. Attention was focused on characterizing the occurrence of peaks near 2850 and 2920 cm^{-1} which were due to the symmetric (SSV) and asymmetric (ASSV) CH_2 stretching vibrations, respectively, which are sensitive to perturbations in the amount and the conformational order of the SC intercellular lipids.

RESULTS AND DISCUSSION

Particle size and uniformity in size distribution values of NFT loaded microemulsions are given in Table 2.

Table 2: Particle size and PI of microemulsions (mean±SD, n=3).

Formulation	Droplet Size (nm)	(PI)
ME 1	66.52±0.23	0.184±0.01
ME 2	78.42±1.27	0.171±0.01

Changes in SC SSV and ASSV peak positions and ASSV peak area and heights after application of microemulsion components and micro-emulsions are shown in Fig. 1 and Fig. 2, respectively.

As can be seen from Fig. 1 OL and CRRH decreased the conformational order of the SC lipids markedly as revealed by the frequency shifts of ASSV and SSV. This observation is attributable to the existence of fluid domains within the more solid SC lipids after treatment with these components.

All components including the surfactants, oil and co-surfactant examined extracted SC intercellular lipids in some extent compare to control. In particular, microemulsions ME1 and ME2 was led to significant decrease in both ASSV peak height and areas compare to that of control (Fig. 2). The possible synergy between the components in the form of a microemulsion formulation may be due to an increased perturbation of SC structure.

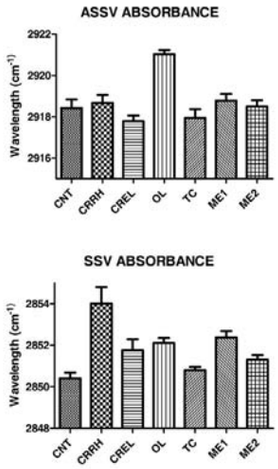

Fig 1: Changes in ASSV and SSV peak positions

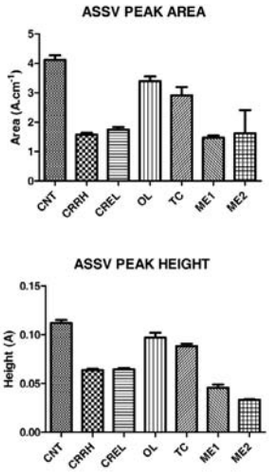

Fig. 2: Changes in ASSV peak area and heights

CONCLUSION

According to ATR-FTIR data, microemulsion carrier systems formulated in our study would be expected to enhance the permeation of NFT, highly lipophilic drug, through SC and that would provide localization of antifungal compound in dermis. To confirm this expectation permeation of NFT through porcine skin will be also investigated.

ACKNOWLEDGEMENT

This work was supported by Scientific Research Projects Coordination Unit of Istanbul University. Project Number:512.

REFERENCES

1. Alam S, Iqbal Z, Ali A, et al. Microemulsion as a potential transdermal carrier for poorly water soluble anti-fungal drug itraconazole. J Disp Sci Technol. 2010; 31: 84-94.
2. Heuschkel S, Goebel A, Neubert RHH. Microemulsions-modern colloidal carrier for dermal and transder-mal drug delivery. J Pharm Sci. 2008; 2: 603-631.

FORMULATION AND EVALUATION OF IN SITU MUCOADHESIVE VAGINAL GEL FORMULATIONS OF CLOTRIMAZOLE

S. Y. Karavana, S. Rençber, Z. Ay Şenyiğit, E. Baloğlu*

Ege University, Faculty Pharmacy, Department of Pharmaceutical Technology, 35100, Bornova-İzmir

INTRODUCTION

Clotrimazole (CLO) is local antifungal agent and it plays an important role in the treatment of vaginal infections and diseases caused by both candidasis and other fungi [1]. This investigation was aimed to develop an in situ mucoadhesive gel formulation of CLO for vaginal administration. The course of development includes formulation of in situ mucoadhesive gel formulations using cold method [2], determination of their gelation temperatures, pH values, mechanical properties, mucoadhesion properties, rheological properties and their syringeability. In situ gels were prepared using poloxamer (PLX) 407 and 188 and hydroxypropylmethylcellulose (HPMC) K100 M and E50.

MATERIALS AND METHODS

Materials

CLO, PLX 188 and 407, HPMC E50 and K 100M were obtained from Sigma (Germany), BASF Chemical Company (Germany) and Colorcon Ltd. (USA), respectively. All other materials were of analytical grade.

Methods

Preparation of gel formulations: HPMC E50, HPMC K100M, PLX 407 and PLX 188 combinations with different ratios were prepared by using the cold method. The certain amount of polymers were added to distilled water at 4°C with gentle mixing and then allowed to dissolve overnight at the same temperature [3]. The compositions of formulations are given in Table 1.

Measurement of Gelation Temperature and pH: Determination of gelation temperature and pH studies were carried out on AR 2000 controlled stress/controlled rate rheometer (T.A. Instruments, Surrey, England) and pH meter (WTW series pH 720), respectively. The geometry was a stainless steel plate/plate (PP35Ti, frequency:0.01 Hz, heat rate:2°C/60 min, temperature:7-80°C). The sol-gel transition temperature graph was determined by sweeping temperature as a function of the viscosity (η*).

Table 1: The composition, gelation temperature and pH values of the formulations (*1% of CLO was added, **GT:Gelation temperature)

F	PLX 407 (%)	PLX 188 (%)	HPMC K100 M (%)	HPMC E 50 (%)	GT* (°C)	pH
F1	20	10	0.5	-	34.5±0.0	6.5±0.1
F1*	20	10	0.5	-	34.5±0.03	6.9±0.1
F2	20	10	-	0.5	34.47±0.02	7.3±0.1
F2*	20	10	-	0.5	34.48±0.02	6.9±0.1

Texture Profile Analysis of Formulations: Textural analysis was performed using Software-controlled penetrometer at 37°C. [TA-TX Plus, Stable Micro System, UK]. From the resultant force-time curve mechanical parameters were derived [4].

Mucoadhesion Studies: The mucoadhesive properties of formulations were evaluated Software-controlled penetrometer at 37°C. Mucin disc was attached to the lower end of the probe of the instrument with cyanoacrylate glue. The probe holding the musin disc was lowered on to the surface of the gel with a constant speed of 0.1 mm.s^{-1} and a contact force of 0.05 N were applied. After keeping in contact for 120 s, the probe was then moved vertically upward at a constant speed of 0.1 mm.s–1. The area under the curve was calculated from force-distance plot as the mucoadhesion [4].

Rheological Measurements: The rheological analysis of the formulations was performed at both 20±0.1°C and 37±0.1°C using Haake Mars Rheometer, in flow mode, and in conjunction with parallel steel plate geometry (PP35 Ti). Oscillatory analysis of each formulation under examination was performed after determination of its linear viscoelastic region at 20±0.1°C and 37±0.1°C. Frequency sweep analysis was performed over the frequency range of 0.1–10.0 Hz following application of a constant stress and standard gap size was 0.3 mm for each sample.

Syringeability of the Formulations: The syringeability of the formulations was examined using a software controlled penetrometer in compression mode. A filled 2 ml syringe was held in place with a clamp and the upper probe of the texture analyzer moved downwards until it came in contact with the syringe barrel base. A constant force of 0.5 N was applied to the base and the work required to expel the contents for a barrel length of 30 mm was measured. The area under the resulting curve was used to determine the work of expulsion.

RESULTS AND DISCUSSION

The gelation temperatures and pH values were shown in Table 1. Table 2 shows the mechanical properties and syringeability of the formulations. Mechanical properties of formulation have been directly applicable to the design of topical formulations. It was observed that the presence of active substance affected the mechanical properties of the formulations. Syringeability of the formulations was presented the effect that content of the formulation have on the force required to expel the product. Addition of active substance affected syringeability of formulations. On the other way, using different polymer type in formulation didn't change syringeability values of formulations. All the formulations presented pseudoplastic flow at 37±0.1°C, and those of Newtonian fluid at 20±0.1°C. In the rheological studies, elasticity modulus was low in the solution stage but increased drastically at the temperature required to form a gel. Oscillatory measurements by varying the frequency showed that the elasticity modulus of the formulations was higher than viscosity modulus at higher frequency points except F1* (0.9Hz). F1* also showed the decrease of the viscosity modulus with increasing frequency. This phenomenon could be due to the higher crosslink of the poloxamer molecules with HPMC K100M than HPMC E50. In addition, the presence of CLO provided higher elasticity comparing with other formulations. Greater elasticity of this formulation would be expected to enhance retention at the site of application (Figure 1 and 2).

Table 2: Mechanical, mucoadhesive and syringeability properties of the formulations (n=5)

F	H (N) ±SD	C (N.mm) ±SD	A (N.mm) ±SD	Ch ±SD	M (mJ) ±SD	S (N.sec)
F1	0.020 ±0.001	0.079 ±0.031	0.067 ±0.026	0.735 ±0.041	0.077 ±0.056	11.130 ±1.986
F1*	0.050 ±0.002	0.242 ±0.028	0.186 ±0.099	0.773 ±0.337	0.043 ±0.011	20.863 ±5.165
F2	0.016 ±0.001	0.043 ±0.005	0.035 ±0.003	0.572 ±0.007	0.082 ±0.040	13.663 ±2.893
F2*	0.012 ±0.001	0.037 ±0.003	0.037 ±0.015	0.901 ±0.214	0.047 ±0.009	26.575 ±2.816

H: Hardness C: Compressibility, A: Adhesiveness, Ch: Cohesiveness, M: Mucoadhesion, S: Syringeability

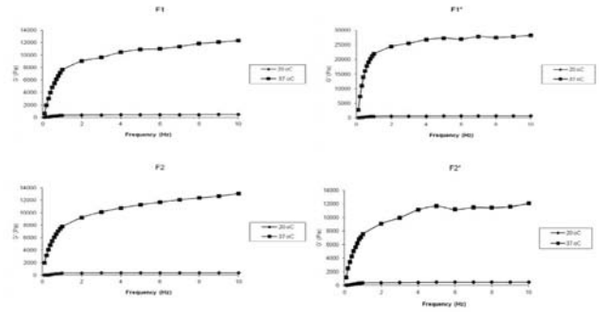

Fig. 1: Frequency-dependence of viscoelastic properties of the formulations at 20°C and 37°C.

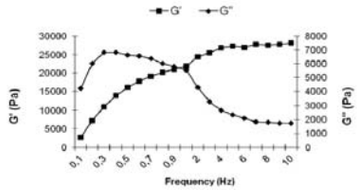

Fig. 2: Frequency-dependence of viscoelastic properties of F1* formulation at 37°C.

CONCLUSIONS

In conclusion, in situ mucoadhesive vaginal gel formulation of PLX 188 :P 407:HPMC K100M-20:10:0.5 and CLO was found valuable for further studies.

REFERENCES

1. Czeizel A.E, Kazy., Vargha P., Eur J Obs Gynecol 111, 135–140, 2003.
2. Chang J.Y., Oh Y., Choi H, Kim Y., Kim C., Int J Pharm 241, 155–163, 2002.
3. Choi H.G, Oh Y.K, Kim C.K., Int J Pharm; 65:23–32, 1998.
4. Jones, D.S., Woolfson, A.D., Brown, A.F., J Control Release, 67, 357–368, 2000.

EVALUATION OF ORGANOGELS PREPARED BY HIGH SPEED HOMOGENIZATION AND MICROIRRADIATION METHOD

E.H. Gokce, A. Yurdasiper*, E. Korkmaz, Ö. Abaci, Ö. Özer

University of Ege, Faculty of Pharmacy, Department of Pharmaceutical Technology, 35100, Izmir, Turkey;
University of Ege, Faculty of Science, Basic Industrial Microbiology, 35100, Izmir, Turkey

INTRODUCTION

Carbopol gels are generally formulated in an aqueous solvent and neutralization of the polymer ensuring polymer hydration and gel formation. Usually its acidic nature has been neutralized with a base like triethanolamine to form strong gels (1). However the addition of such a base is not always suitable for some drug substances. Moreover the addition of water insoluble drugs in such systems may cause non-homogeneous and non-transparent dispersions. Therefore hydrophilic water miscible cosolvents can be used to produce formulations called organogels (2). Bonacucina et al. recently prepared organogels by heating the system up to 80ºC for 30 min, successfully (1).

The aim of this work is to prepare organogels of Carbopol 974P NF, in Polyethyleneglycol 400 (PEG 400) avoiding long time heating and neutralization agents by using a novel technique; high speed homogenization and microirradiation. Triclosan is used as a model drug (solubility in water: 10µg/ml). The prepared organogels have been compared with the gels prepared by heating. The rheological properties of the formulations have been evaluated. In vitro microbial efficacy and the accumulation of triclosan in the rat skin have been investigated comparatively with a commercial product available in the market.

MATERIALS AND METHODS

Carbopol 974P NF (C974), PEG 400 and Triclosan (TCS) have been purchased from Lubrizol (Belgium), Fluca (Italy) and Sigma Aldrich (UK), respectively.

Methods

C974, at concentrations ranging from 1-4% (F1-4) was dispersed in 25ml of PEG 400 and the dispersion was homogenised (Ultraturrax T25) for 5 min at 24000 rpm. TCS was added to system (1% w/w) before homogenisation. Two methods of gel preparation were used using this homogenised dispersion. In the first method, the dispersion was heated at 80ºC in a water bath under mechanic stirring at 200 rpm until a homogeneous and transparent system was formed (F-h). In the second method the dispersion was poured into glass Petri dishes and exposed to microirradiation (600w) for 2 min and spontaneously a transparent system was formed (F-mw).

Rheological analysis

Frequency sweep: The sample was exposed to a step-wise increasing frequency at constant stress (1 Pa); 0.05-50 Hz frequency range at 25 °C. (Fig 1 and 2)

Viscometry test: Flow measurements were performed at the 0.05-10 Pa range of stress at 25°C. (Fig 3 and 4) (Haake Mars Advanced Modular System)

DSC analysis

The samples were sealed in aluminum pans under nitrogen air atmosphere at a flow rate of 20 ml/min and evaluated in 25-100°C temperature ranges (Perkin Elmer 8000). (Fig 5)

Ex vivo studies

Rat abdominal skin was excised immediately after the animal sacrifice and purified from the surrounding tissue. The skin was placed in Franz diffusion cell at 37°C and 0.35 mg of the formulations was evaluated. The formulations (F4-h and F4-mw) were kept in contact for 24 h and then the skin samples were homogenized and the accumulated TCS were extracted with ethanol during 24 h with the aid of a horizontal shaker. The samples were evaluated with a validated HPLC method, (HP Agilent 1200) equipped with a UV detector set at 281nm, using C18 column (250mm×4.6mm; Waters, Alltech). The mobile phase consisting of acetonitrile:water (90:10) was fluxed at 1ml/min. The measurements were carried out for six samples per experiment (Fig 6).

Microbiological efficacy studies

The formulations were transferred to Saboraud's glucose agar (SAG) plates for quantitative cultures. SAG plates were incubated for 48 hr at 37°C, and the colonies of *Streptococcus aerous* were counted. All data represent six separate experiments.

Statistical analysis

Differences among groups were statistically evaluated by one-way ANOVA followed by Tukey's multiple comparison test. The level of significance was set at $p < 0.05$.

RESULTS AND DISCUSSION

The formulations prepared with 1% C974 were liquid dispersions. The storage modulus (G') of the dispersions at the concentration of 2% C974 were slightly higher than the viscose modulus (G"). However the formulations prepared at 3% and 4% of C974 performed gel characteristics and no significant differences was seen between the gels prepared with

these two methods. As the concentrations of the polymer increased in PEG 400, the elastic properties also increased ($p<0.05$).

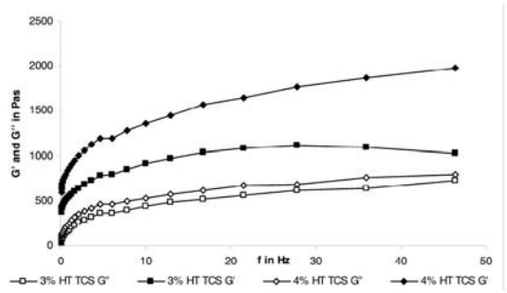

Fig. 1: Frequency sweep of C974 gels in PEG 400 prepared at at 80ºC.

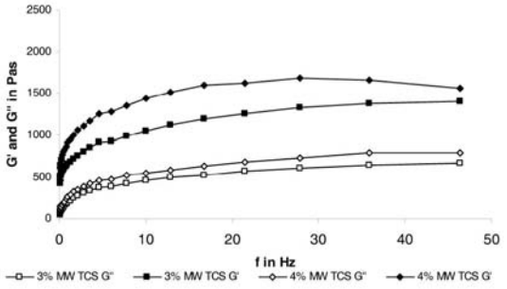

Fig. 2: Frequency sweep of C974 gels in PEG 400 prepared with microirradiation.

The viscosity profiles indicated a shear-thinning system for formulations of 3% and 4% of C974 and as the polymer concentration increased in the system the viscosity increased ($p<0.05$). At lower concentrations the systems resembled to viscous liquids. The organogels prepared with heat using C974 at 4% concentration were more viscous compared to gels prepared with microirradiation upto 50 Pa ($p<0.05$).

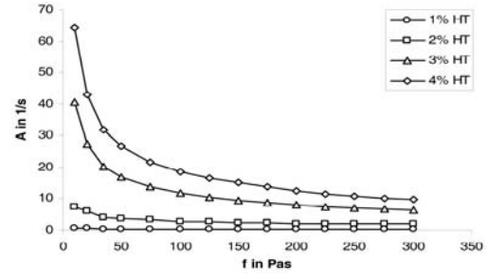

Fig. 3: Viscosity profile of C974 gels in PEG 400 prepared at at 80ºC.

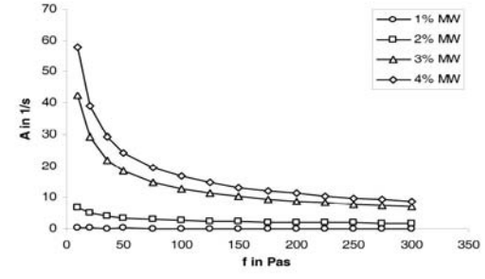

Fig. 4: Viscosity profile of C974 gels in PEG 400 prepared with microirradiation

DSC data revealed that TCS was dissolved in PEG 400 during gel preparation. TCS melting peak has been disappeared in formulations prepared with both methods.

The gels either prepared with heat or microirradiation enabled more than 2 fold accumulation of TCS in comparison to commercial product at the same drug concentration ($p<0.05$).

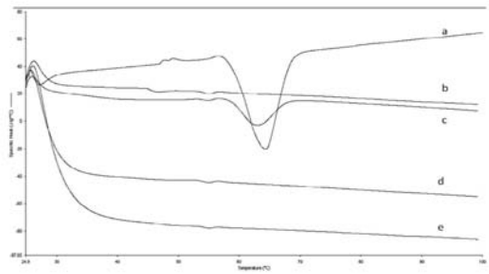

Fig 5: DSC thermograms of a)TCS b) C974 c) physical mixture d) 4% of C974 gels in PEG 400 prepared at at 80ºC e)4% of C974 gels in PEG 400 prepared with microirradiation.

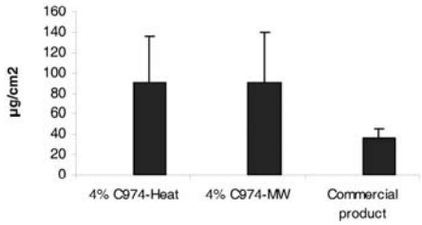

Fig. 6: The amount of TCS accumulated in rat abdominal skin, there is significant differences between commercial product and organogels ($p < 0.05$)

The microbiological studies revealed that the formulations performed effective antimicrobial activity and this activity was significantly greater than TCS suspension in water and commercial product but the same for both organogels.

CONCLUSION

By the choice of the appropriate concentration, gelation of the polymer will occur by high speed homogenization and microirradiation. In light of the known properties of C974, C974 in PEG400 is thought to be an ideal candidate for the formulation of such platforms. This system can be suggested as promising topical delivery gel system for lipophilic drugs.

REFERENCES

1. Bonacucina G, Martelli S, et al. Rheological, mucoadhesive and release properties of Carbopol gels in hydrophilic cosolvents Int. J. Pharm. 2004; 282:115-130.
2. Jones DS, Muldoon B, et al. An examination of the rheological and mucoadhesive properties of poly(acrylic acid) organogels designed as platforms for local drug delivery to the oral cavity. J. Pharm. Sci. 2007; 96: 2632-2646.

OPTIMIZATION OF A HPLC METHOD FOR DETERMINATION OF BETAMETHASONE DIPROPIONATE IN GINGIVAL CREVICULAR FLUID

L. Bogdanovska[1,*], R. Petkovska[1], M. Popovska[2], A. Dimitrovska[1]

[1] University "Ss Cyril and Methodius", Faculty of Pharmacy, Vodnjanska 17, 1000 Skopje, Macedonia; [2] University "Ss Cyril and Methodius", Faculty of Dentistry, Vodnjanska 16, 1000 Skopje, Macedonia

INTRODUCTION

Scaling and root planning (SRP) are the bases of non-surgical therapy in the treatment of periodontitis. Betamethasone dipropionate is often used in dentistry, after the nonsurgical, conventional treatment for periodontitis, because of its topical anti-inflammatory and immunosuppressive actions although the precise mechanism for its activity is unknown. It has greater antiinflammatory potential in relation to other topical corticosteroids (1). Gingival crevicular fluid (GCF) is a serum transudate or inflammatory exudate which plays very important role in the oral defence mechanism (2). Drugs that are distributed in gingival fluid may therefore be very important for the treatment of periodontal disease (3).

The aim of our study was to optimise a HPLC method for determination of betamethasone dipropionate in gingival crevicular fluid after topical application of betamethasone dipropionate 0.5 mg/g cream on the inflamed gingiva.

MATERIALS AND METHODS

Materials

Methanol (HPLC-grade) was supplied by Merck (Darmstadt, Germany) and analytical grade monobasic potassium phosphate was purchased from Fluka. Betamethasone dipropionate and aclo- methasone dipropionate (used as an internal standard) reference standards were used to prepare stock standard solutions.

Whatmann 3MM Chromatography paper strips 2x5mm (Whatmann Lab Sales Ltd., Maidstone, Kent,UK) were used for GCF collection.

Preparation standard solutions

Standard solutions were prepared each day in concentrations of 0.1, 0.25, 0.5, 0.75, 1 and 2 µg/ml each containing 2 µg/ml aclomethasone as an internal standard, using mobile phase as diluting agent.

Collection of Gingival Crevicular Fluid

GCF was collected from ten volunteers 21 to 65 years old, suffering from moderate periodontitits. The applied volume of the cream was 0.1 ml to each volunteer and specimens were taken 15 minutes after treatment.

GCF samples were collected using Whatmann paper strips. The paper strips were inserted into the deepest periodontal pockets (PD≥4 mm) until minimal resistance was felt and were left there for 30 s (4). Average volume of GCF collected on the paper strips was 0.4 µL. Samples containing blood were not included for analysis. All the samples were frozen at - 20°C until analysis.

Extraction procedure

Samples were extracted using MeOH:H_2O (70:30, v/v) mixture. The final extract volume was 500 µL. Aclomethasone internal standard (10 µL 100 µg/ml solution) was added to each extract.

Chromatography

The HPLC analysis was conducted on Agilent 1100 series equipped with UV Diode Array Detector. The chromatographic separation was performed on Purospher STAR RP 18-e 120 Å, 150 x 4.6 mm, 5µm using LiChroCART® 4-4 guard column at 25 °C. The mobile phase was methanol: 0.04M KH_2PO_4 (70:30, v/v) with flow rate of 1.3 ml min^{-1}. The injection volume was 100 µl. UV detection was performed at 245 nm. The runtime was 14 min.

RESULTS AND DISCUSSION

Validation

The HPLC method was validated according to EMEA Guideline for the validation of bioanalytical methods (5). The retention times for aclomethasone (IS) and betamethasone dipropionate were 6.5 and 11 min, respectively.

The method was linear in the concentration range from 0.1-2 µg/ml (y=0.513x-0.003, R^2=0.997). Recovery of extraction in human GCF was calculated by comparing the peak area ratio from an extracted spiked sample with the peak area of blank GCF containing the same amount of drug. The mean recovery was 98.75%. The precision and accuracy were determined at four concentration levels, 0.1, 0.25, 1, 1.75 µg/ml (Table 1).

Table 1: Within-run and between-run accuracy and precision for betamethasone in GCF

Added (µg/ ml)	Determined (µg/ml)	CV (%)	Accuracy (%)
With-in run accuracy and precision			
0.10	0.11	3.51%	109,06 %
0.25	0.25	4.00%	99,71%
1,00	0.97	2.22%	96.67%
1.75	1.73	4.53%	98.77%
Between run accuracy and precision			
0.10	0.10	4.38%	103.45%
0.25	0.25	3.25%	99.11%
1.00	0.96	2.00%	96.89%
1.75	1.77	5.71%	100.97%

The selectivity of the method was demonstrated as the resolution of the beta- methasone dippropionate peak from other peaks and absence of interfering peaks (Fig.2).

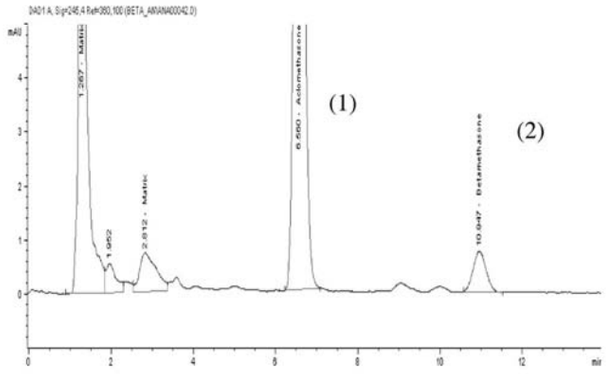

Fig. 2: Representative chromatogram of GCF sample. Peaks: (1)-aclomethasone dipropionate (internal standard, 2µg/ml; (2)-betamethasone dipropionate, 0.15µg/ml

Analysis of betamethasone dipropionate in human GCF

Results from patients show that betamethasone dipropionate applied as a cream penetrates well into human crevicular fluid as evidenced by the levels obtained (Table 2).

This may have implications in the basis of non-surgical therapy for periodontitis.

Table 2: Concentration of betamethasone in patient samples

Patient	Concentration applied (µg/ml)	Concentration determined (µg/ml)	%
No.1	0.25	0.2375	95.00
No.2	0.25	0.2369	94.76
No.3	0.25	0.2198	87.92
No.4	0.25	0.2223	88.90
No.5	0.25	0.2298	91.92
No.6	0.25	0.2350	94.00
No.7	0.25	0.2284	91.36
No.8	0.25	0.2151	86.04
No.9	0.25	0.2173	86.92
No.10	0.25	0.2138	85.52

CONCLUSION

The data presented in this study indicate that the HPLC method used for the determination of betamethasone dipropionate in human crevicular fluid samples showed parameters of precision, accuracy, linearity, and specificity in the limits of validation criteria. Additionally the recovery of extraction in human GCF was satisfactory.
The HPLC method are therefore suitable and applicable for the analysis of betamethasone dipropionate in human crevicular fluid.

REFERENCES

1. Fachin EVF, Zaki AE. Histology and lysosomal cytochemistry of the postsurgicaly inflamed dental pulp after topical application of steroids.I.Histological study. J.Endod. 1991 ; 17(9) : 457-60
2. Kinney,S.J., Rameseier,A.C, Gianobille V. W. Oral Fluid-Based Biomarkers of alveolar bone loss in periodontitis. Ann.N.Y. Acad.Sci.1098: (2007); 230-251
3. Babinchak J.T. Oral ciprofloxacin therapy for prosthetic valve endocarditis due to Actinobacillus actinomycetemcomitans. Clin.Infect.Dis. 1995; 21(6) : 1517-1518
4. Lamster B.I, Ahlo K.J. Analysis of gingival crevicular fluid as applied to the diagnosis of oral and systemic diseases.Ann.NY.Acad.Sci. 2007;1098:216-229
5. EMEA. Guideline on validation of bioanalytical methods. EMEA/CHMP/EWP/192217/2009

A NEW METHOD FOR MONITORING OXIDATIVE STRESS MARKERS IN EXHALED BREATH CONDENSATE

K. Syslová[1,*], P. Kačer[1], M. Kuzma[2], Š. Vlčková[3], Z. Fenclová[3], J. Lebedová[3], D. Pelclová[3]

[1] Institute of Chemical Technology, Technická 5, 166 28 Prague 6, Czech Republic; [2] Institute of Microbiology, Vídeňská 1083, 142 20 Prague 4, Czech Republic; [3] Department of Occupational Medicine, 1st Medical Faculty, Charles University, Na Bojišti 1, 120 00 Prague 2, Czech Republic.

INTRODUCTION

Oxidative stress can be defined as the body imbalance between production of reactive oxygen species (ROS) and biological system ability to readily detoxify the reactive intermediates or easily repair the resulting damage. ROS generated close to cell membranes oxidize membrane phospholipids (membrane lipid peroxidation), which can be further transformed in a chain reaction. Endoge-nously generated aldehydic lipid peroxi-dation products are malondialdehyde, α,β-unsaturated aldehydes (mainly 4-hydroxynonenal and 4-hydroxyhexenal) and saturated aldehydes (hexanal, heptanal and nonanal). Aldehydes are formed by lipid peroxidation of ω-6 (arachidonic acid, linoleic acid) and ω-3 (oleic acid) polyunsaturated fatty acids. The aldehydes (biomarkers) quantification in various body fluids (exhaled breath condensate, plasma and urine) represent an interesting tool for oxidative stress induceddiseases diagnostics.

MATERIALS AND METHODS

The work presents a new method for the determination of aldehyde-biomrkers in body fluids based on the LC-ESI/MS/MS. Malondialdehyde, 4-hydro-xynonenal, and saturated aldehydes (n-C6 to C13 aldehydes) were quantified after derivatization with Girard's reagent T. LC-ESI-MS/MS operated in neutral loss (NL) mode was used for its exceptionally high degree of selectivity and sensitivity.

RESULTS AND DISCUSSION

It was developed very sensitive and easy-to-use protocol for high throughput analysis of carbonyl compounds in the EBC. Optimized electrospray ionization conditions established the limits of detection at 12 pg/ml and 16 pg/ml of the EBC for the most prominent oxidative stress markers MDA, and 4-HNE respectively. The validation results demonstrated that the LC–MS/MS method is precise (≥ 91.3%), accurate (≥ 89.3%) and selective and can be used for the determination of carbonyl compounds in the EBC.

CONCLUSIONS

The developed method enabled unequivocal parallel determination of several oxidative-stress biomarkers at the only one analysis run. The method was tested on real clinical samples collected from patients with different oxidative stress induced disorders (silicosis, asbestosis) and compared to the control group of healthy subjects.

ACKNOWLEDGEMENT

The work was supported by the Ministry of Health of the Czech Republic (Grant NS 10298-3/2009) and Grant Agency of the Czech Republic (Grant GA CR 203/08/H032).

SYNTHESIS AND ANTIMICROBIAL ACTIVITY OF NEW PYRAZOLINE DERIVATIVES

A. Özdemir[1,*], G. Turan-Zitouni[1], Z. A. Kaplancıklı[1], M. D. Altıntop[1], F. Demirci[2]

[1] Anadolu University, Faculty of Pharmacy, Department of Pharmaceutical Chemistry, 26470, Eskisehir, Turkey; [2] Anadolu University, Faculty of Pharmacy, Department of Pharmacognosy, 26470, Eskisehir, Turkey.

INTRODUCTION

In recent decades, problems of multidrug resistant micro-organisms have reached an alarming level in the world. Resistance to a number of antimicrobial agents (β-lactam antibiotics, macrolides, quinolones, and vancomycin) among a variety of clinically significant species of bacteria is becoming increasingly major global problem. They pose a serious challenge to the scientific community hence emphasis has been laid on the development of new antimicrobial agents. Pyrazolines are five-membered heterocyclic compounds containing two nearby nitrogen atom on their chemical scaffold. Several pyrazoline derivatives possess important pharmacological activities including antimicrobial activity (1) and therefore they are useful materials in drug research. In addition, several 1,3,4-oxadiazole derivatives were reported to exhibit good antimicrobial activity (2). In view of the above observations, we have designed and synthesized new 2-pyrazoline derivatives, bearing oxadiazole, thienyl and phenyl functionality in the same molecule, as potential antimicrobial agents.

MATERIALS AND METHODS

Chemistry

All chemicals were obtained from Aldrich Chemical Co. All melting points (m.p.) were determined by Gallenkamp apparatus and are uncorrected.

Elemental analyses were performed on a Perkin Elmer EAL 240 elemental analyser. Spectroscopic data were recorded with the following instruments: ^{1}H-NMR (Bruker 400 MHz spectrometer) and ^{13}C-NMR (Bruker 100 MHz spectrometer) and MS-FAB (VG Quattro Mass spectrometer).

1-(2-Thienyl)-3-aryl-2-propen-1-ones / 5-Aryl-3-(2-thienyl)-2-pyrazolines: Chalcones and pyrazolines were synthesized according to the literature method (1).

1-(Chloroacetyl)-3-(2-thienyl)-5-aryl-2-pyrazolines:
These compounds were prepared according to the literature method (1).

5-(2-Cyclohexylethyl)-[1,3,4]-oxadiazolin-2-thione:
That compound was synthesized by using a literature procedure (3).

1-[[5-(2-Cyclohexylethyl)[1,3,4] oxadiazole-2-yl]thioacetyl]-3-(2-thienyl)-5-aryl-2-pyrazoline derivatives (1a-f):
A mixture of 1-(chloroacetyl)-3-(2-thienyl)-5-aryl-2-pyrazoline (0.01 mol), 5-(2-cyclohexylethyl)-[1,3,4]-oxadiazolin-2-thione (0.01 mol), and K_2CO_3 (0.01 mol) in acetone (50 mL) was refluxed for 8h. After cooling, the solution was evaporated until dryness. The residue was washed with water and recrystallized from ethanol.

Microbiology
The study was designed to compare MICs obtained by the broth microdilution method (4). The observed data on the antimicrobial activity of the compounds, the control drugs and the test microorganisms are given in Table 1.

RESULTS AND DISCUSSION

In the present work, six new compounds **(1a-f)** were synthesized (Fig 1). Their structures were determined by IR, ^{1}H-NMR, ^{13}C-NMR, FAB$^+$-MS spectral data and elemental analyses. All compounds gave satisfactory elemental analysis. The ^{1}H-NMR spectral data were also consistent with the assigned structures. In the 400 MHz ^{1}H-NMR spectrum of compounds, the CH_2 protons of the pyrazoline ring resonated as a pair of doublet of doublet at 3.07-3.22 ppm, 3.79-3.92 ppm. The CH proton appeared as doublet of doublet at 5.48-5.61 ppm. The CH_2 protons of acetyl group are observed at 4.50-4.69 ppm as two doublets. These geminal protons are observed as two doublets owing to possible two different conformations since rigid protons were occurred. In the ^{13}C-NMR spectra of the compounds, the signal due to the carbonyl carbon (C=O) appears at 168.00-168.08 ppm. ^{13}C-NMR chemical shift values of the carbon atoms at 41.83-42.90 ppm (C-4), 58.88-59.98 ppm (C-5) and about 146.84-151.61 ppm (C-3) corroborate the 2-pyrazoline character deduced from the ^{1}H-NMR data. The compounds have a signal at 35.36-35.64 ppm due to S-CH_2 carbon. The mass spectra of compounds showed [M+1] peaks, in agreement with their molecular formula.
The results indicated that all of the tested compounds were inactive against the test organism.

CONCLUSIONS

The results indicated that all of the tested compounds were inactive against the test organism. The reason for this respect may be the low solubility in polar solvents of such compounds. Regarding the antimicrobial level of the tested derivatives when compared to the previous study (5), it seems to be less active against the tested microorganism which does not mean they would be inactive against other pathogenic microorganisms. So it is worthwhile to test these substances against other microorganism strains and isolates.

ACKNOWLEDGEMENT

This study was supported by Anadolu University Scientific Research Project Commission with 1001S41 number of Project.

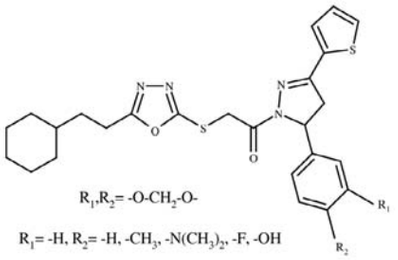

Fig. 1: Synthesis of target molecules (1a-f)

Table 1. Antimicrobial activities of the compounds (mg/mL)

	A	B	C	D	E	F	G	H
1a	>1.25	1.25	1.25	>1.25	1.25	1.25	1.25	1.25
1b	1.25	>1.25	1.25	>1.25	1.25	1.25	1.25	1.25
1c	>1.25	1.25	1.25	1.25	1.25	1.25	1.25	>1.25
1d	>1.25	1.25	1.25	1.25	1.25	1.25	1.25	>1.25
1e	1.25	1.25	1.25	1.25	1.25	1.25	1.25	1.25
1f	>1.25	1.25	1.25	1.25	>1.25	1.25	1.25	>1.25
Ref.1	0.031	0.031	0.5	0.031	0.015	0.031	-	-
Ref.2	-	-	-	-	-	-	0.12	0.25

Reference 1: Chloramphenicole, **Reference 2:** Ketoconazole
A: *Escherichia coli* (NRRL B-3008), **B:** *Staphylococcus aureus* (ATCC 6538), **C:** *Pseudomonas aeruginosa* (ATCC 27853), **D:** *Proteus vulgaris* (NRRL B-123), **E:** *Salmonella typhimurium* (ATCC 13311), **F:** Methicillin-resistant *Staphylococcus aureus* (MRSA) (clinic isolate) **G:** *Candida albicans* (NRRL Y-12983) **H:** *Candida parapsilosis* (NRRL Y-12696).

REFERENCES

1. Turan-Zitouni G, Özdemir A, Güven K. Synthesis of some 1-[(N,N-disubstitutedthiocarbamoylthio)acetyl]-3-(2-thienyl)-5-aryl-2-pyrazoline derivatives and investigation of their antibacterial and antifungal activities. Arch. Pharm. 2005; 338(2-3): 96-104.
2. Padmavathi V, Reddy GS, Padmaja A, Kondaiah P, Shazia A. Synthesis, antimicrobial and cytotoxic activities of 1,3,4-oxadiazoles, 1,3,4-thiadiazoles and 1,2,4-triazoles. Eur. J. Med. Chem. 2009; 44: 2106-2112.
3. Andrushko AP, Demchenko AM, Krasovskii AN, Rusanov EB, Chernega AN, Lozinskii MO. Reactions of α-Halo Ketones with 5-Benzyl and 5-Phenoxymethyl-2H,3H-1,3,4-oxadiazole-2-thiones. Russ. J. Gen. Chem. 2001; 71(11): 1754-1758.
4. Koneman EW, Allen SD, Winn WC, in: Colour Atlas and Textbook of Diagnostic Microbiology, Lippincott Raven Pub, Philadelphia, 1997, pp. 86-856.
5. Özdemir A, Turan-Zitouni G, Kaplancıklı ZA, Revial G, Demirci F, İşcan G. Preparation of some pyrazoline derivatives and evaluation of their antifungal activities. J. Enzym. Inhib. Med. Chem. 2010; 25(4): 565-571.

SYNTHESIS AND THERMAL STUDY OF NEW 4-HYDROXY-3-BENZOYL-2-(2-(4-PHENYL-1-PIPERAZINYL)ACETYL)-2H-BENZO-1,2-THIAZINE 1,1-DIOXIDE

B. Szczęśniak-Sięga[1*], E. Krzyżak[2], W. Malinka[1]

[1] Department of Chemistry of Drugs, Wrocław Medical University, ul. Tamka 1, 50-137 Wrocław, Poland; [2] Department of Inorganic Chemistry, Wrocław Medical University, ul. Szewska 38, 50-139 Wrocław, Poland

INTRODUCTION

We search for new anti-inflammatory agents devoid of the limitations and side effects of the classical non steroidal anti-inflammatory drugs. Our previous investigation revealed that some 4-arylpiperazinyl derivatives of pyrido[3,2-e]-1,2-thiazine 1,1-dioxide exhibited significant peripheral analgesic activity and have sedative influence on the CNS in mice. Moreover, several of these pyridothiazines possess peroxyl radical scavenging activity of equal potency to that found in NAC (N-acetyl-L-cysteine, as reference substance) (1). In the light of nonspecific CNS effects (analgesia, depression of locomotor's activity, prolongation of barbiturate induced sleeping time) further investigation was carried out into syntheses of analogues with reduced central activity in relation to peripheral analgesic activity. For this purpose we decide to substitute pyridine with benzene ring. In this way we receive structures suggestive to piroxicam, an antiphlogistic and analgesic agent. Herein we present synthesis and calorimetric studies one of new benzo-1,2-thiazines derivative.

MATERIALS AND METHODS

Materials

The starting material for the synthesis of the compound mentioned above was 1,1-dioxo-1,2-benzothiazol-3-one (saccharin, Sigma-Aldrich) **1** (Fig.1). It was condensed with 2-bromoacetophenone in dimethylformamide (DMF) in the presence of triethylamine giving compound **2**. Then compound **2** was rearranged to the corresponding benzo-1,2-thiazine ring **3**. The mechanism of rearrangement has been studied recently in our laboratory (2). The new final compound was prepared by alkylation of benzothiazine with 4-phenyl-1-(2-chloracetyl)piperazine. The separated product was purified by the crystallization from ethanol and toluene **4** (M.p.:142-146°C-ethanol and 172-176°C-toluene). The structures of the obtained compounds were confirmed by elemental and spectral (IR, H^1NMR) analyses.

Methods

Thermal analysis is quite a fast and accurate technique, allowing one to receive information about the changes in the thermal properties of new substances, which in this case is very useful, because our new compound shows some aberrant properties. We used the differential scanning calorimetry (DSC), because it is one of the thermal analysis methods very common to record such characteristics. Calorimetric measurements were performed with a Mettler Toledo DSC 25 measuring cell with TC15 TA Controller. Samples weighing 3–4 mg were characterized in sealed 40µL aluminium pans with perforated lids and subjected to thermal analysis under a flowing argon atmosphere ($30 cm^3 min^{-1}$). Analysis was carried out from 30°C to about 20 degree above melting temperature using heating rate of 5°C min^{-1} with an identical empty sample pan as reference. DSC curves measured for the compound obtained from ethanol and toluene are shown on Figure 2.

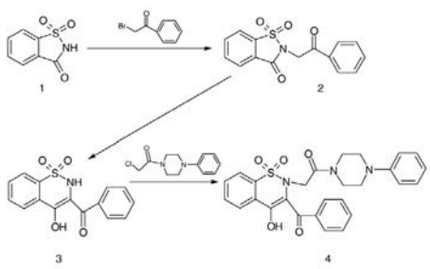

Fig. 1: Scheme of synthesis of new benzo-1,2-thiazines derivative.

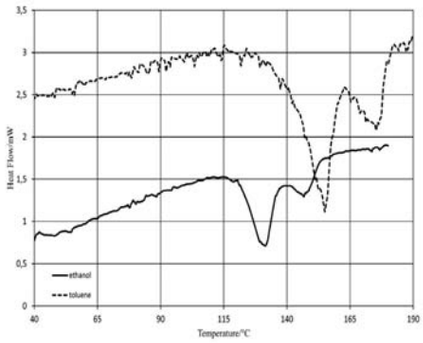

Fig. 2: DSC curves for the new compound crystallized from ethanol and toluene.

RESULTS AND DISCUSSION

There are two exothermic thermal effects on the DSC curve at 121°C, 144°C (ethanol) and 146°C, 168°C (toluene). This result is rather surprising. For pure substance only one exothermic peak should be recorded. On the other hand, corresponding to the data obtained from H^1NMR, IR experiments and elementary analysis, the solvent should not affect the synthesis result. It seems that two thermal effects on the DSC curves are related to keto-enol tautomerism, stabilized by strong intermolecular O-H×××O hydrogen bonding. The same kind of tautomeric equilibrium in the similar compound has been reported (3) (Fig.3). However, our hypothesis requires further study.

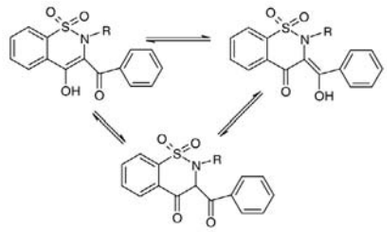

Fig. 3: Three possible tautomeric form of new benzo-1,2-thiazines derivative.

CONCLUSIONS

The new synthesized compound, 4-hydroxy-3-benzoyl-2-(2-(4-phenyl-1-piperazinyl)acetyl)-2H-benzo-1,2-thiazine 1,1-dioxide, with potential analgesic activity, in its thermal properties studies shows two different thermal effects, which may suggest existence of two or more crystalline forms of this structure. While two different melting points for the same compound from two solvents can lead us to conclusion that it may be the conformational polymorphism, the same as the two forms of piroxicam pivalate (4). Interchangeable understanding of this phenomenon needs further investigations.

REFERENCES

1. Malinka W, Kaczmarz M, Filipek B, Sapa J, Glod B, Preparation of novel derivatives of pyridothiazine-1,1-dioxide and their CNS and antioxidant properties, Farmaco 2002; 57: 737-746.
2. Zawisza T, Malinka W, A novel system: 2H-pyrido[3,2-e]-1,2-thiazine-1,1-dioxide. Synthesis and properties of some derivatives, Farmaco 1986; 41: 819-826.
3. Karczmarzyk Z, Keto–enol tautomerism in crystals of 3-[hydroxy(phenyl)methyl]-2,5,7-trimethyl-2,3-dihydropyrido[3,2-e][1,2]thiazin-4-one 1,1-dioxide and 3-(1-hydroxyethylidene)-2,5,7-trimethyl-2,3-dihydropyrido[3,2-e][1,2]-thiazin-4-one 1,1-dioxide, Acta Cryst. 2008; C64: o590-o594.
4. Caira MR, Zanol M, Peveri T, Gazzaniga A, Giordano F, Structural characterization of two polymorphic forms of piroxicam pivalate, J. Pharm. Sci. 1998; 87: 1608-1614.

CHEMICAL CHARACTERIZATION, ANTIBACTERIAL ACTIVITY ASSESMENT AND INCLUSION IN CYCLODEXTRINES OF SATUREJA MONTANA L. ESSENTIAL OILS

E. Haloci[1*], S. Manfredini[1], V. Papajani[2], S. Bertuani[1], P. Ziosi[1], A. Petre[3]

[1] Ferrara University, Pharmaceutical Department, Ferrara, Italy; [2] Tirana University, Medicine Faculty, Pharmaceutical Department, Rr.Dibres, Tirana, Albania; [3] Tirana University, Natural Sciences Faculty, Nutrition and Microbiology Department,Tirana,Albania

INTRODUCTION

Essential oils are lipid soluble well-known ingredient often applied to the skin for their important properties that ranges from antimicrobial, to antinflammatory and skin whitening. Current applications of these volatile compounds turn out to be complicated because of chemical and physical properties. This is one of the major problems for their uses; therefore, microencapsulation could be the solution to problems of stability, evaporation and controlled release. Moreover, some of their components are also provided by side effects such are skin sensitizing activity, thus behaving as allergens. For these reasons, direct contact with skin should be avoided. *Satureja Montana* L. also provides of interesting antimicrobial properties. To explore their dermatological application we investigate the antimicrobial activity and their inclusion in cyclodextrine complexes, in order to achieve better stability in emulsions and better compatibility with skin application. This study is part of a major project divided in four steps. First step was the extraction of the essential oil by hydro-distillation by Clevenger type apparatus, second one was the characterization by GS/FID of essential oils obtained, and third one was screening the antimicrobial activity of the extracted essential oils (the presenting paper). The last one will be preparation of essential oil complexes with cyclodextrine and analysis of their chemical, physical, antibacterial activity and biodisponibility properties.

MATERIALS AND METHODS

MATERIALS and APPARATUS: Gas/Fid TipVarianCP3800, Clevenger Apparatus. Standards: Carvacrol, p-cymen, y-terpinen, borneol, thymol were obtained from Sigma Aldrich Company. Bacterias: Staphylococcus aureus, Escherichia coli, yeast Aspergillus flavia, Claudosporium herbarum, Samples of *S.montana L.*:

Origin	Traditional Pharmacy - M1	Elbasan - M2	Kerraba - M3	Kruja - M4	Scutatri Mauntains - M5
Altitude	150 m	300 m	950 m	740 m	1000 m

Extraction of the essential oils

A hundred grams of dried aerial plant material were subjected to hydro-distillation for 3 hours using a Clevenger-type apparatus to produce oils. The essential oils obtained were dried over anhydrous sodium sulphate and stored in sealed vials at low temperature (2°C).

GAS/FID Identification and quantification of Main components

GC/FID analysis of the essential oil was performed using a Varian CP-3800 instrument equipped with a capillary column.VF:1ms, Film thickness 0.25 mm (L) 25mx (ID) 0.25mmx (OD) 0.39mm.

Helium was used as the carrier gas at the constant flow of 1.2 ml/min and split ratio 1:30. The oven temperature was held at 50°C for 1 min, then programmed to 280°C at a rate of 5 °C /min. Injection volume was 1µl. The injector temperature was 250 and detector (FID) temperature 300°C. Identification was done by comparing the RI of samples with those of standards. Percentages of main components were obtained by serial dilution of standards in hexane. (Tab.2)

Antimicrobial activity of essential oils

The essential oil of samples was tested for antibacterial activity by the disc diffusion method using 100µL of suspension of the tested microorganisms, containing 2.0 x 106 colony forming units (cfu mL–1) for bacteria and 2.0x105 spore mL–1 for fungal strains. Mueller—Hinton agar and dextrose agar were distributed to sterilized Petri dishes with a diameter of 9 cm. The filter paper discs (6 mm in diameter) were individually impregnated with10µL and 30µL of the essential oils dissolved in dimethylsulfoxide (DMSO). The Petri dishes were kept at 4°C for 2 h. The plates inoculated with bacteria incubated at 37°C for 24 h and at 30 °C for 48 h for the yeasts. The diameters of the inhibition zones were measured in millimetres. Negative controls were set up with equivalent quantities of DMSO. Studies were performed in triplicate. In addition, positive controls antibiotic discs such as Cefuroxime, ciprofloxacin, tetracycline and nystatin were used for comparison.

Synergism of main components

Many studies deal with the fact that the components of *Satureja Montana* L. essential oil are in synergy with each other. To study this phenomenon we compared the inhibition zone of each standard and their mixture too.

RESULTS AND DISCUSSION

The sample from Scutari Mountains has the highest (0.65 ml) amount of essential oil and its yields have the highest % of carvacrol and thymol too.

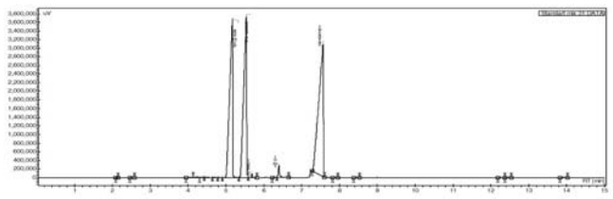

Fig. 1: Standarts chromatograms obtained by Gas/FID.

Table 2: Comparative % of important components of *Satureja Montana* L essential oil from different altitudes in Albania.

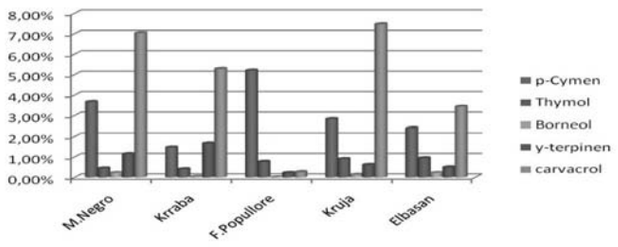

Table 3: Comparative Antimicrobial activity (Mean of Inhibition zone) of *Satureja Montana* L. essential oil samples and positive controls

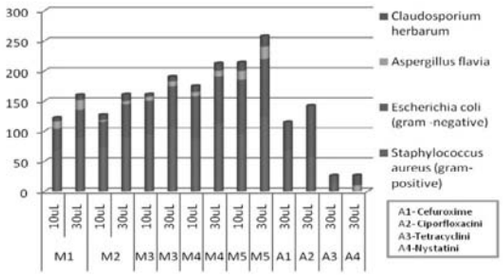

Table 4: Comparative Antimicrobial activity (inhibition zone in mm) of five standards (main components of *Satureja Montana* L.) and their mixture

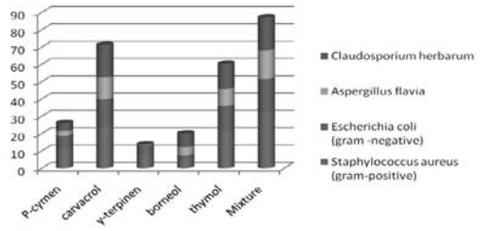

CONCLUSIONS

- Satureja Montana L samples from Shkodra mountains (M5) and Kruja (M4) ones has higher concentration of carvacrol and thymol then the other (Tab2)

-Satureja Montana essential oils with high % of carvacrol and thymol (M5>M>M3) showed higher antimicrobial activity and especially against gram positive bacterial than those gram negative ones (Tab3)

-Main components are synergist to each other as seen by the graphic (Tab 4)

REFERENCES

1. Identification of essential oil components by gas chromatography and mass spectroscopy. Carol Stream, IL. USA: Allured Publishing Corporation.
2. AKGÜL, A., KIVANC,M., SERT, S., 1991: Effect of carvacrol on growth and toxin production by Aspergillus flavus and Aspergillus parasiticus. Sci. Aliment. 11, 361–370.
3. AKGÜL, A., ÖZCAN, M., CHIALVA, F., MONGUZZI, F., 1999: Essential Oil of Four TurkishWild-Growing Labiatae Herbs: Salvia cryptantha Montbr. et Auch., Oil Res. 11,209–
4. M A Botelho, N A P Nogueira, G M Bastos, S G C Fonseca, T L G Lemos, F J A Matos, et al. Antimicrobial activity of the essential oil from Lippia sidoides, carvacrol and thymol against oral pathogens. Brazilian journal of medical and biological research (2007)

SYNTHESIS OF SOME BENZOFURAN AND THEIR ANTITUBERCULOSIS ACTIVITY

G. Turan-Zitouni[1*], A. Özdemir[1], Z. A. Kaplancıklı[1], M. D. Altıntop[1]

[1]Anadolu University, Faculty of Pharmacy, Department of Pharmaceutical Chemistry, 26470, Eskisehir, Turkey.

INTRODUCTION

Tuberculosis, an infectious disease caused by *Mycobacterium tuberculosis*, is the primary cause of mortality in the world. Mycobacteria are widespread organisms that are becoming increasingly significant intracellular pathogens that establish an infection in oxygen-rich macrophage of the lung. Resistance of *Mycobacterium tuberculosis* strains to anti-mycobacterial agents is an increasing problem worldwide. However, powerful novel anti-TB drugs with new mechanism of action have not been developed in the last 45 years. In spite of severe toxicity on repeated dosing of isoniazid (INH), it is still considered to be a first line drug for chemotherapy of tuberculosis (1). Benzofuran and its derivatives exhibit various biological activities. Such derivatives were investigated as antibacterial (2) or antifungal (2) agents. The current work describes the synthesis of new benzofuran moiety with encouraging anti-mycobacterial activity against *M. tuberculosis* H37Rv.

MATERIALS AND METHODS

Chemistry

All chemicals were obtained from Aldrich Chemical Co. All melting points (m.p.) were determined by Gallenkamp apparatus and are uncorrected. The purity of the compounds was routinely checked by thin layer chromatography (TLC) using silica gel 60G (Merck). Elemental analyses were performed on a Perkin Elmer EAL 240 elemental analyser. Spectroscopic data were recorded with the following instruments: IR, Shimadzu 435 IR spectrophotometer; ^{1}H-NMR (Bruker 250 MHz spectrometer) and MS-FAB (VG Quattro Mass spectrometer).

O-(Substituted-2,3-dihydrobenzofuran-3-ilidenamino)(4-substitutedphenyl) thiocarbamate:

A mixture of benzofuran-3-one oxime (0.025 mol), 4-substitutedphenyl isothiocyanate (0.025 mL), and triethylamine (10 drops) in anhydrous diethylether was stirred under reflux in a nitrogen atmosphere for 20 h. The reaction was controlled by TLC using chloroform/methyl alcohol (9:1) as eluent. The reactional mixture was evaporated until dryness. The residue was recrystallized from hexane.

Antituberculosis activity and cytotoxicity

The initial screen is conducted against *M. tuberculosis* H37Rv (ATCC 27294) in BACTEC 12B medium using the Microplate Alamar Blue Assay (MABA) (3). Rifampicin was used as a reference drug. Three of the compounds showed significant antituberculosis activity as can be inferred from Table 1. The VERO cell cytotoxicity assay (4) is done in parallel with the TB Dose Response assay. Viability is assessed using Promega's Cell
Titer-Glo Luminescent Cell Viability Assay (5).

RESULTS AND DISCUSSION

In the present work, six new compounds **(1a-f)** were synthesized (Fig 1). Their structures were determined by IR, ^{1}H-NMR, FAB$^+$-MS spectral data and elemental analyses. All compounds gave satisfactory elemental analysis. The IR data were very informative and provided evidence for the formation of the expected
structures. In the IR spectra, some significant stretching bands due N-H, C=S and C=N were at 3280-3260 cm^{-1}, 1250-1220 cm^{-1}, 1620-1600 cm^{-1}, respectively. The ^{1}H-NMR spectral data were also consistent with the assigned structures. In the 400 MHz ^{1}H-NMR spectrum of compounds, the CH_2 protons of the benzofuran ring resonated as a singlet at 5,39-5,45ppm. The NH proton appeared as singlet at 10.55-10.65 ppm and all the other aromatic and aliphatic protons were observed at expected regions. The mass spectra of compounds showed [M+1] peaks, in agreement with their molecular formula.

The results of antituberculosis and cytotoxicity screening of newly prepared compounds (**1a-f**) are expressed in Table 1. The very important result was observed at antituberculosis activity screening for three of the compounds. The compounds **1a**,**1b**, and **1c** showed high antituberculosis activity (IC_{50}: 4.296, 6.208, 6.122 µg/mL and IC_{90}: 7.457, 7.029, 8.188 µg/mL) and low cytotoxicity (CC_{50}: 2.152, 1.525, 2.451 µg/mL). Because of SI value of the compound **1a**,**1b** and **1c**≥10, further tests are in progress.

CONCLUSIONS

A series of novel *O*-(Substituted-2,3-dihydrobenzofuran-3-ilidenamino) (4-substitutedphenyl) thiocarbamates **1** were synthesized and their

antituberculosis activities and toxicity have been evaluated. Among these series, compounds **1a** (R_1:H, R_2:H, R_3:NO_2),**1b** (R_1:H, R_2:OCH_3, R_3:NO_2), and **1c** (R_1:H, R_2:Cl, R_3:NO_2) showed significant antituberculosis activity. SAR observation showed that a benzofuran structure and a substitution on phenyl affect the activity. We concluded from our investigations that **1a**, **1b**, and **1c**
may be considered promising for the development of new antituberculosis agents with their antituberculosis activity and toxicity screening.

ACKNOWLEDGEMENT

Authors are thankful to the Tuberculosis Antimicrobial Acquisition and Coordinating Facility (TAACF) in the USA for the in vitro evaluation of antimycobacterial activity and cytotoxicity.

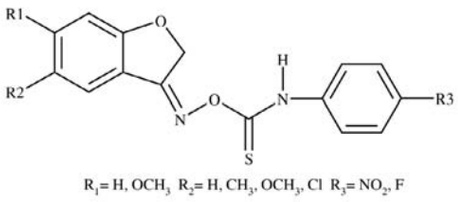

Fig. 1: Synthesis of target molecules (1a-f)

Table 1: Antituberculosis activity and cytotoxicity of the compounds

Comp.	MABA: H37Rv data		Cell Titer-Glo: Vero Cell CC_{50} (μg/mL)	SI (μg/mL)
	IC_{50} (μg/mL)	IC_{90} (μg/mL)		
1a	4,296	7,457	16,05	2,152
1b	6,208	7,029	10,723	1,525
1c	6,122	8,188	20,073	2,451
1d	12.412	13,514	-	-
1e	30,404	67,913	-	-
1f	12,519	25,977	-	-

REFERENCES

1. Ali MA, Shaharyar M, Siddiqui AA., Synthesis, structural activity relationship and anti-tubercular activity of novel pyrazoline derivatives. Eur. J. Med. Chem. 2007; 42: 268-271.
2. Bhovi VK, Bodke YD, Biradar S, Swamy BEK, Umesh S A., Facile Synthesis of Bromo-Substituted Benzofuran Containing Thiazolidinone Nucleus Bridged with Quinoline Derivatives: Potent Analgesic and Antimicrobial Agents. Phosphorus Sulfur 2010; 185: 110-116.
3. Collins LA, Franzblau SG., Microplate alamar blue assayversus BACTEC 460 system for high-throughput screening of compounds against Mycobacterium tuberculosis and Mycobacterium avium. Antimicrob. Agents Chemother. 1997; 41: 1004-1009.
4. Lara-Díaz VJ, Gaytán-Ramos AA, Dávalos-Balderas AJ, Santos-Guzmán J, Mata-Cárdenas BD, Vargas-Villarreal J, Barbosa-Quintana A, Sanson M, López-Reyes AG, Moreno-Cuevas JE. Microbiological and toxicological effects of perla black bean (Phaseolus vulgaris L.) extracts:in vitro and in vivo studies. Basic Clin. Pharmacol. Toxicol., 2009; 104: 81-86.
5. CellTiter-Glo® Luminescent Cell Viability Assay, Promega Corporation's,http://www.promega.com/tbs/tb288/tb288.html June 2009.

NEW DUAL FLUORESCENT-SPIN PROBES AND TRAPS

J. Mravljak[1*], T. Ojsteršek[2], M. Sollner Dolenc[1]

[1] University of Ljubljana, Faculty of Pharmacy, Aškerčeva cesta 7, 1000 Ljubljana, Slovenia; [2] Krka d.d. Novo mesto, Šmarješka Cesta 6, 8501 Novo mesto, Slovenia

INTRODUCTION

Dual fluorescent-spin compounds are composed of two molecular subfunctionality (a fluorescent chromophore and a stable nitroxide radical) tethered together by a spacer (1). The nitroxide is a strong intramolecular quencher of fluorescence from the chromophore fragment. When spin-trap (amine moiety) is oxidized by short-lived reactive free radical (like $O_2^{\bullet-}$ or $HO^{\bullet}$) the molecule becomes EPR active and the fluorescence decrease (Fig. 1)(2).

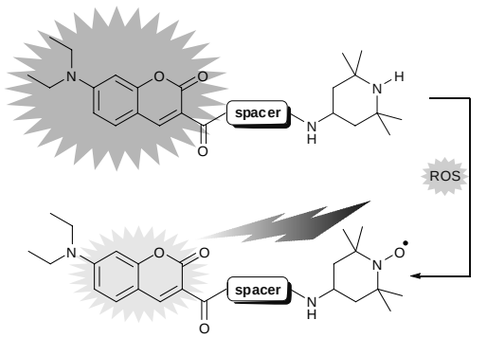

Fig. 1: Reaction of spin trap oxidation to nitroxide and fluorescence quenching.

Probing biological and nonbiological environments allow us to study molecular dynamics and the micropolarity of the media in the vicinity of fluorophore and nitroxide. Dual compounds besides keeping all the properties of fluorescence and nitroxide spin probes possess new principle advantages in the investigation of photochemical and photophysical processes. The organic synthetic chemistry allows us to optimize florescence, EPR and the redox properties of such dual molecules by adapting spacer, the fluorophore structure and the nitroxide fragment (1, 3). The aim of this study was to synthesize new dual probes and spin traps to investigate the influence of the distance between nitroxide and aminocoumarine on florescence quenching.

MATERIALS AND METHODS

Synthesis

Synthetic strategy is presented in Fig. 2.
Starting from carboxylic acid of 7-amino- coumarine (**1**) (4) 2,2,6,6-tetramethylpiperidin-4-amine (amine, Q = H) or 4-amino-2,2,6,6-tetramethylpiperidin-1-oxyl (nitroxide, Q = $O^{\bullet}$) was introduced by peptide coupling. To increase the distance between the nitroxide and the flouorphore amino acid spacer (glycine, β-alanine, γ-aminobutyric acid or 5-aminovalerianic acid) was introduced using the same method of peptide coupling.

Measurements of fluorescence

Fluorescence spectra were measured with a microtiter plate reader (TECAN Infinite M1000). Emission spectra were recorded for DMSO solutions of compounds **2** – **19** at excitation wavelength of 380 nm. From these results percent of fluorescence quenching vas calculated according to eq.

$$fluoresc.quenching = \left(\frac{nitroxide\ emiss.}{amine\ emiss.}\right) \times 100\%$$

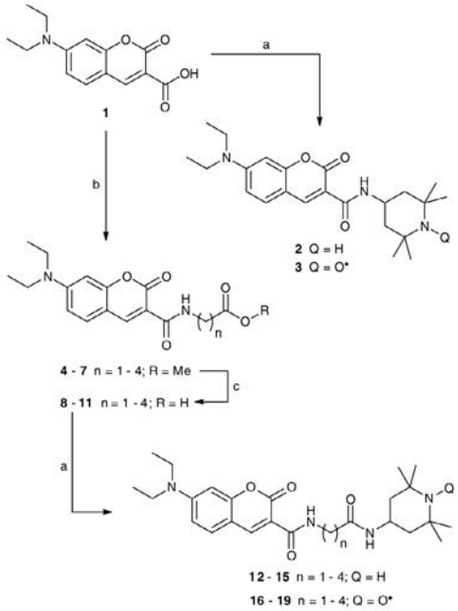

Fig. 2: Scheme of the synthesis. *Reagents and conditions:* (a) TBTU, NMM, DCM, 2,2,6,6-tetramethylpiperidin-4-amine or 4-amino-2,2,6,6-tetramethylpiperidin-1-oxyl; (b) TBTU, NMM, DCM, $H_2N(CH_2)_nCOOMe$; (c) conc. HCl, 1,4-dioxane.

RESULTS AND DISCUSSION

Emission spectra of amines (**2**, **12**, **13**, **14** and **15**) have the same shape and very similar fluorescence intensity. On the other hand emission spectra of nitroxides (**3**, **16**, **17**, **18** and **19**) preserved the shape but fluorescence intensity decreased (Fig. 3).

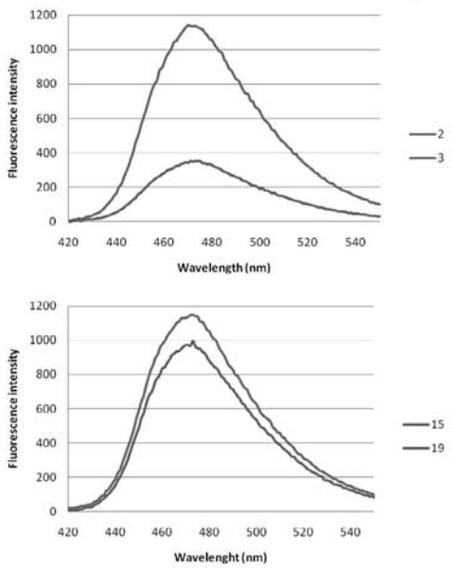

Fig. 3: Fluorescence emission spectra of 2, 3, 15 and 16 in DMSO at a concentration 10^{-6} M; excitation at 380 nm.

The highest quenching of fluorescence was achieved when nitroxide was bound directly to amino-coumarine (without using a spacer) thus the distance between the two molecular subfunctionalities was the smallest. Introducing a spacer into the molecule resulted in a decreased quenching of fluorescence (Fig. 4).

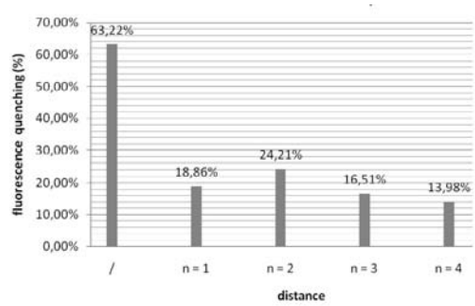

Fig. 4: Fluorescence quenching by nitroxide.

Increasing the length of the spacer resulted in a decrease of fluorescence quenching when β-alanine (n = 2), γ-aminobutyric acid (n = 3) and 5-aminovalerianic acid (n = 4) was used as a spacer, respectively. Using glycine (n = 1) as a spacer decrease quenching of fluorescence in comparison to using β-alanine although the distance between nitroxide and amino-coumarine is smaller in the case of glycine. This can be attributed to differences in polarity of compounds **12**, **16** and **13**, **17** in the region of the spacer which can in combination with differences in solvation (different thickness of solvent around the compounds due to differences in solvent attraction (5)) effect fluorescence (emission) spectra of mentioned compounds through altering quantum yield via reorientation/relaxation of dipolar moments of solvent molecules around the dipolar moment of the excited state of the amino-coumarine fluorophore.

REFERENCES

1. Likhtenshtein GI, Nitroxides in Physicochemistry, in: Likhtenshtein GI (Ed.), Nitroxides, Wiley-VCH Verlag GmbH & Co. KGaA, 2008, pp. 269-301.
2. Likhtenshtein GI, Nitroxide Redox Probes and Traps, Nitron Spin Traps, in: Likhtenshtein GI (Ed.), Nitroxides, Wiley-VCH Verlag GmbH & Co. KGaA, 2008, pp. 239-268.
3. Pajk S, Garvas M, Strancar J, Pecar S. Nitroxide-fluorophore double probes: a potential tool for studying membrane heterogeneity by ESR and fluorescence. Org. Biomol. Chem. 2011.
4. Ma Y, Luo W, Quinn PJ, Liu Z, Hider RC. Design, synthesis, physicochemical properties, and evaluation of novel iron chelators with fluorescent sensors. J. Med. Chem. 2004; 47: 6349-6362.
5. Lakowicz JR. Principles of fluorescence spectroscopy, 3rd ed. Springer: New York, 2006.

DISCOVERY OF D-GLUTAMIC ACID BASED INHIBITORS OF BACTERIAL MUR-D LIGASE

T. Tomašić[1], N. Zidar[1], D. Blanot[2], S. Gobec[1], D. Kikelj[1], L. Peterlin Mašič[1*]

[1] University of Ljubljana, Faculty of Pharmacy, Aškerčeva 7, 1000 Ljubljana, Slovenia; [2] Enveloppes Bactériennes et Antibiotiques, IBBMC, UMR 8619 CNRS, Univ Paris-Sud, 91405 Orsay, France

INTRODUCTION

The escalating emergence of bacterial strains resistant to most of the currently available antibiotics has compromised the treatment of bacterial infections and led to increased morbidity and mortality worldwide. Development of effective antibacterial drugs, necessitating novel mechanisms of action and more chemical diversity than current drugs, is therefore essential to combat bacterial drug-resistance. (1) Peptidoglycan is an essential cell wall polymer unique to prokaryotic cells that preserves cell integrity by withstanding high internal osmotic pressure and maintaining a defined cell shape. The biosynthesis of peptidoglycan – a viable source of targets for development of novel antibacterials – is a multi-step process comprising intracellular assembly of the UDP-MurNAc-pentapeptide, which is subsequently translocated through the cytoplasmic membrane and incorporated into the growing peptidoglycan layer. ATP-dependent Mur ligases (MurC to MurF) catalyze a series of reactions leading to UDP-MurNAc-

pentapeptide. The fact that Mur ligases are vital for the survival of bacteria makes them attractive targets for antibacterial drug discovery. (2)

RESULTS AND DISCUSSION

Recently, we have designed, synthesized and biologically evaluated several series of Mur inhibitors, including multi-target inhibitors of Mur ligases (3, 4) and a series of MurD-selective inhibitors represented by the most potent compounds **1-10** (5-8).

Biological activity

Target compounds **1-10** were assayed for inhibition of MurD ligase from *E. coli* (Table 1 and 2). The Malachite green assay, which detects orthophosphate generated during the enzymatic reaction, was used. The results are presented as IC_{50} values. (7, 8) They show that incorporation of the fluorine or hydroxyl group on a ring reduces MurD inhibition. Introduction of carboxylate-containing acyl substituents, such as oxalyl, malonyl and succinyl groups, on the amino group between rings resulted in the most potent series of MurD inhibitors, with IC_{50} values down to 3 μM. In general, rhodanine-based compounds **8-10** were an order of magnitude better than the thiazolidine-2,4-dione-based compounds **5-7**. MurD inhibition by thiazolidine-2,4-diones **5-7** was dependent mainly on the chain length of the *N*-acyl substituent. Compound **6**, with a malonyl group, was the most potent in the series, with an IC_{50} of 15 μM, followed by oxalyl-substituted compound **5** with an IC_{50} of 40 μM. The weakest inhibitor was compound **7**, with a succinyl moiety, which had an IC_{50} of 105 μM. The same trend is also seen in the rhodanine series that exhibited IC_{50} values of 5 μM (**8**), 3 μM (**9**) and 7 μM (**10**), confirming the malonyl moiety as the optimal chain length. (7, 8) Compound **9** was found to inhibit *E. faecalis* growth weakly, with an MIC of 128 μg/mL, while compound **10** inhibited the growth of both Gram-positive bacteria with an MIC of 128 μg/mL. All compounds were inactive against Gram-negative bacteria. (8)

Table 1. Inhibitory activities of compounds **1-4** against MurD ligase from *E. coli*.

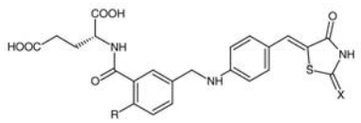

compd	X	R	MurD IC_{50}
1	O	H	85 μM
2	S	H	45 μM
3	S	F	253 μM
4	S	OH	124 μM

Table 2: Inhibitory activities of compounds **5-10** against MurD ligase from *E. coli.*

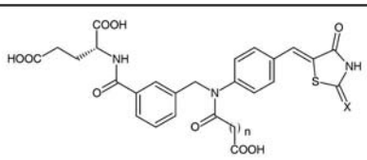

compd	X	n	MurD IC_{50}[a]
5	O	0	40 μM
6	O	1	15 μM
7	O	2	105 μM
8	S	0	5 μM
9	S	1	3 μM
10	S	2	7 μM

Standard deviations were within ±10% of the means. [a]Concentration of the inhibitor, where residual activity of the enzyme is 50%.

X-Ray Crystallography

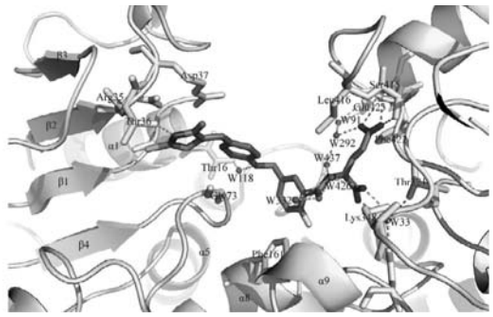

Fig. 1: X-ray binding mode of inhibitor **3** (in magenta) in the active site of MurD from *E. coli* (PDB entry: 2Y68). Hydrogen bonds between **3** and MurD active site residues (in yellow) and crystal water molecules (in red) are presented as dashed green lines.

The binding mode of inhibitor **3** in the MurD active site was determined by solving the crystal structure of the MurD-**3** complex (PDB entry: 2Y68). (8)

CONCLUSIONS

We have designed, synthesized and evaluated a series of novel D-glutamic acid-based inhibitors of *E. coli* MurD ligase. The crystal structure of MurD ligase in complex with **3** shows a binding mode in the MurD active site that served as a foundation for the structure-based design of the most potent series of MurD inhibitors **8-10** with IC_{50} values between 3 and 7 μM. Inhibition of MurD ligase in the low micromolar range makes compounds **8-10**, to the best of our knowledge, the most potent D-glutamic acid-based MurD inhibitors reported to date.

REFERENCES

1. Chopra I, Schofield, C.; Everett, M.; O'Neill, A.; Miller, K.; Wilcox, M.; Frere, J. M.; Dawson, M.; Czaplewski, L.; Urleb, U.; Courvalin, P. Treatment of health-care-associated infections caused by Gram-negative bacteria: a consensus statement. Lancet Infect. Dis. 2008, 8, 133-139.
2. Vollmer, W.; Blanot, D.; de Pedro, M. A. Peptidoglycan structure and architecture. FEMS Microbiol. Rev. 2008, 32, 149-167.
3. Šink, R.; Kovač, A.; Tomašić, T.; Rupnik, V.; Boniface, A.; Bostock, J.; Chopra, I.; Blanot, D.; Peterlin Mašič, L.; Gobec, S.; Zega, A. Synthesis and biological evaluation of N-acylhydrazones as inhibitors of MurC and MurD ligases. ChemMedChem 2008, 3, 1362-1370.
4. Tomašić, T.; Zidar, N.; Kovač, A.; Turk, S.; Simčič, M.; Blanot, D.; Müller-Premru, M.; Filipič, M.; Grdadolnik, S. G.; Zega, A.; Anderluh, M.; Gobec, S.; Kikelj, D.; Peterlin Mašič, L. 5-Benzylidenethiazolidin-4-ones as Multi-target Inhibitors of Bacterial Mur Ligases. ChemMedChem 2010, 5, 286-295.
5. Tomašić, T.; Zidar, N.; Rupnik, V.; Kovač, A.; Blanot, D.; Gobec, S.; Kikelj, D.; Peterlin Mašič, L. Synthesis and biological evaluation of new glutamic acid-based inhibitors of MurD ligase. Bioorg. Med. Chem. Lett. 2009, 19, 153-157.
6. Zidar, N.; Tomašić, T.; Šink, R.; Rupnik, V.; Kovač, A.; Turk, S.; Patin, D.; Blanot, D.; Contreras Martel, C.; Dessen, A.; Müller Premru, M.; Zega, A.; Gobec, S.; Peterlin Mašič, L.; Kikelj, D. Discovery of novel 5-benzylidenerhodanine and 5-benzylidenethiazolidine-2,4-dione inhibitors of MurD ligase. J. Med. Chem. 2010, 53, 6584-6594.
7. Tomašić, T.; Kovač, A.; Simčič, M.; D.; Blanot, D.; Golič Grdadolnik S.; A.; Gobec, S.; Kikelj, D.; Peterlin Mašič, L. Novel 2-Thioxothiazolidin-4-one Inhibitors of Bacterial MurD Ligase Targeting d-Glu- and Diphosphate-binding Sites. Eur. J. Med. Chem. 2011, accepted for publication.
8. Tomašić, T.; Zidar, N.; Šink, R.; Kovač, A.; D.; Blanot, D.; Contreras Martel, C.; Dessen, A.; Müller Premru, M.; Zega, A.; Gobec, S.; Kikelj, D.; Peterlin Mašič, L. Structure-based design of a series of D-glutamic acid based inhibitors of bacterial MurD Ligase. J. Med. Chem. 2011, accepted for publication.

ACETYLCHOLINESTERASE INHIBITORY EFFECTS OF SOME BENZOTHIAZOLE-PIPERAZINE DERIVATIVES

U. Demir-Özkay[1*], O. D. Can[1], Y. Özkay[2]

[1] Anadolu University, Faculty of Pharmacy, Department of Pharmacology, 26470, Eskişehir, Turkey; [2] Anadolu University, Faculty of Pharmacy, Department of Pharmaceutical Chemistry, 26470, Eskişehir, Turkey

INTRODUCTION

The turnover regulation and level of acetylcholine in neurons and synaptic junction play an essential role in various neural disorders, such as Alzheimer's disease, senile dementia, myasthenia gravis and Parkinson's disease. It is well-known that acetylcholinesterase (AChE) degrades acetylcholine in nerve synapses. Inhibitors of this enzyme increase the signal transmission in synapses by prolonging the effect of acetylcholine. Thus, these agents are beneficial for the symptoms of mentioned neurological diseases. However, AChE inhibitors also have adverse effects due to cholinergic stimulation in the brain and peripheral tissues (1,2). Therefore, the searching for new AChE inhibitors, which may cause lower side effects, is extensively investigated. In the light of above knowledge, we designed a compact system including benzothiazole and piperazine pharmacophores, which were the main substructures of some previously reported AChE inhibitors (3,4). AChE/butyrylcholinesterase (BChE) inhibitory activities of synthesized benzothiazole/piperazine derivatives were evaluated in this study.

MATERIALS AND METHODS

Materials

Reagents used in the syntheses were purchased from Merck (Darmstad, Germany) and Sigma-Aldrich (Steinheim, Germany). Donepezil hydrochloride, AChE-E.C.3.1.1.7., Type VI-S, from Electric Eel, 500 units were purchased from Sigma-Aldrich (Steinheim, Germany). The other chemicals used in enzymatic assay were obtained from Fluka (Buchs, Switzerland).

Synthesis of Benzothiazole-piperazines (2a-2e)

Title compounds were prepared in two reaction steps. First of all, 2-aminobenzothiazole (0.03 mol, 4.5 g) in benzene : triethyl amine mixture (100 mL : 5 mL) was acetylated with chloroacetyl chloride (0,033 mol, 2.63 mL) to give 2- chloro-N-(benzothiazol-2-yl)acetamide (**1**). Secondly, N-Benzothiazol-2-yl-2-substituted acetamides (**2a-2e**) were synthesized in acetone by the reaction of compound **1** (0.0025 mol, 0.566 g) and appropriate 1-substituted piperazine (0.0025 mol), with the presence of K_2CO_3 (0.0025 mol, 0.345 g). Products were recrystallized from absolute ethanol.

Acetylcholinesterase/butyrylcholinesterase activity assay

Enzyme activity was investigated using a slightly modified colorimetric method of Ellman et al. (5). The evaluation of enzyme activity was performed using a specific chromogenic reagent, DTNB. The measurements were carried out as follows: Stock solutions of the synthesized compounds were prepared in 2% DMSO. The enzyme activity was determined in the presence six different concentrations of a test compound. Each concentration was assayed in triplicate. The samples were investigated immediately after preparation. Prior to use, all solutions were adjusted to 20 °C. Enzyme solution (100 mL) and test compound solution (100 µL) were added into a cuvette containing the phosphate buffer (3.0 mL, 0.1 M; pH = 8.0). After 5 min. incubation, required aliquots of the DTNB solution (100 mL) and of the acetylthiocholine iodide (20 µL) or butyrylthiocholine iodide (20 µL) were added. After rapid and immediate mixing the absorption was measured at 412 nm. As a reference, an identical solution of the enzyme without the inhibitor is processed following the same protocol. Donepezil was used as a positive control.

RESULTS AND DISCUSSION

Chemistry

In the present work five N-Benzothiazol-2-yl-2-substituted acetamide compounds (**2a-2e**) were synthesized. Structures of the compounds were elucidated by spectral analyses. Significant stretching bands in the IR spectra were observed at expected regions. Stretching bands for N-H and C=O groups were observed at 3284-3234 cm^{-1} and 1691-1705 cm^{-1}, respectively. In the 500 MHz ^1H NMR spectra protons belonging to 3th and 5th positions of piperazine ring gave multiplet at 2.36-3.47 ppm. Protons of 2nd and 6th positions of the piperazine were observed at 2.64-3.64 ppm as multiplet. Acetyl ($COCH_2$) group protons were observed as a singlet at 3.56-3.96 ppm. Aromatic protons were recorded at 6.84-8.02 ppm. Protons of amide group (NHCO) gave peaks at 10.96-12.10 as a singlet. The mass spectra (Es-Ms) of compounds showed [M+1] peaks, in agreement with their molecular formula.

Cholinesterase activity

The inhibitory potency against AChE was evaluated by Ellman's test (5). The IC_{50} values are shown in Table. Donepezil was used as a reference drug. As seen in the Table, phenyl substituted compound **2a** possess a poor inhibitory activity on both AChE and BChE. The compounds **2b** and **2c** showed moderate inhibitory activity. Besides, the compounds **2d** and **2e** indicated notable activity, which was comparable with the reference drug donepezil.

Table: AChE IC50 (µ/M) and BChE IC50 (µ/M) of synthesized compounds. Results are presented as the mean ± SEM.

Comp.	R	AChE IC_{50} (µ/M)	BChE IC_{50} (µ/M)	Selectivity*
2a		22.6 ± 3.07	104.8 ± 9.15	4.64
2b		0.52 ± 0.072	28.9 ± 4.63	55.6
2c		0.13 ± 0.019	16.6 ± 1.27	127.7
2d		0.061 ± 0.0044	8.74 ± 0.36	143.3
2e		0.086 ± 0.0029	9.27 ± 0.41	107.8
Donepezil		0.023 ± 0.0015	4.18 ± 0.34	181.7

*** BChE IC_{50} (µ/M) / AChE IC_{50} (µ/M)**

CONCLUSIONS

Benzothiazole-piperazine compounds indicated different levels of AChE inhibitory potential. Compounds **2b**-**2e**, carrying benzyl groups possess significant inhibitory potency against AChE, whereas this activity is not observed for BChE. As a result, this selective AChE enzyme inhibitory activity depends on the substitution pattern on the benzyl rings.

REFERENCES

1. Kapková P, Stiefl N, et al. Synthesis, biological activity, and docking studies of new acetylcholinesterase inhibitors of the bispyridinium type. Arch. Pharm (Weinheim). 2003; 336: 523-540.
2. Mukherjee PK, Kumar V, et al. Acetylcholinesterase inhibitors from plants. Phytomed. 2007; 14: 289-300.
3. Nagel AA, Liston DR, et al. Design and synthesis of 1-heteroaryl-3-(1-benzyl-4-piperidinyl)propan-1-one derivatives as potent, selective acetylcholinesterase inhibitors. J. Med. Chem. 1995; 38: 1084-1089.
4. Sadashiva CT, Narendra Sharath Chandra JN, et al. Synthesis and efficacy of 1-[bis(4-fluorophenyl)-methyl]piperazine derivatives for acetylcholinesterase inhibition, as a stimulant of central cholinergic neurotransmission in Alzheimer's disease. Bioorg. Med. Chem. Lett. 2006; 16: 3932-3936.
5. Ellman GL, Courtney KD, et al. A new and rapid colorimetric determination of acetylcholinesterase activity. Biochem. Pharmacol. 1961; 7: 88-95.

ANTIMICROBIAL EFFECT OF SOME NEW 2,5-DISUBSTITUTED BENZIMIDAZOLES

Y. Özkay[1*], Y. Tunalı[2], H. Karaca[2], İ. Işıkdağ[1]

[1] Anadolu University, Faculty of Pharmacy, Department of Pharmaceutical Chemistry, 26470, Eskişehir, Turkey; [2] Anadolu University, Faculty of Pharmacy, Department of Pharmaceutical Microbiology, 26470, Eskişehir, Turkey

INTRODUCTION

Discovery of new antimicrobial agents to treat infections has been one of the most important medical aim for many years. Because the resistance of fungi and bacteria to current antimicrobial drugs is a major public health threat throughout the world (1, 2). Benzimidazole and hydrazone are important pharmacophores in the development of new antimicrobial agents. There are some reports about antimicrobial potency of both benzimidazole and hydrazone compounds (3, 4). Depending on this respect, we have recently reported a study (5) including antimicrobial activity of some new compounds, which carry benzimidazole and hydrazone pharmacophores on the same chemical skeleton. Results of such study indicated the importance of chloro substituent on antimicrobial activity. Therefore, in the present study we synthesized some novel benzimidazole-hydrazone derivatives which carry one or two chloro substituent at different positions.

MATERIALS AND METHODS

Materials

All chemicals used in syntheses were obtained from Merck (Germany), Sigma-Aldrich (Germany) or Acros (Belgium) companies. Human pathogenic as *gram* (+) bacteria *Staphylococcus aureus* NRRL B-767, *Bacillus cereus* NRRL B-3711, and *Enterococcus faecalis* ATCC 29212, as *gram* (-) bacteria, *Klebsiella pneumoniae* NRRL B-4420, *Pseudomonas aeruginosa* ATCC 254992 and *Yersinia enterocolitica*, as yeast *Candida globrata* (isolates obtained from Faculty of Medicine Osmangazi University, Eskisehir, Turkey) were used in antimicrobial assays.

Synthesis of target compounds (1-14)

4-(5-Substituted-*1H*-benzimidazol-2-yl)-benzoic acid N-substituted-benzylidene hydrazide derivatives (**1-14**) were synthesized in accordance with our recent study (5).

Antimicrobial assay

Antimicrobial activity assay was performed according to CLSI reference M7-A7 broth microdilution method as described in our recent study (5). Chloramphenicol, Nifuroxazide, and Ketoconazole were used as standard agents.

RESULTS AND DISCUSSION

Chemistry

In the present study, fourteen 4-(5-Substitue-*1H*-benzimidazol-2-yl)-benzoic acid N-substituebenzylidene hydrazide derivatives (**1-14**) were synthesized. Reaction sequence is shown in the Scheme. Some physiochemical characteristics of the products are given in Table 1. Structure elucidations of the final compounds were performed by spectral data. Characteristic stretching absorption of C=O groups were observed at 1687-1664 cm^{-1}. The stretching absorption at about 3396-3304 and 1617-1402 cm^{-1} were recorded for N-H bonds and C=C and C=N double bonds, respectively. In the ^1H NMR spectra, all of the aromatic and aliphatic protons were observed at estimated areas. N-H protons of benzimidazole and hydrazone gave peaks at 12.88-13.06 ppm as a broad and at 8.59-8.78 ppm as a singlet, respectively. C-H proton of azomethine group gave a singlet at 8.37-8.64 ppm. Aromatic protons of the compounds were recorded at the area of 7.04-8.16 ppm. M+1 peak in the mass spectra (ES-MS) were in agreement with the calculated molecular weight of the compounds.

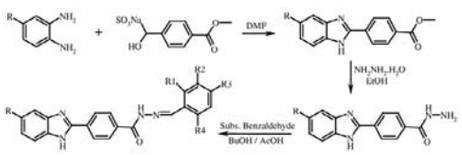

Scheme: Reaction sequence of the compounds **1-14**.

Table 1: Some physiochemical characteristics of the compounds **1-14**.

No	R	R1	R2	R3	R4	Molecular Formula	M.P. (°C)
1	-Cl	-H	-H	-H	-H	$C_{21}H_{15}ClN_4O$	260
2	-Cl	-Cl	-H	-H	-H	$C_{21}H_{14}Cl_2N_4O$	281
3	-Cl	-H	-Cl	-H	-H	$C_{21}H_{14}Cl_2N_4O$	170
4	-Cl	-H	-H	-Cl	-H	$C_{21}H_{14}Cl_2N_4O$	298
5	-Cl	-Cl	-H	-Cl	-H	$C_{21}H_{13}Cl_3N_4O$	252
6	-Cl	-Cl	-Cl	-H	-H	$C_{21}H_{13}Cl_3N_4O$	289
7	-Cl	-Cl	-H	-H	-Cl	$C_{21}H_{13}Cl_3N_4O$	174
8	$-CH_3$	-H	-H	-H	-H	$C_{22}H_{18}N_4O$	202
9	$-CH_3$	-Cl	-H	-H	-H	$C_{22}H_{17}ClN_4O$	179
10	$-CH_3$	-H	-Cl	-H	-H	$C_{22}H_{17}ClN_4O$	304
11	$-CH_3$	-H	-H	-Cl	-H	$C_{22}H_{17}ClN_4O$	296
12	$-CH_3$	-Cl	-H	-Cl	-H	$C_{22}H_{16}Cl_2N_4O$	207
13	$-CH_3$	-Cl	-Cl	-H	-H	$C_{22}H_{16}Cl_2N_4O$	292
14	$-CH_3$	-Cl	-H	-H	-Cl	$C_{22}H_{16}Cl_2N_4O$	188

Antimicrobial activity

Antimicrobial effects of the compounds **1-14** are presented in Table 2. They exhibited poor antibacterial activity against *gram (+)* bacteria *S. aureus B. cereus*, and *E. faecalis.* Similarly, antifungal activity of the compounds (**1-14**) was not important against *Candida globrata*. However, tested compounds showed comparable antibacterial activity to reference drugs against *gram* (-) bacteria. Against *P. aeruginosa*, all compounds, showed greater activity than Nifuroxazide. Such activity was equal to Chloramphenicol. Antibacterial activity of the compounds **1-3**, **5**, **14** against *K. pneumonia* was equal to Nifuroxazide. The other compounds in the series showed greater activity than Nifuroxazide on the same bacterial strain. The compounds (**1-14**), indicated better antibacterial effect than Nifuroxazide aginst *Y. enterocolitica*. Besides, activity of the compounds **4** and **11** was equal activity to that of Chloramphenicol

Table: MIC values (µg/mL) of the compounds 1-14 against various microorganisms.

No	A	B	C	D	E	F	G
1	200	200	200	50^a	50^{bc}	50^b	400
2	200	200	400	50^a	50^{bc}	50^b	200
3	100	200	200	50^a	50^{bc}	50^b	200
4	100	200	200	25^b	50^{bc}	25^{bc}	200
5	100	200	200	50^a	50^{bc}	50^b	200
6	100	200	400	25^b	50^{bc}	50^b	200
7	100	200	400	25^b	50^{bc}	50^b	200
8	100	200	200	25^b	50^{bc}	50^b	200
9	100	200	200	25^b	50^{bc}	50^b	200
10	200	200	400	25^b	50^{bc}	50^b	200
11	200	200	200	25^b	50^{bc}	25^{bc}	200
12	100	200	400	25^b	50^{bc}	50^b	200
13	100	200	200	25^b	50^{bc}	50^b	200
14	100	400	200	50^a	50^{bc}	50^b	200
Ref1	25	100	100	50	100	100	-
Ref2	12.5	6.25	12.5	12.5	50	25	-
Ref3	-	-	-	-	-	-	12.5

A: *S. aureus,* **B:** *B. cereus,* **C:** *E. faecalis,* **D:** *K. pneumonia,* **E:** *P. aeruginosa,* **F:** *Y. enterocolitica,* **G:** *C. globrata,* **Ref1**: Nifuroxazide, **Ref2**: Chloramphenicol, **Ref3**: Ketoconazole [a]Equal MIC value to Ref1 [b]Lower MIC value than Ref1 [c]Equal MIC value to Ref1

CONCLUSIONS

When compared with our recent study (5), results of antimicrobial activity screening revealed that methyl or chloro substitution of benzimidazole ring at 5th position has not essential effect on antimicrobial activity. The compounds **4** and **11**, carrying 4-chlorobenzylidene residue showed best antibacterial potency in the series.

REFERENCES

1. Turan-Zitouni G, Kaplancikli ZA et al. Synthesis and antimicrobial activity of 4-phenyl/cyclohexyl-5-(1-phenoxyethyl)-3-[N-(2-thiazolyl)acetamido]thio-4H-1,2,4-triazole derivatives. Eur. J. Med. Chem. 2005; 40: 607-613.
2. Hegde JC, Girisha KS, et al. Synthesis and antimicrobial activities of a new series of 4-S-[41-amino-51-oxo-61-substituted benzyl-41,51-dihydro-11,21,41-triazin-3-yl] mercaptoacetyl-3-arylsydnones. Eur. J. Med. Chem. 2008; 43: 2831-2834.
3. Pawar NS, Dalal DS et. al. Studies of antimicrobial activity of N-alkyl and N-acyl 2-(4-thiazolyl)-1H-benzimidazoles. Eur. J. Pharm. Sci. 2004; 21: 115-118.
4. Chornous V A, Bratenko MK, et al. Synthesis and antimicrobial activity of pyrazole-4-carboxylic acid hydrazides and N-(4-pyrazoyl)hydrazones of aromatic and heteroaromatic aldehydes. Pharm. Chem. J. 2001; 35: 203-205.
5. Ozkay Y, Tunali Y, et al. Antimicrobial activity and a SAR study of some novel benzimidazole derivatives bearing hydrazone moiety. Eur. J. Med. Chem. 2010; 45: 3293-3298.

SYNTHESIS AND ANTIFUNGAL ACTIVITY OF SUBSTITUTED UREA AND THIOUREA DERIVATIVES CONTAINING 1,2,4-TRIAZOLE MOIETY

B. Koçyiğit-Kaymakçıoğlu[1*], A. Ö. Çelen[1], N. Tabanca[2], D. E. Wedge[3]

[1] Marmara University, Faculty of Pharmacy, Department of Pharmaceutical Chemistry, 34668, İstanbul, Turkey; [2] National Center for Natural Products Research, Research Institute of Pharmaceutical Sciences, The University of Mississippi, University, MS 38677 USA; [3] Mississippi University,Department of Agriculture, Agricultural Research Service, Natural Products Utilization Research Unit, Mississippi, 38667 USA

INTRODUCTION

Thioureas are important sulphur and nitrogen-containing compounds and they have been useful substances in drug research in recent years (1). Some urea derivatives possess valuable biological and pharmacological activities such as, antituberculosis, antibacterial and anticonvulsant properties (2-3). Most of these compounds include heterocyclic rings as oxadiazole, thiadiazole, triazole, and pyrazole. From these ring systems, the 1,2,4-triazole nucleus has been incorporated in to a wide variety of therapeutically interesting molecules to transform them in to better drugs. Drugs such as fluconazole and itraconazole are the best examples of potent antifungal molecules possessing the triazole nucleus (4).

The development of antimicrobial resistance has increased recently and there is a need of synthesis for new antimicrobial agents which will be more selective, potent and less toxic. As part of a program to discovering new agrochemicals for disease control, a series of urea and thiourea derivatives containing 1,2,4-triazole ring, were synthesized and tested for growth inhibition of several plant pathogenic fungi from the genera *Colletotrichum*, *Botrytis*, *Fusarium* and *Phomopsis using* 96-well microtiter plate assays.

MATERIALS AND METHODS

Chemistry

0.500 g (3.3 mmol) 4-(Aminophenyl)acetic acid is solved in acetone at 100°C. Then, a solution of corresponding isocyanate/ isothiocayanate (3.3 mmol) in 5 mL acetone is added as three parts per 30 minutes. After 6-8 hours, reaction is finalized by TLC control. Solid material of **1a-e** and **2a-e** is filtered and recrystallized with a suitable solvent. In the second step, treatment of these compounds (**1a-e**, **2a-e)** with equimolar thiocarbohydrazide at 130-140°C in oil bath about 2-3 hours, gave new urea and thiourea derivatives which containing 1,2,4-triazole (**3a-e, 4a-e**).

Antifungal activity

A standardized 96-well micro-dilution broth assay developed by Wedge and Kuhajek (5) for the discovery of natural fungicidal agents was used to evaluate the antifungal activity of test compounds. This 96-well microtiter assay is used to determine and compare the sensitivity of fungal plant pathogens to natural and synthetic compounds with known fungicidal standards. Isolates of *Colletotrichum acutatum* Simmonds, *Colletotrichum fragariae* Brooks, *Colletotrichum gloeosporioides* (Penz.) Penz & Sacc. In Penz, *Botrytis cinerea* Pers.:Fr, *Fusarium oxysporum* Schlechtend:Fr, *Phomopsis obscurans* (Ellis and Everh.) *B. sutton*, and *P. viticola* Sacc., were used to evaluate the antifungal activity of the test compounds using *in vitro* micro-dilution broth assay. Each fungal species is challenged in a dose-response format so that the final test compounds concentrations of 0.3, 3.0 and 30.0 µM are achieved (in duplicate) in the different columns of the 96-well plate.

RESULTS AND DISCUSSION

Compounds **1a-e** and **2a-e** were prepared by refluxing equimolar 4-(aminophenyl)acetic acid and various isocyanates and isothiocyanates in acetone. The reaction of the compounds **1a-e** and **2a-e** with thiocarbohydrazide in oil bath afforded the corresponding 1,2,4-triazoles (**3a-e, 4a-e**). The chemical structures of all compounds were characterized by various spectroscopic methods and elementel analysis. General formula of target compounds is described in Figure 1.

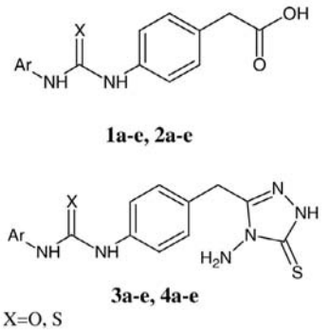

Fig. 1: General formula of synthesized compounds

All synthesized compounds were tested for growth inhibition of several plant pathogenic fungi from the genera *Colletotrichum*, *Botrytis*, *Fusarium* and *Phomopsis using* 96-well microtiter plate assays. The 96-well microbioassay system is a liquid broth culture system in a dose-response format to evaluate each compound. Microbioassay results indicated that the five most active compounds were **1b** (X: S, Ar: 4-ClC_6H_5), **1c** (X: S, Ar: 4-$OCH_3C_6H_5$), **3d** (X: S, Ar: 4-$NO_2C_6H_5$), **3f** (X: S, Ar: 2,4,6-ClC_6H_2), and **4e** (X: O, Ar: 4-FC_6H_5), against *Phomopsis obscurans* and *P. viticola. Phomopsis* cane and leaf spot (*P. viticola*) causes serious economic losses to the vine grape industry in the United States of America and Europe, while *P. obscurans* causes *Phomopsis* leaf blight and fruit rot of strawberry.

CONCLUSIONS

A series of urea and thiourea derivatives bearing 1,2,4-triazole ring were synthesized and tested for their antifungal activity against several plant pathogenic fungi. Compounds **1b, 1c, 3d**, **3f** and **4e** showed potential for further development for control of *Phomopsis* species, which cause small fruit blight, leaf spot, and rot.

REFERENCES

1. Mahajan A, Yeh S, Nell M, Van Rensburg CJ, Chibale K. Synthesis of new 7-chloroquinolinyl thioureas and their biological investigation as potential antimalarial and anticancer agents. Bioorg. Med. Chem. Lett. 2007;17: 5683–5685.
2. Koçyiğit-Kaymakçıoğlu B, Rollas S, Körceğez E, Arıcıoğlu F. Synthesis and biological evaluation of new N-substituted-N-(3,5-di/1,3,5-trimethylpyrazole-4-yl)thiourea/urea derivatives. Eur J. Pharm. Sci. 2005; 26(1): 97-103.
3. Khan SA, Singh N, Saleem K. Synthesis, characterization and in vitro antibacterial activity of thiourea and urea derivatives of stereoids. Eur. J. Med. Chem. 2008; 43(10): 2272-2277.
4. Ashok M, Holla BS, Boja P. Convenient one pot synthesis and antimicrobial evaluation of some new Mannich bases carrying 4-methylthiobenzyl moiety. Eur. J. Med. Chem. 2007; 42: 1095-1101.
5. Wedge DE, Kuhajek JM. A microbioassay for fungicide discovery. SAAS Bulletin Biochem. Biotech. 1998; 11: 1-7.

DESIGN, SYNTHESIS AND ANTIPROLIFERATIVE ACTIVITIES OF CINNAMIC AND HYDROCINNAMIC ACID LIPOPHILIC DERIVATIVES

F. Roleira[1*], C. Tomé[1], T. Bernardo[2], T. Serafim[2], P. Oliveira[2], C. Varela[1], F. Borges[3], R. Carvalho[4], E. Tavares-da-Silva[1]

[1] CEF, Pharmaceutical Chemistry Group, Faculty of Pharmacy, Coimbra University, Portugal; [2] CNC, Centre for Neuroscience and Cellular Biology, Coimbra University, Portugal; [3] CIQUP, Chemistry Dep, Faculty of Sciences, Porto University, Portugal; [4] CNC, Life Sciences Dep, Faculty of Science and Technology, Coimbra University, Portugal

INTRODUCTION

Diet-associated phenolic compounds, specifically hydroxycinnamic acids and derivatives, are known to display relevant antioxidant properties as well as biological activity towards several tumor cells (1). In addition, it has been demonstrated that their growth-inhibitory potency is strongly dependent on their structural characteristics. Despite all the interesting biological effects of hydroxycinnamic acids their bioavailability presents some limitations. Although working well in aqueous media, their hydrophilic nature is usually a restriction to cross membranes (2) and reach intracellular targets. In a recent work, we demonstrated that lipophilic derivatives of caffeic and ferulic acids have increased citotoxicity, against three different human breast cancer cell lines, when compared with the original hydrophilic acids (3).

In order to develop new and more effective phenolic agents suitable for chemopreventive and/or chemotherapeutic purposes, amide derivatives of several cinnamic acids (**Fig.1**) were designed and synthesized. Subsequently, the compounds were screened in terms of cytotoxicity on two different human breast cancer cell lines, namely MCF-7 and HS578T and on one non-transformed human fibroblast cell line (BJ), which was used as a non-tumor cell control. In addition, three amide derivatives of cinnamic/hydrocinnamic acids without hydroxyl groups as well as the parent acid compounds were tested for comparative purposes.

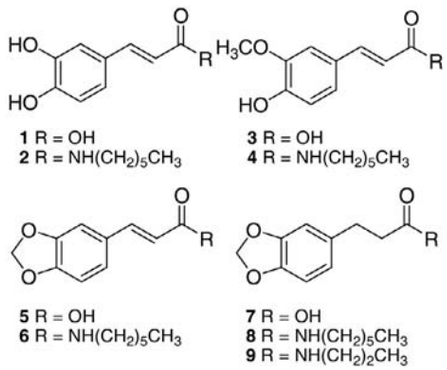

Fig. 1: Cinnamic and hydrocinnamic acids and their lipophilic derivatives screened in human breast cancer cell lines.

MATERIALS AND METHODS

Materials

Cinnamic and hydrocinnamic acids as well as sulforhodamine B were obtained from Apin Chemicals Lda. or Sigma-Aldrich Chemical Co.

Methods

The synthesis of the amides (**2**, **4**, **6**, **8** and **9**) (**Fig.1**), was accomplished by the reaction of the respective cinnamic or hydrocinnamic acids (**1**, **3**, **5**, and **7**) with hexylamine or propylamide, in dimethylformamide (DMF), in the presence of the coupling agent (benzotriazol-1-yloxy)tris(dimethylamino) phosphonium hexafluorophosphate (BOP), at room temperature, according our previous report (4).

Cell proliferation assays were conducted in order to evaluate the effect of the test compounds on tumour and non-tumour cell lines, following the protocol described previously by our laboratory (3). The test compounds were added to each well one day after seeding $1x10^4$ cells/ml in 48-well plates. Appropriate vehicle controls were also performed. Cells were harvested and analyzed for time lengths ranging from 1 to 7 days. Cell density was determined by the sulforhodamine B (SRB) assay. After SRB labelling, absorbance was measured in a spectrophotometer at 540 nm. The amount of released dye is proportional to the number of cells present in the sample, and is a reliable indicator of cell proliferation (5). Results are expressed as percentage of control values (no compound) for each time point.

RESULTS AND DISCUSSION

From the results obtained, one evident finding is that the original cinnamic and hydrocinnamic acids (**1**, **3**, **5** and **7**) did not inhibit the proliferation of any of the cell lines used. This is probably because its hydrophilicity does not favour the intracellular accumulation of the compounds. In fact, compound **1** (logD 0.16) and compound **3** (logD 0.42) have relative low lipophilicity compared to that of the new compounds, where **2** (logP 3.61) and **4** (logP 3.58) (4).

Among the amide derivatives, compound **2** showed a general inhibition of proliferation of all cell lines tested. The most striking effect was seen after 7 days of incubation when around 80-90% inhibition of proliferation of MCF-7, BJ and HS578T cells was observed. MCF-7 cells were particularly susceptible to compound **4**, especially for longer incubation periods (Fig. 2). On the other hand, we have amide derivatives **6**, **8** and **9**, which do not demonstrate any particular effect on the inhibition of the cell lines used. These compounds were tested do disclose the importance of the hydroxyl groups in the cvtotoxicitv effects.

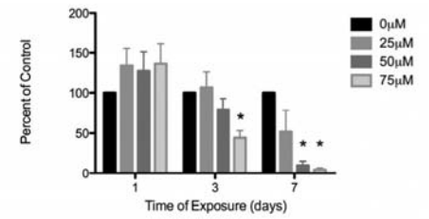

Fig. 2: Effects of compound 4 on MCF-7 cell proliferation. Notice the large inhibition of cell proliferation for longer time points (7 days), which was not observed when using the corresponding parent compound.

CONCLUSIONS

The results obtained showed that the increased lipophilicity of the amide derivatives seems to be crucial for the compounds enter in the cell and exert their activity (compound **2** and **4**). In addition, the presence of hydroxyl groups in the molecules is essential to supply them with antiproliferative activity in the studied cell lines since compounds **6**, **8** and **9** do not present any activity.

ACKNOWLEDGMENTS

This study was funded by a research grant from the Portuguese Foundation for Science and Technology (Portugal), PTDC/QUI-QUI/101409/2008.

REFERENCES

1. Fiuza SM, Gomes C, Teixeira LJ, Girao-da-Cruz MT, Cordeiro MN, Milhazes N, Borges F, Marques MP. Phenolic acid derivatives with potential anticancer properties-a structure-activity relationship study. Part 1: methyl, propyl and octyl esters of caffeic and gallic acids. Bioorg. Med. Chem. 2004; 12: 3581-3589.
2. Gao S, Hu M. Bioavailability challenges associated with development of anti-cancer phenolics. Mini Rev. Med. Chem. 2010; 10: 550-567.
3. Serafim T, Carvalho F, Marques M, Calheiros R, Silva T, Garrido J, Milhazes N, Borges F, Roleira F, Silva E, Jon Holy J, Oliveira P. Lipophilic caffeic and ferulic acid derivatives presenting cytotoxicity against human breast cancer cells. Chem Res Tox 2011; in press.
4. Roleira F, Siquet C, Orru E, Garrido E, Garrido J, Milhazes N, Podda G, Paiva-Martins F, Reis S, Carvalho R, Tavares-da-Silva E, Borges F. Lipophilic phenolic antioxidants: Correlation between antioxidant profile, partition coefficients and redox properties. Bioorg. Med. Chem. 2010; 18: 5816–5825
5. Lin Z, Hoult J, Raman A. Sulphorhodamine B assay for measuring proliferation of a pigmented melanocyte cell line and its application to the evaluation of crude drugs used in the treatment of vitiligo. J. Ethnopharmacol. 1999; 66: 141-150.

SYNTHESIS OF NEW PYRROLO-[2,3-D]PYRIMIDINES DERIVATIVES AS SRC KINASE INHIBITORS

K. T. Çetin[1*], S. Dinçer[1], and S. Ölgen[2]

[1] University of Ankara, Faculty of Science, 06100, Tandogan, Ankara, Turkey; [2] University of Ankara, Faculty of Pharmacy, Department of Pharmaceutical Chemistry, 06100, Tandoğan, Ankara, Turkey

INTRODUCTION

Src is the most widely studied of the largest family of nonreceptor protein tyrosine kinases, namely Src family kinases (SFKs). In many studies, these proteins have been shown to play a critical role in cellular growth and proliferation, angiogenesis, invasion and metastasis (1). The activation of Src in human cancers may occur through a variety of mechanisms that include domain interaction and structural remodeling in response to various activators or upstream kinases and phosphatases. Since Src has prominent roles in invasion and tumor progression and development of metastasis, Src became a promising target for cancer theraphy (2). Several small molecule inhibitors of Src are currently investigated in clinical trials. These Src inhibitors include heterocyclic ATP analogs, pyrazolo-[2,3-*d*]pyrimidines, pyrrolo-[2,3-*d*]pyrimidines, pyrido-[2,3-*d*]pyrimidines, quinolines, and olomucines (1). In this work, we have prepared new Pyrrolo-[2,3-*d*]pyrimidines derivatives and evaluate for their Src kinase inhibitory activities (Scheme 1).

MATERIALS AND METHODS

Materials

Methyl formate, chloroacetonitrile, 2,6-diamino-4-hydroxypyrimidine, palladium on C, sodium acetate, 1,1′-carbonyldiimidazole, dimethylformamide, sodium sulphate, ethyl acetate, p-chlorophenylacetic acid, methanol, hexane, p-chlorophenoxyacetic acid, hydrochloric acid, dichloromethane, silicagel, 4-(3,4-dimethoxyphenyl)butyric acid, p-thiomethylbenzoic acid, 5-methyl thiophen carboxylic acid were purchased from Aldrich, Merck and Riedel companies. Src enzyme kit (Promega) were purchased from invitrogen.

Synthesis

*5-(Cyano)-2-aminopyrrolo[2,3-d]pyrimidine-4(3H)-one (**PreQ$_o$**, compound **3**).* 4.76 mL (0.077 mol) of methyl formate was added to a stirred mixture of 3.57 g (0.066 mol) $NaOCH_3$ in anhydrous toluene at 0ºC. 4.18 mL (0.066 mol) of chloroacetonitrile was added as dropwise over 30 min at 0ºC. The reaction mixture was stirred at 0ºC for 3h. 100 mL of water was added and extracted with toluene (2X100 mL). The aqueous phase was cooled at 0ºC and acidified to pH 4 using 5N HCl. The aqueous phase was extracted with 3X100 mL EtOAc. The organic phase was dried over Na_2SO_4, concentrated to dryness to give crude compound, which was used without further prufication, 3.98 g of chloro(formyl) acetonitrile **1** was obtained as an oily compound, which was used without further prufication for next step. 5.36 g (0.065 mol) of NaOAC was dissolved in 118 mL of distilled water. 4.12 g (0.033 mol) 2,6-diamino-4-hydroxy pyrimidine **2** was added and the mixture was heated at 100ºC. Compound **1** in 62 mL of water was added and mixture was refluxed for 5h. It was cooled to rt and precipitate was formed. It was collected by filtration and washed with copious amount of water and acetone. The compound was dissolved in 6 mL of 6N KOH. It was boiled with charcahol, filtered over celite. The pH was adjusted to 6 at 0ºC with 30% HCl. The yellow solid was collected and dried in vacuo oven at 50 ºC for 24 h. 2.21 g pure compound **3, *PreQ$_o$*** was obtained.

*2-Amino-5-[aminomethyl]pyrrolo[2,3-d]pyrimidine-4(3H)-one (compound **4**, **PreQ$_1$**).* $PreQ_o$ (0.1 g, 0.57 mmol) was suspended in 100 mL MeOH and 25 mL of HCl. 5%Pd/C (0.135 g, 1.3 mmol) was added. The compound was reacted with a hydrogenation gase (3 atm) at room temperature and stirred for 24 h. The catalyst was filtered off from celite and the solvent was evaporated to dryness. The precipitate was purified by silicagel column chromatography.

*The general synthesis of 2-Amino-pyrrolo[2,3-d]pyrimidine-4(3H)-one-5-(substituted) amide derivatives (compounds **5-9**).* 1 mmol appropriate acide was dissolved in DMF and 1.2 mmol CDI was added at 0ºC. The mixture was stirred at rt for 1h and 1 mmol $PreQ_1$ was added and it was stirred at 50 ºC for 12-24 h.

Assay for Src family tyrosine kinase activities

The activity measurement were performed using ProFluor Src-Family Kinase Assay protocol (Promega) with some modifications of the manufacturer's protocol. Briefly, the molecules were mixed with Src-family kinase R110 substrate, in enzyme and control substrate bearing reaction buffer and the kinase reaction was initiated with the addition of ATP. The fluorescence of the liberated R110 was read at a wavelength of 525 nm (E x 460 nm). The decrease in fluorescence of each well inversely relates to kinase activity of the enzyme within the wells and comparison performed with respect to control wells. The IC_{50} values were determined by nonlinear regression analysis.

RESULTS AND DISCUSSION

Chemistry

The starting compound **1** was synthesized with the reaction of methyl formate and chloroacetonitrile in anhydrous toluen. To obtain compound **3** (**PreQ$_0$**), 2,6-diamino-4-hydroxy pyrimidine **2** was reacted with compound **1** in presence of sodium acetate. **PreQ1** (compound **4**) was prepared by reduction of cyano to amine group using H_2/Pd in 1M HCl (**Scheme 1**) (3). The synthesis of amide derivatives of Pyrrolo-[2,3-*d*]pyrimidine (compounds **5-10**) were achieved by the reaction of 2-Amino-5[aminomethyl] pyrrolo[2,3-d]pyrimidine-4(3H)-one **(PreQ1)** and corresponding acide derivatives in presence of 1,1′-carbonyldiimidazole (CDI) in DMF (**Scheme 2**).

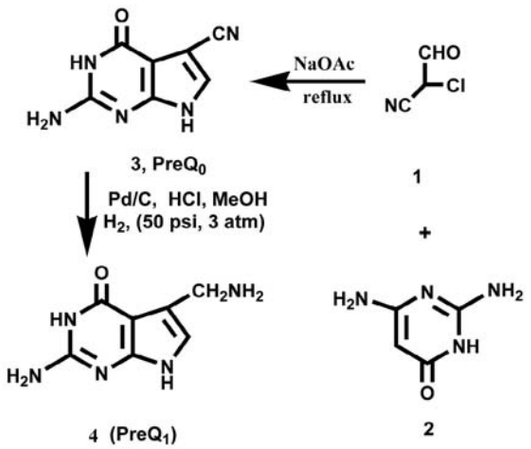

Scheme 1: Synthesis of PreQ0 and PreQ1 (3).

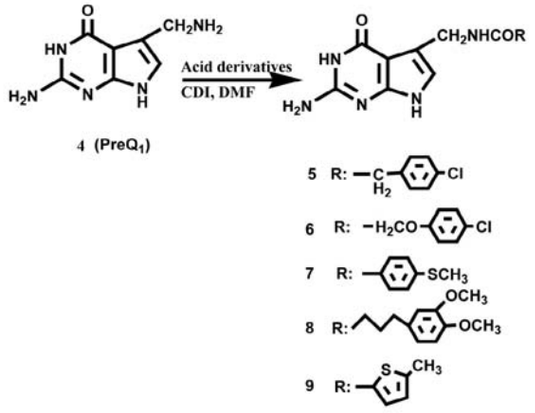

Scheme 2: Synthesis amide derivatives of PreQ1.

Biological Evaluation

The compounds were analyzed for their inhibitory activity toward Src tyrosine kinase (4). Compounds have been screened for their inhibitory potencies against Src kinase and SAR-results so far will be presented.

REFERENCES

1. Rucci N, Susa M, Teti A. Inhibition of pretein kinase c-Src as a therapeutic approach for cancer and bone metastases. Anti-Cancer Agents in Med. Chem. 2008; 8: 342-349.
2. Saad F and Lipton A. Src kinase inhibition: Targeting bone metastases and tumor growth in prostate and breast cancer. Cancer Treatment Reviews 2010; 36: 177-184.
3. Gangjee A, et al. Synthesis, antifolate, and antitumor activities of classical and nonclassical 2-amino-4-oxo-5-substituted-pyrrolo[2,3-d] pyrimidines. J. Med. Chem. 2001; 44: 1993-2003.
4. Technical Bulletin, ProFluor Src Family Kinase of products V1271, Revised 6/09, Printed in USA.

SYNTHESIS AND ANTIMICROBIAL ACTIVITY OF SOME CARBAZOLE DERIVATIVES

Z. A. Kaplancıklı[1], L. Yurttaş[1*], G. Turan-Zitouni[1], A. Özdemir[1], R. Ozic[2]

[1] Anadolu University, Faculty of Pharmacy, Department of Pharmaceutical Chemistry, 26470, Eskisehir, Turkey; [2] Anadolu University, Faculty of Science, Department of Microbiology, 26470, Eskisehir, Turkey.

INTRODUCTION

There is no doubt that the existing arsenal of antimicrobial agents we have in hand for the treatment of infectious diseases is insufficient to protect us over the long term. The primary reason for this state of affairs is the inexorable drive of evolution that leads to antimicrobial resistance (1). This condition need to develop new and efficacious antimicrobial agents.

It is known that carbazole skeleton bearing natural products fused with heterocyclic ring have drawn significant attention due to excellent pharmacological activities (2).

A large number of natural and synthetic carbazole derivatives have been reported to exhibit diverse biological activities such as antimicrobial, antitumor, antiviral, anti-inflammatory, antimalarial, antidiarrhoeal and other biological properties such as immunosuppression neuroprotection and pancreatic lipase inhibition (3).

In light of these observations, it is designed and synthesised carbazole including compounds as potential antimicrobial agent.

MATERIALS AND METHODS

Chemistry

All chemicals were purchased from Sigma-Aldrich Chemical Co. All melting points (m.p.) were determined by Electrothermal 9100 digital melting point apparatus and are uncorrected. Spectroscopic data were recorded with the following instruments: ^{1}H-NMR (Bruker 400 MHz spectrometer) and ^{13}C-NMR (Bruker 100 MHz spectrometer) and MS-FAB (VG Quattro Mass spectrometer).

2-Chloro-*N*-(9-Ethyl-9*H*-carbazole-3-yl)acetamide:

To obtain this compound, 9-Ethyl-9*H*-carbazole-3-amine (0,05 mol) and triethylamine (0.06 mol) were dissolved in tetrahidrofuran with constant stirring. Later, the mixture was cooled in an ice bath, and chloroacetyl chloride (0.06 mol) was added drop wise with stirring. The reaction mixture thus obtained was further agitated for 1 h at room temperature. The precipitate was filtered; the solvent was evaporated to dryness.

***N*-(9-Ethyl-9*H*-carbazole-3-yl)-2-(substituted phenoxy)acetamide derivatives:**

A mixture of 2-chloro-*N*-(9-Ethyl-9*H*-carbazole-3-yl)acetamide (1.65 mmol, 0.5g), the appropriate substitue phenol derivatives (1.98 mmol) and K_2CO_3 (1.98 mmol, 0.3 g) in acetonitril was refluxed for 6 hours. The cooled mixture was filtered and recrystallized from alcohol.

Microbiology

Antimicrobial activities of compounds were tested using microbroth dilution method (4). The observed data the control drugs and the test microorganisms are given in Table 1.

RESULTS AND DISCUSSION

In this study, eight compounds **(1a-f)** were synthesized (Fig 1). The structure elucidation of the compounds were determined by ^{1}H-NMR, ^{13}C-NMR and FAB$^+$-MS spectral data. The ^{1}H-NMR spectral data were also consistent with the assigned structures. In the 400 MHz ^{1}H-NMR spectrum of compounds, the CH_2 protons of the acetamide group resonated at 4.75 ppm as a singlet peak, and N-H of it is at 10.04 ppm. For 9-ethyl substitution, CH_3 protons are observed at 1.31 ppm as triplet, and CH_2 protons are at 4.43 ppm as quartet. Other characteristic peaks due to aromatic protons were observed as expected. In the ^{13}C-NMR spectra of the compounds, the signal of carbonyl carbon (C=O) appears at 166.27 ppm, acetyl carbon at 67.52 ppm, methyl carbon at 16.16 ppm, methylene carbon at 36.95 ppm. In the MS spectra, the electron spraying technique with positive polarity mode was applied and M+1 peaks were detected as base peak.

For antimicrobial activity, MIC's were recorded as the minimum concentration of the compounds, which inhibits the growth of tested microorganisms which are *Staphylococcus aureus, Listeria. Monocytogenes, Escherichia coli, Pseudomonas aeruginosa*, *Micrococcus luteus, Bacillus subtilis, Candida albicans.* The MIC values are generally within the range of 40–500 μg ml^{-1}, against all evaluated strains. Most of the compounds tested were showed significant antifungal activity against *C. albicans,* when compared with ketokonazole. It was also observed that these compounds have antimicrobial activity against all tested bacteria according to standart drug streptomycin. Especially compound 1c is highly effective against all of the evaluating microbial strains.

CONCLUSIONS

A series of carbazole-based compounds were synthesized via an easy, convenient and efficient synthetic route. The antimicrobial results showed that carbazoles including acetamino moiety have valuable antibacterial and antifungal effects. The most active compound is *N*-(9-Ethyl-9*H*-carbazole-3-yl)-2-(4-ethylphenoxy)acetamide (1c) against P. aeruginosa with a MIC value of 40.625 μg/mL.

When we consider activity results according to subtituents of methyl, ethyl chloro and nitro groups on phenyl moiety, we noticed methyl, ethyl and nitro substituents are increasing activity further comparing with chloro substituent.

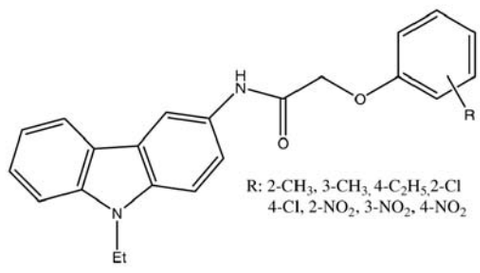

Fig. 1: Synthesis of target molecules (1a-h)

Table 1: Antimicrobial activities of the compounds (μg/mL)

	A	B	C	D	E	F	G
1a	187.5	93.75	93.75	93.75	187.5	187.5	187.5
1b	250	125	125	125	250	250	250
1c	81.25	40.625	40.625	40.625	81.25	81.25	81.25
1d	500	250	250	250	500	500	500
1e	500	250	250	250	500	500	500
1f	500	250	250	250	250	500	250
1g	281.25	140.625	140.625	140.625	281.25	281.25	281.25
1h	393.75	196.875	196.875	196.875	196.875	393.75	393.75
Ref.1	31.25	7.81	31.25	125	15.625	15.625	-
Ref.2	-	-	-	-	-	-	250

Reference 1:Sytreptomycin; **Reference 2:** Ketoconazole.
A: *S. aureus* (NRRL B-767), **B**: *L. monocytogenes* (ATCC-7644), **C**: *E. coli* (ATCC-25922), **D**: *P. aeroginosa* (ATCC-254992), **E**: *M. luteus* (NRLL B-4375), **F**: *B. subtilis* (NRS-744), **G**: *C. albicans* (ATCC-22019)

REFERENCES

1. Brown ED, Wright GD. New Targets and Screening Approaches in Antimicrobial Drug Discovery. Chem. Rev. 2005; 105: 759-774.
2. Surendıran T, Balasubramanian S, Sıvaraj.D. Microwave Assisted Synthesis of Novel 1,2,3,4-Tetrahydrocarbazolyl thiazolidin-4-ones and Azetidin-2-ones and its Biological Behavior. E-J. Chem. 2009; 6(S1), 374-S380.
3. Gu W, Wang S. Synthesis and antimicrobial activities of novel 1H-dibenzo[a,c]carbazoles from dehydroabietic acid. Eur. J. Med. Chem. 2010; 45: 4692-4696.
4. Winn W, Allen S, Janda W, Koneman E, Procop G, Schreckenberger P, Woods G. Color Atlas and Textbook of Diagnostic Microbiology (Lippincott Williams &Wilkıns), Sixth Edition, 2006, p. 945.

DC-SIGN ANTAGONISTS WITH MANNOSE ANCHOR

M. Anderluh[1*], N. Obermajer[2], U. Švajger[3], A. Bernardi[4]

[1] Department of Medicinal Chemistry, Faculty of Pharmacy, Aškerčeva 7, SI-1000 Ljubljana, Slovenia; [2] Department of Biotechnology, Jozef Stefan Institute, Jamova 39, SI-1000 Ljubljana, Slovenia; [3] Blood Transfusion Center of Slovenia, Šlajmerjeva 6, 1000 Ljubljana, Slovenia; [4] Dipartimento di Chimica Organica e Industriale, Università di Milano, via Venezian 21, I-20133 Milano, Italy.

INTRODUCTION

DC-SIGN is a C-type lectin on dendritic cells that binds invading pathogens and mediates an adaptive immune response from T cells (1). Some pathogens (as HIV-1) bind to DC-SIGN and use it as entering point to DCs. Accordingly, inhibition of pathogen interaction with DC-SIGN specific inhibitors is considered as a plausible concept for new anti-infectives. DC-SIGN specifically binds branched mannose and fucose-containing ligands on the pathogen surface with high affinity and their oligosaccharides with modest affinity (2). We have recently reported a pseudo-1,2-mannobioside with moderate antiviral activity in the Ebola infection model (IC_{50} = 0.62 mM), while its azide derivative, inhibited DC-SIGN adhesion with IC_{50} = 1.1 mM, as measured by surface-plasmon resonance (3).

MATERIALS AND METHODS

All the Materials and Methods details can be found in the work of Obermajer et al. (4).

RESULTS AND DISCUSSION

To improve binding affinities of starting mannoside **1**, we have designed glycoconjugates based on pseudo-1,2-mannobioside that could bind into hydrophobic binding pockets on DC-SIGN CRD unoccupied by native ligands. We have sought to modify the structure of the pseudo-disaccharide **1** to include hydrophobic functionalities capable of interacting with one, or possibly both, proposed binding sites (Figure 1).

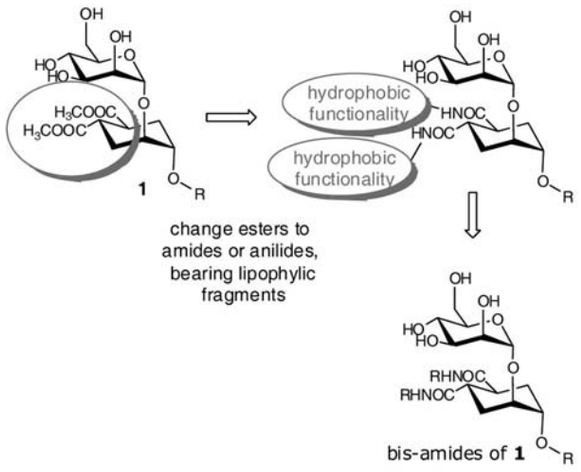

Fig. 1: The design of substituted 1,2-mannobioside mimics and general structure of the bis-amide derivatives of 1.

These binding pockets were identified by careful examination of crystal structure of DC-SIGN CRD in complex with tetramannoside Man_4 (PDB code: 1SL4, Figure 2).

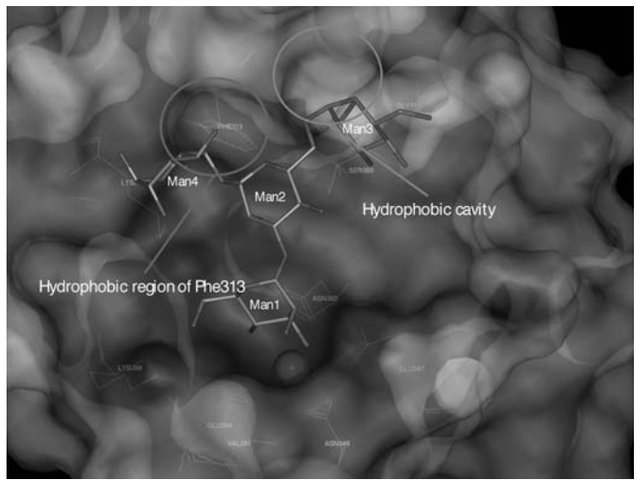

Fig. 2: Crystal structure of DC-SIGN CRD (shown as solvent–accessible surface coloured by electrostatic potential) in complex with Man4 (shown as tubes) with proposed binding regions unoccupied by Man4. Mannose residues and important amino acid residues for Man4 binding are labelled with red and green, Ca2+ coordinated by Man1 residue is presented as a blue sphere.

This crystal structure was taken as a starting-point for docking studies. We have used FlexX 3.1.2 (BioSolveIT GmbH) with PharmMetal pharmacophore around Ca^{2+} to dock target compounds as it correctly accounts for complex interactions between Ca^{2+} (406) and Man1 residue. Docking protocol was validated (docked pose superimposed to the Man4 pose as seen in its X-ray complex) and designed compounds docked to support the design (4). The detailed synthetic protocol of the designed compounds is described in the work of Obermajer et al. (4).
The affinity of the synthesized compounds to DC-SIGN was evaluated by an in vitro assay that measures inhibition of DC-SIGN-mediated immature dendritic cell adhesion to mannan-coated plates (5). Preliminary single-point tests were used to identify candidates for IC_{50} measurement (Table 1.).

Table 1: IC50 of DC-SIGN specific antibodies (H200, 1B10), reference compound 2, and compounds 26-33 and 44-47 in the DC adhesion test.

Compound	IC_{50} [μM]	R^2
H200	6.095 ± 1.040*	0.966
1B10	1.454 ± 0.651*	0.967
2	299 ± 30.0	0.994
26	344 ± 10.4	0.999
27	339 ± 7.69	0.982
28	6,86 ± 0.24**	0.988
29	29,5 ± 2.28	0.995
30	90,0 ± 1.87	0.967
31	44,2 ± 13.2	0.986
32	252 ± 22.4	0.988
33	12,8 ± 3.42	0.982
44	12,5 ± 3.90	0.989
45	26,6 ± 0.72	0.999
46	45,8 ± 9.3	0.980
47	111 ± 2.10	0.971

The results strongly indicate that majority of the hydrophobic functionalities selected were plausible and have increased potency as DC-SIGN inhibitors when compared to starting compound **1** and reference compound **2**, which inhibited DC adhesion only weakly.

CONCLUSIONS

We have synthesized promising candidates and determined their affinities to DC-SIGN by an in vitro assay that measures inhibition of DC-SIGN-mediated immature dendritic cell adhesion. Additionally, we have performed docking studies to rationalize the results and to suggest further optimization. The assay data demonstrate that our efforts to design and synthesize mannose-based DC-SIGN inhibitors resulted in compounds, which inhibit DC-SIGN-mediated adhesion in low micromolar range.

REFERENCES

1. Švajger U, Anderluh M, Jeras M, Obermajer N. Cell. Signal. 2010; 22: 1397-1405.
2. Guo Y, Feinberg H, Conroy E et al. Nat. Struct. Mol. Biol. 2004; 11: 591-598.
3. Reina JJ, Sattin S, Invernizzi D et al. ChemMedChem 2007; 2: 1030–1036.
4. Obermajer N, Sattin S, Colombo C, Bruno M et al. Mol. Div. 2011; 15: 347-360.
5. Obermajer N, Švajger U, Jeras M, et al. Anal. Biochem. 2010; 406: 222-229.

DESIGN AND SYNTHESIS OF NOVEL UDP-MUR-NAC, UDP-MUR-NAC-L-ALA AND UDP-MUR-NAC-L-ALA-D-GLU MIMETICS

R. Frlan[1*], A. Obreza[1]

[1] *University of Ljubljana, Faculty of Pharmacy, Aškerčeva 7, 1000 Ljubljana, Slovenia*

INTRODUCTION

Mur ligases are essential enzymes involved in the cytoplasmic steps of peptidoglycan synthesis which remain attractive, yet unexploited targets (1). In a search for new compounds with the potential to inhibit MurB, MurC, MurD and MurE, we focused initially on an analysis of the active sites of these enzymes. After the initial docking of small peptide fragments into active sites of ligases MurB-MurE using E-Hits (2) a general structure for good enzyme inhibition was proposed, which consisted of peptide mimetic, diphosphate mimetic and phenyl substitute for sugar residue, which orients both mimetics towards the proper conformation and, to some level restricts the molecule's degrees of freedom (**Fig. 1**) (3).

RESULTS AND DISCUSSION

The overall synthetic approach is outlined in **Fig. 2**. The synthesis of UDP-Mur-*N*Ac mimetics was started from 3-nitrobenzenesulfonyl chloride (**4**), which was coupled with Gly-OMe hydrochloride (**2**) to give sulfonamide **3**, followed by the transformation of the methyl ester into the corresponding amide **4** via aminolysis (4). Compound **7** was then synthesized from **4** in three steps. Compound **4** readily reacted with ethylchloroformate in the presence of NaH as a base to give **5**, followed by catalytic hydrogenation of the nitro functional group to give the aromatic amine **6** in 58% yield upon crystallization.

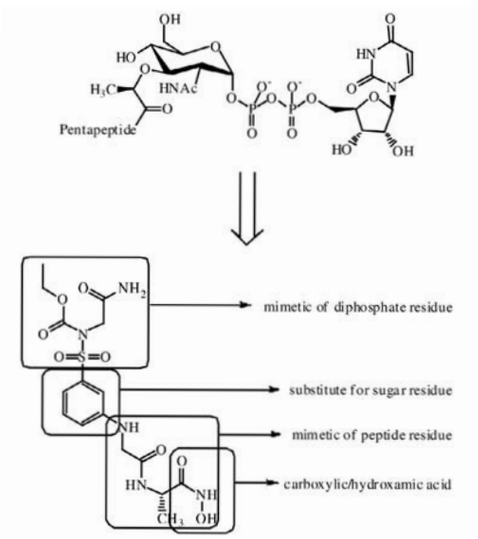

Fig. 1: General principles of new potential MurB-MurE inhibitors design.

Compound **6** was then treated with glyoxylic acid monohydrate under the conditions of reductive amination using $NaCNBH_3$ (5). The product obtained was used for further reactions with various amino acid derivatives followed by hydrogenolysis of the benzyl ester moiety under conditions of heterogeneous catalytic transfer hydrogenation using Pd/C as catalyst and ammonium formate (6) as hydrogen donor to give UDP-Mur-*N*Ac-L-Ala mimetics **9a-9d**.

Our modelling procedure for **9d** revealed that the mode of binding for one of the conformations of the molecule is similar to that of UMA (UDP-MurNAc-L-Ala), which is also presented in **Fig. 3**. Comparison of UMA and **9d** reveals that the sulfonocarbamate moiety forms 6 H-bonds with the active site, according to our model, and could mimic diphosphate. Furthermore, an

additional interaction with Asp 175, which is not present in the binding mode of UMA, is also seen. However, inhibitory activity has to be measured, and will be reported in due course before any firm conclusions can be made.

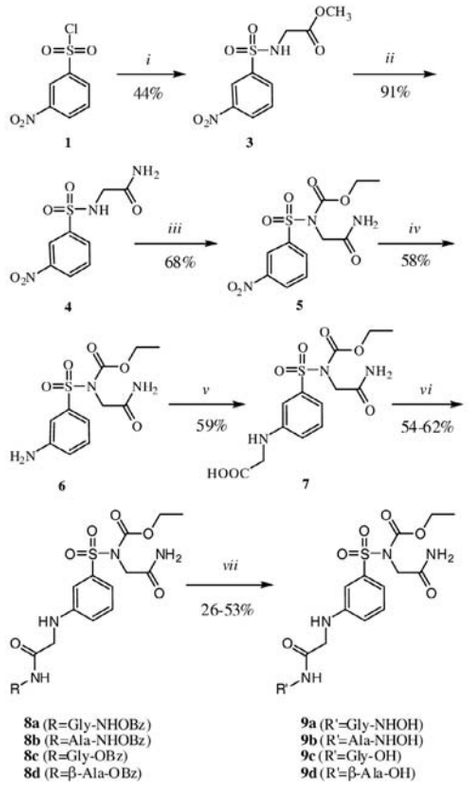

Fig. 2: Synthesis of UDP-Mur-NAc mimetic compounds i. H2NCH2COOMe (2), Et3N, CH2Cl2, ii. NH3(g), CH3OH, iii. ClCOOCH2CH3, NaH, DMF, iv. H2/Pd/C, MeOH:THF=1:1, v. OHC-COOH•H2O, MeOH, NaCNBH3, vi. R-NH2 · HCl, EDC, HOBt, NMM, CH2Cl2, vii. NH4HCO2, Pd/C, MeOH

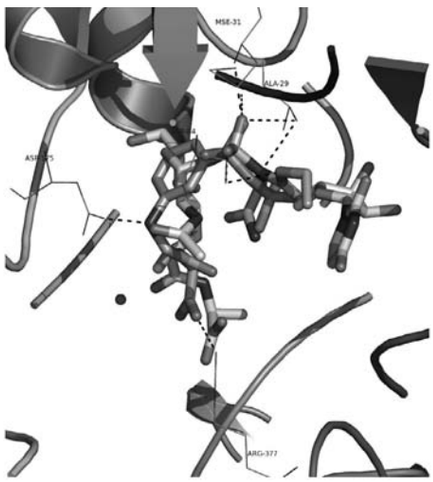

Fig. 3: Binding mode of 9d in the active site of MurC. Binding mode of UMA is also given as a comparison.

CONCLUSIONS

In conclusion, new compounds with the potential to inhibit MurB, C, D and E have been synthesized. The peptide fragments, which strongly resemble the peptide chains of UDP-Mur-*N*Ac, UDP-Mur-*N*Ac-L-Ala and UDP-Mur-*N*Ac-L-Ala were introduced, and linked to a phenyl fragment attached to a sulfonocarbamoyl mimetic of diphosphate. The biological activity of the synthesized compounds is under investigation.

REFERENCES

1. Van Heijenoort J. Recent advances in the formation of the bacterial peptidoglycan monomer unit. Nat. Prod. Rep. 2001, 18: 503–519.
2. Zsoldos Z, Reid D, Simon A, Sadjad SB, Johnson AP. eHiTS: an innovative approach to the docking and scoring function problems. Curr Protein Pept Sci 2006; 7: 421-435.
3. Frlan R, Perdih F, Cirkvenčič N, Pečar S, Obreza A. Design And Synthesis Of Novel Udp-Mur-Nac, UDP-Mur-Nac-L-Ala And Udp-Mur-Nac-L-Ala-D-Glu Mimetics. Acta Chim. Slov.. 2009, 56: 580-590
4. Poloński T. Optical activity of lactones and lactams—IV : Chiroptical properties of 4-imidazolidinones. Tetrahedron 1985, 41: 611-616.
5. Borch RF, Bernstein MD, Durst HD. Cyanohydridoborate anion as a selective reducing agent J. Am. Chem. Soc. 1971, 93: 2897-2904.
6. Johnstone RAW, Wilby AH, Entwistle ID. Heterogeneous catalytic transfer hydrogenation and its relation to other methods for reduction of organic compounds. Chem. Rev. 1985, 85: 129-170.

DESIGN AND SYNTHESIS OF PIPERIDINYL ANALOGUES OF UDP-N-ACETYLMURAMOYL-L-ALANINE

A. Obreza

University of Ljubljana, Faculty of Pharmacy, Aškerčeva 7, 1000 Ljubljana, Slovenia

INTRODUCTION

The widespread emergence of bacterial strains that are resistant to the variety of antibiotics currently available on the market has generated an urgent need for the development of novel antimicrobial agents active against previously unexploited targets. One of the best known and most studied targets is the complex biosynthesis of peptidoglycan. Peptidoglycan is an essential component of the bacterial cell wall, conferring mechanical resistance and maintaining a defined cell shape. Any perturbation of the multi-step peptidoglycan biosynthesis may lead to cell lysis. Among many enzymes involved in the synthesis of peptidoglycan, there are also Mur ligases, enzymes that are essential for bacteria, highly specific and occur only in prokaryotic cells. Two critical enzymes called UDP-*N*-acetylmuramic acid: L-alanine ligase (MurC) and UDP-*N*-acetyl-muramoyl-Lalanine: D-glutamate ligase (MurD) catalyzes the addition of L-alanine to UDP-*N*-acetylmuramic acid and the formation of the peptide bond between UDP-*N*-acetylmuramoyl-L-alanine and D-glutamate, respectively (1).

We were interested in the design, synthesis and biological evaluation of novel inhibitors of MurC and MurD. MurC catalyzes the ATP-dependent ligation of *L*-alanine and UDP-Mur*N*Ac to form UDP-Mur*N*Ac-*L*-Ala, while MurD catalyzes the addition of *D*-glutamate to the product of MurC catalyzed reaction to form UDP-Mur*N*Ac-dipeptide (Figure 1) (2).

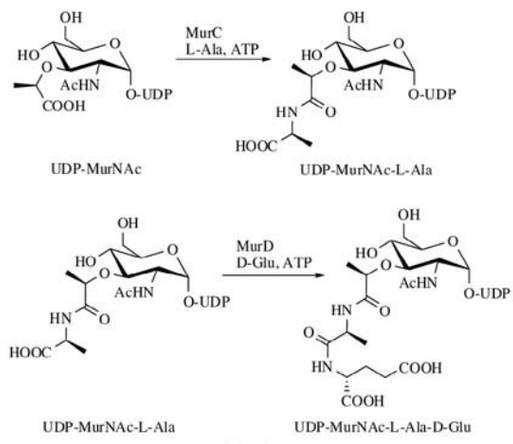

Fig. 1: Reactions catalyzed by bacterial enzymes MurC and MurD.

RESULTS AND DISCUSSION

Based on our previous studies in the field of new antimicrobial drug design (3-5) and reaction mechanisms of MurC and MurD we synthesized a series of compounds that could act as inhibitors of one or both enzymes. They were derivatives of 3-hydroxypiperidine, which represents part of the structure, that imitates the *N*-acetyl-D-glucosamine part of the UDP-*N*-acetylmuramoil-L-alanine. Piperidine ring is a suitable substitution for N-acetylglucosamine part of a molecule since it simplifies the structure and enables the synthesis of numerous derivatives. Substrates for Mur-ligases also do not form many interactions with enzymes in sugar part. More important are interactions with amino acid chain which remains unchanged in new derivatives, and in pyrophosphate group of substrate. This group is ionized, resulting in poor bioavailability of hitherto published substances and was therefore replaced with aromatic sulfonamides, carboxamides and urea derivatives. Malonic and succinic acid derivatives were also synthesized. Schematic presentation of all changes in the structure of UDP-Mur*N*Ac-*L*-Ala is shown in Figure 2.

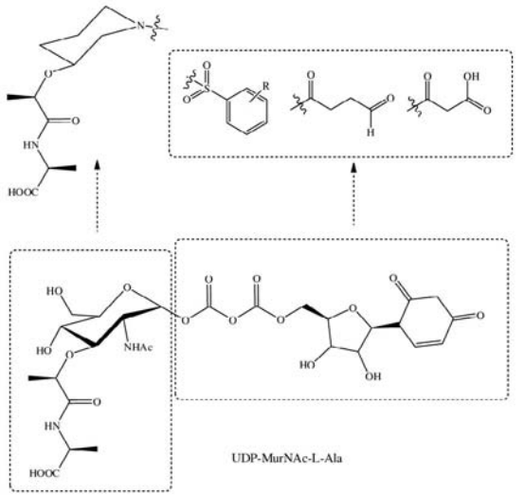

Fig. 2: Modifications in the structure of UDP-N-acetylmuramoyl-L-alanine.

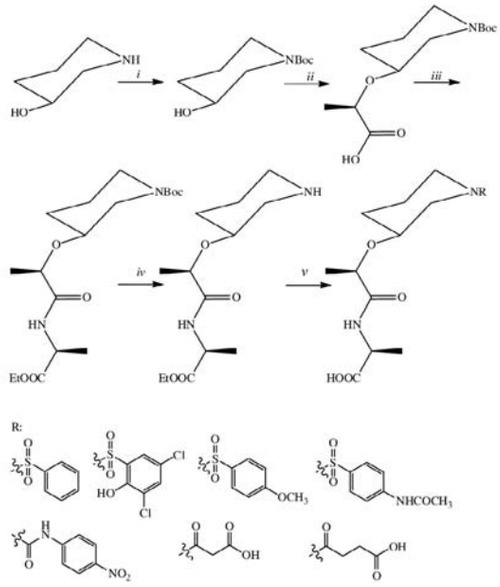

Fig. 2: Synthesis of UDP-N-acetylmuramoyl-L-alanine analogues. i: $(BOC)_2O$/NaOH; *ii*: 1. Cl-$CH(CH_3)$-COOH/NaH; 2. H^+; *iii*: NH_2-$CH(CH_3)$-COOEt, EDC, Hobt, Et_3N; *iv*: HCl(g)/AcOH; *v*: 1. Cl-CO-R^1, Cl-SO_2R^1 or $R^1C_6H_4$-NCO/Et_3N; 2: NaOH/dioxan/water; 3. H^+.

Synthesis of UDP-Mur*N*Ac-*L*-Ala analogs is presented in Figure 3. 3-Hydroxypiperidine was used as a starting reagent. Its secondary amino group was protected with $(Boc)_2O$ and the lactoyl fragment introduced on hydroxylic group with 2-cloropropanoic acid after pretreatment with NaH. L-Ala-OEt was introduced by coupling reaction using Hobt and EDC. After the removal of Boc- protecting group, different sulfonamides and carboxamides were formed and all protecting groups removed to yield seven products, which will be biochemically evaluated in near future.

ACKNOWLEDGMENTS

This work was supported by the European Union FP6 Integrated Project EUR-INTAFAR (Project No. LSHM-CT-2004-512138) under the thematic priority of Life Sciences, Genomics and Biotechnology for Health. The support from the Ministry of Higher Education, Science and Technology of the Republic of Slovenia and the Slovenian Research Agency is also acknowledged.

REFERENCES

1. J. van Heijenoort J. Nat. Prod. Rep. 2001; 18: 503–519.
2. Barreteau H, Kovač A, Boniface A, Sova M, Gobec S et al. FEMS Microbiol. Rev. 2008; 32: 168–207.
3. Frlan R, Kovač A, Blanot D, Gobec S, Pečar S, et al. Molecules. 2008; 13: 11–30.
4. Frlan R, Perdih F, Cirkvenčič N, Pečar S, Obreza A. Acta Chim. Slov. 2009; 56: 580–590.
5. Frlan R, Kovač A, Blanot D, Gobec S, Pečar S, et al. Acta Chim. Slov. 2011; in press.

DISCOVERY OF NEW INHIBITORS OF D-ALANINE: D-ALANINE LIGASE

E. Arsovska[1*], V. Škedelj[1], M. Hrast[1], I. Chopra[1], S. Gobec[1], A. Zega[1]

[1] University of Ljubljana, Faculty of Pharmacy, Aškerčeva 7, 1000 Ljubljana, Slovenia; [2] Institute of Molecular and Cellular Biology and Antimicrobial Research Centre, University of Leeds, Leeds LS 9JT, U.K.

INTRODUCTION

Emergence of bacterial resistance to most current antibiotics has created an urgent need for searching for new antibacterial targets and developing new antimicrobial agents (1). Among the enzymes involved in peptidoglycan synthesis, D-alanyl-D-alanine ligase (Ddl), which catalyzes the ligation of D-Ala-D-Ala in the assembly of peptidoglycan precursors, is considered as an important antimicrobial drug target(2), since bacteria with an inactive, mutated protein are unable to reproduce unless using an alternative pathway for cell wall analysis (3). Ddl belongs to the ATP-grasp enzyme superfamily, which is characterized by an unusual nucleotide-binding fold, referred to as ATP-grasp fold. Sequence alignment of the enzymes from this enzyme superfamily revealed conserved motifs in the ATP-binding domain, suggesting that by targeting the ATP-binding site of bacterial members of the ATP-grasp superfamily a multi-target antibacterial compound with the potential to reduce the development of target-based resistance can be designed (4). Therefore we synthesized a series of pyridopyrimidines, previously described as ATP-competitive inhibitors of another bacterial member of ATP-grasp superfamily and tested them in an in vitro assay for their inhibition of *E. coli* DdlB (5).

MATERIALS AND METHODS

Assay for determining Ddl inhibition

Compounds were tested with the malachite green method in which orthophosphate generated during the reaction is measured. Each compound was tested in duplicate at a concentration of 500 μM for its ability to inhibit DdlB activity. Assays were performed at 37°C in a mixture (final volume: 50 μL) containing 50 mM Hepes (pH 8.0), 5mM $MgCl_2$, 10 mM $(NH_4)_2SO_4$, 700 μM D-Ala, 500 μM ATP and purified DdlB (diluted in 50 mM Hepes and 1 mM DTT). After 20 min of incubation, 100 μL of Biomol reagent

was added and absorbance was read at 650 nm after 5 min. To exclude possible nonspecific (promiscuous) inhibitors, all compounds were also tested in presence of Triton X-114 (0.005 %).

RESULTS AND DISCUSSION

A series of 15 pyridopyrimidines were designed and synthesized for this study and evaluated for their ability to inhibit DdlB from *E. coli*. Most of them reduced the activity of the target enzyme, among which compound **1** proved to be the most promising inhibitor of DdlB with an IC_{50} value of 340 μM.

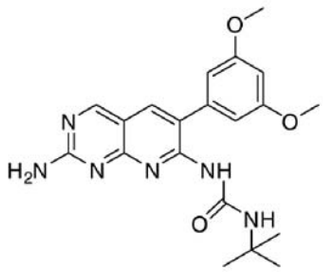

Fig. 1: Structural formula of compound **1**

CONCLUSIONS

Our future work will be focused on the synthesis of new derivatives in order to explore the chemical space and improve the inhibitory activity of pyridopyrimidine-based inhibitors. Based on the inhibitory activities we will be able to determine structural requirements for Ddl inhibition.

REFERENCES

1. Boucher, H. W.; Talbot, G. H.; Bradley, J. S.; Edwards Jr., J. E.; Gilbert, D.; Rice, L. B.; Scheld, M.; Spellberg, B.; Bartlett, J. Bad bugs, no drugs: NO ESKAPE! An update from the Infectious Diseases Society of America. Clin. Infect. Dis. 2009, 48, 1-12.
2. Tytgat, I., Colacino, E., Tulkens, P. M., Poupaert, J. H., Prévost, M., Van Bambeke, F. DD-ligases as a potential target for antibiotics: past, present and future. Curr Med Chem 2009, 16, 2566-2580
3. Baptista M., Depardieu F., Reynolds P., Courvalin P., Arthur M: Mutations leading to increased levels of resistance to glycopeptides antibiotics in VanB-type enterococci. Mol. Microbiol. 1997, 25, 93-105
4. Galperin, M. Y., Koonin, E.V. A diverse superfamily of enzymes with ATP-dependent carboxylate-amine/thiol ligase activity, Protein Science,1997, 6, 2639-2643
5. Miller, J. R.; Dunham, S.; Mochalkin, I.; Banotai, C.; Bowman, M.; Buist, S.; Dunkle, B.; Hanna, D.; Harwood, H. J.; Huband, M. D.; Karnovsky, A.; Kuhn, M.; Limberakis, C.; Liu, J. Y.; Mehrens, S.; Mueller, W. T.; Narasimhan, L.; Ogden, A.; Ohren, J.; Vara Prasad J. V. N.; Shelly, J. A.; Skerlos, L.; Sulavik, M.; Thomas, V. H.; VanderRoest, S.; Wang, L.; Wang, Z.; Whitton, A.; Zhu, T.; Stover, C. K. A class of selective antibacterials derived from a protein kinase inhibitor pharmacophore. Proc. Natl. Acad. Sci. U.S.A. 2009, 106, 1737-1742.

SYNERGISM IN THE EXTRACTION OF PARACETAMOL FROM THE AQUEOUS NaCl SOLUTIONS BY THE DIETHYL ETHER/1-BUTANOL BINARY SOLVENT MIXTURES

G. M. Nikolić[1*], J. V. Živković[1], M. G. Nikolić[2], F. Miljković[1]

[1] University of Niš, Faculty of Medicine, Department of Chemistry, Bulevar dr Zorana Đinđića 81, 18000 Niš, Serbia; [2] University of Niš, Faculty of Natural Sciences and Mathematics, Department of Chemistry, Višegradska 33, 18000 Niš, Serbia

INTRODUCTION

Paracetamol (acetaminophen, N-acetyl-*p*-aminophenol) is one of the most widely used analgesic and antipyretic drugs. Since misuse of paracetamol may lead to serious toxic effects (eg. hepatic necrosis) its determination in various samples is of paramount importance (1).

Numerous methods for paracetamol determination include the liquid-liquid extraction step during the sample preparation for the analysis and diethyl ether alone or in combination with some other organic solvents (2) is often used for such purpose. However, as in the case of some other phenolic compounds (3), paracetamol is poorly extracted with diethyl ether. To overcame this problem the salting-out or/and extraction with binary mixtures of organic solvents (synergism) may be used (3,4).

The aim of this work was to study synergic effect in the extraction of paracetamol with the diethyl ether/1-butanol binary solvent mixture from aqueous NaCl solution.

MATERIALS AND METHODS

Materials

All the chemicals used in this study were of analytical grade quality and have been used without further purification. Stock solution of paracetamol (0.01 mol dm^{-3}) was prepared by dissolving exactly weighted mass of pure substance in doubly distilled water and 0.01 mol dm^{-3} solution of HCl was added to adjust the pH value to ~2. Just before each series of extractions stock solution was diluted 100 times with solution of NaCl (4 mol dm^{-3}). Extraction was performed by the shake-flask method for each binary solvent mixture composition in triplicate.

Measurements and calculations

Evolution 60 UV/Vis scanning spectrophotometer (Thermo Scientific, USA) was used for absorbance measurements. The absorbances of aqueous phases were measured at 243 nm and the distribution ratio (D) of paracetamol was calculated by using the equation where

$$D = \frac{A_0 - A}{A} \times \frac{V_{aq}}{V_{org}}$$

A_0 and A were absorbances of the aqueous phases before and after extraction, and V_{aq} and V_{org} were the volumes of aqueous and organic phase, respectively. Synergic effect in the extraction of paracetamol was quantified by calculating the synergic coefficient, K_c, according to the equation (5)

$$K_c = log\ (D_{mix}/D_{add})$$

where D_{mix} represented experimental and D_{add} theoretically predicted distribution ratio values, respectively.

Theoretically predicted distribution ratio was calculated as

$$D_{add} = D_1 \times x_1 + D_2 \times (1 - x_1)$$

where D_1 and D_2 represented distribution ratios of paracetamol for pure solvents, and x_1 was mole fraction of one pure solvent in binary mixture.

RESULTS AND DISCUSSION

The dependence of paracetamol distribution ratio on the composition of diethyl ether/1-butanol binary mixture is shown in Fig.1.

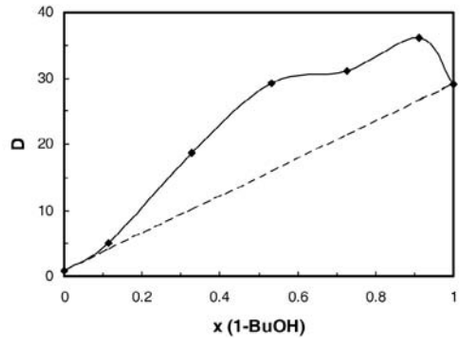

Fig. 1: Dependence of paracetamol distribution ratio on the composition of diethyl ether/1-butanol binary mixture. Dashed line corresponds to the dependence of theoretically predicted distribution ratios (Dadd) on the binary mixture composition.

Distribution ratios of paracetamol was higher than theoretically predicted values in the whole composition range for the extraction by the diethyl ether/1-butanol binary mixture with the maximum value obtained for the binary mixture richest in 1-butanol whose extraction efficacy was much greater than for diethyl ether. Similar results have been reported in the literature for the extraction of ascorbic and nicotinic acids by the ethyl acetate/1-butanol and butyl acetate/1-butanol binary solvent mixtures (5). The distribution ratio values of paracetamol and synergic coefficients for the various compositions of binary solvent mixture used in this study are listed in Table 1. where j (1-BuOH) and x (1-BuOH) present the volume and mole fractions of 1-butanol in the binary mixture, respectively.

Table 1: The values of distribution ratios of paracetamol and synergic coefficients for the various compositions of binary solvent mixture used in this study.

ϕ (1-BuOH)	x (1-BuOH)	D_{mix}	D_{add}	K_c
0	0	0.79	0.79	-
0.1	0.113	5.07	3.98	0.105
0.3	0.329	18.73	10.08	0.269
0.5	0.534	29.21	15.88	0.265
0.7	0.727	31.13	21.33	0.164
0.9	0.911	36.12	26.53	0.134
1	1	29.04	29.04	-

Although the maximum distribution ratio value in our experiments was obtained for the binary mixture richest in 1-butanol, the maximum values of synergic coefficients correspond to the binary mixtures with considerable content of diethyl ether. This result was probably the consequence of the large difference in distribution ratios of paracetamol for pure solvents so the addition of 1-butanol in diethyl ether had more profound influence on the extraction efficacy increase than the addition of diethyl ether in 1-butanol.

The results of this study indicate that diethyl ether/1-butanol binary mixture in combination with salting-out effect of NaCl may be used for the very efficient extraction during the aqueous sample preparation step for the determination of paracetamol.

ACKNOWLEDGMENTS

This work was supported by the Ministry of Education and Science of the Republic of Serbia under the Project No. 172044.

REFERENCES

1. Espinosa Bosch M, Ruiz Sánchez AJ, Sánchez Rojas F, Bosch Ojeda C, Determination of paracetamol : Historical evolution. J. Pharm. Biomed. Anal. 2006; 42: 291-321.
2. Li H, Zhang C, Wang J, Jiang Y, Paul Fawcett J, Gu J, Simultaneous quantitation of paracetamol, caffeine, pseudoephedrine, chlorpheniramine and cloperastine in human plasma by liquid chromatography-tandem mass spectrometry. J. Pharm. Biomed. Anal. 2010; 51: 716-722.
3. Nikolić GM, Perović JM, Nikolić RS, Cakić MM, Salting-out extraction of catechol and hydroquinone from aqueous solutions and urine samples. Facta Universitatis Ser. Pys. Chem. Techn. 2003; 2: 293-299.
4. Korenman Yal, Extraction of organic compounds: General regularities and application to analysis. J. Anal. Chem. 2002; 57: 1064-1071.
5. Mokshina NYa, Erina OV, Pakhomova OA, Savushkin RV, Synergism in the extraction of ascorbic and nicotinic acids by binary solvent mixtures. Russ. J. Phys. Chem. A 2007; 81: 1964-1967.

DIVERSELY SUBSTITUTED 1,3,5-TRIAZINES AS HITS IN DIFFERENT DRUG DISCOVERY PROGRAMS

I. Sosič[1*], B. Mirković[1], B. Štefane[2,3], A. Kovač[1,4], J. Kos[1,5], S. Gobec[1]

[1] University of Ljubljana, Faculty of Pharmacy, Aškerčeva cesta 7, 1000 Ljubljana, Slovenia; [2] Faculty of Chemistry and Chemical Technology, University of Ljubljana, Aškerčeva 5, 1000 Ljubljana, Slovenia; [3] EN-FIST Centre of Excellence, Dunajska 156, 1000 Ljubljana, Slovenia; [4] Lek Pharmaceuticals d.d., Verovškova 57, 1526 Ljubljana, Slovenia; [5] Department of Biotechnology, Jožef Stefan Institute, Jamova 39, 1000 Ljubljana, Slovenia

INTRODUCTION

1,3,5-Triazines constitute a class of heterocyclic compounds that have been well known for a long time, and still represent the object of considerable interest, mainly due to their applications in different fields, such as the production of polymeric photostabilisers (1) and herbicides (2). Some 1,3,5-triazines also display other important biological properties, of which it is worth mentioning antineoplastic activity (3) and antimalarial activity (4). 1,3,5-Triazines have also been recognized as antibacterial compounds (5). Recently, Maeda *et al.* described a series of novel 4,2-di(substituted)amino-1,2-dihydro-1,3,5-triazine derivatives that were evaluated for their antiseptic properties by MIC and MBC tests against Gram-positive and Gram-negative bacteria (6).

Herein we briefly describe our approaches in the discovery of derivatives of 1,3,5-triazines as inhibitors of MurF and cathepsin B enzymes.

MATERIALS AND METHODS

Assay for determining MurF inhibition

The inhibitory activity of the compounds against MurF from *E. coli* was tested for their ability to inhibit the addition of D-Ala-D-Ala to UDP-Mur*N*Ac-L-Ala-g-D-Glu-*meso*-A_2pm. The detection of orthophosphate generated during the reaction was based on the colorimetric Malachite green method (7) with slight modifications in a mixture (final volume, 50 µl) containing 50 mM Hepes, pH 8.0, 50 mM $MgCl_2$, 100 µM UDP-Mur*N*Ac-L-Ala-g-D-Glu-*meso*-A_2pm, 600 µM D-Ala-D-Ala, 500 µM ATP, purified MurF from *E.coli* (diluted with 50 mM Hepes, 1 mM dithiothreitol), and 500 µM of the tested compound dissolved in DMSO. The final concentration of DMSO was 5% (v/v). The mixture was incubated at 37 °C for 20 min and then quenched with 100 µl of Biomol® reagent. The absorbance was measured after 5 min at 650 nm. All the experiments were run in duplicates. The IC_{50} value was determined by measuring the residual activity at seven different inhibitor concentrations and represents the concentration of the inhibitor for which RA is 50%.

Assay for determining cathepsin B and cathepsin H inhibition. The substrates Z-Arg-Arg-AMC (Calbiochem) and Arg-AMC (Biomol) were used to assess the activities of catB and catH, respectively. Five µl of the relevant substrate (all at 5 µM) and 5 µl of the respective compound (final concentration 50 µM) were added into the wells of a black microplate. The reaction was initiated by addition of 90 µl enzyme (final concentration 5 nM for both cathepsins). Formation of the fluorescent degradation products of the AMC substrates was continuously monitored at 460 nm ±10 nm with excitation at 380 nm ±20 nm, at 37 °C. All assay mixtures contained 5% (v/v) DMSO and 0.01% of Triton X-100, to prevent false-positive inhibition due to the formation of compound aggregates. All measurements were performed in duplicate.

RESULTS AND DISCUSSION

A search for new MurF inhibitors

As a part of our efforts to identify new, small-molecule inhibitors of the intracellular steps of peptidoglycan biosynthesis, the virtual high-

throughput screening (VHTS) of the National Cancer Institute "Diversity Set" bank of compounds was performed. We identified the triazine derivative NSC 209931 (Fig. 1) as a promising inhibitor of MurF (IC_{50} = 63 μM) (8). Based on this encouraging result, a series of new 1,3,5-triazines were designed and synthesized as putative MurF inhibitors (9). All the synthesised compounds were tested for their inhibitory activity of the MurF enzyme from *E. coli;* however, only compound **1** (Fig. 1) turned out to display significant inhibitory activity, with an IC_{50} value of 450 μM.

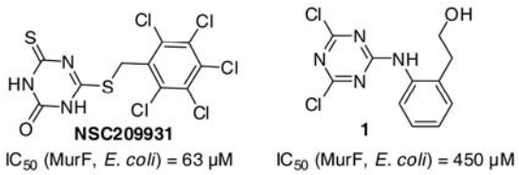

Figure 1: Structural formulae of a NCI hit compound and compound **1**.

1,3,5-Triazines as cysteine protease inhibitors

As it has been claimed that the triazine nitrile scaffold is privileged in its nature towards cysteine proteases (10), we screened this library of variously 2,4,6-trisubstituted-1,3,5-triazines against two different cysteine proteases, cathepsins B and H. All of these compounds were practically inactive against both of these cathepsins at 50 μM, except for compound **2** (Fig. 2), which had a 6-substituted 4-benzylthio-1,3,5-triazin-2(1*H*)-one core. Compound **2** showed high inhibitory activity against catB (K_i = 16 μM), whereas it showed no inhibition of catH.

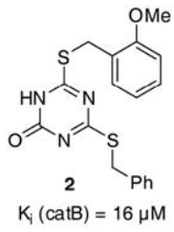

Figure 2: Structural formula of cathepsin B inhibitor.

As compound **2** is unique in the series (it has two different hydrophobic substituents on positions 4 and 6 of the 1,3,5-triazine scaffold), our future work will be focused on the synthesis of new derivatives in order to explore the chemical space of these compounds and to address as many noncovalent interactions with the enzyme as possible. Based on the inhibitory activities we will be able to determine the structural requirements for catB inhibition.

REFERENCES

1. Hollink E, Simanek EE, Bergbreiter DE. Strategies for Protecting and Manipulating Triazine Derivatives. Tetrahedron Lett. 2005; 46: 2005-2008, and references cited therein.
2. Giencke W, Willms L, Dietrich H, et al. Substituted 2-amino-1,3,5-triazines, their preparation, and their use as herbicides and plant growth regulators, U.S. Patent 10/262,001, October 01, 2002.
3. Moon H-S, Jacobson EM, Khersonsky SM, et al. A Novel Microtubule Destabilizing Entity from Orthogonal Synthesis of Triazine Library and Zebrafish Embryo Screening. J. Am. Chem. Soc. 2002; 124: 11608-11609.
4. Melato S, Prosperi D, Coghi P, et al. A combinatorial approach to 2,4,6-trisubstituted triazines with potent antimalarial activity-combining conventional synthesis and microwave-assistance. ChemMedChem 2008; 3: 873-876.
5. Yakhontov LN, Vakhatova GM. Khim. Farm. Zh. 1981; 15: 27-44.
6. Maeda S, Kita T, Meguro K. Synthesis of novel 4,6-di(substituted)amino-1,2-dihydro-1,3,5-triazine derrivatives as topical antiseptic agents. J. Med. Chem. 2009; 52: 597-600.
7. Lanzetta PA, Alvarez LJ, Reinach PS, et al. An improved assay for nanomole amounts of inorganic phosphate. Anal. Biochem. 1979; 100: 95-97.
8. Turk S, Kovač A, Boniface A, et al. Discovery of new inhibitors of the bacterial peptidoglycan biosynthesis enzymes MurD and MurF by structure-based virtual screening. Bioorg. Med. Chem. 2009; 17: 1884-1889.
9. Sosič I, Štefane B, Kovač A et al. The synthesis of novel 2,4,6-trisubstituted 1,3,5-triazines: a search for potential MurF enzyme inhibitors. Heterocycles, 2010; 81: 91-115.
10. Mott BT, Ferreira RS, Simeonov A, et al. Identification and Optimization of Inhibitors of Trypanosomal Cysteine Proteases: Cruzain, Rhodesain, and TbCatB J. Med. Chem. 2010; 53: 52-60.

EVALUATION OF SYNTHETIC SERINE PROTEASE INHIBITORS AS INDUCERS OF APOPTOSIS IN BURKITT LYMPHOMA CELLS

M. Gobec[1*], A. Obreza[1], M. Prijatelj[1], I. Mlinarič-Raščan[1]

[1]*University of Ljubljana, Faculty of Pharmacy, Aškerčeva cesta 7, 1000 Ljubljana, Slovenia*

INTRODUCTION

The role of serine proteases is well established in numerous crucial physiological processes making them interesting targets for therapeutic intervention. Recently, it has been shown that several serine proteases actively participate in the process of apoptosis [1]. The inhibition of either chymotrypsin- or trypsin-like proteases with *N*-tosyl-L-phenylalanine chloromethyl ketone (TPCK) or *N*-tosyl-L-lysine chloromethyl ketone (TLCK), respectively, induces apoptosis in various cell lines [2,3,4]. Their role in programmed cell death indicates the use of serine protease inhibitors as alternative therapeutic agents for the modulation of apoptotic events. This led us to initiate a search for inhibitors against thrombin, factor Xa, trypsine and/or chymotrypsin as apoptosis-inducing agents. We recently evaluated twenty serine protease inhibitors for growth inhibitory and apoptosis inducing capacity.

MATERIALS AND METHODS

Cell culture

Ramos cells were maintained in RPMI 1640 medium (Sigma-Aldrich), supplemented with 10% fetal bovine serum (Gibco, Grand Island, NY, USA), 2 mM L-glutamine, 100 U/ml penicillin, 100 μg/mL streptomycin and 50 μM 2-mercaptoethanol (all from Sigma-Aldrich), in a humidified chamber at 37°C and 5% CO_2.

Metabolic activity assay

The metabolic activity of cells was assessed conducting the tetrazolium MTS test using the CellTiter 96® Aqueous One Solution Cell Proliferation Assay (Promega).

Cell cycle analysis

Ramos cells were treated with compound of interest for 48 h. After that cells were harvested, rinsed in cold PBS and fixed with 80% ethanol at –20°C for 15 min. Samples were then rehydrated in PBS for 15 min and stained with propidium iodine buffer. After 15 min of incubation samples were analysed by flow cytometry.

Caspase-3 (DEVDase) activity.

Caspase-3 activity was measured in total cell lysates as described previously [4,5]. Briefly, after the incubation cells were resuspended in 200 μl of ice-cold caspase lysis buffer, sonicated, left on ice (30 min) and then centrifuged (14000 g, 15 min, 4°C). Cell lysates (20 μg of protein) were incubated for 30 min at 37°C in caspase reaction buffer followed by the addition of 100 μM Ac-DEVD-AFC peptide substrate (Sigma). Immediately after the addition of the substrate, the fluorescence intensity was monitored continuously for 30 min with a fluorescence microplate reader (Tecan Safire 2). Data were expressed as increase in fluorescence as a function of time.

RESULTS AND DISCUSSION

Our previous investigations showed that serine protease inhibitors induce caspase-mediated apoptosis [5]. Therefore we have tested twenty recently synthesized azaphenylalanine-based compounds which possess inhibitory properties against trypsin, thrombin, factor Xa, and/or alpha-chymotrypsin for cytotoxic effects towards Burkitt lymphoma cells. After 24 h treatment at 50 μM concentration with compound of interest, a subgroup of four serine protease inhibitors that caused severe inhibition of metabolic activity were identified (Table 1).

Table 1: Structural formulae of serine protease inhibitors that exhibit cytotoxic effects.

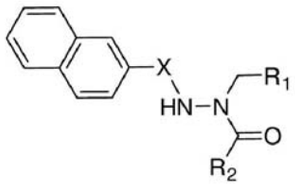

	X	R1	R2
1	CO	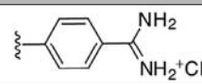	
2	SO_2	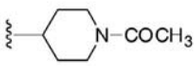	
3	SO_2	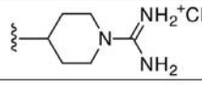	
4	SO_2	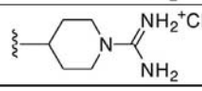	

With analysis of the cell cycle we determined that the decrease of metabolic activity was due to increased population of cells in sub-G0 phase (Fig. 1).

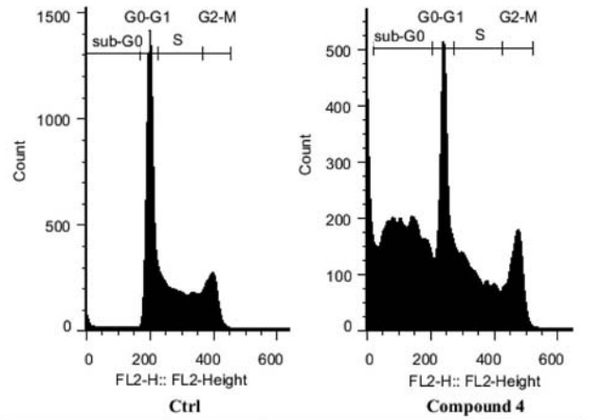

Sample	Ctrl	1	2	3	4
% of cells in sub-G0 phase	3,1	40,5	59,2	41,1	40,4

Fig. 1: (A) Representative cell cycle obtained from flow cytometer after staining cells with propidium iodine. Presented are untreated (left) and treated cells (right). The table presents percentage of cells in sub-G0 phase after 48 h treatment with compound of interest.

To elucidate the mode of cell death provoked by compounds, we examined whether the observed cytotoxic effect in Ramos cells is caused by caspase dependent apoptosis. Protein extracts were prepared from untreated and from Ramos cells incubated in the presence of 50 μM inhibitors for 4 and 16 h. Caspase 3/7 activity, determined with Ac-DEVD-AFC substrate, peaked after 16 h of incubation and subsequently decreased (data not shown) (Fig. 2). This demonstrates a correlation between caspase activation and decreased cell viability, indicating caspase-dependent apoptosis induced by the inhibitors.

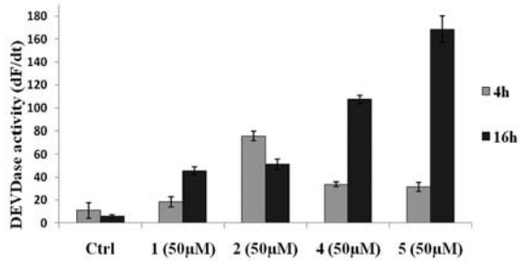

Fig. 2: Ramos cells were incubated with 50 μM inhibitors for indicated times. Caspase 3/7 activity was determined spectrofluorimetrically by measuring DEVDase activity in whole cell lysates using fluorogenic Ac-DEVD-AFC substrate.

CONCLUSION

Molecules regulating cell death constitute prominent therapeutic targets. We have evaluated 20 serine protease inhibitors and identified four compounds that are cytotoxic toward Burkitt lymphoma cells through activation of caspase-dependent apoptosis. These novel inducers of apoptosis could serve as a lead in identifying new targets for anticancer therapy.

REFERENCES

1. Hedstrom L. Serine Protease Mechanism and Specificity. Chem Rev 2002; 102: 4501-4524.
2. King MA, et al. Pro- and anti-apoptotic effects of an inhibitor of chymotrypsin-like serine proteases. Cell Cycle 2004; 3: 1566-1571.
3. Zhu H, et al. Apoptosis in human monocytic THP.1 cells involves several distinct targets of N-tosyl-L-phenylalanyl chloromethyl ketone (TPCK). Cell Death Differ 1997; 4: 590-599.
4. Murn J, et al. Internucleosomal DNA cleavage in apoptotic WEHI 231 cells is mediated by a chymotrypsin-like protease. Genes Cells 2004; 9: 1103-1111.
5. Celhar T, et al. Azaphenylalanine-based serine protease inhibitors induce caspase-mediated apoptosis. Eur J Pharmacol 2009; 602: 15-22.

MONITORING OF LIPOIC ACID PROTECTIVE ROLE BY LIVER ENDONUCLEASES ACTIVITY IN ACUTE INTOXICITY WITH CADMIUM AND LEAD

J. Jovanović[1], R. Nikolić[1], N. Krstić[1*], G. Kocić[2]

[1] Department of Chemistry, Faculty of Science and Mathematics, University of Niš, Višegradska Street 33, 18000 Niš, Serbia; [2] Faculty of Medicine, University of Niš, Bulevar dr Zorana Đinđića 81, 18000 Niš, Serbia

INTRODUCTION

Heavy metals as pollutants in the working and living environment are a serious health and environmental problem.

Ways of Cd and Pb intake include air polluted with fossil fuels combustion products, cigarette smoke, food packaging materials contaminated with these metals in some stage of productions. From the atmosphere, soil, water (surface and groundwater), Cd and Pb are entered and retained in the plants, and further through the food chain and drinking water take into the human body. These are not essential metals, but entered into the organism can be found in almost all tissues and organs of mammals. As a metal with a cumulative effect Pb is competitive with essential metals (Fe, Ca, Cu, Zn) for their many functions in the body (1). Systematic exposure to Cd leads to increased excretion of calcium and bone damage, as well as changes of activities of many enzymes (2). According to physicochemical properties Cd and Pb easily inhibit the physiological activity of the enzyme with active -SH groups, which have presented by many authors. In the literature, there is insufficient data about the influence of these metals on enzyme activity that is not related to the presence of -SH groups.

Lipoic acid (LA), is a cyclic disulfide (Fig. 1), and it`s through the carboxyl groups associated with the protein part of enzymes as amide. Primarily, it participate in

the oxidative decarboxylation of 2-oxoacids, and the active -SH centers in reduced form represent the places that can easily bind heavy metals. It is known, that LA has antioxidative effect. LA as a lipo- and hydrosolubile compound easily passes through the membrane into the cytoplasm and participates in the protection of free reactive radicals, the regulation of gene expression, etc. (3).

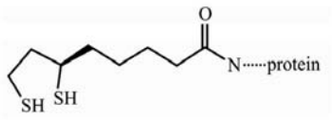

Fig. 1: Lipoic acid binding with protein

Liver endonucleases (acid and alkaline DNase) are hydrolases that degrade both native, and denatured DNA molecules. The main role of DNase is reflected in the regulation of synthesis and degradation of endogenous and exogenous DNA, modified DNA in reparation and removal of circulating DNA from the organism. According to the literature, DNase are considered as the main executors of apoptosis, responsible for internucleosomal fragmentation of DNA cellular in apoptosis. Internucleosomal DNA fragmentation, as a biochemical marker of apoptosis, presents separation of chromosomal DNA into fragments oligonucleosome size (4).
This study was performed in order to investigate the protective role of LA, in acute intoxicity of Cd and Pb, by the activity of liver endonucleases (acid and alkaline DNase).

MATERIALS AND METHODS

Materials

The research was carried out on white Wistar female rats, 6 weeks old, weight 220±20 g. The experimental animals were raisen in the laboratory conditions on a normal dietary regime in the vivarium on Faculty of Medicine (University of Niš). During three weeks of the experiment animals were dosing treated with $CdCl_2$ and $Pb(CH_3COO)_2$ injected intraperitoneally. Total doses were below the lethal dose (Pb <0.1 g/kg, Cd <1 mg/kg), with appropriate control group and group that beside Cd and Pb was treated with LA (12 mg/kg). Biological material were analyzed according to the working standards in biochemical laboratories.

Methods

The liver endonuclease activity was measured spectrophotometrically in 10% homogenate, according to the method of Bartholeyns (5).
Statistical analysis. Statistical data were interpretated using the Student's t-test (Microsoft Office Excel).

RESULTS AND DISCUSSION

Result of the determination of acid and alkaline DNase activity of experimental animals that were intoxicated $CdCl_2$ and $Pb(CH_3COO)_2$, as mean as the results of measurements of the same in the presence of LA, are shown in Figure 2a for acid, and Figure 2b for alkaline Dnase. Results are shown as mean value ± SD in international units per gram of protein.

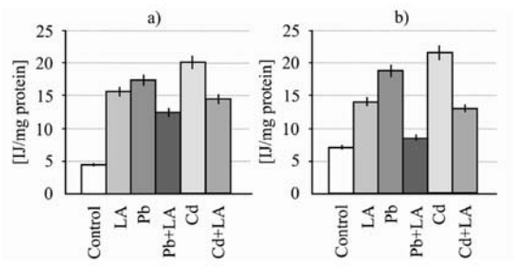

Fig. 2: Results of the determination activity of: a) acid and b) alkaline DNase

Results of the determination of liver enzymes, acid and alkaline DNase, showed that Cd and Pb multiply and statistically significant, increase the value of these enzymes ($p < 0.01$). It is assumed that Cd probable cause oxidative damage of DNA, proteins and lipids, which lead to apoptosis. Cd can cause increased production of free radicals, so we can talk about the genotoxic effects of this metal on the enzymatic and nonenzymatic components of antioxidant defense system of the organism. DNA damages and genotoxic effects in the cell can be increased when the cells are exposed to the influence of Pb, leading to the activation of DNase, which will participate in the degradation of DNA as the ultimate effect of activation of apoptosis, i.e. programmed cellular death (2). LA is not just an antioxidant, but also is a possible antidote for poisoning with Cd and Pb. The addition of LA, a day after exposure to these metals during the experiment, the effect of poisoning is partly reduced, and the value of DNases is lower.

CONCLUSIONS

LA is not only an effective antioxidant, but also detoxicant which in reduced form over two free-SH group can build a stable mercaptides, and so block the heavy metals and reduces their toxic effects.

ACKNOWLEDGMENTS

This work was supported by the Ministry of Education and Science of the Republic of Serbia under the Project No. TR31060.

REFERENCES

1. Sayeda AL, Newairy A, Protective role of flax lignans against lead acetate induced oxidative damage and hyperlipidemia in rats. Food Chem. Tox. 2009; 47: 813–818.
2. Wu C, Wang L, Liu C, Gao F, Su M, Wu X, Hong F, Mechanism of Cd2+ on DNA cleavage and Ca2+ on DNA repair in liver of silver crucian carp. Fish Physiol. Biochem. 2008; 34: 43-51.
3. Gaurav D, Preet S, Dua KK, Chronic cadmium toxicity in rats: treatment with combined administration of vitamins, amino acids, antioxidants and essential metals. J. Food Drug Anal. 2010; 18(6): 467–470.
4. Counis MF, L-DNase II, a Molecule That Links Proteases and Endonucleases in Apoptosis, Derives from the Ubiquitous Serpin Leukocyte Elastase Inhibitor. Mol. Cell. Biol. 1998; 18: 3612-3619.
5. Kocić G, Pavlović D, Pavlović R, Nikolić G, Cvetković T, Stojanović I, Kocić R, Sodium nitroprusside and pre-oxynitrite effect on hepatic DNases: An in vitro and in vivo study. Comp. Hepatol. 2004; 3(6): 1-9.

SPECTROSCOPIC STUDY OF PARACETAMOL–BIOMETAL (M^{2+}) ION COMPLEXES

R. S. Nikolić[1*], G. M. Nikolić[2], N. S. Krstić[1]

[1] University of Niš, Faculty of Natural Sciences and Mathematics, Department of Chemistry, Višegradska 33, 18000 Niš, Serbia; [2] University of Niš, Faculty of Medicine, Department of Chemistry, Bulevar dr Zorana Đinđića 81, 18000 Niš, Serbia

INTRODUCTION

Paracetamol (PA) is an analgesic antipyretic drug with no anti-inflamatory effects and is commonly used for the relief of fever, headaches and other minor aches and pains. Due to its extensive use paracetamol was very well characterized by various techniques. However, there are not much literature data on the characterization of its complexes with metal ions.
Some recent studies provided data about the structure of paracetamol complexes with Cu^{2+}, Zn^{2+} and Fe^{2+} ions (1), and even the pharmacological activity of Zn^{2+}-paracetamol complex was investigated following the polarographic and IR spectroscopic characterization (2).
The aim of this study was to use UV/Vis and IR spectroscopic methods for the charaterization of paracetamol complexes with Cu^{2+} and Co^{2+} because these techniques proved to be very usefull for the investigation of similar complexes (3,4).

MATERIALS AND METHODS

Materials

All the chemicals used in this study were of analytical grade quality and have been used without further purification. The PA solution ($c=1\cdot10^{-3}$ mol

dm^{-3}) was prepared by dissolving exactly weighted mass of PA in EtOH-H_2O 1:1 mixture. Synthesis of the complexes was performed by refluxing solutions of PA and metal chlorides in the molar ratios 1:1 and 1:2 at 60 °C for about 4 hours.

Spectroscopic measurements

Specord UV/VIS spectrophotometer (Carl Zeiss, Jena) was used for recording UV/Vis absorption spectra of the studied compounds in solution.

The IR spectra of the studied compounds were recorded on Bomem Michaelson Series MB FTIR spectrometer by using KBr pellet technique. Solid synthesis products for the IR measurements were obtained by the slow evaporation of solvent and subsequent drying of solid under mild conditions to constant mass.

RESULTS AND DISCUSSION

Preliminary investigations of interaction of biologically important alkaline earth metal ions Mg^{2+} and Ca^{2+} with paracetamol in neutral and weakly acidic solutions (pH=5.5) showed that these ions do not affect the UV/Vis spectrum of PA. Interaction between paracetamol and transition metal ions in solution was reflected by the appearance of new absorption bands in UV/Vis spectra as shown in Fig.1.

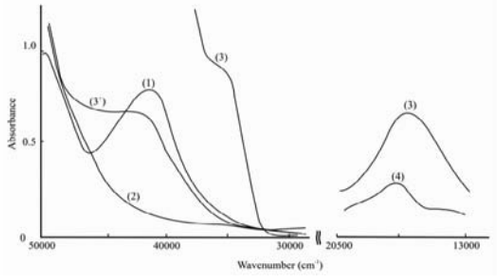

Fig. 1: UV/Vis spectra of: (1) PA, (2) $CuCl_2$, (3) PA+Cu^{2+} ratio 1:2, (3´) PA+Cu^{2+} ratio 1:1, (4) PA+Co^{2+} ratio 1:2.

The characteristic features of these new absorption bands (λ_{max}=593 nm, $\varepsilon=2.95\cdot10^4$ for Cu-PA=1:2 and λ_{max}=574 nm, $\varepsilon=0.7\cdot10^3$ for Co-PA=1:2) indicate the participation of –NH– group of paracetamol in comlex formation because λ_{max} for complexes with only O-donor ligands have much higher values (5).

Characteristic parts of the FTIR spectra of paracetamol, Cu-PA=1:2 and Co-PA=1:2 complexes obtained in weakly acidic solutions (pH=5.5) are shown in Fig.2.

Changes in the IR spectrum of paracetamol upon complexation with Cu^{2+} ion were the same as those already reported in the literature (1). Complexation of paracetamol with Co^{2+} caused changes in the IR spectrum of paracetamol with the similar pattern as for the Cu^{2+} ion but the changes in band position and relative intensities were more pronounced in the case of complex with Co^{2+} ion. The assignments for the specific bands in IR spectra of paracetamol and complexes is given in Table 1.

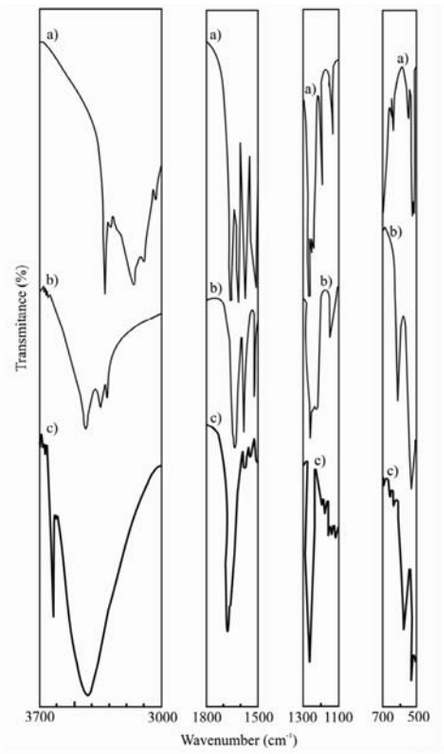

Fig. 2: Comparative IR spectra of: a) PA, b) PA+Cu2+ and c) PA+Co2+

Table 1: The IR band assignments for PA and complex PA–M(II) ions

Assignment	Wavenumber(cm^{-1})		
	PA	PA+Cu^{2+}	PA+Co^{2+}
ν(OH)	3252	3400	3633
ν(C=O)	1653	1640	1660
ν(C–O)	1260	1250	1260
δ(CNH)	1170	1160	1160
ν(M–N)	/	531	520
ν(M–O)	/	607	603

Most notable features of the IR spectra of the paracetamol-M(II) ion complexes in comparison to the IR spectrum of pure paracetamol were the appearance of M–L vibrations (M–N at 520-530 cm^{-1} and M–O at 600-610 cm^{-1}) and retention of the strong band corresponding to the stretching vibration of O–H group. While appearance of the M–L bands confirmed the formation of true complexes, the retention of strong stretching O–H vibration indicated that phenolic -O–H group of paracetamol was not directly involved in the complex formation.

REFERENCES

1. El-Shahawy AS, El-Nady A.M, Ahmed SM, Sayed NK, Some CNDO calculations and structural spectroscopic studies of paracetamol complexes. Spectrosc. Lett. 2006; 39: 163-179.
2. Choure R, Vaidya N, Polarographic and pharmacological study of Zn(II)-paracetamol complex. Curr. Pharma Res. 2011; 1: 123-126.
3. Zayed MA, El-shahat MF, Abdullah SM, The use of IR, magnetism, reflectance, and mass spectra together with thermal analyses in structure investigation of codeine phosphate complexes of d-block elements. Spectrochim. Acta A 2005; 61: 1955-1964.
4. Nakamoto K, Infrared and Raman Spectra of Inorganic and Coordination Compounds, Part B, John Wiley & Sons Inc., Hoboken, New Jersey, 2009.
5. Mitić Ž, Cakić M, Nikolić GM, Nikolić R, Nikolić GS, Pavlović R, Santaniello E, Synthesis, physicochemial and spectroscopic characterization of copper(II)-polysaccharide pullulan complexes by UV-vis, ATR-FTIR, and EPR. Carbohyd. Res. 2011; 346: 434-441.

SYNTHESIS OF NOVEL OXINDOLE DERIVATIVES AS INHIBITORS OF C-SRC TYROSINE KINASE

Z. K. Kurt*, and S. Ölgen

Ankara University, Faculty of Pharmacy, Department of Pharmaceutical Chemistry, Tandogan, Ankara, 06100 Turkey

INTRODUCTION

The c-Src ($pp60^{c\text{-}Src}$), a member of Src family kinases (SFKs), regulates many fundamental cellular processes, including cell growth, differentiation, proliferation, migration, adhesion, invasion and angiogenesis. Overexpression, deregulation or mutations of c-Src have been observed in many cancers including colon, breast, pancreatic, gastrointestinal system, lung, ovary, prostate, and skin (1, 2). In addition, c-Src and SFKs have a central role in the processes of osteoclast-mediated bone resorption and the pathogenesis of bone metastases (3). Recently, c-Src is reported as an attractive and fundamental target for cancer research. Development of new small molecule Src inhibitors is important approach to decrease tumor growth and prevent metastases. In this present work, 5-chloro-3-(substituted-benzylidene)-indolin-2-one and 1-benzyl-5-chloro-3-(substituted-benzylidene)-indolin-2-one derivatives were synthesized and evaluated for their inhibitory activity against c-Src.

MATERIALS AND METHODS

Materials

Melting points were measured with a capillary melting point apparatus (Electrothermal, Essex, UK). The Nuclear Magnetic Resonance (1H-NMR) spectra were recorded on Varian Mercury 400 NMR spectrometer 400 MHz (Varian Inc., Palo Alto, CA, USA). The chemicals shift values were expressed in parts per million (ppm) relative to tetramethylsilane as an internal Standard. Mass spectra were recorded on a Waters ZQ Micromass LC-MS spectrometer (Waters Corporation, Milford, MA, USA) Elemental analysis was taken on a Leco-932 CHNS-O analyzer. Analytical TLC was carried out on Merck 0.2 mm pre-coated silica gel (60 F-254) aluminium sheets (Merck), visualization by irradiation with an UV lamp. Profluor® SRC-Family Kinase Assay Kit (700 Wells), (from Invitrogen) was used to analyze the biological activity of the compounds synthesized in this study.

Reagents: 3-fluoro-benzaldehyde, 3-nitro-benzaldehyde, 2-nitro-5-chloro-benzaldehyde were purchased from Fluka. 2,4-difluoro-benzaldehyde (Aldrich), hydrazine hydrate (Merck), 5-chloro-isatine (Aldrich), benzyl bromide (Acros), anhydrous sodium sulfate (Merck), ethyl acetate (Merck), hexane (Merck), anhydrous dimethylformamide (Aldrich), NaH (Fluka) piperidine (BDH), and ethanol (Riedel) were used for reactions.

Synthesis

*Synthesis of 1-benzyl-5-chloro-isatine (**1b**)*

5-Chloro isatine (0.5 g, 0.002 mol) was dissolved in DMF (3 mL) and the solution was cooled to 0°C. NaH (0.167 g, 0.006 mol) was added and the mixture stirred for 15 min at 0°C and then benzyl bromide (0.7 mL, 0.005 mol) was added dropwise to the reaction mixture and stirred for 1 hour at room temperature. It was diluted with water and extracted with EtOAc (3x50 mL). The combined organic phase dried over anhydrous Na_2SO_4. Evaporation of the solvent gave crude compounds, which were purified by column chromatography (hexane/ ethylacetate, 9:1) and 0.5 g pure compound was obtained with 66.84% yield (4).

*Synthesis of 5-Chlorooxindole (**2a**) and 1-Benzyl-5-chlorooxindole (**2b**)*

5-Chloro-isatine **(1a),** (2.12 g, 0.01 mol) and 1-benzyl-5-chloro-isatine **(1b)**, (0.9 g, 3.67 mmol) were dissolved in 10 ml and 3 ml hydrazine hydrate, respectively and refluxed

at 140 °C for 4 h. The reaction mixture was poured into ice-cold water and acidified by 6 N HCl. After standing at room temperature for 2 days, 1.065 g pure 5-chlorooxindole **(2a)** and 1-benzyl-5-chlorooxindole **(2b)** were obtained, respectively. Yield, 54 % for (2a) and 79 % (for 2b) (5).

*General Synthesis of 5-Chloro-3-(substituted-benzylidene)-indolin-2-ones (**3a-6a**) and 1-benzyl-5-chloro-3-(substituted-benzylidene)-indolin-2-ones (**3b-6b**) Derivatives.*

A reaction mixture of 5-chlorooxindole and 1-benzyl-5-chlorooxindole (1 eq), the aldehyde (1.2 eq), and piperidine (0.1 eq) in ethanol (1-2 ml/1 mmol) was stirred at 90 °C for 3-5 h. The mixture was cooled and the precipitate filtered and washed cold ethanole (5). The pure compounds were obtained with 10-80 % yield.

Assay for Src family tyrosine kinase activities

The activity measurement were performed using ProFluor Src-Family Kinase Assay protocol (Invitrogen) with some modifications of the manufacturer's protocol (6). Briefly, the molecules were mixed with Src-family kinase R110 substrate, in enzyme and control substrate bearing reaction buffer and the kinase reaction was initiated with the addition of ATP. After incubating the plate at 22°C for 60 min, protease solution was added to each well and incubated for 60 min at room temperature. The reaction of protease was terminated with the addition of inhibitor, the fluorescence of the liberated R110 was read at a wavelength of 525 nm (E x 460 nm). The decrease in fluorescence of each well inversely relates to kinase activity of the enzyme within the wells and comparison performed with respect to control wells. The IC_{50} values were determined by nonlinear regression analysis.

RESULTS AND DISCUSSION

Chemistry

Synthesis of 5-chlorooxindole **(2a)** and 1-benzyl-5-chlorooxindole **(2b)** were achieved by a Wolff-Kishner reduction of 5-chloroisatine **(1a)** and 1-benzyl-5-chloroisatine **(1b)** with hydrazine hydrate, respectively. 5-Chloro-3-(substitutedbenzylidene)indolin-2-ones **(3a-6a)** and 1-benzyl-5-chloro-3-(substitutedbenzylidene)indolin-2-ones (**3b-6b)** were prepared by condensation of indolin-2-ones (**2a** and **2b**) with the equivalent amount of aldehydes in EtOH in the presence of piperidine.

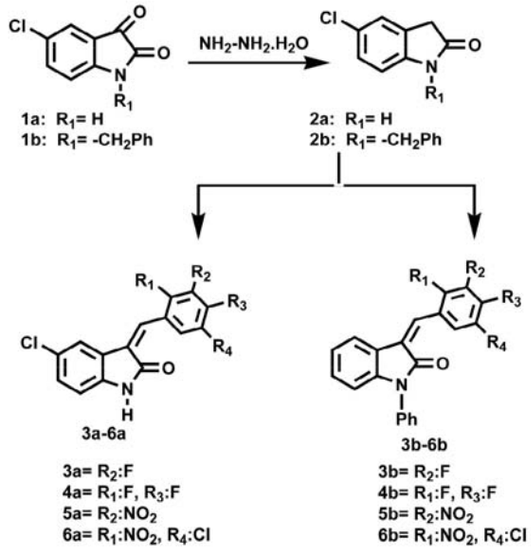

Scheme 1: Synthesis of 5-chloro-3-(substitutedbenzylidene)-indolin-2-one and 1-benzyl-5-chloro-3-(substitutedbenzylidene)-indolin-2-one derivatives.

We have tested the synthesized compounds for their Src kinase inhibitory potencies. Comparative results in terms of structure relationships will be discussed in detail.

REFERENCES

1. Kilic Z, Işgör Y G, Olgen S, Synthesis and pp60c-Src Tyrosine kinase inhibitory activities of novel indole-3-imine and amine derivatives substituted at N1 and C5. Arch. Pharm. Chem. Life Sci. 2009; 342: 333-343.
2. Lieu C, Kopetz S, The Src family of protein tyrosine kinases: A new and promising target for colorectal cancer therapy. Clinical Colorectal Cancer 2010; 9: 89-94.
3. Saad F, Lipton A, Src kinase inhibition: Targeting bone metastases and tumor growth in prostate and breast cancer. Cancer Treatment Reviews 2010; 36: 177–184.
4. Everett S A, Naylor M A, et al. Iminoxyl radicals and stable products from the one-electron oxidation of 1-methylindole-3-carbaldehyde oximes. J. Chem. Soc. Perkin Trans. 2. 2001; 10: 1989-1997.
5. Ölgen S, Götz C, Jose J, Synthesis and biological evaluation of 3-(Substituted-benzylidene)-1,3-dihydro indolin derivatives as human protein kinase CK2 and p60c-Src tyrosine kinase inhibitors. Biol. Pharm. Bull. 2007; 30(4): 715-718.
6. Technical Bulletin, ProFluor Src Family Kinase of products V1271, Revised 6/09, Printed in USA.

SYNTHESIS OF SOME THIADIAZOLE DERIVATIVES AS NEW ANTICONVULSANT AGENTS

Z.A. Kaplancıklı[1], M.D. Altıntop[1*], A. Özdemir[1], G. Turan-Zitouni[1], Ö.D. Can[2]

[1] Anadolu University, Faculty of Pharmacy, Department of Pharmaceutical Chemistry, 26470 Eskişehir, Turkey; [2] Anadolu University, Faculty of Pharmacy, Department of Pharmacology, 26470 Eskişehir, Turkey

INTRODUCTION

Medicinal chemists have carried out considerable research for thiadiazoles due to their effect on central nervous system (1). Some studies have confirmed that thiadiazole derivatives exhibit a wide spectrum of biological effects including anticonvulsant activity (2).

Hydrazones have also been found to possess anticonvulsant activity (3).

In this present study, we described the synthesis of some thiadiazole derivatives bearing hydrazone moiety and focused on their potential anticonvulsant effects.

MATERIALS AND METHODS

Materials

All reagents were purchased from commercial suppliers and were used without further purification. Melting points were determined on Electrothermal 9100 melting point apparatus (Weiss-Gallenkamp, Loughborough, UK) and are uncorrected. ^{1}H-NMR and ^{13}C-NMR spectra were recorded on Bruker 500 MHz and 125 MHz spectrometer (Bruker, Billerica, USA), respectively. Mass spectra were recorded on a VG Quattro Mass spectrometer (Agilent, Minnesota, USA). Elemental analyses were performed on a Perkin Elmer EAL 240 elemental analyser (Perkin-Elmer, Norwalk, USA).

General procedure for the synthesis of the compounds

Ethyl 2-[(5-methyl-1,3,4-thiadiazol-2-yl)thio]acetate (1)

A mixture of 5-methyl-1,3,4-thiadiazole-2-thiol (0.05 mol) and ethyl chloroacetate (0.05 mol) in the presence of potassium carbonate (0.05 mol) in acetone was refluxed for 10 h. The reaction mixture was cooled, filtered and the crude product was solved in water and then extracted with ether (4).

2-[(5-methyl-1,3,4-thiadiazol-2-yl)thio)]acetohydrazide (2)

A mixture of the ester (**1**) (0.05 mol) and hydrazine hydrate (0.1 mol) in ethanol was stirred at room temperature for 3 h and then filtered (4).

N′-[(Aryl)methylidene]-2-[(5-methyl-1,3,4-thiadiazol-2-yl)thio]acetohydrazide

(3a-o)

A mixture of the hydrazide (**2**) (0.01 mol) and aldehydes/ketones (0.01 mol) was refluxed in ethanol for 5 h, filtered and crystallized from ethanol.

Pharmacology

Assessment of anticonvulsant activity against PTZ-induced seizures

In order to evaluate the presence of anticonvulsant activity, PTZ-induced seizure tests were performed. PTZ at a dose of 80 mg/kg was applied to mice (n=10) to induce seizure. Time to appearance of first seizure (latency, sec), percentage inhibition of convulsions, and percentage inhibition of death were recorded. Mice were observed over a period of 30 min, the absence of an episode of clonic spasm of at least 5 s duration indicated the compound's ability to abolish the effect of PTZ on seizure threshold, and these animals were accepted as protected (5). Diazepam (3 mg/kg) was used as a reference drug.

RESULTS AND DISCUSSION

Initially, ethyl 2-[(5-methyl-1,3,4-thiadiazol-2-yl)thio)]acetate (**1**) was synthesized via the reaction of 5-methyl-1,3,4-thiadiazole-2-thiol with ethyl chloroacetate in the presence of potassium carbonate. Then, this ester (**1**) was converted to the corresponding hydrazide derivative (**2**). The treatment of acetohydrazide derivative (**2**) with various aldehydes/ketones gave the target compounds (**3a-o**) (Fig 1).

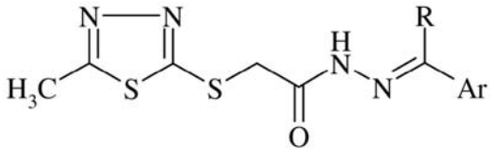

R: H, Ar: 2-pyridyl, 3-pyridyl, 4-pyridyl, 2-furyl, thiophen-2-yl, 5-methyl-2-furyl, 5-methylthiophen-2-yl, 1H-pyrrol-2-yl, 1-methyl-1H-pyrrol-2-yl, 1H-indol-3-yl, 1-naphthyl, biphenyl-4-yl; R: CH_3, Ar: 2-furyl, thiophen-2-yl, 1H-indol-3-yl

Fig. 1: The general structure of the target compounds (3a-o)

The structures of the compounds (**3a-o**) were confirmed by ^{1}H-NMR, ^{13}C-NMR and FAB$^+$-MS spectral data and Elemental analyses. In the ^{1}H-NMR spectra of the compounds (**3a-o**), the signal due to the hydrazone proton appeared at 11.0-13.8 ppm. The signal due to the -S-CH_2- protons gave rise to a singlet peak at 4.0-5.0 ppm. The signal due to the methyl protons attached to thiadiazole ring was observed in the region 2.6-2.7 ppm. In their ^{13}C-NMR spectra, the signal due to the -S-CH_2- carbon appeared at 35-40 ppm. The signal due to the hydrazone carbon was observed at 168-172 ppm. The signal due to the methyl carbon attached to thiadiazole ring was observed in the region 15.0-20.0 ppm. The other aromatic and aliphatic protons and carbons were observed at expected regions. In the mass spectra of all compounds (**3a-o**), the M+1 peak is observed. All compounds gave satisfactory elemental analysis.

The pharmacological results indicated that compounds **3d**, **3e**, **3f**, **3g**, **3h**, **3i**, **3j** (100 mg/kg) significantly delayed the onset of PTZ-induced tonic convulsions. These compounds also inhibited the convulsions and prevented the PTZ-induced deaths in a certain percentage of animals (Table 1). These data clearly indicated the presence of anticonvulsant effect for above-mentioned test compounds against PTZ-induced convulsions. Among these derivatives, compounds **3h** and **3j** were the quite active compounds. This outcome confirms that 1H-pyrrol and 1H-indol groups may have a considerable influence on anticonvulsant activity.

Table 1: The effects of test compounds (100 mg/kg) and Diazepam (3 mg/kg) on seizures induced by PTZ in mice.

Groups	Latency (sec)	% Protection	% inhibition of death
Control	112,7±16,4	0	20
Dzm	>30***	100	100
3a	308,8±124,6	0	20
3b	248,2±71,2	0	20
3c	93,5±20,8	0	10
3d	911,5±193,4*	10	40
3e	886,2±221,0*	10	30
3f	858,5±112,2*	10	30
3g	862,3±211,8*	10	20
3h	1088,3±228,6***	40	70
3i	958,2±186,7*	20	50
3j	1198,8±207,9***	50	70
3k	517,8±119,6	0	30
3l	199,8±105,8	0	20
3m	563,2±124,0	0	30
3n	384,2±142,7	0	20
3o	223,8±57,3	0	10

Values are given as mean ± SEM. Significance against control values, *p<0.05; ***p<0.001; One-way ANOVA, post-hoc Tukey test, n=10.

CONCLUSIONS

In conclusion, we synthesized some thiadiazole derivatives and evaluated their anticonvulsant effects. Among these derivatives, compounds **3h** and **3j** were the quite active derivatives. This result can be attributed to 1H-pyrrol and 1H-indol groups, respectively.

REFERENCES

1. Pattanayak P, Sharma R, Sahoo PK. Synthesis and evaluation of 2-amino-5-sulfanyl-1,3,4-thiadiazoles as antidepressant, anxiolytic, and anticonvulsant agents. Med. Chem. Res. 2009; 18: 351-361.
2. Clerici F, Pocar D. Synthesis of 2-Amino-5-sulfanyl-1,3,4-thiadiazole Derivatives and Evaluation of Their Antidepressant and Anxiolytic Activity. J. Med. Chem. 2001; 44: 931-936.
3. Rollas S, Küçükgüzel ŞG. Biological Activities of Hydrazone Derivatives. Molecules 2010; 12: 1910-1939.
4. Kidwai M, Kumar P. Microwave-induced syntheses of 6-(substituted aryl)-3-[(5-methyl-1,3,4-thiadiazol-2-ylsulfanyl)methyl]-1,2,4-triazolo[3,4-b][1,3,4]thiadiazoles. J. Chem. Res.-S. 1996; 5: 254-255.
5. Ya'u J, Yaro AH, Abubakar MS, Anuka JA, Hussaini IM. Anticonvulsant activity of Carissa edulis (Vahl) (Apocynaceae) root bark extract. J. Ethnopharmacol. 2008; 120 (2): 255-258.

CHARACTERISTICS OF LOW-DENSITY AND HIGH-DENSITY LIPOPROTEIN SUBCLASSES IN PEDIATRIC RENAL TRANSPLANT RECIPIENTS

Aleksandra Zeljkovic[1*], Jelena Vekic[1], Vesna Spasojevic-Kalimanovska[1], Zorana Jelic-Ivanovic[1], Amira Peco-Antic[2], Mirjana Kostic[2], Dragan Vasic[2] and Slavica Spasic[1]

[1] Department of Medical Biochemistry, Faculty of Pharmacy, University of Belgrade, Vojvode Stepe 450, Belgrade, Serbia; [2] School of Medicine, University of Belgrade, Belgrade, Serbia

INTRODUCTION

Renal transplant recipients often suffer from dyslipidemia which is one of the principal risk factors for cardiovascular disease (1). This study sought to determine characteristics of high-density lipoprotein (HDL) and low-density lipoprotein (LDL) particles and their associations with carotid intima-media thickness (cIMT) in a group of pediatric renal transplant recipients. We also examined the influence of immunosuppressive therapy on measured LDL and HDL particle characteristics (2).

MATERIALS AND METHODS

HDL size and subclass distribution were determined by gradient gel electrophoresis, while concentrations of small, dense LDL (sdLDL)-cholesterol (sdLDL-C) and sdLDL-apolipoproteinB (sdLDL-apoB) by heparin-magnesium precipitation method in 21 renal transplant recipients and 32 controls.

RESULTS AND DISCUSSION

Renal transplant recipients had less HDL 2b ($P<0.001$), but more HDL 3a ($P<0.01$) and 3b ($P<0.001$) subclasses. They also had increased sdLDL-C ($P<0.01$) and sdLDL-apoB ($P<0.05$) levels. The proportion of the HDL 3b subclasses was a significant predictor of increased cIMT ($P<0.05$). Patients treated with cyclosporine had significantly higher sdLDL-C and sdLDL-apoB concentrations ($P<0.05$) when compared with those on tacrolimus therapy.

CONCLUSIONS

Pediatric renal transplant recipients have impaired distribution of HDL and LDL particles. Changes in the proportion of small-sized HDL particles are significantly associated with cIMT. Advanced lipid testing might be useful in evaluating the effects of immunosuppressive therapy.

REFERENCES

1. Siirtola A, Antikainen M, Ala-Houhala M, et al. Serum lipids in children 3 to 5 years after kidney, liver, and heart transplantation. Transpl Int 2004;17:109-19.
2. Seymen P, Yildiz M, Türkmen MF, Titiz MI, Seymen HO. Effects of cyclosporine-tacrolimus switching in post-transplantation hyperlipidemia on high-density lipoprotein 2/3, lipoprotein A1/B, and other lipid parameters. Transplantation proceedings 2009;41:4181-3.

SYNTHESIS OF NEW DIBENZ[b,e]OXEPINS AND THEIR ANTIMICROBIAL INVESTIGATIONS

C. Limban[1*], A.V. Missir[1], M.T. Căproiu[2], M.C. Chifiriuc[3], G.M. Nițulescu[1], I.C. Chiriță[1], D.C. Nuță[1], L. Moruşciag[1], R. Guță[4]

[1] Pharmaceutical Chemistry Department, Faculty of Pharmacy, "Carol Davila" University of Medicine and Pharmacy, 6 Traian Vuia, 020956, Bucharest, Romania; [2] The Organic Chemistry Center of Romanian Academy "Costin D. Nenitescu" 202B Splaiul Independentei, 77208, Bucharest, Romania; [3] National Institute for Research in Microbiology and Immunology Cantacuzino, 103 Splaiul Independentei, 050096, Bucharest, Roumania; [4] National Institute for Chemical- Pharmaceutical Research & Development- ICCF, 112 Av. Vitan, 031229, Bucharest, Romania

INTRODUCTION

The compounds with dibenz[b,e]oxepin structure are known as biologically active compounds with a broad range of activities, including antidepressant, anxiolytic, anticholinergic, antihistaminic, antipsychotic, analgesic, antipyretic and anti-inflammatory effects.

Natural and synthetic dibenzoxepins possess good antibacterial activity. Leptosphaerin D, an analogue of Arugosin F, is a new polyketide with dibenz[b,e]oxepin structure who have been isolated from solid cultures of the ascomycete fungus *Leptosphaeria* sp. showed antimicrobial and antifungal effects against the plant pathogens *Fusarium nivale* and *Piricularia oryzae* (1).

A series of new imidazole derivatives of 6,11-dihydrodibenz[b,e]oxepins (2) are antifungal and antibacterial agents.

This study reports the synthesis, spectral analyses and antimicrobial investigations of new dibenz[b,e]oxepin derivatives incorporating an oximino moiety.

MATERIALS AND METHODS

The target compounds were prepared from 11-hydroximino-6,11-dihydro-dibenz[b,e] oxepin as shown in Figure 1.

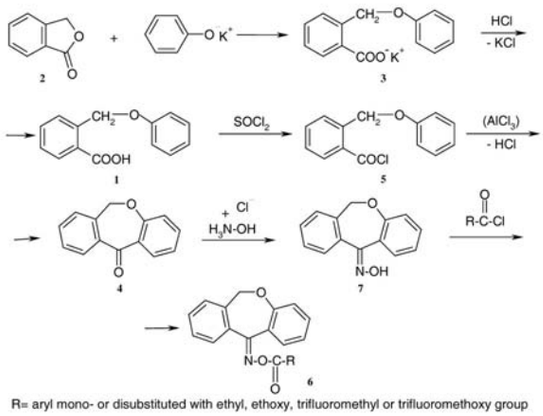

Fig. 1: The pathway for the synthesis of the new dibenz[b,e]oxepins

The necessary oxime was synthesized using the procedure reported earlier (3).
The structures of the obtained compounds were elucidated by elemental and spectral (IR, NMR) data.
Melting points are uncorrected and were determined in open capillary tubes on an Electrothermal 9100 apparatus.
Elemental analyses were done on a Perkin Elmer CHNS/O Analyser Series II 2400 apparatus and the results were within ± 0.4 % of the theoretical values.
IR spectra were recorded on a FT- IR Bruker Vertex 70 spectrophotometer.
NMR spectra were recorded on a Varian Unity Inova 400 instrument operating at 400 MHz for ^{1}H and 100 MHz for ^{13}C.

Antimicrobial assay
The antimicrobial activity of the investigated compounds was tested against the following Gram- positive (coagulase- positive, methicillin resistant *Staphylococcus aureus* 1268) and Gram- negative (*Morganella morganii* 2, *Pseudomonas aeruginosa* 1246, *Salmonella arizonae* 23, *Proteus vulgaris* 12, *Klebsiella planticola* 8, *Escherichia coli* 13147) strains.
Quantitative assay of the antimicrobial activity was performed by a binary micro dilution method, in 96 multi-well plates, in order to establish the Minimal Inhibitory Concentration (MIC) (mg/mL).

RESULTS AND DISCUSSION

Synthesis of the new compounds was accomplished in three steps.
In the first stage, the 2-phenoxymethylbenzoic acid (**1**) was prepared by treating the phtalide (**2**) with potassium phenoxyde in xylene. The resulting 2-phenoxymethylbenzoic acid potassium salt (**3**) shows a good solubility in a potassium hydroxide aqueous solution and thus was separated from xylene. The aforementioned acid was precipitated using a mineral acid solution. The potassium salt of phenol was obtained using phenol and potassium hydroxide in xylene, the resulting water being removed by azeotropic distillation.
The 6,11-dihydro-dibenz[b,e]oxepin-11(6H)-one (**4**) was synthesized in the second stage by a Friedel-Crafts cyclization of the 2-phenoxymethylbenzoic acid chloride (**5**) in dry 1,2-dichloroethane. The acid chloride was obtained by refluxing the corresponding acid with thionyl chloride in 1,2-dichloroethane.
The new compounds (**6**) were prepared by acylation of the 11-hydroximino-6,11-dihydro-dibenz[b,e]oxepin (**7**) with various substituted benzoic acid chlorides, in dry benzene in the presence of anhydrous pyridine as a proton fixator. The oxime was obtained by treating the 6,11-dihydro-dibenz[b,e]oxepin-11(6H)-one with hydroxylamine hydrochloride in presence of pyridine.
The new compounds are solid, crystallized, white or light yellow.

Antimicrobial activity
Several of the tested compounds exhibited good antimicrobial activity, with MIC values lower than DMSO, against *E. coli*, *P. vulgaris*, *M. morganii* and *Ps. aeruginosa*.
The good antimicrobial activity against the enterobacterial strains was correlated with the *orto*- substitution of the compounds with ethoxy or trifluoromethyl groups.
The anti- *Pseudomonas* activity was improved by the same *orto*- substitution with trifluoromethyl group as well as by the *para*- substitution with trifluoromethoxy group.
The *orto*- substitution with trifluoromethyl conferred the respective compounds good antimicrobial properties against *M. morganii* and *E. coli* and the presence in *orto*-of an ethoxy group improved the antimicrobial effect on *P. vulgaris*.

CONCLUSIONS

An efficient procedure for the synthesis of new dibenz[b,e]oxepin derivatives has been developed. The structures were elucidated by elemental analyses and spectral (IR, ^{1}H-NMR and ^{13}C-NMR) data. The new compounds were screened for *in vitro* antibacterial activity.

ACKNOWLEDGEMENTS

The authors acknowledge support for this work from the Romanian Ministry of Education, Research, Youth and Sport through the PN-II 42095/ 2008 grant.

REFERENCES

1. Lin J, Liu S, Sun B, Niu S, Li E, Liu X, Che Y, Polyketides from the Ascomycete Fungus Leptosphaeria sp. J. Nat. Prod. 2010; 73: 905–910.
2. Hoehn H, Imidazole derivatives of 6,11-dihydro-dibenz[b,e]oxepines and 6,11-dihydro-dibenz[b,e]thiepines, U.S. Patent 4169205, sep. 25, 1979.
3. Limban C, Missir AV, Chiriță IC, Caproiu MT, Draghici C, Nițulescu GM, Novel dibenz[b,e]oxepins derivatives, Rev. Chim. (Bucharest) 2009; 60: 1313- 1317.

FOLLOWUP OF EVEROLIMUS BLOOD CONCENTRATIONS AS AN IMMUNOSUPPRESSIVE AGENT AFTER HEART TRANSPLANTATION

P. Finderle[1*], J. Osredkar[1]

[1] University Medical Centre Ljubljana, Clinical Institute of Clinical Chemistry and Biochemistry, Njegoševa cesta 4, 1525 Ljubljana, Slovenia

INTRODUCTION

Everolimus is a macrolide immunosuppressive agent with anticarcinogenetic properties and is used in solid-organ transplantation. It acts as a growth factor-stimulated T cell proliferation inhibitor and it is metabolized by the hepatic and intestinal cytocrome P450 system. Because of intra- and inter- individual variations in drug absorption, distribution, metabolism, and elimination, Everolimus concentrations has to be monitored in post-transplantation dosage adjustment to reduce risk of toxicity (1,2). The most commonly reported side effects were stomatitis, rash, fatigue, diarrhoea, oedema, abdominal pain, fever, headache, nausea, and infections (3). In therapeutic concentrations Everolimus is predominately partitioned into erythrocytes, which makes whole blood the preferred laboratory analysis matrix.
For monitoring Everolimus concentrations, several HPLC methods are available mostly in combination with mass spectrometry detections. These methods are expensive and not readily available in most clinical laboratories, and requires extensive sample preparation (1,2). A simplest method available for all laboratories was introduced by Thermo Scientific; the QMS® Everolimus Immunoassay is based on the competitive particle-enhanced turbidimetry method.

MATERIALS AND METHODS

In the introduction of Everolimus testing in our laboratory, we followed four heart transplant patients over the past year. We used the QMS® Everolimus Immunoassay (Thermo Scientific) applicated on the biochemical analyser Hitachi Modular (Roche Diagnostics).

We used haemolysate samples obtained from K3EDTA whole blood. Sample pre-treatment included precipitation with methanol and QMS® Everolimus Precipitation reagent and centrifugation at 4.000 rpm, 18 °C, 25 minutes. In the analysis reaction the Everolimus-coated microparticles reagent is rapidly agglutinated in the presence of the anti-Everolimus antibody reagent and in the absence of any competing drug in the sample. When a sample containing Everolimus is added, the agglutination reaction is partially inhibited which is monitored as a slowing of the rate of absorbance change.

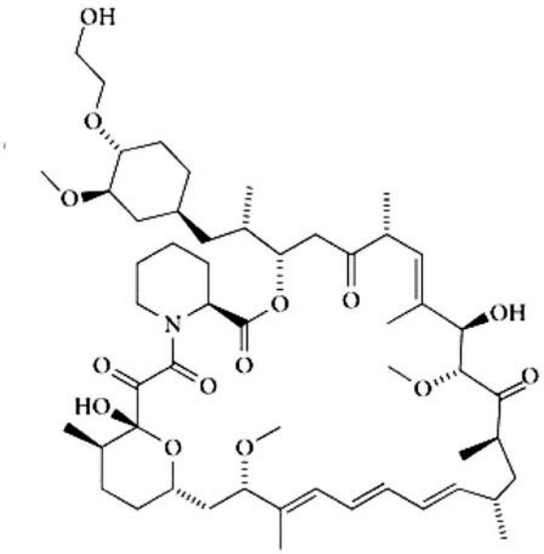

Everolimus

(1*R*,9*S*,12*S*,15*R*,16*E*,18*R*,19*R*,21*R*,23*S*,24*E*,26*E*,28*E*,30*S*, 32*S*,35*R*)-1,18- dihydroxy-12-{(1*R*)-2-[(1*S*,3*R*,4*R*)-4-(2-hydroxyethoxy)-3methoxycyclohexyl]-1 -methylethyl}-19,30-dimethoxy-15,17,21,23,29, 35-hexamethyl-11,36-dioxa-4-aza-tricyclo[30.3.1.0^{4,9}] hexatriaconta-16,24,26,28-tetraene-2,3,10,14,20-pentaone; $C_{53}H_{83}NO_{14}$; M_r = 958.2

Fig. 1: Everolimus structure and chemical name.

RESULTS AND DISCUSSION

Studies have shown good applicability of QMS® Everolimus assay in the follow up of post-transplantant patients. Correlation with LC-MS method among 41 heart transplant patient samples gave a correlation coefficient of 0.92, slope 1.00, and y-intercept -0.15. Precision tests with patient sample pool showed a %CV of 9,45 and 6,62 in the low and high concentration range, respectively. Cross-reactivity with drugs that are routinely administered with Everolimus was not detectable.

All four patients we followed were heart-transplanted and on Everolimus immunosuppressive therapy. The concentrations monitored through the post-transplantation period are shown in figure 2. It is perceived that after an increase of Everolimus concentrations in the initial weeks of therapy observation, there was a decrease presumably on the account of a lower drug dose.

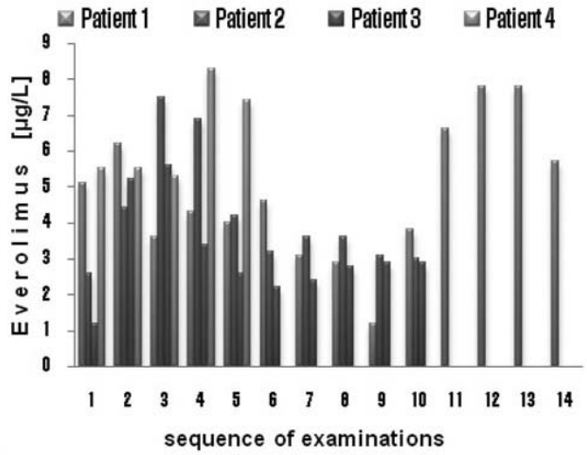

Fig. 2: Graphical view of Everolimus concentrations through patients examinations over the past year for 4 heart-transplant patients.

CONCLUSIONS

The goal of every physician is to obtain the optimum balance between therapeutic efficacy and the occurrence of adverse events. Because of pharmacokinetics and pharmacodynamics variability in patients it is difficult to apply a standard therapeutic protocol (4). The therapeutic drug monitoring of immunosuppressant drugs such as Everolimus aids in patient management in post-transplantation therapy. The assay for Everolimus concentration monitoring presented in this work is a quick and convenient test which can be accessible to most clinical laboratories.

REFERENCES

1. Khoschsorur G. Simultaneous measurement of sirolimus and everolimus in whole blood by HPLC with ultraviolet detection. Clin. Chem. 2005, 51: 1721-1723.
2. Annesley TM, Clayton L. Simple extraction protocol for analysis of immunosuppresant drugs in whole blood. Clin. Chem. 2004, 50:1845-1848.
3. Nordqvist C. Afinitir (everolimus) for rare pancreatic cancer approved by FDA. Medical news today 2011, http://www.medicalnewstoday.com/articles/224560.php.
4. Johnston A. Holt DW. Therapeutic drug monitoring of immunosuppressant drugs. J. Clin. Pharmacol. 1999, 47: 339-350.

*UGT1A1*28* GENOTYPE AFFECTS THE IN VITRO GLUCURONIDATION OF BISPHENOL A

T. Trdan*, R. Roškar, J. Trontelj, A. Mrhar

Department of Biopharmacy and Pharmacokinetics, University of Ljubljana, Faculty of Pharmacy, Aškerčeva cesta 7, 1000 Ljubljana, Slovenia

INTRODUCTION

Bisphenol A (BPA) is a chemical that is used worldwide as essential component of polycarbonate plastic and human exposure to BPA is thought to be of importance, especially because of its estrogenic activity (1). BPA is efficiently glucuronidated to BPA monoglucuronide (BPAG), which has been identified as the predominant metabolite in humans (2). Contrary to BPA, BPAG does not exhibit estrogenic activity (3). Among the UDP-glucuronosyltransferases (UGTs), the UGT2B15 showed the highest activity of BPA glucuronidation, followed by the UGT1A9, UGT2B7, UGT1A1, UGT2B4 and UGT1A3 (4). It has already been shown that UGT2B15 variant having D85Y substitution markedly reduced the intrinsic clearance compared to the wild type (5). As BPA is conjugated also with UGT1A1 which is commonly polymorphic and consequently causes a decreased UGT1A1 activity (6), we have decided to study the association of *UGT1A1* genotype with *in vitro* BPA glucuronidation.

MATERIALS AND METHODS

Materials

Human liver microsomes genotyped for *UGT1A1 *1/*1, *1/*28, *28/*28* variants, Solution A (uridine 5'-diphospho-glucuronic acid (UDPGA)), Solution B (Tris-HCl, $MgCl_2$, alamethicin) were from BD Gentest, bisphenol A, bisphenol A–d16 (BPA_{d16}) from Sigma Aldrich. Bisphenol A glucuronide, bisphenol A glucuronide-d16 ($BPAG_{d16}$) were synthesized and characterised in our laboratory.

Microsomal incubations

The incubation mixture contained 50 µg/mL of human liver microsomes, 8 mM $MgCl_2$, 50 mM Tris-HCl, 25 µg/mL alamethicin, 2 mM UDPGA and 0.5 - 100 µM BPA. Firstly, microsomes were mixed with Solution B and kept on ice for 15 min. Then bisphenol A dissolved in methanol was added and the mixture was preincubated at 37˚C for 10 min. Final methanol concentration in incubation was 1%. To initiate the reaction, UDPGA was added resulting in a final volume of 150 µL. The reaction was carried out for an additional 4 min. The assays were terminated by adding 450 µL of ice cold methanol containing 5 µM BPA_{d16} and 0.5 µM $BPAG_{d16}$ as internal standards. The incubation mixture was left at – 20˚C for 48 hours and then centrifuged at 1300*g* for 100 min at 4˚C. The supernatant was subjected to LC-MS/MS for the determination of BPA and BPAG.

Data analysis

Glucuronidation activities were determined on three replicates. Apparent kinetic parameters were analyzed using substrate inhibition kinetics model:

$$v = \frac{V_{max} * S}{K_m + S * (1 + \frac{S}{K_{si}})} \quad \text{(Eq. 1)}$$

where represents the reaction velocity, is the maximum velocity, S is the substrate concentration, K_m is the Michaelis-Menten constant and K_{si} is constant of substrate inhibition. Goodness of fit to substrate inhibition equation was assessed by visual inspection of Michaelis-Menten plots, determination of the r^2 values and standard error (SE). Kinetic parameters such as K_m, V_{max} and K_{si} for BPA glucuronidation were estimated by analyzing Michaelis-Menten plots using the Enzyme Kinetics Module 1.3 from Sigma Plot 11.0.

Intrinsic clearance (Cl_{int}) was calculated as V_{max}/K_m. The differences in glucuronidation levels among *UGT1A1* genotypes were tested using z-test with Holm's correction.

RESULTS AND DISCUSSION

Incubation of BPA with each of genotyped human liver microsomes in the presence of UDPGA led to the formation of BPAG, which exhibited a substrate inhibition enzyme kinetics. Nonlinear regression curves based on the substrate inhibition equation and determined apparent kinetic parameters are shown in Figure 1 and Table 1.

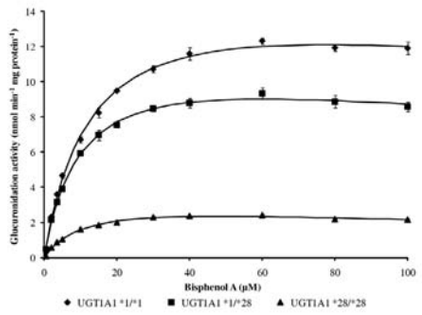

Fig. 1: Michaelis-Menten plots for BPA glucuronidation by human liver microsomes genotyped for the UGT1A1*28 polymorphism

Table 1: Apparent kinetic parameters for the BPA glucuronidation by human liver microsomes genotyped for the UGT1A1*28 polymorphism

UGT1A1 genotype	K_m (µM)	V_{max} (mmol min^{-1} mg^{-1})	K_{si} (µM)	Cl_{int} (ml min^{-1} mg^{-1})	r^2
*UGT1A1*1/*1*	13.1 (1.1)	16.2 (0.9)	455.0 (121.5)	1.24 (0.12)	0.993
*UGT1A1*1/*28*	10.0 (0.9)	12.0 (0.5)	356.1 (89.1)	1.19 (0.12)	0.988
*UGT1A1*28/*28*	10.6 (0.9)	3.4 (0.1)	221.9 (36.5)	0.32 (0.03)	0.989

Values in table are presented as mean (standard error).

The K_m values of all tested human liver microsomes ranged from 10.0 to 13.1 µM and did not significantly differ among the *UGT1A1* variants. The V_{max} determined in the incubation with *UGT1A1 *1/*1* human liver microsomes did not differ significantly from *UGT1A1 *1/*28* microsomes. On the contrary, V_{max} determined in the incubation with *UGT1A1 *28/*28* human liver microsomes was significantly lower from both, the wild type homozygotes and the heterozygotes. The same was observed for the calculated intrinsic clearances that are presented in Figure 2.

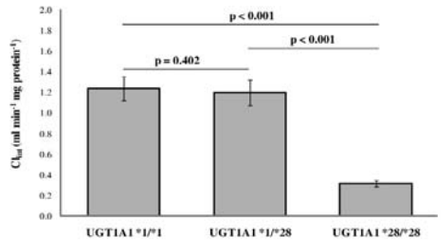

Fig. 2: BPA intrinsic clearance determined by human liver microsomes genotyped for the UGT1A1*28 polymorphism.

CONCLUSIONS

Our results suggest that BPA importantly interacts with UGT1A1 in human and that the common *UGT1A1*28* polymorphism, when present in a homozygous state, may significantly decrease the BPA clearance, which may lead to its higher toxicity, such as hormone disruption and reproductive effects. Our results show that BPA metabolism may be significantly influenced by a person's genotype and this discovery may present an important fact for the currently on going worldwide BPA risk assessment.

REFERENCES

1. Kang J-H, Kondo F, Katayama Y. Human exposure to bisphenol A. Toxicol. 2006; 226: 79-89.
2. Völkel W, Colnot T, Csanady GA et al. Metabolism and kinetics of bisphenol A in humans at low doses following oral administration. Chem. Res. Toxicol. 2002; 15: 1281-1287.
3. Matthews JB, Twomey K, Zavharewski TR. In vitro and in vivo interactions of bisphenol a and its metabolite, bisphenol a glucuronide, with estrogen receptors α and β. Chem. Res. Toxicol. 2001; 14: 149-157
4. Hanioka N, Naito T, Narimatsu S. Human UDP-glucuronosyltransferase isoforms involved in bisphenol A glucuronidation. Chemosphere. 2008; 74: 33-36.
5. Hanioka N, Oka H, Nagaoka K et al. Effect of UDP- glucuronosyltransferase 2B15 polymorphism on bisphenol A glucuronidation. Arch. Toxicol. 2011. DOI 10.1007/s00204-011-0690-5.
6. Bosma PL, Chowdhury NR, Goldhoorn BG, et al. The genetic basis of the reduced expression of bilirubin UDP- glucuronosyltransferase 1 in Gilbert's syndrome. N. Engl. J. Med. 1995; 333: 1171-1175.

A COMPARISON OF TWO RNA ISOLATION METHODS TO DETERMINE SOD1 AND SOD2 GENE EXPRESSION IN HUMAN BLOOD AND MONONUCLEAR CELLS

A. Vujovic*, V. Spasojevic-Kalimanovska, N. Bogavac-Stanojevic, S. Spasic, J. Kotur-Stevuljevic, Z. Jelic-Ivanovic

Department of Medical Biochemistry, Faculty of Pharmacy, University of Belgrade, Vojvode Stepe 450, Belgrade, Serbia

INTRODUCTION

In the current study two RNA isolation techniques were compared and their abilities to produce high-quality RNA were evaluated. mRNA expression profiles of SOD1 (Cu/Zn superoxide dismutase) and SOD2 (Mn superoxide dismutase) genes were measured by real-time PCR.

MATERIALS AND METHODS

From a pool of fresh human citrate whole blood and ten healthy individuals RNA was isolated with the TRIzol™ extraction method (TRI) (1) and with the 6100 Nucleic AcidPrepStation (ABI) (2). The concentration and purity of RNA extracts were determined spectrophotometrically. RNA integrity was evaluated by electrophoresis on a 1% agarose gel (3). PCR was performed on a 7500 Real-Time PCR System. The student's *t*-test was applied to compare normally distributed variables.

RESULTS AND DISCUSSION

Both protocols gave similar RNA quantities when adjusted to the initial blood volume. Relative quantification values obtained from the TRI method for SOD1 were significantly higher ($P<0.01$) and for SOD2 were significantly lower ($P<0.05$) than those obtained from the ABI method, respectively. Coefficients of variation for gene expression parameters in SOD1 and SOD2 analyses were lower when the TRI method was used.

CONCLUSIONS

The TRI method was generally more consistent in yielding pure RNA in comparison to the ABI and better reproducibility in gene expression analyses was apparent.

REFERENCES

1. Chomczynski P, Sacchi N. Single-step method of RNA isolation by acid guanidinium thiocyanate-phenol-chloroform extraction. Anal Biochem 1987: 162; 156-9.
2. Applied Biosystems Protocol. Isolation of Total RNA from Whole Blood and from Cells Isolated from Whole Blood. 2004 Part Number 4332809 Rev. B.
3. Sambrook, J., Russel, D.W. Molecular Cloning: A Laboratory Manual. CSH Laboratory Press, Cold Spring Harbor, NY 2001.

ANTIMICROBIAL ACTIVITY OF COPPER AND ZINC-DOPED HYDROXYAPATITE NANOPOWDERS

Jelena Stankovic[1], Vojislav Stanic[2], Suzana Dimitrijevic[3], Miodrag Mitric[2], Bojan Jokic[3], Ilija Plecas[2], Slavica Raicevic[2]

[1] *Faculty of Pharmacy, University of Belgrade, 11001 Belgrade, Serbia*
[2] *Vinca Institute of Nuclear Sciences, University of Belgrade, P.O. Box 522, 11001 Belgrade, Serbia*
[3] *Faculty of Technology and Metallurgy, University of Belgrade, 11001 Belgrade, Serbia*

Inorganic antimicrobial materials are made of heavy metal ions having biocidal action such as silver, zinc or copper, and calcium phosphate, zeolite or other silica substrate. Among them, one of the calcium phosphates, synthetic hydroxyapatite (HAP, $Ca_{10}(PO_4)_6(OH)_2$), is the most promising because of its biocompatibility, good cation exchange rate with metals, and high affinity for the pathogenic microorganisms. The objective of this research is to synthesize the monophasic Cu(II) and Zn(II) doped hydroxyapatite nanopowders with high crystallinity and to examine their antimicrobial activity.. The antimicrobial activity against *Escherichia coli* (*E. coli*, ATCC 25922), *Staphylococcus aureus* (*S. aureus*, ATCC 25923) and *Candida albicans* (*C. albicans*, ATCC 24433) was evaluated in vitro by agar diffusion method and by liquid challenge method in buffer solution. The results of antimicrobial disk diffusion tests showed that only $CuHAP_2$ affects *E. coli* and *C. albicans*. There is no inhibition zone for *S. aureus*. The results of the quantitative antimicrobial tests in liquid medium demonstrate that all metal-doped HAP samples show viable cells reduction of all microorganism species.

Antimicrobial activity of samples with copper and zinc was similar. We suppose that the reason for this similarity is that the greater quantity of incorporated Zn(II) ions was in the surface of ZnHAP samples particles.

Key words: hidroxyapatite, nanoparticle, antimicrobial

REFERENCES

1. Carson KC, Bartlett JG, Tan TJ and Riley TV, In vitro susceptibility of methicillin-resistant Staphylococcus aureus and methicillin-susceptible Staphylococcus aureus to a New antimicrobial, copper silicate, Antimicrob. Agents Chemother. 2007; 51, 4505–4507.
2. Zhou Y, Xia M, Ye Yand Hu C, Antimicrobial ability of Cu2+-montmorillonite, Appl. Clay Sci. 2004; 27: 215–218.

POPULATION PHARMACOKINETICS OF VANCOMYCIN IN HOSPITALIZED ADULT PATIENTS AT A MALAYSIAN TERTIARY CARE HOSPITAL

C. Long*, N. Che Amin, M. Manan[1]

[1] *Faculty of Pharmacy, Universiti Teknologi MARA (UiTM), 42300 Malaysia*

INTRODUCTION

Population pk is fundamental in measuring the variability such as age, sex, weight and disease state within the selected population for optimizing the dosing regimen. There is no data reported on the vancomycin pk in Malaysian adult therefore it is crucial to obtain estimates of the variability in the local population. This study aims to conduct a population pk analysis in order to obtain pk data for vancomycin in adult patients at Tengku Ampuan Rahimah Hospital (TARH), a tertiary care public hospital in Malaysia.

MATERIALS AND METHODS

Data were collected retrospectively from the patient medical record and TDM forms from 2009 to 2010. Inclusion criteria consist of adult patients ranges from 18-65 years of age, at least one pre- and post-vancomycin serum concentration been determined, calculated creatinine clearance must be more than 15ml/min. Patients were excluded if complete medical records could not be obtained, patients who were on hemodialysis and transplant patients. Creatinine clearance (CLcr), was estimated by the Cockcroft-Gault equation. Pk parameters such as CL, Ke, Vd, and t1/2 were estimated by fitting one-compartment infusion model with first-order elimination to serum vancomycin concentration. Vancomycin serum concentrations were measured at the Clinical Pharmacokinetic Unit using fluorescence polarization immunoassay (FPIA) method with TDx assay system (Abbott Laboratories, Chicago,IL).

RESULTS AND DISCUSSION

Serum vancomycin concentration data (n=398 points) of 60 patients (32 male and 28 female patients) were included and analyzed. The patients had an average age of 45 and an average weight of 66. The patients' demographic parameters such as gender, age, body weight, creatinine clearance (ClCr) and serum electrolytes were analyzed to identify their potential influences or correlations on vancomycin pk. Table 1 summarises the estimated mean population pk parameter values. From data analysis the inter-individual variability of ke, t1/2 and Vd were 65%, 64% and 36% respectively and the estimated pk parameters are different among patient subgroups of impaired and normal renal function.

Parameters (Mean ± SD)	Male	Female	Total
K_e, hr^{-1}	0.19 ± 0.10	0.14 ± 0.11	0.17 ± 0.11
$t_{1/2}$, hr	4.76 ± 2.64	7.62 ± 4.52	6.09 ± 3.88
C_{max}, mg/L	23.31 ± 8.80	28.99 ± 9.44	25.96 ± 9.47
$C_{min,}$ mg/L	7.29 ± 5.12	12.05 ± 7.56	9.51 ± 6.76
$V_{d,}$ L/kg	0.60 ± 0.25	0.70 ± 0.32	0.64 ± 0.28

Table 1: Estimated mean population pk parameter values (n=60).

CONCLUSIONS

The pk parameter values for vancomycin in adult patients in the involved hospital were estimated. The results of this analysis indicate that the population estimates for vancomycin pk parameters were generally in agreement with literature values. Wide inter-patient variability justified the practice of routine TDM. The renal function of patient influenced the disposition of vancomycin. The pk parameters defined according to local population and its renal function can assist clinician in determining accurate vancomycin empirical therapy regime.

TRACKING OF THE MICROWAVE INDUCED SUPRAMOLECULAR STRUCTURAL CHANGES OF POLYMERS WITH POSITRON ANNIHILATION LIFETIME SPECTROSCOPY

B. Szabó[1*], M. Molnár[2], K. Süvegh[3], R. Zelkó[4]

[1] Gedeon Richter Plc., Formulation R&D, Gyömrői Str. 19-21, H-1103 Budapest, Hungary; [2] Laboratory of Nuclear Chemistry, Eötvös Loránd University/HAS Chemical Research Center, 1518 Budapest 112, P.O. Box 32, Hungary; [3] Department of Organic Chemistry, Eötvös Loránd University, 1518 Budapest 112, P.O. Box 32, Hungary; [4] University Pharmacy Department of Pharmacy Administration, Semmelweis University, Hőgyes Endre Str. 7-9, H-1092 Budapest, Hungary

INTRODUCTION

Controlled drug release is one of the most examined research area of pharmaceutical sciences. However, the investigation and modification of the structure of applied polymers become more and more important. Microwave treatment is frequently used in order to modify the polymeric structure and recently several studies deal with the effect of such treatments on the drug release characteristics of biopolymers (1). Any phenomenon involving the free volume change can be detected with positron annihilation lifetime spectroscopy (PALS) therefore it can be recommended in pharmaceutical industrial stability studies (2,3). The influence of microwave irradiation in the case of samples stored under controlled conditions was also investigated and it was found that the stored samples reacted less sensitively to the treatment (4).

The aim of this study was to investigate the influence of microwave treatment and storage on the structural changes of frequently applied polymeric excipients, two types of Carbopol and Sodium alginate, by PALS technique.

MATERIALS AND METHODS

Materials

Sodium alginate (Aldrich, batch number: 0063ITB) Carbopol 71G (Noveon, batch number: TW56GAJ066) Carbopol Ultrez 10 NF (Lubrizol, batch number: 0100648897).

Storage conditions

Samples of the pure substances were stored in closed containers at 40 °C ± 2 °C and 75% ± 5% relative humidity (achieved by oversaturated NaCl solution) for 1 week.

Microwave treatment

Milestone Multisynth AFC-FO 300 microwave reactor was applied for the treatment of various polymers with the following measuring parameters.
Maximum power: 800 W
Maximum pressure: 20 bar
Maximum temperature: 250 °C and 300 °C
Vessel volume: 10 ml
The selected programs are below:
400 W, 4 minutes (constant power)
800 W, 4 minutes (changing power).
The temperature profile was the same in both cases.

Positron annihilation lifetime spectroscopy (PALS)

For the positron lifetime measurements, a positron source made of carrier-free $^{22}NaCl$ was used. Its activity was around 105 Bq and the active material was sealed between two very thin Ti foils. Lifetime spectra were measured with a fast-fast coincidence system (5) based on BaF_2 /XP2020Q detectors and Ortec electronics. Every spectrum was recorded in 4096 channels of an analyser card and each contained 107 coincidence events. Several parallel spectra were measured at each concentration to increase the reliability. The lifetime spectra were evaluated individually by the RESOLUTION computer code (6); the indicated errors are the standard deviations of the lifetime parameters obtained.

RESULTS AND DISCUSSION

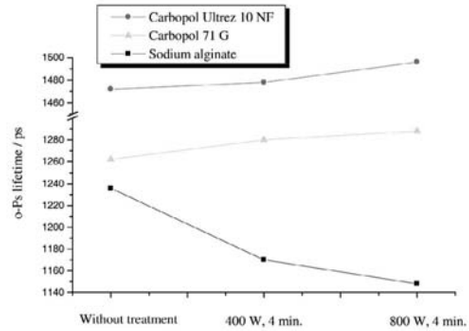

Fig. 1: The effect of microwave treatment on the o-Ps lifetime values of polymers

Fig. 1 illustrates that the microwave treatment slightly increased the o-Ps lifetime values in Carbopol polymers while remarkable decrease could be observed in the case of Sodium alginate. Along with the increase of power the extent of changes also increased. The microwave treatment resulted in the loss of crystal water of Sodium alginate thus decreasing the o-Ps lifetime values and consequently the polymeric free volumes. In contrast to Sodium alginate, the o-Ps values of Carbopols increased as a result of microwave

treatment. The latter could be explained by the effect of elevated temperature which increased the distance between the polymeric chains.

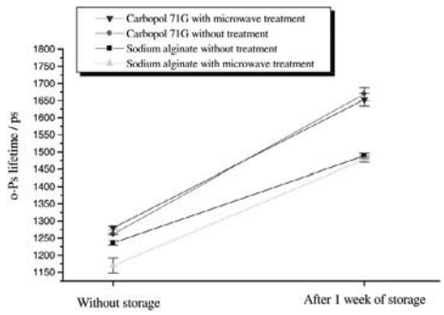

Fig. 2: The effect of storage on the changes of polymers induced by microwave treatment

It is clearly seen from Fig. 2 that the significant differences of o-Ps lifetime values of unstored samples disappeared after 1-week storage. After this short time storage period there were no significant differences in the o-Ps lifetime values of stored (microwave-treated and untreated) samples, consequently the effect of microwave treatment on the supramolecular structure of the examined polymers could be considered reversible.

REFERENCES

1. Wong TW, Chan LW, Kho SB, Sia Heng PW. Design of controlled-release solid dosage forms of alginate and chitosan using microwave. J. Control. Release 2002; 84: 99-114.
2. Pintye-Hódi K, Süvegh K, Marek T, Zelkó R. Tracking of the effects of the plasticizer on the water uptake and free volume changes of methylcellulose. Polym. Adv. Technol. 2007; 18: 921-924.
3. Süvegh K, Zelkó R. Physical Aging of Poly(vinylpyrrolidone) under Different Humidity Conditions. Macromolecules. 2002; 35: 795-800.
4. Wong TW, Chan LW, Kho SB, Sia Heng PW. Aging and microwave effects on alginate/chitosan matrices J. Control. Release 2005; 104: 461-475.
5. Mackenzie IK, In: Brandt W, Dupasquier A (Eds.), Positron Solid-State Physics. Experimental methods of annihilation time and energy spectrometry. North-Holland, Amsterdam, 1990, p. 196.
6. Kirkegaard P, Eldrup M, Mogensen OE, Pedersen N.J. Program system for analysing positron lifetime spectra and angular correlation curves. Comput. Phys. Commun. 1981; 23: 307–338.

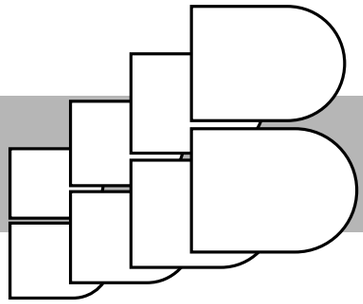

INDEX

G

H

I

J

K

L

M

N

O

P

R

S

Š

T

U

V

W

Y

Z

Ž